ISSN 0914-9457

日本磁気共鳴医学会雑誌

JAPANESE JOURNAL OF MAGNETIC RESONANCE IN MEDICINE

第44回日本磁気共鳴医学会大会　講演抄録集
2016年9月　大宮ソニックシティ

MR

VOL.36
SUPPLEMENT
2016

一般社団法人　日本磁気共鳴医学会

JSMRM2016 第44回日本磁気共鳴医学会大会開催にあたって

JSMRM 2016、第44回日本磁気共鳴医学会大会（通称、MR学会）を2016年9月9日（金）～11日（日）に大宮ソニックシティにて開催いたしますので一言ご挨拶を申し上げます。

テーマを「MRI Now and Beyond」としました。MRIの現状の把握と未来への展望を探るものです。今大会ではまず、現状の把握として、今、でできることと残る課題を検討します。そして未来への展望として、近い将来への現有技術の展開と、さらに未来へのseedingの展望を試みたいと思います。
今回JSMRM 2016の新しい点を挙げますと、

1. 国際化の推進
すべての抄録・スライド・ポスターを英語としました。口頭発表形式の一部を英語とし、海外からの一般演題募集を開始しました。公式名称もJSMRM2016とします。韓国MR学会KSMRM（Korean Society of Magnetic resonance in Medicine）との共催シンポジウムは昨年から毎年の相互開催となり、今大会でも両国間の学術的・人的交流をさらに深めたいと思います。

2. 会期を金曜日−日曜日としました。
従来の木曜日−土曜日から1日後ろにずらしました。従来に比べて、病院勤務の方々には出席しやすいかと期待しております。

3. 抄録集のスリム化
大会の抄録集は厚くなる一方です。今大会もアプリを使用したWEB参照を出来るようにしますが、紙の抄録集の要望も高いのも事実です。そこで今回は、抄録集への掲載は一般演題と教育講演のみとし、シンポジウムなど特別講演の抄録・CVはありません。お忙しいところを手弁当で来ていただいているシンポジウム発表者の負担を少しでも軽減する意図もあります。また各社のワークインプログレスも廃止しました。このようにして抄録集の減量を図ります

4. 第一展示場を出席者の憩いの場とします。
会場で一番広い、第一展示場で機器展示を行います。飲料も提供します。埼玉県は全国第4位の日本酒生産県ですが、あまり知られておりません。今回は「文楽」酒造様のご厚意により、午後に限って、日本酒の試飲会を行います。会期2日目の土曜日18時からは全員懇親会・優秀ポスター表彰式を第一展示場で行います。アトラクションとして東京大学音楽部管弦楽団ホルンセクションOB・OGの演奏があります。また「テスラ」のよしみで、会期期間中、テスラモーターズの電気自動車「テスラ」、プレミアムEVセダン「モデルS」を展示しております。

5. 緊急シンポジウムを追加
先日報道され、会員の多くが関心もお持ちと思われる、fMRIデータ解析の問題点について、解説・検討の場を設けます。

最後に、今回の大宮ソニックシティは、私にとって思い入れが強い会場です。1997年に板井悠二・筑波大学放射線科主任教授が第25回大会長をなされ、私が実行委員長を務めた会場です。当時は参加者が1000名ちょっと、口演会場も4会場と、現行の2000名近い参加者、5会場よりは、小規模な、こじんまりとした学会でした。

思い入れの多い大宮の地で、皆様をお迎えするのをスタッフ一同、心待ちにしております。

JSMRM2016 第44回日本磁気共鳴医学会大会　大会長
埼玉医科大学 放射線科
新津　守

日本磁気共鳴医学会歴代会長

第 1 代	有水　昇	1981(昭和56)年7月～1989(平成元)年9月
第 2 代	佐久間貞行	1989(平成元)年9月～1991(平成 3)年9月
第 3 代	高橋　睦正	1991(平成 3)年9月～1993(平成 5)年9月
第 4 代	舘野　之男	1993(平成 5)年9月～1996(平成 8)年3月
第 5 代	亘　弘	1996(平成 8)年4月～1998(平成10)年3月
第 6 代	高橋　睦正	1998(平成10)年4月～2000(平成12)年3月
第 7 代	宮坂　和男	2000(平成12)年4月～2002(平成14)年3月
第 8 代	渡部　徳子	2002(平成14)年4月～2004(平成16)年3月
第 9 代	杉村　和朗	2004(平成16)年4月～2006(平成18)年3月
第10代	犬伏　俊郎	2006(平成18)年4月～2008(平成20)年3月
第11代	荒木　力	2008(平成20)年4月～2010(平成22)年6月
第12代	梅田　雅宏	2010(平成22)年7月～2012(平成24)年9月
第13代	新津　守	2012(平成24)年9月～2014(平成26)年9月
第14代	巨瀬　勝美	2014(平成26)年9月～2016(平成28)年9月
第15代	原田　雅史	2016(平成28)年9月～

歴代大会長

第 1 回	1981(昭和56)年	有水　昇	東　京
第 2 回	1982(昭和57)年	有水　昇	東　京
第 3 回	1983(昭和58)年	松沢　大樹	仙　台
第 4 回	1984(昭和59)年	亀井　裕孟	つくば
第 5 回	1985(昭和60)年(春)	飯尾　正宏	東　京
第 6 回	1985(昭和60)年(秋)	飯沼　武	東　京
第 7 回	1986(昭和61)年(春)	古瀬　和寛	中津川
第 8 回	1986(昭和61)年(秋)	鳥塚　莞爾	京　都
第 9 回	1987(昭和62)年(春)	亘　弘	岡　崎
第10回	1987(昭和62)年(秋)	青野　要	岡　山
第11回	1988(昭和63)年(春)	荒田　洋治	東　京
第12回	1988(昭和63)年(秋)	竹中　榮一	東　京
第13回	1989(平成元)年(春)	金沢　洋子	福　岡
第14回	1989(平成元)年(秋)	舘野　之男	東　京
第15回	1990(平成 2)年(春)	曽我美　勝	岐　阜
第16回	1990(平成 2)年(秋)	佐久間貞行	名古屋
第17回	1991(平成 3)年(春)	井上　多門	東　京

第18回	1991(平成 3)年(秋)	高橋　睦正	熊　本
第19回	1992(平成 4)年(春)	遠藤　真広	東　京
第20回	1992(平成 4)年(秋)	入江　五朗	札　幌
		宮坂　和男	
第21回	1993(平成 5)年	能勢　忠男	つくば
第22回	1994(平成 6)年	小塚　隆弘	大　阪
第23回	1995(平成 7)年	渡部　徳子	東　京
第24回	1996(平成 8)年	湯浅　龍彦	大　磯
第25回	1997(平成 9)年	板井　悠二	大　宮
第26回	1998(平成10)年	成瀬　昭二	京　都
第27回	1999(平成11)年	多田　信平	東　京
第28回	2000(平成12)年	西川　弘恭	京　都
第29回	2001(平成13)年	上野　照剛	つくば
第30回	2002(平成14)年	蜂屋　順一	東　京
第31回	2003(平成15)年	荒木　　力	山　梨
第32回	2004(平成16)年	犬伏　俊郎	大　津
第33回	2005(平成17)年	平敷　淳子	東　京
第34回	2006(平成18)年	三森　文行	つくば
第35回	2007(平成19)年	杉村　和朗	神　戸
第36回	2008(平成20)年	田中　邦雄	旭　川
第37回	2009(平成21)年	吉川　宏起	横　浜
第38回	2010(平成22)年	巨瀬　勝美	つくば
第39回	2011(平成23)年	興梠　征典	北九州
第40回	2012(平成24)年	富樫かおり	京　都
第41回	2013(平成25)年	原田　雅史	徳　島
第42回	2014(平成26)年	梅田　雅宏	京　都
第43回	2015(平成27)年	青木　茂樹	東　京
第44回	2016(平成28)年	新津　　守	大　宮

ご 案 内

1．会期および会場

会　期：2016年9月9日（金）・10日（土）・11日（日）

会　場：大宮ソニックシティ

〒330-8669　埼玉県さいたま市大宮区桜木町1-7-5

TEL：048-647-4558

総合受付：	ソニックシティホール	1F　大ホール前ホワイエ
ＰＣ受付：	〃	〃
クローク：	〃	〃
大会本部：	〃	1F　楽屋
第１会場：	〃	1F　大ホール
第２会場：	〃	2F　小ホール
第３会場：	〃	4F　国際会議室
第４会場：	ソニックシティビル	4F　401・402会議室
第５会場：	〃	4F　403・404会議室
委員会会場：	〃	9F　903・904・905会議室
ポスター受付：	〃	1F　第2-5展示場前ホワイエ
ポスター会場：	ソニックシティホール	B1F　第2-5展示場
PDFポスター会場：	〃	B1F　第2-5展示場
機器展示会場：	〃	B1F　第1展示場

2．参加者へのご案内

1）参加費

	当日参加
本学会　正会員	12,000円
本学会　学生会員	4,000円
一般参加者	15,000円
基礎系学生・外国人留学生（非会員）	6,000円

＊学生の方は「学生証」等、在学を証明できるものを受付で提示してください。

＊熊本・九州地方で被災した大学・研究機関に所属の学生の支援を目的として参加費の免除制度を設けています。希望者は当日登録の際にお申し出ください。

2）登録受付時間

9月 9 日（金）7：15～17：00

9月10日（土）7：30～17：00

9月11日（日）7：30～12：00

3）事前登録者

ネームカードは事前に郵送させていただいております。ネームカードに付いております「プログラム抄録集引換券」と引き換えに、所定場所にてプログラム抄録集とネームカードホルダーをお受け取りください。

＊プログラム抄録集引換所：9月9日（金）7：15～11：00　ソニックシティホール　1F　エントランスホール

9月9日（金）11：00以降～　総合受付横

4）当日登録者
記名台にて当日登録用紙に必要事項を記入し、「当日登録受付」にて当日参加費を支払い、ネームカード（参加証、領収書）と抄録集をお受け取りください。ネームカードには、可能な限り日本語とローマ字併記にて、ご所属、ご氏名を必ずご記入ください。大会の国際化推進のため、ご協力をお願いいたします。

5）抄録集を別途ご希望の方
参加費には、抄録集が1冊含まれます。追加で購入を希望される方は、「総合受付」にお申し出ください。1冊4,000円（税込）です。配送希望の場合、送料を実費ご負担いただきます。

6）ランチョンセミナーについて
ランチョンセミナーではチケット（入場整理券）を配布します。チケットをお持ちの方が優先的に入場となります。
配布場所：ソニックシティホール　B1F　第1展示場前ホワイエ
配布時間：9月9日（金）9：30～11：00
　　9月10日（土）、9月11日（日）8：00～11：00
（無くなり次第終了。残数がある場合、11：00以降は会場前にて配布します）
※チケットはセミナー開始5分後に無効となります。セミナー開始5分以降はチケットをお持ちの方でもご入場いただけない場合もございますのでご了承ください。

7）全員懇親会
9月10日（土）18：00より、ソニックシティホール　B1F　第1展示場にて開催いたします。会費は無料です。お食事やお飲み物をご用意しておりますので、お誘い合わせの上、是非ご参加ください。

8）総会
9月9日（金）16：30～17：30　第5会場（ソニックシティビル　4F　403-404会議室）にて開催いたします。

9）クローク
ソニックシティホール　B1F　大ホール前ホワイエのクロークをご利用ください。

10）無線LANについて
大会期間中は展示会場（ソニックシティホール　B1F　第1展示場）および第1会場（ソニックシティホール　1F　大ホール）で無線LANが使えます。

11）日本磁気共鳴医学会への入会手続き
一般演題の発表者で未入会の方は、学会事務局にご連絡の上、至急入会手続きをお済ませください。
一般社団法人日本磁気共鳴医学会事務局
〒105-0012　東京都港区芝大門2-12-8　浜松町矢崎ホワイトビル2F
TEL：03-6721-5388　FAX：03-6721-5433

12）大会HP上（http://www.c-linkage.co.jp/jsmrm44/）にて、オンラインで演題検索・閲覧やスケジュール登録ができる抄録アプリの紹介ページをご案内しています。パソコンでご利用いただけるWeb版と、iPhoneやAndroid等に対応した電子抄録アプリ（JSMRM2016）をご用意しておりますので是非ご活用ください。アプリダウンロードページのURLは、iOS（App Store）用が<https://goo.gl/P3lNNR>、Andoroid（Google Play）用が<https://goo.gl/VKALG0>となっております。なお、抄録の閲覧には、ネームカードに印刷されているパスワードの入力が必要です。

3．会員のみなさまへ

会員へのメール配信サービスをより充実させるため、下記の二次元バーコードもしくは下記アドレスの日本磁気共鳴医学会ホームページより各種変更手続きに進みメールアドレス等の登録をお願いします。

http://www.jsmrm.jp/

4．アプリについて

「jsmrm2016」または「日本磁気共鳴医学会」で検索してください。iOS版とAndroid版を用意しております。

←iOS版　←Android版　←メール登録

お　願　い

・ネームカード（参加証、兼領収書）の再発行は行いませんので紛失しないようご注意ください。
・ネームカードは、各会場への入場券となりますので、大会期間中は必ずご着用ください。
・ネームカードホルダーを記名台にご用意しておりますので、ご自由にお取りください。
・会場内での呼び出しは行いません。参加者への連絡は、総合受付で申し受け、受付付近のメッセージボードに掲示します。呼び出しが予想される方は掲示板をご確認ください。
・会場内では携帯電話のスイッチをお切りいただくか、マナーモードに設定してください。
・大会長の許可のない掲示・展示・印刷物の配布・録音・写真撮影・ビデオ撮影は固くお断りいたします。

発表者へのご案内

1．口頭発表演者の方へ

1）パワーポイントによるコンピュータ（以下、PC）発表のみとなります。講演に使用できるPCプロジェクターは1台（スクリーン1面）のみです。

2）B1F ホワイエにて「PC 受付」を設けております。発表されるセッションの開始 30分前までに「PC 受付」にお越し頂き、試写を行ってください。

受付時間：9月 9 日（金）7：15～17：00
9月11日（土）7：30～17：00
9月12日（日）7：30～12：00

3）一般演題の発表時間は、10分（講演7分、質疑3分）です。
計時は発表終了1分前に黄色ランプが点灯、終了時に赤色ランプを点灯してお知らせします。円滑な進行のため、時間厳守でお願いいたします。

4）演台上には、モニター、キーボード、マウスをご準備しております。演台に上がると最初のスライドが表示されますので、その後の画像切替等の操作は各自で行ってください。

5）データをお持込の方へ

・発表データは Windows に限り、CD-RもしくはUSBメモリーでの受付に対応しております。
※動画や音声をご使用される場合、Macintosh にて作成したデータをご使用される場合は、ご自身のPCをご持参ください。「6）PCをお持込の方へ」をご参照ください。

・ご発表データのファイル名は、「演題番号、氏名」をご入力ください。
※例「O-1-001○○○○.ppt」もしくは、「O-1-001○○○○.pptx」
・データのフォントは、Windows に設定されている標準的なフォントをご使用ください。
【日本語】MSゴシック・MSPゴシック・MS明朝・MSP明朝
【英　語】Arial、Arial Black、Arial Narrow、Century、Century Gothic、
Courier、Courier New、Georgia、Times New Roman
・画面の解像度はXGA（1024×768）です。このサイズより大きい場合、スライドの周囲が切れる等の支障が出ます。
・必ず事前にご自身でウイルスチェックを行ってください。
・セッションの進行に影響が出るため、発表者ツールは使用できません。発表原稿が必要な方は、あらかじめプリントアウトをお持ちください。
・ご発表のデータは、学会終了後、責任を持って消去いたします。

6）PCをお持込の方へ
・お持込のPCが動作不良等でご利用できない場合に備え、発表ファイルをバックアップしたCD-RもしくはUSBメモリーをお持ちください。
・PC受付にて動作確認を行った後、ご自身で会場左手前方のPCオペレーター席までPC本体をお持ちください。発表後は、忘れずにPCをお受け取りください。
・会場にはPCプロジェクターにつながった、D-Sub 15ピン（ミニ）オスのケーブルを用意しております。
※HDMIやMini Display PortなどD-Sub15ピン以外の接続はお受けできません。
・PCのACアダプターは必ず各自ご持参ください。
・スクリーンセーバー、ウイルスチェック、並びに省電力設定（Macintoshの場合はホットコーナーも）はあらかじめ解除しておいてください。解除されておりませんと発表中にスクリーンセーバー等が作動してしまうことがあります。
・試写後は、PCの設定を変更しないでください。PCの電源を切ったり、スリープモードに入ったときに設定が変わってしまう場合がありますので、ご自分のPCの設定をよく理解しておいてください。

2．ポスター発表演者の方へ

【紙ポスター】

1）ポスターの貼付は9月9日（金）9：00～11：00の間にお願いします。
2）発表の行われるセッション開始時間の10分前までに、ご自分のポスターパネルの前で待機してください。
3）発表時間は6分（講演3分、質疑3分）です。
4）ポスター発表の中で、内容の優れたものには大会長賞を授与します。選考結果は、9月10日（土）午後に受賞したポスターパネルに掲示し、お知らせします。受賞したポスター発表者は総合受付においでください。また、同日18：00からの全員懇親会（ソニックシティホールB1F　第1展示場）にて授賞式を行いますので、ご参加ください。
5）ポスターを掲示するパネルは1種類です。サイズは8ページの図面のとおりです。
ポスター発表の先生方は各自ご自身のパネルサイズを確認の上、作成をお願いいたします。
6）演題番号（サイズ：20cm×20cm）は大会事務局で準備します。
7）タイトル・所属・氏名は発表者がご用意ください。（ポスター掲示図面をご参照ください。）
8）ポスター受付にて、ポスターを貼りつけるための専用マジックテープをお渡しいたします。
ポスターの撤去は9月11日（日）12：00～13：30の間に行い、忘れずにお持ち帰りください。万一、お忘れの場合はすべて破棄いたしますので、ご了承ください。

9）結論が見やすいように、Conclusionの英語文と要旨の日本語文はポスターの上部に配置してください。
10）利益相反（COI）の開示もポスター内に必ず含めてください。

【ポスターパネル】

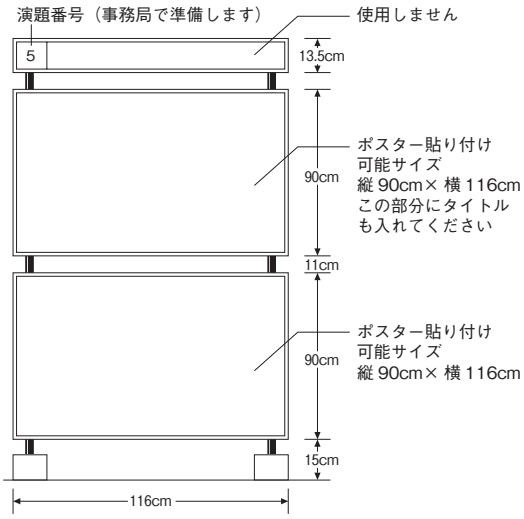

・パネル上：横116cm × 縦90cm、パネル下：横116cm × 縦90cmですので、これに合わせて作成をお願いします。タイトル、演者名、所属はこのパネル上内に入れて作成してください。
・ポスターの貼付方法は専用マジックテープを使用して、パネルにポスターを貼り付けます。粘着テープ、ピン等は使用できません。専用マジックテープはポスター会場でお渡しします。

【PDFポスター】
PDFポスター原稿を、下記会場内の閲覧用PCにて自由に閲覧いただけます。
PDFポスター会場：ソニックシティホール　B1F　第2-5展示場
※PDFポスター原稿はA4サイズで作成し、事前提出いただいたデータを掲載いたします。
※データ内に、利益相反（COI）の開示もポスター内に必ず含めてください。

座長の先生方へのお願い

1）参加登録受付後、総合受付付近「座長受付」にお越しください。また、担当いただくセッションの開始15分前までに、口頭発表ご担当の先生は会場右手前前方の次演者席に、ポスター発表ご担当の先生はご担当いただくポスター会場のフロアにあるポスター受付（ソニックシティホールB1F　第2-5展示場前ホワイエ）にお越しください。座長リボンと指示棒、演者よみがなリストをお渡しいたします。
2）プログラムの円滑な進行のため、各セッションの時間管理を厳密にお願いします。
3）各座長は、全ポスターの中から、学術奨励賞候補となる演題を3題推薦してください。推薦用紙は、座長受付でお渡しいたしますので、9月10日（土）13時までに推薦用紙に記入の上、総合受付にご提出ください。
4）シンポジウム、教育講演、ランチョンセミナー、イブニングセミナーを含めて、本大会ではすべての演者の略歴・CVは準備しておりません。現所属のアナウンスのみでお願いします。

ポスター会場

〔B1F 第2～5展示場〕

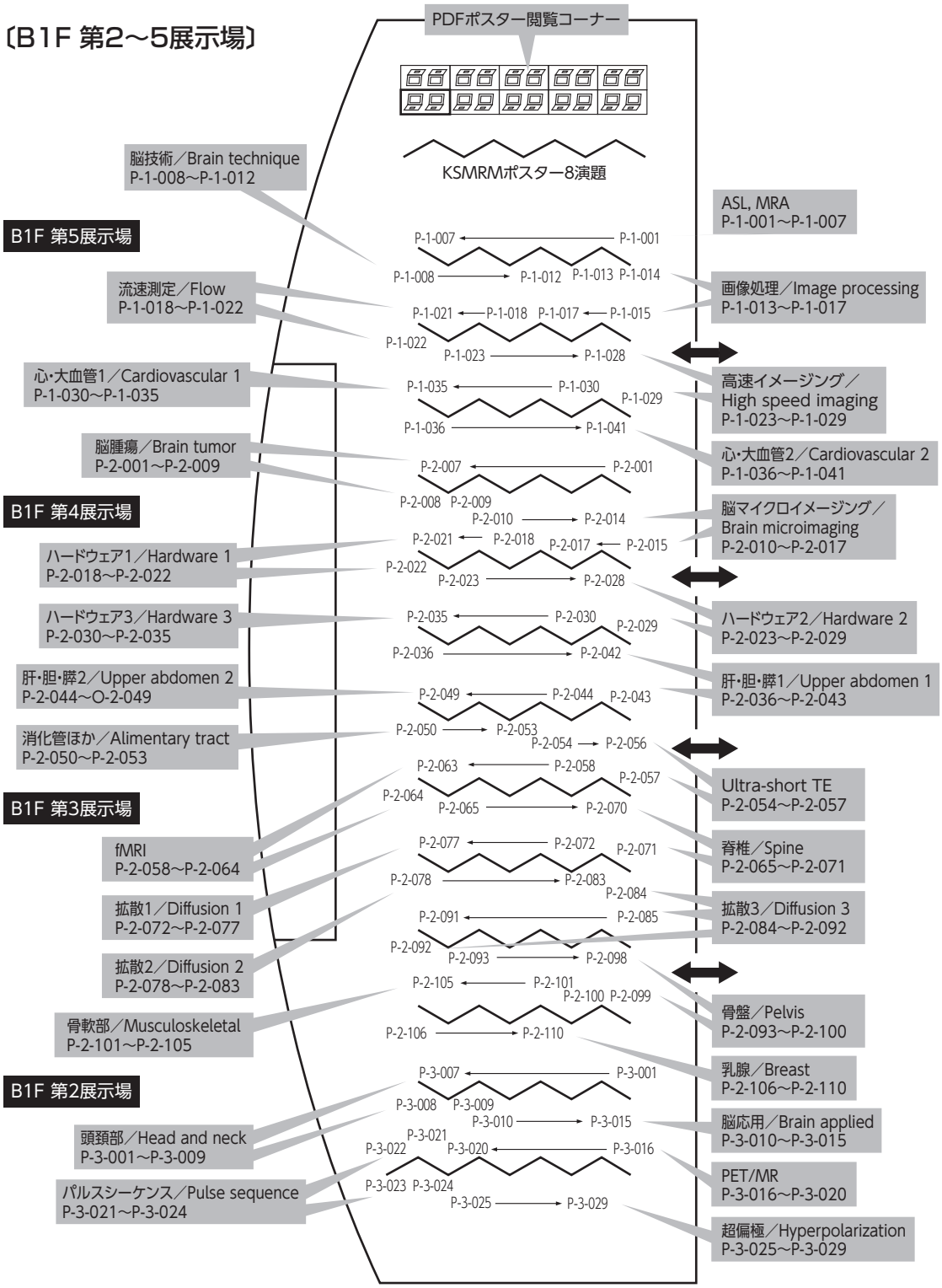

会場のご案内

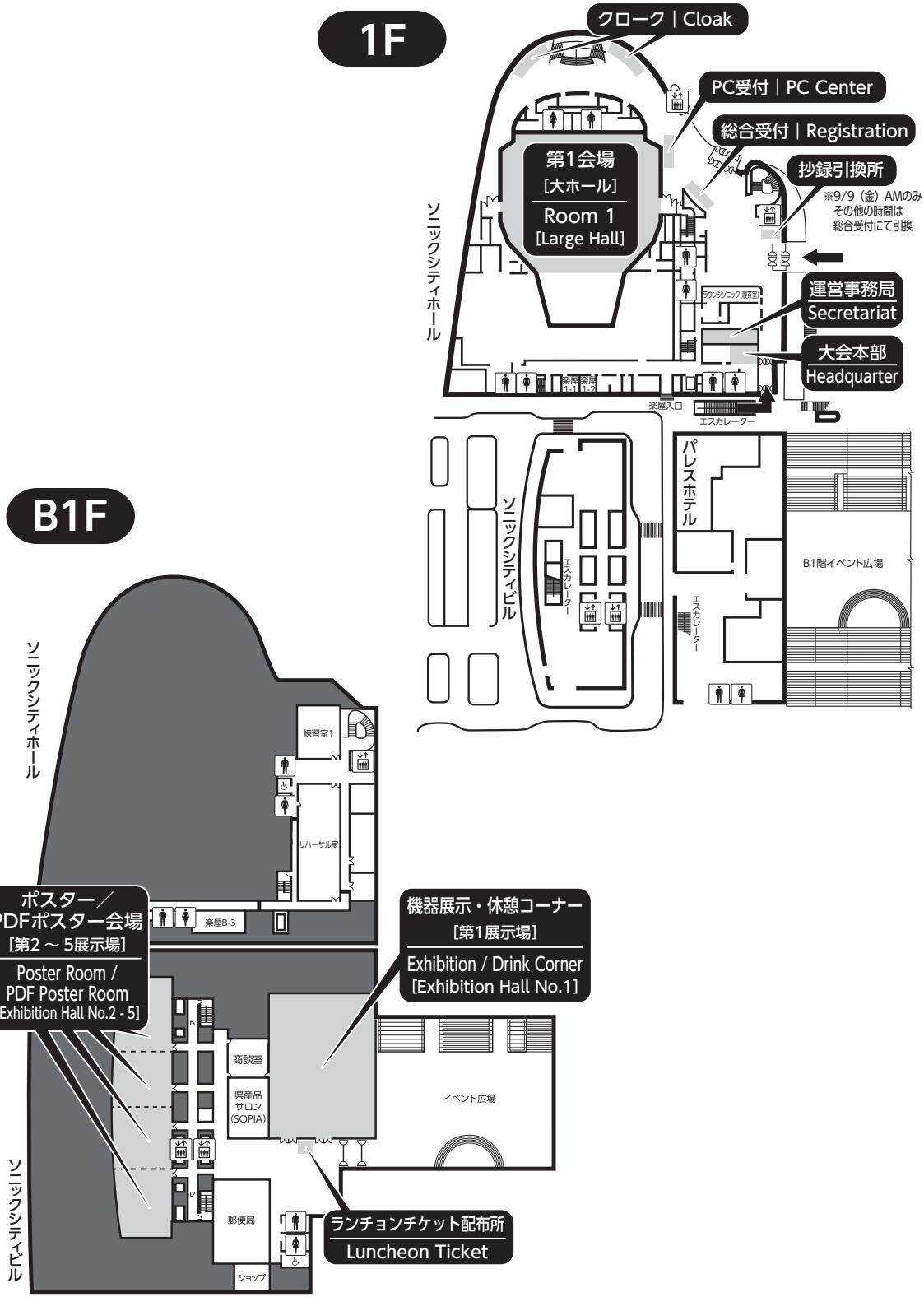
1F
クローク｜Cloak
PC受付｜PC Center
総合受付｜Registration
抄録引換所
※9/9（金）AMのみ
その他の時間は
総合受付にて引換
第1会場
[大ホール]
Room 1
[Large Hall]
ソニックシティホール
運営事務局
Secretariat
大会本部
Headquarter
楽屋入口
エスカレーター
パレスホテル
ソニックシティビル
B1階イベント広場
B1F
練習室1
リハーサル室
楽屋B-3
ポスター／
PDFポスター会場
[第2 ～ 5展示場]
Poster Room /
PDF Poster Room
[Exhibition Hall No.2 - 5]
機器展示・休憩コーナー
[第1展示場]
Exhibition / Drink Corner
[Exhibition Hall No.1]
商談室
県産品
サロン
(SOPIA)
イベント広場
郵便局
ショップ
ランチョンチケット配布所
Luncheon Ticket

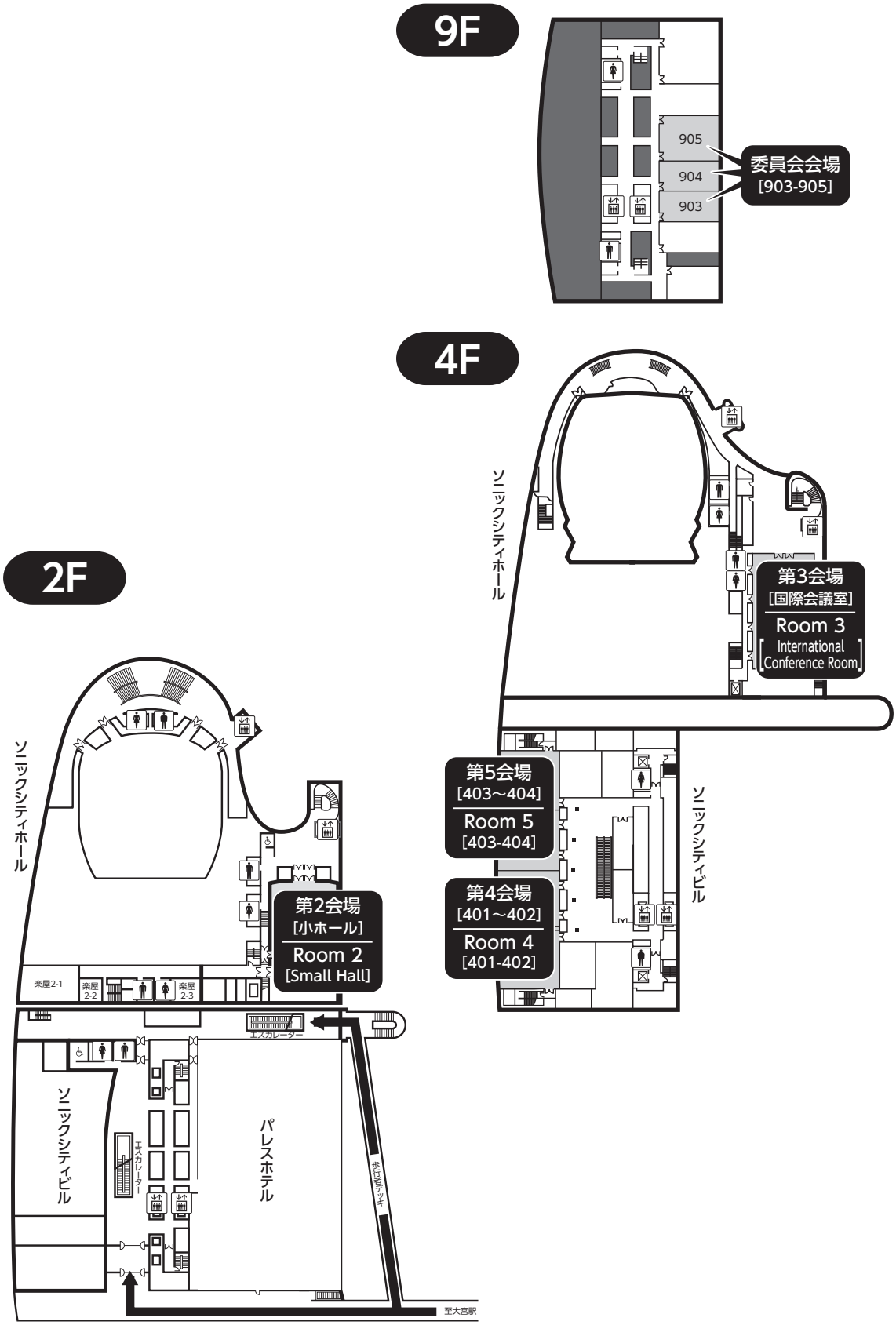
9F
905
904
903
委員会会場
[903-905]
4F
ソニックシティホール
第3会場
[国際会議室]
Room 3
International Conference Room
第5会場
[403～404]
Room 5
[403-404]
第4会場
[401～402]
Room 4
[401-402]
ソニックシティビル
2F
ソニックシティホール
第2会場
[小ホール]
Room 2
[Small Hall]
楽屋2-1
楽屋2-2
楽屋2-3
エスカレーター
ソニックシティビル
パレスホテル
エスカレーター
歩行者デッキ
至大宮駅

第44回日本磁気共鳴医学会大会　各種委員会一覧

委員会名	時　間	場　所
9月8日（木）		
理事会	16：00～18：30	ソニックシティビル　9F　905
9月9日（金）		
広報委員会	11：30～12：00	ソニックシティビル　9F　905
編集委員会	12：00～13：00	ソニックシティビル　9F　905
将来計画委員会	13：00～14：00	ソニックシティビル　9　F905
国際交流委員会	14：00～15：00	ソニックシティビル　9F　905
総会	16：30～17：30	第5会場（ソニックシティビル　4F　403～404）
7TMR装置の安全使用小委員会	18：00～19：00	ソニックシティビル　9F　903
デバイス評価小委員会	18：00～19：00	ソニックシティビル　9F　904
9月10日（土）		
安全性評価委員会	7：40～8：40	ソニックシティビル　9F　905
KSMRM会合	12：00～13：00	ソニックシティビル　9F　905
医療経済委員会	14：10～15：10	ソニックシティビル　9F　905

スタディグループ＆プロジェクト研究開催一覧

スタディグループ＆プロジェクト研究名	時　間	場　所
9月9日（金）		
躯幹部における拡散強調画像スタディグループ	17：40～18：00	第1会場（ソニックシティホール 1F　大ホール）
プロジェクト）q-space imaging有用性確立にむけた、基礎的研究と臨床応用に関する研究	18：00～19：00	第1会場（ソニックシティホール 1F　大ホール）
次世代diffusion MRを用いた脳のmicrostructureの解析と臨床応用	19：00～20：00	第2会場（ソニックシティホール 2F　小ホール）
前臨床MRI	19：00～20：00	第3会場（ソニックシティホール 4F　国際会議室）
MR適合性研究会	19：00～20：00	第4会場（ソニックシティビル 4F　401～402）
3次元シネ位相コントラスト法による血行動態解析の医療への利用促進を図るスタディグループ	18：00～20：00	第5会場（ソニックシティビル 4F　403～404）
MRイメージングおよび画像解析における数理問題の研究とソフトウェア開発	18：00～19：00	ソニックシティビル　9F　905
9月10日（土）		
プロジェクト）定量的画像バイオマーカーとしてのMRelastography 実現に向けた評価法の確立と推奨撮像プロトコルの作成	18：00～19：30	第2会場（ソニックシティホール 2F　小ホール）
位相画像情報の臨床応用	17：30～19：00	第4会場（ソニックシティビル 4F　401～402）
超偏極による他核MRSIの高感度計測	17：10～18：10	ソニックシティビル　9F　905

大会第１日目

	ソニックシティホール			ソニックシティビル	
	第１会場	第２会場	第３会場	第４会場	第５会場
	1F　大ホール	2F　小ホール	4F　国際会議室	4F　401 ～ 402	4F　403 ～ 404
8:00		**教育講演1** [J] 脳神経1 8:00～9:00	**教育講演2** [J] 腹部骨盤1 8:00～9:00	**教育講演3** [J] 乳腺 8:00～9:00	**教育講演4** [J] 基礎1 8:00～9:00
9:00	**シンポジウム1** [J] 関節MRIのすべて 9:00～11:40	**緊急シンポジウム** [J] クラスターレベルでの統計論拡論の注意点～fMRIデータ統計解析にまつわる最近の論争をめぐって～ 9:10～10:00	**一般演題** [E] 脳MRA O-1-019～025 9:10～10:20	**一般演題** [J] 頭頸部1 O-1-057～062 9:10～10:10	**一般演題** [J] 安全性 O-1-088～093 9:10～10:10
10:00		**シンポジウム2** [J] 前立腺MRI：これからの前立腺癌診療のために 10:10～11:40	**一般演題** [E] 脳ASL O-1-026～031 10:30～11:30	**一般演題** [J] 頭頸部2 O-1-063～068 10:10～11:10	**一般演題** [J] 画像処理 O-1-094～100 10:20～11:30
11:00					
12:00	**ランチョンセミナー1** [J] 富士製薬工業㈱ 12:00～12:50	**ランチョンセミナー2** [J] ㈱フィリップス エレクトロニクスジャパン 12:00～12:50	**ランチョンセミナー3** [J] シーメンスヘルスケア㈱ 12:00～12:50	**ランチョンセミナー4** [J] バイエル薬品㈱ 12:00～12:50	**ランチョンセミナー5** [J] 日本メドトロニック㈱ 12:00～12:50
13:00					
14:00	**シンポジウム3** [J] 匠の技① MRS・fMRIと心臓MRIを磨く匠の技 13:10～14:50	**一般演題** [J] 脳拡散1 O-1-006～012 13:10～14:20	**一般演題** [E] 肝臓1 O-1-032～037 13:10～14:10	**一般演題** [J] ファントム O-1-069～074 13:10～14:10	**一般演題** [J] 腹部 O-1-101～106 13:10～14:10
15:00	**シンポジウム4** [J] Synthetic MR imagingの現状と展望 15:00～16:30	**一般演題** [J] 脳拡散2 O-1-013～018 14:20～15:20	**一般演題** [E] 肝臓2 O-1-038～043 14:10～15:10	**一般演題** [J] 磁場 O-1-075～078 14:20～15:00	**一般演題** [J] 応用 O-1-107～111 14:20～15:10
16:00		**シンポジウム5** [J] 脳画像ビッグデータを扱う 15:55～17:50	**一般演題** [E] ハードウェア O-1-044～050 15:20～16:30	**一般演題** [J] Elastography1 O-1-079～082 15:10～15:50 **一般演題** [J] Elastography2 O-1-083～087 15:50～16:40	
17:00	**一般演題** [J] Body diffusion O-1-001～005 16:50～17:40		**一般演題** [E] パルスシーケンス1 O-1-051～056 16:40～17:40		**総会** 16:30～17:30
18:00	**スタディグループ** 躯幹部における拡散強調画像 スタディグループ 17:40～18:00	**イブニングセミナー1** [J] 第一三共㈱ 18:00～18:50	**イブニングセミナー2** [J] GEヘルスケアジャパン㈱ 18:00～18:50	**イブニングセミナー3** [J] [E] コニカミノルタ ジャパン㈱ 18:00～18:50	**スタディグループ** 3次元シネ位相コントラスト法による血行動態解析の医療への利用促進を図るスタディグループ 18:00～20:00
19:00	**プロジェクト研究** q-space imaging有用性確立にむけた、基礎的研究と臨床応用に関する研究 18:00～19:00	**スタディグループ** 次世代diffusion MRを用いた脳microstructureの解析と臨床応用 19:00～20:00	**スタディグループ** 前臨床MRI 19:00～20:00	**スタディグループ** MR適合性研究会 19:00～20:00	
20:00					

[J]：日本語セッション　[E]：英語セッション

9月9日(金)

ソニックシティビル			ソニックシティホール			
委員会会場			ポスター /PDF ポスター会場			機器展示・休憩コーナー
9F 903	9F 904	9F 905	B1F 第 2 ～ 5 展示場			B1F 第 1 展示場
			ポスター貼付 9:00～11:00			機器展示 9:00～17:00
		広報委員会 11:30～12:00				
		編集委員会 12:00～13:00				
		将来計画委員会 13:00～14:00	ポスター ASL, MRA P-1-001～007 13:10～13:55	ポスター 画像処理 P-1-013～017 13:10～13:40	ポスター 心・大血管1 P-1-030～035 13:10～14:00	
		国際交流委員会 14:00～15:00	ポスター 脳技術 P-1-008～012 14:30～15:00	ポスター 流速測定 P-1-018～022 14:00～14:30	ポスター 心・大血管2 P-1-036～041 14:30～15:20	
				ポスター 高速イメージング P-1-023～029 15:15～16:00		
7TMR装置の安全使用小委員会 18:00～19:00	デバイス評価小委員会 18:00～19:00	スタディグループ MRイメージングおよび画像解析における数理問題の研究とソフトウェア開発 18:00～19:00				

8:00 9:00 10:00 11:00 12:00 13:00 14:00 15:00 16:00 17:00 18:00 19:00 20:00

大会第２日目

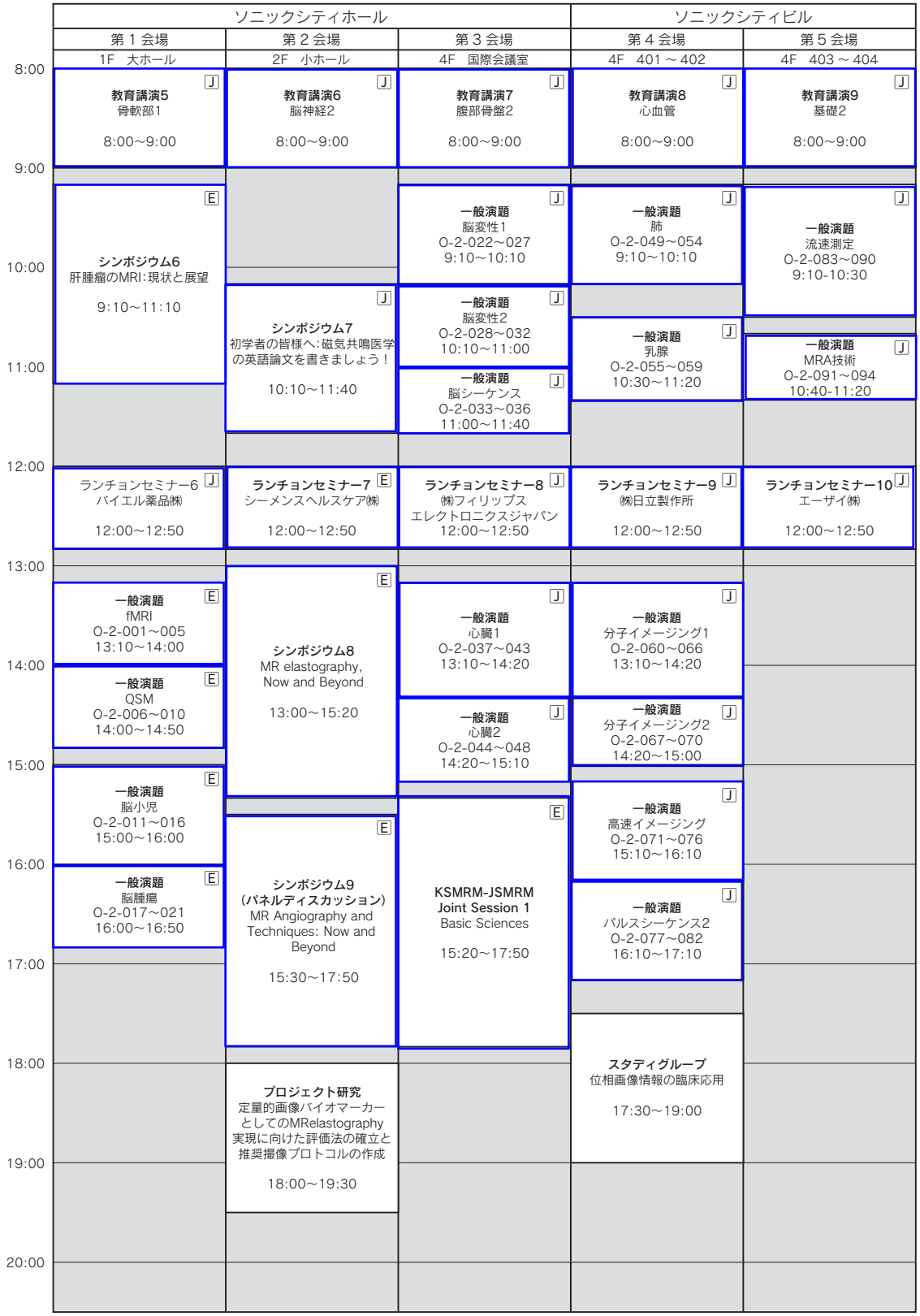

J：日本語セッション　E：英語セッション

9月10日(土)

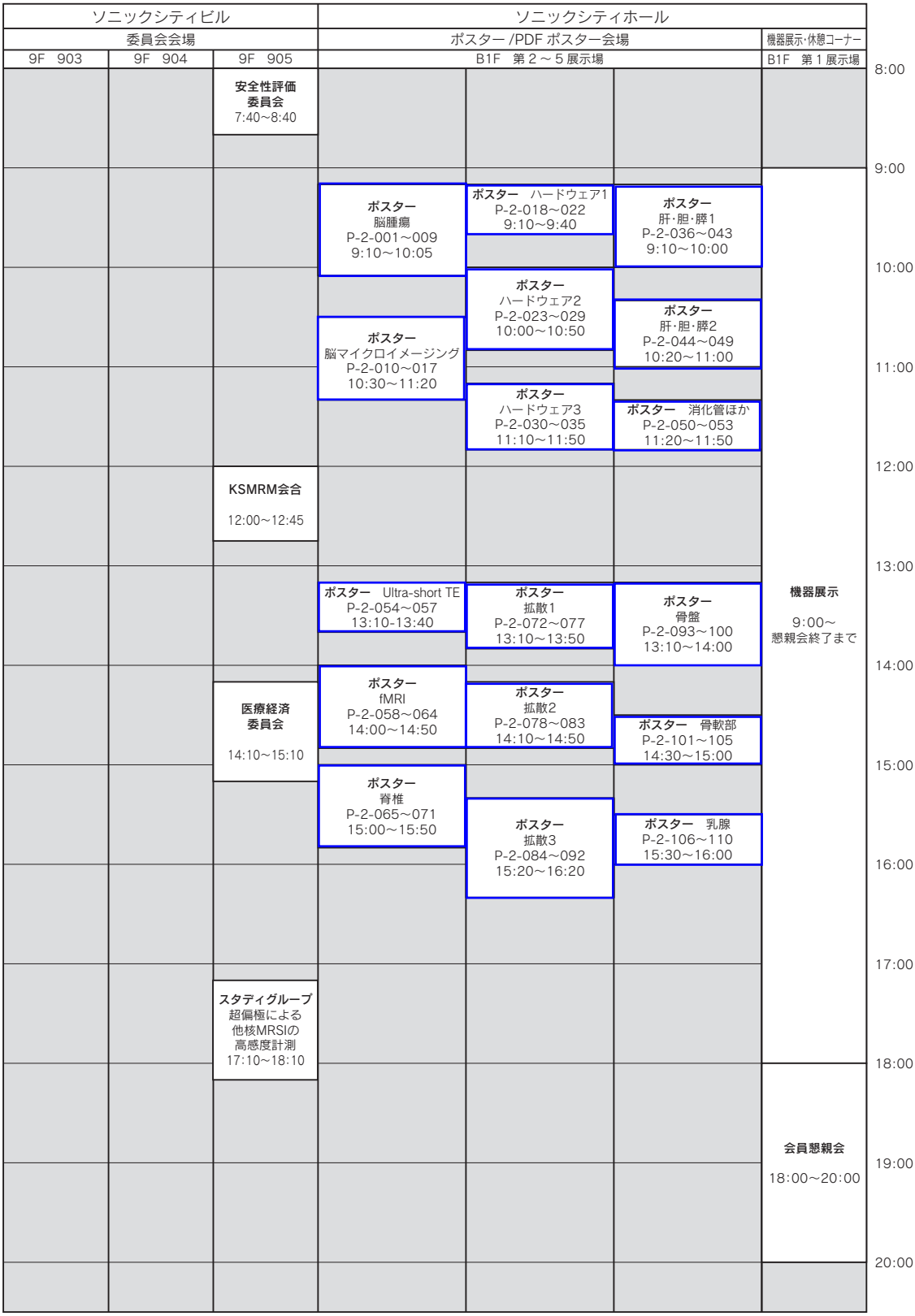
ソニックシティビル
委員会会場
9F 903
9F 904
9F 905
安全性評価
委員会
7:40~8:40
KSMRM会合
12:00~12:45
医療経済
委員会
14:10~15:10
スタディグループ
超偏極による
他核MRSIの
高感度計測
17:10~18:10
ソニックシティホール
ポスター /PDF ポスター会場
B1F 第 2 ~ 5 展示場
ポスター
脳腫瘍
P-2-001~009
9:10~10:05
ポスター
脳マイクロイメージング
P-2-010~017
10:30~11:20
ポスター Ultra-short TE
P-2-054~057
13:10-13:40
ポスター
fMRI
P-2-058~064
14:00~14:50
ポスター
脊椎
P-2-065~071
15:00~15:50
ポスター ハードウェア1
P-2-018~022
9:10~9:40
ポスター
ハードウェア2
P-2-023~029
10:00~10:50
ポスター
ハードウェア3
P-2-030~035
11:10~11:50
ポスター
拡散1
P-2-072~077
13:10~13:50
ポスター
拡散2
P-2-078~083
14:10~14:50
ポスター
拡散3
P-2-084~092
15:20~16:20
ポスター
肝·胆·膵1
P-2-036~043
9:10~10:00
ポスター
肝·胆·膵2
P-2-044~049
10:20~11:00
ポスター 消化管ほか
P-2-050~053
11:20~11:50
ポスター
骨盤
P-2-093~100
13:10~14:00
ポスター 骨軟部
P-2-101~105
14:30~15:00
ポスター 乳腺
P-2-106~110
15:30~16:00
機器展示·休憩コーナー
B1F 第 1 展示場
機器展示
9:00~
懇親会終了まで
会員懇親会
18:00~20:00
8:00
9:00
10:00
11:00
12:00
13:00
14:00
15:00
16:00
17:00
18:00
19:00
20:00

大会第３日目

	ソニックシティホール			ソニックシティビル	
	第１会場 1F　大ホール	第２会場 2F　小ホール	第３会場 4F　国際会議室	第４会場 4F　401～402	第５会場 4F　403～404
8:00		**教育講演10** [J] 骨軟部2 8:00～9:00	**教育講演11** [J] 脳神経3 8:00～9:00	**教育講演12** [J] 撮像技術 8:00～9:00	**教育講演13** [J] 安全 8:00～9:00	
9:00		**一般演題** [E] 骨軟部1 O-3-001～004 9:10～9:50		**教育講演14** [J] 基礎3 9:00～10:00	
10:00	**シンポジウム10** [J] 匠の技② 乳腺MRI撮像と拡散強調画像を磨く匠の技 9:10-11:50	**一般演題** [J] 骨軟部2 O-3-005～008 9:50～10:30	**KSMRM-JSMRM Joint Session 2** [E] What's hot in neuroimaging field? Japan and Korea 9:10-11:40	**一般演題** [J] 骨盤 O-3-014～019 10:10～11:10	
11:00		**一般演題** [J] 骨軟部3 O-3-009～013 10:50～11:40			
12:00	**ランチョンセミナー11** [J] 東芝メディカルシステムズ㈱ 12:00～12:50	**ランチョンセミナー12** [J] GEヘルスケア・ジャパン㈱ 12:00～12:50	**ランチョンセミナー13** [J] ㈱日立製作所 12:00～12:50	**ランチョンセミナー14** [J] セント・ジュード・メディカル㈱ 12:00～12:50	
13:00					
14:00					
15:00					
16:00					
17:00					
18:00					
19:00					
20:00					

[J]：日本語セッション　[E]：英語セッション

9月11日(日)

ソニックシティビル			ソニックシティホール			
委員会会場			ポスター /PDF ポスター会場			機器展示・休憩コーナー
9F 903	9F 904	9F 905	B1F 第 2 ～ 5 展示場			B1F 第 1 展示場
			ポスター 頭頸部 P-3-001～009 9:10～10:10	**ポスター** 脳応用 P-3-010～015 9:10～9:50	**ポスター** パルスシーケンス P-3-021～024 9:10～9:40	**機器展示** 9:00～12:00
				ポスター PET/MR P-3-016～020 10:20～10:50	**ポスター** 超偏極 P-3-025～029 10:10～10:40	
			ポスター撤去 12:00～13:00			

8:00
9:00
10:00
11:00
12:00
13:00
14:00
15:00
16:00
17:00
18:00
19:00
20:00

Day 1

	Sonic City Hall			Sonic City Building	
	Room 1	Room 2	Room 3	Room 4	Room 5
	1F, Large Hall	2F, Small Hall	4F, International Conference Room	4F, 401 ~ 402	4F, 403 ~ 404
8:00		[J] **Educational Lecture 1** CNS 1 8:00~9:00	[J] **Educational Lecture 2** Abdomen and Pelvis 1 8:00~9:00	[J] **Educational Lecture 3** Breast 8:00~9:00	[J] **Educational Lecture 4** MR basics 1 8:00~9:00
9:00	[J] **Symposium 1** Joint MRI: Now and Beyond 9:00~11:40	[J] **Special Symposium** 9:10~10:00	[E] **Oral** Brain MRA O-1-019~025 9:10~10:20	[J] **Oral** Head and neck 1 O-1-057~062 9:10~10:10	[J] **Oral** Safety O-1-088~093 9:10~10:10
10:00		[J] **Symposium 2** Prostate MRI. Now and Beyond 10:10~11:40	[E] **Oral** Brain ASL O-1-026~031 10:30~11:30	[J] **Oral** Head and neck 2 O-1-063~068 10:10~11:10	[J] **Oral** Image processing O-1-094~100 10:20~11:30
11:00					
12:00	[J] **Luncheon Seminar 1** Fuji Pharma Co., Ltd. 12:00~12:50	[J] **Luncheon Seminar 2** Philips Electronics Japan, Ltd. 12:00~12:50	[J] **Luncheon Seminar 3** Siemens Healthcare K.K. 12:00~12:50	[J] **Luncheon Seminar 4** Bayer Yakuhin, Ltd. 12:00~12:50	[J] **Luncheon Seminar 5** Medtronic Japan Co., Ltd. 12:00~12:50
13:00	[J] **Symposium 3** The art of MR meisters: fMRI and cardiac MRI 13:10~14:50	[J] **Oral** Brain diffusion 1 O-1-006~012 13:10~14:20	[E] **Oral** Liver 1 O-1-032~037 13:10~14:10	[J] **Oral** Phantom O-1-069~074 13:10~14:10	[J] **Oral** Abdomen O-1-101~106 13:10~14:10
14:00		[J] **Oral** Brain diffusion 2 O-1-013~018 14:20~15:20	[E] **Oral** Liver 2 O-1-038~043 14:10~15:10	[J] **Oral** Magnetic field O-1-075~078 14:20~15:00	[J] **Oral** Applied science O-1-107~111 14:20~15:10
15:00	[J] **Symposium 4** Synthetic MR imaging : Now and Beyond 15:00~16:30		[E] **Oral** Hardware O-1-044~050 15:20~16:30	[J] **Oral** Elastography1 O-1-079~082 15:10~15:50	
16:00		[J] **Symposium 5** Big Data for MRI: Now and Beyond 15:55~17:50		[J] **Oral** Elastography2 O-1-083~087 15:50~16:40	
17:00	[J] **Oral** Body diffusion O-1-001~005 16:50~17:40		[E] **Oral** Pulse sequence 1 O-1-051~056 16:40~17:40		**General Assembly** 16:30~17:30
18:00	**Study Group** 17:40~18:00	[J] **Evening Seminar 1** DAIICHI SANKYO CO., LTD. 18:00~18:50	[J] **Evening Seminar 2** GE Healthcare Japan Corporation 18:00~18:50	[J] [E] **Evening Seminar 3** Konica Minolta Japan, Inc. 18:00~18:50	**Study Group** 18:00~20:00
19:00	**Project Study** 18:00~19:00	**Study Group** 19:00~20:00	**Study Group** 19:00~20:00	**Study Group** 19:00~20:00	
20:00					

[J] : Japanese Session [E] : English Session

Friday, September 9

Sonic City Building			Sonic City Hall			
Conference Room			Poster /PDF Poster Room			Exhibition / Drink Corner
9F, 903	9F, 904	9F, 905	B1F, Exhibition Hall No.2 ~ No.5			B1F, Exhibition Hall No.1
			Poster Installation 9:00~11:00			
		Public Information Committee 11:30~12:00				
		Editional Committee 12:00~13:00				
		Future Planning Committee 13:00~14:00	**Poster** ASL, MRA P-1-001~007 13:10~13:55	**Poster** Image processing P-1-013~017 13:10~13:40	**Poster** Cardiovascular 1 P-1-030~035 13:10~14:00	**Exhibition** 9:00~17:00
		International Relationship Committee 14:00~15:00	**Poster** Brain technique P-1-008~012 14:30~15:00	**Poster** Flow P-1-018~022 14:00~14:30	**Poster** Cardiovascular 2 P-1-036~041 14:30~15:20	
				Poster High speed imaging P-1-023~029 15:15~16:00		
Subcommittee 18:00~19:00	**Subcommittee** 18:00~19:00	**Study Group** 18:00~19:00				

8:00
9:00
10:00
11:00
12:00
13:00
14:00
15:00
16:00
17:00
18:00
19:00
20:00

Day 2

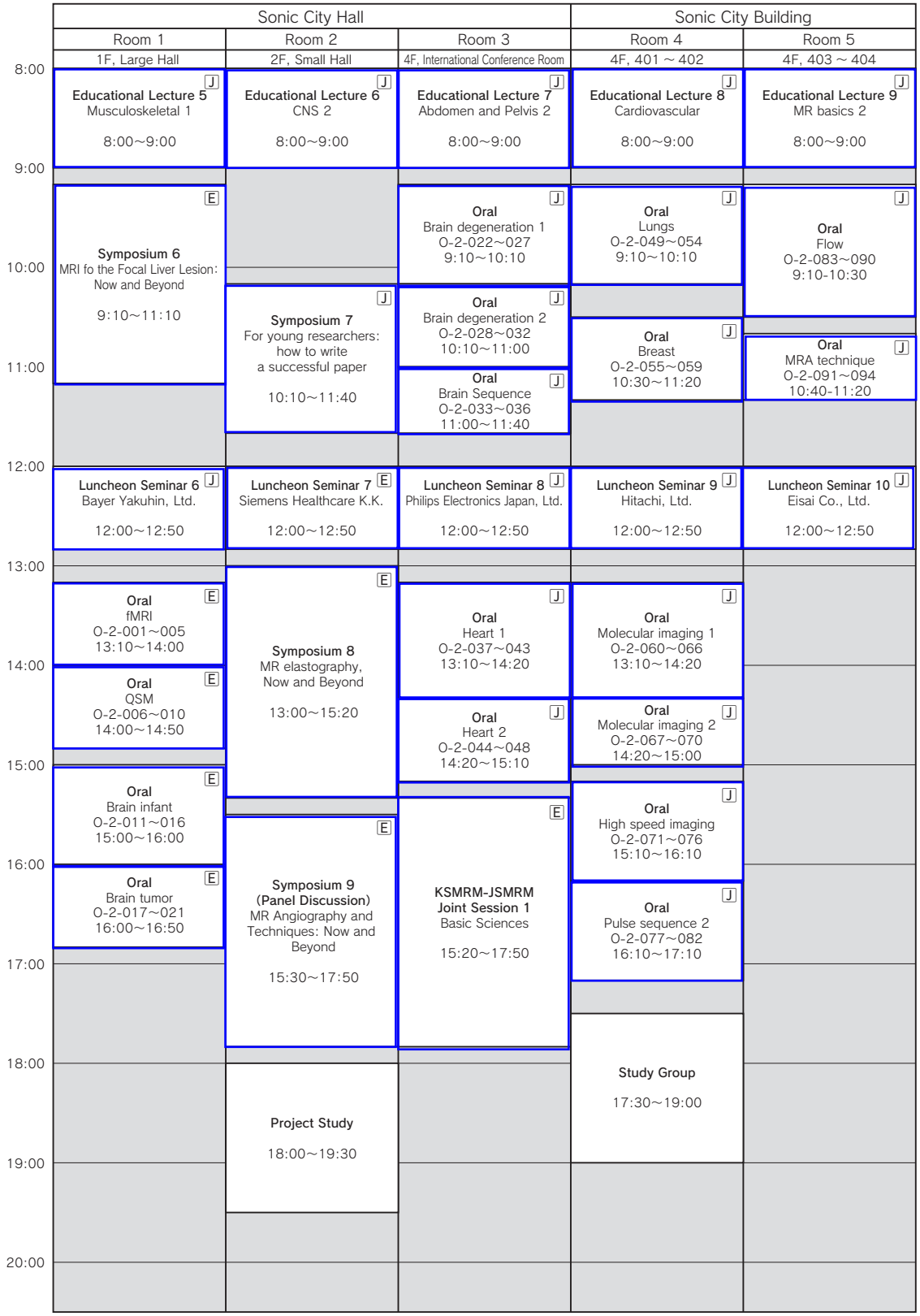

J : Japanese Session E : English Session

Saturday, September 10

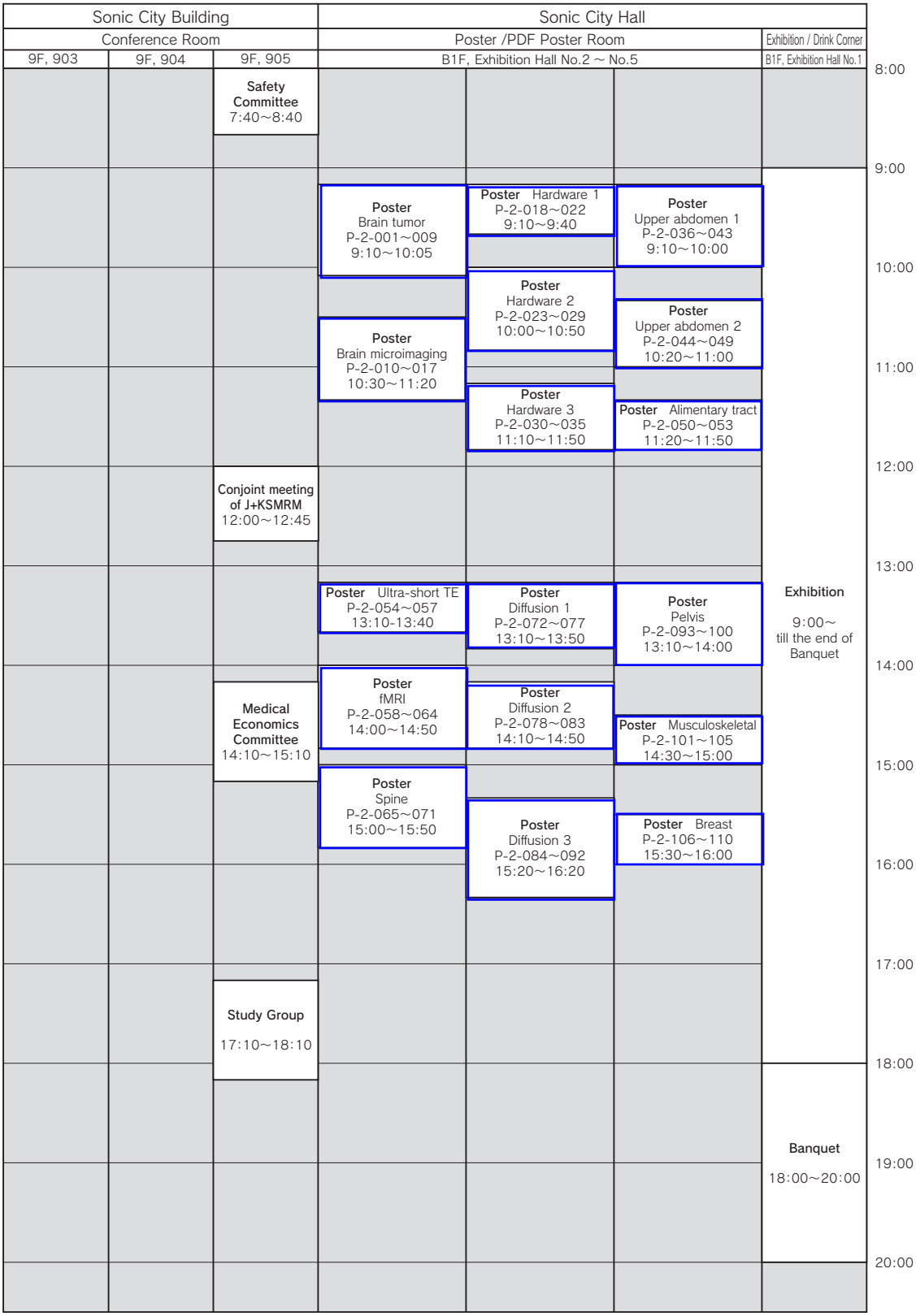

Day 3

	Sonic City Hall			Sonic City Building	
	Room 1	Room 2	Room 3	Room 4	Room 5
	1F, Large Hall	2F, Small Hall	4F, International Conference Room	4F, 401 ~ 402	4F, 403 ~ 404
8:00	[J] **Educational Lecture 10** Musculoskeletal 2 8:00~9:00	[J] **Educational Lecture 11** CNS 3 8:00~9:00	[J] **Educational Lecture 12** Imaging technique 8:00~9:00	[J] **Educational Lecture 13** Safety 8:00~9:00	
9:00	[J] **Symposium 10** The art of MR meisters: breast MRI and DWI 9:10-11:50	[E] **Oral** Musculoskeletal 1 O-3-001~004 9:10~9:50	[E] **KSMRM-JSMRM Joint Session 2** What's hot in neuroimaging field? Japan and Korea 9:10-11:40	[J] **Educational Lecture 14** MR basics 3 9:00~10:00	
10:00		[J] **Oral** Musculoskeletal 2 O-3-005~008 9:50~10:30		[J] **Oral** Pelvis O-3-014~019 10:10~11:10	
11:00		[J] **Oral** Musculoskeletal 3 O-3-009~013 10:50~11:40			
12:00	[J] **Luncheon Seminar 11** Toshiba Medical Systems Corporation 12:00~12:50	[J] **Luncheon Seminar 12** GE Healthcare Japan Corporation 12:00~12:50	[J] **Luncheon Seminar 13** Hitachi, Ltd. 12:00~12:50	[J] **Luncheon Seminar 14** St. Jude Medical Co., Ltd. 12:00~12:50	
13:00					
14:00					
15:00					
16:00					
17:00					
18:00					
19:00					
20:00					

[J] : Japanese Session [E] : English Session

Sunday, September 11

Sonic City Building			Sonic City Hall			
Conference Room			Poster /PDF Poster Room			Exhibition / Drink Corner
9F, 903	9F, 904	9F, 905	B1F, Exhibition Hall No.2 ~ No.5			B1F, Exhibition Hall No.1
						8:00
			Poster Head and neck P-3-001~009 9:10~10:10	**Poster** Brain applied P-3-010~015 9:10~9:50	**Poster** Pulse sequence P-3-021~024 9:10~9:40	9:00
				Poster PET/MR P-3-016~020 10:20~10:50	**Poster** Hyperpolarization P-3-025~029 10:10~10:40	**Exhibition** 9:00~12:00 10:00
						11:00
			Poster Removal 12:00~13:00			12:00
						13:00
						14:00
						15:00
						16:00
						17:00
						18:00
						19:00
						20:00

第44回日本磁気共鳴医学会大会 プログラム委員（50音順）

青木伊知男	量子科学技術研究開発機構・放医研
青木　茂樹	順天堂大学医学部・大学院医学研究科 放射線医学教室 放射線診断学講座
阿部　　修	日本大学医学部 放射線医学系 画像診断学分野放射線腫瘍学分野
井田　正博	東京都保健医療公社 荏原病院 放射線科
井上　快児	埼玉医科大学 放射線科
内野　　晃	埼玉医科大学国際医療センター画像診断科
扇　　和之	日本赤十字社医療センター 放射線診断科
大友　　邦	国際医療福祉大学
大野　良治	神戸大学大学院 放射線医学分野
押尾　晃一	慶應義塾大学医学部 放射線診断科
小澤　栄人	埼玉医科大学 放射線科
小畠　隆行	量研機構 放射線医学総合研究所
小原　　真	株式会社フィリップスエレクトロニクスジャパン
桃沢　宏之	GEヘルスケア・ジャパン株式会社 技術本部 MR研究室
楫　　靖	獨協医科大学 放射線医学講座
角谷　眞澄	信州大学医学部 画像医学教室
金澤　　右	岡山大学大学院医歯薬学総合研究科 放射線医学
川光　秀昭	神戸大学医学部付属病院
紀ノ定保臣	岐阜大学大学院 医学系研究科
黒田　　輝	東海大学情報理工学部情報科学科
興梠　征典	産業医科大学 放射線科学教室
後閑　武彦	昭和大学医学部放射線医学講座
巨瀬　勝美	筑波大学数理物質系 物理工学域
佐久間　肇	三重大学医学部 放射線医学教室
佐々木真理	岩手医科大学 医歯薬総合研究所
陣崎　雅弘	慶應義塾大学医学部 放射線診断科
杉村　和朗	神戸大学大学院医学研究科放射線医学分野
鈴木　政司	埼玉医科大学 放射線科
瀬尾　芳輝	獨協医科大学 医学部
高原　太郎	東海大学工学部 医用生体工学科
竹原　康雄	浜松医科大学医学部附属病院 放射線部
土井　　司	社会医療法人 高清会 高井病院
富樫かおり	京都大学 放射線医学講座
長縄　慎二	名古屋大学 放射線科
成瀬　昭二	京都岡本記念病院
新津　　守	埼玉医科大学 放射線科
原田　雅史	徳島大学 放射線医学分野
尾藤　良孝	株式会社日立製作所ヘルスケアビジネスユニット
平井　俊範	宮崎大学医学部 病態解析医学講座 放射線医学分野
増谷　佳孝	広島市立大 大学院 情報科学研究科
松村　　明	筑波大学医学医療系 脳神経外科
三木　幸雄	大阪市立大学大学院 医学研究科 放射線医学教室
南　　学	筑波大学 放射線医学
宮崎美津恵	東芝メディカルシステムズ株式会社
宮地　利明	金沢大学医薬保健研究域
村上　卓道	近畿大学医学部放射線医学教室放射線診断学部門
村瀬　研也	大阪大学大学院医学系研究科保健学専攻医用物理工学講座
村田　勝俊	シーメンスヘルスケア株式会社
山下　康行	熊本大学大学院生命科学研究部放射線診断学
山田　　惠	京都府立医科大学大学院 放射線診断治療学講座
吉川　宏起	駒澤大学 医療健康科学部
渡邉　英宏	国立研究開発法人国立環境研究所 環境計測研究センター

第44回日本磁気共鳴医学会大会
口演座長一覧

（50音順）

相田　典子　神奈川県立こども医療センター放射線科
磯田　裕義　京都大学医学部付属病院 先制医療・生活習慣病研究センター
入江　裕之　佐賀大学 放射線科
内野　　晃　埼玉医科大学 国際医療センター 画像診断科
扇　　和之　日本赤十字社医療センター 放射線診断科
小畠　隆行　量研機構 放射線医学総合研究所
北垣　　一　島根大学医学部
工藤　與亮　北海道大学病院 放射線科
小山　　貴　倉敷中央病院 放射線診断科
坂井　修二　東京女子医科大学
妹尾　淳史　首都大学東京 放射線学科
長尾　充展　東京女子医科大学 画像診断・核医学講座
沼野　智一　首都大学東京大学院 人間健康科学研究科 放射線科学域
畠中　正光　札幌医科大学 放射線診断学
増谷　佳孝　広島市立大 大学院 情報科学研究科
松田　哲也　京都大学 情報学研究科
三好　光晴　GEヘルスケア・ジャパン株式会社
門澤　秀一　神鋼記念病院
吉浦　　敬　鹿児島大学大学院医歯学総合研究科放射線診断治療学分野
吉満　研吾　福岡大学医学部放射線医学教室
赤羽　正章　NTT東日本関東病院 放射線部
井上　優介　北里大学医学部 画像診断学
内田　幸司　えだクリニック整形外科リハビリテーション科 PICTORUいずも画像診断室
江原　　茂　岩手医科大学 放射線科
押尾　晃一　慶應義塾大学医学部 放射線診断科
桧沢　宏之　GEヘルスケア・ジャパン株式会社 技術本部 MR研究室
木村　浩彦　福井大学 医学部 放射線医学
五味　達哉　東邦大学医療センター大橋病院 放射線科
齋藤　尚子　埼玉医科大学国際医療センター 画像診断科
杉本　英治　自治医科大学医学部放射線医学講座
豊田　圭子　帝京大学医学部放射線科学講座
長縄　慎二　名古屋大学 放射線科
野口　智幸　国立国際医療研究センター病院 放射線診療部
前田　正幸　三重大学 先進画像診断学講座
松下　　明　茨城県立医療大学付属病院脳神経外科
松村　　明　筑波大学医学医療系 脳神経外科
村田　勝俊　シーメンスヘルスケア株式会社
横沢　　俊　株式会社日立製作所 研究開発グループ
吉川　宏起　駒澤大学 医療健康科学部
渡谷　岳行　東京大学医学部附属病院 放射線科

ポスター座長一覧

（50音順）

粟井　和夫　広島大学 放射線診断学
井田　正博　荏原病院 放射線科
今井　　裕　東海大学医学部 画像診断学
上谷　雅孝　長崎大学 放射線科
大久保敏之　帝京大学ちば総合医療センター 放射線科
岡本浩一郎　新潟大学 脳研究所
紀ノ定保臣　岐阜大学大学院 医学系研究科
巨瀬　勝美　筑波大学 数理物質科学研究科
鈴木　雄一　東京大学医学部附属病院 放射線部
拝師　智之　株式会社エム・アール・テクノロジー
平井　俊範　宮崎大学 放射線科
堀　　雅敏　大阪大学大学院医学系研究科 放射線統合医学講座
丸山　克也　シーメンスヘルスケア株式会社
村瀬　研也　大阪大学大学院医学系研究科保健学専攻医用物理工学講座
渡邉　嘉之　大阪大学医学部放射線医学講座
礒田　治夫　名古屋大学 脳とこころの研究センター
市川　智章　埼玉医科大学国際医療センター 画像診断科
上口　貴志　情報通信研究機構
扇谷　芳光　昭和大学医学部 放射線医学講座 放射線科学部門
岡田　知久　京都大学 脳機能総合研究センター
小原　　真　株式会社フィリップスエレクトロニクスジャパン
久保　　均　福島県立医科大学 先端臨床研究センター
鈴木　清隆　新潟大学脳研究所 統合脳機能研究センター
豊田　圭子　帝京大学医学部放射線科学講座
畑　　純一　理化学研究所 脳科学総合研究センター
細矢　貴亮　山形大学医学部画像医学講座
松永　尚文　山口大学大学院医学系研究科 放射線医学分野
南　　学　筑波大学 放射線医学
渡邉　英宏　国立環境研究所

Symposium
シンポジウム

Friday, September 9, 9:00～11:40　　Room 1 (Sonic City Hall, 1F, Large Hall)

Symposium 1「Joint MRI：Now and Beyond」

シンポジウム1「関節MRIのすべて」

Chairs：Hajime Fujimoto（Numazu City Hospital Department of Radiology）
Takashi Tabuchi（Kurashiki Central Hospital Department of Medical Technology）
座　長：藤本　　肇（沼津市立病院 放射線科）
田渕　　隆（倉敷中央病院 医療技術部）

S1-1　Knee

膝 （開会の辞を含む）

Mamoru Niitsu（Department of Radiology, Saitama Medical University）
新津　　守（埼玉医科大学 放射線科）

S1-2　Hip joint

股関節

Tsutomu Inaoka（Toho University Sakura Medical Center Department of Radiology）
稲岡　　努（東邦大学佐倉病院 放射線科）

S1-3　Ankle and foot

足・足関節

Eiji Fukuba（PICTORU Izumo Imaging Center）
福庭　栄治（PICTORUいずも画像診断室）

S1-4　Technique for lower extremities

下肢の撮像のコツ

Masanori Komi（University of Miyazaki Hospital Department of Radiology）
小味　昌憲（宮崎大学医学部附属病院 放射線部）

S1-5　Shoulder

肩

Ryuji Sashi（Yaesu Clinic Department of Radiology）
佐志　隆士（八重洲クリニック 放射線科）

S1-6　Elbow and hand

肘・手

Kaoru Kitsukawa（St. Marianna University School of Medicine, Department of Radiology）
橘川　　薫（聖マリアンナ医科大学放射線医学講座）

S1-7　Technique for upper extremities

手の外科領域の上肢撮像のコツ

Kiyoko Kazama（Department of Radiology Niigata Hand Surgery Foundation Niigata Hand Care Center）
風間　清子（一般財団法人 新潟手の外科研究所 新潟手の外科研究所病院 放射線科）

Friday, September 9, 9:10～10:00　　Room 2 (Sonic City Hall, 2F, Small Hall)

Special Symposium

緊急シンポジウム「クラスターレベルでの統計的推論の注意点 ～ fMRIデータ統計解析にまつわる最近の論争をめぐって～」

Chair：Takayuki Obata（National Instititute of Radiological Scinences）
座　長：小畠　隆行（量研機構 放射線医学総合研究所）

SS-1　Is debugging needed for fMRI software?

fMRIソフトウェアに『バグ』が見つかったというのは本当か？

Noriaki Yahata（Department of Molecular Imaging and Theranostics, National Institute of Radiological Sciences, National Institutes for Quantum and Radiological Science and Technology）
八幡　憲明（量研機構 放射線医学総合研究所 分子イメージング診断治療研究部）

SS-2　Why 70 percent false positive rate? -Lecture for statistical cluster inference-

偽陽性70%はなぜ出たのか ～統計的クラスター推論の解説～

Atsushi Kawaguchi（Saga University Faculty of Medicine Center for Comprehensive Community Medicine）
川口　　淳（佐賀大学医学部 附属地域医療科学教育研究センター）

Friday, September 9, 10:10～11:40　　Room 2 (Sonic City Hall, 2F, Small Hall)

Symposium 2「Prostate MRI. Now and Beyond」

シンポジウム2「前立腺MRI：これからの前立腺癌診療のために」

Chairs：Yasushi Kaji（Dokkyo Medical University, Department of Radiology）
Takehiko Gokan（Showa University School of Medicine Department of Radiology）
座　長：楫　　靖（獨協医科大学放射線医学講座）
後閑　武彦（昭和大学医学部放射線医学講座）

S2-1　Recent progress for the prostatic cancer

最近の前立腺癌診療について

Yasushi Kaji（Dokkyo Medical University, Department of Radiology）
楫　　靖（獨協医科大学放射線医学講座）

S2-2　Diffusion-weighted MR imaging of the prostate gland -current status and future directions-

前立腺癌DWI: 現在と将来

Hiroshi Shinmoto（National Defense Medical College, Department of Radiology）
新本　　弘（防衛医科大学校 放射線医学講座）

S2-3　Evaluation of prostate cancer -PSA v.s. MRI-

前立腺MRIはPSA検査を越えるか

Kazuhiro Katahira（Kumamoto chuo hospital Department of Radiology）
片平　和博（熊本中央病院 放射線科）

S2-4　Standardization of prostate MRI Pi-RADS v2 and beyond

前立腺MRI：Pi-RADS v2で示された標準化の実践

Satoru Takahashi（Kobe University Hospital, Department of Radiology）
高橋　　哲（神戸大学附属病院 放射線部）

S2-5　The role of whole body MRI for metastases

全身MRI による転移診断

Katsuyuki Nakanishi（Department of Diagnostic Radiology, Osaka Medical Center for Cancer & Cardiovascular Diseases）
中西　克之（大阪府立成人病センター 放射線科）

Friday, September 9, 13:10～14:50　　Room 1 (Sonic City Hall, 1F, Large Hall)

Symposium 3「The art of MR meisters: fMRI and cardiac MRI」

シンポジウム3「匠の技①　MRS・fMRIと心臓MRIを磨く匠の技」

Chairs：Hideto Toyoshima（Research Institute for Brain and Blood Vessels-Akita Department of Radiology）
Hisashi Kitagawa（The Jikei University Daisan Hospital）
座　長：豊嶋　英仁（秋田県立脳血管研究センター 放射線科診療部）
北川　　久（東京慈恵会医科大学附属第三病院）

S3-1　Professional skills for MRS measurement

MRSの匠の技

Hitoshi Kubo（Fukushima Medical University, Advanced Clinical Research Center）
久保　　均（福島県立医科大学 先端臨床研究センター）

S3-2　An approach for optimizing acquisition parameters on fMRI using multiband technique

Multiband技術を用いたfMRIにおける最適パラメータを探るためのアプローチ

Yasuhiro Shimada（ATR-Promotions, Brain Activity Imaging Center）
島田　育廣（ATR-Promotions, 脳活動イメージングセンタ）

S3-3　A retrospect and prospect technics of late gadolinium enhancement for cardiac MRI

心臓MRIの遅延造影撮像技術：臨床の工夫と展望

Takashige Yoshida（Tokyo Metropolitan Police Hospital）
吉田　学誉（財団法人自警会 東京警察病院）

S3-4　The technical method for magnetic resonance coronary angiography -technical idea and problem at 3.0Tesla MRI-

心臓MRIの冠動脈撮像技術：3Tでの工夫と課題

Kei Fukuzawa（Toranomon Hospital Department of Radiology）
福澤　　圭（国家公務員共済組合連合会 虎の門病院 放射線部）

Friday, September 9, 15:00～16:30　　Room 1 (Sonic City Hall, 1F, Large Hall)

Symposium 4「Synthetic MR imaging : Now and Beyond」

シンポジウム4「Synthetic MR imaging の現状と展望」

Chairs：Taro Takahara（Department of Biological Engineering, Tokai University, School of Biological Engineering）
Masaaki Hori（Department of Radiology, Juntendo University）
座　長：高原　太郎（東海大学工学部医用生体工学科）
堀　　正明（順天堂大学医学部放射線医学講座）

S4-1　Synthetic MRI-contrast adjustment, quantitative analysis and myelin map-

Synthetic MRI：コントラスト調整から定量解析、ミエリンマップまで

Akifumi Hagiwara（Juntendo University Hospital, Department of Radiology）
萩原　彰文（順天堂大学医学部附属順天堂医院 放射線科）

S4-2　Principle and Aim of the Synthetic MR imaging

Marcel Warntjes（Synthetic MRI）

S4-3　Synthetic MRI of the Brain

頭部領域におけるSynthetic MRI

Hirokazu Fujiwara（Keio University Department of Diagnostic Radiology）
藤原　広和（慶應義塾大学放射線診断科）

S4-4 **Synthetic MRII Outside the Brain**

Taro Takahara（Department of Biological Engineering, Tokai University, School of Biological Engineering）

高原　太郎（東海大学 工学部 医用生体工学科）

Friday, September 9, 15:55～17:50　　Room 2 (Sonic City Hall, 2F, Small Hall)

Symposium 5「Big Data for MRI: Now and Beyond」

シンポジウム5「脳画像ビッグデータを扱う」

Chairs：Yukunori Korogi（University of Occupational and Environmental Health, Department of Radiology）

Kuni Ohtomo（International University of Health and Welfare）

座　長：興梠　征典（産業医科大学 放射線科学教室）

大友　　邦（国際医療福祉大学）

S5-1 **Industry 4.0 enabled by IoT, big data and AI**

IoT、ビッグデータが支える産業4.0

Naoyuki Nomura（Metadata Inc.）

野村　直之（メタデータ株式会社）

S5-2 **Current status of neuroimaging in a big data science**

脳画像ビッグデータの現状

Makoto Sasaki（Institute for Biomedical Sicneces, Iwate Medical University）

佐々木真理（岩手医科大学 医歯薬総合研究所）

S5-3 **Brain Big Data Accumulation in Neuroscience and Social Implementation**

脳科学での集積と社会実装

Yoshinori Yamakawa（Impulsing Paradigm Change through Disruptive Technologies Program）

山川　義徳（内閣府革新的研究開発推進プログラム シニアマネージャー）

S5-4 **Data correction and utilization of medical checkup**

検診での集積と利活用

Fumio Yamashita（Iwate Medical University Institute for Biomedical Sciences）

山下　典生（岩手医科大学 医歯薬総合研究所）

S5-5 **Application of big data on brain imaging to clinical practice and trials**

医療での集積と利活用

Kazunori Toyoda（Dept of Cerebrovascular Medicine, National Cerebral and Cardiovascular Center）

豊田　一則（国立循環器病研究センター 脳血管内科）

Saturday, September 10, 9:10～11:10　　Room 1 (Sonic City Hall, 1F, Large Hall)

Symposium 6「MRI fo the Focal Liver Lesion：Now and Beyond」

シンポジウム6「肝腫瘤のMRI：現状と展望」

Chairs：Tomoaki Ichikawa（Saitama Medical University International Medical Center Department of Diagnostic Radiology）
Kazuhiko Ueda（Cancer Institute Hospital of JFCR）
座　長：市川　智章（埼玉医科大学国際医療センター 画像診断科）
上田　和彦（がん研究会有明病院画像診断部）

S6-1　Hepatocellular adenoma

肝腺腫

Hiroki Haradome（Nihon University School of Medicine）
原留　弘樹（日本大学医学部 放射線医学系 画像診断学分野）

S6-2　Combined hepatocellular carcinoma and cholangiolocellular carcinoma

混合型肝癌、細胆管細胞癌

Hiroyuki Morisaka（Saitama Medical University International Medical Center, Department of Diagnostic Radiology）
森阪　裕之（埼玉医科大学 国際医療センター）

S6-3　Hyperplastic hepatocellular nodules

肝細胞性過形成結節

Norihide Yoneda（Kanazawa University Hospital Department of Radiology）
米田　憲秀（金沢大学附属病院）

S6-4　2.Malignant lesions of the liver and their masquerades

Sukru Mehmet Erturk（Department of Radiology, Adiyaman University）

Saturday, September 10, 10:10～11:40　　Room 2 (Sonic City Hall, 2F, Small Hall)

Symposium 7「For young researchers: how to write a successful paper」

シンポジウム7「初学者の皆様へ：磁気共鳴医学の英語論文を書きましょう！」

Chairs：Toshiaki Miyati（Institute of Medical, Pharmaceutical and Health Sciences, Kanazawa University）
Susumu Kanazawa（Department of Radiology, Okayama University Graduate School of Medicine, Dentistry and Pharmaceutical Sciences）
座　長：宮地　利明（金沢大学医薬保健研究域）
金澤　　右（岡山大学大学院医歯薬学総合研究科 放射線医学）

S7-1　How to write a paper in English after daily clinical work

臨床業務に従事しながら英語論文を書くには

Naoki Ohno（Faculty of Health Sciences, Institute of Medical, Pharmaceutical and Health Sciences, Kanazawa University）
大野　直樹（金沢大学 医薬保健研究域 保健学系）

S7-2　Importance of response file and technique to make English sentences

レスポンスファイルの重要性と英文を作るための技

Masami Goto（Kitasato University Department of School of Allied Health Sciences）
後藤　政実（北里大学 医療衛生学部）

S7-3　English paper writing for non-native speakers

明日からのらくらく論文執筆

Eriko Maeda（The University of Tokyo, Department of Radiology）
前田恵理子（東京大学 放射線科）

S7-4 **Elements of an effective paper for the journals JMRI and MRM**
Stephen J. Riederer（Department of Radiology, Mayo Clinic）

Saturday, September 10, 13:00～15:20 Room 2 (Sonic City Hall, 2F, Small Hall)

Symposium 8「MR elastography, Now and Beyond」

シンポジウム8

Chairs：Utaroh Motosugi（Department of Radiology, University of Yamanashi）
Mikio Suga（Chiba University, Center for Frontier Medical Engineering）
座　長：本杉宇太郎（山梨大学 医学部 放射線医学講座）
菅　　幹生（千葉大学 フロンティア医工学センター）

S8-1 **Principle of MRE**
Tetsuya Wakayama（GE Healthcare Japan）
若山　哲也（GEヘルスケア・ジャパン株式会社 研究開発部 MRI研究室）

S8-2 **Clinical application of MRE1**
MREの臨床応用1
Kengo Yoshimitsu（Department of Radiology, Faculty of Medicine, Fukuoka University）
吉満　研吾（福岡大学医学部放射線医学教室）

S8-3 **Clinical application of MRE**
臨床におけるMREの有用性
Shintaro Ichikawa（Department of Radiology, University of Yamanashi）
市川新太郎（山梨大学医学部 放射線科）

S8-4 **Future direction**
Richard L. Ehman（Department of Radiology, Mayo Clinic）

Saturday, September 10, 15:30～17:50 Room 2 (Sonic City Hall, 2F, Small Hall)

Symposium 9「MR Angiography and Techniques: Now and Beyond」

シンポジウム9

Chairs：Mitsue Miyazaki（Toshiba Medical Systems）
Stephen J. Riederer（Department of Radiology, Mayo Clinic）
座　長：宮崎美津恵（東芝メディカルシステムズ株式会社）
Stephen J. Riederer（Department of Radiology, Mayo Clinic）

S9-1 **Technical Aspects of Contrast-Enhanced MRA: Current Status and New Applications**
Stephen J. Riederer（Department of Radiology, Mayo Clinic）

S9-2 **Contrast Enhanced MR Angiography Revisited**
造影MR Angiography再考
Yasuo Takehara（Hamamatsu University Hospital）
竹原　康雄（浜松医科大学附属病院）

S9-3 **Non-Contrast MRA Techniques**
Mitsue Miyazaki（Toshiba Medical Systems）
宮崎美津恵（東芝メディカルシステムズ株式会社）

S9-4 **Non-contrast-enhanced MR angiography in the past present and future**
非造影MR angiographyの臨床応用；過去，現在，今後
Katsumi Nakamura（Tobata Kyoritsu Hospital, Department of Radiology）
中村　克己（戸畑共立病院 放射線科）

S9-5 **True Tracer for Water-Time-SLIP Application to the Cerebrospinal Fluid-**
理想的な水のトレーサースタディー タイムスリップ法の脳脊髄液への応用
Shinya Yamada（Toshiba RInkan Hospital Neurosurgey Hydrocephalus CSF center）
山田　晋也（東芝林間病院 脳神経外科 水頭症 脳脊髄液センター）

S9-6 **Pancreaticobiliary application of non-contrast enhanced MR angiography Pancreatic juice depiction**
非造影MRAの膵胆道疾患への応用：膵液の描出
Reiji Sugita（Sendai City Medical Hospital, Department of Radiology）
杉田　礼児（仙台オープン病院 放射線科）

Sunday, September 11, 9:10～11:50　　Room 1 (Sonic City Hall, 1F, Large Hall)

Symposium 10「The art of MR meisters: breast MRI and DWI」

シンポジウム10「匠の技②　乳腺MRI撮像と拡散強調画像を磨く匠の技」

Chairs：Akio Ogura（Gunma Prefectural College of Health Sciences）
Hajime Tanji（Northern Fukushima Medical Center）
座　長：小倉　明夫（群馬県立県民健康科学大学）
丹治　　一（北福島医療センター）

S10-1 **Effect of the Menstrual Cycle in Breast MR Imaging**
乳腺MRIのポジショニングと撮像時期
Mariko Kajihara（FUJIFILM Medical Co.,Ltd.）
梶原万里子（富士フイルムメディカル株式会社 モダリティソリューション部）

S10-2 **Fat suppression technique in Breast MRI**
乳腺MRIにおける脂肪抑制技術
Yasuo Takatsu（Osaka Red Cross Hospital, Department of Radiology）
高津　安男（大阪赤十字病院 放射線診断科部）

S10-3 **Breast DWI and Dynamic study**
乳腺DWIとダイナミックスタディ
Takayuki Tamura（Hiroshima University Hospital Department of Clinical Support）
田村　隆行（広島大学病院 診療支援部画像診断部門）

S10-4 **The effective ROI setting method for the breast MRI using DPS map**
乳腺MRIでTICを得るためのROI設定
Akio Ogura（Gunma Prefectural College of Health Sciences）
小倉　明夫（群馬県立県民健康科学大学）

S10-5 **Suppression techniques of distortion of DWI**
DWIの歪抑制技術
Mitsuyuki Takahashi（Department of Radiology, Yokohama Sakae Kyosai Hospital, Federation of National Public Service Personnel Mutual Associations）
高橋　光幸（国家公務員共済組合連合会 横浜栄共済病院 放射線技術科）

S10-6 **Diffusion-weighted Imaging fat suppression technique**
DWIの脂肪抑制技術
Hajime Tanji（Northern Fukushima Medical Center）
丹治　　一（北福島医療センター）

S10-7 **Effect of imaging parameters on the accuracy of apparent diffusion coefficient**
ADCの測定精度について
Masanori Ozaki（GE Healthcare Japan Corporation）
尾﨑　正則（GEヘルスケア・ジャパン株式会社）

S10-8 **A basic knowledge of the motion with DWI**
DWIの動きに対する考え方
Isao Muro（Tokai University Hospital Department of Radiological Technology）
室　伊三男（東海大学医学部付属病院放射線技術科）

KSMRM-JSMRM Joint Session

Saturday, September 10, 15:20～17:50　Room 3 (Sonic City Hall, 4F, International Conference Room)

KSMRM-JSMRM Joint Session 1「Basic Sciences」

Chairs：Chang-Beom Ahn（Kwangwoon University, Seoul, Korea）
Kagayaki Kuroda（Course of Electrical and Electronic Engineering, School of Engineering, Tokai University）

座　長：Chang-Beom Ahn（Kwangwoon University, Seoul, Korea）
黒田　　輝（東海大学大学院工学研究科電気電子工学専攻）

Opening remarks
Yongmin Chang（Kwangwoon University and Hospital）

KJS1-1 **Functional and Theranostic Contrast Agents**
機能的およびセラノスティック造影剤
Ichio Aoki（National Institute of Radiological Sciences, QST）
青木伊知男（量子科学技術研究開発機構・放医研）

KJS1-2 **Electrical property imaging**
Dong Hyun Kim（Yonsei University）

KJS1-3 **Visualization of Electromagnetic Phenomena**
Masaki Sekino（The University of Tokyo, Department of Electrical Engineering and Information Systems）
関野　正樹（東京大学 大学院工学系研究科 電気系工学専攻）

KJS1-4 **MR Temperature Imaging Technique using Keyhole Method**
Chi-Woong Mun（Department of Biomedical Engineering, Inje University）

KJS1-5 **A quantitative measurement of water exchange between hindered and restricted diffusion compartments**
Hindered/ Restricted diffusion compartment間における水交換の定量的評価
Yasuhiko Tachibana（Applied MRI Research, Department of Molecular Imaging and Theranostics, National Institute of Radiological Sciences）
立花　泰彦（放射線医学総合研究所 分子イメージング診断治療研究部 医工連携画像研究チーム）

KJS1-6 **Functional MRS**
Geon-Ho Jahng（Radiology, Kyung Hee University Hospital at Gangdong）

Sunday, September 11, 9:10～11:40　　Room 3 (Sonic City Hall, 4F, International Conference Room)

KSMRM-JSMRM Joint Session 2「What's hot in neuroimaging field? Japan and Korea」

Chairs：Kei Yamada（Kyoto Prefectural University of Medicine, Graduate School of Medical Science）
Sang Joon Kim（Radiology, Asan Medical Center）
座　長：山田　　惠（京都府立医科大学大学院医学研究科 放射線診断治療学）
Sang Joon Kim（Asan Medical Center）

KJS2-1 CEST

Ji Eun Park（Department of Radiology and Research Institute of Radiology, Asan Medical Center）

KJS2-2 Clinical application of CEST/APT imaging

CEST/APTイメージングの臨床応用

Osamu Togao（Department of Clinical Radiology, Graduate School of Medical Sciences, Kyushu University）
栂尾　　理（九州大学大学院医学研究院 臨床放射線科学分野）

KJS2-3 radiogenomics

Seung Hong Choi（Department of Radiology, Seoul National University Hospital）

KJS2-4 The Role of Radiomics in Neuroimaging

中枢神経領域におけるラジオミクスの有用性

Khin Khin Tha（Department of Radiation Medicine, Hokkaido University）
タ　キンキン（北海道大学大学院医学研究科放射線医学分野）

KJS2-5 diffusion

Seung-Koo Lee（Department of Radiology, Yonsei University College of Medicine）

KJS2-6 Diffusion

拡散MRI

Koji Sakai（Kyoto Prefectural University of Medicine, Graduate School of Medical Science）
酒井　晃二（京都府立医科大学大学院医科学研究科）

Educational Lecture
教育講演

Friday, September 9, 8:00～9:00　　Room 2 (Sonic City Hall, 2F, Small Hall)

Educational Lecture 1「CNS 1」

教育講演1「脳神経1」

Chair：Toshiaki Taoka（Nagoya University, Department of Radiology）
座　長：田岡　俊昭（名古屋大学 放射線科）

EL1-1 Head MRI and water molecules

頭部MRIと水分子

Koji Sakai（Department of Radiology, Graduate School of Medical Science, Kyoto Prefectural University of Medicine）
酒井　晃二（京都府立医科大学 大学院医学研究科 放射線診断治療学）

EL1-2 **Innovation for generating clinically useful new contrast**

臨床に役立つ新しいコントラストを生み出すための工夫

Masami Yoneyama（MR Clinical Science, IS Buisiness Group, Philips Electronics Japan）

米山　正己（株式会社 フィリップスエレクトロニクスジャパン ISビジネスグループ MRクリニカルサイエンス）

Friday, September 9, 8:00～9:00　　Room 3 (Sonic City Hall, 4F, International Conference Room)

Educational Lecture 2「Abdomen and Pelvis 1」

教育講演2「腹部骨盤1」

Chair：Junko Takahama（Nara Medical University）

座　長：高濱　潤子（奈良県立医科大学 放射線科・総合画像診断センター）

EL2-1 **MRI of Prostate Cancer in the TZ and the AFMS: Intraprostatic Patterns of Spread and the Relative Frequency of the Locations**

前立腺移行域がんのMRI: 発生部位と進展様式からのアプローチ

Hiroshi Shinmoto（Department of Radiology, National Defense Medical College）

新本　　弘（防衛医科大学校 放射線医学講座）

EL2-2 **The acute gynecologic abdomen ; role of MR imaging in diagnosis**

産婦人科急性腹症の画像診断 - MRI が寄与できること -

Ayako Tamura（Department of Radiology, Tokyo-Kita Medical Center）

田村　綾子（東京北医療センター 放射線科）

Friday, September 9, 8:00～9:00　　Room 4 (Sonic City Building, 4F, 401～402)

Educational Lecture 3「Breast」

教育講演3「乳腺」

Chair：Hidetake Yabuuchi（Department of Health Sciences, Kyushu University Graduate School of Medical Sciences）

座　長：藪内　英剛（九州大学大学院医学研究院保健学部門）

EL3-1 **Non-mass enhancement at breast MRI**

Non-mass enhancement at breast MRI: 鑑別のための Key findings

Youichi Machida（Department of Radiology, Kameda Kyobashi Clinic）

町田　洋一（医療法人鉄蕉会 亀田京橋クリニック 放射線科／医療法人鉄蕉会 亀田メディカルセンター 乳腺科）

EL3-2 **MRI of benign breast lesions: Key imaging findings for making correct diagnosis**

乳腺良性病変のMR-pathologic correlation: 鑑別のためのKey findings

Mariko Goto（Department of Radiology, Kyoto Prefectural University of Medicine）

後藤眞理子（京都府立医科大学大学院医学研究科 放射線診断治療学）

Friday, September 9, 8:00～9:00　　Room 5 (Sonic City Building, 4F, 403～404)

Educational Lecture 4「MR basics 1」

教育講演4「基礎1」

Chair：Yoshio Machida（Tohoku University Graduate School of Medicine）
座　長：町田　好男（東北大学大学院医学系研究科）

EL4-1　Basics of RF Pulses

RFパルスの基礎

Yoshitaka Bito（Hitachi, Ltd. Healthcare Business Unit）
尾藤　良孝（株式会社日立製作所 ヘルスケアビジネスユニット）

EL4-2　Basic principles of MRA

MR angiographyの基礎

Atsushi Ono（Kousei Hospital Medical Support Division）
小野　　敦（光生病院 診療支援部／大阪大学大学院 医学系研究科 医用物理工学講座）

Saturday, September 10, 8:00～9:00　　Room 1 (Sonic City Hall, 1F, Large Hall)

Educational Lecture 5「Musculoskeletal 1」

教育講演5「骨軟部1」

Chair：Kaoru Kitsukawa（St. Marianna University School of Medicine, Department of Radiology）
座　長：橘川　　薫（聖マリアンナ医科大学放射線医学講座）

EL5-1　Magnetic Resonance Neurography for Peripheral Nerve Disorders

末梢神経疾患の画像診断：MR neurographyを中心に

Shuji Nagata（Kurume University School of Medicine）
長田　周治（久留米大学 医学部）

EL5-2　Bone Marrow MRI

骨髄のMRI

Yoshiko Hayashida（University of Occupational and Environmental Health）
林田　佳子（産業医科大学 放射線科学教室）

Saturday, September 10, 8:00～9:00　　Room 2 (Sonic City Hall, 2F, Small Hall)

Educational Lecture 6「CNS 2」

教育講演6「脳神経2」

Chair：Hiroshi Oba（Teikyo University School of Medicine, Department of Radiology）
座　長：大場　　洋（帝京大学医学部放射線科）

EL6-1　Drug-induced imaging features in the central nervous system

中枢神経領域における薬剤に起因する画像所見

Satoshi Matsushima（Department of Radiology Jikei University School of Medicine）
松島　理士（東京慈恵会医科大学 放射線医学講座）

EL6-2　MR Imaging for neonatal hypoxic-ischemic encephalopathy

新生児低酸素性虚血性脳症のMRI

Katsumi Hayakawa（Iwate Prefectural Kamaishi Hospital）
早川　克己（岩手県立釜石病院）

Saturday, September 10, 8:00～9:00　　Room 3 (Sonic City Hall, 4F, International Conference Room)

Educational Lecture 7「Abdomen and Pelvis 2」

教育講演7「腹部骨盤2」

Chair：Satoshi Goshima（Gifu University Department of Radiology）
座　長：五島　　聡（岐阜大学 放射線科）

EL7-1　Liver tumors: differential diagnosis and pitfalls on MR imaging

MRIによる肝腫瘍の診断法とピットフォール

Yoshihiko Fukukura（Kagoshima University, Department of Radiology）
福倉　良彦（鹿児島大学 放射線診断治療学分野）

EL7-2　MRI of pancreatic disease -common and uncommon findings-

膵疾患のMRI　～common and uncommon findings～

Katsuhiro Sano（Department of Diagnositc Radiology, Saitama Medical University International Medical Center）
佐野　勝廣（埼玉医科大学国際医療センター 画像診断科）

Saturday, September 10, 8:00～9:00　　Room 4 (Sonic City Building, 4F, 401～402)

Educational Lecture 8「Cardiovascular」

教育講演8「心血管」

Chair：Noriko Oyama-Manabe（Hokkaido University Hospital）
座　長：真鍋　徳子（北海道大学病院）

EL8-1　Clinical use of 4D flow MRI in cardiac disease

心疾患における4Dフロー MRIの臨床利用

Michinobu Nagao（Tokyo Women's Medical University, Diagnostic Imaging & Nuclear Medicine）
長尾　充展（東京女子医科大学 画像診断学・核医学講座）

EL8-2　Cardiac MRI in the Patients with Rheumatic Diseases

膠原病患者における心臓MRI

Yasuyuki Kobayashi（Department of Advanced Biomedical Imaging Informatics, St.Marianna University School of Medicine, Kawasaki, Japan）
小林　泰之（聖マリアンナ医科大学 医学部 先端生体画像情報研究講座）

Saturday, September 10, 8:00～9:00　　Room 5 (Sonic City Building, 4F, 403～404)

Educational Lecture 9「MR basics 2」

教育講演9「基礎2」

Chair：Masayuki Yamaguchi（National Cancer Center Division of Functional Imaging）
座　長：山口　雅之（国立がん研究センター 機能診断開発分野）

EL9-1　Introduction to MR Fingerprinting

MR fingerprinting入門

Yasuhiko Terada（Faculty of Pure and Applied Sciences, University of Tsukuba）
寺田　康彦（筑波大学 数理物質系 物理工学域）

EL9-2　Introduction of Radiomics – Basics of Machine Learning

Radiomics入門: 機械学習の基礎

Natsumaro Kutsuna（Graduate School of Frontier Sciences, The University of Tokyo）
朽名　夏麿（東京大学 大学院新領域創成科学研究科）

Sunday, September 11, 8:00～9:00　　Room 1 (Sonic City Hall, 1F, Large Hall)

Educational Lecture 10「Musculoskeletal 2」

教育講演10「骨軟部2」

Chair：Ryuji Sashi（Yaesu clinic）
座　長：佐志　隆士（八重洲クリニック）

EL10-1　Shoulder joint (rotator cuff)

肩関節（腱板）

Shin Hitachi（Tohoku University Hospital, Diagnostic Radiology）
常陸　　真（東北大学病院 放射線診断科）

EL10-2　Imaging Diagnosis of Shoulder joint(Glenoid lip,rotator interval,biceps brachii tendon)

肩関節の画像診断（関節唇、腱板疎部、上腕二頭筋長頭腱疾患）

Daisuke Amano（Meirikai Chuo General Hospital Department of Radiology）
天野　大介（明理会中央総合病院 放射線科）

Sunday, September 11, 8:00～9:00　　Room 2 (Sonic City Hall, 2F, Small Hall)

Educational Lecture 11「CNS 3」

教育講演11「脳神経3」

Chair：Yukio Miki（Osaka City University Department of Diagnostic and Interventional Radiology）
座　長：三木　幸雄（大阪市立大学 放射線科）

EL11-1　Imaging features of meningioma variants

髄膜腫の稀な亜型の画像診断

Akira Kunimatsu（Department of Radiology, Graduate School of Medicine, The University of Tokyo）
國松　　聡（東京大学大学院 医学系研究科 放射線医学講座）

EL11-2　Neuroimaging of mucopolysaccharidoses

ムコ多糖症の中枢神経画像

Satoshi Doishita（Osaka City University Graduate School of Medicine, Department of Diagnostic and Interventional Radiology）
土井下　怜（大阪市立大学大学院 医学研究科 放射線診断学・IVR学）

Sunday, September 11, 8:00～9:00　　Room 3 (Sonic City Hall, 4F, International Conference Room)

Educational Lecture 12「Imaging technique」

教育講演12「撮像技術」

Chair：Hitoshi Kubo（Fukushima Medical University, Advanced Clinical Research Center）
座　長：久保　　均（福島県立医科大学 先端臨床研究センター）

EL12-1　Think about what to do the MRI imaging in children

小児のMR検査はどうするべきかを考える

Akihiro Ishikuro（Osaka Prefectural Medical Center for Respiratory and Allergic Diseases）
石黒　秋弘（地方独立行政法人大阪府立病院機構 大阪府立呼吸器・アレルギー医療センター 放射線科）

EL12-2　Imaging techniques in MR angiography of the body

体幹部MR angiographyの撮像技術

Hirofumi Hata（Department of Radiology, Kitasato University Hospital）
秦　　博文（北里大学病院 放射線部）

Sunday, September 11, 8:00～9:00　　Room 4 (Sonic City Building, 4F, 401～402)

Educational Lecture 13「Safety」

教育講演13「安全」

Chair：Masafumi Harada（Tokushima University Department of Radiology）
座　長：原田　雅史（徳島大学 放射線医学分野）

EL13-1　Safety management of MR conditional device

条件付きMRI対応デバイス患者の安全管理

Toshio Tsuchihashi（Department of Radiology, Nippon Medical School Hospital）
土橋　俊男（日本医科大学付属病院放射線科）

EL13-2　Current status and challenging future of MR conditional device

条件付きMRI対応デバイスの現状と今後の課題

Kenichi Yokoyama（Department of Radiology, Kyorin University, School of Medicine）
横山　健一（杏林大学 医学部 放射線医学教室）

Sunday, September 11, 9:00～10:00　　Room 4 (Sonic City Building, 4F, 401～402)

Educational Lecture 14「MR basics 3」

教育講演14「基礎3」

Chair：Kazuhiro Nakamura（Research Institute for Brain and Blood Vessels Akita）
座　長：中村　和浩（秋田県立脳血管研究センター）

EL14-1　Basics of quantitative DCEMRI

定量的 DCEMRI の基礎

Hideto Kuribayashi（Siemens Healthcare）
栗林　秀人（シーメンスヘルスケア株式会社）

EL14-2　Clinical application of quantitative DCEMRI

定量的DCEMRIの臨床応用

Akira Yamada（Shinshu University School of Medicine, Department of Radiology）
山田　　哲（信州大学 医学部 画像医学教室）

Luncheon Seminar
ランチョンセミナー

Friday, September 9, 12:00～12:50　　Room 1 (Sonic City Hall, 1F, Large Hall)

Luncheon Seminar 1

ランチョンセミナー1

Chair：Kaori Togashi（Department of Diagnostic Imaging and Nuclear Medicine, Kyoto University）
座　長：富樫かおり（京都大学大学院医学研究科 放射線医学講座）

LS1-1　The management of risks in contrast-enhanced MRI

MRI造影剤のリスクマネージメントについて

Makoto Iida（Department of Diagnostic Radiology, Hiroshima University Hospital）
飯田　　慎（広島大学大学院 放射線部）

LS1-2 **The indication and practical procedures of the gynecologic MRI based on the The Japanese Imaging Guideline 2016**

あなたのその検査、世界標準ですか？－画像診断ガイドライン2016年版から学ぶ産婦人科MRの適応と実際－

Yumiko Tanaka（Diagnostic Imaging Department, The Cancer Institute Hospital, Japanese Foundation for Cancer Research）

田中優美子（がん研有明病院 画像診断部 婦人科領域）

sponsored by Fuji Pharma Co., Ltd.
共催：富士製薬工業株式会社

Friday, September 9, 12:00～12:50　　Room 2 (Sonic City Hall, 2F, Small Hall)

Luncheon Seminar 2「The latest topics in clinical applications for Abdomen and Cardiac」

ランチョンセミナー2「腹部・心臓 最新アプリケーション」

Chair：Yasuyuki Yamashita（Biomedical Informatics, Integrated Medical and Pharmaceutical Sciences, Department of Diagnostic Radiology, Kumamoto University）

座　長：山下　康行（熊本大学大学院 生命科学研究部 放射線診断学）

LS2-1 **Clinical significance of New Advanced MRI Technique**

MRI技術が及ぼす臨床的意義

Satoshi Goshima（Department of Radiology, Gifu University）

五島　　聡（岐阜大学医学部附属病院放射線部）

LS2-2 **New potential of Cardiac MRI**

心臓MRIの新しいポテンシャル

Noriko Oyama-Manabe（Hokkaido University Hospital）

真鍋　徳子（北海道大学病院）

sponsored by Philips Electronics Japan, Ltd.
共催：株式会社フィリップス エレクトロニクスジャパン

Friday, September 9, 12:00～12:50　　Room 3 (Sonic City Hall, 4F, International Conference Room)

Luncheon Seminar 3「Cardiac MRI: The leading edge of clinical study」

ランチョンセミナー3

Chair：Kei Takase（Diagnostic Radiology, Tohoku University of Medicine）

座　長：高瀬　　圭（東北大学大学院医学系研究科 放射線診断学分野）

LS3-1 **CMR future delivered by Compressed sensing**

Compressed sensingが切り開くCMRの未来

Masashi Nakamura（Department of Radiology, Ehime University Graduate School of Medicine）

中村　壮志（愛媛大学大学院医学系研究科 愛媛大学医学部 器官・形態領域 放射線医学）

LS3-2 **Can unstable plaque diagnosis with HIP (High Intensity Plaque) influence on disease prevention and treatment policy?**

HIP（High Intensity Plaque）による不安定プラーク診断は予防と治療方針に影響を与えるか？

Teruo Noguchi（Department of Cardiovascular Medicine, National Cerebral and Cardiovascular Center）

野口　暉夫（国立循環器病研究センター病院 心臓血管内科部門）

sponsored by Siemens Healthcare K.K.
共催：シーメンスヘルスケア株式会社

Friday, September 9, 12:00～12:50　　Room 4 (Sonic City Building, 4F, 401～402)

Luncheon Seminar 4

ランチョンセミナー4

Chair：Katsuyoshi Ito（Department of Radiology, Kawasaki Medical School）
座　長：伊東　克能（川崎医科大学放射線医学（画像診断1））

LS4　Optimized examination protocol and scan parameter of EOB-MRI
EOB-MRIの最適撮像法 -GALIREO study（国内45施設における多施設試験）の結果を含めて-
Takamichi Murakami（Department of Radiology, Kindai University School of Medicine）
村上　卓道（近畿大学医学部放射線医学教室放射線診断学部門）

sponsored by Bayer Yakuhin, Ltd.
共催：バイエル薬品株式会社

Friday, September 9, 12:00～12:50　　Room 5 (Sonic City Building, 4F, 403～404)

Luncheon Seminar 5「B1+rms control on MR-conditional implantable devices」

ランチョンセミナー5「条件付きMRI対応植込み型デバイスにおけるB1+rms制御」

Chair：Tsukasa Doi（Kouseikai Takai Hospital）
座　長：土井　　司（社会医療法人 高清会 高井病院）

LS5-1　SAR and B1rms
SARとB1+rms
Tomoya Yamaguchi（Suzuka Saisei Hospital）
山口　智也（峰和会 鈴鹿回生病院 放射線科）

LS5-2　How to control B1rms
B1+rmsの制御方法に関して
Toshio Tsuchihashi（Nippon Medical School Hospital）
土橋　俊男（日本医科大学付属病院 放射線科）

sponsored by Medtronic Japan Co., Ltd.
共催：日本メドトロニック株式会社

Saturday, September 10, 12:00～12:50　　Room 1 (Sonic City Hall, 1F, Large Hall)

Luncheon Seminar 6「Clinical application of Gadovist in Japan」

ランチョンセミナー6「本邦におけるガドビストの臨床応用」

Chair：Hajime Sakuma（Department of Radiology, Mie University Graduate School of Medicine）
座　長：佐久間　肇（三重大学大学院 医学系研究科 放射線医学講座）

LS6-1　Contrast-enhanced cardiac MR using Gadovist
Gadovistを用いた造影心臓MR
Yasuo Amano（Department of Radiology, Nihon University School of Medicine）
天野　康雄（日本大学医学部 放射線医学系 画像診断学分野）

LS6-2　Magnetic Resonance Angiography for the Aorta and Branches Using Gadovist
大動脈・分枝動脈のガドビスト造影MR Angiography
Yasuo Takehara（Department of Radiology, Hamamatsu University School of Medicine, University hospital）
竹原　康雄（浜松医科大学医学部附属病院 放射線部）

sponsored by Bayer Yakuhin, Ltd.
共催：バイエル薬品株式会社

Saturday, September 10, 12:00～12:50　　Room 2 (Sonic City Hall, 2F, Small Hall)

Luncheon Seminar 7

ランチョンセミナー7

Chair：Kazuro Sugimura（Kobe University）
座　長：杉村　和朗（神戸大学大学院医学研究科 内科系講座放射線医学分野）

LS7　Simultaneous Multi-Slice (SMS) acquisition
Stephen F. Cauley（Biomedical Engineering, Massachusetts General Hospital）

sponsored by Siemens Healthcare K.K.
共催：シーメンスヘルスケア 株式会社

Saturday, September 10, 12:00～12:50　Room 3 (Sonic City Hall, 4F, International Conference Room)

Luncheon Seminar 8「The latest topics in clinical applications for Neurology」

ランチョンセミナー8「脳神経領域 最新アプリケーション」

Chair：Toshihide Ogawa（Division of Radiology, Department of Pathophysiological Therapeutic Science, School of Medicine, Tottori University Faculty of Medicine）
座　長：小川　敏英（鳥取大学医学部 医学科 病態解析医学講座 画像診断治療学分野）

LS8-1　Diagnosis of Dementia using MRI
MRIによる認知症の画像診断
Hiroshi Matsuda（Integrative Brain Imaging Center, National Center of Neurology and Pyschiatry）
松田　博史（国立精神・神経医療研究センター脳病態統合イメージングセンター）

LS8-2　Evaluation of clinical efficacy of the CINEMA
CINEMAの臨床的有用性について
Kayoko Abe（Department of Diagnostics imaging and Nuclear Medicine, Tokyo Women's Medical University）
阿部香代子（東京女子医科大学 画像診断学・核医学講座）

sponsored by Philips Electronics Japan, Ltd.
共催：株式会社フィリップス エレクトロニクスジャパン

Saturday, September 10, 12:00～12:50　　Room 4 (Sonic City Building, 4F, 401～402)

Luncheon Seminar 9

ランチョンセミナー9

Chair：Makoto Sasaki（Institute for Biomedical Sciences, Iwate Medical University）
座　長：佐々木真理（岩手医科大学 医歯薬総合研究所）

LS9　Utility of neuroimaging diagnosis in dementia – case-based imaging review –
一筋縄ではいかない認知症の画像診断 -画像検査が有用であった症例を中心に-
Keita Sakurai（Tokyo Metropolitan Medical Center of Gerontology）
櫻井　圭太（東京都健康長寿医療センター放射線診断科）

sponsored by Hitachi, Ltd.
共催：株式会社日立製作所

Saturday, September 10, 12:00～12:50　　Room 5 (Sonic City Building, 4F, 403～404)

Luncheon Seminar 10「Topics of Gadolinium contract agents」

ランチョンセミナー10「Gd造影剤の有効性と安全性に関するトピックス」

Chair：Yukio Miki（Department of Diagnostic and Interventional Radiology, Osaka City University Graduate School of Medicine）

座　長：三木　幸雄（大阪市立大学大学院 医学研究科 放射線診断学・IVR学教室）

LS10-1　The gadolinium deposition in the brain 3rd years experiences and future goal

ガドリニウムの脳内残留問題　～3年間で判明した事実とこれから～

Tomonori Kanda（Department of Radiology, Teikyo University School of Medicine）

神田　知紀（帝京大学医学部放射線科学講座）

LS10-2　Efficacy and Safety of Gadolinium Contrast Agents: Based on the TRUTH study, etc

Gd造影剤の有効性と安全性：TRUTH study等を踏まえて

Toshinori Hirai（Department of Radiology, Faculty of Medicine, University of Miyazaki）

平井　俊範（宮崎大学医学部 病態解析医学講座 放射線医学分野）

sponsored by Eisai Co., Ltd.

共催：エーザイ株式会社

Sunday, September 11, 12:00～12:50　　Room 1 (Sonic City Hall, 1F, Large Hall)

Luncheon Seminar 11「Creative ideas and Ingenuity encompasses Toshiba Medical's MRI System」

ランチョンセミナー11「MRIをとりまく創意と工夫」

Chair：Shigeki Aoki（Juntendo University Graduate School of Medicine Department of Radiology）

座　長：青木　茂樹（順天堂大学医学部・大学院医学研究科 放射線医学教室 放射線診断学講座）

LS11-1　Innovative Usage of Olea Software and Silent Sequence

Oleaソフトウェアと静音シーケンスの新たな使い方

Tsutomu Katoh（Sumitomo Besshi Hospital）

加藤　　勤（医療法人住友別子病院）

LS11-2　Ingenuity learned from GARON

忘れられない『画論』の知恵

Toshiaki Nitatori（Kyorin University School of Medicine Department of Radiology）

似鳥　俊明（杏林大学医学部 放射線医学教室）

sponsored by Toshiba Medical Systems Corporation

共催：東芝メディカルシステムズ株式会社

Sunday, September 11, 12:00～12:50　　Room 2 (Sonic City Hall, 2F, Small Hall)

Luncheon Seminar 12「3T MRI Neuro Applications -Clinical use and beyond-」

ランチョンセミナー12「3T MRI 頭部アプリケーションの実践」

Chair：Osamu Abe（Department of Radiology, Nihon University School of Medicine）

座　長：阿部　　修（日本大学医学部 放射線医学系 画像診断学分野放射線腫瘍学分野）

LS12-1　Zero TE（Z-TE）MRA

Michimasa Suzuki（Department of Radiology, Juntendo University）

鈴木　通真（順天堂大学医学部・大学院医学研究科 放射線医学教室放射線診断学講座）

LS12-2 **MAGiC (* including SyMRI), – Faster, Further, Deeper–**

Masaaki Hori（Department of Radiology, Juntendo University）

堀　　正明（順天堂大学医学部・大学院医学研究科 放射線医学教室放射線診断学講座）

sponsored by GE Healthcare Japan Corporation

共催：GEヘルスケア・ジャパン 株式会社

Sunday, September 11, 12:00～12:50　Room 3 (Sonic City Hall, 4F, International Conference Room)

Luncheon Seminar 13

ランチョンセミナー13

Chair：Yoshiteru Seo（Dokkyo Medical University Department of Regulatory Physiology）

座　長：瀬尾　芳輝（獨協医科大学 医学部 生理学（生体制御））

LS13 **Clinical research and application in musculoskeletal MRI**

骨関節領域におけるMRIを用いた臨床研究と臨床応用

Taiki Nozaki（Department of Diagnostic Radiology, Tokyo Medical and Dental University/ Department of Radiology, St.Luke's International Hospital）

野崎　太希（東京医科歯科大学 放射線診断科 / 聖路加国際病院 放射線科）

sponsored by Hitachi, Ltd.

共催：株式会社日立製作所

Sunday, September 11, 12:00～12:50　Room 4 (Sonic City Building, 4F, 401～402)

Luncheon Seminar 14

ランチョンセミナー14

Chair：Toshiko Nakai（Division of Advanced Therapeutics for Cardiac Arrhythmias, Department of Medicine, Nihon University School of Medicine）

座　長：中井　俊子（日本大学医学部 先端不整脈治療学分野）

LS14 **How can an AIMD be MR-conditional?: Tips on Safety Testing and Conditional Imaging**

体内埋込み型デバイスはいかにして条件付MRI対応となりうるのか：安全性試験と撮像条件の要点

Kagayaki Kuroda（School of Information Science and Technology Tokai University）

黒田　　輝（東海大学情報理工学部 情報科学科）

sponsored by St. Jude Medical Co., Ltd.

共催：セント・ジュード・メディカル株式会社

Evening Seminar
イブニングセミナー

Friday, September 9, 18:00～18:50　　Room 2 (Sonic City Hall, 2F, Small Hall)

Evening Seminar 1「Imaging Approaches for Dementia」
イブニングセミナー1「認知症の画像診断」

Chair：Kei Yamada（Kyoto Prefectural University of Medicine Department of Radiology）
座　長：山田　　惠（京都府立医科大学大学院医学研究科 放射線診断治療学）

ES1-1　What does functional imaging tell us about dementia?
機能診断から見た認知症画像診断
Hitoshi Shimada（Department of Functional Brain Imaging Research, National Institute of Radiological Sciences, National Institutes for Quantum and Radiological Science and Technology）
島田　　斉（量子科学技術研究開発機構 放射線医学総合研究所 脳機能イメージング研究部）

ES1-2　What does morphological imaging tell us about dementia?
形態診断から見た認知症画像診断
Harushi Mori（The University of Tokyo Department of Radiology, Graduate School of Medicine）
森　　墾（東京大学大学院 医学系研究科・医学部 生体物理医学専攻 放射線医学講座 放射線診断学分野）

sponsored by DAIICHI SANKYO CO., LTD.
共催：第一三共株式会社

Friday, September 9, 18:00～18:50　　Room 3 (Sonic City Hall, 4F, International Conference Room)

Evening Seminar 2「Body MRI Update」
イブニングセミナー2「体幹部アプリケーションの最新知見」

Chair：Masahiro Jinzaki（Department of Radiology, Keio University School of Medicine）
座　長：陣崎　雅弘（慶應義塾大学医学部 放射線診断科）

ES2-1　MR Protocol for Liver Cirrhosis
肝硬変における実践的MRプロトコル
Utaroh Motosugi（Department of Radiology, University of Yamanashi）
本杉宇太郎（山梨大学医学部 放射線医学講座 放射線診断科）

ES2-2　Fast Imaging Techniques for Dynamic MRI
最新の高速シーケンスとダイナミックMRIへの応用
Takayuki Masui（Department of Radiology, Seirei Hamamatsu General Hospital）
増井　孝之（社会福祉法人聖隷福祉事業団総合病院 聖隷浜松病院 放射線科）

sponsored by GE Healthcare Japan Corporation
共催：GEヘルスケア・ジャパン株式会社

Friday, September 9, 18:00～18:50　　Room 4 (Sonic City Building, 4F, 401～402)

Evening Seminar 3「Fundamentals and Applications of the lumbar spine MRI」

イブニングセミナー3「腰椎MRIの基礎から応用まで」

Chair：Kunihiko Fukuda（The Jikei University School of Medicine）
座　長：福田　国彦（東京慈恵会医科大学 放射線医学講座）

ES3-1　Basis of the lumber spine MRI

腰椎MRIの基本

Yasuhiro Kawahara（NAGASAKI ROSAI HOSPITAL）
川原　康弘（独立行政法人労働者健康安全機構 長崎労災病院 放射線科）

ES3-2　Herniated lumber disks / Real-time MR imaging evaluation during continuous traction

椎間板ヘルニア：連続牽引中のリアルタイムMRIによる評価

Tae-Sub Chung（Gangnam Severance Hospital of the Yonsei University）

sponsored by Konica Minolta Japan, Inc.
共催：コニカミノルタジャパン株式会社

Day 1……Room 1 (Sonic City Hall, 1F, Large Hall)

Body diffusion　16：50～17：40

Chair：Masaaki Akahane（NTT Medical Center Tokyo）
座　長：赤羽　正章（NTT東日本関東病院 放射線部）

O-1-001　3D-Histogram Analysis using ADC-map in Liver Magnetic Resonance Image
肝臓MR検査におけるADC-map を用いた3D-ヒストグラム解析
中野　雅浩（JA愛知厚生連 海南病院 診療協同部 放射線技術科）
Masahiro Nakano, Takahiro Natsume, Seiji Kamei, Tatsuya Wakahara

O-1-002　Diffusion-tensor imaging of the median nerve: Correlation with nerve conduction study
正中神経における拡散テンソルと神経伝達速度との相関性の検討
酒井　亮介（東邦大学医療センター 佐倉病院 中央放射線部）
Ryosuke Sakai, Masahiro Sogawa, Hiroyuki Nakazawa, Mitsuyuki Tozawa, Stutomu Inaoka, Hitoshi Terada, Osamu Takahashi

O-1-003　Computed diffusion-weighted 3.0-T MR imaging for pancreatic adenocarcinoma
膵管癌の描出におけるcomputed DWIの有用性
大塚　洋和（鹿児島大学病院 臨床技術部 放射線部門）
Hirokazu Otsuka, Yoshihiko Fukukura, Yuichi Kumagae, Koji Takumi, Hiroto Hakamada, Takashi Iwanaga, Takurou Fujisaki, Yasumasa Saigo, Tomoyuki Okuaki, Takashi Yoshiura

O-1-004　Diffusion Tensor Tractography of the Peripheral Nerve by Computed DWI
Computed DWIによる末梢神経のDiffusion Tensor Tractography
原田　邦明（株式会社日立製作所 ヘルスケアビジネスユニット）
Kuniaki Harada, Yasuo Kawata, Ryuji Shirase, Masahiro Takizawa, Yoshitaka Bito

O-1-005　A phantom study about high intensity rim around simple cyst on computed DWI in the liver
肝臓におけるComputed DWI：肝嚢胞周囲に発生する高輝度アーチファクトの原因についての検討
掛川　貴史（山梨大学医学部附属病院 放射線部）
Takashi Kakegawa, Utaroh Motosugi, Kazuyuki Sato, Tetsuya Wakayama, Hiroshi Kumagai, Hajime Sakamoto, Hiroshi Onishi

Day 1……　Room 2 (Sonic City Hall, 2F, Small Hall)

Brain diffusion 1　13：10～14：20

Chair：Hirohiko Kimura（University of Fukui, Department of Radiology）
座　長：木村　浩彦（福井大学 医学部 放射線医学）

O-1-006　Comparison of 16ch and 32ch multi-channel head coil in the diffusion weighted image
16chと32chコイルの撮像条件の検討
田尻　智美（済生会熊本病院 中央放射線部）
Satomi Tajiri, Takashi Okigawa, Takeshi Ohta, Takashi Sakamoto, Hiroki Arimura, Hiroyuki Hazeyama, Suguru Kawamura, Daisuke Masuda, Megumi Katayama, Yuuki Yamaguchi, Hirofumi Wada, Masahiro Kosaka, Kentarou Haraoka, Miho Kitamura, Masato Ikedo, Mitsue Miyazaki

O-1-007　Computed FLAIR-DWI Technique combined with DWI, PDW, T2W and T1W Imagings
複数コントラストのDWI画像を用いたComputed FLAIR-DWIの検討
高井　雄紀（東芝メディカルシステムズ株式会社 MR事業部 MR開発部グループ）
Yuki Takai, Tokunori Kimura, Hiroshi Kusahara, Naotaka Sakashita

O-1-008 Novel evaluation method for image distortion of magnetic resonance image
MRIにおける新しい画像歪評価法の提言
金子　瑶平（さいたま市立病院）
Yohei Kaneko, Akio Ogura, Isao Fujita, Aoi Kamakura, Tomoya Kitaoka

O-1-009 Differentiation of grade III and IV gliomas by intravoxel incoherent motion MR imaging
IVIMによるグレードIIIとIVグリオーマ鑑別
上村　清央（鹿児島大学大学院医歯学総合研究科 放射線診断治療学分野）
Kiyohisa Kamimura, Masanori Nakajo, Yoshihiko Fukukura, Takashi Iwanaga, Hirofumi Hirano, Takashi Yoshiura

O-1-010 Usefulness of the correction software for the MPG eddy current distortion of the diffusion weighted image
拡散強調画像のMPG渦電流歪みに対する補正ソフトの有用性
齋藤　孝明（飯山赤十字病院 放射線科）
Takaaki Saito, Masato Kobayashi, Akihiro Yamashiro

O-1-011 Correlation between brain DTI and proton MR Spectroscopy estimates for patients with chronic pain: a study using FSL TBSS
股関節慢性疼痛患者におけるbrain DTI and MRS estimatesの関連－FSL　TBSSを用いた比較研究
山本　　誠（地方独立行政法人 さんむ医療センター）
Makoto Yamamoto, Tomonori Shigemura, Yutaka Suzuki, Kouichi Takai, Takayuki Obata, Akio Sakamoto

O-1-012 Examination of the clinical usefulness of DKI with the 1.5T MRI system
1.5T MRI装置によるDKIの臨床有用性の検討
西村　祥循（日本医科大学武蔵小杉病院 放射線科）
Yoshiyuki Nishimura, Shigeki Ikeda, Atsunari Kurose, Tooru Takahashi

Brain diffusion 2　　１４：２０～１５：２０

Chair：Takashi Yoshiura（Department of Radiology, Graduate School of Medical and Dental Sciences）
座　長：吉浦　　敬（鹿児島大学大学院医歯学総合研究科放射線診断治療学分野）

O-1-013 Estimation of optimum imaging conditions using the Monte Calro simulation in QSI
QSIにおけるMonte Calro simulationを用いた最適撮像条件の推定
八木　一夫（首都大学東京大学院 人間健康科学研究科 放射線科学域）
Kazuo Yagi, Masakazu Sato, Junichi Hata, Yasuhiko Tachibana, Norio Sekine

O-1-014 Detection of abnormal cerebral hemodynamic change by intravoxel incoherent motion analysis in bilateral common carotid artery occlusion rat
IVIMを用いた両側総頸動脈閉塞ラットにおける脳血行動態異常の検出
藤原　俊朗（岩手医科大学 医学部 脳神経外科学講座）
Shunrou Fujiwara, Yuki Mori, Daniela Martinez de la Mora, Kuniaki Ogasawara, Yoshichika Yoshioka

O-1-015 Acute cerebral blood flow decrease after subarachnoid hemorrhage in mice with continuous arterial spin labelling
CASL法により検討したくも膜下出血モデルマウスにおける急性期脳血流量の低下
中村　和浩（秋田県立脳血管研究センター）
Kazuhiro Nakamura, Tatsushi Mutoh, Kazumasu Sasaki, Yasuyuki Taki, Toshibumi Kinoshita, Tatsuya Ishikawa

O-1-016 Generalized fractional anisotropy of diffusion spectrum imaging and reaction time to investigate neurotransmission speed
拡散スペクトラム画像法の拡散異方性指標と課題反応時間の関係
松尾香弥子（獨協医科大学 医学部 精神生物学講座）
Kayako Matsuo, Yasuo Takehara

O-1-017 Image Quality Improvement of Computed DWI
Computed DWIにおける画質改善方法の開発
河田　康雄（株式会社日立製作所 ヘルスケアビジネスユニット）
Yasuo Kawata, Ryuji Shirase, Kuniaki Harada, Hiroyuki Itagaki

O-1-018 Evaluation of white matter microstructure in the cases of tuberous sclerosis (TS) using neurite orientation dispersion and density imaging (NODDI)
Neurite orientation dispersion and density imaging (NODDI)による結節性硬化症症例の白質の変化の検討
田岡　俊昭（名古屋大学 附属病院 放射線科）
Toshiaki Taoka, Noriko Aida, Yuta Fujii, Hisashi Kawai, Toshiki Nakane, Shinji Naganawa

Day 1…… Room 3 (Sonic City Hall, 4F, International Conference Room)

Brain MRA　　9：10～10：20

Chair：Akira Matsushita（Ibaraki Prefectural University of Health Sciences, Department of Neurosurgery）
座 長：松下　　明（茨城県立医療大学付属病院脳神経外科）

O-1-019 Visualization of the lenticulostriate arteries on postcontrast MRA using Gd-BT-DO3A
高濃度1.0mol/L非イオン性MRI用造影剤Gd-BT-DO3Aによるレンズ核線条体動脈描出の有用性
一坂　秀一（東京逓信病院 放射線科）
Shuichi Ichisaka, Toshiyuki Terashima, Motoyuki Yamashita, Kazuhiro Tsuchiya

O-1-020 ASL-based Non-contrast MRDSA with 3D Data Acquisition: Initial Clinical Experience in Intracranial Major Trunk Stenoocclusive Diseases
ASLを用いた非造影のMRDSAによる頭蓋内主幹動脈閉塞・狭窄における側副血行の評価の初期経験
土屋　一洋（東京逓信病院 放射線科）
Kazuhiro Tsuchiya, Miho Gomyo, Arisa Ohara, Shichiro Katase, Isao Miyazaki, Nanae Kawano, Naotaka Sakashita

O-1-021 Demonstration of the lenticulostriate arteries by modified 3D-TOF MRA
1.5T 3D-TOF MRAによる大脳基底核穿通枝動脈の描出
山下　素幸（東京逓信病院 放射線科）
Motoyuki Yamashita, Kazuhiro Tsuchiya, Shuichi Ichisaka

O-1-022 The fusion image of 3D-TOF-MRA and T2W-SPACE in evaluation of vertebro-basilar artery dissection
3D-TOF-MRA 元画像とT2WI-SPACE像のfusion像による解離性椎骨脳底動脈瘤の評価
池田　宏明（獨協医科大学病院 放射線科）
Hiroaki Ikeda, Yos Misu, Mayuko Ajima, Kensuke Inamura, Sadaharu Hiki, Hiroaki Arakawa, Shigeko Kuwajima, Yasukazu Shioyama, Tsutomu Ishukawa, Yasushi Kaji

O-1-023 Characteristic of the vascular wall heartbeat imaging in the pulse wave synchronization combination MRA in the subarachnoid hemorrhage case
くも膜下出血症例における脈波同期併用MRA血管壁拍動イメージングの特徴
古川　研治（釧路孝仁会記念病院 診療放射線科）
Kenji Furukawa, Tsuyoshi Nikaidou, Koki Yamamoto

O-1-024 Improved 4D-TOF using subtraction image by iMSDE
iMSDEを併用したサブトラクション法による4D-TOFの改良
高野　晋（東海大学 医学附属病院 診療技術部 放射線技術科）
Susumu Takano, Tetsuo Ogino, Shuhei Shibukawa, Nao Kajihara, Tomohiko Horie, Tetsu Niwa, Isao Muro

O-1-025 Silent MRA of cerebral arteriovenous malformation and dural arteriovenous fistula
Silent MRAによる脳動静脈奇形、硬膜動静脈瘻描出能の検討
藤原　広和（慶應義塾大学 医学部 放射線診断科）
Hirokazu Fujiwara, Suketaka Momoshima, Jun Kurasawa, Masahiro Jinzaki

Brain ASL　　10：30～11：30

Chair：Tomoyuki Noguchi（National center for Global health and Medicine）
座　長：野口　智幸（国立国際医療研究センター病院 放射線診療部）

O-1-026 Effect of background suppression on arterial spin labeling CBF quantification
ASLにおけるbackground suppressionによるCBF値への影響
豊嶋　英仁（秋田県立脳血管研究センター 放射線科診療部）
Hideto Toyoshima, Masanobu Ibaraki, Kazuhiro Nakamura, Kazuhiro Takahashi, Toshibumi Kinoshita, Josef Pfeuffer, Hideto Kuribayashi

O-1-027 3D volumetric analysis of ASL high signal intensity on tumor might be useful in differentiating Glioblastoma and Brain metastasis
悪性神経膠腫と転移性脳腫瘍の鑑別のためのASL高信号の3D容積解析の有用性について
ガンボルドムングンバガナ（徳島大学 放射線科）
Ganbold Mungunbagana, Takashi Abe, Masafumi Harada, Delgerdalai Khashbat, Yuki Kanazawa

O-1-028 Parenchymal hematoma of acute ischemic stroke: Prediction with hyperemic lesion on arterial-spin labeling MRI
急性期脳梗塞におけるASLを用いたParenchymal Hematomaの予測
新甫　武也（宮崎大学 医学部 臨床神経科学講座 脳神経外科分野）
Takeya Niibo, Hajime Ohta, Ichirou Ikushima, Shirou Miyata, Kazuchika Yonenaga, Hideo Takeshima

O-1-029 Perfusion abnormalities on 3D arterial spin labeling at 3T MR in pediatric and adolescent patients with migraine
小児片頭痛患者における3D ASL（arterial spin labeling）での灌流異常について
上谷　浩之（熊本大学 画像診断治療科）
Hiroyuki Uetani, Mika Kitajima, Takeshi Sugahara, Hironori Kikuchi, Kohei Yamada, Tomoo Hirahara, Sadahiro Yamamura, Yasuyuki Yamashita

O-1-030 4D MR Angiography with pCASL Combined with CENTRA-Keyhole (4D-PACK): Visualization of Distal Cerebral Arteries in Moyamoya Disease
CENTRA-Keyholeを用いた4D-PCASL MRA:モヤモヤ病における末梢血管の描出
栂尾　理（九州大学大学院医学研究院 臨床放射線科学分野）
Osamu Togao, Akio Hiwatashi, Makoto Obara, Koji Yamashita, Kazufumi Kikuchi, Ryo Somehara, Ryotaro Kamei, Hiroshi Honda

O-1-031 Non-contrast enhanced 4D intracranial MR angiography based on pseudo-continuous arterial spin labelling (PCASL) with CENTRA-Keyhole (4D-PACK)
キーホールを用いたpseudo-contious arterial spin labeling(PCASL)頭蓋内非造影ダイナミックMRA撮像
小原　真（フィリップスエレクトロニクスジャパン）
Makoto Obara, Osamu Togao, Tomoyuki Okuaki, Shuhei Shibukawa, Masami Yoneyama, Marc Van Cauteren

Liver 1　　13：10～14：10

Chair：Tatsuya Gomi（Toho-University）
座 長：五味　達哉（東邦大学医療センター大橋病院 放射線科）

O-1-032 Feasibility of measuring the T1 relaxation times for characterization of malignant liver tumors
T1測定による肝悪性腫瘍の鑑別
岩永　崇（鹿児島大学病院 臨床技術部 放射線部門）
Takashi Iwanaga, Yoshihiko Fukukura, Yuichi Kumagae, Tomonori Saito, Masashi Sasaki, Takuro Fujisaki, Yasumasa Saigo, Hiroshi Imai, Takashi Yoshiura

O-1-033 Biliary Tract Enhancement during the Hepatobiliary Phase inEOB-MRI:Correlation with Non-invasive Biomarker Associated with Liver Function and Fibrosis
EOB造影MRI肝細胞造影相における胆道系濃染と肝機能に関する検討
梶田　公博（岐阜大学医学部附属病院 放射線部）
Kimihiro Kajita, Yoshifumi Noda, Takayuki Miura, Ryohei Yaegashi, Shogo Maeda, Hiroki Kato, Shinichi Shoda, Satoshi Goshima, Masayuki Matsuo

O-1-034 Long-term observation of hypovascular hypointense nodules (HHNs) on gadoxetic acid-enhanced MRI
EOB-MRIにおける乏血性低信号結節の長期観察研究
清水　辰哉（山梨大学 医学部 放射線科）
Tatsuya Shimizu, Utaroh Motosugi, Katsuhiro Sano, Shintaro Ichikawa, Hiroshi Onishi

O-1-035 Hypovascular hypointense nodules detected by EOB-MRI as a risk factor for multicentric recurrence of hepatocellular carcinoma after hepatectomy
乏血性肝細胞相低信号結節は肝細胞癌術後の多中心性再発の予測因子となるか？
松田　正樹（山梨大学 医学部 放射線科）
Masaki Matsuda, Shintaro Ichikawa, Utaroh Motosugi, Masanori Matsuda, Hiroshi Onishi

O-1-036 Pancreas Signal Intensity Changes among T Stages in Patients with Pancreatic Ductal Adenocarcinoma
膵癌T stageによる膵実質の信号変化に関する検討
野田　佳史（岐阜大学 放射線科）
Yoshifumi Noda, Satoshi Goshima, Hiroshi Kawada, Nobuyuki Kawai, Hiromi Koyasu, Masayuki Matsuo

O-1-037 Recognition of anterior peritoneal reflection in rectal MRI: A single centre experience among southern Chinese
Wai Keung Lo, Deyond YW Siu, PP Iu, PYY Lau, Danny HY Cho

Liver 2　　14：10～15：10

Chair：Takeyuki Watani（Department of Radiology, University of Tokyo Hospital）
座 長：渡谷　岳行（東京大学医学部附属病院 放射線科）

O-1-038 Bayesian prediction for insufficient liver enhancement in gadoxetic acid-enhanced hepatobiliary phase imaging
ベイズ理論を用いた肝実質へのガドキセト酸取り込み低下症例の予測
森　優喜（山梨大学 医学部 放射線医学講座）
Yuki Mori, Utaroh Motosugi, Tatsuya Shimizu, Shintaro Ichikawa, Hiroshi Onishi

O-1-039 Transient respiratory motion during gadoxetic acid-enhanced arterial phase imaging: a study using accelerated 3D gradient echo sequence
EOB造影MRI動脈相における呼吸性アーチファクト：Turbo LAVA FLEXを用いた検討
佐藤　兼是（山梨大学 医学部附属病院 放射線部）
Kazuyuki Sato, Utaroh Motosugi, Tatsuya Shimizu, Shintaro Ichikawa, Takashi Kakegawa, Hiroshi Kumagai, Hajime Sakamoto, Hiroshi Onishi

O-1-040 Dynamic contrast enhanced MR imaging of the heptopancreatobiliary regions in combined use of parallel imaging and compressed sensing
圧縮センシング及びパラレルイメージングを併用した造影ダイナミック検査：肝胆膵領域の評価
増井　孝之（聖隷浜松病院 放射線科）
Takayuki Masui, Motoyuki Katayama, Kei Tsukamoto, Mitsuteru Tsuchiya, Yuki Baba, Yuji Iwadate, Kennichi Mizuki, Naoyuki Takei, Harumi Sakahara, Kang Wang, Koji Yoneyama

O-1-041 Study of LAVA method using compressed sensing in the abdominal area on a 3T wide bore system
腹部領域における圧縮センシングを用いたLAVA法の検討
小出　若葉（聖隷浜松病院 放射線部）
Wakaba Koide, Koji Yoneyama, Yuki Takayanagi, Takayuki Masui, Yuji Iwadate, Kang Wang

O-1-042 Study of 3DLAVA using CS in the upper abdominal region
上腹部領域における圧縮センシングを用いた3DLAVAの検討
高柳　有希（総合病院 聖隷浜松病院 放射線部）
Yuki Takayanagi, Koji Yoneyama, Wakaba Koide, Takayuki Masui, Yuji Iwadate, Naoyuki Takei, Kang Wang

O-1-043 T1ρ and T2 values, and T1ρ/T2 ratio for the assessment of liver function
T1&rho値、T2値、T1&rho/T2比を用いた肝機能評価
高山　幸久（九州大学大学院医学研究院 放射線医療情報・ネットワーク講座）
Yukihisa Takayama, Akihiro Nishie, Yoshiki Asayama, Kousei Ishigami, Yasuhiro Ushijima, Daisuke Okamoto, Nobuhiro Fujita, Tomoyuki Okuaki, Hiroshi Honda

Hardware　15：20～16：30

Chair：Suguru Yokosawa（Hitachi, Ltd. Research & Development Group）
座 長：横沢　俊（株式会社日立製作所 研究開発グループ）

O-1-044 Design of oval gradient coils using current potential and singular value decomposition
特異値分解法を用いた楕円筒型勾配磁場コイルの設計
松澤　晃樹（筑波大学 数理物質科学研究科 電子・物理工学専攻）
Koki Matsuzawa, Mitsushi Abe, Katsumi Kose, Yasuhiko Terada

O-1-045 Development of the MRI software platform (II)
MRI software platformの開発（2）
巨瀬　勝美（筑波大学 数理物質系 物理工学域）
Katsumi Kose, Ryoichi Kose, Tomoyuki Haishi

O-1-046 Development of a multi-circular shimming system for a 1.5 T/280 mm horizontal bore superconducting magnet
1.5T/280mm水平ボア超伝導磁石のためのマルチサーキュラーシムシステムの開発
山田　諒太（筑波大学 数理物質科学研究科）
Ryota Yamada, Katsumi Kose, Yasuhiko Terada

O-1-047 Basic study of 3T Transmit / Receive Knee Coil for High Resolution Imaging
高分解能画像を意図した3T膝用送受信コイルの基礎的検討
太田　美幸（東芝メディカルシステムズ株式会社）
Miyuki Ota, Keiji Tahira, Noah Deetz, Xiaoyu Yang, Hiroyuki Fujita

O-1-048 Effects of dual-frequency parallel transmit pulse design on a water-fat phantom image at 7 T
7T MRI水脂肪ファントム画像における二重周波数パラレルトランスミットパルス設計の効果検討
岩舘　雄治（GEヘルスケア・ジャパン 研究開発部）
Yuji Iwadate, Tsuyoshi Matsuda, Tsuyoshi Metoki, Kohsuke Kudo, Makoto Sasaki, Hiroyuki Kabasawa

O-1-049 RF shimming mitigating left-right difference in hip joint imaging using 4-channel transmit coil
股関節撮像における左右差を考慮した4チャンネルRF shimmingの開発
小高　晃弘（株式会社日立製作所 ヘルスケアビジネスユニット）
Akihiro Odaka, Kosuke Ito, Chikako Moriwake, Masahiro Takizawa

O-1-050 Effect of load size and load position on coupling between the elements of an array coil
Effect of load position on array elements coupling
Shubham Gupta（理化学研究所 脳科学総合研究センター 認知機能表現研究チーム）
Shubham Gupta, Allen Waggnar, Keiji Tanaka, Kang Cheng

Pulse sequence 1　16：40～17：40

Chair：Koichi Oshio（Department of Diagnostic Radiology, Keio University School of Medicine）
座 長：押尾　晃一（慶應義塾大学医学部 放射線診断科）

O-1-051 Peak Correction Algorithm in Radial Sampling for Abdominal Imaging
腹部撮像向けラディアルサンプリング法におけるピーク補正アルゴリズム
西尾　慧祐（株式会社日立製作所 ヘルスケアビジネスユニット）
Keisuke Nishio, Yasuhiro Kamada, Kuniharu Oka, Masahiro Takizawa

O-1-052 Quiet Gradient Pulse Shape Composed of Plural Lobes
複数パルスからなる傾斜磁場パルスの低騒音化
黒川　眞次（株式会社日立製作所 ヘルスケアビジネスユニット）
Shinji Kurokawa, Yo Taniguchi, Yukari Yamamoto, Hisaaki Ochi, Takashi Tsuneki, Hiroyuki Itagaki, Yoshitaka Bito

O-1-053 Evaluation of spatially-selective excitation pulse for improving the inhomogeneous MRI signal intensity due to conducting samples
導電性を有する試料のMRI撮像時に生じるRF電磁波の不均一を改善する空間選択的な励起パルスの評価
禹　　泰城（東京大学 大学院工学系研究科）
Taeseong Woo, Dongmin Kim, Takao Someya, Masaki Sekino

O-1-054 Improved 2D Look Locker method: assessment of T1 value measurement accuracy
2D Look Locker法によるT1値測定精度の検討
中川　貞裕（旭川医科大学病院 診療技術部 放射線技術部門）
Sadahiro Nakagawa, Toshiharu Moriya, Masakazu Uno, Takafumi Nakata, Kunihiro Iwata

O-1-055 SWIFT microimaging for brain tissues from an aceruloplasminemia patient
SWIFTマイクロイメージング
三森　文行（国立環境研究所）
Fumiyuki Mitsumori, Naoharu Kobayashi, Garwood Michael, Hiroaki Miyajima

O-1-056 Magnetic resonance image reconstruction for non-Cartesian sampling schemes using nonlinear differential equation
非線形微分方程式を用いた非デカルト・サンプリングのための磁気共鳴画像再構成
山口　雄作（四国こどもとおとなの医療センター 放射線科）
Yusaku Yamaguchi, Takeshi Kojima, Tetsuya Yoshinaga

Day 1…… Room 4 (Sonic City Building, 4F, 401～402)

Head and neck 1　　9：10～10：10

Chair：Keiko Toyoda（Teikyo University School of Medicine, Department of Radiology）
座 長：豊田　圭子（帝京大学医学部放射線科学講座）

O-1-057 Temporal bone fusion image by using MRI and CT; Assessment of the misregistration arise from cerebellopontine angle
小脳橋角部MRIとCTによるFusion画像作成における位置ずれの検討
小北　修平（大阪警察病院 医療技術部 放射線技術科）
Shuhei Ogita, Satoru Tominaga, Yasuo Fujisawa, Toru Shinohe, Atsushi Tanaka

O-1-058 The visualization of facial nerve canals: A comparative study between PETRA sequence and other 3D sequences
顔面神経管の描出: PETRAと他の3D撮像法との比較
奥知　左智（京都大学大学院医学研究科 画像診断学・核医学）
Sachi Okuchi, Yasutaka Fushimi, Tomohisa Okada, Akira Yamamoto, Tsutomu Okada, Takuya Hinoda, Kaori Togashi

O-1-059 Comparison between 64-channel and 20-channel head and neck coil: Preliminary Study
64 channel、20 channel 頭頸部コイルの比較の初期経験
伏見　育崇（京都大学大学院医学研究科 放射線医学講座（画像診断学・核医学））
Yasutaka Fushimi, Tomohisa Okada, Akira Yamamoto, Tsutomu Okada, Akihiko Sakata, Sachi Okuchi, Gosuke Okubo, Moritaka Yamauchi, Takuya Hinoda, Takayuki Yamamoto, Hikaru Fukutomi, Yusuke Yokota, Kaori Togashi

O-1-060 Evaluation of cervical carotid plaque volume using 3D T1-VISTA: Comparison of manual measurement and automatic measurement by the in-house software
3D T1-VISTA法を用いた頸部頸動脈プラーク容積評価：マニュアル計測と自動計測ソフトの比較
磯嶋　志保（三重大学 医学部附属病院 中央放射線部）
Shiho Isoshima, Katsuhiro Inoue, Ryohei Nakayama, Shinichi Takase, Tsunehiro Yamahata, Masayuki Maeda

O-1-061 Necrotic cervical nodes: Usefulness of diffusion-weighted MR imaging in the differentiation of suppurative lymphadenitis from malignancy
拡散強調画像を用いた壊死を伴う頸部化膿性リンパ節炎と悪性リンパ節の鑑別
三浦　賢征（岐阜大学医学部附属病院 放射線部）
Takayuki Miura, Kimihiro Kajita, Ryohei Yaegashi, Syogo Maeda, Hiroki Kato, Shinichi Shoda, Hiroki Kato, Satoshi Goshima, Masayuki Matsuo

O-1-062 Asymmetry of the labyrinthine signal on Delayed FLAIR: a comparison of unilateral incidental vestibular schwannoma and endolymphatic hydrops cases
Delayed FLAIRでの迷路信号の左右非対称：片側偶発前庭神経鞘腫例と片側内リンパ水腫例の比較
長縄　慎二（名古屋大学大学院 医学系研究科 量子医学）
Shinji Naganawa, Toshiki Nakane, Hisashi Kawai, Toshiaki Taoka, Michihiko Sone

Head and neck 2　　10：10～11：10

Chair：Naoko Saito（Saitama Medical University International Medical Center, Department of Diagnostic Radiology）
座 長：齋藤　尚子（埼玉医科大学国際医療センター 画像診断科）

O-1-063 Usefulness of radial volumetric interpolated breath-hold examination (radial VIBE) for pharyngolaryngeal lesion: comparison with conventional VIBE
咽喉頭領域のMRI撮像におけるradial VIBEの有用性の検討：通常のVIBEとの比較
内匠　浩二（鹿児島大学 医学部 放射線科）
Koji Takumi, Yoshihiko Fukukura, Hiroto Hakamada, Yuichi Kumagae, Takashi Yoshiura

O-1-064 Visualization of nigrosome 1 using multi echo imaging technique in consideration of T_2 star relaxation
T_2スター緩和を考慮したマルチエコー法によるnigrosome 1の描出能の検討
荒井　信行（名古屋市立大学病院 中央放射線部）
Nobuyuki Arai, Hirohito Kan, Harumasa Kasai, Hiroshi Kunitomo, Masahiro Takizawa, Kazuyoshi Omori, Yasujiro Hirose

O-1-065 Artery selective 3D TOF with asymmetrically RF shimmed Pre-Saturation pulse with 4-channel RF transmit at 3T
非対称RF shimを用いたプリサチュレーションパルスによる頸動脈選択3D TOFの開発
伊藤　公輔（株式会社日立製作所ヘルスケアビジネスユニット）
Kosuke Ito, Atsushi Kuratani, Takashi Nishihara, Yukio Kaneko, Masahiro Takizawa

O-1-066 Motion insensitive neck MRA using radial TOF
ラディアルスキャンTOF法を用いた頚部MRA
笠井　治昌（名古屋市立大学病院 中央放射線部）
Harumasa Kasai, Hiroto Kan, Nobuyuki Arai, Masahiro Takizawa, Yoshimasa Matsuda, Kazuyoshi Omori, Yasujiro Hirose

O-1-067 Measurement of blood flow of normal parotid glands using pseudo-continuous arterial spin labeling
Arterial Spin Labeling（ASL）法を用いた健常者耳下腺血流量の計測
井上　勝博（三重大学 医学部附属病院 中央放射線部）
Katsuhiro Inoue, Shiho Isoshima, Shinichi Takase, Tsunehiro Yamahata, Maki Umino, Makoto Obara, Masayuki Maeda

O-1-068 Comparative examination of the Separate acquisition method and Alternate acquisition method in non-contrast MRDSA using Time-SLIP
Time-SLIPを使用した非造影MRDSAにおける交互収集法と分割収集法の比較検討
小泉　達也（順天堂大学 医学部附属 浦安病院 放射線科）
Tatsuya Koizumi, Takashi Iwasaki, Shinsuke Kyogoku, Takao Kimizuka, Daisuke Tsuge, Nao Kikuchi, Saori Shiota, Takeshi Udagawa, Nanae Kawano

Phantom　　13：10～14：10

Chair：Katsutoshi Murata（Siemens Healthcare K.K.）
座　長：村田　勝俊（シーメンスヘルスケア株式会社）

O-1-069 Changes in material properties due to phase transition temperature movement and water content by PNIPAAm-based gel that takes into account QSI-Pantom
QSI－Pantomを考慮したPNIPAAm系ゲルの複合合成による相転移温度移動と含水量による材料特性の変化
八木　一夫（首都大学東京 大学院 人間健康科学研究科 放射線学域）
Kazuo Yagi, Atsuya Ikeda, Naoyuki Kurimoto, Masashi Ueda, Madoka Nanao, Seiichi Sugimoto, Tadashi Inaba

O-1-070 Development of a phantom simulating cell density for diffusion-weighted magnetic resonance imaging
拡散強調画像における細胞密度模擬ファントムの作成
三賀山諒司（九州大学大学院 医学系学府 保健学専攻）
Ryoji Mikayama, Hidetake Yabuuchi, Ryoji Matsumoto, Koji Kobayashi, Yasuo Yamashita, Mitsuhiro Kimura, Satoshi Kawanami, Hiroshi Honda

O-1-071 Comparisons of DTI measures among five different MRI scanners using anisotropic diffusion phantom
異方性拡散ファントムによるMRI装置間のDTI測値の比較
酒井　晃二（京都府立医科大学）
Koji Sakai, Toshiaki Nakagawa, Ryusuke Nakai, Hiroyasu Ikeno, Toru Osawa, Shun Higotani, Seiji Yamaguchi, Hiroaki Takadama, Kei Yamada

O-1-072 Reproducibility of our standardization phantom for evaluation of fractional anisotropy (FA) derived from diffusion tensor imaging (DTI)
拡散テンソルイメージング自作標準化ファントムにおけるFractional Anisotropy (FA) の再現性評価
木村　光宏（九州大学大学院 医学系学府 保健学専攻）
Mitsuhiro Kimura, Hidetake Yabuuchi, Ryoji Matsumoto, Koji Kobayashi, Yasuo Yamashita, Ryoji Mikayama, Satoshi Kawanami, Hiroshi Honda

O-1-073 Analysis of the fluid flow image of phantom push-pull pump by 2 dimensional steady state free precession time spatial spin labeling inversion pulse
2D SSFP Time-SLIP法を用いた擬似拍動ファントムによる流体動画像の解析
酒井　貴寛（駒澤大学大学院 医療健康科学研究科）
Takahiro Sakai, Kohki Yoshikawa, Shinya Yamada

O-1-074 Metal Artifact reduction with MAVRIC-SL: in vitro assessment with implant phantom
MAVRIC-SLによる金属アーチファクト低減効果の検討
内藤　　舞（慶應義塾大学病院 放射線技術室）
Mai Naito, Sari Motomatsu, Yoshinobu Nunokawa, Yasutomi Shimada, Takashi Asakura, Souta Oguro, Hirokazu Fujiwara, Shigeo Okuda, Masahiro Jinzaki, Atsushi Nozaki

Magnetic field　　14：20～15：00

Chair：Koji Uchida（Eda Clinic Orthopedic Rehabilitation PICTORU Izumo Imaging Room）
座　長：内田　幸司（えだクリニック整形外科リハビリテーション科 PICTORUいずも画像診断室）

O-1-075 Quantitative evaluation of the magnetic field distortion mapping
磁場歪みマッピングの定量的評価
金田　貴彦（北海道大学大学院 保健科学院 保健科学専攻）
Takahiko Kaneda, Toru Yamamoto

O-1-076 Metal artifact reduction by SEMAC in 3T
3.0T における金属アーチファクト低減効果（SEMAC）の基礎的検討
近藤　敦之（埼玉医科大学病院）
Atsushi Kondo, Shinichi Watanabe, Maiko Isono, Hiroshi Imai, Taishi Unezawa, Tomio Yamasaki, Iichiro Osawa, Kaiji Inoue, Eito Kozawa, Mamoru Niitsu

O-1-077 MRI-based radiotherapy planning using foamed polyethylene therapeutic immobilization base plate for head and neck
発泡ポリエチレン製頭頚部放射線治療用固定具がMR画像に与える影響
宮本　昌宜（神戸大学医学部附属病院 医療技術部 放射線部門）
Masanori Miyamoto, Yuuichirou Somiya, Katsusuke Kyotani, Yuuichi Aoyama, Satoru Takahashi, Hideaki Kawamitsu

O-1-078 Sensitivity Correction Algorithm for 32-Channel Head Coil at 3T
3T向け32チャンネル頭部コイルに対応する感度補正アルゴリズム
鎌田　康弘（株式会社日立製作所 ヘルスケアビジネスユニット）
Yasuhiro Kamada, Miki Tachibana, Kuniaki Harada, Takeshi Taniguchi, Kazuyuki Kato, Masahiro Takizawa, Hiroyuki Itagaki

Elastography 1　　15：10～15：50

Chair：Tomokazu Numano（Tokyo Metropolitan University）
座　長：沼野　智一（首都大学東京大学院 人間健康科学研究科 放射線科学域）

O-1-079 Assessment of MR Elastography System using 0.3 T Open MRI
0.3Tオープン型MRIによるMRエラストグラフィシステムの評価
吉田　洋樹（千葉大学 大学院 工学研究科）
Hiroki Yoshida, Mikio Suga, Masashi Sekine

O-1-080 Influences of partial volume effect in MR elastography
MR Elastographyにおけるパーシャルボリューム効果の影響
伊東　大輝（首都大学東京大学院 人間健康科学研究科 放射線科学域）
Daiki Ito, Tomokazu Numano, Kazuyuki Mizuhara, Masaki Misawa, Takaaki Onishi, Toshikatsu Washio, Naotaka Nitta

O-1-081 Comparison between Zero-Interpolation Filling(ZIP) and Compressed Sensing(CS)
Zero-Interpolation Filling(ZIP)とCompressed Sensing(CS)の比較
藤田　各務（東京電機大学 工学研究科）
Kagami Fujita, Kazuyuki Mizuhara, Toshikatsu Washio

O-1-082 Development of a Highly Viscous Tissue-Mimicking Phantom for Magnetic Resonance Elastography That Has Low Glycerin Content
低グリセリン濃度で高粘性なMRエラストグラフィ用生体模擬ファントムの開発
石井　孝樹（千葉大学 工学部 メディカルシステム工学科）
Kouki Ishii, Mikio Suga, Riwa Kishimoto, Takayuki Obata

Elastography 2　　15：50～16：40

Chair：Kengo Yoshimitsu（Department of Radiology, Faculty of Medicine, Fukuoka University）
座　長：吉満　研吾（福岡大学医学部放射線医学教室）

O-1-083 Propagate shear waves to the PM efficiently in MR Elastography
大腰筋MREにおいて効率的に大腰筋にせん断波を加える方法
大西　孝明（首都大学東京大学院 人間健康科学研究科 放射線科学域）
Takaaki Onishi, Tomokazu Numano, Daiki Ito, Kazuyuki Mizuhara, Kouichi Takamoto, Hisao Nishijyo, Naotaka Nitta

O-1-084 Optimization of imaging planes for MR elastography of the supraspinatus muscle
棘上筋MR Elastographyにおける撮像位置の最適化
伊東　大輝（首都大学東京大学院 人間健康科学研究科 放射線科学域）
Daiki Ito, Tomokazu Numano, Takaaki Onishi, Kazuyuki Mizuhara, Koichi Takamoto, Hisao Nishijyo, Masaki Misawa

O-1-085 Simultaneous MR elastography and Fat/Water Imaging acquisitions
MR elastographyと 脂肪/水 画像の同時収集
沼野　智一（首都大学東京大学院 人間健康科学研究科 放射線科学域）
Tomokazu Numano, Daiki Ito, Takaaki Onishi, Kazuyuki Mizuhara, Koichi Takamoto, Hisao Nishijyo, Masaki Misawa, Naotaka Nitta

O-1-086 Magnetic resonance elastography for uterine fibroids
子宮筋腫に対するMRエラストグラフィ
大宮　慶惠（山梨大学 医学部 放射線科）
Yoshie Omiya, Shintaro Ichikawa, Utaroh Motosugi, Tetsuya Wakayama, Takashi Kakegawa, Hiroshi Kumagai, Hiroshi Onishi

O-1-087 Vlidity and Reliability of Magnetic Resonance Elastography for Staging Hepatic Fibrosis in Patients with Alcoholic Hepatitis
アルコール性肝障害の線維化ステージングにおけるMRエラストグラフィの有用性
佐々木　優（山梨大学 医学部 放射線科）
Yu Sasaki, Shintaro Ichikawa, Utaroh Motosugi, Tetsuya Wakayama, Takashi Kakegawa, Hiroshi Kumagai, Hiroshi Onishi

Day 1…… Room 5 (Sonic City Building, 4F, 403～404)

Safety　　9：10～10：10

Chair：Atsushi Senoo（Tokyo Metropolitan University Department of Radiologic Science）
座 長：妹尾　淳史（首都大学東京 放射線学科）

O-1-088 Part.1 Examination of the effect of RF shielding, using an electromagnetic wave shield material offered commercially in MRI
第1法　MRIにおける市販電磁波遮蔽材を用いたRF遮蔽効果の検討
谷口　正成（一般財団法人 住友病院 放射線技術科）
Masanari Taniguchi, Toshihiko Nishida, Hidekazu Niikawa, Daichi Shimokawa, Tatsuya Kuwagaki, Kota Uematsu, Akira Tamada, Hideki Matsui

O-1-089 Part.2 Application experiment of electromagnetic wave protective clothing for capsule endoscopy in MRI head area scans
第2報　頭部領域におけるカプセル内視鏡用電磁波防護服の応用
谷口　正成（一般財団法人 住友病院 放射線技術科）
Masanari Taniguchi, Toshihiko Nishida, Hidekazu Niikawa, Daichi Shimokawa, Tatsuya Kuwagaki, Kota Uematsu, Akira Tamada, Hideki Matsui

O-1-090 The Safety of MR Conditional Cochlear Implant at the 1.5 Tesla Magnetic Resonance Imaging System
1.5T MRI装置における条件付きMRI対応人工内耳の安全性
高橋　大輔（北福島医療センター 放射線技術科）
Daisuke Takahashi, Akio Ogura, Norio Hayashi, Shinya Seino, Ryosuke Kawai, Tsuyoshi Matsuda, Tsukasa Doi, Toshio Tsuchihashi

O-1-091 Torque abnormality of the Ti alloy material in a static magnetic field: magnetic susceptibility anisotropy effect
Ti合金材料の静磁場中でのトルク異常性：磁化率異方性効果
川平　慎悟（北海道大学大学院 保健科学院）
Shingo Kawahira, Minghui Tang, Takahiko Kaneda, Toru Yamamoto

O-1-092 Analysis of RF burning by electromagnetic simulation
RF熱傷事故例の電磁界シミュレーション解析
菊地　　侑（北海道大学 大学院 保健科学院）
Yu Kikuchi, Takuya Haruyama, Minghui Tang, Toru Yamamoto

O-1-093 Web-based searchable magnetic resonance imaging safety information system for medical implant compatibility in Japan
日本における体内留置インプラントのMRI検査の適合性検索システムの開発
藤原　康博（熊本大学 大学院 生命科学研究部）
Yasuhiro Fujiwara, Hitoshi Fujioka, Tomoko Watanabe, Maiko Sekiguchi, Ryuji Murakami

Image processing　　10：20～11：30

Chair：Yoshitaka Masutani（Hiroshima City University Graduate School of Information Sciences）
座 長：増谷　佳孝（広島市立大学大学院 情報科学研究科）

O-1-094 PSF and MTF measurement with MR magnitude images using single thin-plate phantom method
絶対値画像と単板ファントムを用いたPSFおよびMTF計測
吉田　　礼（栗原市立栗原中央病院）
Rei Yoshida, Takeo Hikichi, Yoshio Machida

O-1-095 Signal-to-noise ratio measurement using the identical region of interest method by trend correction
トレンド補正を用いた同一関心領域法によるSignal to Noise Ratio測定の検討
石川　和希（独立行政法人 国立病院機構 四国こどもとおとなの医療センター 放射線科）
Kazuki Ishikawa

O-1-096 Evaluation of Brain atrophy after radiotherapy using Voxel Based Morphometry (VSRAD advance2); Fundamental Assessment
VSRAD advence2 を用いた頭部放射線治療後萎縮計測のための基礎的検討
伊藤　猛（長岡赤十字病院 放射線治療科）
Takeshi Ito, Tadatoshi Iihama, Naoki Kawamoto

O-1-097 Evaluation of Temporal Filter for LV Myocardial Strain Analysis in Wall Motion Tracking
Wall Motion Tracking(WMT)を用いた左室心筋ストレイン解析におけるTemporal filterの検討
佐野雄一郎（東芝メディカルシステムズ株式会社 MRI営業部）
Yuichiro Sano, Tatsuya Ohkubo, Yuichi Yamashita, Shuhei Takemoto, Seiya Kai

O-1-098 Workflow Improvement Using the Automatic Tracking Method for MRCA
MRCAにおける冠動脈芯線の自動追跡法を用いたワークフロー軽減の検討
竹本　周平（東芝メディカルシステムズ株式会社 営業本部 MRI営業部）
Shuhei Takemoto, Tatsuya Ohkubo, Yuichi Yamashita, Seiya Kai, Yoichirou Sano, Yoshimori Kassai, Nobuyasu Ichinose, Shuhei Bannae, Takuma Igarashi

O-1-099 Evaluation of Ventricular Torsion by Feature Tracking Cine MRI
Feature Tracking Cine MRIによる心室の捻れ運動の評価
河窪　正照（帝京大学 福岡医療技術学部）
Masateru Kawakubo, Yuzo Yamasaki, Junji Morishita, Michinobu Nagao

O-1-100 Automated planning of 2D MRA in bolus tracking
ボーラストラッキングにおける2次元MRA画像の自動位置決めの検討
後藤　隆男（GEヘルスケアジャパン株式会社）
Takao Goto, Mirai Araki

Abdomen　　13：10～14：10

Chair：Hiroyuki Irie（Department of Radiology, Saga University）
座 長：入江　裕之（佐賀大学 放射線科）

O-1-101 A pilot study of dixon vibe with Controlled aliasing in parallel imaging results in higher acceleration (CAIPIRINHA)
CAIPIRINHAを用いたdixon vibeの基礎的検討
香川　福宏（医療法人 高松画像診断クリニック）
Fukuhiro Kagawa, Tomoko Takaichi, Hiroaki Yasuda, Yoshihito Matsumoto, Kei Yokomine, Junpei Yamaguchi, Hiroki Ogura

O-1-102 Comparing the results of intravoxel incoherent motion diffusion-weighted imaging calculated by different estimation methods
IVIM-DWIの計算法の比較：肝細胞癌の悪性度診断
市川新太郎（山梨大学 医学部 放射線科）
Shintaro Ichikawa, Utaroh Motosugi, Hernando Diego, Hiroyuki Morisaka, Hiroshi Onishi

O-1-103 Computed Diffusion-Weighted Image for Abdominal MRI
腹部MRIにおけるComputed DWIの有用性
吉川　武（神戸大学大学院 医学研究科 先端生体医用画像研究センター）
Takeshi Yoshikawa, Yoshiharu Ohno, Katsusuke Kyotani, Yoshimori Kassai, Koya Nishiyama, Yuji Kishida, Kazuro Sugimura

O-1-104 Abdominal Fast Advanced Spin Echo Diffusion-Weighted Imaging
腹部FASE-DWI
吉川　武（神戸大学大学院 医学研究科 先端生体医用画像研究センター）
Takeshi Yoshikawa, Katsusuke Kyotani, Yoshiharu Ohno, Yoshimori Kassai, Koya Nishiyama, Shinichiro Seki, Yuji Kishida, Kazuro Sugimura

O-1-105 Noninvasive assessment of liver fibrosis by using phase information
位相情報を用いた肝線維症の非侵襲的評価
三尾　素平（福岡大学筑紫病院 放射線部）
Motohira Mio, Tetsuya Yoneda, Kazuki Tani, Tatsuo Toyofuku, Toshihiro Maeda, Masatoshi Matsushima, Syoichi Morimoto

O-1-106 Initial experience of MR Enterography using DISCO technique
Crohn病のMR Enterographyに於けるDISCO法を用いた自由呼吸下Gd造影撮像の検討
鈴木　達也（慶應義塾大学 医学部 放射線診断科）
Tatsuya Suzuki, Shigeo Okuda, Shunsuke Matsumoto, Hirokazu Fujiwara, Akihiro Tanimoto, Masahiro Jinzaki, Yoshinobu Nunokawa, Sari Motomatsu, Rikiya Fujishiro, Yasutomi Shimada, Atsushi Nozaki

Applied science　14：20～15：10

Chair：Kohki Yoshikawa（Komazawa University Faculty of Health Sciences）
座　長：吉川　宏起（駒澤大学 医療健康科学部）

O-1-107 Can dermal tissue be enhancing with Gadolinium-chelate contrast material?
ガドリニウム造影剤により皮膚は造影されるのか？
山本　憲（京都大学大学院 医学研究科 放射線医学講座（画像診断学・核医学））
Akira Yamamoto, Yasutaka Fushimi, Tsutomu Okada, Tomohisa Okada, Kaori Togashi

O-1-108 Visualizing the Structure of the Hippocampus
海馬構造の描出について
宮武　祐士（おさか脳神経外科病院 放射線部）
Yuji Miyatake, Sunao Nakata, Yasuaki Kamada, Yuko Takahashi, Naomi Honjo

O-1-109 Local Magnetic Field Inhomogeneity Correction Pad; Utlity for Improvement of B0 Inhomogeneity on MR System as Compared with $MnCl_2$ concentration
人体における局所磁場不均一補正用パットの最適な塩化マンガン濃度について
京谷　勉輔（神戸大学医学部附属病院 医療技術部 放射線部門）
Katsusuke Kyotani, Hideaki Kawamitsu, Kazuya Sato, Satoru Takahashi, Kazuro Sugimura

O-1-110 Comparison between two consecutive acquisition methods (DCE-MRDSA-DSC vs. MRDSA-DSC) using a 1.0-M Gd-based contrast agent
1.0M Gd造影剤を用いたDCE-MRDSA-DSC 3連続撮像とMRDSA-DSC 2連続撮像の比較検討
五明　美穂（杏林大学 医学部 放射線医学教室）
Miho Gomyo, Kazuhiro Tsuchiya, Arisa Ohara, Shichirou Katase, Masanaka Watanabe, Toshiaki Nitatori

O-1-111 Heart rate measurement by T_{1w}-MRI and infrared photoplethysmography of *Mytilus galloprovincialis*
実験動物としての海洋生物III：MRI法と赤外プレチスモグラフィー法による心拍測定
瀬尾　芳輝（獨協医大 医学部 生理学（生体制御））
Yoshiteru Seo, Toshiyuki Sazi, Morio Togawa, Osamu Nagata, Mika Yokoi-Hayakawa, Yoshie Imaizumi-Ohashi, Masataka Murakami

Day 2……Room 1 (Sonic City Hall, 1F, Large Hall)

fMRI　　13：10～14：00

Chair：Akira Matsumura（Department of Neurosurgery, University of Tsukuba）
座 長：松村　　明（筑波大学医学医療系 脳神経外科）

O-2-001 Detecting sequential activation in sub-second resolution during semantic memory test using simultaneous EEG-fMRI measurement
EEG-fMRI同時計測による意味記憶課題中のサブセカンドレベルでの連続的な脳活動の検出
水野　健吾（名古屋大学大学院 医学系研究科 医療技術学専攻 医用量子科学分野）
Kengo Mizuno, Epifanio Bagarinao, Satoshi Maesawa, Saea Tohira, Hirohisa Watanabe, Toshiharu Nakai, Haruo Isoda

O-2-002 Transiently altered brain connectivity after cataract surgery -resting fMRI study-
白内障術後の一過性脳接続性変化　－安静時fMRIによる検討－
吉田　正樹（東急病院眼科）
Masaki Yoshida, Masahiro Ida, Yuri Masaoka, Nobuyoshi Koiwa, Akira Yoshikawa, Keiko Watanabe

O-2-003 Recovery of motor network in acute stroke: Transcranial magnetic stimulation motor evoked potential and resting state functional MRI
急性期脳卒中における運動機能ネットワークの回復：経頭蓋磁気刺激と安静時機能的MRI所見の関係
松下　　明（茨城県立医療大学付属病院脳神経外科）
Akira Matsushita, Hada Hada, Kousaku Saotome, Tomohiko Masumoto, Aiki Marushima, Kei Nakai, Yoshiyuki Sankai, Masashi Yamazaki, Akira Matsumura

O-2-004 A New fMRI analysis method to visualize the difference of the brain activation timing
脳賦活タイミングの違いを描出するための新しいfMRI解析法
丸山　純人（国際医療福祉大学 保健医療学部 放射線・情報科学科）
Sumito Maruyama

O-2-005 Serial Autocorrelations and Multiband fMRI
Allen Waggoner（理化学研究所 脳科学総合研究センター）
Allen Waggoner, Topi Tanskanen, Keiji Tanaka, Kang Cheng

QSM　　14：00～14：50

Chair：Kohsuke Kudo（Hokkaido University Hospital Department of Diagnostic and Interventional Radiology）
座 長：工藤　與亮（北海道大学病院 放射線科）

O-2-006 Improved Visualization of Cerebral Blood Vessels by Using Wider Band Dipole Inversion in Quantitative Susceptibility Mapping
広帯域双極子場を用いた定量的磁化率マッピングによる脳血管の視認性の向上
梅本　勇哉（京都大学 大学院医学研究科 人間健康科学系専攻）
Yuya Umemoto, Tomohiro Ueno, Shin-ichi Urayama, Toshihiko Aso, Hidenao Fukuyama, Naozo Sugimoto

O-2-007 Quantitative Susceptibility Mapping with Reduced Inhomogeneity and Improved Accuracy of Fat Susceptibility for Prostate Imaging
前立腺定量的磁化率マッピングにおけるムラ低減および脂肪内精度改善手法
佐藤　良太（株式会社日立製作所 研究開発グループ）
Ryota Sato, Toru Shirai, Yo Taniguchi, Takenori Murase, Atsushi Kuratani, Taisei Ueda, Takashi Tsuneki, Yoshitaka Bito, Hisaaki Ochi, Yoshihisa Soutome

O-2-008 Quantitative Susceptibility Mapping using Adaptive Edge-preserving Filtering: Comparison with COSMOS in Multi-echo data of Human Brain
適応的エッジ保存フィルタを用いた定量的磁化率マッピング法：ヒト複数エコー画像によるCOSMOSとの比較
白猪　亨（株式会社 日立製作所 研究開発グループ）
Toru Shirai, Ryota Sato, Yo Taniguchi, Takenori Murase, Atsushi Kuratani, Taisei Ueda, Takashi Tsuneki, Yoshitaka Bito, Yoshihisa Soutome, Hisaaki Ochi

O-2-009 Quantitative Susceptibility Mapping Reconstruction Using Ill-Conditioned Points Weighted Dipole Inversion
Ill-Conditioned Point Weighted Dipole Inversionを利用したQuantitaive susceptibility mapping再構成法
菅　博人（名古屋市立大学病院 中央放射線部）
Hirohito Kan, Nobuyuki Arai, Harumasa Kasai, Masahiro Takizawa, Yoshimasa Matsuda, Kazuyoshi Omori, Yasujiro Hirose

O-2-010 Clinical application of QSM and neuromelanin imaging of the dorsolateral substantia nigra in the diagnosis of Parkinson's disease
パーキンソン病診断における定量的磁化率マッピングと神経メラニンを用いた背外側黒質領域評価の有用性
高橋　洋人（Osaka University Graduate School of Medicine）
Hiroto Takahashi, Yoshiyuki Watanabe, Hisashi Tanaka, Masahito Mihara, Hideki Mochizuki, Tian Liu, Yi Wang, Noriyuki Tomiyama

Brain infant　15：00～16：00

Chair：Noriko Aida（Kanagawa Children's Medical Center, Radiology）
座 長：相田　典子（神奈川県立こども医療センター放射線科）

O-2-011 Susceptibility changes from neonate to childhood on quantitative susceptibility mapping
定量的磁化率マッピングを用いた小児期の磁化率変化の検討
日野田卓也（京都大学 大学院医学研究科 放射線医学講座（画像診断学・核医学））
Takuya Hinoda, Yasutaka Fushimi, Tomohisa Okada, Akira Yamamoto, Tsutomu Okada, Kaori Togashi

O-2-012 Relationship between contrast enhancement of basal ganglia perivascular space and endolymphatic hydrops
基底核血管周囲腔造影効果と内リンパ水腫の関係
大橋　俊夫（総合上飯田第一病院 放射線科）
Toshio Ohashi, Toshio Katagiri, Kayao Kuno, Shinji Naganawa

O-2-013 A small number of abnormal functional connections in the brain predicts adult autism spectrum disorder
安静時脳機能磁気共鳴画像を用いた機械学習による自閉スペクトラム症の神経基盤研究
八幡　憲明（放射線医学総合研究所）
Noriaki Yahata, Giuseppe Lisi, Ryuichiro Hashimoto, Jun Morimoto, Kazuhisa Shibata, Yuki Kawakubo, Hitoshi Kuwabara, Miho Kuroda, Takashi Yamada, Megumi Fukuda, Hiroshi Imamizu, Hidehiko Takahashi, Yasumasa Okamoto, Kiyoto Kasai, Nobumasa Kato, Yuka Sasaki, Takeo Watanabe, Mitsuo Kawato

O-2-014 Pituitary Gland and Postsphenoid Ossification in Fetal Specimens
胎児標本MRIにおける下垂体、後蝶形骨化中心の画像所見
伏見　育崇（京都大学大学院医学研究科 放射線医学講座（画像診断学・核医学））
Yasutaka Fushimi, Tomohisa Okada, Mitsunori Kanagaki, Akira Yamamoto, Tsutomu Okada, Kaori Togashi

O-2-015 Influence on Sound effect and Image quality with Quiet DWI
Quiet DWIによる静音効果と画質への影響
市場　義人（シーメンスヘルスケア株式会社 カスタマーサービス事業本部 アプリケーション部）
Yoshito Ichiba, Takasi Ueda, Terumasa Takemaru, Tsubasa Kaji, Kanae Yamamoto

O-2-016 The Quiet Fast Advanced Spin Echo DWI Sequence with Optimized Variable Refocusing Flip Angle
FASE法DWIを用いた静音化シーケンスの開発とVariable Refocusing Flip Angleパターンの最適化
近藤　大貴（東芝メディカルシステムズ株式会社 MRI事業部）
Hiroki Kondo, Nobuyasu Ichinose, Masaaki Umeda, Yoshimori Kassai, Kota Watanabe, Ayumi Katsunuma, Keiichiro Ishi

Brain tumor　16：00～16：50

Chair：Akira Uchino（Saitama Medical University International Medical Center, Department of Diagnostic Radiology）
座 長：内野　晃（埼玉医科大学 国際医療センター 画像診断科）

O-2-017 Evaluation of peritumoral signal change: Initial experience with neurite orientation dispersion and density imaging (NODDI)
脳腫瘍周囲の異常信号について：NODDIの初期経験
門田　善仁（宮崎大学 医学部 放射線診断学講座）
Yoshihito Kadota, Minako Azuma, Takanori Yano, Masahiro Enzaki, Toshiya Azuma, Toshinori Hirai, Masaaki Hori, Shigeki Aoki

O-2-018 The usefulness of T2*WI for the detection of cavernous angioma in long-term survivors of childhood embryonal tumors treated by cranial irradiation
小児期胎児性腫瘍に対する放射線治療後の海綿状血管腫検出におけるT2*強調画像の有用性
山崎　文之（広島大学病院 脳神経外科）
Fumiyuki Yamasaki, Takeshi Takayasu, Ryo Nosaka, Yuji Akiyama, Taiichi Saito, Fusao Ikawa, Kazuhiko Sugiyama, Kaoru Kurisu

O-2-019 Differentiation of glioblastoma and primary central nervous system lymphoma by using MR image-based speeded up robust features
造影MRIのSURF特徴量を用いた膠芽腫と原発性中枢神経悪性リンパ腫の鑑別：診断困難例への応用可能性
國松　聡（東京大学大学院 医学系研究科 放射線医学講座）
Akira Kunimatsu, Kouhei Kamiya, Yuichi Suzuki, Yasushi Watanabe, Natsuko Kunimatsu, Kaoru Sumida, Akifumi Hagiwara, Harushi Mori

O-2-020 MR imaging for the prediction of TERT promoter mutations in patients with wild-type IDH1 Glioblastoma
MRIを用いた膠芽腫患者におけるTERT遺伝子変異の予測
山下　孝二（九州大学 臨床放射線科学分野）
Koji Yamashita, Akio Hiwatashi, Osamu Togao, Kazufumi Kikuchi, Ryo Somehara, Ryotaro Kamei, Ryusuke Hatae, Hiroshi Honda

O-2-021 NSsaFe: Observational study on the incidence of Nephrogenic Systemic Fibrosis in patients with renal impairment following gadoterate meglumine administration
Bodo Kress, Andreas Gottschalk

Day 2…… Room 3 (Sonic City Hall, 4F, International Conference Room)

Brain degeneration 1　9：10～10：10

Chair：Hajime Kitagaki（Shimane University Faculty of Medicine Department of Radiology）
座 長：北垣　一（島根大学医学部）

O-2-022 A case of seronegative neuromyelitis optica
Seronegative neuromyelitis opticaの一例
森本　伶美（社会医療法人 仁生会 細木病院）
Remi Morimoto, Shino Kousaki, Kazuo Kitaoka, Tadashi Horimi, Masahiko Ikeuti, Naoto Oosawa, Hirokazu Furutani

O-2-023 Hippocampal susceptibility changes in Parkinson disease and Parkinson disease with dementia/Lewy body dementia: QSM assessment
パーキンソン病および認知症を伴うパーキンソン病/レビー小体型認知症における海馬の磁化率変化: QSMの検討
宮田　真里（産業医科大学 放射線科）
Mari Miyata, Shingo Kakeda, Jyunji Moriya, Hidekuni Narimatsu, Toru Sato, Hiroaki Adachi, Yi Wang, Yukunori Korogi

O-2-024 Differentiation of Progressive Supranuclear Palsy from Parkinson Disease by Quantitative Susceptibility Mapping
進行性核上性麻痺の診断における定量的磁化率マップの有用性
東　美菜子（宮崎大学 医学部 放射線科）
Minako Azuma, Mika Kitajima, Kazumichi Yamada, Satoshi Yamashita, Mamoru Hashimoto, Manabu Ikeda, Yasuhiko Iryo, Yoshihito Kadota, Takanori Yano, Yasuyuki Yamashita, Toshinori Hirai

O-2-025 Quantitative assessment of intracranial aneurysm wall enhancement using magnetic resonance imaging
瘤壁造影効果の定量評価: 破裂-未破裂脳動脈瘤の比較
面高　俊介（白河厚生総合病院 脳神経外科）
Shunsuke Omodaka, Hidenori Endo, Kuniyasu Niizuma, Miki Fujimura, Takashi Inoue, Teiji Tominaga

O-2-026 Usefulness of CE 3D SPGR and TRICKS in the estimation of occluded dural sinus for transvenous embolization of dural arteriovenous fistulas
硬膜動静脈瘻経静脈的塞栓術前における造影 3D SPGRと3D time-resolved MRAの有用性
森川　　実（長崎大学病院 放射線科）
Minoru Morikawa, Hideki Ishimaru, Reiko Ideguchi, Nobutaka Horie, Takayuki Matsuo, Masataka Uetani

O-2-027 Serial change of brain temperature measured using magnetic resonance spectroscopy in patients with ischemic stroke
脳梗塞急性期症例におけるMRSによる脳温経時的評価
石田　朋久（さいたま赤十字病院 脳外科）
Tomohisa Ishida, Takashi Inoue, Hidenori Endo, Ryo Itabashi, Nobuo Noshita, Toshie Takahashi, Kuniyasu Niizuma, Miki Fujimura, Teiji Tominaga

Brain degeneration 2　　10：10～11：00

Chair：Masayuki Maeda（Mie University School of Medicine Department of Advanced Diagnostic Imaging）
座　長：前田　正幸（三重大学 先進画像診断学講座）

O-2-028 Quantitative susceptibility mapping (QSM) evaluation of Infantile neuroaxonal dystrophy: a case report
定量的磁化率マッピング（QSM）を用いた乳児軸索ジストロフィの評価
藤原　拓也（大阪大学大学院 医学系研究科 放射線統合医学講座 放射線医学教室）
Takuya Fujiwara, Yoshiyuki Watanabe, Hisashi Tanaka, Hiroto Takahashi, Atsuko Arisawa, Shin Nabatame, Yi Wang, Noriyuki Tomiyama

O-2-029 Neurite Orientation Dispersion and Density Imaging (NODDI) of Nigrostriatal Pathway in Parkinson Disease
パーキンソン病の黒質線条体神経線維の神経突起イメージングによる評価
中澤　美咲（首都大学東京人間健康科学研究科放射線科学域）
Misaki Nakazawa, Christina Andica, Koji Kamagata, Ryo Ueda, Sho Murata, Taku Hatano, Ayami Okuzumi, Osamu Abe, Michimasa Suzuki, Masaaki Hori, Kanako Kumamaru, Nobutaka Hattori, Shigeki Aoki

O-2-030 Application of Neurite Orientation Dispersion and Density Imaging for Normal-appearing White Matter in Neuromyelitis Optica
NODDIを用いた視神経脊髄炎におけるNormal-appearing White Matterの検討
高村　朋宏（山梨大学医学部放射線科）
Takamura Tomohiro, Shou Murata, Koji Kamagata, Masaaki Hori, Michimasa Suzuki, Shigeki Aoki

O-2-031 Neuromelanin-sensitive MR imaging of Machado-Joseph disease
Machado-Joseph 病の神経メラニンイメージング
越智　　誠（長崎北病院 放射線科）
Makoto Ochi, Yoko Nakao, Akira Satoh, Makiko Seto, Mitsuhiro Tsujihata

O-2-032 A multi-parametric quantitative MRI model that assesses myelin and edema for evaluating white-matter damage in patients with multiple sclerosis
髄鞘と浮腫の状態を評価するマルチパラメトリック定量MRIによる多発性硬化症患者における白質障害の評価
萩原　彰文（東京大学大学院 医学系研究科 放射線医学講座）
Akifumi Hagiwara, Masaaki Hori, Misaki Nakazawa, Christina Andica, Mariko Yoshida, Michimasa Suzuki, Nao Takano, Hideo Kawasaki, Nozomi Hamasaki, Shuji Sato, Shigeki Aoki

Brain Sequence　　11：00～11：40

Chair：Shinji Naganawa（Department of Radiology, Nagoya University Graduate School of Medicine）
座　長：長縄　慎二（名古屋大学 放射線科）

O-2-033 Improvement of time resolution with EPI sequence using Simultaneous Multi-Slice (SMS)
Simultaneous Multi-Slice (SMS) を使用したEPIシーケンスの時間分解能向上
竹丸　輝政（シーメンスヘルスケア株式会社 カスタマーサービス事業本部 アプリケーション部）
Terumasa Takemaru, Takashi Ueda, Yoshito Ichiba, Tsubasa Kaji, Kanae Yamamoto

O-2-034 Brain morphometric analysis using artificial intelligence: Development of Alzheimer's disease score
人工知能を用いた脳形状画像解析: Alzheimer's disease scoreの開発
椎野　顯彦（滋賀医科大学 神経難病センター）
Akihiko Shiino, Yutaro Iwamoto, Chen Yen-Wei

O-2-035 Evaluation of Cerebral and Cervical MR Scan Designs for DBS Patients within SAR Limits
DBS患者に対するSARを考慮した頭部および頸髄MR撮像プロトコルの検討
鈴木　智明（名古屋セントラル病院 中央放射線室）
Tomoaki Suzuki, Tomoki Nishihata, Teruhisa Ohno, Tsutomu Minoura, Takumi Kuwahara, Shigenori Takebayashi

O-2-036 Effect of three-dimensional fast spin-echo method imaging parameters using variable refocusing flip angle on T1-weighted image contrast
Variable refocusing flip angleを用いた3D FSE法の撮像パラメータがT1強調画像コントラストに与える影響
塚本　一真（独立行政法人国立病院機構 四国こどもとおとなの医療センター 放射線科）
Kazuma Tsukamoto, Fukuhiro Kagawa, Yusaku Yamaguchi

Heart 1　　13：10～14：20

Chair：Tetsuya Matsuda（Kyoto University Graduate School of Informatics）
座　長：松田　哲也（京都大学 情報学研究科）

O-2-037 Improvement of B1 inhomogeneity in the arterial visualization of FBI using ultrasound gel
FBI法における超音波検査用ゼリーを用いたB1不均一の改善および画質改善の試み
的場　博輝（社会医療法人 共愛会 戸畑共立病院）
Hiroki Matoba, Akiyoshi Yamamoto, Yuuya Kuroki, Daiji Uchiyama, Seigo Yoshida, Katsumi Nakamura, Mitsue Miyazaki

O-2-038 Impacts of the pulmonary, systemic and single right ventricular trabeculations on volume assessed by threshold-based segmentation MR algorithm
閾値ベース磁気共鳴セグメンテーション・アルゴリズムによる肉柱構造が肺、体及び単右心室容量に及ぼす影響
稲毛　章郎（榊原記念病院小児循環器科）
Akio Inage, Naokazu Mizuno, Jun Matsuda

O-2-039 Can sufficient pretreatment information of peripheral artery disease be obtained by Non-contrast MR Angiography Fresh Blood Imaging ?
PAD患者のFBIと血管造影の比較
沖川　隆志（済生会熊本病院 中央放射線部）
Takashi Okigawa, Akira Sasao, Takeshi Ohta, Satomi Tajiri, Miho Kitamura, Masahiro Kosaka, Mitsue Miyazaki, Hiroyuki Hazeyama, Suguru Kawamura, Daisuke Masuda, Megumi Katayama, Hirofumi Wada

O-2-040 Early Experience With 3-T WH MRCA Using an Automatic Motion Probe Setting Function: Comparison Against Conventional Balanced SSFP 1.5-T WH MRCA
Motion Probe自動設定機能を用いた3T冠動脈MRA初期経験 -1.5T従来法との比較-
石村理英子（杏林大学医学部放射線医学教室）
Rieko Ishimura, Toshiya Kariyasu, Kenichi Yokoyama, Toshiaki Nitatori, Tatsuya Yoshioka, Isao Miyazaki, Shigehide Kuhara, Nobuyasu Ichinose, Shuhei Bannae

O-2-041 Coronary flow velocity reserve on left main trunk using 3T-MRI can predict coronary artery disease as ^{15}O-labeled Water PET
3T　MRI計測による冠血流速度予備能の冠動脈病変診断能評価
菊池　穏香（北海道大学病院 放射線診断科）
Yasuka Kikuchi, Noriko Oyama-Manabe, Fumi Kato, Rie Mimura, Keita Sakamoto, Satoshi Yabusaki, Kohsuke Kudo, Hiroki Shirato

O-2-042 Clinical usefulness of FBI using with variable refocusing flip angle at 3T MRI - comparison with conventional FBI in peripheral arteries -
3T MRIにおける可変再収束フリップアングル法を用いたFBI法の臨床的有用性-従来法によるFBI法との比較-
山本　晃義（社会医療法人 共愛会 戸畑共立病院）
Akiyoshi Yamamoto, Hiroki Matoba, Yuuya Kuroki, Daiji Uchiyama, Seigo Yoshida, Katsumi Nakamura, Mitsue Miyazaki, Keiichirou Ishi

O-2-043 Usability Evaluation of Cardiac MRI Assist applications
心臓MRI検査の撮像アシスト機能のユーザビリティ評価
篠田　健輔（東芝メディカルシステムズ株式会社 MRI事業部）
Kensuke Shinoda, Shuhei Takemoto, Shuhei Nitta

Heart 2　　14：20～15：10

Chair：Michinobu Nagao（Tokyo Women's Medical University, Diagnostic Imaging and Nuclear medicine）

座 長：長尾　充展（東京女子医科大学 画像診断・核医学講座）

O-2-044　Basic Study on the Accuracy of T1 Values Obtained Using the Polarity Corrected TI Prep Method in Both 1.5-T and 3-T MRI Systems

Polarity Corrected TI prep法を用いた1.5Tと3TでのT1値測定精度の基礎的検討

安達　卓哉（杏林大学医学部付属病院 放射線部）

Takuya Adachi, Isao Miyazaki, Toshiaki Nitatori, Kenichi Yokoyama, Shigehide Kuhara, shuhei Bannae, Yoshimori Kassai

O-2-045　Creating Myocardial T1-map on the MRI Scanner without the Use of a Dedicated Protocol

専用プロトコルを用いないコンソール上での心筋T1マップ作成

畠山　憲重（長野中央病院）

Norishige Hatakeyama, Kazuki Sakata, Yuuya Ishizawa, Megumi Sakurai, Kouta Ishizaka, Hiroshi Imai

O-2-046　Myocardial T1 values of healthy volunteers measured with SMART1Mapping on 1.5T and 3T scanners

SMART1Mapping法を用いた心筋T1値計測：1.5Tおよび3T装置における正常値の検討

松本　俊亮（慶應義塾大学医学部放射線診断科）

Shunsuke Matsumoto, Shigeo Okuda, Tatsuya Suzuki, Hirokazu Fujiwara, Akihiro Tanimoto, Masahiro Jinzaki, Yoshinobu Nunokawa, Sari Motomatsu, Rikiya Fujishiro, Yasutomi Shimada, Atsushi Nozaki

O-2-047　Evaluation of T1 Value Measurement for ECV Mapping Using the Polarity Corrected Variable TI Prep Tool

Polarity Corrected Variable TI Prep Toolを用いたECV算出を目的としたT1値測定精度の検討

高済　英彰（福島県立医科大学附属病院 放射線部）

Hideaki Takasumi, Shinya Seino, Hironobu Ishikawa, Takashi Kanezawa, Naoki Watanabe, Takanori Sato, Shuhei Bannae

O-2-048　Evaluation of the influence of heart rate on T1 value determined from MOLLI method in Phantom

MOLLI法を使用したT1値測定における心拍数変化の影響の検討

持木　瑞規（群馬県立心臓血管センター 放射線課）

Mizunori Mochiki, Satoshi Tomioka, Toshihiko Ino, Hatsuo Kigure

Day 2…… Room 4 (Sonic City Building, 4F, 401～402)

Lungs　　9：10～10：10

Chair：Shuji Sakai（Tokyo Women's Medical University）

座 長：坂井　修二（東京女子医科大学）

O-2-049　The usefulness of the BLADE application in breath-hold lung MRI

肺野MRIにおける呼吸停止下T2W-BLADE法の有用性

山下　達也（明成会 塩川医院）

Tatsuya Yamashita

O-2-050 Comparison between 1.5T and 3T of UTE in the optical evaluation of the pulmonary vascular
肺血管におけるUltrashort TE(UTE)の1.5Tと3Tの比較
太田　雄（済生会熊本病院 中央放射線部）
Takeshi Ohta, Takashi Okigawa, Satomi Tajiri, Hiroyuki Hazeyama, Suguru Kawamura, Daisuke Masuda, Megumi Katayama, Hirofumi Wada, Masahiro Kosaka, Kenntaro Haraoka, Miho Kitamura, Mitsue Miyazaki, Masato Ikedo

O-2-051 Comparison of the Capability for Therapeutic Outcome Prediction among Dynamic CE-Perfusion MRI and ADCT and PET/CT in NSCLC Patients
Dynamic CE-MRIおよびADCTとPET/CTにおける非小細胞肺癌患者における保存的治療効果予測能の比較
大野　良治（神戸大学大学院医学研究科内科系講座放射線医学分野 機能・画像診断学部門）
Yoshiharu Ohno, Yuji Kishida, Shinichiro Seki, Takeshi Yoshikawa, Yoshiko Ueno, Yasuko Fujisawa, Masao Yui, Shigeharu Ohyu, Kouya Nishiyama, Katsusuke Kyotani, Kazuro Sugimura

O-2-052 Dynamic Perfusion MRI at 3T System: Appropriate Contrast Media Injection Protocol for Perfusion Measurement as Compared with Dynamic Perfusion ADCT
3T 造影Perfusion MRIにおける至適造影法の検討：造影Perfusion ADCTとの比較
大野　良治（神戸大学大学院医学研究科 内科系講座 放射線医学分野 機能・画像診断学部門）
Yoshiharu Ohno, Yuji Kishida, Shinichiro Seki, Takeshi Yoshikawa, Shigeharu Ohyu, Masao Yui, Yoshimori Kassai, Kazuro Sugimura

O-2-053 CEST Imaging: Comparison of the Capability for Differentiation of Malignant from Benign Pulmonary Lesions with DWI and FDG-PET/CT
CEST Imagingにおける良・悪性肺病変鑑別能診断能のDWIおよびPET/CTとの対比
大野　良治（神戸大学大学院医学研究科内科系講座放射線医学分野 機能・画像診断学部門）
Yoshiharu Ohno, Yuji Kishida, Shinichiro Seki, Masao Yui, Takeshi Yoshikawa, Yoshiko Ueno, Kouya Nishiyama, Katsusuke Kyotani, Mitsue Miyazaki, Kazuro Sugimura

O-2-054 Comparison of the Capability for the IASLC/ ITMIG Thymic Epithelial Tumor Staging among PET/MRI, Whole-Body MRI, PET/CT and Conventional Examination
PET/MRI，全身MRI，PET/CTおよび通常画像検査における胸腺上皮性腫瘍の病気診断能の比較
大野　良治（神戸大学大学院医学研究科内科系講座放射線医学分野 機能・画像診断学部門）
Yoshiharu Ohno, Yuji Kishida, Shinnichiro Seki, Takeshi Yoshikawa, Yoshiko Ueno, Kota Aoyagi, Masao Yui, Yoshimori Kassai, Hitoshi Yamagata, Koya Nishiyama, Katsusuke Kyotani, Kazuro Sugimura

Breast　　10：30～11：20

Chair：Shuichi Monzawa（Shinko Hospital）
座 長：門澤　秀一（神鋼記念病院）

O-2-055 Comparison of method that image quality improvement. In Computed DWI of Abdominal region using 3T-MR scanner
3T-MR装置を用いた腹部のComputed DWIにおける画質改善法の比較
白勢　竜二（株式会社 日立製作所 ヘルスケアビジネスユニット）
Ryuji Shirase, Yasuo Kawata, Kuniaki Harada, Masahiro Takizawa, Hiroyuki Itagaki, Yoshitaka Bito

O-2-056 Optimal b-value in computed diffusion-weighted imaging for detecting breast cancer
乳癌に於けるcomputed DWIの最適なb値の検討
田島　祐（東京医科大学病院 放射線科）
Yu Tajima, Kazuhiro Saito, Taiyo Harada, Natsuhiko Shirota, Yoichi Araki, Noriko Kobayashi, Nobutaka Yoshimura, Koichi Tokuuye

O-2-057 Shrinking phenomenon of ductal carcinoma in situ on cDWI; Is it depend on pathological grade?
cDWIにおいて信号が消失してしまう非浸潤性乳管癌とその悪性度の関係について
那須　克宏（筑波大学大学院 人間総合医学研究科 疾患制御医学専攻 応用放射線医学分野）
Katsuhiro Nasu, Hiroaki Takahashi, Manabu Minami

O-2-058 Diagnostic Performance of Maximum Slope in High Resolution Ultrafast Dynamic Contrast Enhanced Breast MRI using KWIC
超高速撮像法(KWIC撮像法)を用いた造影超早期のMSによる診断能の評価
大橋　茜（京都大学 医学部付属病院 放射線診断科）
Akane Ohashi, Masako Kataoka, Shotaro Kanao, Mami Iima, Natsuko Onishi, Makiko Kawai, Rena Sakaguchi, Ayami Oono, Masakazu Toi, Weiland Elizabeth, Kaori Togashi

O-2-059 the investigation of IVIM and non-Gaussian diffusion MRI in the lactating and non-lactating breasts
授乳期・非授乳期乳腺におけるIVIM・非ガウス拡散MRIの検討
飯間　麻美（京都大学 大学院 医学研究科 放射線医学講座）
Mami Iima, Masako Kataoka, Shotaro Kanao, Makiko Kawai, Natsuko Onishi, Akane Ohashi, Rena Sakaguchi, Ayami Oono, Kaori Togashi

Molecular imaging 1　　13：10～14：20

Chair：Takayuki Obata（National Instititute of Radiological Scinences）
座 長：小畠　隆行（量研機構 放射線医学総合研究所）

O-2-060 Material design of sugar -PEG-modified liposome encapsulating the nano magnetic material
ナノ磁性体を内包した糖PEG修飾リポソームの材料設計
八木　一夫（首都大学東京 大学院人間健康科学研究科）
Kazuo Yagi, Daichi Mizutani, Yoshihiro Yazu, Hiroyuki Kawabata, Seiichi Sugimoto, Masataka Kubo, Tadashi Inaba

O-2-061 Evaluation of the sugar coating type material due to the formation of ferrite nanoparticles by liquid phase synthesis and colloidal material method
液相合成法によるフェライト磁性ナノ粒子の生成とコロイドマテリアル法による糖被膜型磁性体の磁気特性評価
八木　一夫（首都大東京 大学院人間健康科学研究科）
Kazuo Yagi, Daichi Mizutani, Hiroyuki Kawabata, Takanori Tanaka, Yoshihiro Yazu, Yujiro Harada, Seiichi Sugimoto, Masataka Kubo, Tadashi Inaba

O-2-062 Absolute quantitation of glutamate and γ-aminobutyric acid on highly resolved 2D constant time ^{1}H spectra using 2D FT with shared time domain data
高分解2D ^{1}H定時間MRSの開発～ 時間領域データの共有再構成法を用いたグルタミン酸、GABAの絶対定量化 ～
渡邉　英宏（国立環境研究所 環境計測研究センター 画像・スペクトル計測研究室）
Hidehiro Watanabe, Nobuhiro Takaya

O-2-063 Development of nitroxide-based theranostic probes for septic mouse brain
マウス脳内REDOXイメージング用theranosticプローブの開発
藤井　博匡（札幌医科大学 医療人育成センター）
Hirotada Fujii, Miho Emoto, Shingo Sato

O-2-064 Quantitative measurement of susceptibility/R2* values of SPIO-labeled bone marrow stromal cells in gel phantom
ゲルファントムにおけるSPIO標識骨髄間質細胞の磁化率・R2*定量解析
原田太以佑（北海道大学病院 放射線診断科）
Taisuke Harada, Kohsuke Kudo, Toru Shirai, Yoshitaka Bito, Hideo Shichinohe, Chengbo Tan, Ziefeng Wang, Kiyohiro Houkin, Hiroki Shirato

O-2-065 ^{13}C MRS reveals changes in muscle glycogen content during rapid weight loss and recovery
^{13}C MRSを用いた急速減量と回復による筋グリコーゲン動態の描出
高橋　英幸（国立スポーツ科学センター）
Hideyuki Takahashi, Emi Kondo, Keisuke Shiose, Takuya Osawa, Keiko Motonaga, Shiori Ouchi, Akiko Kamei, Kohei Nakajima, Katsuya Maruyama

O-2-066 Examination of the glutathione measurement in the human brain
ヒト脳内におけるグルタチオン測定の検討
村瀬　智一（明治国際医療大学 医療情報学ユニット）
Tomokazu Murase, Masahiro Umeda, Yuko Kawai, Ayako Mandai, Toshihiro Higuchi

Molecular imaging 2　14：20～15：00

Chair：Yusuke Inoue（Kitasato University School of Medicine, Department of Diagnostic Radiology）
座　長：井上　優介（北里大学医学部 画像診断学）

O-2-067 Correlation between quantitative values depending on CEST effect and indices of MT and NOE for APT-CEST imaging
APT-CEST imagingのCEST効果の定量値とMT及びNOE指標との関連
原田　雅史（徳島大学大学院 放射線医学分野）
Masafumi Harada, Sonoka Hisaoka, Maki Ohtomo, Mitsuhiro Kinoshita, Saho Irahara, Mitsuharu Miyoshi, Yuki Kanazawa

O-2-068 Dependence of the duration and power of saturation pulse on chemical exchange saturation transfer in pH sensitive amide proton transfer imaging
pH強調APTイメージングにおける飽和パルスの持続時間と強度の影響
徳永　千晶（九州大学病院 医療技術部 放射線部門）
Chiaki Tokunaga, Tatsuhiro Wada, Osamu Togao, Yasuo Yamashita, Kouji Kobayashi

O-2-069 Multiple pools model fitting map with CEST Peak Extraction Spectrum in brain tumor patients
脳腫瘍患者でのCEST Peak Extraction Spectrumを用いたMultiple pools model fitting map
三好　光晴（GEヘルスケア・ジャパン研究開発部）
Mitsuharu Miyoshi, Masafumi Harada, Yuki Kanazawa, Hiroyuki Kabasawa

O-2-070 Effect of the readout RF pulse on amide proton transfer imaging contrast in brain tumor: comparison between single-shot and multi-shot turbo spin echo
Readout RFパルスが脳腫瘍のamide proton transferイメージングに及ぼす影響
和田　達弘（九州大学病院 医療技術部 放射線部門）
Tatsuhiro Wada, Osamu Togao, Chiaki Tokunaga, Yasuo Yamashita, Kouji Kobayashi

High speed imaging　15：10～16：10

Chair：Hiroyuki Kabasawa（GE Healthcare Japan Global MR Applications and Workflow）
座　長：椛沢　宏之（GEヘルスケア・ジャパン株式会社 技術本部 MR研究室）

O-2-071 Magnetic Resonance Compressed Sensing using Higher-density Sampling in Restricted Signal Space
部分空間高密度サンプリングを使用したMR圧縮センシング
松本　知之（宇都宮大学 大学院工学研究科 情報システム科学専攻）
Tomoyuki Matsumoto, Mone Shibuya, Satoshi Ito

O-2-072 Compressed Sensing Image Reconstruction using Non-randomly Sampled Signa
信号の非ランダムサンプリングを利用した圧縮センシング画像再構成
伊藤　聡志（宇都宮大学 大学院工学研究科 情報システム科学専攻）
Satoshi Ito, Kazuki Sekine

O-2-073 Simultaneous multi slice turbo spin echo imaging of the knee joint for examination time reduction
SMSTSE法による膝関節MRI検査の撮像時間短縮
采澤　大志（埼玉医科大学病院 中央放射線部）
Taishi Unezawa, Takahiro Watanabe, Atushi Kondou, Takashi Ogino, Shinichi Watanabe, Tomio Yamasaki, Masashi Suzuki, Hiroshi Imai, Mayuko Haraikawa, Iichiro Osawa, Kaiji Inoue, Eito Kozawa, Mamoru Niitsu

O-2-074 Selection of Mixed Acceleration Factors in Combined Parallel imaging and Compressed Sensing in 3D Time of Flight
3DTOF パラレルイメージと圧縮センシング併用におけるアクセラレーションファクター選択の検討
竹井　直行（GE ヘルスケア・ジャパン 研究開発部 MR研究室）
Naoyuki Takei, Masayuki Kanamoto, Tatsuya Yamamoto, Hirohiko Kimura, Hiroyuki Kabasawa

O-2-075 Evaluating Vessel Depictability in Total Variation Compressed Sensing MR Angiography Using Numerical Phantom
数値ファントムを用いたTotal Variationによる圧縮センシングMRアンギオグラフィにおける血管描出能の検討
三浦　洋亮（東北大学 大学院 医学系研究科）
Yousuke Miura, Toshiki Saito, Yoshio Machida

O-2-076 NMR microscopy accelerated by MR Fingerprinting
MR指紋法によるNMRマイクロスコピーの高速化
寺田　康彦（筑波大学 数理物質系 物理工学域）
Yasuhiko Terada

Pulse sequence 2　16：10～17：10

Chair：Kazuyuki Ohgi（Japanese Red Cross Medical Center）
座 長：扇　　和之（日本赤十字社医療センター 放射線診断科）

O-2-077 Effect of scanner noise reduction at Quiet sequence
Quiet sequenceによる騒音軽減効果
中井　浩大（名古屋大学医学部付属病院 医療技術部 放射線部門）
Kodai Nakai, Shinji Naganawa, Toshiaki Taoka, Hisashi Kawai, Kazusige Ichikawa, Yasuo Sakurai, Minako Kawamura, Katsuhiro Sakakibara, Yutaka Katou, Yasuo Andou, Kiminori Bokura, Isami Konishi

O-2-078 Phase unwrapping method considering phase variance between dynamic phases for dynamic fat-water separation imaging
時間軸方向のフェーズアンラップを用いた水脂肪分離法によるダイナミック撮像の基礎検討
中井　則正（株式会社日立製作所 ヘルスケアビジネスユニット）
Norimasa Nakai, Hiroyuki Itagaki, Masahiro Takizawa

O-2-079 Improving T2 weighted imaging of the Abdomen: Using fast BLADE Sequences
Fast BLADEシーケンスの腹部T2WIへの応用
植田　隆史（シーメンスヘルスケア株式会社 カスタマーサービス事業本部 アプリケーション部）
Takashi Ueda, Terumasa Takemaru, Yoshito Ichiba, Tsubasa Kaji, Kanae Yamamoto

O-2-080 How Flexible Can TEs Be in Two-Point Dixon with Out-Of-Phase and In-Phase Model?
2ポイントDixon水脂肪分離法におけるTE柔軟性の検討
岩舘　雄治（GEヘルスケア・ジャパン 研究開発部）
Yuji Iwadate, Kang Wang, Aya Shiobara, Yasuo Adachi, Akira Yamada, Yoshihiro Kito, Yasunari Fujinaga, Atsushi Nozaki, Masumi Kadoya, Horoyuki Kabasawa

O-2-081 Variation among scanners in signal intensity of in/out-of-phase images using dual echo sequences
Dual echo法を用いたin/out-of-phase画像信号強度の機種依存性について
茂木　俊一（城西クリニック 放射線科）
Shunichi Motegi, Yasuo Takatsu, Kouichi Ujita, Norio Hayashi, Mitsuomi Matsumoto, Yoshito Tsushima

O-2-082 Basic study of fat fraction measurement by difference of slice thickness using 6point-Dixon method
6point-Dixon法を用いたスライス厚の違いによる脂肪含有率測定の基礎的検討
神岡　尚吾（広島大学病院 診療支援部 画像診断部門）
Shogo Kamioka, Yuji Akiyama, Takayuki Tamura, Kazushi Yokomachi, Yuuji Takahashi, Yoshiko Iwakado, ryuji Akita, Kazuo Awai

Day 2…… Room 5 (Sonic City Building, 4F, 403～404)

Flow　　9：10～10：30

Chair：Hiroyoshi Isoda（Preemptive Medicine and Lifestyle-related Disease Research Center Kyoto University Hospital）
座　長：磯田　裕義（京都大学医学部付属病院 先制医療・生活習慣病研究センター）

O-2-083 Study on two-dimensional spatial selective pulse for non-enhanced MRA slice selective spin labeling
非造影MRA向けスライス選択スピンラベリング用2次元局所励起パルスの検討
瀬川　陽子（株式会社 東芝 研究開発センター）
Yoko Segawa, Koji Akita, Masao Yui, Kazuya Okamoto

O-2-084 Analysis of Directions of Cardiac- and Respiratory-driven Cerebrospinal Fluid Motions using Asynchronous Phase Contrast Technique
非同期位相コントラスト法に基づく心拍動性及び呼吸性脳脊髄液運動の方向の解析
春原紗依子（東海大学 工学研究科 電気電子工学専攻）
Saeko Sunohara, Satoshi Yatsushiro, Toru Yamada, Ken Takizawa, Mitsunori Matsumae, Nao Kajiwara, Kagayaki Kuroda

O-2-085 Effect of Difference between Phase Contrast and Time-SLIP Techniques in View of Observation
位相コントラスト法とTime-SLIP法の観測方法の違いの影響
八ツ代　諭（東海大学大学院 総合理工学研究科 総合理工学専攻）
Satoshi Yatsushiro, Saeko Sunohara, Toru Yamada, ken Takizawa, Mitsunori Matsumae, Nao Kajiwara, Kagayaki Kuroda

O-2-086 Abnormal Hemodynamics and Wall Shear Stress within the Saccular Aneurysm in Contrast to Fusiform Aneurysm in the Abdominal Aorta
腹部大動脈瘤における嚢状瘤と紡錘状瘤の壁剪断応力および異常血行動態の解析
杉山　将隆（浜松医科大学 放射線科）
Masataka Sugiyama, Yasuo Takehara, Naoki Ooishi, Marcus Alley, Tetsuya Wakayama, Hatsuko Nasu, Mika Kamiya, Shuhei Yamashita, Yohei Ito, Harumi Sakahara

O-2-087 Serial blood flow measurements of the brain arteries before and after carotid artery stenting
頸動脈ステント前後のfast-cine位相画像による脳動脈血流量測定
田中　　壽（大阪大学 医学部 放射線科）
Hisashi Tanaka, Hajime Nakamura, Yoshiyuki Watanabe, Hiroto Takahashi, Atsuko Arisawa, Takuya Fujiwara, Noriyuki Tomiyama

O-2-088 The effects of the gadolinium-based contrast agent injection on 4D flow
In vivoでの造影前後の4D flowの精度検証
松本　卓弥（総合病院 聖隷三方原病院 画像診断部）
Takuya Matsumoto, Tomoyasu Amano, Mutsuki Tanaka, Mamoru Takahashi, Tomoyuki Okuaki, Hideo Yamamoto

O-2-089 Hemodynamic Assessments of Hepatic Vasculatures using 4D-PCA and MRFD
4D-PCAとMRFDによる肝血管の血行力学的評価
吉川　　武（神戸大学大学院 医学研究科 先端生体医用画像研究センター）
Takeshi Yoshikawa, Katsusuke Kyotani, Yoshiharu Ohno, Yuji Kishida, Shinichiro Seki, Koya Nishiyama, Kazuro Sugimura

O-2-090 Reproducibility of the carotid arterial hemodynamic analysis using 3D cine phase contrast MRI
頸動脈を対象とした3次元シネ位相コントラスト磁気共鳴法の血流動態解析の再現性
七条　来夢（名古屋大学 医学部 保健学科 放射線技術科学専攻）
Raimu Shichijou, Atsushi Fukuyama, Tomoya Watanabe, Kenta Ishiguro, Haruo Isoda

MRA technique　　10：40～11：20

Chair：Mitsuharu Miyoshi（GE Healthcare Japan）
座　長：三好　光晴（GEヘルスケア・ジャパン株式会社）

O-2-091 Application of Variable Refocusing Flip Angle (vFA) in FBI for 6-min Three-Station Peripheral MRA at 3T
3T MRIを用いた非造影下肢FBIにおけるVariable Refocusing Flip Angle パターンの最適化
宮崎美津恵（TOSHIBA MEDICAL RESEARCH INSTITUTE）
Mitsue Miyazaki, Keiichiro Ishi, Xiangzhi Zhou, Masaaki Umeda, Nobuyasu Ichinose, Akiyoshi Yamamoto, Katsumi Nakamura

O-2-092 Evaluation of Multiple Phases Silent MRA
Multiple Phase Silent MRAの基礎的検討
坂下　尚孝（東芝メディカルシステムズ株式会社 医用システム研究開発センター）
Naotaka Sakashita, Masaaki Umeda, Yoshimori Kassai, Masao Yui, Seiji Nozaki, Andrew Wheaton, Deepak Bhat, Aiming Lu

O-2-093 Selective Hepatic Artery Imaging Using VASC-ASL with Beam IR Sequence
Beam IRパルスを用いた選択的肝動脈撮像
西原　　崇（株式会社日立製作所 ヘルスケアビジネスユニット）
Takashi Nishihara, Kuniaki Harada, Ryuji Shirase, Noriko Itabashi, Kuniharu Oka, Hiroyuki Itagaki

O-2-094 Study of short-acquisition time imaging of whole brain Black Blood MRA imaging with 3D Gradient Echo EPI sequence
FE型マルチショット3D EPI法による短時間全脳Black Blood MRAの検討
高橋沙奈江（杏林大学医学部付属病院 放射線部）
Sanae Takahashi, Kenji Hamada, Isao Miyazaki, Nanae Kawano, Hiroshi Kusahara

Day 3…… Room 2 (Sonic City Hall, 2F, Small Hall)

Musculoskeletal 1　　9：10～9：50

Chair：Hideharu Sugimoto（Jichi Medical University Department of Radiology）
座 長：杉本　英治（自治医科大学医学部放射線医学講座）

O-3-001 Simultaneous Acquisition of quantitative T1ρ and T2 measurement in knee cartilage
膝軟骨における定量的T1ρおよびT2同時撮影
奥秋　知幸（Philips Healthcare）
Tomoyuki Okuaki, Kosuke Morita, Seitaro Oda, Takeshi Nakaura, Makoto Obara, Yasuyuki Yamashita, Marc Van Cauteren

O-3-002 Feasibility of diffusion kurtosis imaging for differentiation between schwannomas and soft tissue sarcomas
拡散尖度画像における神経鞘腫と軟部肉腫の鑑別の有用性
中條　正典（鹿児島大学大学院医歯学総合研究科 放射線診断治療学分野）
Masanori Nakajo, Yoshihiko Fukukura, Kiyohisa Kamimura, Takashi Iwanaga, Tomoyuki Okuaki, Takashi Yoshiura

O-3-003 Effectiveness of whole-body MRI for the evaluation of patients with rheumatoid arthritis receiving biologic agents: a retrospective study
全身MRIによる関節リウマチのスコアリング評価
神島　　保（北大 保健科学研究院）
Tamotsu Kamishima, Michihito Kono, Shinsuke Yasuda, Keita Sakamoto, Atsushi Noguchi, Toshiyuki Watanabe, Yuka Shimizu, Kenji Oku, Toshiyuki Bohgaki, Olga Amengual, Tetsuya Horita, Tatsuya Atsumi

O-3-004 Evaluation of treatment effect in soft-tissue sarcoma with multiparametric voxel-based analysis of SUVs and ADCs in a PET/MR system
PET/MR装置を用いたSUVとADCのvoxel-based analysis：軟部肉腫の治療効果判定への応用
鷺山　幸二（九州大学医学研究院大学院 臨床放射線科学分野）
Koji Sagiyama, Yuji Watanabe, Ryotaro Kamei, Sungtak Hong, Satoshi Kawanami, Yoshihiro Matsumoto, Hiroshi Honda

Musculoskeletal 2　　9：50～10：30

Chair：Masamitsu Hatakenaka（Sapporo Medical University, Department of Diagnostic Radiology）
座 長：畠中　正光（札幌医科大学 放射線診断学）

O-3-005 Hospital factors associated with early MR imaging for low back pain in working-age subjects: a Japanese Claims Database study
若年・壮年患者の良性腰椎疾患に対する「早期」MRI検査頻度と病院因子：大規模レセプトデータベース解析
佐野由起子（順天堂大学医学部 放射線診断学講座）
Yukiko Sano, Kanako Kumamaru, Michimasa Suzuki, Masaaki Hori, Ryusuke Irie, Atsushi Nakanishi, Shigeki Aoki

O-3-006 An Experimental Investigation of Artifact Reduction by BLADE Combined with SyngoWARP(VAT)
syngoWARP(VAT)を併用したBLADEによるアーチファクト低減の基礎的検討
井隈　美鶴（マツダ病院 画像診断科）
Mitsuru Ikuma, Yoshihide Asao, Akitoshi Sunada, Yoshiko Nakamura, Toshiharu Shimokawa, Kumiko Miyake

O-3-007 High-resolution MRI of both hands using aliasing phenomenon
折り返しを利用した両手指高分解能撮像法の考案
加藤　広士（国家公務員共済組合連合会 新別府病院 放射線科）
Hiroshi Kato, Kentarou Abiru, Kyouichi Misaka

O-3-008 Ultrashort time-to-echo quantitative magnetic resonance imaging of the triangular fibrocartilage: comparison between pronation and neutral position
Ultra-short TE（UTE）を用いた三角線維軟骨評価：回内位と正常位との比較
藤崎　瑛隆（産業医科大学 放射線科）
Akitaka Fujisaki, Takatoshi Aoki, Hidekuni Narimatsu, Sho Watanabe, Chie Kuwahara, Atsushi Nozaki, Yukunori Korogi

Musculoskeletal 3　　10：50～11：40

Chair：Shigeru Ehara（Iwate Medical University Department of Radiology）
座 長：江原　　茂（岩手医科大学 放射線科）

O-3-009 Vertebral strength prediction in diabetic patients: quantification of bone marrow fat content obtained by IDEAL-IQ
IDEAL-IQ法を用いた骨髄脂肪定量化による糖尿病患者の骨強度解析
山口　晋平（産業医科大学 放射線科）
Shinpei Yamaguchi, Takatoshi Aoki, Masami Fujii, Michiko Kobayashi, Chihiro Chihara, Yoshiko Hayashida, Yukunori Korogi, Yosuke Okada, Yoshiya Tanaka

O-3-010 Acute neck pain in patients with inflammation : Dose MRI contribute to the diagnosis?
炎症を有する頚部痛患者へのMRIは診断に貢献するのか
結城　雅子（北摂総合病院 放射線科）
Masako Yuki, Yoshifumi Narumi

O-3-011 Usefulness of simultaneous acquisition of MR MicroNeurography and T2*mapping for assessment of carpal tunnel syndrome
手根管症候群におけるMicroNeurographyと同時取得するT2*mapの有用性
小澤由莉子（八重洲クリニック）
Yuriko Ozawa, Masami Yoneyama, Satoshi Tatsuno, Koji Fujita, Takashi Miyamoto, Yuji Inoue, Nozomu Koyama

O-3-012 Reliability of MR quantification of rotator cuff muscle fatty degeneration using a Two-point Dixon technique
2-Point Dixon法による棘上筋脂肪変性の定量評価の信頼性の検討、Goutallier分類による定性評価との比較
堀内　沙矢（聖路加国際病院 放射線科）
Saya Horiuchi, Taiki Nozaki, Atsushi Tasaki, Akira Yamakawa, Yasuhito Kaneko, Starkey Jay, Takeshi Hara, Yasuyuki Kurihara, Hiroshi Yoshioka

O-3-013 Improvement of 3D MR Neurography in the extremities using phase-cycling modified diffusion-sensitized driven equilibrium (pc-mDSDE)
四肢領域におけるphase-cycling modified DSDEを用いた3D MR Neurographyの改善法の検討
坂井　上之（東千葉メディカルセンター 放射線部）
Takayuki Sakai, Atsuya Watanabe, Masami Yoneyama, Kiichi Nose, Noriyuki Yanagawa

Day 3…… Room 4 (Sonic City Building, 4F, 401～402)

Pelvis　　10：10～11：10

Chair：Takashi Koyama（Kurashiki Central Hospital Department of Diagnostic Radiology）
座　長：小山　　貴（倉敷中央病院 放射線診断科）

O-3-014　MR spectroscopy of the testis: The reduction in creatine signals is a potential marker of irreversible ischemic damage
精巣のMRS：非可逆的な虚血障害ではクレアチン信号が低下する
山口　雅之（国立がん研究センター 先端医療開発センター 機能診断開発分野）
Masayuki Yamaguchi, Hidehiro Watanabe, Nobuhiro Takaya, Fumiyuki Mitsumori, Hirofumi Fujii

O-3-015　Validation of Adaptive Brachytherapy using 3T MRI in Gynecological Cancer Patients: Impact of Sequential Evaluation of ADC and T2 values
3テスラMRIを用いた婦人科癌小線源治療患者のADC値とT2値の経時変化：放射線抵抗性予測の可能性について
京谷　勉輔（神戸大学医学部附属病院 医療技術部 放射線部門）
Katsusuke Kyotani, Satoru Takahashi, Kenji Yoshida, Ryo Nishikawa, Yuuichirou Somiya, Hideaki Kawamitsu, Ryohei Sasaki, Kazuro Sugimura

O-3-016　Comparison of the diagnostic accuracy of multiparametric MRI and 18F-FDG PET/CT in the differentiation between uterine sarcoma and benign leiomyoma
子宮肉腫と子宮筋腫の鑑別におけるmultiparametric MRIとPET/CTの診断能の比較
中川　雅貴（熊本大学 医学部 放射線診断学）
Masataka Nakagawa, Tomohiro Namimoto, Kie Shimizu, Fumi Sakamoto, Shinnya Shiraishi, Seitarou Oda, Takeshi Nakaura, Daisuke Utsunomiya, Yasuyuki Yamashita

O-3-017　演題取り下げ

O-3-018　Evaluation of prostate cancer on synthetic FOCUS DWI by using the PI-RADS version 2.0
前立腺癌のSynthetic FOCUS DWI: PIRADS version2における有用性についての検討
片山　元之（聖隷浜松病院 放射線科）
Motoyuki Katayama, Takayuki Masui, Kei Tsukamoto, Kenichi Mizuki, Yuki Baba, Masako Sasaki, Tetsuya Wakayama, Mitsuharu Miyoshi

O-3-019　Effect and optimization of Gadobutrol (Gd-BT-DO3A) injection speeds on uterus DCE-MRI
子宮DCEにおけるガドブトロールGd-BT-DO3Aの注入速度の変化がもたらす影響と至適条件の検討
伊東　直博（社会医療法人愛仁会 千船病院 技術部 放射線科）
Naohiro Itou, Akira Tsubota, Ryouta Nakamura, Noriaki Kuriyama, Hiroya Tanaka, Yutaka M.D Tanaka

Day 1…… Poster Room (Sonic City Building, B1F, Exhibition Hall No.2～No.5)

ASL, MRA　　13：10～13：55

Chair：Haruo Isoda（Brain & Mind Research Center, Nagoya University）
座　長：礒田　治夫（名古屋大学 脳とこころの研究センター）

P-1-001　Carotid-Anterior Cerebral Artery Anastomosis Diagnosed by MR Angiography
内頸動脈―前大脳動脈吻合のMRA診断
内野　　晃（埼玉医科大学 国際医療センター 画像診断科）
Akira Uchino, Naoko Saito

P-1-002 Study of readout sequence for 3D whole brain ASL
全脳撮像を対象とした3D ASLのリードアウトシーケンスの検討
吉澤　延之（株式会社 日立製作所 ヘルスケアビジネスユニット）
Nobuyuki Yoshizawa, Hiroyuki Itagaki

P-1-003 Utility of multiphase ASL and 4DMRA for evaluating patients with acute neurological disorder
multiphase ASLと4DMRA の救急頭部領域における有用性
田中　茂子（若草第一病院 放射線科）
Shigeko Tanaka, Shiromaru Ishida, Masayuki Fujioka

P-1-004 Rapid-Basal ganglia pCASL which can be applied pre endovascular therapy protocol for acute ischemic stroke
虚血性脳卒中に対する血管内治療術前検査として適応可能な基底核レベルの高速pCASL
大浦　大輔（小樽市立病院 放射線室）
Daisuke Oura, Kyohei Abe, Tomoka Kadoya, Takumi Yokohama

P-1-005 Evaluation of water permeability for ischemic lesion in the brain using DW-ASL
DW-ASLを用いた脳虚血領域におけるwater permeabilityの評価
藤間　憲幸（北海道大学病院放射線診断科）
Noriyuki Fujima, Tomoyuki Okuaki, Takuya Aoike, Suzuko Aoike, Hiroyuki Sugimori, Kohsuke Kudo

P-1-006 Usefulness of silent MRA for follow-up of intracranial aneurysms treated with pipeline embolization device
パイプラインステントによる治療後のフォローアップに対するSilent MRAの有用性
高野　　直（順天堂大学大学院 医学研究科 放射線医学）
Nao Takano, Michimasa Suzuki, Ryusuke Irie, Munetaka Yamamoto, Shuji Sato, Nozomi Hamasaki, Tomoya Muroi, Shiori Hamagawa, Haruyoshi Hoshito, Masaaki Hori, Hidenori Oishi, Shigeki Aoki

P-1-007 a evaluation of the metal artifact reduction by MR-angiography in neurosurgery
脳神経外科領域におけるMR-angiographyによる体内金属アーチファクト低減の検討
木村　紀行（札幌白石記念病院 放射線部）
Noriyuki Kimura, Hideyuki Osanai, Hideki Hirata, Kenta Yamanaka, Shouta Fukushima

Brain technique　　１４：３０～１５：００

Chair：Kouichirou Okamoto（Brain Research Institute, Niigata University）
座　長：岡本浩一郎（新潟大学 脳研究所）

P-1-008 The Advantages of Synthetic MRI in pediatric patients
小児疾患におけるSynthetic MRIの臨床応用
アンディカ　クリスティナ（順天堂大学医学部放射線科）
Christina Andica, Akifumi Hagiwara, Misaki Nakazawa, Aki Hattori, Sho Murata, Nao Takano, Masaaki Hori, Shigeki Aoki

P-1-009 Altered resting state functional connectivity after autogenic training
自律神経訓練後のresting state functional connectivityの諸変化
雫石　　崇（日本大学 医学部 放射線医学系 画像診断学分野）
Takashi Shizukuishi, Osamu Abe, Takahiro Shinozaki, Akihiko Wada, Haruyasu Yamada, Ryutaro Kohashi, Yoshiki Imamura

P-1-010 Evaluation of clincal single atlas-based attenuation correction for integrated PET/MR
TOF-PET/MR臨床機で用いられているsingle atlas-based methodによる頭部吸収補正
関根　鉄朗（日本医科大学 放射線科）
Tetsuro Sekine, Buck Alfred, Delso Gaspar, Ter Voert Edwin, Huellner Martin, Veit-Haibach Patrick, Warnock Geoffrey

P-1-011 VR images of the cerebellopontine angle using 3D-FIESTA: comparison with 3D-SPGR
3D-FIESTAを用いた小脳橋角部近傍のVR表示：3D-SPGRとの比較も含め
四家　洋介（総合南東北病院 診療放射線科）
Yosuke Shike, Mika Kokubun, Takashi Konno, Hidekazu Yamazaki, Natsuru Kobiyama, Noriaki Tomura, Syunsuke Sato

P-1-012 Relationship of cerebral gray and white matter contrast in different inversion time using ultra-short echo time sequence (PETRA)
Ultra-short TEシーケンス（PETRA法）におけるTI値の違いによる脳白質・灰白質コントラストの検討
塩田　正和（手稲渓仁会病院）
Masakazu Shioda, Ken Masuyama, Syun Akimoto, Kazuya Akiyoshi

Image processing　13：10～13：40

Chair：Kenya Murase（Department of Medical Physics and Engineering, Course of Health Science, Graduate School of Medicine, Osaka University）
座 長：村瀬　研也（大阪大学大学院医学系研究科保健学専攻医用物理工学講座）

P-1-013 Three-dimensional target tracking method for MRgHIFU using image matching technique with liver deformation volumes
3次元画像マッチング手法を用いた肝MRgHIFUのターゲット追尾
熊本　悦子（神戸大学 情報基盤センター）
Etsuko Kumamoto, Daisuke Kokuryo, Tatsuhiko Matsumoto, Kagayaki Kuroda

P-1-014 Error in QSI analysis for slow flow in a noisy environment
ノイズの多い環境中における遅い流れのQSI解析に対する誤差評価
長田　晃佳（筑波大学大学院 数理物質科学研究科 電子・物理工学専攻）
Akiyoshi Nagata, Yasuhiko Terada, Katsumi Kose

P-1-015 Rapid T_1 Measurement using Fast imaging
高速撮像法によるT1計測の撮像時間短縮化
俵　　紀行（日本医療大学 保健医療学部 診療放射線学科）
Noriyuki Tawara, Atsushi Nishiyama

P-1-016 Accelerating Imaging Reconstruction by GPGPU Computing in Magnetic Resonance Compressed Sensing for Phase-varied Images
GPGPUを利用したMR位相画像の圧縮センシング再構成の高速化
市村　亮祐（宇都宮大学 大学院工学研究科 情報システム科学専攻）
Ryosuke Ichimura, Satoshi Ito

P-1-017 Denoising of MR images using Fast Composite Splitting Algorithm
FCSAを用いたMR画像の雑音除去法
奥木　稜平（宇都宮大学 大学院工学研究科 情報システム科学専攻）
Ryohei Okugi, Satoshi Ito

Flow　14：00～14：30

Chair：Yoshiyuki Watanabe（Osaka University Department of Radiology）
座 長：渡邉　嘉之（大阪大学医学部放射線医学講座）

P-1-018 Asymmetry of pulmonary perfusion and pulmonary regurgitation in Tetralogy of Fallot after repair
Fallot四徴症術後患者における phase contrast MRI による肺血流評価
小川　　遼（愛媛大学大学院 医学系研究科放射線医学）
Ryo Ogawa, Tomoyuki Kido, Masashi Nakamura, Teruhito Kido, Teruhito Mochizuki, Takashi Higaki

P-1-019 Study on scan parameters for 4Dflow using kat-ARC
kat-ARC用いた4Dflow：撮像パラメータの検討
藤代　力也（慶應義塾大学病院 放射線技術室）
Rikiya Fujishiro, Shigeo Okuda, Atsushi Nozaki, Yoshinobu Nunokawa, Yasutomi Shimada, Masahiro Jinzaki

P-1-020 Four-dimensional Phase Contrast MRI Iliac Artery with Fat Suppression Techniques
4D-PC MRIを用いた腸骨動脈における脂肪抑制法の比較
福島　沙知（倉敷中央病院 放射線技術部）
Sachi Fukushima, Kenichi Nakagawa, Shohei Naruishi, Hiroaki Kameiyama, Noriyoshi Morimoto, Takashi Tabuchi

P-1-021 Visualization of Blood Flow for Renal Artery using Four-dimensional Flow Analysis: Optimization of Fat Suppression Parameters
4D-Flow解析を用いた腎動脈血流可視化法: 脂肪抑制法のパラメータ適正化
亀井山弘晃（倉敷中央病院 放射線技術部）
Hiroaki Kameiyama, Syohei Naruishi, kenichi Nakagawa, Sachi Fukushima, Noriyoshi Morimoto, Takashi Tabuchi

P-1-022 Visualization of Blood Flow for Renal Artery using Four-dimensional Flow Analysis : Optimization of slice orientation and k-space trajectory
4D Flow解析を用いた腎動脈血流可視化法：スライス断面とk空間の収集方法の適正化
成石　将平（倉敷中央病院 放射線技術部）
Syohei Naruishi, Hiroaki Kameiyama, Kenichi Nakagawa, Sachi Fukushima, Noriyoshi Morimoto, Takashi Tabuchi

High speed imaging　　15：15～16：00

Chair：Toshinori Hirai（University of Miyazaki, Department of Radiology）
座　長：平井　俊範（宮崎大学 放射線科）

P-1-023 Fast 3D Multi-Parameter Mapping of Relaxation Times and Susceptibility Using RF-Spoiled Gradient Echo
RF-Spoiled Gradient Echoを用いた緩和時間と磁化率の高速3Dマッピング
谷口　　陽（株式会社日立製作所 研究開発グループ）
Yo Taniguchi, Suguru Yokosawa, Tomoki Amemiya, Toru Shirai, Ryota Sato, Hisaaki Ochi, Yoshihisa Soutome

P-1-024 Quantification error due to B0 inhomogeneity in MR fingerprinting
MR指紋法におけるB0不均一性由来の定量誤差
小林　優太（筑波大学大学院 数理物質科学研究科 電子・物理工学専攻）
Yuta Kobayashi, Yasuhiko Terada

P-1-025 Spiral imaging for a 9.4T/54mm vertical bore superconducting magnet
9.4T/54mm縦型開口径超伝導磁石におけるSpiral imagingの開発
瀬戸井綾菜（筑波大学 数理物質科学研究科 電子・物理工学専攻）
Ayana Setoi, Nao Kodama, Katsumi Kose

P-1-026 Development of spiral imaging for a 1.5T/280mm horizontal bore superconducting magnet
1.5T/280mm水平開口超伝導磁石におけるスパイラルイメージングの開発
瀬戸井綾菜（筑波大学 数理物質科学研究科 電子・物理工学専攻）
Ayana Setoi, Katsumi Kose

P-1-027 3D MR Compressed Sensing using Higher-density Sampling in Restricted Signal Space
信号収集領域の制限による信号収集の高密度化を利用した3次元MR撮像の圧縮センシング
松本　知之（宇都宮大学 大学院工学研究科 情報システム科学専攻）
Tomoyuki Matsumoto, Satoshi Ito

P-1-028 Compressed Sensing of 3D MR Phase-varied Images using Multi-scale Sparsify Transform
マルチスケール・スパース化変換を利用した3次元MR位相画像の圧縮センシング
渋谷　萌音（宇都宮大学 大学院工学研究科 情報システム科学専攻）
Mone Shibuya, Satoshi Ito

P-1-029 Study on Multi-sparsified Transform Compressed Sensing for MR Angiography
MR血管画像に対するマルチスケール・スパース化変換圧縮センシングの基礎検討
生井　勇己（宇都宮大学 大学院工学研究科 情報システム科学専攻）
Yuki Namai, Satoshi Ito

Cardiovascular 1　　13：10～14：00

Chair：Takashi Ueguchi（National Institute of Information and Communications Technology）
座　長：上口　貴志（情報通信研究機構）

P-1-030 Novel cardiac 4D flow imaging using arterial spin labeling with modified flow sensitive alternating radio frequency: analysis of pulmonary artery flow
ASLによる肺動脈4D-flow画像の至適条件検討
後藤　康裕（東京女子医科大学病院 中央放射線部）
Yasuhiro Goto, Michinobu Nagao, Kenji Fukushima, Masami Yoneyama, Hitoshi Tadenuma, Mamoru Takeyama, Shuji Sakai

P-1-031 Study of parameter to improve the accuracy of cardiac function evaluation at free breath in cardiac cine magnetic resonance imaging
Free-Breathによる心臓シネMRIにおいて心機能評価の精度向上を目的とした撮影条件の検討
原　久美子（倉敷中央病院 放射線技術部）
Kumiko Hara, Kenichi Nakagawa, Noriyoshi Morimoto, Takashi Tabuchi

P-1-032 Development of the myocardial color map by Look-Locker method
Look-Locker法による心筋Color MAPの検討
立石　敏樹（国立病院機構山形病院 放射線科）
Toshiki Tateishi, Atsuko Idogawa, Hiroya Rikimaru, Akihiro Satou, Nobuyuki Kihara, Hiroshi Oonishi, Takeshi Shinozaki

P-1-033 Implication of late gadolinium enhancement magnetic resonance imaging in the management of a patient with Emery-Dreifuss muscular dystrophy
エメリードレフィス型筋ジストロフィーの管理におけるガドリニウム遅延造影を用いた磁気共鳴画像の意義。
山澤　弘州（北海道大学病院 小児科）
Hirokuni Yamazawa, Atsuhito Takeda, Gaku Izumi, Osamu Sasaki, Jiro Abe, Daisuke Sasaki, Noriko Oyama-Manabe

P-1-034 Improvement of contrast enhancement MRA with the tube for exclusive use of injecting contrast media and saline together in carotid arteries
頸動脈造影MRA撮像における混合専用チューブを用いた造影剤生理食塩水同時混同注入の有用性
浜口　明巧（札幌麻生脳神経外科病院 放射線科）
Akiyoshi Hamaguchi, Naoko Hamaguchi, Tetsuji Hayashi

P-1-035 A study on asynchronous extremity non-contrast MRA by FE3D method with MTC
MTC併用FE3D法における非同期四肢非造影MRAの検討
矢澤　真一（日本私立学校振興・共済事業団 東京臨海病院）
Shinichi Yazawa, Ichirou Iijima, Atsushi Yamaki

Cardiovascular 2　　14：30～15：20

Chair：Naofumi Matsunaga（Department of Radiology, Yamaguchi University Graduate School of Medicine）

座 長：松永　尚文（山口大学大学院医学系研究科 放射線医学分野）

P-1-036 Comparison of the imaging plane of the non-contrast-enhanced coronary artery visualization in 3 Tesla MRI

3 Tesla MRIにおける非造影冠動脈描出の撮像断面の比較

渡邉　城大（埼玉県済生会栗橋病院 放射線技術科）

Kunihiro Watanabe, Mayumi Ootani, Kazuihiro Maruyama, Nobuyasu Ichinose, Shinichi Kitane, Tomoko Miyata, Kouki Kurita

P-1-037 Morphology-Matching-Based R-Wave Detection For Noise-Robust ECG Gating: Evaluation of the R-wave detection accuracy

モルフォロジーマッチングによるR波検出技術を用いたロバスト心電図同期法：検出性能の評価

川上　毅人（東芝メディカルシステムズ株式会社 MRI事業部 MRI開発部）

Taketo Kawakami, Takami Yoshida, Makoto Hirohata, Shigehide Kuhara, Akio Mori

P-1-038 Comparison of whole-heart unenhanced coronary MRA using multi-shot gradient echo EPI and TFE coronary MRA in healthy volunteers at 3T MRI

Multi-shot EPIを用いた非造影冠動脈MRAの検討

中浦　　猛（熊本大学 医学部 画像診断解析学）

Takeshi Nakaura, Kosuke Morita, Seitaro Oda, Daisuke Utsunomiya, Tomohiro Namimoto, Mika Kitajima, Yasuyuki Yamashita

P-1-039 Examination of Three-dimensional T1-Weighted Black- Blood Turbo Spin-Echo: The Vessel Wall Imaging in the Aortic Arch

3D T1強調black-blood turbo spin echoの検討：大動脈弓部の血管壁画像

中河　賢一（倉敷中央病院 放射線技術部）

Kenichi Nakagawa, Noriyoshi Morimoto, Sachi Fukushima, Takashi Tabuchi

P-1-040 Non-contrast enhanced MR-Venography using 3D-T1FFEEPI in lower extremity

3D-T1FFEEPIを用いた下肢MR-Venography

古牧　伸介（川崎医科大学附属川崎病院 中央放射線部）

Shinsuke Komaki, Katsuhiro Kida, Yukako Hayashi, Akihiko Tabuchi

P-1-041 Investigation to the stent makers about MRI examination start time after implanted of stent to coronary artery and peripheral arteries

冠動脈および末梢血管ステント挿入後の MRI検査可能時期に関するステントメーカー各社の見解の調査

蛸井　邦宏（山形県立新庄病院 放射線部）

Kunihiro Takoi, Shuichi Otake, Shintaro Saito, Soichi Ono, Toshiro Shibasaki, Yuitu Narasaki, Takatomo Itagaki

Day 2…… Poster Room (Sonic City Building, B1F, Exhibition Hall No.2～No.5)

Brain tumor　　9：10～10：05

Chair：Takaaki Hosoya（Yamagata University Faculty of Medicine, Dept. of Diagnostic Radiology）

座 長：細矢　貴亮（山形大学医学部画像医学講座）

P-2-001 CEST APTimaging of Intracranial Tumor with anaplastic transformation

悪性転化した脳腫瘍のCEST APTimage

若山　季樹（東京都保健医療公社 荏原病院 放射線科）

Toshiki Wakayama, Masahiro Ida, Katsutoshi Murata, Kenji Saitou, Takashi Ueda, Fumiaki Kawakami, Toshiyuki Onodera, Atsushi Senoo, Akira Yamashita

P-2-002 Comparison of MR-permeability imaging from MET-PET in differentiating radiation necrosis from recurrent tumors after gamma knife radiosurgery
脳転移へのガンマナイフ治療後の再発、壊死の鑑別における、MR-permeability imagingとMET-PETの比較
戸村　則昭（脳神経疾患研究所附属 総合南東北病院 神経放射線診断科）
Noriaki Tomura, Mika Kokubun, Yasuhiro Kikuchi

P-2-003 Predicting the Consistency of Meningioma with T1ρ at 3T-MR: Preliminary Study
T1ρによる髄膜腫の硬さの評価
北島　美香（熊本大学 医学部 画像診断・治療科）
Mika Kitajima, Shigetoshi Yano, Hiroyuki Uetani, Tomoyuki Okuaki, Yasuyuki Yamashita

P-2-004 Differentiation of meningioma and high-grade glioma using dynamic susceptibility contrast and dynamic contrast-enhanced MRI
髄膜腫と悪性神経膠腫の鑑別におけるMR灌流画像の有用性の検討
村山　和宏（藤田保健衛生大学 医学部 放射線医学）
Kazuhiro Murayama, Takashi Fukuba, Shigeharu Ohyu, Ayako Ninomiya, Masato Ikedo, Kazuhiro Katada, Hiroshi Toyama

P-2-005 Pattern difference in the area with T2-hyperintensity: comparison between gliomas and edema by using texture analysis
T2強調像での高信号域におけるテクスチャ解析による検討: gliomaと浮腫との比較
川井　　恒（名古屋大学 医学部附属病院 放射線科）
Hisashi Kawai, Toshiaki Taoka, Toshiki Nakane, Shinji Naganawa

P-2-006 Morphologic features of intratumoral susceptibility signals on PRESTO for predicting the WHO grade of gliomas
PRESTO-MRIによる腫瘍血管形態評価の試み：神経膠腫悪性度診断への応用
李　　麗（東北大学 医学系研究科 放射線診断科）
Li Li, Shunji Mugikura, Takaki Murata, Toshiaki Akashi, Shiho Sato, Masayuki Kanamori, Mika Watanabe, Hajime Tamura, Shoki Takahashi, kei Takase

P-2-007 Improvement of Brain T1 Weighted Images Quality using Spin Echo Sequence at 3.0T
SE法による3T頭部T1強調画像の画質改善
松下　　利（岡山大学病院 医療技術部 放射線部門）
Toshi Matsushita, Seiichirou Ohno, Shunsuke Fuji, Akira Kurozumi, Takatugu Yamauchi, Naoki Nishida, Akira Nagano, Seiji Tahara

P-2-008 Differentiation among GBM, and Primary CNS Lymphoma Using Whole-Tumor Histogram Analysis of the nCBV and minimum ADC in Enhancing Lesions
リンパ腫とGBMの鑑別診断：CBVとADC画像のヒストグラム解析
包　　是星（大阪大学 医学研究科 放射線医学）
Shixing Bao, Yoshiyuki Watanabe

P-2-009 Evaluation of optimal injection rate in gadovist enhanced MR dynamic study
ガドビストダイナミックMRI至適注入速度の検討
中村　　誠（三豊総合病院 診療技術部 放射線科）
Makoto Nakamura, Shinya Azuma, Masashi Kiyohara, Hironori Kurokawa

Brain microimaging　　10：30～11：20

Chair：Junichi Hata（RIKEN Brain Science Institute）
座 長：畑　　純一（理化学研究所 脳科学総合研究センター）

P-2-010 Anatomical Development of Hippocampus and its Related Regions in Common Marmosets
コモンマーモセットの海馬体とその関連領域の形態的発達
植松　明子（慶應義塾大学大学院 医学研究科 生理学教室）
Akiko Uematsu, Junichi Hata, Yuji Komaki, Fumiko Seki, Erika Sasaki, Hideyuki Okano

P-2-011 Age-related changes in magnetization transfer ratio with atlas based whole brain analysis in common marmoset development
コモンマーモセットの脳発達に伴うMagnetization Transfer Ratioの変化
西尾　真鈴（首都大学東京 健康福祉学部 放射線学科）
Marin Nishio, Yuji Komaki, Fumiko Seki, Junichi Hata, Akiko Uematsu, Ryosuke Ishihara, Ryutaro Yano, Erika Sasaki, Akira Furukawa

P-2-012 Postmortem MRI properties of common marmoset brain during formaldehyde-fixed
コモンマーモセット脳における標本固定の影響
羽賀　　柔（首都大学東京 健康福祉学部 放射線学科）
Yawara Haga, Junichi Hata, Akiko Uematsu, Takaaki Kaneko, Yukiko Nagawa, Marin Nishio, Yuji Komaki, Fumiko Seki, Noriyuki Kishi, Erika Sasaki, Hideyuki Okano, Akira Furukawa

P-2-013 Impacts of difference of transparency reagents on mouse brain
透明化試薬の違いによるマウス脳への影響
名川友紀子（首都大学東京大学院 人間健康科学研究科）
Yukiko Nagawa, Junichi Hata, Akiko Uematsu, Fumiko Seki, Yuji Komaki, Ryutaro Yano, Masakazu Sato, Ryousuke Ishihara, Hideyuki Okano, Kazuo Yagi, Norio Sekine

P-2-014 Depiction of Neural Microstructures by Ultra High Field MRI
超高磁場MRIによる小型霊長類脳構造のマイクロイメージング
畑　　純一（理化学研究所 脳科学総合研究センター）
Junichi Hata, Akiko Uematsu, Takaaki Kaneko, Makoto Fukushima, Fumiko Seki, Yuji Komaki, Yukiko Nagawa, Keigo Hikishima, Noriyuki Kishi, Erika Sasaki, Hideyuki Okano

P-2-015 Four-dimensional in vivo MRI for tracking individual immune cells in mouse brain
マウス生体脳内における4次元免疫細胞追跡の検討について
森　　勇樹（大阪大学 免疫学フロンティア研究センター 生体機能イメージング）
Yuki Mori, Daniela Martinez de la Mora, Atsuki Tashita, Syoji Kobashi, Ikuhiro Kida, Yutaka Hata, Yoshichika Yoshioka

P-2-016 Gd-enhancement differences between mouse strains as shown by 3D MR histology
三次元MR組織学的評価法を用いたガドリニウム造影能のマウス系統間の違い
森　　勇樹（大阪大学 免疫学フロンティア研究センター 生体機能イメージング）
Yuki Mori, Kiyoyuki Osugi, Daniela Martinez de la Mora, Yoshichika Yoshioka

P-2-017 High resolution 3-D T2-weighted imaging of human fetus
ホルマリン固定胎児標本蝸牛構造描出：臨床機による0.1mm等方性撮像の試み
山本　　憲（京都大学大学院 医学研究科 放射線医学講座（画像診断学・核医学））
Akira Yamamoto, Yasutaka Fushimi, Tsutomu Okada, Tomohisa Okada, Yutaka Yamaguchi, Rena Miyazaki, Haruyuki Makishima, Shigehito Yamada, Kaori Togashi

Hardware 1　　9：10～9：40

Chair：Kiyotaka Suzuki（Niigata University Brain Research Institute）
座　長：鈴木　清隆（新潟大学脳研究所 統合脳機能研究センター）

P-2-018 Development of portable MRI for early detection of baseball elbow
野球肘初期診断用ポータブルMRIの開発
田辺　亮勝（筑波大学大学院 数理物質科学研究科 電子・物理工学専攻）
Katsumasa Tanabe, Syuhei Oka, Yoshikazu Okamoto, Katsumi Kose, Yasuhiko Terada

P-2-019 Potential and Problems of MRI simulators
MRI simulatorの可能性と問題点
巨瀬　勝美（筑波大学 数理物質系 物理工学域）
Katsumi Kose, Ryoichi Kose

P-2-020 GPU optimized general purpose MRI simulator
GPUに最適化した汎用MRIシミュレータの開発
巨瀬　亮一（株式会社 エム・アール・テクノロジー）
Ryoichi Kose, Katsumi Kose

P-2-021 Development of a multi-channel hub-unit for 8 digital transceivers using a console-PC and software for NMR/MRI
汎用PCで制御するNMR/MRI用デジタルトランシーバを多チャンネル化するハブユニットの開発
拝師　智之（株式会社エム・アール・テクノロジー）
Tomoyuki Haishi, Seitaro Hashimoto, Hisao Mizukami, Hiroshi Hasegawa, Masaru Aoki

P-2-022 Development of a fast analog-to-digital converter-haed performing rf under-sampling of MRI signals and an optical fiber link upto 400MHz
400MHzまでのMRI信号をアンダーサンプリングでデジタル化するAD変換ヘッドと光接続リンクの開発
拝師　智之（株式会社エム・アール・テクノロジー）
Tomoyuki Haishi, Shin-ichi Morisaka, Hiroshi Hasegawa, Masaru Aoki

Hardware 2　　10：00～10：50

Chair：Tomoyuki Haishi（MRTechnology, Inc.）
座　長：拝師　智之（株式会社エム・アール・テクノロジー）

P-2-023 Reduction of B1+ Inhomogeneity Using 4-channel RF Shimming for Partial Region in Cervical Spine Imaging at 3T
4チャンネルRFシミングを用いた，頸椎撮像での部分領域に対するB1+不均一低減効果の検討
金子　幸生（株式会社日立製作所 研究開発グループ）
Yukio Kaneko, Kosuke Ito, Masahiro Takizawa, Yoshihisa Soutome, Hideta Habara, Yusuke Seki, Tetsuhiko Takahashi, Yoshitaka Bito, Hisaaki Ochi

P-2-024 Elliptical Birdcage Coil with Identical Ring Capacitor Value
同一容量のリングキャパシタを用いた楕円バードケージコイルの開発
五月女悦久（株式会社日立製作所 研究開発グループ）
Yoshihisa Soutome, Shin-ichiro Suzuki, Hideta Habara, Takahide Shimoda, Yoshitaka Bito

P-2-025 Electromagnetic Field Analysis of Split Transmit Body Coil for Wide-bore MRI
ワイドボアMRI向け分割型照射ボディコイルの電磁界解析
五月女悦久（株式会社日立製作所 研究開発グループ）
Yoshihisa Soutome, Hisaaki Ochi, Yoshitaka Bito

P-2-026 Development of 32ch Head receiver coil for 3T high-field MRI
3T高磁場MRIにおける32ch 頭部用コイルの開発
加藤　和之（株式会社日立製作所 ヘルスケアビジネスユニット）
Kazuyuki Kato, Takeshi Taniguchi, Takahide Shimoda, Koenig Steven, Napier Christophor

P-2-027 Optimization of scan protocol for 32ch Head receiver coil
32チャンネル頭部用コイルにおける撮像プロトコルの最適化
立花　美紀（株式会社 日立製作所 ヘルスケアビジネスユニット）
Miki Tachibana, Kuniaki Harada, Ryuji Shirase, Takeshi Taniguchi, Takahide Shimoda, Kazuyuki Kato, Yasuhiro Kamada, Chikako Moriwake

P-2-028 Comparison of B1+ distribution between 8ch and 2ch RF transmit coils at 7T
7T 装置における8ch送信コイルと2ch送信コイルによるB1+分布の比較
松田　　豪（岩手医科大学 医歯薬総合研究所 超高磁場MRI診断・病態研究部門）
Tsuyoshi Matsuda, Tsuyoshi Metoki, Yuji Iwadate, Hiroyuki Kameda, Taisuke Harada, Kohsuke Kudo, Makoto Sasaki

P-2-029 Development of the Head Coil with Comfort Design
快適性を考慮した頭部用RFコイルの開発
今井　聡志（東芝メディカルシステムズ株式会社）
Satoshi Imai, Sadanori Tomiha, Zachary Bauer, Xiaoyu Yang, Hiroyuki Fujita, Shinji Mitsui

Hardware 3　　11：10～11：50

Chair：Katsumi Kose（University of Tsukuba）
座 長：巨瀬　勝美（筑波大学 数理物質科学研究科）

P-2-030 Correction for eddy current effect of field cycle MRI using rotary magnet
磁石回転型Field Cycle MRIにおけるEddy Currentの効果と補正
小林　竜馬（九州大学 先端融合医療レドックスナビ研究拠点）
Ryoma Kobayashi, Hideo Utsumi

P-2-031 Magnetic Field Shimming Calculation (HiSHIM) Using TSVD Regularization With Descritization and Limitation of Iron Pieces Placements
打ち切り特異値分解正則化計算を用いたMRI用磁石用シミング計算手法(HiSHIM)の開発
阿部　充志（日立製作所 研究開発グループ エネルギーイノベーションセンタ）
Mitsushi Abe, Kenji Sakakibara

P-2-032 Applications to MRI magnets of shimming calculation method HiSHIM
MRI用磁石のシミング計算手法HiSHIMの装置適用
榊原　健二（株式会社日立製作所 ヘルスケアビジネスユニット）
Kenji Sakakibara, Mitsushi Abe, Hikaru Hanada, Takuya Fujikawa, Akihiro Shimada

P-2-033 Study of optimal design of oval shaped gradient coil pattern using DUCAS
DUCASによる楕円傾斜磁場コイルパターン最適化設計手法の検討
今村　幸信（株式会社 日立製作所 研究開発グループ）
Yukinobu Imamura, Takeshi Kawamura, Tatsuhiko Kawakami, Mitsushi Abe, Akira Kurome, Shin Hoshino

P-2-034 Development of an insertable gradient coil for a 1.5T/280mm horizontal bore superconducting magnet
1.5T/280mm水平開口型超伝導磁石のための挿入型勾配磁場コイルの開発
矢野　順也（筑波大学 数理物質科学研究科 電子・物理工学専攻）
Junya Yano, Yuta Kobayashi, Yasuhiko Terada, Katsumi Kose

P-2-035 Development of field monitoring system using field cameras for a 1.5 T superconducting magnet system
1.5T超伝導磁石におけるField Cameraを用いた磁場モニタリングシステムの開発
小林　優太（筑波大学大学院 数理物質科学研究科 電子・物理工学専攻）
Yuta Kobayashi, Katsumi Kose, Yasuhiko Terada

Upper abdomen 1　　9：10～10：00

Chair：Kazuo Awai（Hiroshima University Department of Diagnostic Radiology）
座 長：粟井　和夫（広島大学 放射線診断学）

P-2-036 Free breathing 3D radial sequence for contrast enhanced examination of the liver: comparison with e-THRIVE
非呼吸停止下における3D radial sequenceとe-THRIVEの比較評価
吉田　学誉（財団法人自警会 東京警察病院 放射線科）
Takashige Yoshida, Yuki Furukawa, Kohei Yuda, Yuki Matsuzaka, Toru Sagami, Nobuo Kawauchi

P-2-037 Investigating the relationship between proton density fat fraction and T2* value using six-point DIXON MRI: A fat-water-iron phantom study
6point-DIXON MRIにおける肝臓脂肪含有量とT2*値の関係の検討：水・脂肪・鉄ファントムによる検討
福澤　　圭（虎の門病院 放射線部）
Kei Fukuzawa, Satoshi Saito, Hidesato Suzuki, Shougo Yoda, Chiharu Yoshihara, Masakatsu Tano

P-2-038 Evaluation of the image quality on respiratory navigator-gated three-dimensional spoiled gradient-recalled echo pulse sequence (3D FSPGR)
Navigator gating法を用いた横隔膜同期併用3D fast SPGR法の画質評価－息止め3D fast SPGR法との比較－
松芳　圭吾（磐田市立総合病院 医療技術部 第1放射線診断技術科）
Keigo Matsuyoshi, Masaki Terada, Masanori Oosugi, Kenichi Ootsubo, Yukina Anzawa, Mika Koitabashi

P-2-039 The evaluation of Single breath hold Whole body 3D Balanced MRCP with 32ch torso coil in 1.5T
1.5T 32ch torso coilを用いたSingle breath hold Whole body 3D Balanced MRCPの検討
大西　宏之（王子会神戸循環器クリニック 放射線技術科）
Hiroyuki Ohnishi, Hiroyuki Fukuya, Hiroko Yamamoto

P-2-040 Magnetic resonance imaging for abdominal radiotherapy planning
腹部放射線治療計画に有用なMRI撮像方法の検討
山崎　達也（香川大学 医学部 附属病院 放射線部）
Tatsuya Yamasaki, Takuya Kobata, Akihiro Ooishi, Takashi Ishimori, Kazuo Ogawa, Yasuhiro Sasakawa

P-2-041 Basic Study on Silent Navigator
Silent Navigator の基礎的検討
布川　嘉信（慶應義塾大学病院 放射線技術室）
Yoshinobu Nunokawa, Rikiya Fujishiro, Yasutomi Shimada, Takashi Asakura, Shigeo Okuda, Hirokazu Fujiwara, Masahiro Jinzaki, Atsushi Nozaki, Yuji Iwadate

P-2-042 Comparison of respiratory navigator-gating techniques in 2D SPGR imaging of the liver
2D SPGR法における横隔膜同期技術の比較
秦　　博文（北里大学病院 放射線部）
Hirofumi Hata, Yusuke Inoue, Ai Nakajima, Shotaro Komi, Yutaka Abe, Keiji Matsunaga, Hiroki Miyatake

P-2-043 Evaluation of the numbers of pancreatic peripheral branches identified by 3D MRCP; Comparison of 3D TSE, 3D T2 SPACE and 3D T2 SPACE ZOOMit
膵管分枝の描出能に関する研究、3種類のMRCPの比較検討
堀　　郁子（松江市立病院 放射線科）
Ikuko Hori, Yoshiko Kanasaki, Motoki Ametani, Masahiro Moriyama, Atsuya Kawaguchi, Toshihide Ogawa

Upper abdomen 2　　10：20～11：00

Chair：Tomoaki Ichikawa（Saitama Medical University International Medical Center Department of Diagnostic Radiology）
座 長：市川　智章（埼玉医科大学国際医療センター 画像診断科）

P-2-044 In vivo MR evaluation of gallstones using three dimensional ultra-short echo time imaging
three dimensional ultra-short echo time imagingを用いたin vivoでの胆石の評価
高橋　　護（聖隷三方原病院 放射線科）
Mamoru Takahashi, Yasuo Takehara, Norihiro Tooyama, Katsutoshi Ichijo, Tomoyasu Amano, Takuya Matsumoto, Tomoyuki Okuaki, Yukiko Fukuma, Harumi Sakahara

P-2-045 Effect of food intake for Intravoxel incoherent motion and T2* in the healthy liver
食事摂取による肝IVIM, T2*緩和時間への影響
齋藤　和博（東京医科大学 放射線医学分野）
Kazuhiro Saito, Yoichi Araki, Yu Tajima, Taiyo L Harada, Takahiro Shimizu, Koichi Tokuuye

P-2-046 Improvement of fatty liver with resistance training and low carbon diet - Quantitative evaluation with mDIXON method
レジスタンス運動と低糖質食による脂肪肝改善効果ー mDIXON法による定量的評価
高原　太郎（東海大学 工学部 医用生体工学科）
Taro Takahara, Toshiki Kazama, Munetaka Haida, Seism Sawano, Satoshi Tatsuno, Yuriko Ozawa, Yoshio Umezaki

P-2-047 Scan Time Shortening of the Hepatic Arterial Phase of Liver Magnetic Resonance Imaging and the Influence of Reference Scan
肝臓MRI検査の動脈相における撮像時間の短縮とリファレンススキャンの影響の検討
辻　　良憲（国家公務員共済組合連合会 虎の門病院 放射線部）
Yoshinori Tsuji, Satoshi Saitoh, Junji Takahashi, Naomi Tagaya, Mariko Hiramoto, Chisato Abe, Yasutaka Tanuma, Akira Sawayama

P-2-048 High and ultra-high b-value diffusion-weighted MRI for the evaluation of hepatic focal lesions with 3-T MRI
3T MRI 超高b値(b=2000)を用いたADCによる肝腫瘍鑑別能の従来法との比較
浪本　智弘（熊本大学 医学部 放射線診断科）
Tomohiro Namimoto, Masataka Nakagawa, Kie Shimizu, Masafumi Kidoh, Seitaro Oda, Takeshi Nakaura, Daisuke Utsunomiya, Yasuyuki Yamashita

P-2-049 Comparative evaluation of computed diffusion weighted imaging based on the mono-exponential and bi-exponential model
Bi-ExponentialモデルおよびMono-Exponentialモデルに基づくcDWIの基礎的検討
甲斐　征八（東芝メディカルシステムズ株式会社）
Seiya Kai, Yuichi Yamashita, Tatsuya Ohkubo, Syuhei Takemoto, Yuichiro Sano

Alimentary tract　　11：20～11：50

Chair：Yutaka Imai（Tokai University School of Medicine）
座 長：今井　　裕（東海大学医学部 画像診断学）

P-2-050 Mediastinal MRI can predict respectability of a locally advanced esophageal cancer after chemoradiation therapy
化学放射線療法後局所進行食道癌の切除の可否を縦隔MRIは予測可能である。
小野寺祐也（社会医療法人 恵佑会札幌病院 放射線診断科）
Yuya Onodera, Taisuke Harada, Osamu Manabe, Hiroaki Takahashi, Toshinao Takenouchi, Masao Hosokawa

P-2-051 Preoperative 3T MR imaging for rectal cancer of ZOOMit T2 SPACE 3D: A comparative study with T2W
ZOOMIT T2 SPACE 3Dの直腸癌に対する術前3T MRI：T2Wとの比較研究
井藤　千里（香川大学 医学部 放射線医学講座）
Senri Ito, Yuko Fukuda, Kenichi Tanaka, Akihiro Oishi, Kazuo Ogawa, Yoshihiro Nishiyama

P-2-052 q-Space MR Imaging of Colorectal Carcinoma Ex Vivo: Evaluation of Histologic Grades and Lymph Node Metastasis
大腸癌のQSIによるEx Vivoでの評価：組織学的分化度とリンパ節転移の検討
山田　一郎（東京医科歯科大学 大学院医歯学総合研究科 画像診断・核医学分野）
Ichiro Yamada, Keigo Hikishima, Norio Yoshino, Naoyuki Miyasaka, Shinichi Yamauchi, Hiroyuki Uetake, Masamichi Yasuno, Yukihisa Saida, Ukihide Tateishi, Daisuke Kobayashi, Yoshinobu Eishi

P-2-053 A pictorial review of the impact of adding diffusion-weighted MR imaging to other MR sequences for assessment of renal pelvic carcinoma
腎盂癌におけるMR拡散強調像の有用性について：他撮影条件との比較
吉田　理佳（島根大学 医学部 放射線科）
Rika Yoshida, Takeshi Yoshizako, Kazumi Araki, Megumi Nakamura, Shinji Andou, Takashi Katsube, Nobuko Yamamoto, Hajime Kitagaki

Ultra-short TE　　13：10～13：40

Chair：Yasutomi Kinosada（Gifu University Graduate School of Medicine）
座　長：紀ノ定保臣（岐阜大学大学院 医学系研究科）

P-2-054　Investigation of the Non-contrast Head Magnetic Resonance Angiography using mUTE 4D-MRA
mUTE 4D-MRAを用いた非造影頭部MRA描出の試み
山内智恵美（東芝メディカルシステムズ株式会社 MRI営業部）
Chiemi Yamauchi, Hisae Chiba, Shin Takamatu, Yoshihito Miyamoto, Tsutomu Katou

P-2-055　A functional study of the description in carotid artery using Ultra short TE
Ultra short TEを用いた頸動脈描出における基礎的検討
宮本　良仁（医療法人 住友別子病院 放射線部）
Yoshihito Miyamoto, Tsutomu Katou, Shin Takamatsu, Chiemi Yamauchi, Tomonari Ishida, Hisae Chiba

P-2-056　Noise estimation of phantom phase image in ultra-short echo time imaging
ultra-short echo time 位相画像のノイズ推定.
松元　友暉（徳島大学 大学院 保健科学教育部）
Yuki Matsumoto, Yuki Kanazawa, Natsuki Ikemitsu, Toshiaki Sasaki, Hiroaki Hayashi, Mitsuharu Miyoshi, Masafumi Harada, Hideki Otsuka

P-2-057　Feasibility study of visualizing tree-ring structures of dried wood with Ultra-short Echo Time (UTE) MR-imaging for chronological measurements
Ultra-short TEによる乾燥木材の年輪年代計測の試み
森　　美加（杏林大学 保健学部 診療放射線技術学科）
Mika Mori, Shigehide Kuhara, Kuninori Kobayashi, Masahisa Yamada, Atsushi Senoo

fMRI　　14：00～14：50

Chair：Tomohisa Okada（Kyoto University, Human Brain Research Center）
座　長：岡田　知久（京都大学 脳機能総合研究センター）

P-2-058　Odor induced autographical memory associated with activity in the posterior parts of the brain as well as limbic olfactory areas
香りによる自伝的記憶の想起　－帯状回後部領域賦活の検討－
渡辺　慶子（昭和大学 医学部 内科学講座神経内科学部門）
Keiko Watanabe, Yuri Masaoka, Masaki Yoshida, Nobuyoshi Koiwa, Akira Yoshikawa, Masahiro Ida, Mitsuru Kawamura, Kenjiro Ono, Masahiko Izumizaki

P-2-059　Respiratory-related neural activities in medulla and limbic system during resting and olfactory states -fMRI study-
安静時、嗅覚刺激時の呼吸に同期した辺縁系、延髄の脳活動
政岡　ゆり（昭和大学 医学部 生体調節機能学）
Yuri Masaoka, Masahiro Ida, Masaki Yoshida, Nobuyoshi Koiwa, Keiko Watanabe, Akira Yoshikawa, Ikuo Homma, Masahiko Izumizaki

P-2-060　Detecting the olfactory responses in the mouse whole brain using a cryogenic probe
クライオプローブを用いたマウス全脳の匂い応答の検出
舩津　大嗣（熊本大学大学院生命科学研究部 構造生命イメージング分野）
Hirotsugu Funatsu, Sosuke Yoshinaga, Naoya Yuzuriha, Shunsuke Kusanagi, Mitsuhiro Takeda, Hiroaki Terasawa

P-2-061　An fMRI study of the evaluation system for analgesic agents on allodynia-specific pain
アロディニア特異的な痛みに対する鎮痛薬評価系に関するfMRI研究
杠　　直哉（熊本大学大学院 生命科学研究部 構造生命イメージング分野）
Naoya Yuzuriha, Sosuke Yoshinaga, Hiroshi Sato, Sokichi Honda, Keisuke Tamaki, Toshihiro Sekizawa, Akihiko Fujikawa, Mitsuhiro Takeda, Hiroaki Terasawa

P-2-062 Optimization of the awake mouse MRI method using mouse clothes for a cryogenic coil system
Awake mouse MRI 測定法における極低温プローブに適応可能なマウス服の最適化
中田　悦史（熊本大学大学院 生命科学研究部 構造生命イメージング分野）
Etsushi Nakata, Shunsuke Kusanagi, Kazunari Kimura, Rikita Araki, Mitsuhiro Takeda, Sosuke Yoshinaga, Hiroaki Terasawa

P-2-063 Atlas based whole brain analysis with the graph theoretical approach in resting state functional connectivity MRI of neuropathic pain model mice
神経因性疼痛モデルマウスのグラフ理論に基づいた全脳網羅的解析
小牧　裕司（慶應義塾大学 医学部 生理学教室）
Yuji Komaki, Fumiko Seki, Keigo Hikishima, Masaya Nakamura, Hideyuki Okano

P-2-064 Operant Learning fMRI
オペラント学習 fMRI
久恒　辰博（東京大学 大学院新領域創成科学研究科）
Tatsuhiro Hisatsune, Keisuke Sakurai, Naohiro Jomura, Jun Kaneko

Spine　15：00～15：50

Chair：Toshiyuki Okubo（Department of Radiology, Teikyo University Chiba Medical Center）
座　長：大久保敏之（帝京大学ちば総合医療センター 放射線科）

P-2-065 Fat suppression effect　STIRon 3D-TSE with improved motion-sensitized driven equilibrium (iMSDE) for MR neurography
iMSDE併用STIR3DTSE法を用いた神経叢描出における脂肪抑制効果
梶原　　直（東海大学 医学部附属病院 診療技術部 放射線技術科）
Nao Kajihara, Kouki Hayasaka, Susumu Takano, Syuhei Shibukawa, Makoto Obara, Masami Yoneyama, Tetsu Niwa, Tomohiko Horie

P-2-066 Usefulness of Fast Spoiled Gradient Echo with three point DIXON method in the cervical spinal cord MR Myelography
頚髄MR Myelographyにおける3point DIXON法併用Fast Spoiled Gradient Echo法の有用性
上薗　博史（東海大学 医学部付属 大磯病院 放射線技術科）
Hiroshi Uezono, Yuhei Otsuka, Shiho Sakamura, Yumiko Iida

P-2-067 Depiction of brachial plexus in MRI: Low-RFA STIR-PROPELLER method vs T2FSE-IDEAL method
Low-RFA STIR-PROPELLER法とT2FSE IDEAL法における腕神経叢描出の比較検討
小野浩二郎（千葉県こども病院 検査部 放射線科）
Kojiro Ono, Takayuki Sakai, Yasuhiro Oikawa, Akira Shirayama, Atsushi Senoo

P-2-068 MR imaging of the cervical spine with respiratory gating
呼吸同期併用頸椎MRIの検討
小玉　亮一（長崎北病院 放射線科）
Ryoichi Kodama, Takeshi Ideguchi, Satoru Koura, Toshimasa Fujishita, Makoto Ochi

P-2-069 Impact of image quality due to the imaging section in Variable refocus flip angle 3D FSE (Cube)
Variable refocus flip angle 3D FSE (Cube)における撮像断面による画質の影響
小泉　百未（聖隷佐倉市民病院 放射線科）
Yumi Koizumi, Masaru Sonoda, Hideki Nagatomo

P-2-070 Evaluation of chronic inflammatory demyelinating polyradiculoneuropathy with MR neurography/T2 mapping (SHINKEI Quant)
MR neurography/T2 mapping同時収集シーケンス(SHINKEI Quant)を用いた慢性炎症性脱髄性多発神経炎の評価
樋渡　昭雄（九州大学 臨床放射線科学）
Akio Hiwatashi, Osamu Togao, Koji Yamashita, Kazufumi Kikuchi, Ryo Somehara, Ryotaro Kamei, Masami Yoneyama, Hiroshi Honda

P-2-071 Investigation of the Coronal Lumbar 3D-MERGE Imaging
腰椎冠状断面における3D-MERGEの検討
二階堂　剛（社会医療法人孝仁会 釧路脳神経外科 診療放射線科）
Tsuyoshi Nikaidou, Kenji Furukawa, Kouki Yamamoto

Diffusion 1　　13：10～13：50

Chair：Masatoshi Hori（Osaka University Graduate School of Medicine, Department of Radiology）
座 長：堀　雅敏（大阪大学大学院医学系研究科 放射線統合医学講座）

P-2-072 Is repeatability of voxel-wise ADC value satisfactory?
ボクセル単位のADC値の再現性は十分でない
小野寺耕一（札幌医科大学 医学部 放射線診断学）
Koichi Onodera, Naoya Yama, Mitsuhiro Nakanishi, Masamitsu Hatakenaka

P-2-073 The clinical assessment of upgraded Computed Diffusion-Weighted MR Imaging for prostatic cancer
前立腺癌診断における改良後Computed DWIの有用性の検討
黒川　浩典（三豊総合病院 放射線診断・IVR科）
Hironori Kurokawa, Atsushi Okamura, Shumiyo Iwata

P-2-074 Optimum b-value for WDS (weighted diffusion subtraction) in prostate cancer imaging
前立腺WDS(weighted diffusion subtraction)における至適b値
押尾　晃一（慶應義塾大学 医学部 放射線診断科）
Koichi Oshio, Hiroshi Shinmoto

P-2-075 Examination of imaging parameters by field-of-view optimized and constrained undistorted single-shot using computed diffusion weighted image
computed DWIを併用したFOCUSによる撮像条件の検討
五十嵐太郎（一般財団法人神奈川県警友会 けいゆう病院）
Taro Igarashi, Mitsuyuki Takahashi, Hiroki Hori, Tetsuichi Hondera

P-2-076 A model of water diffusion in isotropic tissue: a relationship between diffusion kurtosis and tissue microstructure
等方的組織内水拡散モデル：拡散尖度と組織微細構造との関係
田村　元（東北大学大学院医学系研究科医用物理学分野）
Hajime Tamura, Akiko Shimauchi, Naoko Mori, Tatsuo Nagasaka, Hideki Ota

P-2-077 The usefulness of Q-ball imaging tractography versus diffusion tensor tractography in gamma knife radiosurgery
ガンマナイフ治療患者におけるQ-ball imaging tractographyの有用性検討
鈴木　雄一（東京大学 医学部 附属病院 放射線部）
Yuichi Suzuki, Hirotaka Hasegawa, Minoru Mitsuda, Akihiro Kasahara, Kanako Matsuda, Takeo Sarashina, Yasushi Watanabe, Kenji Ino, Masahiro Shin, Jiro Sato, Keiichi Yano, Nobuto Saito, Akira Kunimatsu

Diffusion 2　　14：10～14：50

Chair：Manabu Minami（University of Tsukuba, Dept. of Diagnostic & Interventional Radiology）

座 長：南　　学（筑波大学 放射線医学）

P-2-078 Correlation between DWI bi-exponential estimates and PET hypoxia imaging activities in head and neck carcinoma

拡散強調MRIのbi-exponentialパラメーターと低酸素イメージングパラメーターとの関連性

今泉　晶子（放射線医学総合研究所 医工連携画像研究チーム）

Akiko Imaizumi, Takayuki Obata, Masayuki Inubushi, Mitsuru Koizumi, Kyosan Yoshikawa, Ming-Rong Zhang, Katsuyuki Tanimoto, Rintaro Harada, Takashi Uno, Tsuneo Saga

P-2-079 Intravoxel incoherent motion diffusion imaging of the liver in Fontan circulation: Comparison with the liver in normal circulation

Fontan循環肝臓のIntravoxel incoherent motion(IVIM)-DWI：正常循環との比較

小野浩二郎（千葉県こども病院 検査部 放射線科）

Kojiro Ono, Kazuhiro Shiraga, Takumi Okubo, Hirofumi Watanabe, Hiromichi Nakajima, Atsushi Senoo, Akira Shirayama

P-2-080 Comparison of image artifacts between DWIBS using single-shot TSE (TSE-DWIBS) and DWIBS using echo-planner imaging (EPI-DWIBS) at 3T MRI scanner

3T-MRIにおける直接冠状断TSE-DWIBSとEPI-DWIBSのアーチファクトの比較

鈴木　真（東京女子医科大学病院 中央放射線部）

Makoto Suzuki, Yuki Hachiman, Masami Yoneyama, Yu Nishina, Satoru Morita

P-2-081 Basic study on Parameters of Direct Coronal Diffusion-weighted Whole Body Imaging with Background Body Signal Suppression without SENSE

SENSEを用いないDirect Coronal DWIBSにおける撮像条件の基礎的検討

佐藤　広崇（草加市立病院 医療技術部 放射線科）

Hirotaka Sato, Hirokazu Kato, Mamoru Okubo, Junrou Yamamoto, Tsuneaki Nakagawa, Namiko Matsui

P-2-082 FOCUS(Fov Optimized and Constrained Undistorted Single-shot) for the whole body DWI: A comparison of image quality between FOCUS and conventional DWI

Whole Body Coronal DWIにおけるFOCUSと従来撮像法における画像の比較

松永　奈美（GEヘルスケア・ジャパン株式会社 MRマーケティング）

Nami Matsunaga, Masanori Ozaki

P-2-083 Effect of imaging object on optimal b-value sampling for intravoxel incoherent motion imaging

Intravoxel incoherent motion imagingにおいて撮像対象がb値の最適化に与える影響

横沢　俊（株式会社 日立製作所 研究開発グループ）

Suguru Yokosawa, Hisaaki Ochi, Yoshihisa Soutome, Yoshitaka Bito

Diffusion 3　　15：20～16：20

Chair：Masahiro Ida（Tokyo Metropolitan Ebara Hospital Department of Radiology）

座 長：井田　正博（荏原病院 放射線科）

P-2-084 Ventricular volumetry and anterior thalamic radiation on DTI of idiopathic normal pressure hydrocephalus after a lumboperitoneal shunt

LPシャント術前後のiNPHの脳室体積測定と拡散テンソルトラクトグラフィ解析

齊藤　麻美（横浜市立大学）

Asami Saito, Koji Kamagata, Ryo Ueda, Misaki Nakazawa, Andica Christina, Sho Murata, Madoka Nakajima, Masakazu Miyajima, Kouhei Kamiya, Masaaki Hori, Kanako Kumamaru, Michimasa Suzuki, Hajime Arai, Shigeki Aoki

P-2-085 Cortico-subcortical white matter connectivity disruption in schizophrenia
皮質-皮質下構造間コネクティビティに着目した統合失調症の白質神経回路異常の検討
奥畑　志帆（京都大学大学院 工学研究科）
Shiho Okuhata, Satoki Yoda, Naohiro Okada, Noriaki Yahata, Kiyoto Kasai, Tetsuo Kobayashi

P-2-086 Investigation of DWI by multiplexed sensitivity encoding (MUSE)
MUSE法を用いたDWIの検討
野崎　　敦（GEヘルスケア・ジャパン 研究開発部）
Atsushi Nozaki, Hiroyuki Kabasawa, Yoshinobu Nunokawa, Rikiya Fujishiro, Shigeo Okuda, Hirokazu Fujiwara, Masahiro Jinzaki

P-2-087 Functional and structural reorganization before and after repetitive transcranial magnetic stimulation plus intensive occupational therapy
脳卒中後上肢片麻痺患者を対象としたrTMS・集中的OT併用療法前後の機能と構造の再編成
上田　　亮（首都大学東京大学院 人間健康科学研究科 放射線科学域）
Ryo Ueda, Naoki Yamada, Masahiro Abo, Atsushi Senoo

P-2-088 Simultaneous Multi-Slice RESOLVE DWI: comparison of single shot technique by Diffusion tensor and Kurtosis tractography
拡散テンソル・拡散尖度画像におけるSMS-RESOLVEの有用性の検討
福永　一星（順天堂大学医学部附属 順天堂医院 放射線科・部）
Issei Fukunaga, Masaaki Hori, Nozomi Hamasaki, Shuji Sato, Ryo Ueda, Hideo Kawasaki, Nao Takano, Syo Murata, Kouhei Tsuruta, Haruyosi Hoshito, Katsutoshi Murata, Shigeki Aoki

P-2-089 Optimal strategy for measuring intraventricular temperature using acceleration motion compensation DWI
加速度補正型DWIによる脳温度測定
渋川　周平（東海大学 医学部 付属病院 放射線技術科）
Shuhei Shibukawa, Naoki Ohno, Toshiaki Miyati, Susumu Takano, Tetsu Niwa, Tetsuo Ogino, Tomohiko Horie, Nao Kajihara

P-2-090 Brain structural connectivity and five-factor personality measures in healthy adults
脳内ネットワークとNEO-FFI性格検査の5因子との関係：正常成人における検討
上田　一生（産業医科大学 医学部 放射線科）
Issei Ueda, Shingo Kakeda, Keita Watanabe, Koichiro Sugimoto, Natsuki Igata, Asuka Katsuki, Junji Moriya, Reiji Yoshimura, Osamu Abe, Yukunori Korogi

P-2-091 Relationship between a BDNF gene polymorphism and the brain structural networks in major depressive disorder patients: a connectome analysis with DTI
BDNF遺伝子Val166Met多型におけるうつ病患者の脳内ネットワーク変容:テンソル画像を用いたコネクトーム解析
杉本康一郎（産業医科大学 医学部 放射線科）
Koichiro Sugimoto, Shinzo Kakeda, Keita Watanabe, Issei Ueda, Natsuki Igata, Asuka Katsuki, Junji Moriya, Reiji Yoshimura, Osamu Abe, Yukunori Korogi

P-2-092 Quantitative comparison between conventional and accelerated NODDI maps of the brain
脳NODDI解析：線形化・凸最適化による高速法と原法との解析結果の対比
上口　貴志（情報通信研究機構 脳情報通信融合研究センター）
Takashi Ueguchi, Ikuhiro Kida, Yasushi Kobayashi, Ken-ichi Okada, Yoshinori Kadono, Sachiko Yamada, Guoxiang Liu

Pelvis　　13：10～14：00

Chair：Yoshimitsu Ohgiya（Showa University School of Medicine Department of Radiology, Division of Radiology）

座 長：扇谷　芳光（昭和大学医学部 放射線医学講座 放射線科学部門）

P-2-093 Value of automated quantitative 6-point Dixon MR imaging in distinguishing for cystic ovarian lesions

卵巣ののう胞性腫瘤の鑑別診断における6-point Dixonの有用性に関する検討

清水　紀恵（熊本大学医学部附属病院 中央放射線部）

Kie Shimizu, Tomohiro Namimoto, Masataka Nakagawa, Masahumi Kidou, Takeshi Nakaura, Seitaro Oda, Daisuke Utsunomiya, Yasuyuki Yamashita

P-2-094 Evaluation of depth of myometrial invasion in endometrial cancer: Comparison of reduced FOV DWI and DCE-MRI

子宮体癌における筋層浸潤の評価：Reduced FOV DWIおよびDCE-MRIによる検討

竹内麻由美（徳島大学 医学部 放射線科）

Mayumi Takeuchi, Kenji Matsuzaki, Masafumi Harada

P-2-095 MR Imaging Characteristics of Ovarian Endometrioid Carcinoma Resembling Sex-Cord Stromal Tumor

卵巣のEndometrioid Carcinoma Resembling Sex-Cord Stromal TumorのMR所見の評価検討

小澤　栄人（埼玉医科大学 放射線科）

Eito Kozawa, Iichirou Oosawa, Kaiji Inoue, Tomomi Katou, Masanori Yasuda, Kousei Hasegawa, Tomoaki Ichikawa, Mamoru Niitsu

P-2-096 Feasibility of diffusion kurtosis imaging as a tool for differentiation between benign and malignant uterine lesions

子宮病変の良悪性診断における拡散尖度MR画像の有用性の検討

熊谷　雄一（鹿児島大学 医学部歯学部付属病院 放射線科）

Yuichi Kumagae, Yoshihiko Fukukura, Koji Takumi, Hiroto Hakamada, Takashi Iwanaga, Masashi Sasaki, Takuro Fujisaki, Tomoyuki Okuaki, Takashi Yoshiura

P-2-097 Post contrast 3D isotropic VIBE images at earlier phase for diagnosis of myometrial invasion of uterine endometrial cancer

造影早期の 3D isotropic VIBE 画像による子宮内膜癌の筋層浸潤評価

高畑　暁子（京都府立医科大学 放射線科）

Akiko Takahata, Kouji Sakai, Mariko Goto, Sachimi Yamada, Kei Yamada

P-2-098 Evaluation of motion artifact using readout segmented echo-planer imaging in pelvic imaging

骨盤部撮像でのreadout segmented echo-planer imagingの体動による影響の評価

斉藤　宏明（新潟大学医歯学総合病院 診療支援部 放射線部門）

Hiroaki Saito, Tatsuya Kondo, Tsutomu Kanazawa

P-2-099 Prenatal diagnosis of tuberous sclerosis complex with different renal appearance using MRI

腎所見が異なる結節性硬化症のMRIによる出生前診断

桑島　成子（獨協医大 放射線医学教室）

Shigeko Kuwashima

P-2-100 Quantitative analysis of circulatory function for prostate tumors using reference tissue model in DCE-MRI studies

ダイナミック造影MRIにおける参照領域法を用いた前立腺腫瘍の循環動態の定量評価

生駒　洋子（量子科学技術研究開発機構 放射線医学総合研究所）

Yoko Ikoma, Takayuki Obata, Yasuhiko Tachibana, Tokuhiko Omatsu, Riwa Kishimoto, Hiroshi Tsuji

Musculoskeletal　14：30～15：00

Chair：Masataka Uetani（Nagasaki University Department of Radiology）
座 長：上谷　雅孝（長崎大学 放射線科）

P-2-101 The influence Echo Space exerts on T2 contrast
Echo SpaceがT2コントラストに及ぼす影響
園田　　優（聖隷佐倉市民病院 放射線科）
Masaru Sonoda, Yumi Koizumi

P-2-102 Study of upper limb imaging Positions in consideration of the static magnetic field inhomogeneity
静磁場不均一を考慮した上肢撮像体位の検討
岡田　敦彦（国立病院機構 大阪医療センター 医療技術部 放射線科）
Atsuhiko Okada

P-2-103 Analysis of muscle activity using T2 relaxation time and T2w-MRI by progressive resistance exercise on wrist flexion
T2強調画像とT2緩和時間による手関節屈曲漸増抵抗運動の活動筋分析
秋山　純和（人間総合科学大学 保健医療学部 リハビリテーション学科）
Sumikazu Akiyama, Masayoshi Takamori, Kazuya Yoshida, Hayato Ishizaka, Tomoyuki Haishi, Hiroshi Otsuka, Yoshiteru Seo

P-2-104 Muscle activity analysis of the Extensor digiti minimi muscle and Extensor indicis muscle by MRI method
MRI法による示指伸筋と小指伸筋の筋活動分析
吉田　一也（獨協医科大学 生理学（生体制御））
Kazuya Yoshida, Sumikazu Akiyama, Masayoshi Takamori, Hiroshi Otsuka, Yoshiteru Seo

P-2-105 Optimization of MR Arthrography Protocol of the Shoulder using 3D-FSE Sequence with Variable Refocusing Flip Angle
Fat Sat Variable Refocusing Flip Angle 3D-T2-FSE法を用いた肩関節MR Arthrographyの基礎的検討
本寺　哲一（昭和大学 藤が丘病院 放射線室）
Tetsuichi Hondera, Junya Nakashima, Toshiyuki Takahashi, Ken Shinohara, Kyoichi Kato, Yasuo Nakazawa

Breast　15：30～16：00

Chair：Katsuya Maruyama（Siemens Healthcare K.K.）
座 長：丸山　克也（シーメンスヘルスケア株式会社）

P-2-106 Usefulness of auto scale subtraction in the Contrast-enhanced breast MRI
乳腺造影MRIでのauto scale subtractionの有用性
千嶋　昭夫（メディカルスキャニング新宿）
Akio Chishima, Keiichi Doutanuki, Tatsuya Miyazaki, Yuu Katou

P-2-107 An evaluation of silicon imaging using the 3-point DIXON method
3point-DIXON法を用いたシリコンイメージの検討
坪内　隆将（木沢記念病院 放射線技術課）
Takamasa Tsubouchi, Saki Yoshimura, Kenji Sakou, Rikiya Syouji, Hiroki Nishibori, Mika Takagi

P-2-108 Does fat suppression method Influence on T1 measurement?: Oil-in-water emulsion phantom study
T1値測定に脂肪抑制法は影響を与えるか？：油-水-エマルジョンファントムによる検討
池野　寛康（京都府立医科大学附属病院 放射線部）
Hiroyasu Ikeno, Koji Sakai, Hiroshi Imai, Toshiaki Nakagawa, Mariko Goto, Tsunao Kishida, Osamu Mazda, Kei Yamada

P-2-109 Retrospective Study of Injection Condition in Breast MRI
乳腺MRIにおける造影剤注入条件に関する後方視的検討
小塚　雪乃（東京都保健医療公社 豊島病院 放射線科）
Yukino Kozuka, Satoshi Honda, Yoichi Okada, Toshiyuki Onodera, Masanori Yamamoto, Kikuo Fujinami, Akira Yamashita

P-2-110 Evaluation of an MRI-Powered Robotic Sysytem for Cryoablation
MRガイド下凍結治療支援ロボットシステムの基礎的評価
五月女康作（筑波大学 サイバニクス研究センター）
Kousaku Saotome, Ryutaro Ouchi, Akira Matsushita, Mitsuhiro Tozaki, Kenji Suzuki, Yoshiyuki Sankai

Day 3…… Poster Room (Sonic City Building, B1F, Exhibition Hall No.2～No.5)

Head and neck　　9：10～10：10

Chair：Keiko Toyoda（Department of Radiology, Teikyo University School of Medicine）
座　長：豊田　圭子（帝京大学医学部放射線科学講座）

P-3-001 Optimization of the imaging of sagittal section Turbo Spin Echo-DWI in the pituitary region
下垂体領域における矢状断Turbo Spin Echo-DWIの撮像条件の最適化
圓崎　将大（宮崎大学医学部附属病院 放射線部）
Masahiro Enzaki, Toshiya Azuma, Tomomi Sumiyoshi, Takanori Yano, Yoshihito Kadota, Minako Azuma, Toshinori Hirai

P-3-002 Semi-automated segmentation to evaluate hypertrophy of the brachial plexus in chronic inflammatory demyelinating polyneuropathy
慢性炎症性脱髄性多発神経障害における腕神経叢肥厚解析のための領域分割法
川口　拓之（産業技術総合研究所 人間情報研究部門）
Hiroshi Kawaguchi, Hajime Yokota, Hiroki Mukai, Kazumoto Shibuya, Hitoshi Shimada, Shoichi Ito, Tetsuya Suhara, Takashi Uno, Satoshi Kuwabara

P-3-003 Evaluation of new hemodynamic and structural imaging of the subclavian arteries using Turbo-CINEMA
Turbo-CINEMA法を用いた鎖骨下動脈領域における描出能の検討
蓼沼　　仁（東京女子医科大学病院 中央放射線部）
Hitoshi Tadenuma, Kayoko Abe, Masami Yoneyama, Yasuhiro Goto, Mamoru Takeyama, Syuji Sakai

P-3-004 PET/MR versus PET/CT in the Initial Staging of Head and Neck Cancer
初発頭頸部癌ステージングに対するPET/CTとPET/MRの診断能比較；PET/CT/MR機での検討
関根　鉄朗（日本医科大学 放射線科）
Tetsuro Sekine, Barbosa Felipe, Kuhn Felix, Burger Irene, Delso Gaspar, Ter Voert Edwin, Veit-Haibach Patrick, Huellner Martin W

P-3-005 Local resectability assessment of head and neck cancer, PET/MR versus PET/CT
頭頸部癌の切除可能性評価に対するPET/CTとPET/MRの診断能比較
関根　鉄朗（日本医科大学 放射線科）
Tetsuro Sekine, Barbosa Felipe, Delso Gaspar, Ter Voert Edwin, Veit-Haibach Patrick, Huellner Martin W

P-3-006 Comparison of the image quality of turbo spin echo- and echo-planar diffusion-weighted images of the oral cavity region
口腔領域でのturbo spin echo (TSE) DWIとecho-planar imaging (EPI) DWIの比較検討
平田健一郎（熊本大学 医学部 画像診断科）
Kenichiro Hirata, Takeshi Nakaura, Tomoyuki Okuaki, Masafumi Kidoh, Seitaro Oda, Daisuke Utsunomiya, Tomohiro Namimoto, Mika Kitajima, Hideki Nakayama, Yasuyuki Yamashita

P-3-007 Utility of PROPELLER DWI in head and neck region
頭頚部領域におけるPROPELLER DWIの有用性
嶋田　諭（国保直営総合病院 君津中央病院）
Satoshi Shimada, Hazuki Watanabe, Takashi Tsukaya, Ryu Emura, Hironori Yamamoto

P-3-008 Endolymphatic volume ratio measurement using region growing method
内リンパ体積比の定量（用手法と Region growing 法の比較）
小川絵莉子（総合上飯田第一病院 放射線科）
Eriko Ogawa, Toshio Ohashi, Toshio Katagiri, Kayao Kuno, Shinji Naganawa

P-3-009 Optimization of Variable Flip Angle 3D T1WI MPV (Multi Planar Voxel) in Head and Neck Imaging
Variable Flip Angle 3DT1WI（MPV：Multi Planer Voxel）の頭頸部での最適化
河野奈々恵（東芝メディカルシステムズ株式会社）
Nanae Kawano, Ayako Ninomiya, Miho Kitamura, Hiroshi Kusahara

Brain applied　9：10～9：50

Chair：Yuichi Suzuki（The University of Tokyo Hospital Department of Radiology）
座 長：鈴木　雄一（東京大学医学部附属病院 放射線部）

P-3-010 Anatomical labeling with belief propagation in Bayes estimation for human brain
信念伝播法を用いたベイズ推定による脳画像の自動ラベリング手法の検討
山本　詩子（京都大学 情報学研究科 システム科学専攻）
Utako Yamamoto, Masayuki Ohzeki, Tomoyuki Hiroyasu, Megumi Nakao, Tetsuya Matsuda

P-3-011 Tissue time intensity curve behavior of gadobutrol bolus injection
脳灌流MRIにおけるガドブトロールの組織信号強度の検討
山田　将大（トヨタ記念病院 放射線科）
Masahiro Yamada, Toshiaki Taoka, Yasushi Niinomi, Ai Kawaguchi, Kenji Yasuda, Yoichi Ohashi, Takahito Okuda, Shinji Naganawa

P-3-012 The relationship between diffusional kurtosis imaging with the neurite density in a confocal microscopy of the cleared mouse brain
透明脳マウスにおける次世代拡散MRI(DKI)と共焦点顕微鏡による神経線維密度の関係
入江　隆介（順天堂大学 医学部 放射線科）
Ryusuke Irie, Koji Kamagata, Aurelien Kerever, Suguru Yokosawa, Yosuke Otake, Hisaaki Ochi, Kazuhiko Tagawa, Hitoshi Okazawa, Kohske Takahashi, Kanako Sato, Masaaki Hori, Eri Arikawa-Hirasawa, Shigeki Aoki

P-3-013 Intravoxel incoherent motion analysis using diffusional kurtosis imaging: a simulation study
Diffusional kurtosis imaging を用いた intravoxel incoherent motion 解析: シミュレーションによる検討
梅沢　栄三（藤田保健衛生大学 医療科学部 放射線学科）
Eizou Umezawa, Masahiro Kawasaki, Masayuki Yamada, Takashi Fukuba, Kazuhiro Murayama

P-3-014 Initial examination for the quantitative evaluation of MR-NM image -with DatSCAN-
MRI神経メラニン画像の定量評価に向けた初期検討 -DaTSCANとの比較-
小野寺聡之（東京都保健医療公社 荏原病院 放射線科）
Toshiyuki Onodera, Toshiki Wakayama, Miwa Sasaki, Ken Yashiro, Takashi Ueda, Kenji Saito, Akira Yamashita, Masahiro Ida

P-3-015 Optimization of MR Imaging Parameters for Neuromelanin Imaging of the Substantia Nigra
黒質神経メラニンイメージングの撮像条件最適化
中田　直（おさか脳神経外科病院 放射線部）
Sunao Nakata, Yuji Miyatake, Yasuaki Kamada, Yuko Takahashi, Naomi Honjo

PET/MR　10：20～10：50

Chair：Hitoshi Kubo（Fukushima Medical University, Advanced Clinical Research Center）
座 長：久保　均（福島県立医科大学 先端臨床研究センター）

P-3-016 ADC-corrected SUV derived from voxel-based SUV-ADC scatter plots in FDG-PET/MR hybrid imaging: Concept, techniques, and clinical applications
ADCで補正した新たな定量的指標computed SUV：概念、技術、臨床応用
渡邊　祐司（九州大学大学院 医学研究院 分子イメージング診断学）
Yuji Watanabe, Koji Sagiyama, Ryotaro Kamei, Sungtak Hong, Satoshi Kawanami, Yoshihiro Matsumoto, Hiroshi Honda

P-3-017 PET/MR outperforms PET/CT in suspected occult tumors
原発不明癌に対するPET/CTとPET/MR診断能比較
関根　鉄朗（日本医科大学 放射線科）
Tetsuro Sekine, Barbosa Felipe, Sah Bert-Ram, Cacilia Mader, Delso Gaspar, Ter Voert Edwin, Veit-Haibach Patrick, Huellner Martin W

P-3-018 Clinical evaluation of ZTE attenuation correction for brain FDG-PET/MR imaging, comparison with atlas attenuation correction
Zero-echo-TEによる頭蓋骨推定を用いた頭部PET/MR吸収補正法の検討
関根　鉄朗（日本医科大学 放射線科）
Tetsuro Sekine, Ter Voert Edwin, Warnock Geoffrey, Buck Alfred, Huellner Martin, Veit-Haibach Patrick, Delso Gaspar

P-3-019 Multi atlas-based attenuation correction for brain FDG-PET imaging
PET/MR頭部吸収補正における臨床用single-Atlas法とMulti-Atlas法の比較
関根　鉄朗（日本医科大学 放射線科）
Tetsuro Sekine, Burgos Ninon, Warnock Geoffrey, Huellner Martin, Buck Alfred, Ter Voert Edwin, Ourselin Sebastien, Hutton Brian, Veit-Haibach Patrick, Delso Gaspar

P-3-020 Detection of ground-glass opacity lesions using breath-hold black-blood magnetic resonance imaging of the lungs
Black-blood 脂肪抑制T2強調像を用いた限局性肺すりガラス影検出能の検討
亀井僚太郎（九州大学大学院 医学研究院 臨床放射線科学分野）
Ryotaro Kamei, Yuji Watanabe, Koji Sagiyama, Satoshi Kawanami, Hiroshi Honda

Pulse sequence　9：10～9：40

Chair：Makoto Obara（Philips Electronics Japan）
座 長：小原　真（株式会社フィリップスエレクトロニクスジャパン）

P-3-021 Comparison of fat suppression images by using balanced steady-state free precession sequences: a multi-vendor study
Balanced steady state free precession sequenceにおける脂肪抑制効果の装置間の比較-多施設評価-
上山　毅（彩都友紘会病院 放射線部）
Tsuyoshi Ueyama, Hiroyuki Tarewaki, Yuya Yamatani, Masaaki Kajisako, Kenichirou Yamamura

P-3-022 Comparison of contrasts by using balanced steady-state free precession sequences: a multi-vendor study
Balanced steady-state free precession sequenceにおけるコントラストの装置間の比較-多施設評価
垂脇　博之（大阪大学医学部附属病院 放射線部）
Hiroyuki Tarewaki, Tsuyoshi Ueyama, Yuya Yamatani, Masaaki Kajisako, Kenichirou Yamamura

P-3-023 Consideration of the effect of metal artifact suppression with combination of mDixon-XD and O-MAR
mDIXON-XDとO-MAR併用による金属アーチファクト抑制効果の検討
牛島　大悟（株式会社フィリップスエレクトロニクスジャパン ISビジネスグループ）
Daigo Ushijima, Atsushi Takemura, Yasutomo Katsumata, Akira Suwa, Futoshi Nakagawa

P-3-024 Optimization of a noise reduction parameter using the Brain routine 3 sequences
頭部用シーケンスを用いた静音化パラメータの検討
川又　　渉（秋田県厚生連 かづの厚生病院）
Wataru Kawamata

Hyperpolarization　　10：10～10：40

Chair：Hidehiro Watanabe（National Institute for Environmental Studies）
座 長：渡邉　英宏（国立環境研究所）

P-3-025 Construction of a parahydrogen-induced hyperpolarized 13C MRI system for metabolic imaging
PHIP型の超偏極 13C MRI代謝イメージングシステムの構築
内尾　佳貴（北海道大学大学院 情報科学研究科）
Yoshiki Uchio, Hiroshi Hirata, Shingo Matsumoto

P-3-026 Development of s para-hydrogen induced polarization (PHIP) type hyperpolarizer system for hyperpolarized metabolic 13C MRI
超偏極13C　MRI代謝イメージングのためのパラ水素誘起分極(PHIP)型13C核励起装置の開発
中西沙由里（北海道大学 大学院 情報科学研究科 生命人間情報科学専攻）
Sayuri Nakanishi, Shingo Matsumoto, Hiroshi Hirata

P-3-027 An Attempt to Evaluate the Progression of Lung Cancer in Mice by means of Hyperpolarized ^{129}Xe MRI
超偏極^{129}Xe MRIを用いた肺がんモデルマウスの病態進行評価に対する試み
下川　晃弘（大阪大学大学院 医学系研究科 保健学専攻 医療技術科学分野 医用物理工学講座）
Akihiro Shimokawa, Shota Hodono, Yu Ozaki, Naoto Miyazaki, Atsuomi Kimura

P-3-028 Ultra-Low Field MRI with Optically Pumped Atomic Magnetometer: Hyperpolarized ^{129}Xe Imaging
光ポンピング原子磁気センサ用いた超低磁場MRIの実現：超偏極^{129}Xeイメージング
山本　哲也（京都大学 大学院工学研究科）
Tetsuya Yamamoto, Takenori Oida, Hiroaki Natsukawa, Ingo Hilschenz, Yosuke Ito, Tetsuo Kobayashi

P-3-029 Hyperpolarized xenon imaging with SWIFT approach in ultra-low field MRI
超低磁場MRIにおける超偏極XeのSWIFT法による画像化
笈田　武範（京都大学 大学院工学研究科）
Takenori Oida, Yuki Kaga, Tetsuya Yamamoto, Tetsuo Kobayashi

Day 1~3 …… Poster Room (Sonic City Building, B1F, Exhibition Hall No.2~ No.5)

PDF-001 Comparison of MRI and CT for acute traumatic brain in
頭部外傷に対する急性期MRI,CTの比較検討
藏本　智士（香川県立中央病院 脳神経外科）
Satoshi Kuramoto, Hikari Matsumura, Akira Takeuchi, Atsushi Katsumata, Masamitsu Kawauchi

PDF-002 Diagnostic Imaging of ASL perfusion in the grading of Non-enhancing Astrocytic Tumors
ハシバット　デルゲルダライ（徳島大学放射線科）
Delgerdalai Khashbat, Masafumi Harada, Takashi Abe, Mungunbagana Ganbold

PDF-003 Utility of Dynamic Contrast-Enhanced (DCE) MRI in Predicting Prognosis of Enhancing Lesions Persisting after Completion of Adjuvant Temozolomide in Glioblastoma Patients
Sung-Hye You, Roh-Eul Yoo, Seung Hong Choi

PDF-004 Usefulness of cranial nerve system contrast ehnaced imaging using the MPG combined 3D-GRE (FSBB)
MPG併用3D-GRE(FSBB)を使用した脳神経系造影検査の有用性について
平田　恵哉（金沢医科大学病院 医療技術部 診療放射線技術部門）
Keiya Hirata, Yuuichi Murasaki, Tatsunori Kuroda, Chihiro Watari, Nanako Miyamoto, Saeko Tomida, Tomokazu Oku, Shigeo Miyazaki, Masahiro Kawashima

PDF-005 Initial evaluations of conventional contrast images on a 7T-MRI system
7T-MRIによる通常コントラスト画像の初期評価
岡田　知久（京都大学 大学院 医学研究科）
Tomohisa Okada, Hideto Kuribayashi, Yuta Urushibata, Junko Inoue

PDF-006 Investigation of improved Motion Sensitized Driven Equilibrium (iMSDE) for intracranial contrast-enhanced 3D black-blood imaging
improved Motion Sensitized Driven Equilibrium (iMSDE) を併用した頭部造影3D撮像法の検討
岩本　勝一（函館脳神経外科病院）
Shoichi Iwamoto, Masaaki Ichinoseki, Makoto Obara, Takashi Namiki

PDF-007 The MR-based 3D-reconstruction image of the skull using 3D-FIESTA-C sequence; evaluation of the clinical utility
3D FIESTA-Cを用いたMRI 3D再構成頭蓋骨画像の臨床的有用性についての検討
林　　哲司（札幌麻生脳神経が科病院 放射線科）
Tetsuji Hayashi, Akiyoshi Hamaguchi, Noriyuki Fujima

PDF-008 Tradeoff between image quality and acoustic noise reduction in quiet sequence of turbo spin echo
静音化TSE法における画質と静音化に関する至適条件の検討
高橋　一広（秋田県立脳血管研究センター 放射線科診療部）
Kazuhiro Takahashi, Hideto Toyoshima, Kazuhiro Nakamura, Toshibumi Kinoshita

PDF-009 Study of brain aneurysm 4D FLOW analysis by MRI
MRIによる脳動脈瘤4D―FLOW解析の検討
関根　麻生（メディカルスキャニング お茶の水）
Mau Sekine, Yuu Ishizaka, Tatsuya Miyazaki, Takuma Nishiwaki

PDF-010 Consideration of Neuromelanin Imaging parameters using Simultaneous Multi-Slice Turbo Spin Echo
Simultaneous Multi-Slice Turbo Spin Echoを利用したNeuromelanin Imagingの撮像パラメータの検討
村田　　渉（順天堂大学放射線科・部）
Syo Murata, Koji Kamagata, Katsutoshi Murata, Misaki Nakazawa, Masaaki Hori, Kanako Kumamaru, Michimasa Suzuki, Issei Fukunaga, Asami Saito, Andica Christina, Syuji Sato, Nozomi Hamasaki, Ryo Ueda, Kohei Tsuruta, Haruyoshi Houshito, Shigeki Aoki

PDF-011 A functional study of the number of phase in the head MRA using mUTE 4D-MRA
mUTE 4D-MRAを用いた頭部MRAにおけるphase数の検討
高松　慎（東芝メディカルシステムズ株式会社）
Shin Takamatsu, Chiemi Yamauchi, Hisae Chiba, Yoshihito Miyamoto, Tsutomu Koto

PDF-012 Assessment of the accuracy and precision of the gadolinium concentration map using synthetic MRI
Synthetic MRIを用いたガドリニウム濃度マップの確度と精度についての評価
中澤　美咲（首都大学東京人間健康科学研究科放射線科学域）
Misaki Nakazawa, Akifumi Hagiwara, Christina Andica, Masaaki Hori, Ryo Ueda, Nao Takano, Sho Murata, Shuji Sato, Nozomi Hamasaki, Hideo Kawasaki, Haruyoshi Houshito, Shigeki Aoki, Atsushi Senoo

PDF-013 MRI-based characterization of lifespan development in common marmosets
コモンマーモセットにおける脳発達MRI解析
関　布美子（慶應義塾大学 医学研究科）
Fumiko Seki, Yuji Komaki, Junichi Hata, Akiko Uematsu, Keigo Hikishima, Erika Sasaki, Hideyuki Okano

PDF-014 Comparison of voxel-based morphometry (VBM) analysis and absolute T_1 value analysis
Daehun Kang, Yul-Wan Sung, Seiji Ogawa

PDF-015 Study of carotid plaque depiction performance at the T1WI using 3D MPV
3D MPVによるT1強調画像での頚部プラーク描出能の検討
福場　崇（藤田保健衛生大学病院 放射線部）
Takashi Fukuba, Kazuhiro Murayama, Ayako Ninomiya, Masato Ikedo, Akiyoshi Iwase, Yutaka Kinomura

PDF-016 Analysis of imaging parameters in dynamic imaging of mandibular movement
下顎運動のMRI動的撮像法における撮像パラメータの分析
中井　隆介（中部大学 生命健康科学部）
Ryusuke Nakai, Takashi Azuma, Mariko Wakatsuki, Hideki Hashimoto, Seiji Yamaguchi, Hiroaki Takadama

PDF-017 3D Quantitative MR Lymphography using the improved Motion Sensitized Driven Equilibrium (iMSDE) pre-pulse
iMSDE pre-pulseを用いた定量的な3D MR Lymphography
青池　拓哉（北海道大学病院 医療技術部 放射線部門）
Takuya Aoike, Noriyuki Fujima, Masami Yoneyama, Suzuko Aoike, Kinya Ishizaka, Kohsuke Kudo

PDF-018 Clinical feasibility of dual acceleration 3D-TOF-MRA
2種類の高速撮像法を併用した3D-TOF-MRAの評価
金本　雅行（福井大学 医学部附属病院 放射線部）
Masayuki Kanamoto, Shota Ishida, Naoyuki Takei, Toshiki Adachi, Hiroyuki Kabasawa, Hirohiko Kimura

PDF-019 Study of carotid artery plaque imaging using mDIXON-XD with Inversion Recovery
mDIXON-XDとIR法を用いた頸動脈プラークイメージングの検討
堀野由香梨（国家公務員共済組合連合会 熊本中央病院）
Yukari Horino, Seiichirou Noda, Nobuyuki Toyonari, Masami Yoneyama

PDF-020 Initial Evaluation of the mUTE Sequence in Lung Imaging
mUTEを用いた肺撮像の初期検討
千葉　寿恵（東芝メディカルシステムズ株式会社 MRI営業部）
Hisae Chiba, Yuichi Yamashita, Yasutaka Sugano, Masaaki Umeda, Naotaka Sakashita

PDF-021 Evaluation of the effects of heart rate and corrections in T1 measurement using MOLLI on 3T MRI
3T MRI MOLLI法を用いたT1計測の心拍数の影響と補正法の検討
植木　渉（国立循環器病研究センター）
Wataru Ueki, Yoshiaki Morita, Masaru Shiotani, Mutsumi Adachi, Toshiya Sano, Yoshiaki Komori

PDF-022 Optimum conditions to measure the peripheral vasculature using the balanced TFE technique prior to transcatheter aortic valve implantation
3DBTFE法を用いた径カテーテル大動脈弁留置術前における末梢血管計測のための最適条件の検討
妹尾　大樹（埼玉医科大学国際医療センター 中央放射線部）
Taiki Senoo, Yasuo Sakurai, Masanori Morita, Kenji Abe, Kazuya Okabe, Kasumi Shiga, Yasuyuki Yoshimura

PDF-023 Evaluation of Areas for Blood T1 Value Measurement in ECV Mapping
ECV算出における血液のT1値測定部位の検討
高済　英彰（福島県立医科大学医学部附属病院 放射線部）
Hideaki Takasumi, Shinya Seino, Hironobu Ishikawa, Takashi Kanezawa, Naoki Watanabe, Takanori Sato, Shuhei Bannae

PDF-024 Myocardial T1 mapping using T1-weighted turbo field echo (T1-TFE) sequence at 3.0 T
3.0 T装置におけるT1-weighted turbo field echo (T1-TFE)を用いた心筋のT1マッピング
木田　勝博（岡山赤十字病院 放射線科）
Katsuhiro Kida, Sachiko Goto, Takamasa Kurosaki, Masaki Ikeda, Tsutomu Kajitani, Yoshiharu Azuma

PDF-025 Inducibility of Ventricular Arrhythmia is Correlated to Viability of the Peri-Infarct Region
心室性不整脈の誘発と梗塞周囲における生存領域との関係性の評価
橘　篤志（AIC八重洲クリニック）
Atsushi Tachibana, Junaid Zaman, Hiromi Sano, Michelle Santoso, Phillip Yang

PDF-026 Colorectal Carcinoma: Diffusion Kurtosis MR Imaging Ex Vivo for Evaluation of Histologic Grades and Lymph Node Metastasis
大腸癌：DKIによるEx Vivoでの組織学的分化度とリンパ節転移の検討
山田　一郎（東京医科歯科大学 大学院医歯学総合研究科 画像診断・核医学分野）
Ichiro Yamada, Keigo Hikishima, Norio Yoshino, Shinichi Yamauchi, Naoyuki Miyasaka, Hiroyuki Uetake, Masamichi Yasuno, Yukihisa Saida, Ukihide Tateishi, Daisuke Kobayashi, Yoshinobu Eishi

PDF-027 Evaluation of Lower Digestive Tract Cancer in DWI by Concurrently Using the CHESS and STIR Methods
CHESS法とSTIR法を併用したDWIを用いた下部消化管癌の評価
宮崎　達也（メディカルスキャニングお茶の水）
Tatsuya Miyazaki, Akio Chishima, Yu Ishizaka, Toshihisa Miyamoto, Yuki Ito, Mau Sekine

PDF-028 Liver Iron Quantification in a Nonalcoholic Steatohepatitis Mouse Model by Using MR Imaging at 3.0 T: A Feasibility Study
3テスラMRIを用いた非アルコール性脂肪性肝炎モデルマウスの肝内の鉄の定量に関する検討
大西　裕満（大阪大学大学院医学系研究科 放射線統合医学講座 放射線医学講座）
Hiromitsu Onishi, Masatoshi Hori, Takahiro Tsuboyama, Mitsuaki Tatsumi, Makoto Sakane, Yoshiyuki Watanabe, Noriyuki Tomiyama, Takashi Ueguchi, Guoxiang Liu

PDF-029 Evaluation of spleen with Diffusional Kurtosis Imaging (DKI) in patients with liver disease
拡散尖度画像 Diffusional Kurtosis Imaging（DKI）による肝疾患に伴う脾臓の検討
濱田　雄貴（東京女子医科大学 八千代医療センター 画像検査室）
Yuhki Hamada, Daisuke Yoshimaru, Nozomi Mogi, Ayumu Funaki, Yoshihiro Ikeda

PDF-030 Evaluation of imaging features of fast imaging technique: Comparison of DISCO-LAVAFLEX and LAVA with compressed sensing and ARC
高速画像の特徴の評価：DISCO-LAVAFLEX法と圧縮センシングとARCを併用したLAVA法の比較
米山　浩司（聖隷浜松病院 放射線部）
Kouji Yoneyama, Takayuki Masui, Yuji Iwadate, Naoyuki Takei, Kang Wang

PDF-031 Comparison of two MR elastography (MRE) methods for the pancreas ; conventional-MRE vs. reduced FOV MRE using local excitation technique
通常法MRエラストグラフィ (MRE) と局所励起技術を利用したMREとによる膵臓撮影の比較
伊東　洋平（浜松医科大学 放射線診断学・核医学講座）
Yohei Itoh, Yasuo Takehara, Kenshi Kawamura, Takashi Nakajima, Ikumi Igarashi, Maho Hayashi, Satoshi Usami, Naoko Hyodo, Takasuke Ushio, Yuki Hirai, Nobuko Yoshizawa, Shuhei Yamashita, Hatsuko Nasu, Tetsuya Wakayama, Atsushi Nozaki, Hiroyuki Kabasawa, Harumi Sakahara

PDF-032 Optimization of echo time setting in High speed T2 corrected multi echo MR spectroscopy (HISTO)
HISTO Sequenceにおける設定TEの最適化
栗田　京助（埼玉医科大学病院 中央放射線部）
Kyosuke Kurita, Tsuyoshi Sasaki, Taishi Unezawa, Hiroshi Imai, Mamoru Niitsu

PDF-033 Non-contrast Renal MRA Using Multi-shot gradient echo EPI: Comparison with balanced TFE Sequence in healthy volunteers at 3-T MRI
Multi-shot EPIを用いた腎動脈MRA
森田　康祐（熊本大学医学部附属病院 中央放射線部）
Kosuke Morita, Takeshi Nakaura, Seitaro Oda, Tomohiro Namimoto, Makoto Goto, Masahiro Hashida, Yasuyuki Yamashita

PDF-034 SECURE study: observational post-marketing study on the safety profile of gadoterate meglumine - Final results in 35,499 patients
Bodo Kress, Andreas Gottschalk

PDF-035 Comparison of the MRI sequences in ideal fiducial marker-based radiotherapy for prostate cancer
放射線治療用の金マーカーが留置された前立腺癌に対する種々のMRIシーケンスの比較
広瀬　茂樹（岐阜市民病院 中央放射線部）
Shigeki Hirose, Osamu Tanaka, Mitsuyoshi Hattori, Takamasa Yokoyama, Yuko Yamada

PDF-036 Intraindividual quantitative comparison of 0.5M gadolinium contrast material and 1.0M gadobutrol in female pelvic MR imaging
女性骨盤領域におけるガドビストと従来のガドリニウム造影剤の造影効果に関する対比
藤井　進也（鳥取大学 医学部 画像診断治療学分野）
Shinya Fujii, Takeru Fukunaga, Chie Inoue, Naoko Mukuda, Toshihide Ogawa

PDF-037 Evaluate a clinical value of MAVRIC-SL and SEMAR for detecting a post operative local recurrence of soft tissue tumor around a metal implant
骨軟部悪性腫瘍の人工関節置換術後再発に対するMAVRIC-SLとSEMARを用いた金属アーチファクト低減の比較検討
小黒　草太（慶應義塾大学病院 放射線診断科）
Sota Oguro, Shigeo Okuda, Hirokazu Fujiwara, Kuniaki Ohori, Kazutaka Kikuta, Robert Nakayama, Hideo Morioka, Masahiro Jinzaki

PDF-038 Feasibility of noninvasive and absolute thermometry for knee joint cartilageusing spin-lattice relaxation time
スピン-格子緩和時間による膝関節軟骨の絶対温度分布非侵襲画像化の可能性
木村　智也（東海大学 工学研究科 電気電子工学専攻）
Tomoya Kimura, Kagayaki Kuroda, Kenji Takahashi

PDF-039 Assessment of T2 values of the wrist cartilage in healthy subjects at high-resolution 3T-MRI
高分解能3T-MRIを用いた健常者での手関節軟骨のT2マッピング
船田　重和（聖路加国際病院 放射線科）
Shigekazu Funada, Taiki Nozaki, Junichi Tsuchiya, Saya Horiuchi, Chiharu Osakabe, Yasuyo Teramura, Hiroshi Yoshioka, Hiromi Nakamura, Kazuhiro Umehara, Yasuyuki Kurihara

PDF-040 Evaluation of Shoulder Joint Cartilage Degeneration by Sports disorders Using T2 Mapping at 3T MRI
3T-MRIによるT2mappingを用いたスポーツ障害による肩関節軟骨変性の評価
伊藤　勇輝（メディカルスキャニングお茶の水）
Yuki Ito, Tatsuya Miyazaki, Akio Chishima, Yu Ishizaka, Toshihisa Miyamoto

PDF-041 Signal Processing in Noninvasive Magnetic Resonance Temperature Imaging for Breast Thermotherapy
乳がんの温熱療法のための磁気共鳴による非侵襲温度分布画像化における信号処理
大脇　陽介（東海大学工学研究科電気電子専攻）
Yosuke Owaki, Kenichirou Kurihara, Yutaka Imai, Kagayaki Kuroda

PDF-042 An MR compatible robot system using MR and ultrasound images to assist image guided puncture
MRと超音波画像を併用したイメージガイド下穿刺支援のためのMR対応ロボットシステム
森川　茂廣（滋賀医科大学 神経難病研究センター MR医学研究部門）
Shigehiro Morikawa, Atsushi Yamada, Shigeyuki Naka, Koichiro Murakami, Tohru Tani

PDF-043 fMRI study of clinical "shonishin" stimulation
小児鍼刺激による脳活動の変化の検討
上林紗也果（明治国際医療大学大学院 鍼灸学研究科 鍼灸学専攻 脳神経外科）
Sayaka Kanbayashi, Masahiro Umeda, Yasuharu Watanabe, Yuko Kawai, Tomokazu Murase, Ayako Mandai, Toshihiro Higuchi

PDF-044 A challenge for sub-millisecond fMRI
Yul-Wan Sung, Daehun Kang, Seiji Ogawa

PDF-045 ASL MRI in patients with traumatic brain injury as the imaging of cerebral blood flow compared with Technetium ECD SPECT
ASL MRIを用いた頭部外傷の脳血流評価　Tc ECD SPECTとの比較
柴田　　靖（筑波大学 水戸地域医療教育センター 水戸協同病院 脳神経外科）
Yasushi Shibata, Ryota Mashiko

PDF-046 Optimization of b-value Arrangement for Calculating of Water Permeability Using Diffusion-Weighted Arterial Spin Labeling
DW-ASLを用いたWater Permeabilityの算出におけるb値の最適化
青池寿々子（北海道大学病院 医療技術部 放射線部門）
Suzuko Aoike, Noriyuki Fujima, Tomoyuki Okuaki, Takuya Aoike, Sayaka Takamori, Kinya Ishizaka, Kohsuke Kudo

PDF-047 Pearls and Pitfalls in Arterial Spin-Labeling MR Imaging (ASL-MRI) in Various Intracranial Pathologic Condition
Aleum Lee, Chang Kee-Hyun

PDF-048 Diffusion Kurtosis Imaging (DKI) for the pathophysiology of the hepatocellular carcinoma (HCC)
Diffusion Kurtosis Imaging (DKI)を使用したHCCの病態評価
茂木　　望（東京女子医科大学 八千代医療センター 医療技術部 画像検査室）
Nozomi Mogi, Daisuke Yoshimaru, Yuuki Hamada, Yoshihiro Ikeda, Ayumu Funaki

PDF-049 Examination about the usefulness of the pelvis part sagittal section using RESOLVE in 3T-MRI
3T-MRIにおけるRESOLVEを用いた骨盤部矢状断の有用性についての検討
針生　武瑠（メディカルスキャニング 東京）
Takeru Hariu, Tatsuya Miyazaki, Akio Chishima, Keita Kimura

PDF-050 Basic study of the direct coronal diffusion weighted whole body imaging with background body signal suppression (DWIBS) in Children
小児におけるdirect coronal DWIBSの基礎検討
渡邉　裕文（千葉県こども病院 検査部 放射線科）
Hirofumi Watanabe, Kojiro Ono, Takumi Ookubo, Miwako Suzuki, Akira Shirayama

PDF-051 Diffusion-weighted imaging at 3T requires sufficiently long TR owing to incidental magnetization transfer and crosstalk effects
3T拡散強調像において充分長いTRが必要な理由：MT効果とクロストークの影響
北　　美保（生長会 府中病院 放射線科）
Miho Kita, Kazuhiro Kawano, Morio Sato, Hideto Sakamoto, Seigo Ishii, Tetsuo Sonomura

PDF-052 Application of mASTAR to the Evaluation of Portal Vein Hemodynamics
門脈血流動態把握へのmulti-phase ASTAR（mASTAR）法の応用
二宮　綾子（東芝メディカルシステムズ株式会社 MRI営業部）
Ayako Ninomiya, Miho Kitamura, Naotaka Sakashita, Yuichi Yamashita

PDF-053 Comparison of 2D-Cine PC and 3D-Cine PC in unruptured cerebral aneurysm
未破裂脳動脈瘤における2D-Cine PC法と3D-Cine PC法の比較検討
佐藤　兼也（青森県立中央病院 放射線部）
Kenya Sato, Tetsuhiro Saito, Noriko Maeda, Yoko Yokoyama, Ryoichi Yamauchi, Kazuki Kudo, Atsushi Saito, Hiroshi Midorikawa, Tatsuya Sasaki, Koichi Shibutani, Atsushi Nozaki

PDF-054 Evaluation of Depiction of Peripheral Arteries with mASTAR
mASTAR法を用いた末梢血管描出の検討
北村　美穂（東芝メディカルシステムズ株式会社 MRI営業部）
Miho Kitamura, Ayako Ninomiya, Naotaka Sakashita, Yuichi Yamashita

PDF-055 Labeled peripheral macrophages were found in the spinal cord of chronic constriction injury model mice by MRI
坐骨神経結紮による慢性疼痛モデルマウスの脊髄において末梢マクロファージの浸潤を確認できた
吉田　将太（大阪大学 免疫学フロンティア研究センター）
Shota Yoshida, Yuki Mori, Ting Chen, Yoshichika Yoshioka

PDF-056 The possibility of high-speed imaging of MRI by the reduction of the number of phase encodes
位相エンコード数の低減によるMRIの高速撮像化の可能性
山田　　徹（東海大学大学院 工学研究科 情報理工学専攻）
Toru Yamada, Satoshi Yatsushiro, Saeko Sunohara, Ken Takizawa

PDF-057 Chemical exchange saturation transfer imaging in human brain at 7T
7T ヒト脳化学交換飽和移動 (CEST) イメージング
栗林　秀人（シーメンスヘルスケア株式会社）
Hideto Kuribayashi, Yuta Urushibata, Tomohisa Okada, Benjiamin Schmitt, Kaori Togashi

PDF-058 Measurements of choline contents by ^{1}H-MRS are affected by the position of VOI and navigator tracker in respiratory gating: A phantom study
スピンエコー型ナビゲータを併用した1H-MRSにおいてVOIとトラッカーの設定位置がコリン濃度に及ぼす影響
高森　清華（北海道大学病院 医療技術部 放射線部門）
Sayaka Takamori, Kinya Ishizaka, Satoshi Yabusaki, Suzuko Aoike, Hiroyuki Hamaguchi, Kohsuke Kudo

PDF-059 Relationship between brain metabolite concentrations/volumes during neonatal period and developmental prognosis in premature birth babies
早産児の新生児期における脳内代謝物濃度／脳容積とその予後との関連性
富安もよこ（量研機構 放医研）
Moyoko Tomiyasu, Noriko Aida, Jun Shibasaki, Seiichi Tomotaki, Masahiko Sato, Kouki Kusagiri, Yasutake Muramoto, Yuichi Suzuki, Yukako Kawasaki, Eiji Shimizu, Takayuki Obata

PDF-060 Introduction of 31P MR Spectroscopy measurements to clinical human liver image examination at 3T
31P MRS 計測の肝臓 3T MRI 臨床検査への導入
磯田　裕義（京都大学 医学部 附属病院 先制医療・生活習慣病研究センター）
Hiroyoshi Isoda, Hideto Kuribayashi, Shun Asahina, Katsutoshi Murata, Ryutaro Nakagami, Yoshihiko Kawabata, Kaori Togashi

PDF-061 Hyper-realistic display system with wide field of view to reduce the stress and anxiety for MRI examination
MRI検査における閉所での不安感を解消する広視野バーチャル映像表示技術
石崎　庄治（東芝メディカルシステムズ 株式会社）
Shoji Ishizaki, Yu Ueda, Hiromitsu Takamori, Takashi Sasaki

PDF-062 Considering minimized installation space for a 3T MRI system
3T MRI装置の設置面積削減の検討
石原　隆尋（東芝メディカルシステムズ株式会社）
Takahiro Ishihara, Naoki Imamura, Kazuyuki Soejima

PDF-063 Evaluation of the directional dependency of spatial resolution at MPR processing after using VRFA
VRFA撮像後のMPR処理における空間分解能の方向依存性の検討
加々美　智（福岡リハビリテーション病院）
Satoshi Kagami

PDF-064 Quantitative t2 mapping accelerated by model-based iterative reconstruction
model-based iterative reconstructionを利用したT2マッピングの定量化
小林　謙一（獨協医科大学病院 放射線部）
Kenichi Kobayashi, Kiyotaka Kato, Kiyoshi Oguro, Yasushi Kaji, Hiroshi Imai

PDF-065 Influences of cosmetic pigments for nipple areola tattoo after breast reconstruction on artifacts and magnetic attractive force in MR imaging
乳輪再建術に使用するインクが磁場不均一を及ぼす影響についての検討
前田　晋義（社会医療法人 生長会 府中病院）
Masayoshi Maeda, Mamoru Ishimoto, Kazuhiro Kawano, Miho Kita, Kenichi Takenaka, Gouichi Haraoka, Morio Sato

PDF-066 Psychological Stress in Patients Undergoing MR Imaging -Plethysmogram analysis-
MRI検査時に生じるストレス　－脈波解析－
門間　正彦（茨城県立医療大学 保健医療学部 放射線技術科学科）
Masahiko Monma, Rika Kikuti, Naho Mitimura, Suzuka Wakui, Yoshikazu Shimada, Hiraku Kawamura, Yoshiyuki Ishimori, Mitihiro Kawano

PDF-067 The effect of a homemade dielectric pad with using commercially available ultrasound gel to correct B1 inhomogeneity in body MRA – a phantom study–
生体MRAのB1不均一性に対する超音波検査用ジェルを用いた自作誘電パッドのファントム実験による検証
黒木　佑椰（社会医療法人 共愛会 戸畑共立病院）
Yuuya Kuroki, Akiyoshi Yamamoto, Hiroki Matoba, Daiji Uchiyama, Seigo Yosida, Katsumi Nakamura, Mitsue Miyazaki

PDF-068 Surface marker localization devices with sufficient signal-to-noise ratio: verification with wood
木質材料による良好なSNRと異方性を持つ位置決め用皮膚表面マーカの提案と検証
鈴木　政司（首都大学東京 大学院 放射線）
Masashi Suzuki, Atsushi Senoo

PDF-069 Influence of MR Imaging by changing the k-space Ordering Scheme in 3D – eTHRIVE
3D-eTHRIVEにおけるk-space充填配列によるMR画像への影響
大塚　和人（独立行政法人 国立病院機構 宇都宮病院）
Kazuto Ohtsuka

PDF-070 A Patient-Satisfaction Survey for MRI Using the SERVQUAL Model
MRI患者の満足度影響をSERVQUAL解析
小檜山奈津留（一般財団法人脳神経疾患研究所附属総合南東北病院）
Natsuru Kobiyama

PDF-071 A Patient-Loyalty for MRI with the SERVQUAL Model
MRI検査の患者におけるSERVQUALモデルを用いたロイヤリティ評価
小檜山奈津留（一般財団法人脳神経疾患研究所附属総合南東北病院）
Natsuru Kobiyama

PDF-072 Classification of MRI examinee claustrophobia and examine countermeasures matched each phobia
MRI受検者における閉所恐怖症の切り分けと恐怖症に合った対策の検討
田泉　智明（市立敦賀病院 放射線室）
Tomoaki Taizumi, Satoshi Matsuyama, Atsuyuki Shimizu, Takeshi Yamazaki, Takeshi Hibi

PDF-073 Basic Study on the Relationships between the Scanning Parameters of the mUTE Sequence and Image Contrast
mUTE シーケンスにおける撮像条件とコントラストの関係についての基礎的検討
菅野　康貴（東芝メディカルシステムズ株式会社 MRI営業部）
Yasutaka Sugano, Yuichi Yamashita, Miho Kitamura, Naotaka Sakashita

PDF-074 T1 relaxation time measurement using ultra-short echo-time imaging with inversion recovery pulse
IR パルス併用 Ultra-short echo-time imaging を用いた T1 緩和時間測定
増山　　研（医療法人 渓仁会 手稲渓仁会病院 診療技術部）
Ken Masuyama, Masakazu Shioda, Shun Akimoto, Kazuya Akiyoshi, Hiroyuki Aoki, Yuka Inoko, Hajime Adachi, Toru Yamamoto

EL1-1　頭部MRIと水分子
Head MRI and water molecules

酒井　晃二（京都府立医科大学 大学院医学研究科 放射線診断治療学）
Koji Sakai（Department of Radiology, Graduate School of Medical Science, Kyoto Prefectural University of Medicine）

頭部MRIは水分子とどのように関連して説明されるのであろうか？ MRIはプロトンの緩和過程の違いを画像化したものと捉えることが出来る。水分子を相手にしているのになぜコントラストが得られるのであろうか？これがボクセル内の水分子存在量の違いと組織内および組織間による緩和メカニズムの違いによるものであることは明解であるが、どのようなものなのであろう？日常的に頭部MRI画像を見慣れている我々は、目前の画像について改めて緩和メカニズムを考えて説明を加える機会はほとんどないかもしれない。水分子内のプロトンの緩和メカニズムは、双極子―双極子相互作用、スピン移動など多岐に亘り、複雑に関連し合っている。その基本は、対象となるプロトンとそれ以外との「エネルギーの受け渡し」とエネルギーの増減を伴わない「状態の交換」である。プロトンどうし、プロトンと水分子、プロトンとその他の分子などの間でエネルギーの受け渡しが行われることとスピン間の状態交換により、励起状態から緩和状態に至る。プロトンが置かれた環境に応じて、その緩和過程に違いが生じる。それらはどのように頭部MRIと関係しているのか？緩和メカニズムと水分子について頭部MRIを舞台に再考を試みる。頭部MRIの対象となる病態の検出とその変化過程の観察には、水分子の動きの違いが利用されていることも多い。水分子の動きは、大きく3つに分類できる。1つ目は分子運動であり、2つ目は自己拡散、そして3つ目は流れである。1つ目の動きは、分子が本来もつ性質によるものであり、3つ目は水分子が置かれた環境によるものである。2つ目の自己拡散運動は、1つ目と2つ目の双方によるものである。水分子の自己拡散運動は、周囲の環境に大きく依存する。水分子が置かれた空間サイズや水分子以外との関係、さらに温度などにより変化することは周知である。これらを反映した観察方法は、腫瘍、血管障害、梗塞、変性など多くの疾患の鑑別に用いられてきた。本講演では、頭部MRIにおける水分子の緩和メカニズムと3つの動きを再考し、水分子の存在量・状態・環境と病態との関係ついて考察を加えることも試みる。

EL1-2　臨床に役立つ新しいコントラストを生み出すための工夫
Innovation for generating clinically useful new contrast

米山　正己（株式会社 フィリップスエレクトロニクスジャパン ISビジネスグループ MRクリニカルサイエンス）
Masami Yoneyama（MR Clinical Science, IS Buisiness Group, Philips Electronics Japan）

MRI研究開発の分野では、新たな技術や方法論が絶え間なく開発されている。近年では高速化、あるいは定量化を目的とした開発が非常に増えており、今後の開発の主軸になっていくものと思われる。しかしながら、臨床MRIにおいて未だ最も重要なのはその画像コントラストであり、臨床に役立つ新しいコントラストを生み出すためのパルスシーケンス開発も未だ重要である。また、新しい技術でなくとも、現在の装置にインストールされているシーケンスをユニークな形で組み合わせることで、これまでなかったコントラストを生み出すことが可能なこともある。例えば、T1・T2・magnetization trasferなど生体組織の緩和特性や拡散、動静脈の血流（定常流と加速度流）の違いを強調するために適したプリパルスやパルスシーケンス、あるいはそれらをそれぞれ強調／抑制させる新たなコンビネーションを選択することで、目的となるコントラストを生み出すことができる。
本講演では、臨床に役立つ新しいコントラストを生み出すための技術的な工夫（プリパルス、パルスシーケンスとそれらのコンビネーション）とその考え方について、3D-T1強調高速スピンエコーイメージングやブラックブラッドイメージング、非造影血管イメージング（MR Angiography）や末梢神経イメージング（MR Neurography））など、脳神経領域での応用を中心にこれまでの幾つかの開発経験を例に解説する。

EL2-1　前立腺移行域がんのMRI: 発生部位と進展様式からのアプローチ
MRI of Prostate Cancer in the TZ and the AFMS: Intraprostatic Patterns of Spread and the Relative Frequency of the Locations

新本　弘（防衛医科大学校 放射線医学講座）
Hiroshi Shinmoto（Department of Radiology, National Defense Medical College）

前立腺がんは近年日本においても急増しており、2020年以降において男性がん罹患数が第1位になると予想されている。前立腺がんの診断法としてPSA、直腸診、経直腸的前立腺生検が確立しているが、PSAはその特異度が低いことが欠点である。また経直腸的前立腺生検においても、1) 尿道より腹側にあるがんを見逃しやすい、2) clinically insignificant cancerを検出することがある、3) がんの悪性を低く見積もる可能性がある、などの問題点がある。そのため最近では生検前にMRIを施行する施設も増加している。そのため最近では前立腺MRIに要求されるものは、単に前立腺がんの病期診断だけではなく、がんの正しい局在診断と悪性度予測まで含まれてきている。前立腺MRIはmultiparametric MRIが施行されるようになってから、その診断能は飛躍的に向上している。特に拡散強調ではADC値とグリソンスコアが相関することから、がんの悪性度の判断に有用とされている。しかし従来から診断の難しいとされている移行域に発生する前立腺がんにおいては、今日でも日常診療で診断に困るような症例が多く見受けられる。今回の講演では移行域に発生する前立腺がんに焦点を絞り、その局在や進展形式の特徴に関して解説する。

EL2-2　産婦人科急性腹症の画像診断 - MRI が寄与できること -
The acute gynecologic abdomen ; role of MR imaging in diagnosis

田村　綾子（東京北医療センター 放射線科）
Ayako Tamura（Department of Radiology, Tokyo-Kita Medical Center）

急性腹症で来院された際、消化器疾患に並び、産科・婦人科領域疾患であることは稀ではない。　急性腹症の画像診断は、超音波、CTが主である。臨床所見に加え、これらの検査で診断・治療に至ることが殆どであり、MRI は必須の検査ではない。ただし、特に産婦人科疾患では、CT 上どうしても診断に迷うことがある。症状や検査所見上、治療までに時間的余裕があれば、MRI を追加することで、より正確な診断に結びつくことを少なからず経験する。　産婦人科領域の急性腹症の原因としては、卵巣出血、異所性妊娠破裂、卵巣嚢腫破裂、内膜症性嚢胞破裂、付属器捻転、漿膜下筋腫捻転、子宮筋腫赤色変性、骨盤内炎症性疾患 (pelvic inflammatory disease ; PID) などが挙げられる。　内膜症性嚢胞の破裂は、癒着のために血性腹水が拡がりにくい。MRI では、内膜症性嚢胞の診断が容易であることに加え、少量の血性腹水が癒着した骨盤内を這うように広がる様子や、嚢腫の緊満感低下などを認識しやすい。　卵巣嚢腫破裂では、稀ながら悪性腫瘍を合併していることがあり、CT に比し MRIでは充実部を確認しやすく、悪性腫瘍であれば拡散強調像も役に立つ。　付属器捻転の際には、捻転茎や嚢腫壁の虚血、それに伴ううっ血や浮腫を、早期に拡散強調号高信号として捉えられる。　漿膜下筋腫の捻転は、付属器捻転の診断基準の一つである子宮の偏位は生じにくい。MRI では、腫瘤の由来臓器同定がCTに比し容易なことが多い。　筋腫の赤色変性は、卵巣嚢腫捻転と同様に、出血の信号が見られないかなり早期でも、虚血、うっ血、浮腫を反映して拡散制限が認められ、診断に有用である。　卵管拡張や壁肥厚等は、MRI では消化管との区別がし易く、認識しやすい。このため、異所性妊娠の着床部(卵管膨大部は好発部位)の同定、PIDの際の拡張した卵管や腫大した卵巣の確認が容易である。さらにPIDでは、貯留液が膿性であるかどうか、拡散強調像を用いて評価が可能である。　可能な限りCTと対比しながら、実際に診断に有用であった救急疾患の MRI 画像を呈示したい。

EL3-1　Non-mass enhancement at breast MRI: 鑑別のための Key findings
Non-mass enhancement at breast MRI

町田　洋一（医療法人鉄蕉会 亀田京橋クリニック 放射線科／医療法人鉄蕉会 亀田メディカルセンター 乳腺科）
Youichi Machida（Department of Radiology, Kameda Kyobashi Clinic）
嶋内亜希子、吉田　民子（医療法人鉄蕉会 亀田京橋クリニック 放射線科）

乳房MRIの読影は「足し算」および「引き算」で考えるとわかりやすい。
Non-mass enhancementはsegmental distribution、あるいはclustered ring internal enhancement patternなど、悪性を示唆することが知られている要素が見て取れた場合、加点式に悪性の可能性を見積もっていく。こうすることで精査、つまり生検を必要とする病変を効果的に選定することができる。また一方で、左右対称性のある所見は互いを引き算をすることで、病変と紛らわしい背景乳腺の増強効果を除外することが重要である。
乳房MRI読影においては時に難解な症例にも遭遇し、一筋縄ではいかないことも多い。しかしながら、カテゴリー判定概念の理解や、上記に挙げたポイントなどをあわせた体系的な読影法の習得で、多くの症例は効果的に判定可能である。本講演では、実例や、これまでの文献報告の紹介を交えながら、次の日から役立つ乳房MRIにおけるnon-mass enhancementの読影法を紹介する。

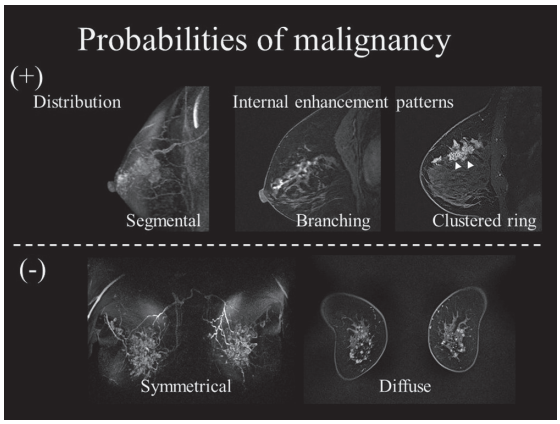

EL3-2　乳腺良性病変のMR-pathologic correlation: 鑑別のためのKey findings
MRI of benign breast lesions: Key imaging findings for making correct diagnosis

後藤眞理子（京都府立医科大学大学院医学研究科 放射線診断治療学）
Mariko Goto（Department of Radiology, Kyoto Prefectural University of Medicine）

現在乳腺診療において、乳房MRIは欠かせないモダリティの1つである。乳房MRIの適応は広く、従来の乳癌の広がり診断から、最近はproblem solvingとしての質的診断が求められる機会も増えてきている。乳房MRIによる乳腺病変の質的診断においては、ACR BI-RADS（Breast imaging-reporting and data system）の診断基準が本邦でもほぼ普及し、これに従えば、比較的正しくMRIによる乳腺病変の良悪性診断を行うことが可能となっている。　しかしながら、BI-RADS MRIの診断基準をもってしても、乳房MRIは高い感度を有するが、特異度は中等度で、偽陽性が多いことが知られている。その一因としては、良性病変に特異的なMRI所見についての知識やエビデンスが不足していることが挙げられる。　そこで本教育講演では、乳腺良性病変に主眼をおき、1．一般的な乳腺良性病変のMRI所見をレビューし、その組織学的背景を理解すること、2．これらの良性病変とよく似たMRI所見を呈しうる悪性病変をレビューし、その組織学的背景について学ぶこと、最後に、3．両者を鑑別するために必要なMRI所見のポイントについて学ぶこと、を目標としたい。

EL4-1　RFパルスの基礎
Basics of RF Pulses

尾藤　良孝（株式会社日立製作所 ヘルスケアビジネスユニット）
Yoshitaka Bito（Hitachi, Ltd. Healthcare Business Unit）

磁気共鳴現象を誘起するためには，ある特定の周波数(RF: Radio Frequency)を有する電磁波の照射が必須である。この電磁波を比較的短時間で照射するRFパルスは，MRIで様々な生体情報を観察する際に使用されるシーケンスの基本となっている。例えば，緩和や磁化移動によるコントラスト生成，脂肪や脳脊髄液の信号抑制，RF trainによる計測高速化，スライス面等の領域選択励起や領域選択抑制，MRAにおけるフリップ角の傾斜照射など様々な面で使用されている。現在のMRIにおいては，これらRFパルスを駆使して，所望の領域からの磁気共鳴信号のみを発生させ，所望のコントラストで高速に信号計測するような技術が搭載されている。さらに詳細な生体情報を高速に取得するために，様々な技術が研究開発されている。このような技術を理解し開発するために，RFパルスの役割について理解することが重要になっている。

本講演では，これらRFパルスの役割について理解するために，RFパルスの基礎について概説する。まず，磁気共鳴現象における磁化とRFパルスとの関係についてBloch Equationに則って基本的な挙動について説明する。次に，単一のRFパルスについて，Small tip angle approximationおよびLarge tip angleにおけるRFパルスの波形設計について説明し，RFパルスによる磁化の励起や反転，RFパルスと同時に傾斜磁場を印加するスライス領域選択励起・選択抑制，ケミカルシフトの影響などについて例示する。次に，複数のRFパルスについて，磁化の基本的な挙動について説明し，Spin echoやそのEcho train，複合RFパルスによる周波数選択，複数のRFパルスと同時に傾斜磁場を印加する空間領域選択や空間・周波数領域選択などについて例示する。これにより，RFパルスの基本的な役割を理解することをめざす。

EL4-2　MR angiographyの基礎
Basic principles of MRA

小野　　敦（光生病院 診療支援部／大阪大学大学院 医学系研究科 医用物理工学講座）
Atsushi Ono（Kousei Hospital Medical Support Division）

MR信号を用いてプロトンの流れと動きを最初に画像化したMR Angiography（MRA）の基本概念であるTime of flight（TOF）効果は、1951年にSuryanによって報告された。それから65年が経過し、MRAの役割は、血管の形態変化や血流の評価から動態イメージングによる詳細な病態把握が可能な診断ツールへと進化している。特に、非造影MRAは、従来のTOF法に始まりarterial spin labeling（ASL）法や4D Flow法に至るまで多岐にわたるため、初学者にとって取り付きにくい領域のひとつになった。各種非造影法を深く理解し、有効に利用するためには、MRIの画像化理論、基本となるシーケンスの特性、各組織の緩和時間や血流動態等の生体情報に加え、流体力学の知識までも総動員しなければならない。他方、非造影技術の応用は、血流のみならず脳脊髄液や膵液の動態と各組織の機能評価にも拡大し、今となってはMRAの枠を超えた非侵襲的診断法として確立されつつある。本講演では、MRAの入門編として、使用頻度が高い代表的な非造影法であるTOF法、Phase Contrast法、高速SE系ならびにSSFP系水強調法、ASL法に焦点をあて、それぞれの原理と特徴の重要な部分を総ざらいし、撮像における要点ならびに有意義な利用法を体系的に概説する。初学者から熟練者までが、今一度MRAの基礎に立ち返り、難解な原理や画像の成り立ちを成書とは違った切り口で見直し、効果的な臨床応用のポイントの理解や再発見につながる機会となるよう解説する。

EL5-1　末梢神経疾患の画像診断：MR neurographyを中心に
Magnetic Resonance Neurography for Peripheral Nerve Disorders

長田　周治（久留米大学 医学部）
Shuji Nagata（Kurume University School of Medicine）

末梢神経疾患のMRI (MR neurography) 検査には、細い末梢神経と周囲臓器との良好なコントラストと高い空間分解能が重要となる。近年、高磁場装置の普及と最適コイルやパラメータの進歩により、これらの問題が解決され、詳細な末梢神経の描出が可能となった。

MR neurographyの基本となるパラメータは、2D FSE T1強調像、T2強調像、脂肪抑制T2強調像であり、適宜、3D FSE T2強調像 (Cube, SPACE, VISTAなど) の再構成やcurved MPRを追加する。拡散強調画像を用いたDWIBSやテンソル画像も神経の全体的な形態的評価に有用である。

本講演では、MR neurographyによる末梢神経疾患の診断のポイントと各疾患における撮像のコツを中心に概説する。末梢神経疾患には、絞扼性神経障害 (Carpal tunnel syndrome、Cubital tunnel syndrome、Morton neuroma、Lumber nerve root entrapment)、外傷性神経障害、炎症性神経障害、放射線神経障害、腫瘍関連性神経障害 (Peripheral nerve sheath tumor、Perineuroma、Neural fibrolipoma、Interneural ganglion、Peripheral neurolymphoma、Metastasis) などがある。

EL5-2　骨髄のMRI
Bone Marrow MRI

林田　佳子（産業医科大学 放射線科学教室）
Yoshiko Hayashida（University of Occupational and Environmental Health）

骨とは常に新陳代謝を行う生きた結合組織である。脳や脊髄、肺、腹部臓器等を保護する保護作用、丈夫なテコ作用を有する。更には、カルシウム塩、脂肪の貯蔵庫でもあり、造血組織である骨髄を有するなど様々な働きを担っている。このため、MRIT1強調画像にて骨髄に異常信号を呈する疾患は、非常に多種多様である。限局性病変には腫瘍性病変が認められ、びまん性病変には、腫瘍浸潤の他に、骨基質の代謝異常による病変、狭義の骨髄異常の病変が存在する。更に骨髄病変のMRI診断をさらに難解にするのは、正常骨髄が生理的に赤色髄から黄色髄へと転換（Conversion）し、ある環境下では再転換（Reconversion）が起こることにあり、この赤色髄の存在が悪性病変との鑑別を困難にしている。まず、骨の機能、骨構造とその生理的な変化について、骨基質（リモデリング）、骨髄（転換、再転換）にわけて復習し、骨基質由来の病変、骨髄由来の病変を紹介する。更に様々な撮像法における正常の赤色髄のMRI画像について疾患を提示しながら説明する。

EL6-1　中枢神経領域における薬剤に起因する画像所見
Drug-induced imaging features in the central nervous system

松島　理士（東京慈恵会医科大学 放射線医学講座）
Satoshi Matsushima（Department of Radiology Jikei University School of Medicine）

現代医療において薬剤は治療の大きな主軸のひとつとなっており、広く治療に用いられていることはいうまでもない。日常診療において画像診断を行う際に、治療効果を含め薬剤による生体内変化がわれわれが読影する画像に反映されることがあり、薬剤が画像所見に与える影響を知っておく必要がある。
読影した画像所見から薬剤性病変の可能性を想起することが可能であれば、薬剤の継続、中止、変更といった治療方針の決定に多大な貢献ができると考える。
本講演では薬剤に起因する血管性病変、抗菌薬・抗てんかん薬・抗腫瘍剤・分子標的治療などを含めさまざまな薬剤に関連した中枢神経領域における画像変化や病変を文献的な考察も加えながら概説する。

EL6-2　新生児低酸素性虚血性脳症のMRI
MR Imaging for neonatal hypoxic-ischemic encephalopathy

早川　克己（岩手県立釜石病院）
Katsumi Hayakawa（Iwate Prefectural Kamaishi Hospital）

1．低酸素性虚血性脳症におけるMRIの役割　MRIの役割として重要なことは、低酸素性虚血性脳症による脳の損傷の評価であり、MRIがその感度や客観性において優れていることがわかっている。二番目の役割は、児の予後評価に果たす役割である。予後評価において、amplitude-integrated EEG(aEEG), MR spectroscopy, visual evoked potential, sensory evoked potentialなどとの比較におけるメタ解析にてMRIの有用性が証明されている。重要なことは、新生児低酸素性虚血性脳症において新生児期の脳は刻々と変化しており、MRIは撮像時点での一過性の画像を見ているに過ぎないということである。拡散強調画像の最適評価日齢は3-5日であり、7日以降はpseudonormalizationが生じて過小評価になることを知っておく必要がある。また、MRSにおいても、生後24時間前後において，pseudonormalizationが生じるので、初期変化がピークとなる生後3-5日において計測する必要がある。このようにMRI,MRSの撮像はそのタイミングが極めて重要であり、生後1週目と2週目では画像がかなり変化するのでピーク時期の撮像することが最大の注意点である。2.低酸素性虚血性脳症のMRI診断の三つのパターン1）peripheral patternは大脳分水嶺領域に虚血が生じるパターンで別名parasagital cerebral injury, watershed patternとか呼ばれるが、大脳白質から一部皮質も含む損傷である。のちほど、瘢痕回（Ulegyria）の原因となる。2）basal ganglia/thalamus injury:中心性損傷であり、その程度は、基底核・視床損傷のみのもの、これにローランド皮質損傷を合併するもの、さらに、この2部位に海馬損傷を合併するもの、と範囲が拡大するにつれて予後が不良になる。3）total brain injury：テント上の脳組織がすべて損傷を受けるパターンであり、生後7日以内の拡散強調画像にて“White cerebrum sign”といわれる所見を呈する。相対的に小脳・脳幹部が低信号を呈するが、大脳にウィンドウを合わせれば見落とすことがある。幼児期の画像では、“multicystic encephalomalacia”を呈する。最も予後不良のパターンである。

EL7-1　MRIによる肝腫瘍の診断法とピットフォール
Liver tumors: differential diagnosis and pitfalls on MR imaging

福倉　良彦（鹿児島大学 放射線診断治療学分野）
Yoshihiko Fukukura（Kagoshima University, Department of Radiology）

MRIは、空間・時間分解能の点においてはCTに劣るものの、MRIは高い組織コントラストや良好な造影剤感受性を有し、放射線被曝がなく安全に撮像できる利点がある。特に、水や脂肪、血流、出血、線維化、分子拡散や組織硬度の評価を同時にこなせる点で唯一無二の検査である。また、従来CTに劣っていた空間分解能や時間分解能の点においても、多チャンネルコイルの開発や3テスラ装置の出現により微細な解剖構造の評価が可能となっており、肝腫瘍性病変の診断にMRIは重要な位置を占めている。特に、Gd-EOB-DTPA造影剤が使用可能となり、肝臓のMRIは病変の描出ならびに良悪性の鑑別に必須の検査となっている。しかしながら、装置の進歩による情報量の増加と共に不必要な情報も増加しており、我々画像診断に携わる人間は、以前にも増して画像の知識のみならず、より多くの臨床・病理組織学的知識を持つことが必要となってくる。したがって、臨床・病理組織学的知識から必要な撮像を選択し、得られた多くの画像情報の中から必要な情報のみを抽出し、有益な情報を統合し、病変の形態的特徴を正確に推測することが診断への近道となる。今回、「MRIによる肝腫瘍の診断法とピットフォール」と称し、肝臓 MRI でみられる信号変化がどのような病理学的背景から出現するのか概略を提示し、MRIによる肝腫瘍の系統的な診断方法ならびにピットフォールについて述べる。

EL7-2　膵疾患のMRI　～ common and uncommon findings ～
MRI of pancreatic disease -common and uncommon findings-

佐野　勝廣（埼玉医科大学国際医療センター 画像診断科）
Katsuhiro Sano（Department of Diagnositc Radiology, Saitama Medical University International Medical Center）

Therapies for panrcreatic diseases include surgical resection, chemotherapy, and radiotherapy, etc. Imaging diagnosis of pancreatic disease is important to choose optimal therapy for the diseases. However, it is sometimes difficult to diagnose pancreatic disease because of rare pancreatic diseases and uncommon image findings. Radiologists have to know imaging and clinical features of common and rare pancreatic diseases with/without uncommon image findings such as pancreatic carcinomas includings mucinous carcinoma, anaplastic / undifferentiated carcinoma, neuroendocrine tumor, acinar cell carcinoma, solid pseudopapillary neopslasm, malignant lymphoma, intraductal neoplasms, cystic neoplasms, and non-neoplastic diseases, etc.

EL8-1　心疾患における4Dフロー MRIの臨床利用
Clinical use of 4D flow MRI in cardiac disease

長尾　充展（東京女子医科大学 画像診断学・核医学講座）
Michinobu Nagao（Tokyo Women's Medical University, Diagnostic Imaging & Nuclear Medicine）

心臓MRIは、複雑な形態の心疾患の画像を死角無く得られる点、再現性の高い心室容量測定が可能な点で心エコーに優る。さらに被ばくがなく造影剤を使わず低侵襲で心機能を測定できる利点がある。従来の位相コントラスト法でも大動脈や肺動脈の流速測定は行われていたが、4次元フローは3次元位相コントラスのデータをより明瞭に可視化するもので新たな心機能評価のツールとして期待されている。4次元フローでは血管内に置いた仮想粒子とその軌跡＝流線により、血流の動態を3次元＋時間軸＝4次元で観察することができる。複数の色の仮想粒子を設定することにより、血管内で渦巻くVortex flowなども観察できる点が従来法とは大きく異なる。さらに血管壁にかかる剪断応力分布を可視化、定量化することも可能である。　我々は、慢性血栓塞栓性肺高血圧症において肺動脈形成術前後の4次元フローイメージで剪断応力に関連する肺動脈幹の渦流の変化を観察した。また複雑心奇形に対して実施される大静脈→導管・心房→肺動脈のフォンタン術のフローイメージでは、再建法によりフォンタン経路の渦流が異なり、肺動脈血流分布に影響する現象を発見した。ここでは、心疾患の病態を反映する4次元フローイメージの活かし方、撮像法の工夫、従来の位相コントラストとの定量結果の違いについて紹介する。

EL8-2　膠原病患者における心臓MRI
Cardiac MRI in the Patients with Rheumatic Diseases

小林　泰之（聖マリアンナ医科大学 医学部 先端生体画像情報研究講座）
Yasuyuki Kobayashi（Department of Advanced Biomedical Imaging Informatics, St.Marianna University School of Medicine, Kawasaki, Japan）
小林ひとみ（日本大学 医学部 血液膠原病内科）

膠原病には様々な臨床症状を呈する多臓器疾患であり、多くの膠原病で心臓病変が認められる。心臓病変があっても臨床的に心症状を現しにくいとされ生命予後を脅かすことが知られており、心臓病変は膠原病における死亡原因の主たる原因の一つである。強皮症や多発性筋炎・皮膚筋炎では心病変が多いことが知られているが、患者数の最も多い関節リウマチにおいても生命予後が約10年短く、その死因の一つに心血管合併症が挙げられている。また、心臓MRIの進歩も著しく、局所心機能評価、心筋パーフュージョン検査、遅延造影やT1マッピングによる心筋性状の評価が臨床的に可能となり、非侵襲的に心臓病変を検出してその程度を定量化できるようになった。膠原病患者における心臓MRIの有用性に関して概説する。

EL9-1　MR fingerprinting入門
Introduction to MR Fingerprinting

寺田　康彦（筑波大学 数理物質系 物理工学域）
Yasuhiko Terada（Faculty of Pure and Applied Sciences, University of Tsukuba）

MRI検査では、T_1やT_2などの組織パラメタの違いを強調した定性画像がしばしば用いられる。組織パラメタの定量画像を得るためには、一般的に複数回のMR撮像が必要である。一方、近年現れたMR Fingerprinting（磁気共鳴指紋法、MRF）では、一度の撮像データから複数の定量画像を得ることができる。定量化できるパラメタとして、T_1、T_2、プロトン密度だけでなく、最近ではdiffusionやperfusionなども報告されている。MRFでは、短時間でこれらの定量画像が同時に得られるため、新しい臨床検査法として大いに期待されている。
MRFでは準備段階として、各組織のパラメタに固有な信号系列（これをMRFでは指紋という）が高感度で得られるようなシーケンスを用意する。このシーケンスに基づき、想定される組織パラメタ値の組み合わせに対して信号系列を計算し、辞書として保管しておく。続いて実際に実験データを取得した後、得られた指紋と辞書内の指紋をパターン認識によって比較し、最も似た指紋をもつ項目の組織パラメタの値を画像化する。
MRFでは、時間、空間的なインコヒーレンスを重視する。前者は、組織パラメタに対する感度を高めるために必要である。MRFではtrue FISP (bSSFP)系やFISP (SSFP)系のパルスシーケンスを改良し、繰り返し時間やフリップ角などをランダムに変えて時間的コヒーレンスを崩すことで、T1やT2に対する感度を高めている。後者の空間的インコヒーレンス性は、高速撮像のために必要である。MRFでは、高速化のためにk空間内をアンダーサンプリングする。これをランダムに行うことで、エリアジングなどのアーチファクトを防ぎつつ、効率的にサンプリングする。
このようにMRFの撮像シーケンスやデータ解析法は複雑である。また、システムの不完全性、例えばB_0やB_1、スライスプロファイルなどの不完全性に対しても大きく影響を受ける場合もあり、MRFの実装のハードルは決して低くない。本稿ではMRFの実装例を交えながら、MRFの原理、撮像法、実装の注意点などや、最近の研究事例についても概説する。

EL9-2　Radiomics入門: 機械学習の基礎
Introduction of Radiomics - Basics of Machine Learning

朽名　夏麿（東京大学 大学院新領域創成科学研究科）
Natsumaro Kutsuna（Graduate School of Frontier Sciences, The University of Tokyo）

近年、生体の可視化法や撮像系の開発と普及、画像データベースの構築など、メディカルイメージング技術をとりまく状況は日増しに進歩している。しかしその一方、得られた画像を評価・解析する過程については、現在もなおほとんどの場合に医師・技師・研究者の目視による判断が重きを占めており、定量化のための画像からの計測工程についても人手に頼っていることが多い。これはイメージングに基づく評価・解析が、さらなる精度とスループットを達成する上での障害となっている。 このような状況下で期待される画像データの評価・解析に対するコンピュータによる支援技術の中でも、最近とくに注目を集めているアプローチである機械学習について、本発表ではとりあげる。機械学習は人工知能の主要な一分野であり、デジタル画像データをはじめデジタル化可能なあらゆる情報(各種の検査値、ゲノム情報、音声、テキストなど)について自動的な分類や評価を、人間に代わって、あるいは人間と協同して、コンピュータで行なうためのアルゴリズムの総称である。 発表ではまず機械学習を教師付き学習・教師無し学習に大別して紹介する。また、機械学習に共通して必須となる特徴抽出工程について、MRIはじめバイオメディカル画像からいかにして形態やテキスチャを数値化して特徴として抽出するのかを説明する。そしてとくに Radiomics において重要度が高いと考えられる教師付き学習について、代表的なアルゴリズムとして k-最近傍法(k-NN)、サポートベクトルマシン(SVM)、決定木、集団学習、ニューラルネットワークをとりあげる。最後に、この数年で急速に研究開発が活発化しているディープラーニング技術の代表格であるディープニューラルネットワーク(DNN)につき、その原理と、なぜDNNが高い性能を備えるのか、従来の機械学習手法との違いはいかなる所にあるのか、その得失はどのような点かについて解説する。全体を通じ、これまで機械学習を利用した経験がない初学者を対象に、極力数式の利用を避け、直観的に本分野の概略を把握できるよう構成する。

EL10-1　肩関節（腱板）
Shoulder joint (rotator cuff)

常陸　真（東北大学病院 放射線診断科）
Shin Hitachi（Tohoku University Hospital, Diagnostic Radiology）

腱板断裂の診断において、MRIは今や必要不可欠な検査であり、治療方針決定に重要な役割を果たしている。以前はMR関節造影が盛んに施行されていたが、高磁場MRIの普及に伴い、現在では非造影のMRIで十分な診断が可能となっている。
腱板断裂は全層断裂、部分断裂に分類される。全層断裂は関節側から滑液包側まで全層性に連続した断裂が認められる。全層断裂の評価では断裂の大きさやや幅の評価の他、術前の評価として、筋肉の萎縮や脂肪変性の程度も重要となっている。部分断裂には関節側、滑液包側、腱内（水平）断裂がある。関節側部分断裂は関節側に限局した断裂であり、滑液包側部分断裂は滑液包側に限局した断裂である。これらは断裂の深さの評価が術式選択に影響を与える。腱内断裂は腱板表面への連続性が無いもので、関節鏡では確認が出来ない。
腱板断裂が存在する側に液体貯留を認めることが多く、どこに液体が貯留しているかで、断裂の部位を類推することができる。肩甲下筋腱舌部の損傷は上腕二頭筋長頭腱の損傷に伴い生じる事が多い。見逃されやすく、hidden lesionと呼ばれ、注意が必要である。

EL10-2　肩関節の画像診断（関節唇、腱板疎部、上腕二頭筋長頭腱疾患）
Imaging Diagnosis of Shoulder joint(Glenoid lip,rotator interval,biceps brachii tendon)

天野　大介（明理会中央総合病院 放射線科）
Daisuke Amano（Meirikai Chuo General Hospital Department of Radiology）

肩関節のMRI画像診断では、日常診療では腱板断裂の有無を診断する頻度が圧倒的に高い。しかし、実際は肩関節の疾患は多岐にわたる。腱板全層断裂に陳旧性長頭腱断裂を合併している症例や、腱板断裂とhidden lesionを合併し、腱板断裂の修復のみでは疼痛の改善の得られない症例など、同一患者で複数の疾患を合併していることも多い。漠然と疑われた疾患のみを想定して読影していると、見逃されてしまう所見が多い分野でもある。骨折や骨性Bankart損傷の評価にはCTも有用であるが、肩関節疾患の画像評価としてはMRIが重要である。今回は、SLAP損傷を中心としたスポーツ障害肩、不安定肩(反復性肩関節脱臼や動揺肩)、腱板疎部疾患(拘縮肩や腱板疎部損傷)、上腕二頭筋長頭腱疾患(長頭腱炎、長頭腱断裂、亜脱臼／脱臼、hidden lesion)など、頻度は高くなくともまれではない疾患について、肩関節の正常解剖を含めて、病態とMRI所見を中心に解説する。

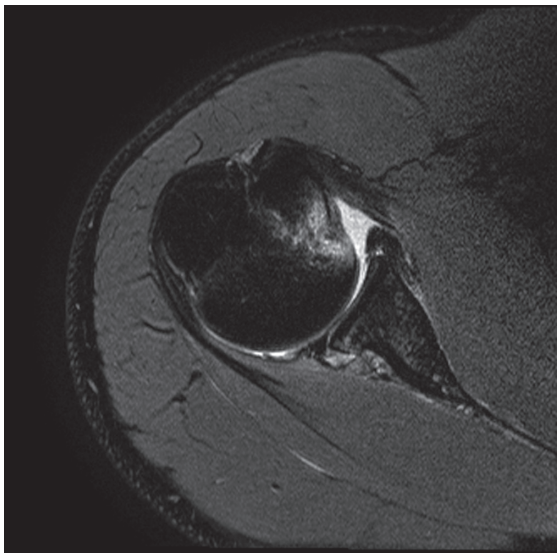

EL11-1　髄膜腫の稀な亜型の画像診断
Imaging features of meningioma variants

國松　聡（東京大学大学院 医学系研究科 放射線医学講座）
Akira Kunimatsu（Department of Radiology, Graduate School of Medicine, The University of Tokyo）

2016年発行の脳腫瘍WHO分類改訂第4版では、髄膜腫の疾患分類に変更は加えられず、異型髄膜腫の診断基準の一項目に脳内浸潤の存在が加えられるにとどまった。そのため、髄膜腫の診断根拠となる知見の根幹は現在も変わらない。髄膜腫の15種類の組織亜型のうち、髄膜皮性髄膜腫が最多で、これに続いて多い線維性髄膜腫、および両者の中間型である移行性髄膜腫という三つの組織亜型だけで、髄膜腫全体の約8割を占める。したがって、髄膜腫の典型的画像所見と理解されているものは、頻度の高いこれら三者の知見に基づくものが多い。残る組織亜型はそれぞれ髄膜腫全体の1～3％程度を占めるに過ぎず、実際に臨床で目にした場合に自信を持って診断することは必ずしも容易ではない。これらの頻度の低い組織亜型は、頻度の高い三組織亜型とは異なる画像的・臨床的特徴を示すことがあり、知っておくとその診断の一助になる。砂粒腫性髄膜腫は濃厚な石灰化を特徴とし、胸椎レベルの脊柱管内に発生することが相対的に多い。腫瘍の大きさのわりに隣接する脳実質の浮腫が強いものには、血管腫性髄膜腫、微小嚢胞性髄膜腫、分泌性髄膜腫がある。さらに、血管腫性髄膜腫は著明なvascularity、微小嚢胞性髄膜腫はT1強調像での明確な低信号、分泌性髄膜腫は頭蓋底部に好発することを特徴とする。拡散制限を示しやすいものには、リンパ球形質細胞に富む髄膜腫、異型髄膜腫、退形成性髄膜腫が含まれ、このうちリンパ球形質細胞に富む髄膜腫では、プラーク状進展を示しやすく、また炎症細胞浸潤を反映して腫瘍境界が不明瞭となりやすい。脊索腫様髄膜腫は拡散促進を示すことが特徴的である。明細胞髄膜腫、乳頭状髄膜腫、ラブドイド髄膜腫は、嚢胞を伴いやすく、また通常の髄膜腫にくらべ若年に発生しやすい。本講演では、日常臨床でたまに遭遇することのある「変な」髄膜腫に関する知識の整理を目標とする。

EL11-2　ムコ多糖症の中枢神経画像
Neuroimaging of mucopolysaccharidoses

土井下　怜（大阪市立大学大学院 医学研究科 放射線診断学・IVR学）
Satoshi Doishita（Osaka City University Graduate School of Medicine, Department of Diagnostic and Interventional Radiology）

ムコ多糖症はライソゾーム蓄積病の一種である。ライソゾーム内にあるグリコサミノグリカン（ムコ多糖）分解酵素の一つが欠損し、細胞内外にグリコサミノグリカンが蓄積することで、中枢神経系を含めた種々の臓器に進行性の障害が引き起こされる。現在までに11種類の原因酵素が特定され、I型（Hurler病やScheie病など）、II型（Hunter病）など7つの病型に分類されている。
ムコ多糖症の中枢神経画像所見として血管周囲腔の拡大が有名であるが、それ以外にも白質異常信号や脳萎縮、脳室拡大、くも膜下腔の拡大、頭蓋頸椎移行部の狭窄、頭蓋骨や脊椎の形態異常など多彩な所見を呈しうる。これらの画像所見の頻度や重症度には病型によって差異があり、各病型の画像所見の傾向を理解しておくことは、特にフォローアップ画像の読影において意義がある。
本講演では、これら頭部および頸髄・頸椎の画像所見を、整理して解説したい。

EL12-1　小児のMR検査はどうするべきかを考える
Think about what to do the MRI imaging in children

石黒　秋弘（地方独立行政法人大阪府立病院機構 大阪府立呼吸器・アレルギー医療センター 放射線科）
Akihiro Ishikuro（Osaka Prefectural Medical Center for Respiratory and Allergic Diseases）

現在のMR検査では、様々な撮像法が検査部位や依頼内容に応じて適宜、臨床利用されている。その中で小児のMR検査については、従来からスピンエコー（SE）法や高速SE法等を主として用い、T1・T2強調画像を取得している。撮像条件で考えてみると、FOVやマトリクス・スライス厚等SNRで厳しい場合も多い事から、撮像時間が延長する傾向にある。その結果、小児にとって長時間に及ぶ検査となる事が多い。環境面では、近年ワイドボア形状により閉鎖空間に対する配慮がなされたMRシステムが登場している。しかし、安静状態による体位保持や、騒音あるいは振動といった問題から、やむを得ず睡眠導入を行う場合も多い。睡眠導入による検査は、体幹部のような部位で特に長い撮像時間を要するシーケンスが中心となる事が多く、検査内容に関しても成人と比較して不十分な場合が少なからず発生する。また、覚醒したままで検査が可能な小児については、プレパレーションを十分に行う等、検査前準備でも長時間必要としたり、煩雑さが伴う事も日常的に存在する。
小児の成長・発達に関しては、新生児期や乳幼児期・学童期など、各々の時期に応じて体格面においても大きく変化する。また、脳実質における髄鞘形成に関しても、出現時期が異なる上にT1・T2強調画像における白質と灰白質のコントラストが加齢と共に変化する等、成人と比較して著しく画像の印象が異なる。その他に先天奇形や、代謝変性疾患・破壊性疾患等、小児特有の疾患に対しては、拡散強調画像や、$T2^{*}$強調画像もしくは磁化率強調画像、MRA・MRスペクトロスコピー等の追加が有用となる場合がある。
本講演では、小児検査に関する注意点や体位保持の方法から、脳実質の加齢に伴う信号変化に関する事や体動補正技術の応用、体幹部については、短時間撮像を実現する高速撮像技術や、呼吸抑制を目的とした呼吸補正・同期撮像、さらに検査環境面では、大幅な騒音軽減を実現した静音化撮像技術等、小児のMR検査はどうするべきなのかについて考えていきたい。

EL12-2　体幹部MR angiographyの撮像技術
Imaging techniques in MR angiography of the body

秦　　博文（北里大学病院 放射線部）
Hirofumi Hata（Department of Radiology, Kitasato University Hospital）

体幹部領域のMR angiography（以下MRA）検査は、体幹部血管領域においてMDCTによるCT angiographyが一般的に施行されることが多くなったため、検査依頼は減少傾向にある。しかし、ヨード造影剤禁忌症例、腎機能低下症例などMRA検査が必要とされるケースもあり、撮像技術を習得しておく必要がある。MRAには造影MRAと非造影MRAがあり、体幹部ではどちらも使用される。造影MRAは細胞外液性Gd造影剤を使用し、T1強調3D GRE法を呼吸停止下で撮像して得られる。撮像タイミング（造影剤到達タイミング）とk-space充填法を把握して撮像することで、動脈のみを描出することが可能である。一方、非造影MRAは3D balanced SSFP法、3D FSE法などで撮像され、T2値が比較的長い血液を高信号として描出する方法が一般的に用いられる。しかし、これらの撮像法では、動脈と静脈の両方が描出されてしまうため、撮像部位、目的によっては、動静脈を分離する必要がある。動静脈を分離する手法として、Inflow効果を利用する手法、心周期の違いによる動脈のFlow void効果の差を利用した方法などが臨床で使用されているが、いずれの手法も被検者の血流状態への依存が強いため、画質が不良になるケースもある。造影、非造影MRAで可能な限り良好な画質を得るためには、MRAの撮像原理を十分に理解しておく必要がある。本講演では、体幹部におけるMRA撮像の技術的な部分について解説する。また、近年では、3D phase contrast法の撮像データから、血流解析を行う研究、臨床応用が行われており、これらの撮像技術についても紹介したい。

EL13-1　条件付きMRI対応デバイス患者の安全管理
Safety management of MR conditional device

土橋　俊男（日本医科大学付属病院放射線科）
Toshio Tsuchihashi（Department of Radiology, Nippon Medical School Hospital）

2012年10月より，本邦においても条件付きMRI対応心臓植込み型電気的デバイス（ペースメーカ，ICD，CRT-D等：以下，条件付きMRI対応デバイス）が承認された．現在，各社から多くの機種が販売され，全国で1500～2000例近いMRI検査が施行されているものと思われる．多くの検査は，問題なく安全に施行できていると考えられるが，一部の検査で機種ごとに決められているMRIの撮像条件や，院内手順を逸脱して検査を施行（予約）したり，非認定施設でMRI対応モードに変更しないで検査を施行したりしている現実がある．ある一定の条件下でのみ検査が施行可能な「条件付きMRI対応デバイス」であるにもかかわらず，「MRI対応デバイス」と理解されてしまっていることが大きな要因の一つではないかと思われる．また，非認定施設では条件付きMRI対応デバイスに関する情報が十分周知されていないことも関係していると思われる．さらに，撮像条件ならびに撮像可能な範囲がメーカやデバイスの組み合わせごとに様々で複雑であることも影響していると考えられる． 条件付きMRI対応デバイスに関しては，各社から次々に新しい機種が登場している．当初MRI非対応であったリードがMRI対応となり，検査が可能となる場合もある．MRI検査時のデバイスのペーシングモードの設定によっても撮像条件が変わる機種が存在する．当初，静磁場強度は1.5Tのみであったが，最近は3.0T対応の機種も増加傾向にある．MRI装置の静磁場強度，静磁場の空間的な勾配，傾斜磁場の性能などハードに関係した制限，SARや最近登場したB1＋rmsなどの撮像条件に関係した制限などが多く存在し，その制限値が機種ごとに異なる現状は，検査現場で一番の問題点となっている．全てを把握しておくことが困難な状況である．この様な中で安全に検査を施行するには，検査現場が必要とする最新情報（撮像条件など）を検査現場からいつでも検索できるシステムの構築が必要ではないかと考える． 今回の講演では，検査現場で実際に発生した事例を紹介しながら安全に検査を施行するための今後の課題について考えてみたい．

EL13-2　条件付きMRI対応デバイスの現状と今後の課題
Current status and challenging future of MR conditional device

横山　健一（杏林大学 医学部 放射線医学教室）
Kenichi Yokoyama（Department of Radiology, Kyorin University, School of Medicine）

2012年秋に我が国に初めて条件付MRI対応ペースメーカが導入され、既に4年が経過しようとしている。この間、ペースメーカのみでなく植え込み型除細動器(ICD)や心臓再同期療法(CRT)などの多種多様な心臓関連のMRI対応デバイスが登場している。また脊髄刺激療法 (SCS)や脳深部刺激システム(DBS)といった心臓以外のデバイスも多く登場し、急速な勢いで日常臨床に浸透している。これらのデバイスの登場により、従来MRI検査が不可能であった多くのデバイス装着患者にとっての恩恵は計り知れない。我が国では患者の安全を第一に考え、関連3学会により検査実施の施設基準や実施条件を定め、一貫して厳密な運用を推進している。各施設の努力により厳密な安全管理がなされているが、検査の適応を十分考慮することや多職種間で密に連携することなど、今後も慎重な運用が望まれる。多種多様なMRI対応デバイスが導入される中、最近では1.5Tのみでなく3Tでの撮像も可能な製品も多く登場している。また撮像条件が各製品で異なることや同じ製品でも時期により撮像条件が変更となることもあり、実際の現場では少なからぬ混乱が生じている。対策の一つとして、全ての製品の情報をいち早く医療従事者に周知できるシステム作りや研修資料の統一化などの取り組みが必要と考えられる。

EL14-1　定量的 DCEMRI の基礎
Basics of quantitative DCEMRI

栗林　秀人（シーメンスヘルスケア株式会社）
Hideto Kuribayashi（Siemens Healthcare）

ダイナミック造影 MRI (Dynamic Contrast-Enhanced MRI: DCEMRI) は、静脈内投与されたガドリニウム系造影剤が腫瘍にどのように取り込まれ、その後排出されるのかを、T1 強調画像の連続撮像によりダイナミックに観察する方法である。造影剤投与後の腫瘍組織の信号変化の形状から、直感的に腫瘍の悪性度を推測することも可能である。例えば、造影された信号強度が時間とともに一定もしくは減衰していく形状を示した腫瘍組織は、悪性度が高いと疑われる。さらに、薬物動態学的アプローチにより、DCEMRI は定量的解析が行え、造影剤が腫瘍の毛細血管から組織へ移行する定数 (K^{trans}) や、移行した先である血管外・細胞外体積が組織の単位体積に占める割合 (v_e)、造影剤が組織から毛細血管へ戻る定数 (k_{ep}) などが求められる (1)。定量的 DCEMRI は同一被験者のがん治療効果の判定や抗がん剤開発のための多施設研究にも期待されるが、信頼される薬物動態パラメータを求めるためには、定量的 MRI 撮像プロトコルが確立されていなければならない。 そこには、造影剤の選択から用量・注入速度、T1 強調画像シーケンスの選択やその連続時間、造影剤投与前に撮っておくべき T1 マップなど、注意すべき点が多い (2)。それらの中には、総撮像時間の短縮や縦断・多施設研究のしやすさを優先させて確立されたものもある。DCEMRI の定量的解析には Tofts の薬物動態モデルが使われることが多いが、そのモデル式は単純に、造影剤濃度の高い毛細血管内と濃度の低い血管外・細胞外体積との間で造影剤がどう行き来し、それらを含む組織体積中の造影剤濃度がどのように時間変化するかを微分方程式であらわしたものである。その一般式への導出には、組織の形態や造影剤濃度の推移から推定した多くの「仮定」がなされており、得られた薬物動態パラメータを評価するには、それらの「仮定」を十分理解しておく必要がある。1. Tofts PS et al. J Magn Reson Imaging 1999;10:223-232.2. Leach MO et al. Eur Radiol 2012;22:1451-1464.

EL14-2　定量的DCEMRIの臨床応用
Clinical application of quantitative DCEMRI

山田　　哲（信州大学 医学部 画像医学教室）
Akira Yamada（Shinshu University School of Medicine, Department of Radiology）

定量的 dynamic contrast-enhanced MR imaging (DCEMRI) は非侵襲的に生体の血流動態・機能を解析可能であり，生検等の侵襲的手技の代替診断法としての臨床応用が期待されている．

本講演の前半では，定量的DCEMRIの臨床応用に必要不可欠な各種MR造影剤（細胞外液性，肝細胞特異性，細網内皮系特異性）の薬物動態，造影剤動態解析モデル（コンパートメントモデル，デコンボリューション法，最大傾斜法），造影剤動態解析によって得られる各種パラメーターの解釈について概説する．

本講演の後半では，具体的な定量的DCEMRIの臨床応用例として，一般的な治療適応判定や治療効果判定への応用の他，当院にて行っている肝細胞特異性DCEMRIの2-in-1-uptake-2-コンパートメントモデル解析による肝細胞癌の分化度診断，肝線維化のステージ診断への応用についても紹介する．

また，定量的DCEMRIの臨床応用においてMR画像上の造影効果の定量化は非常に重要な問題であり，当院にて行っている簡易ファントムを利用した定量的DCEMRIの実例として，定量的DCEMRIで得られるパラメーターと各種肝 MR biomarkers（肝硬度，Fat fraction，R2*，ADC）との相関，定量的DCEMRIで得られるパラメーターと血液検査との組み合わせによる肝障害度推定モデルについても紹介する予定である．

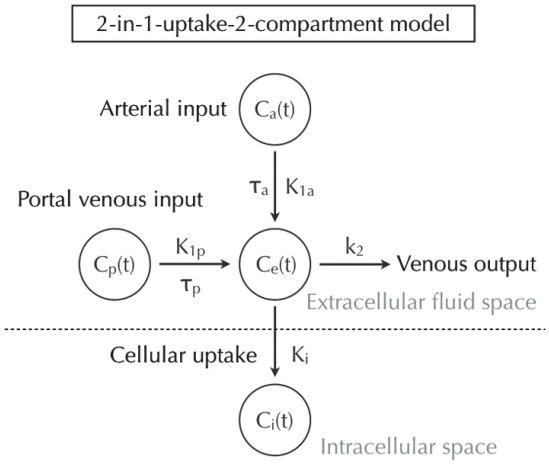

O-1-001　肝臓MR検査におけるADC-map を用いた3D-ヒストグラム解析
3D-Histogram Analysis using ADC-map in Liver Magnetic Resonance Image

中野　雅浩（JA愛知厚生連 海南病院 診療協同部 放射線技術科）
Masahiro Nakano[1], Takahiro Natsume[2], Seiji Kamei[3], Tatsuya Wakahara[1]

[1]Department of Radiological Technology, Kainan Hospital, Aichi Prefectural Welfare Federation, [2]School of Health Science, Fujita Health University, [3]Department of Radiology, Kainan Hospital, Aichi Prefectural Welfare Federation

【要旨】肝臓MR検査で拡散強調画像（b=0, 1000 sec/mm^2）を撮像し、ADC mapを作成した。解析には、Osirixを用いて撮像した画像に対して関心体積を手動で設定し3D-Histgramから算出したパラメータの検討を行った。解析の結果、ADCの最小値と歪度で有意差が認められヒストグラム解析の有用性が示唆された。

Purpose: The purpose of this study is to evaluate the 3D-histogram analysis using ADC-map in the liver MR study.
Methods: Contrast enhanced Liver MR images were obtains were acquired using a 3 Tesla MR scanner (Ingenia, Philips Healthcare) in 12 subjects (Hepatocellular carcinoma (HCC): 4, Hemangioma: 4, Healthy volunteers: 4). Apparent diffusion coefficient (ADC) maps were calculated with b-values of 0 and 1000 s/mm^2 using diffusion weighted imaging. The volume of interests (VOIs) were manually set on ADC maps for 3D-histogram analysis by using T2-weighted images and contrast enhanced T1-weighted images as a reference. Several parameters (mean values, standard deviation, minimum values, maximum values, skewness and kurtosis) were calculated by 3D-histogram analysis. The reduction of ADCs of the liver parenchyma in patients with chronic hepatitis or cirrhosis of the liver have been reported previously. Therefore, the region of interests (ROIs) were set on liver and spleen for evaluation of ADCs in liver parenchyma. The ADCs were normalized by ADCs of the spleen.
Results: There was no significant difference in the normalized ADCs of the liver between the patients with cirrhosis of the liver and healthy volunteers. The mean minimum ADCs values and mean ADCs ratios in the peritumoral regions of HCC were significantly lower than those in hemangioma. Skewness of the histogram in liver hemangioma was not as high as HCC.
Conclusion: Our study shown that the results of ADCs histogram analysis can be used to differentiate HCC from liver hemangioma.

O-1-002　正中神経における拡散テンソルと神経伝達速度との相関性の検討
Diffusion-tensor imaging of the median nerve: Correlation with nerve conduction study

酒井　亮介（東邦大学医療センター 佐倉病院 中央放射線部）
Ryosuke Sakai[1], Masahiro Sogawa[1], Hiroyuki Nakazawa[1], Mitsuyuki Tozawa[1], Stutomu Inaoka[2], Hitoshi Terada[2], Osamu Takahashi[3]

[1]Toho University Sakura Medical Center Central radiology department, [2]Toho University Sakura Medical Center radiological department, [3]Toho University Sakura Medical Center Clinical physiological function testing department

【要旨】本研究は、拡散テンソル法を用いて、末梢神経損傷の新たな診断法を確立することである。上記障害の検査の1つとして神経伝導速度検査がある。解析の結果、拡散テンソルと神経伝達速度に良好な相関関係を認めた。以上の結果から、拡散テンソルが末梢神経障害を診断する上で、有用な手段となることが示唆された。

[Purpose]To assess correlations between FA and ADC values from DTI and nerve conduction studies of the median nerves across the carpal tunnel in healthy adults.
[Materials and Methods]A total of 40 healthy adults(20 males and 20 females; age, 20-59years)were included in this study. DTI of the median nerves of bilateral wrist joints was performed with 3T MRI(Siemens healthcare, Magnetom Skyra) and a flex coil by using a single-shot echo-planar imaging sequence[repetition time(msec)/echo time(msec): 6500/81, b-value: 1400(sec/mm^2)]. FA and ADC values of the median nerves of bilateral wrist joints were measured at three locations of the radial head, proximal portion, and distal portion. In addition, nerve conduction studies of the median nerves of bilateral wrist joints were performed and motor conduction velocities (MCV) and sensory conduction velocities (SCV) were measured. To assess the correlations between FA and ADC values from DTI and MCV and SCV from nerve conduction studies of the median nerves of bilateral wrist joints, Pearson's correlation test was used. P value less than 0.05 indicated a statistically significant difference.
[Results]FA and ADC values from DTI and MCV and SCV from nerve conduction studies of the median nerves of bilateral wrist joints could be measured in all the 40 adults. Although there was no correlation between the FA values and MCV, a good correlation between the FA values and SCV was found ($p<0.001$). There was no correlation between the ADC values, MCV, and SCV.
[Conclusion]FA values from DTI have a good correlation with SCV from nerve conduction studies of the median nerves of the wrist joints in the healthy adults. FA values from DTI may be one of the useful tools for the evaluation of peripheral nerve impairment.

O-1-003　膵管癌の描出におけるcomputed DWIの有用性
Computed diffusion-weighted 3.0-T MR imaging for pancreatic adenocarcinoma

大塚　洋和（鹿児島大学病院 臨床技術部 放射線部門）
Hirokazu Otsuka[1], Yoshihiko Fukukura[2], Yuichi Kumagae[2], Koji Takumi[2], Hiroto Hakamada[2], Takashi Iwanaga[1], Takurou Fujisaki[1], Yasumasa Saigo[1], Tomoyuki Okuaki[3], Takashi Yoshiura[2]
[1]Department of Radiological Technology, Kagoshima University Hospital, Kagoshima, Japan, [2]Department of Radiology, Kagoshima University Graduate School of Medical and Dental Sciences, Kagoshima, Japan, [3]Philips Electronics Japan, Tokyo, Japan

【要旨】膵管癌の描出におけるcomputed DWI（cDWI）の有用性を検討した．b値0と1000から作成したb値1500のcDWIの膵管癌の描出能は，撮像にて得られたb値1500のDWI同様，b値1000のDWIと比して向上した．b値0と1000から作成したb値1500のcDWIは膵管癌の描出に有用と考えられた．

PURPOSE To assess the efficacy of computed DWI (cDWI) for visualizing pancreatic adenocarcinomas. **METHODS** Fifty-five patients with pancreatic adenocarcinoma underwent DWI with b-values of 0, 1000 (DWI_{1000}), 1500 (DWI_{1500}), and 2000 s/mm2 (DWI_{2000}). cDWIs with b-values of 1500 ($cDWI_{1500}$) and 2000 s/mm2 ($cDWI_{2000}$) were generated from b-values of 0 and 1000 s/mm2. We compared the visualization of pancreatic adenocarcinomas (clear hyperintensity; hyperintensity with an unclear distal border; and isointensity) and tumor to pancreas contrast ratio (CR) between DWI and cDWI in each b-value of 1500 and 2000 s/mm2. **RESULTS** DWI and cDWI findings are shown in Table. Incidence of clear hyperintense tumors was significantly higher on $cDWI_{1500}$ than on DWI_{1000} (P=.013). The tumor to distal pancreas CR was higher on $cDWI_{2000}$ than on $cDWI_{1500}$ (P<.001), and on $cDWI_{1500}$ than on DWI_{1000} (P<.001). The tumor to distal pancreas CR was significantly higher on cDWI than on DWI in both b-value of 1500 (P=.004) and 2000 (P<.001). **CONCLUSION** $cDWI_{1500}$ generated from b-values of 0 and 1000 s/mm2 yields higher tumor to distal pancreas CR compared with DWI_{1000}, and improved the delineation of pancreatic adenocarcinoma.

Table. DWI and cDWI findings and tumor-to-pancreas contrast ratio in 55 pancreatic adenocarcinomas

b-value (s/mm^2)	1000	1500		2000	
	DWI	DWI	cDWI	DWI	cDWI
DWI findings					
Clear hyperintensity	31 (56.4%)	44 (80.0%)	44 (80.0%)	47 (85.5%)	39 (70.9%)
Hyperintensity with unclear distal border	21 (38.2%)	9 (16.4%)	9 (16.4%)	5 (9.1%)	10 (18.2%)
Isointensity	3 (5.5%)	2 (3.6%)	2 (3.6%)	3 (5.5%)	6 (10.9%)
Tumor-to-pancreas CR					
Proximal pancreas	0.29 ± 0.13	0.29 ± 0.14	0.31 ± 0.17	0.30 ± 0.15	0.33 ± 0.22
Distal pancreas	0.20 ± 0.16	0.26 ± 0.20	0.29 ± 0.19	0.27 ± 0.18	0.36 ± 0.23

DWI=diffusion-weighted imaging, cDWI=computed diffusion-weighted imaging, CR=contrast ratio

O-1-004　Computed DWIによる末梢神経のDiffusion Tensor Tractography
Diffusion Tensor Tractography of the Peripheral Nerve by Computed DWI

原田　邦明（株式会社日立製作所 ヘルスケアビジネスユニット）
Kuniaki Harada, Yasuo Kawata, Ryuji Shirase, Masahiro Takizawa, Yoshitaka Bito
Healthcare Business Unit, Hitachi, Ltd.

【要旨】高空間分解能データを必要とする末梢神経のDiffusion Tensor Tractographyにおいて、比較的SNRの高いlow b factor DTIからcDWIを用いてhigh b factor DTIに変換したデータで解析することでTractographyの描出能を改善させた。

[Introduction]Diffusion tensor imaging (DTI) with high spatial resolution of the peripheral nerve such as median nerve requires long scan time. Furthermore, the usage of high b-value leads low SNR image, and this causes poor visualization of fiber on the diffusion tensor tractography (DTT). The purpose of this study is to improve visualization of fiber on DTT by using computationally calculating DTI images from low b-value images which have relatively high SNR.
[Methods]3 Tesla MRI scanner (Hitachi, Ltd., Tokyo, Japan) equipped with a hand/wrist coil was used for data acquisition of four healthy volunteers after informed written consent was obtained in accordance with our institutional review board guidelines. Single shot echo-planar diffusion weighted imaging (DWI) using thirteen motion proving gradient directions were performed with two b-values (200, 600 s/mm^2). The imaging parameters were as follows : FOV 120mm, Matrix size 80x128, Thickness 2mm, TR 8000 ms, TE 38.7 ms, and number of signal averages 2. Three different computed DWI (cDWI) image sets with b = 600, 800, and 1000 were generated from low b-value images (b = 200 s/mm^2) by using our custom-made software. DTT Analysis on the Virtual Place (Virtual Place is registered trademark or trademark of AZE Ltd. in Japan and other countries.) was used for generating 3D fiber tracts. These DTT results were compared with those from conventional DWI images.
[Results]DTT results from cDWI relatively showed better visualization of fiber than conventional DTT with b = 600 s/mm^2. However, DTT visualization might be changed by b-value which was used for calculation of cDWI.
[Conclusion]Good DTT visualization of fiber on Peripheral nerves was achieved by using cDWI.

O-1-005　肝臓におけるComputed DWI：肝嚢胞周囲に発生する高輝度アーチファクトの原因についての検討
A phantom study about high intensity rim around simple cyst on computed DWI in the liver

掛川　貴史（山梨大学医学部附属病院 放射線部）
Takashi Kakegawa[1], Utaroh Motosugi[2], Kazuyuki Sato[1], Tetsuya Wakayama[3], Hiroshi Kumagai[1], Hajime Sakamoto[1], Hiroshi Onishi[2]

[1]Department of Radiology, Yamanashi University Hospital, [2]Department of Radiology, University of Yamanashi, [3]GE Healthcare Japan

【要旨】DWI（b値0、500、1000(s/mm2)）から作製したComputed DWI(cDWI)（b値2000）において、肝嚢胞辺縁に高輝度アーチファクトをしばしば確認した。撮像マトリクスを増加させるにつれてb値0のDWIにおいて自作ファントム内模擬嚢胞周囲のトランケーションアーチファクトが減少し、cDWIにおける高輝度アーチファクトも減少した。

Purpose
Computed DWI (cDWI) is a technique to virtually make DWI with arbitrary b value from two or more DWIs obtained with different b alues. A high intensity rim is always observed around cysts in the liver on cDWI with target b value of 2000 s/mm^2 (cDWI2000) calculated from images with b value of 0, 500, and 1000 s/mm^2. In this study, we aimed to study the background of this finding.
Methods
A handmade phantom with liver of a pig in which water-filled balloon was inserted to simulate liver cyst was scanned with clinical 3T MR scanner (Discovery MR750, GE Healthcare). SE-EPI DW images with b values of 0, 500, and 1000 s/mm^2 were obtained with the following matrix size; frequency × phase, 64 × 160,128 × 160,192 × 160,256 × 160,128 × 64,128 × 128,128 × 192,128 × 256. The cDWI2000 by either 3 b values (0, 500, and 1000) or 2 b values (500 and 1000) were evaluated by a radiologist and a MR technologist to see the rim-like high intensity around the cyst (balloon).
Results
The truncation artifacts around the cyst (balloon) on b=0 images were less obvious, as phase/frequency encoding steps increased. Similarly, the rim-like high intensity around the cyst (balloon) on cDWI2000 by 3 b-values (b=0, 500, and 1000) were also less obvious by increasing matrix size. The rim-like high intensity was not as obvious on cDWI2000 by 2 b-values (b=500 and 1000) as that by 3 b-values.
Conclusion
Signal drop around the cyst (balloon) on b=0 images due to truncation artifacts is probably the cause of rim-like high intensity on cDWI2000.

O-1-006　16chと32chコイルの撮像条件の検討
Comparison of 16ch and 32ch multi-channel head coil in the diffusion weighted image

田尻　智美（済生会熊本病院 中央放射線部）
Satomi Tajiri[1], Takashi Okigawa[1], Takeshi Ohta[1], Takashi Sakamoto[1], Hiroki Arimura[1], Hiroyuki Hazeyama[1], Suguru Kawamura[1], Daisuke Masuda[1], Megumi Katayama[1], Yuuki Yamaguchi[1], Hirofumi Wada[1], Masahiro Kosaka[2], Kentarou Haraoka[2], Miho Kitamura[2], Masato Ikedo[2], Mitsue Miyazaki[2]

[1]Department of Radiology, Saiseikai Kumamoto Hospital, [2]Toshiba Medical Systems Corporation

【要旨】多チャンネルコイルは感度やSNRが良いが、DWIは従来と同じ撮像条件では表面の感度が高いため16chや1.5Tと比べて画像歪みが現れ、誤診を招く恐れがある。今回ファントムと健常ボランティアで最適条件の検討を行った。32chコイルは16chや1.5T画像と臨床画像の比較をする場合はパラメータや輝度補正を最適にする必要がある。

PURPOSE: Both 16ch and 32ch head coils have been used for brain image with our hospital's 3tesla MRI system. The multi-channel head coil has good sensitivity and SNR, however distortion occurs especially in the diffusion weighted image (DWI) . So we investigated and compared imaging each of the multi-channel head coils. MATERIALS AND METHODS: These studies were performed with a 3T MRI (Vantage Titan 3T; Toshiba Medical Japan) and Atlas SPEEDER Head coil (16ch coil) and 32ch Head SPEEDER coil were used. First,the phantom was scanned and obtained DWI images, in order to scaled the signal intensity of the images. We evaluated slice thickness and spatial resolution of clinical DWI images of healthy volunteers.RESULTS: In phantom images, the signal intensity using the 32ch coil was higher than the 16ch coil, but was more heterogeneous. The 32ch coil images have high signal intensity at the surface of the phantom compared to the center, the heterogeneity of signal intensity was appeared. In the clinical images of healthy volunteers, signal intensity was higher on the surface of the brain. The sensitivity correction and increasing the spatial resolution were employed to improve the distortions of 32ch coil images.CONCLUSION: The 32ch coil has a higher SNR compared to the 16ch coil, but the signal intensity in the images were heterogeneous. The artifacts decrease the image quality in clinical images. When using the 32ch coil, it is necessary to optimize imaging parameters and correct sensitivity to compare clinical images of the 16ch coil and 1.5T MRI systems.

O-1-007　複数コントラストのDWI画像を用いたComputed FLAIR-DWIの検討
Computed FLAIR-DWI Technique combined with DWI, PDW, T2W and T1W Imagings

高井　雄紀（東芝メディカルシステムズ株式会社 MR事業部 MR開発部グループ）
Yuki Takai[1], Tokunori Kimura[2], Hiroshi Kusahara[1], Naotaka Sakashita[2]

[1]MRI System Division, MRI Development department, Toshiba Medical Systems Corporation, [2]Clinical Application Research and Development Department, Toshiba Medical Systems Corporation

【要旨】我々はTE,b値,TR(TI)がそれぞれ異なる4つの測定画像からT2,ADC,T1mapを作成し,PDW,FLAIRなど任意のコントラストのDWI画像を作成できる新たなcDWIを提案する.特にFLAIR画像に着目し,実測のFLAIR-DWIよりも高いSNR,CNRの画像を提供できることを確認した.さらなる最適化が必要であるが,臨床の診断に有用であると期待される.

[Background]
A computed diffusion imaging (cDWI) was proposed and applied to improve contrast between tumors and the background. More recently a short-TE cDWI technique was proposed to reduce T2 shine-through effects or to further enhance tissues with short T2 and lower ADC. On the other hand, a synthetic MRI technique is gathering attention with shorter acquisition time than actual imaging. The purpose of this study was to propose a new computed DWI technique to generate arbitral combination of imaging parameters of TR (or TI), TE and b in combination of 4 kinds of acquired images, and to assess for volunteer brain imaging. Here Fluid-Attenuated IR (FLAIR)-DWI imaging was particularly focused on as an application of this technique.
[Theory]
Here following methods for computed FLAIR-DWI were compared including measured FLAIR-DWI.
a) FLAIR-mDWI: 1-point directly acquired IR signal at T2W-FLAIR DWI condition was assumed.
b) FLAIR-cDWI by FLAIR-DWI: ADC was calculated with 2 points FLAIR signals.
c) FLAIR-cDWI by T2W-DWI & T1map by short TR-T1W: ADC was calculated with 2 points T2W-SE signals. T1 was calculated using 2 points signals T1W-SE and PDW-SE.
d) FLAIR-cDWI by T2W-DWI & T1map by IR-T1W: ADC was calculated with the same way as method-c. T1 was calculated using 2 points signals of IR-T1W and PDW-SE.
[Result]
For simulations, the background noise SDs were increased in the order of **method d < c < b < a**, reflecting noise propagation effects of quantitative parameters. As the SDs in ADC and in R1 were smaller, SDs in cDWI signals became smaller. Brain tissue provided sufficient SNR even using T1 by TR method despite of poor T1W image. The SNR for the R1 map with T1 by IR was better than with T1 by TR, and therefore those effects reflected on the corresponding cDWI images.

O-1-008　MRIにおける新しい画像歪評価法の提言
Novel evaluation method for image distortion of magnetic resonance image

金子　瑤平（さいたま市立病院）
Yohei Kaneko[1], Akio Ogura[2], Isao Fujita[1], Aoi Kamakura[3], Tomoya Kitaoka[4]

[1]Saitama City Hospital, [2]Gunma Prefectural College of Health Science, [3]Jichi Medical University Hospital, [4]Fujita Health University Hospital

【要旨】NEMA法は撮像法に依存する画像歪評価には不十分なため、基準画像と評価画像で乖離した面積を評価する、面積法を新たに考案した。RFOVの長方形率を変化させたEPI像を対象として、NEMA法と面積法で歪率の理論値との整合性を比較した。結果として、面積法は測定時間も短く理想値に近い測定が可能であった。

Purpose
For evaluation of distortion on the MRI, the method recommended by National Electrical Manufactures Association (NEMA) is commonly used. However, by the NEMA method, it is thought to be inadequate for an evaluation of the distortion on the image using the various imaging techniques. Therefore, we devised a novel evaluation method for the distortion on the MR image.
Material & Methods
The novel evaluation method called the area method is measured the size of the different areas between criteria image and the evaluation image.
The container of the square filled nickel sulfate solution phantom was imaged using an MRI device of 1.5T. The PDWI of SE was as criteria image without the distortion and echo planar image was as a target image with the distortion. For imaging of the EPI, the rectangular rate of RFOV were changed the degree of the distortion.
An agreement degree with the theoretical value of the distortion rate for the RFOV were compared the NEMA method and the area method. In addition, the measurement time of each method was compared.
Results
In the NEMA method, the number for the measurement subject line was stable in its result for 16 lines or more. In addition, the coefficient of correlation with the theoretical value came to have 0.9 or more number for the measurement subject line in 32 or more.
Area method was agree to theoretical value. Also, the measurement time by the NEMA method became significantly long more than the area method.
Conclusion
The area method is suitable for an evaluation of the distortion depending on an imaging sequence because it has a short measurement time, and measurement accuracy is high.

O-1-009　IVIMによるグレードIIIとIVグリオーマ鑑別
Differentiation of grade III and IV gliomas by intravoxel incoherent motion MR imaging

上村　清央（鹿児島大学大学院医歯学総合研究科 放射線診断治療学分野）
Kiyohisa Kamimura[1], Masanori Nakajo[1], Yoshihiko Fukukura[1], Takashi Iwanaga[2], Hirofumi Hirano[3], Takashi Yoshiura[1]

[1]Department of Radiology, Kagoshima University Graduate School of Medical and Dental Sciences, [2]Clinical Engineering Department Radiation Section, Kagoshima University Hospital, [3]Department of Neurosurgery, Kagoshima University Graduate School of Medical and Dental Sciences

【要旨】グリオーマのWHOグレードIIIとIVでは予後が異なり、その鑑別は重要である。IVIMで算出されるD、f、D*やfxD*、ADCといったパラメータがその鑑別に有用であるか検討した。また、各種パラメータとKi-67インデックスとの相関係数を検討した。グレードIIIとIVとの鑑別にはfとfxD*が有用であった。

PURPOSE:The differentiation between WHO grade III and grade IV gliomas is critical since their prognoses could differ substantially. Our purpose was to evaluate the utility of intravoxel incoherent motion (IVIM) imaging in distinguishing grade III from grade IV gliomas.MATERIALS AND METHODS:Findings from 22 consecutive patients with pathologically proven malignant gliomas that included grade IV (16 glioblastomas) and grade III (5 anaplastic oligodendrogliomas and 1 anaplastic astrocytoma) were retrospectively evaluated. The maximum values of the f, D*, product of f and D* (fxD*), and the minimum values of the D and ADC were obtained in each tumor. Each IMIV metric was compared between grade III and grade IV tumors using Mann-Whitney U test. Receiver-operating characteristic (ROC) analysis was performed to determine diagnostic efficiency of each IVIM metric to distinguish grade III from grade IV tumors. In addition, correlation between each IMIV metric and immunohistological Ki-67 proliferation index (PI) was analyzed using Pearson's correlation coefficient. RESULTS: The f and the fxD* were significantly higher in grade IV than in grade III gliomas (14.1% vs. 8.57% and $3.03x10^{-3}mm^2/s$ vs. $1.92x10^{-3}mm^2/s$, $P<0.05$), whereas the other IVIM metrics (D, D*) and the ADC were not significantly different between the two groups. Area under the ROC curve (AUC) was largest for the f in distinguishing grade IV from grade III gliomas (AUC=0.823, $P<0.05$). Moreover, the D* and the fxD* showed a moderate positive correlation with the Ki-67 PI ($r=0.473$ and $r=0.439$, $P<0.05$), whereas the other IVIM metrics and the ADC showed no significant correlation.CONCLUSION:The f and the fxD* were found to be useful in preoperatively distinguishing between grade III and grade IV gliomas.

O-1-010　拡散強調画像のMPG渦電流歪みに対する補正ソフトの有用性
Usefulness of the correction software for the MPG eddy current distortion of the diffusion weighted image

齋藤　孝明（飯山赤十字病院 放射線科）
Takaaki Saito[1], Masato Kobayashi[2], Akihiro Yamashiro[3]

[1]Department of radiology, Iiyama red cross hospital, [2]Department of radiology, Nagano municipal hospital, [3]Department of radiology, Nagano red cross hospital

【要旨】Spin echo型のEPIによる拡散強調画像ではEPIモジュールでの位相方向への歪み、およびMPGの印加に伴う渦電流による歪みが問題となる。今回、装置搭載の補正ソフトの補正効果を検証した。補正によりMPG印加に伴う渦電流による歪みの影響を低減可能であり、特にoff centerでの病変描出能の向上に寄与する可能性が示唆された。

Purpose: Distortion to the phase direction in EPI module and distortion by the eddy current with the applying of motion proving gradient (MPG) become the problem in the diffusion weighted image by spin echo type echo planer imaging (EPI)."Correction of EPI distortions"is software equipped an MRI device.It is software correct the distortion by the eddy current that we can use when we apply MPG more than 6 axes and imaged it.The purpose of our study was to examine a correction effect and a usefulness of "Correction of EPI distortions".
Methods: We imaged a diffusion weighted image using an MRI performance evaluation phantom at a 75mm cephalad position away from the center of the magnetic field.We conducted the following studies with an obtained synthetic image about presence of "Correction of EPI distortions".
1)We acquired profile curve of four directions (phase direction, frequency direction, 45 degrees direction, 135 degrees direction) at four pin away from the center of the magnetic field of the synthetic image which we made. We calculated the diameter of the pin from FWHM (measurements) and calculated the distortion rate.
2)We confirmed a correction effect visually of the software by the image which subtracted a synthetic image from the b0 image.
Results: The distortion rate became small when corrected in "Correction of EPI distortions"in all directions. Difference in pin shape to the b0 image was small when corrected.
Conclusion:"Correction of EPI distortions" made it possible to reduce effect of the distortion by the eddy current with the applying of MPG. We may contribute to improvement of the lesion depiction ability at the position of away from the center of the magnetic field by using this software.

O-1-011　股関節慢性疼痛患者におけるbrain DTI and MRS estimatesの関連－FSL　TBSSを用いた比較研究
Correlation between brain DTI and proton MR Spectroscopy estimates for patients with chronic pain: a study using FSL TBSS

山本　誠（地方独立行政法人 さんむ医療センター）
Makoto Yamamoto[1], Tomonori Shigemura[1], Yutaka Suzuki[1], Kouichi Takai[1], Takayuki Obata[1,2], Akio Sakamoto[1]

[1]General local incorporated administrative agency Sanmu medical center, [2]Applied MRI Research, National Institute of Radiological Sciences

【要旨】FSLの『TBSS』を用いて慢性疼痛患者における視床MRSと内包後脚DTI指標の関連を探索した。疼痛と対応する側において、視床のNAA+NAAg/Crと内包後脚のFAに負の相関を認めた。視床MRSおよび内包DTI指標は慢性疼痛に関連する視床・皮質間の神経線維変化の評価に有用な可能性がある。

PURPOSE: Some reports have suggested that chronic pain affects brain function. Since the thalamus and posterior limb of internal capsule (PL-IC) are on the main pathway of pain information, DTI and proton MR Spectroscopy may reveal brain changes due to chronic pain. We performed DTI examination using spatial normalization to standard brain with Tract-Based Spatial Statistics (TBSS), and compared it with MRS and clinical condition grading methods. We also compared the results using manual region-of-interest (ROI) setting and TBSS methods. METHODS: Twenty-five female patients with osteoarthritis of the hip (mean, 70.5 yr (45-87)) underwent DTI (b=0, 1000s/mm^2; MPG=13 directions) and proton MRS on a 3T MRI scanner. ROIs were positioned on the bi-lateral PL-ICs. Fractional anisotropy (FA) and mean diffusivity (MD) were measured. Proton MRS (TE/TR, 35/2000ms) was performed to obtain NAA, mI, Cho and Cre ratios in bi-lateral thalami. RESULTS: There was significant difference in NAA + NAAG / Cre ($p = 0.032$) between ipsi- and contralateral thalami. There was a significant negative correlation between thalamic NAA + NAAG / Cre and PL-IC FA using TBSS skeleton method ($\rho = -0.61$, $p = 0.003$), while there was no significant correlation using the manual ROI method ($\rho = -0.35$, $p = 0.089$). There was no significant correlation among other MRS and DTI estimates. There was no significant correlation of clinical condition grading with any MRS or DTI estimates.CONCLUSION: We successfully determined the laterality in NAA + NAAG / Cre and correlation between thalamic NAA + NAAG / Cre and PL-IC FA using TBSS. The results suggest that DTI and MRS measure brain changes due to chronic pain, and that the TBSS approach can increase the quality of DTI assessment.

O-1-012　1.5T MRI装置によるDKIの臨床有用性の検討
Examination of the clinical usefulness of DKI with the 1.5T MRI system

西村　祥循（日本医科大学武蔵小杉病院 放射線科）
Yoshiyuki Nishimura, Shigeki Ikeda, Atsunari Kurose, Tooru Takahashi

Nippon Medical school Musashikosugi Hospital

【要旨】DKIは、頭部領域における疾患への臨床応用が期待されている。MRI装置のVer. upに伴いDKIのオンライン解析機能が搭載された。実際に臨床症例における撮像を行い、その有用性を検討した。ルーチンのDWI,ADC,FAと比較してより微細な変化を捉えることが可能となった。今後は撮像時間の短縮にも取り組むことが重要である。

<Purpose>In Diffusion kurtosis imaging(DKI), various clinical applications are expected, such as tumor of the brain, neurodegenerative disease, ischemic cerebrovascular disease. However, the use by the routine was still difficult because an imaging protocol, a method of analysis had not been yet established. In our hospital, as for our system, an online analysis function of DKI was equipped with by version up of January, 2016. Therefore, we actual performed the imaging in the clinical case and examined the usefulness.
<Material and Method>We performed the imaging of DKI in ECHELON OVAL 1.5T Version.5.1 (Hitachi, Ltd. Healthcare Business Unit). The scan parameters of DKI are as follows.TR:6000, TE:92, MPG(motion probing gradient)21 axis, b-factor:1000,2500s/mm^{2}We scanned ten patients in the above-mentioned parameter.
<Results>We were able to catch the more detailed lesion in comparison with standard DWI(Diffusion weighted imaging), ADC(apparent diffusion coefficient), FA(Fractional anisotropy).In this way, it understood that it was very useful to add DKI imaging to examination of the brain.
<Conclusion>We were able to confirm that clinical usefulness improved by adding DKI imaging to a routine examination in a clinical disease. However, it is difficult to add it to all examination because the scan time is long. We want to examine the parameter that useful information is provided in shorter scan time in future.

O-1-013　QSIにおけるMonte Calro simulationを用いた最適撮像条件の推定
Estimation of optimum imaging conditions using the Monte Calro simulation in QSI

八木　一夫（首都大学東京大学院 人間健康科学研究科 放射線科学域）
Kazuo Yagi[1], Masakazu Sato[1,2], Junichi Hata[1,2,3], Yasuhiko Tachibana[4], Norio Sekine[1]

[1]Division of Radiological Sciences, Graduate School of Human Health Sciences, Tokyo Metropolitan University, [2]Department of Radiology, University of Tokyo Hospital, [3]Department of physiology, Keio University School of Medicine, [4]Dartment of Charged Particle Therapy Research, National Institute of Radiological Science

【要旨】QSI においてMonte-Calro法を用いて水分子の拡散シミュレーションを行い、制限微細構造における最適撮像条件の推定を試みた。対象は白質神経と骨格筋線維とし、基本パルスシーケンスはPGSE法を用いた。理想条件、実験機条件、臨床機条件の3条件でシミュレーションを行い、どの程度制限構造を評価できるか比較検討した。

Performs a diffusion simulation of water molecules using a Monte-Calro method in QSI, we tried to estimate the optimal imaging conditions in the limit microstructure.Target structure is a skeletal muscle fiber with a relatively large structure also in white matter nerve and in vivo limit structure, which is a fine limit structure, basic pulse sequence was used PGSE (Pulse Gradient Spin Echo) method.Ideal conditions, experimental machine conditions, to simulate in three conditions of clinical machine conditions, the target structure is gradient magnetic field strength in each condition (ideal conditions: infinity, experimental machine conditions: smaller than 600 [mT / m], clinical machine conditions: the use of smaller than 40 [mT / m]), we can evaluate the degree limiting structure, compared either show any signal attenuation due to changes in configuration parameters were studied.From the results, the diffusion time of how much in the structural evaluation of the target limit structure it was possible to estimate either be required.Further, in this simulation delta, can see the transition of the signal decay curve due to variations in [delta], in limiting structure research conducted numerous [delta] Today, the optimum imaging condition included in the actual imaging data it is considered to be able to be presented.

O-1-014　IVIMを用いた両側総頸動脈閉塞ラットにおける脳血行動態異常の検出
Detection of abnormal cerebral hemodynamic change by intravoxel incoherent motion analysis in bilateral common carotid artery occlusion rat

藤原　俊朗（岩手医科大学 医学部 脳神経外科学講座）
Shunrou Fujiwara[1], Yuki Mori[2], Daniela Martinez de la Mora[2], Kuniaki Ogasawara[1], Yoshichika Yoshioka[2]

[1]Neurosurgery, Department of Medicine, Iwate Medical University, [2]WPI Immunology Frontier Research Center, Osaka University

【要旨】本研究では、IVIM-DWIによって両側総頸動脈閉塞ラットにおける脳血行動態異常が検出可能か動物用11.7TMRIを用いて検討した。BCCA後IVIM-DWIが可能であった7例では、BCCAO前に比べ、BCCAO後の左側皮質においてfivimが有意に上昇していた。

BackgroundBilateral carotid artery occlusion (BCCAO) rat is used as the chronic cerebral hypoperfusion model to assess the longitudinal ischemic effect to the brain. In the previous works, the effect of reduced CBF has been investigated, however, that of CBV has not been done. Here, we investigated whether IVIM-DWI could detect hemodynamic change, especially that of CBV, in BCCAO rat.Materials and Methods We performed surgical treatment to 13 Wistar rats (3 females, 7-9 week-old) as follows: first, a unilateral common carotid artery (CCA) was occluded by ligation with a 4-0 surgical thread; second, another CCA on the contralateral side was occluded 4 days after the previous unilateral occlusion. We performed DWI (multi-shot spin echo EPI sequence; FOV = 25.6x12.8 [mm2]; matrix = 128x64; slice thickness = 0.8 [mm]; 13 b values = 0-3000 [s/mm^2]) on a preclinical vertical 11.7 Tesla MRI (AVANCE II 500WB, Bruker) within 1h after the second surgical treatment. IVIM parameters (f_{ivim}, D*, D and K) were estimated by an original software developed with MATLAB (MathWorks, USA). And also, all parameter values were measured in two region of interest on the left and right side of the cortex. ResultsIn seven rats after BCCAO, all protocols were successfully performed. In quantitative assessment, f_{ivim} after BCCAO significantly increased on the left side (p=0.0313) of the cortex but the right side (p=0.8125) comparing with that before BCCAO. Then, D after BCCAO significantly decreased on the both side (left: p=0.0156; right: p=0.0313). Conclusion In conclusion, f_{ivim} from IVIM analysis has the ability to detect subtle hemodynamic change in the rat brain. CBV in BCCAO rat might be potentially affected by the order of carotid artery occlusion side for BCCAO.

O-1-015　CASL法により検討したくも膜下出血モデルマウスにおける急性期脳血流量の低下
Acute cerebral blood flow decrease after subarachnoid hemorrhage in mice with continuous arterial spin labelling

中村　和浩（秋田県立脳血管研究センター）
Kazuhiro Nakamura[1,2], Tatsushi Mutoh[1,2], Kazumasu Sasaki[1,2], Yasuyuki Taki[2], Toshibumi Kinoshita[1], Tatsuya Ishikawa[1]

[1]Research Institute for Brain and Blood Vessels Akita, [2]Institute of Development Aging and Cancer Tohoku University

【要旨】クモ膜下出血後生じる血管攣縮による脳血流量低下を評価するため、CASL法を用いてくも膜下出血モデルマウスの脳血流量を評価した。その結果SAH直後の脳血流量は明らかな低値として観察された。総頚動脈の反転効率低下など測定上の問題は残るものの、CASL法の有用性が示されたと考えられる。

[Purpose] Subarachnoid hemorrhage (SAH) is severe type of stroke caused by sudden bleeding into subarachnoid space. After SAH, arterial vasospasm appears up to three days in mice. This vasospasm should relate to cerebral blood flow (CBF) decrease. However, laser Doppler flowmetry (LDF) study showed dramatically reduction at SAH quickly returned within thirty minutes in mice. Arterial narrowing cause an increase in flow velocity distal of the vasospasm in LDF. The LDF is detected the blood cell velocity, whereas ASL is reflected the delivery of blood volume to the tissue. Therefore, LDF may not reflect the CBF adequately. To investigate the CBF after SAH, we have applied continuous arterial spin labelling (CASL) for SAH model mice.
[Methods] SAH was induced in thirty-nine male wild-type C57BL/6 mice (22 – 28 g) using endvascular perforation technique. The mice were set in the 4.7-T MRI (Varian Inova) spectrometer within one hour after SAH operation. CASL was performed using a two-coil system with labeling neck coil and quadrature brain surface coil. Average CBF value for the brain area was calculated.
[Results & Discussion] The mortality rate was 7.7% (3/39) at one hour after SAH operation. CASL CBF was 18.3 ± 11.2 ml/100g/min. The value was extremely low CBF than the normal value in mice. CASL CBF was decreased less than 25 % of normal CBF after SAH. It was strange because such extreme reduction caused tissue damage. Even after SAH, infarction area did not observe. CASL CBF might be underestimated in the two-coil system with labeling neck coil. The labeling neck coil only inverts the magnetic spin in the common carotid artery (CCA) and not in the vertebral artery (VA). Endvascular perforation may affect the inverted spin in the CCA.

O-1-016　拡散スペクトラム画像法の拡散異方性指標と課題反応時間の関係
Generalized fractional anisotropy of diffusion spectrum imaging and reaction time to investigate neurotransmission speed

松尾香弥子（獨協医科大学 医学部 精神生物学講座）
Kayako Matsuo[1], Yasuo Takehara[2]

[1]Department of Psychophysiology, Dokkyo Medical University, [2]Department of Radiology, Hamamatsu University Hospital

【要旨】拡散スペクトラム画像法により皮質脊髄路について調べたところ、その拡散指標は反応時間が速い被験者においてより大きかった。皮質に近い部分は反応時間全般に、深部は左右の手の使用に関与するといった部位特異性が認められた。拡散の異方性が大きいほど膜電位の伝達に有利であることが反映されている可能性がある。

INTRODUCTION:
We examined the neural basis of behavioral reaction time (RT) using generalized fractional anisotropy (GFA) of diffusion spectrum imaging (DSI). DSI has an advantage in a tract-based analysis because of its enhanced accuracy.
METHODS:
We introduced a DSI acquisition system to a GE 3T MRI (Discovery MR750): 56 axial slices, TR 8000, TE minimum, slice thickness 2.5, FOV 20*20, in-plane resolution 80 x 80, max b-value 4000 and 101 directions. We acquired DSI of 22 normal controls (F/M = 11/11, age 20-26) who also underwent an RT experiment with 4 conditions of 2 cue modalities (visual or auditory) by 2 response modes (left or right hand button press). We constructed a group template by an LDDMM algorithm and extracted individual fiber tracts. We specifically analyzed the bilateral pair of the corticospinal tract (CST) that ended up to the cortical hand area. Each tract (100 steps) was sectioned into quarters to use as GFA measures.
RESULTS:
Subjects with faster mean RT had greater GFA in the CST at the 4th quarter near the cortex. Moreover, subjects with greater GFA in the 2nd quarter of the left CST reacted faster when using their right hand, whereas subjects with greater GFA in the 1st quarter of the right CST reacted faster when using their left hand (both for visual cues).
DISCUSSION:
Faster RT actually had an association with greater GFA in the CST. We also observed a regional specificity within the CST, i.e., the portion near the cortex indicated faster RT in general, whereas the deeper portions were particularly associated with the left and right specialization. The GFA might reflect efficiencies of neurotransmissions, i.e., when the diffusion anisotropy was greater, the changes in the membrane potentials might transmit faster along the fibers.

O-1-017　Computed DWIにおける画質改善方法の開発
Image Quality Improvement of Computed DWI

河田　康雄（株式会社日立製作所 ヘルスケアビジネスユニット）
Yasuo Kawata, Ryuji Shirase, Kuniaki Harada, Hiroyuki Itagaki
Healthcare Business Unit, Hitachi, Ltd.

【要旨】DWI画像に対して、ADC値が異常となる画素の検出、補正処理の適用後に、Computed DWI画像を計算することによって、Computed DWI画像における輝点ノイズ、ドット抜けを低減する手法を検討した。本手法は、Computed DWI画像の画質を改善する可能性があることを示した。

[Objective]It has been reported that the computed DWI has a possibility to assist the clinical diagnosis of the tumor, e.g. prostate cancer, bladder cancer and breast cancer. However, the bright spot noises and the defective pixels are occurred on the computed DWI by the abnormal value of the apparent diffusion coefficient (ADC). These bright spot noises and the defective pixels prevent the radiologist from diagnosing the tumor. In this paper, we've developed the method to reduce the bright spot noises and the defective pixels for image quality improvement of the computed DWI.[Method]The DWI images were acquired with the b-value 300 s/mm2 by Hitachi 0.4T MRI apparatus. The healthy volunteers were evaluated after informed written consent was obtained in accordance with our institutional review board guidelines. We tried to compare the image quality of the computed DWI (b = 1000 s/mm2) calculated by the following algorithms.(a) Detection and correction of the pixels becoming the abnormal ADC, before the calculation of the ADC (Our method).(b) Cutoff of the abnormal ADC (Conventional Method).(c) Calculation of the computed DWI without (a) and (b).[Result and Conclusion]The bright spot noises and the defective pixels of the computed DWI were reduced by applying our method (a) to the DWI images. This approach may be able to improve the image quality of the computed DWI.

O-1-018　Neurite orientation dispersion and density imaging (NODDI) による結節性硬化症症例の白質の変化の検討
Evaluation of white matter microstructure in the cases of tuberous sclerosis (TS) using neurite orientation dispersion and density imaging (NODDI)

田岡　俊昭（名古屋大学 附属病院 放射線科）
Toshiaki Taoka[1], Noriko Aida[2], Yuta Fujii[2], Hisashi Kawai[1], Toshiki Nakane[1], Shinji Naganawa[1]
[1]Department of Radiology, Nagoya University Hospital, [2]Department of Radiology, Kanagawa Children's Medical Center

【要旨】結節性硬化症症例の白質では、Neurite orientation dispersion and density imaging (NODDI) の細胞内分画 (Ficvf) 画像で、拡散異方性 (FA) 画像と比較して、より広範な異常が検出された。

Objective: Neurite orientation dispersion and density imaging (NODDI) is a multi-compartment models to translate diffusion images using a set of indices that are related to white matter microstructure. Our purpose for the current study is to evaluate the NODDI in the tuberous sclerosis (TS) cases and speculate what are happening in the white matter after stroke.
Materials and Methods: Nine cases of TS were evaluated. Imaging was performed with a 3T clinical scanner. Two shells diffusion data was acquired including b=1000 and 2000 and analyzed with NODDI Matlab toolbox. Intracellular volume fraction (Ficvf) images were evaluated as well as fractional anisotropy (FA) images by scoring intensities of the white matter (3: obvious hyper-signal , 2: partial hyper-signal, 1: slight hyper-signal, 0: same as or lower than gray matter) in projection fiber (PF) and association fiber (AF) area of frontal, parietal, occipital and temporal lobe. These area are classified by existence of cortical tuber on FLAIR image, and mean scores were compared.
Results: In 61 areas with cortical tuber, mean score of PF area were 2.85 on FA and 1.68 on Ficvf, while those of AF area were 2.72 on FA and 0.95 on Ficvf. In 9 areas without cortical tuber, mean score of PF area were 3 on FA and 2.18 on Ficvf, while those of AF area were 3 on FA and 1.63 on Ficvf.
Conclusion: Decreases in FA, which might represent lower packing density of unmyelinated axonal fibers, were not prominent in TS cases. While, Ficvf of the white matter showed significant decrease, which might reflect the lack of maturation with thin non-myelinated fibers, especially in the association fiber area compared to the projection fiber area. These changes could be seen not only in the area with cortical tuber, but the area without them.

O-1-019　高濃度1.0mol/L非イオン性MRI用造影剤Gd-BT-DO3Aによるレンズ核線条体動脈描出の有用性
Visualization of the lenticulostriate arteries on postcontrast MRA using Gd-BT-DO3A

一坂　秀一（東京逓信病院 放射線科）
Shuichi Ichisaka, Toshiyuki Terashima, Motoyuki Yamashita, Kazuhiro Tsuchiya
Department of Radiology, Tokyo Teishin Hospital

【要旨】昨年、従来品と比べて2倍の濃度を有する高濃度（1.0mol/L）ガドリニウム造影剤が発売された。これを用い造影MRAを撮像し、従来品を用いた造影MRAとレンズ核線条体動脈の描出を比較した。結果として高濃度造影剤は、少なくとも従来品と同等かそれ以上の描出が期待できる。

[Purpose] We compared difference in visualization of in the lenticulostriate arteries (LSAs) on between postcontrast MRA using a 0.5-M agent and that using a 1.0-M agent (Gd-BT-DO3A, Gadovist).[Method] We performed postcontrast 3D-TOF MRA after administration of a 0.5-M agent (17 cases; age range, 41-85 years; median, 64) or after that of Gadovist (19 cases, age range, 35-88 years; median, 70). Contrast agent dose was determined according to patient' s body weight. On partial MIP images, we assessed the number of visualized LSAs and a contrast ratio (CR) of the LSAs comparing with the surrounding white matter.[Results] No difference was found between the two groups in the number of visualized LSAs. In the CR assessment, Gadovist yielded a better CR than the 0.5-M agent but the difference was not statistically significant.[Conclusion] Although there was no statistical difference in the present assessments, Gadovist is likely to provide better or at least equal value compared with 0.5-M agents in the demonstration of LSAs on postcontrast MRA.

O-1-020　ASLを用いた非造影のMRDSAによる頭蓋内主幹動脈閉塞・狭窄における側副血行の評価の初期経験
ASL-based Non-contrast MRDSA with 3D Data Acquisition: Initial Clinical Experience in Intracranial Major Trunk Stenoocclusive Diseases

土屋　一洋（東京逓信病院 放射線科）
Kazuhiro Tsuchiya[1], Miho Gomyo[2], Arisa Ohara[2], Shichiro Katase[2], Isao Miyazaki[3], Nanae Kawano[4], Naotaka Sakashita[4]
[1]Department of Radiology, Tokyo Teishin Hospital, [2]Department of Radiology, Kyorin University, [3]Radiology Department, Kyorin University Hospital, [4]Toshiba Medical Systems

【要旨】本研究により3D撮像での非造影のMRDSAは主幹部でのCNRは3D-TOF法のMRAには劣るが、これによって頭蓋内主幹動脈の閉塞・狭窄ならびにその側副血行といった血行動態が比較的短時間に良好に描出可能であることが示された。

[Objective] Arterial spin labeling (ASL) has recently been applied to visualize cerebral arteries as non-contrast MRDSA. We have developed an ASL-based MRDSA sequence that acquires 3D signal data at multiple interval times (multi-TI MRA with signal targeting alternating radiofrequency using asymmetric inversion slab [ASTAR] ASL technique: mASTAR). Our purpose was to assess its clinical feasibility in the diagnosis of stenoocclusive lesions of major intracranial arteries. [Materials and Methods] Six-phase 3D MRDSA was performed using a 3D-FFE sequence with an initial delay of 435 ms followed by 5 phases with a 235-ms interval. In 5 volunteers, we compared the CNR between mASTAR and 3D-TOF MRA at internal carotid artery (ICA) trunk and two portions of the middle cerebral artery (MCA). In 22 patients with stenosis/occlusion of the MCA (n = 11) and ICA (n = 11) including those with moyamoya disease (n = 7) as well as those after bypass surgery (n = 4), we visually scored demonstration of the lesion and that of branches distal to the lesion and bypass recipient vessels between the two methods. [Results] 3D MRDSA by mASTAR yielded six-phase serial images in 5 min 17 sec. In the CNR assessment, mASTAR was inferior to 3D-TOF MRA at the 3 portions. In the patient group, however, as for demonstration of stenosis, the two techniques well corresponded in 21 patients, while discrepancy was noted in 1 patient. Additionally, mASTAR better depicted distal branches in 15 patients, while two methods were equivalent in the remaining 7 patients. [Conclusion] In cerebral major artery stenoocclusive lesions, 3D MRDSA by the mASTAR technique could provide images reflecting hemodynamics in an acceptable scanning time.

O-1-021　1.5T 3D-TOF MRAによる大脳基底核穿通枝動脈の描出
Demonstration of the lenticulostriate arteries by modified 3D-TOF MRA

山下　素幸（東京逓信病院 放射線科）
Motoyuki Yamashita, Kazuhiro Tsuchiya, Shuichi Ichisaka
Department of Radiology, Tokyo Teishin Hospital, Tokyo, Japan

【要旨】大脳基底核領域のラクナ梗塞は線条体動脈などの穿通枝動脈の閉塞により生じる。通常の3D-TOF MRAでは穿通枝動脈の描出は困難である。そこで我々は、1.5T MRI装置を用いた高解像3D-TOF MRAの条件を検討し大脳基底核穿通枝動脈の描出を試みた。検討の結果、高解像3D-TOF MRAによる大脳基底核穿通枝動脈描出は可能である。

[Purpose] Lacunar infarction of the basal ganglia is caused by stenosis or occlusion of the lenticulostriate artery (LSA). Visualization of the normal LSAs by conventional 3D-TOF MRA is difficult. Therefore, we assessed scanning parameters of 3D-TOF MRA in an attempt to improve visualization of the LSAs.
[Method] We employed a 1.5-T system (Achieva, R2.6, Philips) using a SENSE Head coil. Five healthy volunteers were examined with the approval of our IRB. Scanning parameters examined were as follows: (1) slab thickness, (2) flip angle, and (3) initial angle of the TONE pulse. In the obtained images, we selected an LSA branch that was most clearly depicted and assessed its visualization using a five-point grading system We also evaluated its CNR comparing with the white matter.
[Results] LSAs were visualized in all cases. Depiction of the LSAs improved by using thinner slab thickness as well as by increasing the flip angle.
[Conclusion] It is possible to improve the depiction of the LSAs by modification of scanning parameters of 3D-TOF MRA.

O-1-022　3D-TOF-MRA 元画像とT2WI-SPACE像のfusion像による解離性椎骨脳底動脈瘤の評価
The fusion image of 3D-TOF-MRA and T2W-SPACE in evaluation of vertebro-basilar artery dissection

池田　宏明（獨協医科大学病院 放射線科）
Hiroaki Ikeda, Yos Misu, Mayuko Ajima, Kensuke Inamura, Sadaharu Hiki, Hiroaki Arakawa, Shigeko Kuwajima, Yasukazu Shioyama, Tsutomu Ishukawa, Yasushi Kaji
Department of radilogy, Dokkyo Medical University

【要旨】椎骨脳底動脈解離性動脈瘤に関して、3D-TOF-MRA元画像とT2-SPACE像のfusion像で得られる情報について検討した。血栓化解離腔を簡単に検出でき、脳梗塞や、くも膜下出血の原因病変を指摘できた。これまでのBPAS像とMRAの比較による評価に比べて、このfusion法はより簡単で正確に動脈解離を評価できると思われた。

Purpose: To assess the usefulness of the fusion image of 3D-TOF-MRA and 3D-T2W-SPACE in evaluation of dissecting aneurysm of the vertebro-basilar artery (VBA). Methods: 85 patients (median age 58.5 years; 62 men) with clinically suspected VBA dissection were included in this study. First, 3D-TOF-MRA and T2W-SPACE that covers the main trunk of the VBA were obtained using the 3T machine (MAGNETOM Skyra, Siemens Healthcare Japan). Second, the gray scale of the original images of T2W-SPACE were inverted, and fusioned with the source images of 3D-MR angiography on the workstation (SingoVia, Siemens Healthcare Japan). We evaluated the difference between the outline of VBA wall showed by T2W-SPACE and that by MRA, which means the thrombosed clot. Results and Discussion: There were 20 cases showing the difference between the outline of VBA wall and the arterial lumen. We considered this as the thrombosed clot in dissected space. These dissections of VBA might cause the cerebral infarction in 13 cases, and the subarachnoid hemorrhage in one case. We usually evaluate the dissecting aneurysm by comparing basi-parallel anatomic scanning (BPAS) with 3D-TOF-MRA, however the arterial dissection could be showed more easily and precisely using this fusion technique.Conclusion: The VBA dissection may be detected by the fusion of source images 3D-TOF-MRA and 3D-SPACE. This fusion technique is considered to be useful.

O-1-023　くも膜下出血症例における脈波同期併用MRA血管壁拍動イメージングの特徴
Characteristic of the vascular wall heartbeat imaging in the pulse wave synchronization combination MRA in the subarachnoid hemorrhage case

古川　研治（釧路孝仁会記念病院 診療放射線科）
Kenji Furukawa[1], Tsuyoshi Nikaidou[2], Koki Yamamoto[1]
[1]kushiro kojinkai memorial hospital, [2]kushiro neurosurgery

【要旨】くも膜下出血症例に対し脈波同期併用MRAを撮像。血管壁の拍動イメージングより得られた破裂脳動脈瘤とblebの詳細な動きをまとめ報告する。クモ膜下出血症例13例でblebを確認できた症例は9例。blebの拡張率の平均は27%で、9例全てで20%以上であった。本法は破裂予測の一助になりうる。

Purpose: There is a difference between disease rate of the cerebral aneurysm and probability of rupture. Therefore it is important to know the risk assessment of the rupture in necessity of treatment and operation. We have done the pulse wave synchronization MRA in a subarachnoid hemorrhage(SAH) case, then we analyzed the vascular wall exercise of ruptured cerebral aneurysm and bleb with heartbeat image.Method: We scanned pulse wave synchronization 3D TOF MRA in a SAH case and acquired MRA data of 4phase. We make the heartbeat imaging that Cine displayed VR image in each phase of a provided images.And three neurosurgeons performed the evaluation that is motion of the wall of a cerebral aneurysm and a bleb, the expansion degree and depiction.Result: We evaluated it by 13 SAH cases. (1)The degree of expansion averages that is the long axis and short axis of the aneurysm were 7% and 12% respectively. (2) The cases bleb were 9 examples, and an average of the expansion rate of bleb was 27%. And it was more than 20 % by all 9 examples of blebs. (3)Totals of a case with the case the part of the aneurysm expanded 20 % and bleb were 11 examples. Conclusion: The vascular wall heartbeat image of MRA showed motion on a blood vessel wall by a pulse. Therefore we can guess at arteriosclerosis of aneurysm and expansion of bleb. It is very important that we catch movement by the heartbeat of aneurysm and bleb in a rupture prediction

O-1-024　iMSDEを併用したサブトラクション法による4D-TOFの改良
Improved 4D-TOF using subtraction image by iMSDE

高野　　晋（東海大学 医学附属病院 診療技術部 放射線技術科）
Susumu Takano[1], Tetsuo Ogino[2], Shuhei Shibukawa[1], Nao Kajihara[1], Tomohiko Horie[1], Tetsu Niwa[3], Isao Muro[1]
[1]Department of Radiology, Tokai University Hospital, [2]Philips Electronics Japan, [3]Department of Diagnostic Radiology, Tokai University School of Medicine

【要旨】我々は、先行研究にてsaturation pulseを用いた新しい4D-MRA撮像法である4D-TOFを開発し発表を行った。本研究では、従来の4D-TOFよりも頭蓋内血管の描出能を向上させ、ASLベースの4D-MRAよりも高速撮像できるiMSDEを併用したサブトラクション法を考案し、検討を行った。

Purpose:
4D-MRA based arterial spin labeling (ASL) subtracts control images from labeling images. Although ASL could obtain high contrast between intracranial artery and brain tissue, it relatively takes long scan time to require all phase at control images. Hence, We have developed four-dimensional time-of-flight (4D-TOF), a novel 4D-MRA technique using saturation pulse for observing intracranial hemodynamics. Additionally, we apply single-phase subtraction using improved motion sensitized driven equilibrium (iMSDE) for 4D-TOF(sub 4D-TOF) to obtain depiction of intracranial artery and reduce scan time compared with 4D-MRA based ASL.
Methods:
We evaluated eight healthy volunteers, who underwent conventional 4D-TOF and sub 4D-TOF. Mask as subtraction images consist of single-phase TOF by iMSDE that could obtain black blood imaging. Scan time of mask took 1min. The iMSDE T2Prep consisted of 3 directions with flow venc=5,10,20cm/s, echo time=20ms, refocusing pulses=4.To compare conventional 4D-TOF and sub 4D-TOF, the contrast ratio (Rt MCA's ROI/white matter's ROI) was calculated.
Results and Discussion:
The contrast ratio of sub 4D-TOF showed higher values than conventional 4D-TOF especially at early phase. The difference between conventional 4D-TOF and sub 4D-TOF may be understood as follows. Sub 4D-TOF might have kept signal of intracranial artery and suppressed signal of brain tissue because mask obtain black blood signal at brain vascular by iMSDE. We indicated sub 4D-TOF improve depiction of intracranial arteries compared with conventional 4D-TOF in this study.

O-1-025　Silent MRAによる脳動静脈奇形、硬膜動静脈瘻描出能の検討
Silent MRA of cerebral arteriovenous malformation and dural arteriovenous fistula

藤原　広和（慶應義塾大学 医学部 放射線診断科）
Hirokazu Fujiwara, Suketaka Momoshima, Jun Kurasawa, Masahiro Jinzaki
Keio University Department of Diagnostic Radiology

【要旨】Silent MRAはUTE MRIにASLを併用する新しいMRAの撮影技術である。Silent MRAの脳動静脈奇形(AVM)、硬膜動静脈瘻(dAVF)描出能をTOF MRAと比較検討した。Silent MRAはTOF MRAに比べAVM, dAVFを明瞭に描出した。栄養動脈、導出静脈の描出もTOF MRAより良好でAVM, dAVFの診断に有用と考えられた。

Purpose: Silent MRA is a new technique using ultra shot TE MRI combined with arterial spin labeling preparation pulses. The purpose of this study is to evaluate diagnostic ability of silent MRA for cerebral arteriovenous malformation (AVM) and dural arteriovenous fistula (dAVF).Materials and methods: Silent MRA and 3D time-of-flight (TOF) MRA of 10 cases of AVM and 8 cases of dAVF were retrospectively reviewed. All MR images were obtained with a 3 T scanner (SIGNA Pioneer, GE Healthcare Japan). Silent MRA was compared with TOF MRA as to the presence of shunts, feeding arteries and drainage veins. Results: Silent MRA revealed AVM and dAVF more clearly than TOF MRA. Small AVMs adjacent to hematomas and small dAVFs were detected with only silent MRA. Signal intensities of AVM nidus were higher on silent MRA than on TOF MRA. Silent MRA was also superior in visualizing the feeding arteries and drainage veins.Conclusion: Silent MRA is useful for detection and grading of cerebral AVM and dAVF.

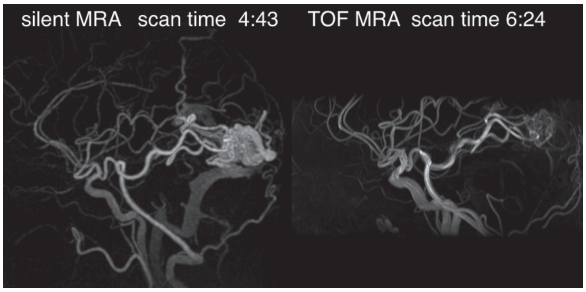

O-1-026　ASLにおけるbackground suppressionによるCBF値への影響
Effect of background suppression on arterial spin labeling CBF quantification

豊嶋　英仁（秋田県立脳血管研究センター 放射線科診療部）
Hideto Toyoshima[1], Masanobu Ibaraki[1], Kazuhiro Nakamura[1], Kazuhiro Takahashi[1], Toshibumi Kinoshita[1], Josef Pfeuffer[2], Hideto Kuribayashi[3]
[1]Research Institute for Brain and Blood Vessels-Akita, [2]Siemens Healthcare GmbH, Germany, [3]Siemens Healthcare KK, Japan

【要旨】【目的】ASLにおけるbackground suppression (BS) によるCBF値の影響を評価した.
【方法】Siemens WIP 3D-pCASLを用いてBSのOn/Offの状態で健常人5名を測定し，画質ならびにCBF値を比較した.
【結果】画質はBS Onのほうが均一性およびSNRが向上した．5スライス全脳のCBF平均値は,BS onのほうが約20％低下した.

Aim: The use of background suppression (BS) is strongly recommended for ASL measurements to improve image quality, by reducing physiological noises and motion artifacts. However, BS pulses are also known to reduce the ASL signals because of pulse imperfection, potentially causing significant underestimation of CBF. The aim of the study is to investigate the effect of BS on quantitative ASL CBF measurements.
Methods: ASL CBF experiments for five healthy volunteers were performed on a 3T scanner (MAGNETOM Verio Dot, Siemens) using 32-channel head receiver array. For each subject, 3D pCASL acquisition was conducted with and without BS (Siemens work-in-progress pulse sequence). Sequence parameters are as follows: labeling duration = 1,800 ms; post labeling delay = 2,000 ms. Image quality and absolute CBF estimates were compared between the results with and without BS. This study was approved by the local ethics committee.
Results: Image uniformity and SNR of CBF maps were significantly superior with BS compared to without BS. Regions-of-interest analysis showed that average CBF values in cortical regions with and without BS were 34.4 and 44.2 (mL/100 g/min), respectively.
Discussion: The present study confirms that background-suppressed ASL provides better image quality, but underestimates absolute CBF values. The degree of reduction in CBF estimates by BS, approximately 20%, seems to be consistent with the measured inversion efficiency of BS pulses (e.g., Garcia DM et al. MRM 2005;54:366-372). Background-suppressed 3D pCASL should be carefully used for application in which the determination of absolute CBF values is essential.

O-1-027　悪性神経膠腫と転移性脳腫瘍の鑑別のためのASL高信号の3D容積解析の有用性について
3D volumetric analysis of ASL high signal intensity on tumor might be useful in differentiating Glioblastoma and Brain metastasis

ガンボルドムングンバガナ（徳島大学 放射線科）
Ganbold Mungunbagana, Takashi Abe, Masafumi Harada, Delgerdalai Khashbat, Yuki Kanazawa
Tokushima University

【要旨】神経膠芽腫25例と脳転移13例についてASLにおける高信号の容積と造影領域の容積を算出し、両者の容積差についてROC解析を行い、診断精度を検討した。その結果、ASLと造影領域の容積差は神経膠芽腫で有意に高値であり、ROC解析でもASLによる血流値による鑑別よりも診断精度が高い結果となった。

Purpose: We aimed to investigate the volume of tumor Arterial spin labeling (ASL) high signal to differentiate Glioblastoma (GBM) from brain metastasis. **Materials and methods:** Thirty-eight patients with a diagnosis of GBM (n=25) and metastasis (n=13) were underwent conventional and ASL MR imaging. The volume of interests were manually placed on tumor lesion with high signal intensity of ASL and contrast enhancing (CE) of post-contrast T1WI by using Synapse Vincent Three dimensions (3D) software. Subtracted tumor volume (ASL-CE) and ratio of tumor volume (ASL/CE) were obtained from ASL and CE+T1WI. Absolute maximal tumor blood flow (TBF) and ratio of TBF (normalized to white matter) were also measured from the tumors. The Mann-Whitney U Test and the receiver operating characteristic (ROC) curve analysis were used to assess the difference of the measurements between tumor groups. **Results:** Subtracted tumor volume is significantly higher in GBM than in metastasis (21.55 ± 22.12 ml versus 3.49 ± 11.59 ml, p <0.001). Ratio of tumor volume is also significantly higher in GBM than in metastasis (3.2 ± 2.4 versus 1.2 ± 0.89, p <0.001) in this study.The diagnostic accuracy values for the differentiation of GBM from metastasis in subtracted tumor volume area under curve of 0.865 (p<0.001) and in ratio area under curve of 0.852 (p <0.001). TBF and TBF ratio of GBM were higher than metastasis, but the differences were not significant (136.5 < 58.16 versus 107.6 ± 64.93 ml/100g/min p=0.85; 5.66 < 2.35 versus 4.26 ± 2.36, p=0.69). **Conclusion:** The volume of tumor ASL high signal intensity might be useful to differentiate GBM from brain metastasis, whereas ASL TBF is insufficient. GBM showed larger lesions with high signal intensity in ASL compared with metastasis.

O-1-028　急性期脳梗塞におけるASLを用いた Parenchymal Hematomaの予測
Parenchymal hematoma of acute ischemic stroke: Prediction with hyperemic lesion on arterial-spin labeling MRI

新甫　武也（宮崎大学 医学部 臨床神経科学講座 脳神経外科分野）
Takeya Niibo[1], Hajime Ohta[2], Ichirou Ikushima[3], Shirou Miyata[2], Kazuchika Yonenaga[3], Hideo Takeshima[1]

[1]Department of Neurosurgery, Faculty of Medicine, University of Miyazaki, [2]Department of Neurosurgery, Miyakonojo Medical Association Hospital, [3]Department of Radiology, Miyakonojo Medical association hospital

【要旨】急性期脳梗塞で発症後6時間以内にMRIを施行されMRAで主幹動脈閉塞を伴っていた136例を対象とした。ASL mapでHyperemic lesion(HL)を健側比でCBF≧250％と定義し、ROC分析でHL volumeとPHに有意な相関（P< 0.001）が認められ、ロジステイック回帰分析でHLはPHの独立した予測因子であった。HLはPHの予測に有用と考えられた。

Background and Purpose-To evaluate whether hypermic lesions detected on arterial-spin labeling MRI could predict cerebral parenchymal hematoma (PH) in acute stroke patients.Methods-We identified patients with acute ischemic stroke who underwent MRI scanning including ASL images within 6 hours of symptom onset and had vessel occlusions (distal internal carotid artery or proximal middle cerebral artery) on the baseline MR angiography. HL volumes defined by relative cerebral blood flow (rCBF)>175, 200, 225, and 250% of contralateral mean were calculated using voxel-based algorithms in symptomatic hemispheres. MRI or CT scans were performed at subacute phase to identify PH. The association between HL and PH was examined using receiver operating characteristic (ROC) analysis and multivariate logistic regression analysis.Results-Of 136 patients, 26 (19.1%) patients developed PH.In the ROC analysis for association between PH and HL across the range of ASL-rCBF thresholds, ASL-rCBF>250% gave an optimal area under the curve of 0.84 (P< 0.001) and ASL-rCBF>250% volumes of >0.5 mL allowed prediction of PH with sensitivity of 96% and specificity of 52%. ASL-rCBF>250% volume and combined endovascular therapy were both independently predictive of PH in multivariate analysis (P< 0.001).Conclusions-HL defined by ASL-rCBF>250% appears to allow for distinguishing patients with acute ischemic stroke who are likely from those who are not likely to develop PH.

O-1-029　小児片頭痛患者における3D ASL（arterial spin labeling）での灌流異常について
Perfusion abnormalities on 3D arterial spin labeling at 3T MR in pediatric and adolescent patients with migraine

上谷　浩之（熊本大学 画像診断治療科）
Hiroyuki Uetani[1,2], Mika Kitajima[1], Takeshi Sugahara[2], Hironori Kikuchi[2], Kohei Yamada[3], Tomoo Hirahara[4], Sadahiro Yamamura[2], Yasuyuki Yamashita[1]

[1]Dept. of Radiology, Graduate School of Medical Sciences, Kumamoto University, [2]Dept. of Radiology, Japanese Red Cross Kumamoto Hospital, [3]Dept. of Pediatrics, Japanese Red Cross Kumamoto Hospital, [4]Dept. of Neurology, National Hospital Organization Kumamoto Medical Center

【要旨】本研究の目的は小児片頭痛患者において、3D ASLでの灌流異常の発生頻度と分布、重症度を調べることである。対象は3T MRIを撮像した連続する小児片頭痛患者44名で、34%に灌流異常を認め、後頭葉に最も多くみられた。小児の片頭痛患者では高頻度にASLで灌流異常がみられ、特に後頭葉優位であった。

The purpose of this study was to determine the prevalence, topography and severity of perfusion abnormalities on 3D ASL at 3T in pediatric and adolescent patients with migraine. The subjects were 44 consecutive patients (20 women, 24 men; age range, 3–18 years) with migraine diagnosed based on criteria of the International Classification of Headache Disorders, third edition and all underwent 3T MRI including 3D ASL. We retrospectively reviewed 3D ASL, DWI, MRA, and conventional MR images. We assessed the severity and distribution of abnormal perfusion on ASL. Abnormal perfusion on ASL was qualitatively evaluated using a 5-point grading system from score −2 (moderate to severe hypoperfusion compared to the normal appearing region) to score +2 (moderate to severe hyperperfusion), and was correlated with conventional MR images and MRA. Of the 44 patients, 15 (34%) exhibited perfusion abnormalities. One had mild hyperperfusion (score +1), 10 had mild hypoperfusion (score −1), and 4 had moderate to severe hypoperfusion (score −2). In 8 of these 15 patients (53%) the occipital lobe was most frequently involved. One patient with sporadic hemiplegic migraine manifested vasoconstriction of the left middle and posterior cerebral artery on MRA, and prominent hypointense cortical and medullary veins in the area corresponding to the vasoconstriction on T2* weighted image. Other MR imeges showed no abnormality in any of the patients. Of the 15 patients with abnormal perfusion, 5 underwent follow up MRI including ASL; the perfusion abnormalities were improved in all. In patients with pediatric and adolescent migraine, 3T ASL showed a high prevelance of abnormal perfusion especially in the occipital lobe with hypoperfusion.

O-1-030　CENTRA-Keyholeを用いた4D-PCASL MRA:モヤモヤ病における末梢血管の描出
4D MR Angiography with pCASL Combined with CENTRA-Keyhole (4D-PACK): Visualization of Distal Cerebral Arteries in Moyamoya Disease

栂尾　　理（九州大学大学院医学研究院 臨床放射線科学分野）
Osamu Togao[1], Akio Hiwatashi[1], Makoto Obara[2], Koji Yamashita[1], Kazufumi Kikuchi[1], Ryo Somehara[1], Ryotaro Kamei[1], Hiroshi Honda[1]

[1]Department of Clinical Radiology, Graduate School of Medical Sciences, Kyushu University, [2]Philips Electronics Japan

【要旨】pCASLにCENTRA-keyhole法を組み合わせた4D-PACKのモヤモヤ病における有用性を検討した。LMAからの逆行性血流を有する中大脳動脈末梢枝の描出は4D-PACKの方がCINEMAよりも優れており、本法は長いtransit timeを有するモヤモヤ病の末梢枝の描出に有用である。

PURPOSE:To evaluate the utility of 4D MR angiography (MRA) using pCASL combined with CENTRA-keyhole technique (4D-PACK) in the visualization of distal cerebral arteries and leptomeningeal anastomosis (LMA) collaterals in Moyamoya disease by comparing with contrast inherent inflow enhanced multi-phase angiography (CINEMA).METHODS:Nine patients with Moyamoya disease who underwent both MRA and DSA were scanned on a Philips 3T scanner. Thirteen cerebral hemispheres that did not received bypass surgeries were analyzed. The 4D-PACK and CINEMA were obtained with the identical spatial resolution and imaging geometry. The label durations in 4D-PACK ranged from 100 ms to 2200 ms, and the post labeling delay in CINEMA ranged from 200 ms to 2200 ms with 200 ms interval. The scan time for 4D-PACK and CINEMA was 5 min 10 sec and 4 min 30 sec, respectively. The maximum contrast-to-noise ratio (CNR) and time to peak (TTP) were measured in 1) distal MCA branches (M3-4) with anterograde flow and 2) distal MCA branches (M4) with retrograde flow via LMA collaterals. RESULTS:In the distal MCAs with anterograde flow, the maximum CNRs were significantly higher in 4D-PACK (38.0 ± 14.7, P=0.007) than in CINEMA (22.1 ± 12.4). The TTP was significantly longer in 4D-PACK (1969 ± 468 ms, P<0.0001) than in CINEMA (923 ± 342 ms). In the distal MCAs with retrograde flow via LMA collaterals, the maximum CNRs were significantly higher in 4D-PACK (27.3 ± 8.6, P<0.0001) than in CINEMA (10.5 ± 4.0). The TTP was significantly longer in 4D-PACK (1908 ± 405 ms, P<0.0001) than in CINEMA (1231 ± 304 ms).CONCLUSION:The 4D-PACK is useful in the evaluation of distal cerebral arteries and LMA collaterals with very long transit time in Moyamoya disease.

O-1-031　キーホールを用いたpseudo-contious arterial spin labeling(PCASL)頭蓋内非造影ダイナミックMRA撮像

Non-contrast enhanced 4D intracranial MR angiography based on pseudo-continuous arterial spin labelling (PCASL) with CENTRA-Keyhole (4D-PACK)

小原　真（フィリップスエレクトロニクスジャパン）
Makoto Obara[1], Osamu Togao[2], Tomoyuki Okuaki[3], Shuhei Shibukawa[4,5], Masami Yoneyama[1], Marc Van Cauteren[3]

[1]Philips Electronics Japan, [2]Graduate School of Medical Sciences, Kyushu University, [3]Philips Healthcare, Asia Pacific, [4]Department of Radiology, Tokai University Hospital, [5]Graduate School of Medical Sciences, Kanazawa University

【要旨】PCASLを用いた頭蓋内ダイナミックアンギオグラフィーにキーホールを併用し高速化を試みた。キーホールなしで得られたデータとの間に血流到達時間において高い相関が得られ、撮像時間が時相1600msまでの撮像で3分以上短縮した。また従来法CINEMAと比較した結果、中大脳動脈末梢において高い血流信号を示した。

PURPOSE: Intracranial four-dimensional magnetic resonance angiography (4D-MRA) using PCASL is introduced. The 4D-PCASL was combined with contrast-enhanced timing-robust angiography (CENTRA) k-space sampling and keyhole (4D-PACK). The aim of this study is to investigate validity of flow dynamic information in 4D-PACK and to investigate arterial visualization ability in 4D-PACK compared with contrast inherent inflow-enhanced multiphase angiography (CINEMA). METHODS: Philips 3T was used. For validation of flow dynamic information, arterial transit time (ATT) was measured in 4D-PCASL and 4D-PACK at multiple regions in middle cerebral artery (MCA) and correlation coefficient was calculated. For the assessment of flow visualization ability, contrast-to-noise ratio (CNR) between MCA and white matter were measured at four MCA segments and compared with CINEMA. Two dynamic schemes were tested for the validation of flow dynamic information: 1. labeling duration from 200ms to 1600ms with 200ms interval (scheme-A) and 3min20sec scan time reduction in 4D-PACK, 2. labeling duration from 100ms to 800ms with 100ms interval (scheme-B) and 2min11sec reduction. For the assessment of flow visualization ability, scheme-A was compared with CINEMA with post labeling delay from 200ms to 1600ms with interval 200ms. Six healthy volunteers were examined with scheme-A and CINEMA. Four healthy volunteers were examined with scheme-B.RESULTS: For the ATT correlation coefficient was consistently higher than 0.9. The CNRs were significantly higher in 4D-PACK compared with CINEMA at M4 segment ($P < 0.05$). CONCLUSION: The 4D-PCASL can be accelerated by keyhole, while retaining inflow dynamic information. This technique is less sensitive to signal saturation effects compared with CINEMA.

O-1-032　T1測定による肝悪性腫瘍の鑑別

Feasibility of measuring the T1 relaxation times for characterization of malignant liver tumors

岩永　崇（鹿児島大学病院 臨床技術部 放射線部門）
Takashi Iwanaga[1], Yoshihiko Fukukura[2], Yuichi Kumagae[2], Tomonori Saito[1], Masashi Sasaki[1], Takuro Fujisaki[1], Yasumasa Saigo[1], Hiroshi Imai[3], Takashi Yoshiura[2]

[1]Department of Radiological Technology, Kagoshima University Hospital, Kagoshima, Japan, [2]Department of Radiology, Kagoshima University Graduate School of Medical and Dental Sciences, Kagoshima, Japan, [3]Siemens Healthcare K.K.

【要旨】肝悪性腫瘍の診断に対するGd-EOB-DTPA造影前後の腫瘍T1値の有用性を評価した．造影前後のT1値および造影剤の取り込みの指標であるRRとΔR1のすべてのパラメータで肝細胞癌と転移性肝腫瘍間に有意差を認めた．腫瘍のT1値は，肝悪性腫瘍の鑑別に有用であると考えられた．

PURPOSE: To evaluate the feasibility of T1 relaxation times for characterization of malignant liver tumors. **METHODS:** Forty-one patients with histologically confirmed 22 hepatocellular carcinomas (HCCs) and 19 metastases underwent dual FA T1 mapping before and 20 min after Gd-EOB-DTPA injection on a 1.5-T MRI system. We compared the T1 relaxation times before and 20 min after Gd-EOB-DTPA injection, reduction rate of T1 relaxation time (RR), and ΔR1 between HCCs and metastases. Receiver operating characteristic (ROC) analysis was carried out to evaluate the diagnostic accuracy for differentiating HCCs from metastases. **RESULTS:** T1 relaxation times before (P=.002) and after Gd-EOB-DTPA injection (P<.001) were significantly lower in HCCs than in metastases (Table). RR and ΔR1 of HCCs were significantly higher than those of metastases (both, P<.001). T1 relaxation times 20 min after Gd-EOB-DTPA injection showed the highest area under the ROC curve (0.945; 95% CI: 0.826, 0.992) with a sensitivity of 100% and specificity of 86.4% at a cut-off value of 853 ms. **CONCLUSION:** T1 relaxation times 20 min after Gd-EOB-DTPA injection of tumors can help characterize malignant liver tumors.

Table. T1 relaxation times of liver and tumors before and 20 min after Gd-EOB-DTPA administration

				HCC vs. metastases	
	Liver	HCC	metastases	P value	AUC
Pre T1 [ms]	740.6±87.0	1247.2±262.7	1627.8±352.6	0.002	0.782
Post T1 [ms]	270.2±67.8	704.4±188.6	1249.7±361.9	<0.001	0.945
RR	0.637±0.072	0.428±0.127	0.230±0.141	<0.001	0.868
ΔR1(×10^3)	2.576±0.947	0.675±0.318	0.212±0.138	<0.001	0.895

HCC=hepatocellular carcinoma, RR=reduction rete of T1relaxation time, AUR=areas under the ROC

O-1-033　EOB造影MRI肝細胞造影相における胆道系濃染と肝機能に関する検討
Biliary Tract Enhancement during the Hepatobiliary Phase inEOB-MRI:Correlation with Non-invasive Biomarker Associated with Liver Function and Fibrosis

梶田　公博（岐阜大学医学部附属病院 放射線部）
Kimihiro Kajita[1], Yoshifumi Noda[2], Takayuki Miura[1], Ryohei Yaegashi[1], Shogo Maeda[1], Hiroki Kato[1], Shinichi Shoda[1], Satoshi Goshima[2], Masayuki Matsuo[1,2]
[1]Gifu University Hospital Radiology services, [2]Gifu University Hospital department of Radiology

【要旨】肝機能障害が疑われた139例を対象に、肝細胞造影相を含めたEOB造影MRIを撮像し、SIR（左右肝管、総肝管、胆嚢管、総胆管/脊柱起立筋信号）を算出した。胆嚢管、総胆管のSIRが、重回帰分析においてChild-pugh分類、MELD score、APRIに対し有意なパラメータとして同定され、肝機能評価に有用である可能性が示された。

＜ Purpose ＞ To evaluate the association between gadoxetic acid-enhanced magnetic resonance (MR) imaging measurements and other laboratory and clinical biomarkers of liver function and fibrosis. ＜ Materials and Methods ＞ This retrospective study was approved by our institutional review board and written informed consent was waived. One hundred thirty nine consecutive patients (89 men and 50 women, age range 33-87 years, mean age 67 ± 12.6 years) with suspected liver disease or liver tumor underwent gadoxetic acid-enhanced MR imaging. MR imaging measurements during the hepatobiliary phase included biliary tract structure-to-muscle signal intensity ratio (SIR) and quantitative liver-spleen contrast ratio (Q-LSC). These measurements were compared with Child-Pugh classification, end-stage liver disease (MELD) score, and aspartate aminotransferase-to-platelet ratio index (APRI).<Results ＞ The SIRs of cystic duct and common bile duct were significantly correlated with Child-Pugh classification (P = 0.012 for cystic duct and P < 0.0001 for common bile duct), MELD score (P = 0.0016 and P = 0.0033), and APRI (P = 0.0022 and P = 0.0015). The sensitivity, specificity, and area under the receiver-operating-characteristic curve were: (74%, 88%, 0.86) with the SIR of common bile duct for the detection of patients with Child-Pugh class B or C; (100%, 87%, 0.94) with the SIR of cystic duct for high MELD score (＞ 10); (65%, 76%, 0.70) with the SIR of common bile duct for APRI (＞ 1.5). ＜ Conclusion ＞ Gadoxetic acid contrast enhancement of cystic duct and common bile duct could be used as biomarkers to assess liver function.

O-1-034　EOB-MRIにおける乏血性低信号結節の長期観察研究
Long-term observation of hypovascular hypointense nodules (HHNs) on gadoxetic acid-enhanced MRI

清水　辰哉（山梨大学 医学部 放射線科）
Tatsuya Shimizu[1], Utaroh Motosugi[1], Katsuhiro Sano[2], Shintaro Ichikawa[1], Hiroshi Onishi[1]
[1]Department of Radiology, University of Yamanashi, [2]Department of Diagnostic Radiology, Saitama Medical University International Medical Center

【要旨】早期肝細胞癌はEOB-MRIでは肝細胞相で低信号を呈する乏血性結節として認められる。今回我々はこのような乏血性低信号結節を長期間にわたってフォローし、多血化の割合とそのリスク因子について調べた。その結果、脂肪抑制T1強調像にて高信号であることと、腫瘍サイズが10mm以上であることが独立したリスク因子であった。

Purpose
Hepatocellular carcinomas (HCCs) commonly develop via hypovascular HCCs also known as early HCCs. Early HCCs show hypointensity on gadoxetic acid-enhanced hepatobiliary phase images. In this study, we call these nodules hypovascular hypointense nodule (HHN). We investigated outcomes of HHNs with long-term observation, and conducted a retrospective study to perform risk analysis of development of hypervascular HCC from HHNs (hypervascularization).
Method
We reviewed the radiological records about the patients who underwent gadoxetic acid-enhanced MRI for the purpose of screening for HCC at our hospital from February 2008 to February 2011. We included all patients who had HHN and follow-up MRI (222 HHNs in 92 patients). Endpoint of this study was the hypervascularization of HCCs. Risk factors of hypervascular HCC were analyzed by univariate and multivariate Cox proportional hazard model with the following factors: age, sex, tumor size, signal intensity on T2-weighted images and fat-saturated T1-weighted images, fat-containing appearance on opposed-phase T1-weighted images, growth rate in size. The incidence rate of hypervascular HCC was assessed using Kaplan-Meier curves.
Result
Median of observation period was 775 days (184-2858). During the follow-up, 123 HHNs became hypervasular HCCs. Incidence rate of hypervascularization at 3 years and 5 years were 41.21% and 68.61%, respectively. Multivariate analysis revealed that, fat-saturated T1-weighted images (1.85 [1.09 - 3.08]), lager tumor size (>10mm, 1.56 [1.01 - 2.41]) were the independent risk factors of hypervascularization.
Conclusion
Cumulative rate of hypervascularization from HHNs were ever-increasing over 5 years. Size of >10 mm were one of the independent risk of becoming hypervascular HCCs.

O-1-035　乏血性肝細胞相低信号結節は肝細胞癌術後の多中心性再発の予測因子となるか？
Hypovascular hypointense nodules detected by EOB-MRI as a risk factor for multicentric recurrence of hepatocellular carcinoma after hepatectomy

松田　正樹（山梨大学 医学部 放射線科）
Masaki Matsuda[1], Shintaro Ichikawa[1], Utaroh Motosugi[1], Masanori Matsuda[2], Hiroshi Onishi[1]
[1]Department of Radiology, University of Yamanashi, [2]Department of First Surgery, University of Yamanashi

【要旨】多血性HCC手術例126名を対象として乏血性肝細胞相低信号結節（HHN）がHCC術後の多中心性再発（術後1年以降の再発）の予測因子となるかを検討した。早期再発症例（術後1年以内の再発）29名を除いた場合、術前にHHNのある群はない群よりも優位に無病生存期間が短かった（術後5年で24.5% vs 70.4%）。

Purpose: To evaluate the presence of hypovascular hypointense nodules (HHN) using EOB-MRI for predicting multicentric recurrence after surgery in patients with HCC.
Methods: We included 126 patients with primary hypervascular HCC who had undergone hepatectomy. The patients were classified into two groups: patients with early recurrence (< 1 year) and those without early recurrence. The preoperative patient characteristics and imaging variables were evaluated to predict multicentric recurrence using Cox proportional hazards regression analysis, which was used to assess disease-free survival (DFS). In this study, multicentric recurrence was defined as a recurrent event that occurs more than 1 year after surgery. Kaplan-Meier analysis was used to compare the prognosis between the groups with and without early recurrence.
Results: The median follow-up period was 36 months. Twenty-nine patients (23.0%) showed early recurrence, while 30 (23.8%) showed multicentric recurrence after surgery. The findings of the univariate analyses revealed that the presence of HHN was significantly associated with DFS, except in patients with early recurrence (P = 0.0139). Multivariate logistic regression analysis with HHN, age, and sex showed that the presence of HHN (P = 0.0231) was an independent predictor of DFS for patients without early recurrence. The results of Kaplan-Meier analysis revealed that for patients without early recurrence, those with HHN had a significantly worse prognosis than those without HHN (P = 0.0081). Five years after the surgery, the DFS of patients with HHN and without HHN was 24.5% and 70.4%, respectively.
Conclusions: HHN detected by EOB-MRI is an indicator of HCC recurrence and prognosis after surgical resection of HCCs in patients without early recurrence.

O-1-036　膵癌T stageによる膵実質の信号変化に関する検討
Pancreas Signal Intensity Changes among T Stages in Patients with Pancreatic Ductal Adenocarcinoma

野田　佳史（岐阜大学 放射線科）
Yoshifumi Noda, Satoshi Goshima, Hiroshi Kawada, Nobuyuki Kawai, Hiromi Koyasu, Masayuki Matsuo
Gifu University Hospital

【要旨】膵癌患者のT stageによる膵実質の信号変化につき検討した。膵頭部癌患者32例、非膵癌患者11名を対象とし、膵体部の信号を各シーケンスで測定した。T1信号、ADC値は、非膵癌患者、T1-2、T3-4と順に有意な低下を認めた。T1信号、ADC値はT stageに応じて低下することが示された。

Purpose: To assess the signal intensity changes of non-tumoral pancreatic parenchyma among T stages in patient with pancreatic ductal adenocarcinoma (PDAC).
Materials and Methods: This retrospective study was approved by our institutional review board and written informed consent was waived. Magnetic resonance (MR) imaging obtained in 32 consecutive patients (18 men, 14 women; mean age, 69.6 ± 8.6 years) who underwent pancreatectomy and 11 normal studies were evaluated. Patients were classified into three groups according to the T stages: normal study (group 1), T = 1 or 2 (group 2), and T = 3 or 4 (group 3). The pancreas-to-muscle signal intensity ratio (SIR) on in- and opposed-phase images, T1- and T2-weighted images, and the apparent diffusion coefficient (ADC) value of the pancreas were measured. The relationships among the T stages and the MR imaging measurements were examined by using logistic regression analysis, Kruskal-Wallis test, and receiver-operating-characteristic (ROC) analysis.
Results: Logistic regression analysis demonstrated that SIR on T1-weighted images (P < 0.0001) and ADC value (P = 0.015) were independently associated with T stages. Group 1 demonstrated significantly higher SIR on T1-weighted images and ADC value (P < 0.05) compared with group 2 and 3. The sensitivities, specificities, and area under the ROC curves (AUCs) in the detection of group 1 were 100%, 88%, and 0.97 with SIR on T1-weighted images, and 82%, 91%, and 0.86 with ADC value, respectively.
Conclusion: The SIR on T1-weighted images and ADC value of the pancreas can be a potential biomarker for the assessment of the changes in pancreatic parenchyma among T stages in patients with PDAC.

O-1-037　Recognition of anterior peritoneal reflection in rectal MRI: A single centre experience among southern Chinese

Wai Keung Lo[1], Deyond YW Siu[1], PP Iu[1], PYY Lau[2], Danny HY Cho[1]

[1]Department of Radiology, Kwong Wah Hospital Hong Kong, China, [2]Department of Surgery, Kwong Wah Hospital Hong Kong, China

Introduction:
The anterior peritoneal reflection is a well-defined landmark separating the intra and extraperitoneal rectum. Its preoperative identification can aid appropriate staging and therapy in patients with primary rectal carcinoma. A previous study in the USA reported good visualization (~80%) of it on rectal MRI, concurred by a study among northern Chinese in Shanghai. However it is well known that ethnic variations exist, and paucity of mesorectal fat thickness has been reported in a case series in Hong Kong. Therefore the purpose of this study is to determine percentage visualization of anterior peritoneal reflection among southern Chinese in Hong Kong.
Methods:
Imaging data for consecutive patients referred for rectal MRI (1.5T Philips Achieva XR) with a presumed diagnosis of rectal carcinoma from November 2015 to May 2016 were retrospectively reviewed. Visibility of the anterior peritoneal reflection was graded on a 5-point scale as the one proposed by Gollub et. Al . Quality of MRI was also graded. Distance from the anal verge to it was measured in a straight line. Relationship to adjacent structures, such as seminal vesicle in men and uterocervical angle in women, as well as other factors that may influence visualization such as bladder distension and uterine version were also recorded.
Results:
The anterior peritoneal reflection was deemed probably or definitely visible in 75%(18) of all(24) rectal MRI studies. Motion artifacts, bladder distension, prostate enlargement and prior hysterectomy were noted in patients whose reflection could not be confidently seen. Mean, median, range of the distance from anal verge were 8.5cm, 8.7cm and 6.1-10.9cm. It is consistently associated with top of the seminal vesicle in men, with much variation in women.
Conclusion:
The anterior peritoneal reflection can be visualized in many southern Chinese. Optimizing image quality by reducing motion artifacts and bladder emptying prior to scan maybe helpful to improve visibility. In men, top of the seminal vesicle can be a reliable landmark to locate the anterior peritoneal reflection.

O-1-038　ベイズ理論を用いた肝実質へのガドキセト酸取り込み低下症例の予測
Bayesian prediction for insufficient liver enhancement in gadoxetic acid-enhanced hepatobiliary phase imaging

森　優喜（山梨大学 医学部 放射線医学講座）
Yuki Mori, Utaroh Motosugi, Tatsuya Shimizu, Shintaro Ichikawa, Hiroshi Onishi

Department of Radiology, University of Yamanashi

【要旨】肝機能低下症例では肝特異性造影剤を十分に取り込めない。ビリルビンなどの指標と取り込み不良症例との関連が先行研究で示唆されているが、検査前に取り込み不良を予測する方法は確立されていない。本研究では、ベイズ理論を用いて複数の指標を組み合わせることで取り込み不良症例の予測が可能であることを証明した。

Purpose: Insufficient liver enhancement due to decreased liver function is a major limitation in gadoxetic acid-enhanced hepatobiliary phase imaging (HBP). Some factors, such as liver stiffness measured by MR elastography (MRE), associate with insufficient liver enhancement. Bayesian prediction is a statistical method which provides posterior probability by combining more than one factor that could predict the event. The purpose of this study was to reveal feasibility and utility of Bayesian method for predicting patients with insufficient liver enhancement. Materials and Methods2068 patients who had undergone MRE and gadoxetic acid-enhanced MR imaging from June 2012 to December 2015 were reviewed. They were excluded if (i) spleen was removed, (ii) blood test results within 2 weeks were unavailable, (iii) γ-GT raised abnormally for reasons other than liver disease. 639 patients who matched these criteria were divided into two groups according to liver-to-portal vein contrast ratio, for which a cut-off value of 1.48 was used. We used student's t-test and logistic regression analysis to determine predictive factors. The feasibility of Bayesian prediction was tested by cross validation.ResultsLogistic regression analysis revealed following factors as independent associates of insufficient liver enhancement in HBP; Alb (odds ratio [OR]=2.52, p<0.001), ChE (OR=1.36, p<0.001), T-Bil (OR=0.51, p=0.001), AST (OR=0.64, p<0.001), ALT (OR=0.91, p<0.001), PT-INR (OR=1.03, p=0.002), and the liver stiffness (OR=0.87, p=0.002). The accuracy of Bayesian methods for predicting insufficient liver enhancement was 74.4%.ConclusionBayesian prediction is feasible to predict patients with insufficient enhancement by serum liver function tests and liver stiffness with MRE.

O-1-039　EOB造影MRI動脈相における呼吸性アーチファクト：Turbo LAVA FLEXを用いた検討
Transient respiratory motion during gadoxetic acid-enhanced arterial phase imaging: a study using accelerated 3D gradient echo sequence

佐藤　兼是（山梨大学 医学部附属病院 放射線部）
Kazuyuki Sato[1], Utaroh Motosugi[2], Tatsuya Shimizu[2], Shintaro Ichikawa[2], Takashi Kakegawa[1], Hiroshi Kumagai[1], Hajime Sakamoto[1], Hiroshi Onishi[2]

[1]Department of Radiology, Yamanashi University hospital, [2]Radiation Medicine, Yamanashi University hospital

【要旨】EOB造影MRI動脈相では一過性の呼吸困難感により呼吸性アーチファクトが多く認められることが知られている.高時間分解能の3次元GRE法を用いた多時相動脈相取得のprotocolまたは撮像時間を短縮したprotocolにより動脈相撮像における呼吸停止失敗・呼吸性アーチファクトを低減できるかを検討した.

Purpose Transient respiratory motion, i.e. breath-hold failure, has been recognized as a cause of artifacts in gadoxetic acid-enhanced arterial phase imaging. The purpose of this study was to examine if breath hold failure and/or respiratory artifacts during arterial phase imaging can be reduced using protocols with multiphasic arterial phase acquisition or shortened acquisition using accelerated 3D gradient echo sequence (3D-GRE) in gadoxetic acid-enhanced MRI.Methods We included the patients who underwent gadoxetic acid-enhanced MRI at our institution using either conventional 3D-GRE for single arterial phase (LAVA, acquisition time=16s, n=148), accelerated 3D-GRE for 6 arterial phases (multiphasic acquisition with DISCO, 24s, n= 257), and another accelerated 3D-GRE for single arterial phase (shortened acquisition with Turbo LAVA, 10s, n=97). The MR technologist assessed the breath-hold success/failure by monitoring the respiratory motion with bellows. The artifacts in the arterial phase images were evaluated by a radiologist with 4-point scale (severe/moderate/mild/no artifacts), for which severe and moderate artifacts were categorized as substantial artifacts. The rates of breath-hold failure and substantial artifacts were compared by Chi-square test.Results Breath-hold was failed in 14% (21/148, control) for conventional 3D-GRE, 18% (47/257, p=0.288 [versus conventional 3D-GRE]) for multiphasic acquisition, and 16% (16/97, p=0.622) for shortened acquisition, respectively. The images had no substantial artifacts in 85% of the patients (127/148, control) for conventional 3D-GRE, 94% (243/257, p<0.001) for multiphasic acquisition, and 96% (16/97, p=0.01) for shortened acquisition, respectively.

O-1-040　圧縮センシング及びパラレルイメージングを併用した造影ダイナミック検査：肝胆膵領域の評価
Dynamic contrast enhanced MR imaging of the heptopancreatobiliary regions in combined use of parallel imaging and compressed sensing

増井　孝之（聖隷浜松病院 放射線科）
Takayuki Masui[1], Motoyuki Katayama[1], Kei Tsukamoto[1], Mitsuteru Tsuchiya[1], Yuki Baba[1], Yuji Iwadate[2], Kennichi Mizuki[1], Naoyuki Takei[2], Harumi Sakahara[3], Kang Wang[2], Koji Yoneyama[1]

[1]Dept of Radioloy, Seirei Hamamatsu General Hospital, [2]Global MR applications and work flow, GE Healthcare, [3]Dept of Radiology, Hamamatsu University School of Medicine

【要旨】上腹部造影ダイナミックMR検査には、高速撮像法が使用される。肝胆膵領域について、パラレルイメージングと圧縮センシングを併用した呼吸停止下造影ダイナミック検査の施行可能性について評価した。臨床3T装置にて、この撮像方法により時間分解能の高い良好な画像が取得可能であることがわかった。

Dynamic contrast study has provided information for characterization of lesions. Faster imaging can be strengthened in combined use of parallel imaging (ARC) and compressed sensing (CS). The purpose was to evaluate feasibility of dynamic contrast study for evaluations of hepatopanceatobiliary regions using turbo LAVA with ARC and CS. Materials and Methods: Fifteen patients (11men, 4 women, mean 75.4years old), who underwent Gd-contrast (Gd-chelate, 0.1mmol/kg) enhanced MR imaging for abdomen at 3T (750 750W, GEHC) were included. Dynamic contrast imaging using turbo LAVA with ARC and CS (one phase; 4-5seconds) were obtained with fluoro-triggering technique. Consecutive 4-5 phases within a breath-held were obtained. Portal phase, Equilibrium phases were obtained, respectively. Image quality and recognition of lesions were evaluated using a five-point scale (1 undiagnostic-5 excellent).Results: All images in dynamic contrast phases were diagnostic [Image quality; mean 4.3 (rank phase1-5; 4.2,4.3,4.5,4.4,4.4, respectively) Lesion recognition 4.5(5,4,3,2,1:34,1,5,1,2 case base)]. Time for image reconstruction was about 5 minutes for each phase.Discussion: Dynamic contrast MR imaging could be successfully obtained with acceptable image quality and lesion recognitions. This technique has several features: high temporal resolution (4-5 seconds for one phase); images reconstructed from Independent data sets (without view share); optimal timing for start of first phase with monitoring contrast-arrival. Compensation of signal intensity drop with ARC by using CS.In conclusion, with ARC and CS, breath-held dynamic contrast MR study for the hepatopancreatobiliary regions can be successfully performed with acceptable image quality and lesion recognitions on clinical 3T magnets.

O-1-041　腹部領域における圧縮センシングを用いたLAVA法の検討
Study of LAVA method using compressed sensing in the abdominal area on a 3T wide bore system

小出　若葉（聖隷浜松病院 放射線部）
Wakaba Koide[1], Koji Yoneyama[1], Yuki Takayanagi[1], Takayuki Masui[2], Yuji Iwadate[3], Kang Wang[4]
[1]Seirei Hamamatsu General Hospital radiation part, [2]Seirei Hamamatsu General Hospital radiology department, [3]Global MR Applications and Workflow, GE Healthcare Japan, [4]Global MR Applications and Workflow, GE Healthcare United States

【要旨】従来の腹部造影ダイナミック撮像では、1相20秒程を要し、早い動脈相の描出が困難であった。LAVA法において圧縮センシングとパラレルイメージング法を組み合わせ、撮像時間と画質変化を検討したところ、画質を保持したまま、時間分解能6.0秒の高速撮像が可能となり有用性が示唆された。

Purpose: Compressed sensing (CS) is a technique to restore the original data from the under-sampled data. In conventional dynamic contrast enhanced imaging in the abdominal area, about 20 seconds are needed for a single phase, so it is difficult to visualize dynamics of the early arterial phase. So by adding the CS, imaging time reduction is expected.in 3D T1-weighted imaging method called LAVA. 3T Wide bore system is now widely used, but comparing with standard bore system, slightly longer imaging time is expected for 3D fast imaging and arrangements of multiple body array coils might be different. Thus we evaluated effects of combination of CS and the parallel imaging method (ARC) against image quality and imaging time, and found optimal acceleration factors on wide bore system. Methods: We performed all scans on GE Discovery 750W MR imaging system. Healthy volunteers were scanned with different combinations of CS Factor (1.0 ~ 1.5) and ARC Factor (phase 2, slice1.0 ~ 2.0). Fixed imaging conditions were: scan plane = axial, FOV = 35cm, slice thickness = 4mm, frequency matrix = 256, phase matrix = 192, phase FOV = 0.8, turbo mode ON, number of slices = 50. Visual evaluation was carried out with a 5-poit scale regarding the artifacts and image quality. Results: When we increased CS Factor, image blurring tended to increase. As we increased the ARC Factor with fixed CS factor, an increase in the artifact was observed. When we fixed the scan time, images with higher CS Factor and lower ARC factor were evaluated with higher quality. Conclusion: The combination of CS and ARC allows a high temporal resolution of 6.0 seconds while maintaining the image quality. The technique was suggested to be useful.

O-1-042　上腹部領域における圧縮センシングを用いた3DLAVAの検討
Study of 3DLAVA using CS in the upper abdominal region

高柳　有希（総合病院 聖隷浜松病院 放射線部）
Yuki Takayanagi[1], Koji Yoneyama[1], Wakaba Koide[1], Takayuki Masui[1,2], Yuji Iwadate[3], Naoyuki Takei[3], Kang Wang[4]
[1]Seirei Hamamatsu General Hospital Radiation Part, [2]Seirei Hamamatsu General Hospital Radiology Department, [3]Global MR Applications and Workflow, GE Healthcare Japan, [4]Global MR Applications and Workflow, GE Healthcare United States

【要旨】圧縮センシング(CS)をパラレルイメージング法(ARC)と組み合わせることにより、撮像時間短縮が期待される。そこで、CSとARC を組み合わせ、3DLAVAの画質変化を視覚評価した。結果、画質を担保したまま、時間分解能5s以下の高速撮像が有用である可能性が示唆された。

[Background] Compressed sensing (CS) is a technique to restore the original data from the under-sampled observed data. LAVA is a useful method as a breath-hold dynamic imaging of the abdomen, but the breath-hold of 20 seconds per single phase is required with the conventional LAVA, which prevents detailed diagnosis of the arterial phase. So, by adding parallel imaging method (ARC) to the CS in LAVA, the imaging time reduction is expected.[Purpose] To examine the LAVA image quality changes bythe different combination of CS and ARC factors.[Method] We used GEHC Discovery MR750 3.0T, and 32ch body array coil. 1) Healthy volunteers were scanned with combinations of the CS (factor = 1.0,1.1,1.2,1.3,1.4,1.5) and ARC (factor = 2 * 1.0,1.2,1.4,1.6,1.8,2.0). Fixed imaging conditions were: scan plane = axial, FOV = 35cm, slice thickness = 4mm, frequency matrix = 288, the phase matrix = 192, phaseFOV = 0.8, turbo ON, and number of slices = 50. 2) Blur, S / N, and artifact were visually evaluated with a five-point scale.[Results] When we gradually increased the CS factor with a fixed ARC factor, blurring of the image was enhanced and artifacts appeared. When we gradually increased the ARC factor with a fixed CS factor, S / N was reduced. Among the combination of CS and the ARC, with a time resolution of 5s, the image quality was good when CS factor was 1.3 or 1.4, and ARC factor was 1.8 or less.[Conclusion] It was suggested that LAVA with the combination of CS and ARC is a potentially useful high-speed imaging technique, while securing the image quality.

O-1-043　T1&rho値、T2値、T1&rho/T2比を用いた肝機能評価
T1ρ and T2 values, and T1ρ/T2 ratio for the assessment of liver function

高山　幸久（九州大学大学院医学研究院 放射線医療情報・ネットワーク講座）
Yukihisa Takayama[1], Akihiro Nishie[2], Yoshiki Asayama[2], Kousei Ishigami[2], Yasuhiro Ushijima[2], Daisuke Okamoto[2], Nobuhiro Fujita[2], Tomoyuki Okuaki[3], Hiroshi Honda[2]

[1]Department of Radiology Informatics and Network, Graduate School of Medical Sciences, Kyushu Univerity, [2]Department of Clinical Radiology, Graduate School of Medical Sciences, Kyushu Univerity, [3]Philips Healthcare Asia Pacific

【要旨】本研究の目的はT1ρ値、T2値、T1ρ/T2比を用いた肝機能評価を検証することである。肝機能が悪化すると肝実質のT1ρ値が上昇する為、T1ρ値が肝機能評価の指標となりえる。T1ρ値とT2値はいずれも水分量を反映した定量的評価法であるが、肝機能評価において、T1ρ値とT2値の対比を行った先行研究はない。

Purpose:To investigate the potential of T1ρ and T2 values, and T1ρ/T2 ratio for assessing liver function.Materials and Methods:A total of 20 patients (18 men, 2 women; mean age, 68.9 yrs) were enrolled in this study. All patients had liver tumors and were scanned liver MRI were performed before the surgery. T1ρ maps were calculated using 4 different times of spin lock pulse (0/20/40/60 ms). T2 maps were calculated using 4 different echo times (0/20/40/60 ms). The number of slices of each map was limited to three because of the breath-hold acquisition. Three slices were set at the level of the hepatic hilum. In addition to T1ρ and T2 maps, three different types of T1ρ/T2 ratio maps were calculated using following different methods; T1ρ/T2 ratio1 = [(T1ρ-T2)/(T1ρ+T2)] × 100%, T1ρ/T2 ratio2 = T1ρ/T2 × 100%, T1ρ/T2 ratio3 = [(T1ρ-T2)/T2] × 100%, respectively. All maps were developed using an in-house software. Mean T1ρ and T2 values, and T1ρ/T2 ratio of the liver parenchyma were measured after drawing a total of 5 regions of interest avoiding vessels or tumors for each patient. Liver function was evaluated by retention rates at 15 min after the injection of indocyanine green (ICG-R15s). A linear regression analysis was performed to assess relationships between those indices and ICG-R15.Results:There were positive relations between ICG-R15 and T1ρ value (R2=0.22, p=0.06), ICG-R15 and T2 value (R2=0.10, p=0.24) and ICG-R15 and T1ρ/T2 ratios (T1ρ/T2 ratio1; R2=0.35,p=0.02, T1ρ/T2 ratio2; R2=0.37,p=0.01, and T1ρ/T2 ratio3; R2=0.36, p=0.01), respectively. Three kind of T1ρ/T2 ratio showed significant positive relation with ICG-R15, though T1ρ and T2 values did not.Conclusion:T1ρ/T2 ratio has a possibility to assess liver function more sensitive than T1ρ or T2 values alone.

O-1-044　特異値分解法を用いた楕円筒型勾配磁場コイルの設計
Design of oval gradient coils using current potential and singular value decomposition

松澤　晃樹（筑波大学 数理物質科学研究科 電子・物理工学専攻）
Koki Matsuzawa[1], Mitsushi Abe[2], Katsumi Kose[1], Yasuhiko Terada[1]

[1]Institute of Applied Physics, University of Tsukuba, [2]Applied Energy Systems Research Department Center for Technology Innovation, Hitachi, Ltd.

【要旨】オープン型MRIシステムでは一般的に円形平板型の勾配磁場コイルが用いられるが、楕円体という評価領域の形状を考慮すると電流効率の面で最適ではない。そこで、本研究では任意形状のコイル設計ができる特異値分解法を用いて、楕円筒型の勾配磁場コイルを設計した。

Open MRI systems often use gradient coils with biplanar geometries. However, the geometry of an imaging volume is spherical or ellipsoidal, and curved geometries that fit the imaging area would outperform biplanar geometries in terms of the gradient efficiency. For proof-of-concept, we designed the gradient coils with the oval geometry. We used a singular value decomposition method (DUCAS) that can design gradients with arbitrary geometries.
The target region was a 150 mm x 150 mm x 50 mm diameter ellipsoidal volume in a 0.3 T permanent magnet. The gradient coil with the oval geometry (158 mm (x) x 108 mm (z) ellipsoidal aperture, 220 mm long) and that with the biplanar geometry (320 mm in diameter, 120 mm gap) were designed. The node weights and initial distribution were set appropriately. The eigenmodes were chosen in ascending order in such a way that the nonlinearity ranged from 7 to 8%.
Table1 summarizes the current efficiency and nonlinearity for the designed coils. The nonlinearity was almost the same for both coils, and the oval coil had the higher current efficiency. In conclusion, the gradient coil with the oval geometry exhibited the high performance.

		Efficiency [mT/m/A]	Nonlinearity [%]
Biplanar	Gx	0.55	7.80
	Gy	0.55	7.80
	Gz	0.64	8.50
Oval	Gx	1.70	7.32
	Gy	0.95	7.00
	Gz	1.47	8.35

Table1: Coil performance of the gradient coils

Fig.1: The designed oval gradient coil with 0.3 T open MRI system

O-1-045　MRI software platformの開発（2）
Development of the MRI software platform (II)

巨瀬　勝美（筑波大学 数理物質系 物理工学域）
Katsumi Kose[1], Ryoichi Kose[2], Tomoyuki Haishi[2]
[1]Institute of Applied Physics, University of Tsukuba, [2]MRTechnology Inc.

【要旨】MRIハードウェアの飛躍的進歩とパルスシーケンスの高機能化に伴い，核磁化の運動は複雑化を増し，MRI simulatorなしでの新規シーケンス開発は不可能な状況となっている．そこで，GPUで高速化したBloch simulatorをコアとしたMRI software platformを開発した．

Introduction
With remarkable progress of MRI hardware and pulse sequences, it has become impossible to develop new MRI sequences without MRI simulators. In this study, we developed an MRI software platform that utilized a GPU optimized Bloch simulator.
Materials and Methods
The figure shows an overview of the MRI software platform. This platform consists of a sequence generator, a Bloch simulator, a reconstructor, and a sequence optimizer. The sequence generator generated CUDA codes from MRI sequence files and numerical phantoms for the Bloch simulator optimized using a GPU. Simulated images were compared with MR images acquired with an MRI system using a 9.4T/54mm vertical bore superconducting magnet.
Results and discussion
Multiple 2D spin-echo (2000/80), 3D FLASH (20/10), 3D GRASS (20/10), and 3D balanced SSFP (20/10) sequences were simulated using the platform and used to acquire MR images with the 9.4T MRI. Identical sequence files were successfully used for both experiments and simulations. The simulations reproduced the experimental results very well and were a few to several times faster than the experiments, which demonstrated usefulness of the software platform.

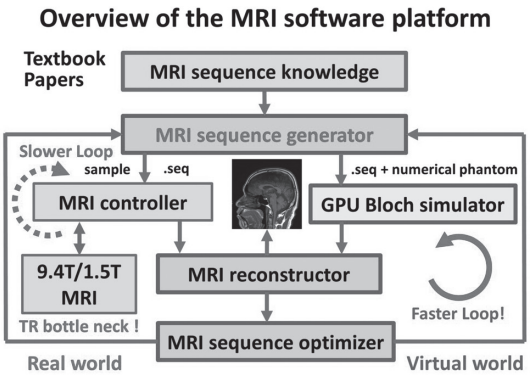

O-1-046　1.5T/280mm水平ボア超伝導磁石のためのマルチサーキュラーシムシステムの開発
Development of a multi-circular shimming system for a 1.5 T/280 mm horizontal bore superconducting magnet

山田　諒太（筑波大学 数理物質科学研究科）
Ryota Yamada, Katsumi Kose, Yasuhiko Terada
Institute of applied science

【要旨】当研究室で利用している1.5 T/280 mm超伝導磁石はマウスやラットの撮像に適しているが，冷凍ポンプの周期的な発振によりB_0のドリフトが発生する．そこで本研究では，マルチサーキュラーシムコイル[1]を用いることでこの問題を解決し，かつダイナミックシミングにも対応できる専用のシムコイルシステムの開発を目的とした．

We have been developing a 1.5 T/280 mm horizontal bore superconducting magnet (SCM; JASTEC, Japan) system that is applicable to mouse and rat imaging. Currently, the SCM system suffers from B_0 drift due to the periodical oscillation of the cooling refrigerator. In this study, we developed a shimming system with a multi-circular shim coil (MCSC) [1] for the SCM system, which uses a set of localized circular current coils and is a flexible device that can compensate for a given B_0 inhomogeneity both statically and dynamically. The proposed shimming system would also utilize for dynamic shimming.
Figure 1 shows design of the MCSC and capability of inhomogeneity correction with third-order terms. The MCSC consisted of circular coils (24 coils, wire diameter 0.5 mm, 30 turns for each coil) fixed on an acrylic pipe (4 mm thick, 700 mm long). The coil current for each was controlled to range from −1 A to +1 A by a home-built 24 ch current power supply operating at single-phase 100 V. The theoretical field maps generated by the MCSC (simulation) agreed with the ideal third-order spherical harmonics term. More accurate field correction may be achieved by increasing the maximum coil current.

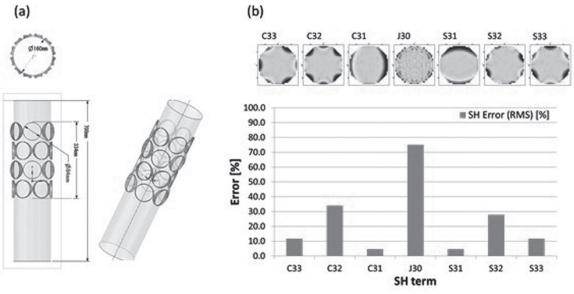

Fig. 1 (a) Multi-Circular Shim Coil (MCSC)
(b) Theoretical errors in the magnetic field generated by the MCSC and ideal spherical harmonic terms

O-1-047　高分解能画像を意図した3T膝用送受信コイルの基礎的検討
Basic study of 3T Transmit / Receive Knee Coil for High Resolution Imaging

太田　美幸（東芝メディカルシステムズ株式会社）
Miyuki Ota[1], Keiji Tahira[1], Noah Deetz[2], Xiaoyu Yang[2], Hiroyuki Fujita[2,3,4]
[1]Toshiba Medical Systems Corporation, [2]Quality Electrodynamics, LLC, [3]Case Western Reserve University, [4]The University of Queensland

【要旨】高分解能画像の撮像のため、3T膝用送受信コイルを開発し、ファントムとボランティアによる画質の評価を行った。コイルの設計により高SNRおよび高速撮像(低g-factor)を可能とすることで、従来の膝用コイルと同等のSNR、撮像時間で高分解能画像を得ることができた。

[Purpose] In the field of orthopedics high-resolution imaging is required, however, signal noise ratio (SNR) decreases. Furthermore higher matrix size introduces longer scan time. In this study, a new transmit and receive knee coil was developed to enable high resolution imaging maintaining the practical SNR and scan time.[Method] The design and arrangement of the coil elements were optimized. In relation to SNR, the aperture diameter was smaller than that of conventional knee coil and it is 154mm which can cover majority of the patient knee size. In relation to scan time, the coil configuration was rearranged to make g-factor low for high acceleration parallel imaging. For the evaluation of the newly designed knee coil, the phantom SNR, g-factor and volunteer image scanned on 3T MRI system (Toshiba Medical Systems Corp.) were compared to ones of the conventional knee coil. In volunteer imaging for high resolution image, the scan time of the new knee coil was adjusted to be equivalent to the one of the conventional knee coil by adjusting the acceleration factor of parallel imaging and oversampling. [Result] In phantom SNR evaluation, the new knee coil showed 1.4 times higher SNR and lower g-factors than the conventional knee coil. In volunteer imaging, parameter changes became available : acceleration factor 1.0 to 1.2 and matrix size 320 × 320 to 416 × 512. The higher resolution imaging could be realized with the same scan time as conventional knee coil.[Conclusion] We developed a knee coil with optimizing design and arrangement of the coil elements for high-resolution imaging. According to SNR and g-factor improvements, the newly designed knee coil was enabled high resolution imaging maintaining the practical SNR and imaging time.

O-1-048　7T MRI水脂肪ファントム画像における二重周波数パラレルトランスミットパルス設計の効果検討
Effects of dual-frequency parallel transmit pulse design on a water-fat phantom image at 7 T

岩舘　雄治（GEヘルスケア・ジャパン 研究開発部）
Yuji Iwadate[1], Tsuyoshi Matsuda[2], Tsuyoshi Metoki[2], Kohsuke Kudo[3], Makoto Sasaki[2], Hiroyuki Kabasawa[1]
[1]Global MR Applications and Workflow, GE Healthcare Japan, [2]Division of Ultrahigh Field MRI, Institute for Biomedical Sciences, Iwate Medical University, [3]Department of Diagnostic and Interventional Radiology, Hokkaido University Hospital

【要旨】7T MRIにおいて二重周波数パラレルトランスミットパルスを設計し、水脂肪ファントムを2チャンネルおよび8チャンネル送信－32チャンネル受信コイルで撮像しその効果を検証した。二重周波数法は従来手法と比較し脂肪領域の励起を均一に行うことがactual flip-angle撮像法により確認された。

Purpose: Parallel transmit pulses with a three-dimensional spoke design are used for uniform excitation especially at ultra-high field MRI such as 7 T. Conventionally, pulse design is performed regarding the resonance frequency of water proton, which may result in non-uniform excitation in the fat region. In this study, we examined the effects of dual-frequency parallel transmit pulse design on a water-fat phantom image at 7 T.
Methods: Parallel transmit pulses were designed with three spokes in k-space based on measured transmit RF field and B0 field maps. Frequencies were set at 0 Hz (water) and −1030 Hz (fat) in the design. A home-made water-fat phantom was scanned on a GE Healthcare 7 T Discovery MR950 imaging system with Nova Medical 2Tx/32Rx and 8Tx/32Rx channel coils. Scans with single-frequency pulses were also performed for comparison. Comparison of single- and dual-frequency methods were repeated twice for both 2Tx and 8Tx coils, and the phantom was re-positioned between the repetitions. The flip angle maps were measured using the actual flip-angle method with repetition times of 30 ms and 150 ms.
Results and Discussion: The average of fat flip angles were increased with the dual-frequency method compared to the single-frequency method. On the other hand, standard deviation of the fat flip angles was decreased with the dual-frequency method, which resulted in reduction of coefficient of variation by 32–56%. Investigation of this technique with human subjects should be performed in the future.
Conclusion: The dual-frequency parallel transmit pulse design improved homogeneity of flip angles of fat excitation in the phantom. This can improve accuracy of fat quantitation in 7 T MRI.

O-1-049　股関節撮像における左右差を考慮した４チャンネルRF shimmingの開発
RF shimming mitigating left-right difference in hip joint imaging using 4-channel transmit coil

小高　晃弘（株式会社日立製作所 ヘルスケアビジネスユニット）
Akihiro Odaka, Kosuke Ito, Chikako Moriwake, Masahiro Takizawa
Healthcare Business Unit, Hitachi, Ltd.

【要旨】3T以上の高磁場MRIでは、RFパルスの照射不均一のために、画像の信号強度にムラが生じる。特に股関節撮像において左右差が問題であった。今回、４チャンネル照射コイルを用いたRF shimmingの目的関数を改良し、股関節撮像における左右差を緩和した。

Purpose: In 3T MRI, inhomogeneous B1 spatial distribution causes left-right difference (LRD) of tissue contrast. An objective function based on Usd (standard deviation divided by mean of B1) was used for RF shimming [1]. In this study, the objective function was modified to mitigate LRD in hip joint region.
Methods: The modified objective function uses LRD and back-forward difference (BFD) in B1 maps acquired with multi Td method [2, 3] instead of Usd. Also, difference between high and low B1 region (HLD) was calculated. The resulting objective function is sum of LRD, BFD, and HLD. 3T MRI system (Hitachi, Ltd.) and 4channel RF transmit coil were used for scanning 22 healthy volunteers after informed written consent was obtained in accordance with our institutional review board guidelines. Difference in B1 map between left and right side was evaluated for Quatrature Drive (QD) and 2 RF shimming modes (previous and proposed).
Results: Differences in B1 map were 0.35 ± 0.03 (QD), 0.11 ± 0.03 (previous), and 0.03 ± 0.02 (proposed).
Conclusions: Proposed method can reduce LRD in hip joint region.
References: [1] Ibrahim, et al; MRI 18(2000) 733-742. [2, 3] Ito, et al. ISMRM 2013; 23: 2598, 2599.

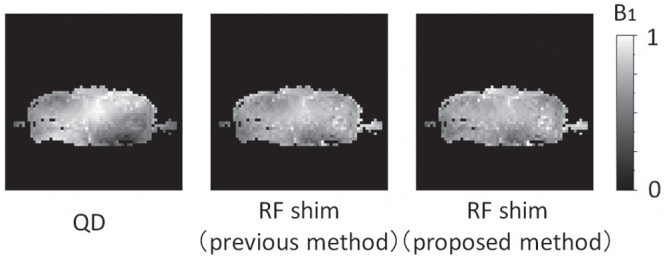

O-1-050　Effect of load position on array elements coupling
Effect of load size and load position on coupling between the elements of an array coil

Shubham Gupta（理化学研究所 脳科学総合研究センター 認知機能表現研究チーム）
Shubham Gupta[1], Allen Waggnar[1], Keiji Tanaka[1], Kang Cheng[1,2]
[1]Cognitive Brain Mapping, Brain Scince institute, RIKEN, [2]fMRI support unit, RRC, Brain Science Institute, RIKEN

【要旨】Not applicable.

Generally the same RF array is used with varying load sizes and positions. These changes can affect the coupling between the array elements. In this study, we simulated a two channel transmit/receive array with a radius of curvature of 85mm (in CST studio) and have analysed two scenarios: 1) Phantoms of different sizes (40 to 80mm), placed concentrically with the coil and 2) A 70mm phantom at various offsets relative to the center of the array (-10mm to 40mm). The coil elements were tuned to 170.33 MHz and the reactive coupling was kept near zero using the inductive decoupling method. For each simulation, Q-factors and coefficients of resistive (Kr) & reactive (Kx) coupling were calculated using 2-port S-parameters. Table 1 shows that when the phantom is big or near the coils, the coils are better loaded i.e. the Q factor is low and the elements are better decoupled (have lower Kr and S12). As the size of phantom decreases or the phantom moves away from the elements, Q-factor, Kr and S12 all increase, demonstrating that when the array is well loaded, the elements are better decoupled.

Table 1	Radius of Phantom					Distance b/w coil center and phantom center					
(in mm)	80	70	60	50	40	-10	0	10	20	30	40
Q11*	4.4	10.8	21.8	48.7	121.7	5.6	10.8	17.7	27.5	42.6	63.1
Q22*	4.5	10.4	20.8	47.3	121.7	5.3	10.4	16.9	26.2	40.6	60.8
S12	-17	-15	-13	-11	-9	-21	-15	-12	-10	-8	-7
Kr	0.18	0.31	0.4	0.45	0.48	0.19	0.31	0.42	0.52	0.61	0.68
Kx	0	0	0	0	0	0	0	0	0	0	0

* Q11 & Q22 are the Q-factors for coil 1 & 2 respectively

O-1-051　腹部撮像向けラディアルサンプリング法におけるピーク補正アルゴリズム
Peak Correction Algorithm in Radial Sampling for Abdominal Imaging

西尾　慧祐（株式会社日立製作所 ヘルスケアビジネスユニット）
Keisuke Nishio, Yasuhiro Kamada, Kuniharu Oka, Masahiro Takizawa
Healthcare Business Unit, Hitachi, Ltd.

【要旨】RADARは、k空間を放射状に計測して体動アーチファクトを抑制するが、ハードウェア誤差により信号のピークがシフトし、画像不均一が生じる。これまでピークシフトの補正アルゴリズムを開発し、頭部では安定した計測を実現した。腹部では補正精度が低下したため、安定に補正できるようアルゴリズムを改良した。

Introduction: RADAR (RADial Acquisition Regime), a kind of non-Cartesian sampling method, acquires signals radially in k-space and is able to suppress image artifact caused by patient motion. However, these kind of sampling methods sometimes have non-uniform images caused by peak position shift of sampled echo signals in the k-space due to hardware error, thus peak shift correction was needed. In previous study, a peak shift correction was developed for achieving stable brain imaging. For abdominal imaging, this correction sometimes did not work well due to an error on the reference data which were used for calculation of echo peak shifts. In this study, we modified the correction algorithm in order to achieve robust abdominal imaging.
Methods: The main cause of the instable results at abdominal region was that signal intensity of reference data varied depending on imaging sequence. We adjusted acquisition scheme of reference data so that signal intensity was not affected by sequence parameter. Furthermore, offset phase in the reference data occurred when imaging slice position was off-centered. This results in image shading due to interference of signal caused by phase difference between echo signals. We also developed an additional phase correction according to imaging slice position. A 3T MRI (Hitachi, Ltd., Tokyo, Japan) and a 28-channel torso coil were used for imaging healthy volunteers after obtaining informed written consent in accordance with our institutional review board guidelines.
Results: The modified algorithm showed good results in the case which result in non-uniform images in the previous algorithm at abdominal region.
Conclusion: The modified algorithm improves robustness of RADAR in the abdominal region.

O-1-052　複数パルスからなる傾斜磁場パルスの低騒音化
Quiet Gradient Pulse Shape Composed of Plural Lobes

黒川　眞次（株式会社日立製作所 ヘルスケアビジネスユニット）
Shinji Kurokawa[1], Yo Taniguchi[2], Yukari Yamamoto[2], Hisaaki Ochi[2], Takashi Tsuneki[1], Hiroyuki Itagaki[1], Yoshitaka Bito[1]
[1]Healthcare Business Unit, Hitachi, Ltd., [2]Research & Development Group, Hitachi, Ltd.

【要旨】複数のパルスからなる傾斜磁場パルスを全体として低騒音化した。模式的なFRFを用い、A特性音圧レベルが最小になるようにパルス形状を数値的に最適化した。最適パルス形状は従来の形状とは大きく異なった。サイン波に比べて10dB低騒音化でき、従来法より静かなパルス形状が存在することを示せた。

INTRODUCTION
In sequence-based acoustic noise reduction, several methods utilizing sinusoidal pulses [1,2] or spline interpolation [3,4] have been presented. These methods, however, are not intended to find the quietest shape for the whole sequence, since they control each pulse individually with predefined shape. The aim of this study is to find the shape of the quietest pulse sequence.
METHODS
A pulse shape during repetition time was represented by a list of discretized gradient amplitudes. The list was numerically optimized to minimize the A-weighted sound pressure level (SPL). We used a synthetic frequency response function in calculation of SPL to make the study generic.
RESULTS AND CONCLUSION
Figure 1 shows the fast spin echo sequence in read-out axis generated by the conventional method and our optimization.The shape of the optimized sequence is quite different from the sinusoidal or low-pass filtered trapezoid.The A-weighted SPL of the optimized sequence is 10 dB lower than that of the sinusoidal.

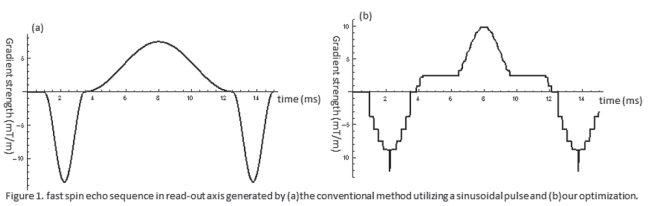

Figure 1. fast spin echo sequence in read-out axis generated by (a)the conventional method utilizing a sinusoidal pulse and (b)our optimization.

REFERENCE
1. F. Hennel, et al. MRM. 1999;42:6-10.2. Y. Taniguchi, et al. JSMRM 2014:P-2-1443. B. Heismann, et al. MRM. 2015;73(3):1104-1109.4. D. M. Grodzki, et al. ISMRM 2015:2544.

O-1-053　導電性を有する試料のMRI撮像時に生じるRF電磁波の不均一を改善する空間選択的な励起パルスの評価
Evaluation of spatially-selective excitation pulse for improving the inhomogeneous MRI signal intensity due to conducting samples

禹　泰城（東京大学 大学院工学系研究科）
Taeseong Woo, Dongmin Kim, Takao Someya, Masaki Sekino

Department of Electrical Engineering and Information System, The University of Tokyo

【要旨】MRI撮像時に測定対象が導体を含む場合，導電性によって渦電流によってRF磁場が不均一に分布し取得した画像を定量的に評価することが難しい．本研究では，導体によって生じるRF磁場の不均一を補正するための空間選択的励起パルスを設計し，補正効果の定量的な評価を行った．

In magnetic resonance imaging (MRI), radiofrequency (RF) field induces eddy current on conductors such as metallic implant. This phenomenon result from inhomogeneity of RF field distribution. Spatially-selective excitation pulse is an established technique for correcting RF field inhomogeneity. However, the compensating effect for conducting samples has not been evaluated in previous researches. In this study, we evaluated the effect of spatially-selective excitation RF pulse for improving the inhomogeneous MRI signal intensity due to conducting samples. We carried out MRI simulations and experiments using different patterns including conductors. Attenuation patterns were prepared for numerical MRI simulation. And different concentration of sodium chloride aqueous solutions were prepared as conducting samples for experiments. According to concentration of sodium chloride, different conductivities were obtained in B1 maps. RF pulse waveform was calculated by analyzing Bloch equation inversely. The effect for correcting RF field inhomogeneity was evaluated by applying designed spatially-selective excitation pulse to each sample. In MRI simulations, designed RF pulse shows a good performance to reduce inhomogeneities of RF field distribution. MRI images acquired by spatially-selective excitation pulse also showed the homogenous signal intensities, compared with conventional RF pulse. Attenuation induced by conductivity of sodium chloride aqueous solutions was compensated by designed pulse. These simulations and experimental results show that spatially-selective excitation pulse has the compensating effect to recover attenuated signal intensities due to conducting samples.

O-1-054　2D Look Locker法によるT1値測定精度の検討
Improved 2D Look Locker method: assessment of T1 value measurement accuracy

中川　貞裕（旭川医科大学病院 診療技術部 放射線技術部門）
Sadahiro Nakagawa, Toshiharu Moriya, Masakazu Uno, Takafumi Nakata, Kunihiro Iwata

Section of Radiological Technology, Department of Medical Technology, Asahikawa Medical University Hospital

【要旨】目的は2D Look Locker（LL）法によるT1値測定の正確性の調査である。LL法によるT1値測定は異なる造影剤濃度を有するバイアルにて5つのEPIfactorと5つのTFEfactorにより取得した。リファレンスとなるT1値はIR法にて取得しLL法との誤差を算出した。TFEfactor、EPIfactorともに低く設定することでより正確なT1値が測定された。

[Purpose]T1 measurement is the gold standard that can be generated using an inversion recovery spin echo sequence (IR-SE). However, the scan time involved in IR-SE-based T1 measurements is long. The 2D Look-Locker (LL) sequence is a widely used fast-T1-measurement method. Generally, the error between LL and IR-SE is approximately 10-30%. To the best of our knowledge, there are not many reports on the effects of both the EPI factor and TFE factor on T1 value measurements using the 2D LL method. The purpose of this study was to compare the T1 measurements obtained from different EPI factors and TFE factors to investigate the accuracy of the T1 value measurements using 2D LL technique.[Materials and Methods]All examinations were performed on a 1.5T MRI with a 32-channel cardiac coil. A validation study was performed using a phantom consisting of seven vials with different concentrations of contrast agent. Reference T1 measurements were first obtained in a single section by using seven spin-echo acquisitions having different inversion times, from 50 ms to 5000 ms. The T1 measurements using the LL scan were obtained by a single scan at five different EPI factors (3-11) and five different TFE factors (3-11); then, the percent errors between the IR-SE and 2D LL technique were calculated. [result]The LL technique exhibited lower percent errors in small EPI and TFE factors than large EPI and TFE factors. The averaged T1 measurements in a phantom consisting with different concentrations of contrast agent exhibited an error of 7.6% using an EPI factor of 7 and a TFE factor of 7. Further, T1 measurements using an EPI factor of 3 and a TFE factor of 3 exhibited an error of 5.9%.[conclusion]The LL technique in both small EPI TFE factors presents accurate T1 measurements.

O-1-055　SWIFTマイクロイメージング
SWIFT microimaging for brain tissues from an aceruloplasminemia patient

三森　文行（国立環境研究所）
Fumiyuki Mitsumori[1], Naoharu Kobayashi[2], Garwood Michael[2], Hiroaki Miyajima[3]
[1]National Institute for Environmental Studies, [2]CMRR University of Minnesota, [3]Hamamatsu Univ. School of Medicine

【要旨】無セルロプラスミン血症患者の死後脳より得たホルマリン固定組織での鉄の存在状態を明らかにするためSWIFT法を用いた16.4T高磁場マイクロイメージング測定を試みた。従来法で用いた組織測定用検出器をテフロン化し、樹脂からの信号混入を防止した。数分程度で組織に蓄積した鉄の粒状構造を描出できた。

[Introduction]　We have reported conventional spin echo microimaging exhibited two forms of iron in the tissue from a patient with aceruloplasminemia, a granular structure (probably insoluble form) and diffusive one (soluble form) [1]. However, we lose significant signal with the conventional method due to very short T_2 of the tissue water. In this paper we attempted a method of SWIFT (SWeep Imaging with Fourier Transformation) [2] for microimaging of tissues with high iron accumulation.[Materials and Methods]　Brain tissues were obtained by an autopsy and chemically fixed with formalin solution. MRI was performed with 16.4T animal MRI spectrometer equipped with a horizontal bore magnet (Agilent). The same design of an RF coil as previously reported was used, but most of Perspex used was replaced with Teflon in order to avoid signal contamination from the resin in the SWIFT measurements. In SWIFT measurements data points are radially sampled on spokes (views). Typically, the number of data points was 192 at each view, and 2k to 128k views were collected. Gap rate was 156.25 kHz. Data were collected with TR of 1.9384 ms and flip angle of a few degrees. Typical FOV was 20mm. [Results and Discussion]　SWIFT microimaging again exhibited the granular structure of iron in the tissue as low signal intensity spots. Resolution of 50 μm was attainable in a few minutes dependent on the number of views collected. Compared with the conventional imaging method, SWIFT is more than 10 times efficient to visualize iron particles with extreme magnetic susceptibility. However, it loses contrast in soluble form of iron with milder T_2 differences.[1] Mitsumori F, Garwood M: Jpn J Magn Reson Med 35, Suppl, O-1-82 (2015).[2] Idiyatullin D et al: J Magn Reson, 181, 342-349 (2006).

O-1-056　非線形微分方程式を用いた非デカルト・サンプリングのための磁気共鳴画像再構成
Magnetic resonance image reconstruction for non-Cartesian sampling schemes using nonlinear differential equation

山口　雄作（四国こどもとおとなの医療センター 放射線科）
Yusaku Yamaguchi[1], Takeshi Kojima[2], Tetsuya Yoshinaga[2]
[1]Department of Radiology, Shikoku Medical Center for Children and Adults, [2]Institute of Biomedical Sciences, Tokushima University

【要旨】磁気共鳴画像再構成の逆問題から導かれた最適化問題を微分方程式系の初期値問題に帰着させ，極限集合への解の収束により画素値を求める方法を提案している．螺旋状軌道で計測空間を充填する超高速撮像法に提案系を適用し，数値実験を行った．提案法は評価関数の最小化に優れ，高品質な再構成画像が得られることがわかった．

Image reconstruction problem in magnetic resonance imaging (MRI) is formulated as a problem of finding a solution satisfying linear equations derived from signals sampled in k-space according to a pulse sequence. When sampling signals are taken at the Cartesian locations using the ordinary pulse sequences represented by, e.g., the spin echo sequence, it is possible to reconstruct an image using the method of two-dimensional Fourier transformation. However, spatial frequency data in the pulse sequence for an ultrafast MRI sequence may be provided with non-Cartesian k-space sampling schemes such as spiral or radial trajectories. The relation between image pixel densities and sampled signals is described through a set of linear equations and the problem of MRI reconstruction becomes a linear inverse problem, which may be generally ill-posed due to the presence of noise and detection error. In this study, we present a novel approach for MRI reconstruction involving a spiral k-space scanning on the basis of the idea of continuous dynamical methods using the minimization of Kullback-Leibler (KL) divergence. Our proposed system is described by nonlinear differential equations and it can not only reconstruct non-negatively constrained tomographic images but also has the property that the KL-divergence measure monotonically decreases along the solution. To evaluate the performance of the proposed method, we compare numerically the convergence properties of proposed method with the conjugate gradient iterative method using simulated noisy phantom data. We demonstrated that the proposed method is more effective than the conventional iterative method in convergence quality, through numerical experiments in the case of noisy phantom data with lower signal-to-noise ratios.

O-1-057　小脳橋角部MRIとCTによるFusion画像作成における位置ずれの検討
Temporal bone fusion image by using MRI and CT; Assessment of the misregistration arise from cerebellopontine angle

小北　修平（大阪警察病院 医療技術部 放射線技術科）
Shuhei Ogita, Satoru Tominaga, Yasuo Fujisawa, Toru Shinohe, Atsushi Tanaka
Division Of Radiological Technology, Department Of Medical Technology, Osaka Police Hospital

【要旨】真珠腫診療にてnon-EPI DWI撮影を実施している。骨組織との関係把握にCT画像とFusion画像作成を試みたが、位置ずれが大きい症例を認めた。ファントムをMRI撮影し、CTはMRIと同角度から50度まで5度ずつ傾けて撮影した。15度以上になると位置ずれは顕著になった。基準部位を臨床画像にて検証し最小の位置ずれは眼窩であった。

Background and Purpose: Recently the utilities of non-EPI DWI were reported at the evaluation of cholesteatoma. To evaluate cholesteatoma lesions, it is important to recognize the anatomy of temporal bone, and therefore creations of fusion image by using non-EPI DWI image and CT image are tried in our hospital. However, there were some cases with large misregistration when used the automatic fusion function on the work station. These cases were needed to create manually, however the reproducibility becomes a problem. Because cerebellopontine angles between MRI scan and CT scan are different in our hospital, we hypothesis that the differences is strongly affect to the misregistration. The purpose of this study was, therefore, to assess the influence of cerebellopontine angle at the fusion images by using CT and MRI. **Method:** Agar fathom with gel was scanned with 3T MRI and 64-MDCT. To access the effect of the scanning angle, the scanning angle was changed from 0 to 50 degrees by five degrees. Fusion images were created by using commercially available software, and these images were visually evaluated. In addition, clinical fusion images were also assessed at the point of the difference of cerebellopontine angle. **Result:** According to increasing the difference of scanning angle between MRI and CT, the misregistration of the fusion image was also increasing. In particular, it was remarkable when the difference of the scanning angle was 15 degrees or more. At the evaluation on clinical fusion images, the effect of the scanning angle had same tendencies. Meanwhile, at the set of the level of orbit as reference point, the misregistration was smallest. **Conclusion:** The difference of cerebellopontine angle was an important factor at the creation of fusion images by using CT and MRI.

O-1-058　顔面神経管の描出: PETRAと他の3D撮像法との比較
The visualization of facial nerve canals: A comparative study between PETRA sequence and other 3D sequences

奥知　左智（京都大学大学院医学研究科 画像診断学・核医学）
Sachi Okuchi, Yasutaka Fushimi, Tomohisa Okada, Akira Yamamoto, Tsutomu Okada, Takuya Hinoda, Kaori Togashi
Department of Diagnostic Imaging and Nuclear Medicine, Graduate School of Medicine, Kyoto University

【要旨】PETRAと他の3Dシーケンス(MPRAGE、T2SPACE)の顔面神経管の描出能の検討のため、顔面神経管を4つの部位に分け、見え方を点数化して比較した。PETRAはT2SPACEとは同程度の描出能であったが、MPRAGEよりは描出が良好であった。PETRAは顔面神経管の描出に有用な検査である。

Purpose: To compare the visualization of the facial nerve canal among PETRA and the other 3D sequences. Methods: Fourteen volunteers (mean age 41, range 31-57 years) were enrolled in this under approval of institutional review board with written informed consent. Scan was conducted using a 3T-MR system (Magnetom Skyra, Siemens, Erlangen, Germany) with a 32-channel head coil for PETRA (axial, TR/TE 4/0.07 ms, FA4°, resolution 0.67 × 0.67 mm, 0.67 mm-thickness, matrix 320 × 320), T2-SPACE (sagittal, TR/TE 1800/273 ms, FA120°, resolution 0.65 × 0.98 mm, 0.8 mm-thickness, matrix 320 ×260) , and MPRAGE (sagittal, TR/TE 1900/2.58 ms, TI 900ms, FA9°, resolution 0.9 × 0.9 mm, 0.9 mm-thickness, matrix 256 × 256). The image volumes of PETRA, T2-SPACE and MPRAGE were reconstructed in axial image of 0.9 mm thickness by using syngo FUSION, and the visualization of the facial nerve canal was evaluated. The facial nerve canals were divided into the four segments (labyrinthine, geniculate ganglion, tympanic, and mastoid). For each of the left and right facial nerve canal, a three-point scale was used: 0 = not visible, 1= partially visible, or 2= excellently visible. The scores were compared among PETRA, T2-SPACE and MPRAGE using Friedman test. A P value less than 0.05 was considered statistically significant. Results: At geniculate ganglion, tympanic and the sum of four segments, the scores of PETRA and T2-SPACE were statistically better than MPRAGE. At labyrinthine and mastoid, there were no significant differences. Conclusion: In the visualization of the facial nerve canal, PETRA was better than MPRAGE. PETRA was useful for the visualization of facial nerve canal.

O-1-059　64 channel、20 channel 頭頸部コイルの比較の初期経験
Comparison between 64-channel and 20-channel head and neck coil: Preliminary Study

伏見　育崇（京都大学大学院医学研究科 放射線医学講座（画像診断学・核医学））
Yasutaka Fushimi[1], Tomohisa Okada[2], Akira Yamamoto[1], Tsutomu Okada[1], Akihiko Sakata[1], Sachi Okuchi[1], Gosuke Okubo[1], Moritaka Yamauchi[1], Takuya Hinoda[1], Takayuki Yamamoto[1], Hikaru Fukutomi[1], Yusuke Yokota[1], Kaori Togashi[1]

[1]Department of Diagnostic Imaging and Nuclear Medicine, Kyoto University Grad uate School of Medicine, [2]Human Brain Research Center, Kyoto University Graduate School of Medicine

【要旨】頭頸部領域は、血管拍動、嚥下や咳嗽などの生理的な動きのため画質低下が生じやすい領域である。今回、2種類の頭頸部コイル（64, 20チャンネル）を使用する機会があったため、両者のSNR計測を行った。使用したシークエンスは3D T1 SPACE, T2 SPACEで、両者とも表面、深部ともに64チャンネル・コイルで高いSNRが得られた。

Background and Purpose: Artifacts associated with physiologic movement such as atrial pulsation, breathing and swallowing decrease the image quality in carotid plaque imaging. The 64 head and neck coil has been introduced to clinical practice. In this study, we compared SNR of 64 channel coil with that of 20 channel coil.Materials and Methods: A phantom was scanned at 3T MR unit (Magnetom Prisma, Erlangnen, Germany). SNR of 3D T1-SPACE and 3D T2-SPACE with 64 and 20 channel head and neck coil was measured by consecutive subtraction. Results: SNR of 3D T1-SPACE and 3D T2-SPACE with 64 channel coil was higher both the surface and the center than that with 20 channel coil. Discussion and Conclusion: Thanks to more coverage of coil elements around the neck area, 64 channel head and neck coil will provide us better 3D MR carotid plaque imaging than 20 channel head and neck coil.

O-1-060　3D T1-VISTA法を用いた頸部頸動脈プラーク容積評価：マニュアル計測と自動計測ソフトの比較
Evaluation of cervical carotid plaque volume using 3D T1-VISTA: Comparison of manual measurement and automatic measurement by the in-house software

磯嶋　志保（三重大学 医学部附属病院 中央放射線部）
Shiho Isoshima[1], Katsuhiro Inoue[1], Ryohei Nakayama[2], Shinichi Takase[1], Tsunehiro Yamahata[1], Masayuki Maeda[3]

[1]Department of Radiology, Mie University Hospital, [2]Ritsumeikan University, College of Science and Engineering, Department of Electronic and Computer Engineering, [3]Department of Advanced Diagnostic Imaging, Mie University School of Medicine

【要旨】3D T1-Volume Isotropic TSE Acquisition（VISTA）法を用い頸動脈プラーク容積をマニュアル計測と自動計測ソフトで比較検討した。13例を対象に検討し、自動計測ソフト値はマニュアル計測値と同等の再現性と妥当性が認められた。

[purpose]We aimed to compare the cervical carotid plaque volume measurements based on the VISTA data between manual method and automatic method using the in-house software. [Method]We used a 3T MR (Ingenia 3.0T MR, Philips) using ds HeadNeck Spine coil.The study was retrospectively performed in 13 patients who underwent plaque MR examinations using 3D VISTA. Plaque volume data were measured by both manual and automatic methods (in-house software), and were respectively compared regarding inter-rater and intra-rater analyses. [Results]Signal intensity ratio (plaque to adjacent muscle) was 2.37 ± 0.34 in 13 cases. The reliability of plaque volume measurements among intra-rater analysis was the following: ICC=1.000, Spearman (r)=0.955, $p<0.01$ for the automatic method; ICC=0.986, Spearman (r)=0.984, $p<0.01$ for the manual method . The reliability of plaque volume measurements among inter-rater analysis was the following: ICC=0.999, Spearman (r)=0.955, $p<0.01$ for the automatic method; ICC=0.98, Spearman (r)=0.852, $p<0.01$ for the manual method. Using Spearman's correlation coefficient, there was a strong correlation between the automatic and the manual methods ($r=0.945$, $p<0.01$). [Conclusion]The automatic method and the manual method showed similar reliability in inter-rater and intra-rater. As the manual method is very complicated and time-consuming, the automatic method used in the current study is practically expected to be very useful.

O-1-061　拡散強調画像を用いた壊死を伴う頸部化膿性リンパ節炎と悪性リンパ節の鑑別
Necrotic cervical nodes: Usefulness of diffusion-weighted MR imaging in the differentiation of suppurative lymphadenitis from malignancy

三浦　賢征（岐阜大学医学部附属病院 放射線部）
Takayuki Miura[1], Kimihiro Kajita[1], Ryohei Yaegashi[1], Syogo Maeda[1], Hiroki Kato[1], Shinichi Shoda[1], Hiroki Kato[2], Satoshi Goshima[2], Masayuki Matsuo[1,2]

[1]Gifu University Hospital Radiology service, [2]Gifu University Hospital department of Radiology

【要旨】壊死を伴う頸部化膿性リンパ節炎と悪性リンパ節の鑑別において拡散強調画像の有用性を検討する。DWI、T1WI、T2WIにおいて壊死領域の信号値を脊髄信号値で除した値(SIR)及び同領域のADC値を算出し、良悪性間の比較を行なった。結果はDWIのSIR及びADC値のみ有意差を認めた。よってDWIのSIR及びADC値の有用性が示された。

Purpose: The purpose of this study was to assess the efficacy of diffusion-weighted (DW) MR imaging for the differentiation between suppurative lymphadenitis and malignancy in necrotic cervical lymph nodes. Materials and methods: Fifteen patients with suppurative lymphadenitis, 40 with squamous cell carcinoma (SCC), eight with lymphoma, and six with thyroid cancer were accompanied by necrotic cervical nodes. All 69 patients underwent 1.5-T MR imaging including DW and 58 underwent gadolinium-enhanced MR imaging. Necrotic area-to-spinal cord signal intensity ratios (SIR) on T1-, T2- and DW images and apparent diffusion coefficients (ADCs) [× 10-3 mm2/s] were correlated with the pathologies. Results: Nineteen necrotic cervical nodes with suppurative lymphadenitis, 67 with SCC, 10 with lymphoma, and 12 with thyroid cancer were identified. SIR on DW images was higher in suppurative lymphadenitis (2.50　± 1.21) than in malignancies (1.29 ± 0.67) ($p<0.01$), and ADC value was lower in suppurative lymphadenitis (0.89 ± 0.21) than in malignancies (1.46 ± 0.46) ($p<0.01$). SIR on T1-weighted images was higher in thyroid cancer (1.95 ± 0.53) than in suppurative lymphadenitis (0.87 ± 0.17), SCC (0.92 ± 0.13), and lymphoma (0.95 ± 0.09) ($p<0.01$). Conclusion: DW imaging with ADC measurements may play a supplementary role in the differentiation of necrotic cervical nodes between suppurative lymphadenitis and malignancy.

O-1-062　Delayed FLAIRでの迷路信号の左右非対称：片側偶発前庭神経鞘腫例と片側内リンパ水腫例の比較
Asymmetry of the labyrinthine signal on Delayed FLAIR: a comparison of unilateral incidental vestibular schwannoma and endolymphatic hydrops cases

長縄　慎二（名古屋大学大学院 医学系研究科 量子医学）
Shinji Naganawa[1], Toshiki Nakane[1], Hisashi Kawai[1], Toshiaki Taoka[1], Michihiko Sone[2]

[1]Department of Radiology, Nagoya University Graduate School of Medicine, [2]Department of Otorhinolaryngology, Nagoya University Graduate School of Medicine

【要旨】ガドリニウム造影剤静注4時間後のDelayed FLAIRでの迷路外リンパ信号の著明な左右差は前庭神経鞘腫の存在可能性を示唆する。血液-外リンパ関門は前庭神経鞘腫例の方が、内リンパ水腫例よりもより透過性が高い。

PurposeTo visualize endolymphatic hydrops (EH), heavily T2w-3D-FLAIR is routinely obtained 4 hours(H) after IV single dose of gadolinium (Delayed FLAIR after IV-SD-GBCA) in our hospital. Among 1500 cases, we incidentally found 9 cases of unilateral vestibular schwannoma (VS). These cases were accompanied by a significant right-left asymmetry of the labyrinthine signal on delayed FLAIR. It is easy to discern a large mass at a glance, but in cases with small masses, we initially noticed an asymmetry of the labyrinthine signal, and then we detected the small mass with careful examination. This signal asymmetry was also observed in unilateral EH cases. The purpose of this study was to retrospectively compare the degree of signal asymmetry between VS and EH cases.Materials and Methods9 cases of unilateral VS (mass size 2-39mm) were found incidentally and 12 cases of unilateral significant EH in both cochlea and vestibule were extracted randomly and included. Both MR cisternography (MRC) and delayed FLAIR were obtained at 4H after IV-SD-GBCA. We set the ROI on the MRC in the scala tympani of the cochlear basal turn and the ROI was copied onto the delayed FLAIR. We calculated the signal intensity ratio (SIR; affected side / Non-affected side).ResultsThe SIR of the VS group was 2.1-4.0 (3.1 +/- 0.7) and that of the EH group was 0.9-1.5 (1.2 +/- 0.2)($p=0.00012$). The SIR was higher than 2.0 in all cases of the VS group and no more than 1.5 in all cases of the EH group.ConclusionThe right-left labyrinthine signal asymmetry of the VS group on a delayed FLAIR was significantly higher than that of the EH group. If the SIR is greater than 2.0, then the images should be examined carefully to diagnose the presence or absence of VS.

O-1-063　咽喉頭領域のMRI撮像におけるradial VIBEの有用性の検討：通常のVIBEとの比較
Usefulness of radial volumetric interpolated breath-hold examination (radial VIBE) for pharyngolaryngeal lesion: comparison with conventional VIBE

内匠　浩二（鹿児島大学 医学部 放射線科）
Koji Takumi, Yoshihiko Fukukura, Hiroto Hakamada, Yuichi Kumagae, Takashi Yoshiura
Departments of Radiology Kagoshima University Graduate School of Medical and Dental Sciences

【要旨】咽喉頭病変のMR検査を施行された22名を対象に、radial VIBE撮像MRIと通常のVIBEを比較し、検討した。質的評価（全体的な画質や粘膜の造影効果、血管の描出、動きによるアーチファクト、病変の視認性、病変辺縁の明瞭さ）では通常のVIBEと比較してradial VIBEが有意に優れていた。

Purpose: To evaluate the usefulness of radial volumetric interpolated breath-hold examination (radial VIBE) for pharyngolaryngeal lesions by comparing with conventional VIBE.Materials and methods: Images from 22 patients who underwent neck MRI at 1.5T for evaluation of pharyngolaryngeal lesion were reviewed. Both contrast-enhanced fat-suppressed T1-weighted radial and conventional VIBE sequences were performed in all patients. We assessed qualitative imaging parameters (overall image quality, mucosal enhancement, vessel clarity, motion artifact, lesion conspicuity, and lesion edge sharpness) using a 5-point scale. We calculated lesion-to-adjacent structure contrast ratio (CR). We compared all qualitative parameters and CR between radial and conventional VIBE images using the Wilcoxon signed-rank test.
Results: Radial VIBE images showed significantly higher scores in all qualitative parameters in comparison with conventional VIBE images. No significant difference was shown in CR between radial and conventional VIBE images (p=0.112). Conclusion: Radial VIBE showed a higher image quality compared to conventional VIBE. Radial VIBE sequence may be applicable for pharyngolaryngeal MRI.

Table. Comparison of imaging parameters between radial VIBE and conventional VIBE sequences.

Imaging parameters	Radial VIBE	Conventional VIBE	p
Qualitative parameters			
Overall image quality	4.7 ± 0.6	3.9 ± 0.9	<0.001
Mucosal enhancement	4.5 ± 0.6	4.0 ± 0.9	0.004
Vessel clarity	4.0 ± 0.6	3.0 ± 0.6	<0.001
Motion artifact	4.7 ± 0.5	3.9 ± 0.8	0.001
Lesion conspicuity	4.5 ± 0.7	3.5 ± 1.1	0.001
Lesion edge sharpness	4.2 ± 0.9	3.3 ± 1.1	0.002
Contrast ratio	0.14 ± 0.06	0.12 ± 0.08	0.112

Data are the mean ± SD

O-1-064　T_2スター緩和を考慮したマルチエコー法によるnigrosome 1の描出能の検討
Visualization of nigrosome 1 using multi echo imaging technique in consideration of T_2 star relaxation

荒井　信行（名古屋市立大学病院 中央放射線部）
Nobuyuki Arai[1], Hirohito Kan[1], Harumasa Kasai[1], Hiroshi Kunitomo[1], Masahiro Takizawa[2], Kazuyoshi Omori[2], Yasujiro Hirose[1]
[1]Nagoya city university hospital, [2]Healthcare Business Unit, Hitachi, Ltd.

【要旨】T_2スター緩和を考慮したマルチエコーによるnigrosome 1の描出について検討した．9エコーによる合成画像を基準とした．delta TEを最短にした条件で最初，中央，最後のTEをそれぞれ一致させ，さらにエコー数を6点，4点と少なくして検討した．TEが極端に短い，または長いエコーが混入するとnigrosome 1の描出能が低下した．

Purpose: A new imaging diagnostic tool that existence of nigrosome 1 located in the caudal and mediolateral part of the substantia nigra pars compacta has a lot to do with Parkinson's disease, then some reports visual assessment of it use combined image from 3D spoiled gradient echo with multi echo technique. We evaluated multi echo in nigrosome 1 in consideration of T_2 star relaxation.Materials and Methods: It was based on a combined image by nine points of echo (first TE/last TE/delta TE, 4.6/66.9/7.5ms). To investigate effective by the T_2 star relaxation, under a condition with delta TE as shortest (i.e. 4.6ms), we made first TE, central TE and last TE consistent with each. Furthermore, we fixed first TE and last TE, and examined fewer echo number, i.e. six and four points of echo. The repetition time and bandwidth were fixed as each parameter using multi echo imaging technique that is being studied. We calculated contrast of the nigrosome 1 and its surrounding substantia nigra in order to assess visualization of nigrosome 1.Results: The shortest delta TE had a significant higher contrast of the nigrosome 1 and substantia nigra. However, contrast significantly decreased when we set the echo train too much in the front or the back, and reduced the number of the echoes.Conclusion: The echoes in each TE are affected by the T_2 star relaxation. When the TE is extremely short or long, the echo causes decreasing visualization of nigrosome 1.

O-1-065　非対称RF shimを用いたプリサチュレーションパルスによる頸動脈選択3D TOFの開発
Artery selective 3D TOF with asymmetrically RF shimmed Pre-Saturation pulse with 4-channel RF transmit at 3T

伊藤　公輔（株式会社日立製作所ヘルスケアビジネスユニット）
Kosuke Ito[1], Atsushi Kuratani[1], Takashi Nishihara[1], Yukio Kaneko[2], Masahiro Takizawa[1]
[1]Healthcare Business Unit, Hitachi, Ltd., [2]Research and Development Group, Hitachi, Ltd.

【要旨】4チャンネル照射コイルを用いた非対称RF shimをプリサチュレーションパルスに適用した。2D励起を用いた頸動脈選択励起方法と比べて、TRの延長が不要なため脳実質と血液とのコントラストが高く、撮像時間も延長しない特徴がある。被検者で検討して効果を確認した。

PURPOSE
Artery selective 3D TOF is used to evaluate collateral blood flow [1]. 2D excited Pre-Saturation pulse (PreSat) was used to saturate blood signal from left or right internal carotid artery (ICA). But 2D excitation caused extension of duration of PreSat, and longer TR was needed. In this study, we applied Regional RF shimming to PreSat without extension of TR to selectively visualize blood flow from ICA [2] and compared with 2D excitation.
Methods
3T MRI system (Hitachi, Ltd.), and 4-channel RF transmit coil were used. 6 volunteers were evaluated after informed written consent was obtained in accordance with our institutional review board guidelines. B_1 map was acquired by multi Td method [3]. 2 region of interest (ROI) for PreSat(+) and (−) were set on the B_1 map at the location of ICAs. RF shimming parameters for PreSat were determined to minimize mean of B_1 in ROI_-, subject to mean of B_1 in ROI_+ is equal to QD. Ratio of mean of B_1 in $ROI_\pm$ was evaluated for 5 volunteers. Also, ratio of signal intensity of blood in ROI_- and white matter was compared between nonselective 3D TOF, 2D excitation, and proposed method for a volunteer. Scan parameters of 3D TOF were as follows ((): case of 2D excitation): TR=20, 18, (23.1) ms, FA=18, 20°.
Results
Mean of B_1 in ROI_- was smaller than that in ROI_+ by 87%. The contrast between blood and white matter was 3.2 in nonselective 3D TOF, 2.8 in 2D excitation, and 3.3 in proposed method.
Conclusions
By applying asymmetrically RF shimmed PreSat to 3D TOF, blood flow from left or right ICA is selectively visualized. The method provides high contrast between blood and brain parenchyma.
References
1. Ito Kenji, et al. J Stroke Cerebrovasc Dis. 23(5), 1019-1023
2. Ito Kosuke, et al. ISMRM 2016; 24: 3177
3. Ito Kosuke, et al. ISMRM 2013; 23: 2597

O-1-066　ラディアルスキャンTOF法を用いた頚部MRA
Motion insensitive neck MRA using radial TOF

笠井　治昌（名古屋市立大学病院 中央放射線部）
Harumasa Kasai[1], Hiroto Kan[1], Nobuyuki Arai[1], Masahiro Takizawa[2], Yoshimasa Matsuda[2], Kazuyoshi Omori[2], Yasujiro Hirose[1]
[1]Department of Central Radiology, Nagoya City University Hospital, [2]Healthcare Business Unit, Hitachi, Ltd.

【要旨】TOFを用いた頸部MRAは、撮像時間が長いため撮像中の患者の動きが問題となる。今回我々は、ラディアルスキャン（RADAR TOF）の特長を利用して頚部MRAに用いた。RADAR TOFは体動抑制効果、取得データ数が少なくても空間分解能が保たれるため、動きそうな部位においては有効な手段となりうると考えられる。

＜Purpose>TOF sequence is widely used for neck MRA. However image artifact caused by patient motion due to long scan time was often observed. Radial scan acquires echo signals radially in k-space and is able to suppress image artifact caused by patient motion. Additionally, it has a feature that spatial resolution of image is kept even if the number of echo signals is reduced. In this study, we apply the radial scan for neck MRA to shorten scan time and improve robustness against the body motion. ＜Methods>Scan time was shortened by reducing the number of echo signals (under-sample condition). The visualization of target vessels was compared between conventional TOF (Conv. TOF) and radial TOF (RADAR TOF) in the under-sample condition. A 3T MRI (TRILLIUM OVAL, Hitachi, Ltd.) was used for imaging healthy volunteers after obtaining informed written consent in accordance with our IRB guidelines. The vessel visualization was evaluated by using line profiles on the carotid bifurcation in the original image for both non-motion and motion cases. The line profiles were compared in the point of separation of two vessels at the carotid bifurcation by using difference between top and bottom signal intensities. For the reference of the vessel visualization, full sampled Conv. TOF image was acquired. ＜Results>RADAR TOF image had higher spatial resolution and smaller truncation artifact than Conv. TOF image at the carotid bifurcation. In the motion case, RADAR TOF still showed a good visualization at the carotid bifurcation compared to the Conv. TOF. ＜Conclusion>RADAR TOF has features which keep the spatial resolution of image in the under-sample condition, and suppresses body motion during scanning. This would work well for scanning the patient who cannot stand for a long time.

O-1-067　Arterial Spin Labeling（ASL）法を用いた健常者耳下腺血流量の計測
Measurement of blood flow of normal parotid glands using pseudo-continuous arterial spin labeling

井上　勝博（三重大学 医学部附属病院 中央放射線部）
Katsuhiro Inoue[1], Shiho Isoshima[1], Shinichi Takase[1], Tsunehiro Yamahata[1], Maki Umino[3], Makoto Obara[2], Masayuki Maeda[4]

[1]Department of Radiology , Mie University Hospital, [2]Philips Electronics Japan, [3]Department of Radiology, Mie University School of Medicine, [4]Department of Advanced Diagnostic Imaging, Mie University School of Medicine

【要旨】Arterial Spin Labeling（ASL）法を用い、健常ボランティア6名による耳下腺血流量の検討を行った。3D-TSE pCASLは2D-EPI pCASLに比べ、視覚的に優れ、測定誤差も小さく耳下腺血流量の計測に有用である。

[Purpose]Arterial spin labeling(ASL) has become to be used in head and neck regions. The purpose of this study is to evaluate the blood flow of normal parotid glands using pseudo-continuous arterial spin labeling(pCASL) including 2D-EPI and 3D-TSE. [Method]The study was performed at a 3T MRI(Ingenia,Philips)using ds HeadNeck Spine coil.Six normal volunteers were evaluated for the measurements of blood flow of parotid glands using 2D-EPI and 3D-TSE pCASL. The common parameters of the two pCASL sequence were the following; post labeling delay=1800ms, matrix=80×80, scan time=5min30s. The quantitative data were achieved using quantitative CBF measurement software(C++ programming language, Philips Healthcare Korea, Republic of Korea). Quantitative data(blood flow and standard deviation) as well as visual assessment of parotid-flow map were compared between each technique. [Results]Visual assessment showed 3D-TSE pCASL map was significantly better in the delineation of parotid glands($p<0.05$). 3D-TSE showed larger parotid blood flow than 2D-EPI(50.3±8.5,37.7±5.9 ml/min/100mg, respectively;$p<0.05$). Standard deviation was significantly smaller in 3D-TSE(13.6, 25.6,respectively;$p<0.05$). [Conclusion]Blood flow of the normal parotid flow was significantly higher in 3D-TSE pCASL than 2D-EPI pCASL. This is probably because of the difference of readout and dimensions between the two techniques. Normal parotid glands was more clearly delineated on 3D-TSE pCASL map, which was due to higher signal-to-noise ratio and lesser distortion of images on 3D-TSE pCASL map. 3D-TSE pCASL is suitable for the measurements of parotid blood flow.

O-1-068　Time-SLIPを使用した非造影MRDSAにおける交互収集法と分割収集法の比較検討
Comparative examination of the Separate acquisition method and Alternate acquisition method in non-contrast MRDSA using Time-SLIP

小泉　達也（順天堂大学 医学部附属 浦安病院 放射線科）
Tatsuya Koizumi[1], Takashi Iwasaki[2], Shinsuke Kyogoku[1], Takao Kimizuka[1], Daisuke Tsuge[1], Nao Kikuchi[1], Saori Shiota[1], Takeshi Udagawa[1], Nanae Kawano[3]

[1]Department of Radiology, Juntendo University Urayasu Hospital, [2]Department of Radiology, Juntendo University Hospital, [3]Toshiba Medical Systems corporation

【要旨】Time-SLIPのAlternate法とSeparate法をファントム、ボランティアにてRR間隔を変化させ比較をした。冠状断では短いRR間隔でContrast ratioが低下したが水平断では低下しなかった。Separate法はAlternate法よりも冠状断では少しの撮像時間の延長で高い画質が得られ、水平断では短時間で同等の画質が得られる可能性がある。

[Purpose]Time-SLIP has an alternate acquisition (AT) method which alternately acquires labeling images and control images to prevent misregistration. However, the AT method has a long imaging time since it acquires a control image for every BBTI. Therefore, we examined the effectiveness of the separate acquisition (ST) method, which acquires the control and labeling images separately and share the control images for each BBTI. **[Material and Methods]**MRI scanner was the Excelart Vantage 1.5T (Toshiba). We put a pseudo blood solution (T1value 1051ms) in phantoms and compared the contrast ratio (CR) with respect to the background signals while varying the RR intervals. The cross-sectional images acquired coronal and axial. We acquired the cerebral MRA images of the seven healthy volunteers (7 males, mean age 42.8 years), and compared in the same way. six radiologists conducted visual evaluations. **[Results]**For the phantom in the coronal cross section, the CR decreased to 0.66, 0.74 in the both AT and ST method of the 1500ms RR intervals. For volunteer scans, there was a significant difference between the coronal images according to the ST method (3000ms) and those according to the AT and ST methods (1500ms) ($p<0.01$). There was no significant difference for the axial images. **[Conclusion]**For the coronal cross section, the ST method rendered images with higher quality than those by the AT method with 1500ms just by setting the RR intervals to 3000ms, i.e., increasing the imaging time for the control images. For the axial cross section, the ST method acquired images of equivalent quality in a shorter amount of time because it is less susceptible to short RR intervals. Therefore, the study implied that the ST method could be effective in cases not affected by misregistration.

O-1-069　QSI－Pantomを考慮したPNIPAAm系ゲルの複合合成による相転移温度移動と含水量による材料特性の変化
Changes in material properties due to phase transition temperature movement and water content by PNIPAAm-based gel that takes into account QSI-Pantom

八木　一夫（首都大学東京 大学院 人間健康科学研究科 放射線学域）
Kazuo Yagi[1,2,3], Atsuya Ikeda[2], Naoyuki Kurimoto[2], Masashi Ueda[1], Madoka Nanao[1], Seiichi Sugimoto[3], Tadashi Inaba[2]

[1]Division of Radiological Sciences, Graduate School of Human Health Sciences, Tokyo Metropolitan University, [2]Graduate School of Engineering, Mie University, [3]Medical and Welfare Engineering,Tokyo Metropolitan College of Industrial Technolog

【要旨】ポリN-イソプロピルアクリルアミド(PNIPAAm)系材料は温度対応材といわれる。これをQSI用ファントムとして利用するため、合成時の水分量を生体の保持する水分量(60-80重量%）に設定し、重合時の温度条件を変化させ、ゲルの内部構造と材料特性に与える影響を調査した。含水量と強度との関係で強度が上昇する領域が発現した。

Purpose: Poly N- isopropyl acrylamide (PNIPAAm) based gel causes a volume phase transition phenomenon in response to temperature change is said to be temperature corresponding material.To use as QSI phantom, set the water content at PNIPAAm-based gel synthesis amount of water retention of biological, changing the temperature condition during the polymerization, investigated the effects on the internal structure and the material properties.Methods: Material design and synthesis of gel: the moisture content of gel material in the synthesis set to approximate the living tissue (60-80% by weight of the moisture content at the time of charging), condensation polymerization of monomers NIPAAm. It is to create a PNIPAAm-based gel.This material to evaluate the temperature response was immersed in cold water solvent (3-5 degree) from the high-temperature water solvent (36-40 degree), performs a weight change test to measure the rate of change in weight of each temperature, the ambient temperature. It was uniaxial tensile test to evaluate the mechanical characteristics due to the change. Result: Phase transition before and after the change in weight, the tensile strength properties, were performed SEM observation.Area specifically strength is increased in relation to water content and strength of the gel was expressed.Conclusion: Material properties of the hydrogel is due to inside of the polymer network structure. Since this material is synthesized by chemical polymerization reactions influences the polymer network in the gel by changing the synthesis conditions, the material properties change.

O-1-070　拡散強調画像における細胞密度模擬ファントムの作成
Development of a phantom simulating cell density for diffusion-weighted magnetic resonance imaging

三賀山諒司（九州大学大学院 医学系学府 保健学専攻）
Ryoji Mikayama[1], Hidetake Yabuuchi[1], Ryoji Matsumoto[2], Koji Kobayashi[2], Yasuo Yamashita[2], Mitsuhiro Kimura[1], Satoshi Kawanami[3], Hiroshi Honda[3]

[1]Department of Health Sciences, Graduate School of Medical Sciences, Kyushu University, [2]Division of Radiology, Department of Medical Technology, Kyushu University Hospital, [3]Department of Clinical Radiology, Graduate school of Medical Sciences, Kyushu University

【要旨】直径10, 15, 20 μmのアクリル系微粒子を用いて細胞を模擬し、細胞密度を段階的に変化させた拡散強調画像標準化ファントムを作成した。ADC値は0.89～1.41 ($\times 10^{-3}$ mm^2 / s) となり、細胞密度とADC値は強い負の相関関係を示した ($r = -0.986$, $P < 0.05$)。発表時はファントムの再現性評価も含めて報告する予定である。

[Purpose] A phantom for diffusion-weighted imaging (DWI) is required to standardize the quantitative evaluation of DWI. However, there is no phantom simulating various cell density of lesions. The purpose of our study was to develop a phantom simulating various cell density of lesions using acrylic fine particles.
[Method] The acrylic fine particles, which are insoluble polymethyl methacrylate (PMMA) with diameters of three kinds (10, 15, and 20 μm, respectively) were used to simulate the human cells. First, we prepared four degree of cell density phantoms by adjusting the volume of 10 μm particles (5, 20, 35 and 50 % volume, respectively), which were dispersed in the detergent diluted with purified water. Second, two degree of cell size phantoms to simulate cell edema were developed. In each phantom, 15 and 20 μm particles were dispersed without change of number (17 and 40 % volume, respectively by referring to 5 % volume of 10 μm particles) in the detergent diluted with purified water. Spearman's rank correlation coefficient was used to test whether a significant correlation existed between apparent diffusion coefficient (ADC) and particle density. A P-value < 0.05 was regarded as indicating a statistically significant difference.
[Result] Each phantom component (particle density of 5, 17, 20, 35, 40 and 50 % volume, respectively) showed ADC values of 1.42, 1.30, 1.30, 1.12, 1.09 and 0.89 ($\times 10^{-3}$ mm^2 / s), respectively. There was a negative correlation ($r = -0.986$, $P < 0.05$) between ADC and particle density.
[Conclusion] A phantom simulating diffusion limitation correlating the increased cell density and size could be developed.

O-1-071　異方性拡散ファントムによるMRI装置間のDTI測値の比較
Comparisons of DTI measures among five different MRI scanners using anisotropic diffusion phantom

酒井　晃二（京都府立医科大学）
Koji Sakai[1], Toshiaki Nakagawa[2], Ryusuke Nakai[3,4], Hiroyasu Ikeno[2], Toru Osawa[2], Shun Higotani[2], Seiji Yamaguchi[3], Hiroaki Takadama[3], Kei Yamada[1]

[1]Kyoto Prefectural University of Medicine, [2]Kyoto Prefectural University Hospital, [3]Chubu University, [4]Kyoto University

【要旨】同じ型式のMRI装置、設定で画像を取得しても、差異は存在すると認識されている。本報では、安価に作成できる異方性拡散ファントムとして、透析用止血圧迫綿を用い、5台のMRI装置間の拡散指標（ADC, FA）の差異、繰り返し測定誤差、日隔変動の差異を比較し、MRI装置間での値の相互利用の可能性を評価した。

Multi-site study gives large statistical power for the results of multi-scanner imaging. Some intrinsic differences among scanners are recognizing as an inevitable property. QIBA is trying to tackle this intrinsic differences to achieve statistically meaningful results from multi-site study. As QIBA's endeavor, isotropic diffusion has already been discussing. In contrast, anisotropic diffusion has been evading the endeavor because of the absence of an appropriate anisotropic diffusion phantom. In this study, we compared DTI measures (ADC, FA) among five different MR scanners (Siemens Skyra 3T, Philips Master 1.5T, Philips Nova 1.5T, Siemens Avanto 3T, and Siemens Sonata 1.5T, 32-ch head coils) at three different sites using commercially available astriction cotton (length = 30 mm, diameter = 20 mm, Hakujuji Co. Ltd., Tokyo, Japan). FOV of DTI was 240 x 240 mm and matrix was 120 x 108 by an EPI technique. A b value of 1,000 s/mm^2 and 10 MPGs were used. Five times acquisitions were longitudinary repeated at approximately 22.0 degree C room temperature. The DTI analysis was performed with Diffusion Toolkit/TrackVis version 0.5.2.2 and tract-based average diffusion metrics were calculated with manually placed ROIs on center slices in three orthogonal directions. The stability of ADC and FA were evaluated by comparing coefficient of variations (CV). The range of averaged CV for five times sequentially acquisition of ADC and FA on five different MR scanners were 0.2-1.0% and 0.9-5.3%, respectively. The range of averaged CV for longitudinary repeated acquisitions of ADC and FA on five different MR scanners were 2.2-3.6% and 2.1-7.8%, respectively. The scan-rescan properties of five different MR scanners were compared using anisotropic diffusion phantom.

O-1-072　拡散テンソルイメージング自作標準化ファントムにおけるFractional Anisotropy (FA) の再現性評価
Reproducibility of our standardization phantom for evaluation of fractional anisotropy (FA) derived from diffusion tensor imaging (DTI)

木村　光宏（九州大学大学院 医学系学府 保健学専攻）
Mitsuhiro Kimura[1], Hidetake Yabuuchi[1], Ryoji Matsumoto[2], Koji Kobayashi[2], Yasuo Yamashita[2], Ryoji Mikayama[1], Satoshi Kawanami[3], Hiroshi Honda[3]

[1]Department of Health Sciences, Graduate School of Medical Sciences, Kyushu University, [2]Division of Radiology, Department of Medical Technology, Kyushu University Hospital, [3]Department of Clinical Radiology, Graduate School of Medical Sciences, Kyushu University

【要旨】拡散テンソルイメージング自作標準化ファントムにおけるFractional Anisotropy (FA) の再現性を評価した。このファントムを2週間間隔で3回撮像したときのFAの再現性は高かった。このファントムは拡散テンソルイメージングにおける定量評価の標準化に有用であると示唆される。

[Purpose] It is necessary to standardize the quantitative evaluation of diffusion tensor imaging (DTI) for a multi-center trial or establishment of a diagnostic criteria, however, there has been no report on the reproducibility of standardization phantom for evaluation of fractional anisotropy (FA) derived from DTI. Thus, the purpose of this study was to examine the reproducibility of standardization phantom composed of different fiber density (FD) and material for evaluation of FA derived from DTI.
[Methods] Two types of fiber material (Fiber1: Ultra-High Molecular weight Polyethylene Fiber and Fiber2: High-Performance Polyethylene Fiber) wrapped in heat shrinkable tubes were used for the phantom. FD was calculated as the ratio of the summed cross-section area of fibers to the sectional area of a tube, and we designed phantoms with three different FD (0.3, 0.4, and 0.5) of each fiber material. The phantoms were examined using DTI protocol on three sessions (Day1, Day15 and Day29), repeated six times a day. One of our authors performed fiber tracking by setting regions of interest in FA map, and measured FA in each FD at two types of fiber material. Spearman's rank correlation coefficient was used to evaluate the relationship between FD and FA ($P < 0.05$). Percent difference, which was decided as the percentage obtained by dividing the difference of two values by the average of two values, was used to evaluate the reproducibility of FA.
[Results] FA showed significant correlations with FD at each fiber material (Fiber1: $r = 0.945$, $P < 0.001$; Fiber2: $r = 0.947$, $P < 0.001$). Percent differences of Day1 and Day15, Day1 and Day29 were within 3%, respectively.
[Conclusion] High reproducibility of our standardization phantom was achieved.

O-1-073　2D SSFP Time-SLIP法を用いた擬似拍動ファントムによる流体動画像の解析
Analysis of the fluid flow image of phantom push-pull pump by 2 dimensional steady state free precession time spatial spin labeling inversion pulse

酒井　貴寛（駒澤大学大学院 医療健康科学研究科）
Takahiro Sakai[1,2], Kohki Yoshikawa[1], Shinya Yamada[3]
[1]Komazawa University Graduate Division of Health Scineces, [2]Toshiba Rinkan Hospital division of Radiology, [3]Toshiba Rinkan Hospital division of Neurosurgery

【要旨】Time-SLIP法は、既存の髄液動態の描出に使用されてきた方法とは大きく異なり、脳脊髄液そのものを内因性トレーサーとして使用することができる。本研究のファントム実験において、作り出した拍動水流の解析を行った結果、この法における脳脊髄液拍動ダイナミクス解析は有用であることが示された。

In Time-SLIP technique, cerebrospinal fluid (CSF) is usable as an endogenous tracer by using RF pulse of MRI. However, the findings of CSF dynamics obtained by this method markedly differ from those obtained by exogenous tracer or MRI Phase-Contrast method, which suggests that existing theory about physiological pulsatile CSF dynamics in the body should be reconsidered. In this study, the experimental pulsatile flow generated by phantom push-pull pump was analyzed to verify accuracy of human CSF pulsatility observed by Time-SLIP technique. The pulsatile flow was generated by push-pull pump at arbitrary stroke volume and pulse rate, imaged by 2D SSFP Time-SLIP method, and we observed and analyzed how the speed and shape of the fluid in a tube labeled with RF pulse are changed by the indicated stroke volume and pulse rate. Semi-automated tracing software was used in motion image analysis. The condition changing the speed and shape of the fluid in a tube labeled with RF pulse by the indicated stroke volume and pulse rate were captured and analyzed with semi-automated tracing software. The results of phantom experiment demonstrated that human CSF pulsatility was exactly captured by 2D real time Time-SLIP. This method suggests to be effective in analysis of pulsatile CSF dynamics.

O-1-074　MAVRIC-SLによる金属アーチファクト低減効果の検討
Metal Artifact reduction with MAVRIC-SL: in vitro assessment with implant phantom

内藤　　舞（慶應義塾大学病院 放射線技術室）
Mai Naito[1], Sari Motomatsu[1], Yoshinobu Nunokawa[1], Yasutomi Shimada[1], Takashi Asakura[1], Souta Oguro[2], Hirokazu Fujiwara[2], Shigeo Okuda[2], Masahiro Jinzaki[2], Atsushi Nozaki[3]
[1]Office of Radiation Technology, Keio University Hospital, [2]Department of Ragiology, Keio University School of Medicine, [3]MR Applications and workflow, Asia Pacific, GE Health Care Japan

【要旨】3種類の金属インプラントを使用し、MAVRIC-SLによる金属アーチファクトの低減効果、および人工股関節の材質によりその効果に差異がないか視覚評価を行った。MAVRIC-SLを用いることで金属インプラント周囲の炎症および腫瘍等の描出能の向上が見込まれ、金属インプラント挿入患者に対する画像診断能の向上が期待される。

[Purpose]To evaluate the artifact reduction around implanted metal devices using MAVRIC-SL (multi-acquisition variable-resonance image combination selective). [Materials and Methods]The subjects were three metal hip implant devices (Titanium (Stryker), cobalt-chromium (Stryker) and stainless-steal (BIOMET) stem hip modules). Each device was fixed to the plastic container with the grid plate, and filled with Vinyl acetate. Each phantom was scanned using 3.0T MRI scanner (SIGNA Pioneer: GE) with TDI Anterior Array coil. Conventional Fast Spin Echo (FSE) and MAVRIC-SL were scanned with the following parameters: FSE-XL (MAVRIC-SL) TR/TE/ETL=500/5.6msec/2 (500msec/6.8msec/8), FOV=30cm, Slice Thickness=5mm, NEX=1 (0.5). Three radiologists were visually evaluated the severity of metal artifact with 5-point scale.[Results] Image distortion was reduced with MAVRIC-SL for all three devices we tested, in comparing to FSE. Stainless-steal caused largest artifacts for both FSE and MAVRIC-SL sequence, followed by Titanium and cobalt-chromium device. Our results suggested that MAVRIC-SL might be useful for detecting tumor and/or inflammation around the metallic implant in the clinical setting.

MAVRIC-SL image artifact comparison with three different metal implants

O-1-075　磁場歪みマッピングの定量的評価
Quantitative evaluation of the magnetic field distortion mapping

金田　貴彦（北海道大学大学院 保健科学院 保健科学専攻）
Takahiko Kaneda[1], Toru Yamamoto[2]

[1]Graduate School of Health Sciences, Hokkaido University, Sapporo, Japan, [2]Faculty of Health Sciences, Hokkaido University, Sapporo, Japan

【要旨】金属インプラントのMRIアーチファクトの原因である磁場歪みの精密測定のため、磁化率が既知の棒状金属試料を対象に、3D GRE法を用い1mm^{3}ボクセルで高分解能磁場歪みマッピングを行った。解析的に予想した磁場歪みと比較することでこの磁場歪みマッピングが数％程度の正確度を有することが確認できた。

Introduction Metallic implants distort static magnetic field of MRI and this distortion causes artifacts that prevent proper diagnosis. The magnetic field distortion ($\delta B/B_0$) map of metallic implants would enable comprehensive comparison of various implants with respect to metallic artifact in MRI. However, the accuracy of the $\delta B/B_0$ mapping has been unknown. To evaluate the accuracy of $\delta B/B_0$ mapping with 3D GRE imaging, we derived the magnetic susceptibility (χ) of a metallic rod from the $\delta B/B_0$ map and compared this obtained value with the value of the material in the literature.
Materials and Methods An Elgiloy rod and a Ti alloy (Ti-4Al-6V) rod (diameter = 1.8 mm, length = 38.8 mm) were placed at the center of the phantom which composed of agar (1wt.%, bottom half) and water (upper half), respectively. The 3D GRE imaging of isotropic voxel of 1 mm3 with 2 different TEs (2.7, 22.7 ms) was performed with a 3-T MR system. Then the $\delta B/B_0$ map was made from 2 phase images of different TEs in the horizontal slice that contained the metallic rod. The χ of each rods was calculated by using the theoretical equation of a magnetic field of a paramagnetic rod with the obtained $\delta B/B_0$ values on the mapping.
Results and Discussion The calculated χ of the Elgiloy rod was 2.8×10^{-3} which was within the various reported values of χ of Elgiloy (2.1×10^{-3} - 4.0×10^{-3}). On the other hand, the χ of Ti-4Al-6V has been exactly reported as 1.8×10^{-4}, and the calculated χ of the Ti alloy rod was 1.9×10^{-4} which agrees well with the value in the literature. Because the $\delta B/B_0$ is theoretically proportional to χ, the $\delta B/B_0$ mapping is reliable within a few percentages.
Conclusion Our employed magnetic distortion mapping with 3D GRE imaging is quantitatively reliable within a few percentage.

O-1-076　3.0T における金属アーチファクト低減効果（SEMAC）の基礎的検討
Metal artifact reduction by SEMAC in 3T

近藤　敦之（埼玉医科大学病院）
Atsushi Kondo[1,2], Shinichi Watanabe[1], Maiko Isono[1], Hiroshi Imai[3], Taishi Unezawa[1], Tomio Yamasaki[1], Iichiro Osawa[1], Kaiji Inoue[1], Eito Kozawa[1], Mamoru Niitsu[1]

[1]Saitama Medical University Hospital, [2]Tokyo Metropolitan University, [3]Siemens Healthcare K.K.

【要旨】ACLスクリューを水中に固定したファントムをTSE、WARP+VAT、SEMACで撮像し、信号低下域を評価した。また、SEMAC factor、スライス厚についても評価した。信号低下域はSEMACが最も少なかった。SEMAC factorが大きく、スライス厚が薄くなるほど信号低下域は減少した。スライス厚2.5mm、SEMAC factor15を至適条件とした。

[Background, purpose]In MR imaging, an artifact from the internal metallic substance distorts the images and may degrades the diagnosis. The newly installed SEMAC (Slice Encoding for Metal Artifact Correction), which acquire several images with an additional slice encoding gradient and synthesize them, can reduce the metal artifacts. However, the increasing the number of slice encode steps (SEMAC factor) extend the acquisition time. We evaluated and examined optimal SEMAC factor, comparing the SEMAC to the conventional imaging. [Method] A phantom with a metallic screw for knee surgery (ligament fixation) sealed with water package was made. The screw orientated 0degree, 45degree, 90 degree to B0 field. The phantom was imaged by TSE, WARP+VAT, SEMAC using MAGNETOM Skyra (3T) and Tx/Rx 15-Channel Knee Coil. The ranges of the signal loss were measured in each setting. The influence of SEMAC factor and slice thickness were also evaluated. The signal decay was decreased in order of TSE (max), WARP+VAT, SEMAC (minimum). The signal of surrounding water was preserved in SEMAC. The signal decay was largest when the screw positioned closer to perpendicular to B0. Increasing the SEMAC factor boosted the artifact reduction and didn't change any more at more than the SEMAC factor of 15. The signal decay was decreased with thinner slice thickness.[Conclusion]Metallic artifacts were decreased by using the SEMAC. Considering the total scanning time, optimal condition with SEMAC factor of 15 and slice thickness of 2.5mm, was employed in our institution.

O-1-077　発泡ポリエチレン製頭頚部放射線治療用固定具がMR画像に与える影響
MRI-based radiotherapy planning using foamed polyethylene therapeutic immobilization base plate for head and neck

宮本　昌宜（神戸大学医学部附属病院 医療技術部 放射線部門）
Masanori Miyamoto[1], Yuuichirou Somiya[1], Katsusuke Kyotani[1], Yuuichi Aoyama[1], Satoru Takahashi[2], Hideaki Kawamitsu[1]

[1]Division of Radiology, Department of Medical Technology, Kobe University Hospital, [2]Department of Radiology, Kobe University Hospital

【要旨】カーボン製頭頚部放射線治療用固定具がB1不均一やSNR低下をまねく。目的は発泡ポリエチレン製頭頚部放射線治療用固定具でSNRとB1不均一を改善することである。ファントムとボランティアのB1の均一性、SNRをImage J で解析した。ファントムとボランティアのB1不均一が改善し、SNRも改善した。

Introduction:We have reported that carbon therapeutic immobilization base plate complicated the image quality of MRI-based planning for head and neck radiotherapy, because eddy current in conductive material shield RF penetration. The purpose of the study was to evaluate the usefulness of the non-conductive foamed polyethylene immobilization base plate in B1 inhomogeneity and SNR of MRI for radiotherapy planning. Materials and Methods:Mineral oil-phantoms were placed on carbon or formed polyethylene therapeutic immobilization base plate for head and neck, and scanned at 3T MR unit. B1 map and SNR map were calculated with and without each base plate, and B1 homogeneity and SNR were analyzed. Five volunteers were also scanned and evaluated in the same way. Results:In phantom study, B1 homogeneity decreased approximately 20% with carbon base plate compare to those without base plate, while foamed polyethylene did not degenerate B1 homogeneity. SNR was reduced approximately 50% with carbon base plate, while 15% with formed polyethylene base plate. In volunteer scan, B1 homogeneity and SNR decreased 20% and 40% with carbon base plate, whereas formed polyethylene base plate caused 5% and 15% reduction, respectively. Conclusions:Non-conductive foamed polyethylene immobilization base plate reduced degeneration of image quality for MRI-based radiotherapy planning.

O-1-078　3T向け32チャンネル頭部コイルに対応する感度補正アルゴリズム
Sensitivity Correction Algorithm for 32-Channel Head Coil at 3T

鎌田　康弘（株式会社日立製作所 ヘルスケアビジネスユニット）
Yasuhiro Kamada, Miki Tachibana, Kuniaki Harada, Takeshi Taniguchi, Kazuyuki Kato, Masahiro Takizawa, Hiroyuki Itagaki

Healthcare Business Unit, Hitachi, Ltd.

【要旨】3T向けに開発された32チャンネル頭部コイルは、従来コイルに比べて計測画像のSNRが高く、撮像のさらなる高速化や高分解能化が期待される。一方で、受信エレメントが小さいため、受信感度の空間分布が急峻になる。今回、32チャンネル頭部コイル向けに感度補正アルゴリズムを改良し、従来法よりも均一な画像を得た。

[Introduction]
In a 32-channel head coil developed for 3T, image SNR (Signal to Noise Ratio) can be increased compared with conventional head coil. Therefore shorter scan time or higher spatial resolution can also be achieved as a result of high SNR. On the other hand, the small receiver element size causes steep sensitivity distribution of coil, and thus inhomogeneous image was usually acquired. In this study, we modify the sensitivity correction algorithm for a 32-channel head coil to acquire homogeneous images.
[Methods]
The sensitivity correction algorithm uses sensitivity maps calculated from low spatial resolution images acquired in a dedicated sequence. These images contain many signal components such as tissue contrast, B1 distribution, and coil sensitivity, and undesired components other than coil sensitivity should be removed to acquire sensitivity maps. In the modified algorithm, target spatial frequency of coil sensitivity is set to higher than that in conventional algorithm in order to acquire steeper sensitivity maps. A 3T MRI scanner (Hitachi, Ltd., Tokyo, Japan) equipped with a 32-channel head coil was used for data acquisition. In the reconstruction process, modified algorithm was applied to correct image inhomogeneity in off-lined software. Evaluations were performed on different image contrasts used in routine head examination with healthy volunteers after obtaining written informed consent in accordance with our institutional review board guidelines.
[Results]
Calculated sensitivity maps in modified algorithm became similar to actual sensitivity distribution of a 32-channel head coil, and this leads more homogeneous images than those in conventional algorithm.
[Conclusions]
Sensitivity correction algorithm is modified for a 32-channel head coil.

O-1-079　0.3Tオープン型MRIによるMRエラストグラフィシステムの評価
Assessment of MR Elastography System using 0.3 T Open MRI

吉田　洋樹（千葉大学 大学院 工学研究科）
Hiroki Yoshida[1], Mikio Suga[1,2], Masashi Sekine[2]

[1]Graduate School of Engineering, Chiba University, [2]Center for Frontier Medical Engineering, Chiba University

【要旨】現在臨床において，MRエラストグラフィ (MRE) は高磁場トンネル型MRIを利用している．本研究では0.3 Tオープン型MRIを用いたMREシステムの構築を目的とした．ファントムを対象とした実験により，低磁場MRIでも振幅対雑音比の高い弾性波画像を取得することで，レオメータ測定値に近い弾性率が得られることを確認した．

Introduction: Conventionally, tunnel-type, high static magnetic field MRI are used for magnetic resonance elastography (MRE). For orthopedics, open MRI is advantageous because it gives patient the flexibility in any chosen position. The purpose of this study was to develop an MRE system using low static magnetic field open MRI and to make a quantitative assessment of the developed system using a viscoelastic polyacrylamide phantom.
Methods: Elasticity measurements were performed using a 0.3 T open MRI (AIRIS Vento, Hitachi medical systems) and a rheometer (MCR 302, Anton-Paar). For imaging the propagation of shear waves using MRI, we used SE-EPI-MRE sequence. The frequency of external vibrations used in the MRE and rheometer measurements were 62.5 Hz and 10 Hz, respectively. To investigate the relationship between the storage modulus and shear wave amplitude, we used a waveform generator to generate waveforms with different amplitudes (0.05, 0.1, 0.25, and 0.5 V). We calculated the amplitude-to-noise ratio obtained from the shear wave images with and without vibration.
Results: The storage moduli obtained from the MRE measurements using waveforms of amplitude 0.05, 0.1, 0.25, and 0.5 V were 1.91 ± 0.30, 2.24 ± 0.31, 2.80 ± 0.31, and 2.84 ± 0.34 kPa, respectively, and the amplitude-to-noise ratios in the four cases were 26.1, 50.2, 106.9, and 146.3. The storage modulus obtained from the rheometer measurement was 2.89 ± 0.05 kPa.
Conclusion: This work demonstrates the feasibility of quantitative estimation of storage modulus using MRE with low static magnetic field open MRI. The storage modulus obtained from the MRE measurement using a large amplitude of vibration is close to that obtained from the measurement using a rheometer.

O-1-080　MR Elastographyにおけるパーシャルボリューム効果の影響
Influences of partial volume effect in MR elastography

伊東　大輝（首都大学東京大学院 人間健康科学研究科 放射線科学域）
Daiki Ito[1,2], Tomokazu Numano[1,2], Kazuyuki Mizuhara[3], Masaki Misawa[2], Takaaki Onishi[1], Toshikatsu Washio[2], Naotaka Nitta[2]

[1]Department of Radiological Science, Graduate School of Human Health Science, Tokyo Metropolitan University, [2]Health Research Institute, National Institute of Advanced Industrial Science and Technology, [3]TOKYO DENKI UNIVERSITY

【要旨】MREでは振動による変位を位相シフト量として可視化するため，ボクセル内が同じ物質で満たされている場合でもパーシャルボリューム効果が起こり得る．本研究では均一なファントムに対し，スライス厚を変えてMREを行った．MREにおいては，可視化できる振動の変位量及び弾性率がスライス厚に依存して変化することが示唆された．

[Objective & Background] Partial volume effect (PVE) is an imaging artefact associated with many imaging modalities. It is well known that the PVE yields averaging the arbitrary values (e.g., signal intensity in MRI) of the materials within a voxel. MR elastography (MRE) is phase contrast technique that is capable of visualizing wave displacements from vibrations. Tissue displacements due to vibrations are encoded into MR phase images (wave images) using motion-sensitized gradients (MSG). Estimates of the local shear wavelengths in the tissue using the wave images provide stiffness images (elastograms). Even in MRE, it is possible to be occurred the PVE on the wave images. In general, the MR signal obtained from a voxel can be considered to be the vector sum of the magnetization of a large number of smaller subelements (isochromats). In MRE, the PVE may occur even if a voxel is filled with the same materials, because phase shifts due to vibrations are different in each isochromat. The changes in wave images may cause to the changes in elastogram. This study was investigated influences of the PVE in MRE.
[Material & Method] All experiments were performed on a 2.0-T animal experiment MR scanner on JSMRM-MRE phantom. MRE data were acquired by a spin echo-based MRE pulse sequence at 200Hz phenumatic vibrations in three MSG directions. A custom-designed vibration pad was used as a pneumatic transducer. We assessed for the changes of the wave images and elastograms by changing slice thickness; 1-19 mm, with a 2 mm step.
[Results & Conclusion] Visualized wave displacements on the wave images decreased with increasing slice thickness and the elastograms changed depend on slice thickness. In MRE, the PVE may be more significant problem compared to other imaging technique.

O-1-081　Zero-Interpolation Filling(ZIP)とCompressed Sensing(CS)の比較
Comparison between Zero-Interpolation Filling(ZIP) and Compressed Sensing(CS)

藤田　各務（東京電機大学 工学研究科）
Kagami Fujita[1], Kazuyuki Mizuhara[2], Toshikatsu Washio[3]
[1]Tokyo Denki University, Graduate school of Engineering, [2]Tokyo Denki University, Faculty of Engineering, [3]Advanced Industrial Science and Technology, Health Research Institute

【要旨】プレパレーションパルスを用いずに、Read out傾斜磁場と外部振動を併用して得られるMRエラストグラフにおいて、より一層の撮像時間の短縮が可能になれば、対象臓器も増えると考えている。Read Outの回数に着目して、ZIPとCSそれぞれのサンプリング率と、得られる再構成画像を比較した。

MR imaging apparatus makes MR Elastography which is image of organs' mechanical properties with its shape image. MR Elaslography takes longer time than usual MR imaging because MR Elaslography uses a sequence with special preparation pulse. In this study, we challenged time of taking signal could be shorten by not hardware but software. We combined compressed sensing (CS) and no preparation pulse MR Elaslography sequence for making mechanical properties map. CS was compared with zero-interpolation filling (ZIP). We use full 2D k-space which taking usual sequence instead of special sequence of CS. Random number that is made by mechanical random number birth device was used for picking up line data from full k space. We used whole data of one read out on the assumption that clinical use. We calculated full k-space as 100% data, and we reduced data every 10 % from full k space to 50 %. Reconstruction of image was calculated by projection over convex sets (POCS) type algorithm. Reconstruct phase images that were calculated from 50% of k-space were almost same as image by ZIP. As the result, we would solve an unbalance of machine time that is reconstruction on software method and shortening time of taking signal.

O-1-082　低グリセリン濃度で高粘性なMRエラストグラフィ用生体模擬ファントムの開発
Development of a Highly Viscous Tissue-Mimicking Phantom for Magnetic Resonance Elastography That Has Low Glycerin Content

石井　孝樹（千葉大学 工学部 メディカルシステム工学科）
Kouki Ishii[1], Mikio Suga[1,2,3], Riwa Kishimoto[3], Takayuki Obata[3]
[1]Faculty of Engineering, Chiba University, [2]Center for Frontier Medical Engineering, Chiba University, [3]Hospital for Charged Particle Therapy, National Institute of Radiological Sciences

【要旨】昨年開発した高粘性ゲルファントムは高グリセリン濃度のため，大型ファントムを均一に作成することが困難である．本研究は，低グリセリン濃度で高粘性なファントムを作成することを目的とした．薬品配合量の調整により生体肝と同程度の粘弾性を達成できることをレオメータによる評価で確認した．

Purpose:MRE is a noninvasive technique for quantitatively measuring tissue viscoelasticity. The measured viscoelasticity can be used as an imaging biomarker. A quantitative phantom is required to assess MRE systems. We had previously developed stable polyacrylamide gel phantoms that contain 70% glycerin (by weight) to achieve the necessary viscosity. However, it is difficult to develop large homogeneous phantoms from gels with high glycerin content. The purpose of this study was to develop a highly viscous phantom with a low glycerin content.Methods:We used varying amounts of acrylamide, glycerin, and cross-linking agents to adjust the mechanical properties of the phantom. Content estimation equations of the chemical agents were obtained through preliminary experiments. Based on these equations, we made two different gel phantom sheets designed to have storage modulus of 3 kPa and 4.5 kPa, each having a loss tangent greater than 0.2. The size of the cylindrical phantoms was ϕ 20 mm × 2 mm. The storage and loss modulus of each phantom were measured using a parallel disc rheometer (MCR302, Anton-Parr). For the measurements, the strain constant was 1% and vibration frequency was 16 Hz. Results:The measured value of the storage modulus for the two phantoms (3.04 kPa and 4.59 kPa) are in good agreement with those we designed. The measured value of the loss modulus for the two phantoms are 0.67 kPa and 0.99 kPa, where the loss tangents are 0.22 and 0.22, respectively. The glycerin content succeeded to be decreased from about 70 % to 40 %.Conclusion:In this study, we successfully developed highly viscous MRE phantoms with a low glycerin content. These phantoms are more representative of human liver tissue than previous phantoms having a high glycerin content.

O-1-083　大腰筋MREにおいて効率的に大腰筋にせん断波を加える方法
Propagate shear waves to the PM efficiently in MR Elastography

大西　孝明（首都大学東京大学院 人間健康科学研究科 放射線科学域）
Takaaki Onishi[1], Tomokazu Numano[1,2], Daiki Ito[1], Kazuyuki Mizuhara[3], Kouichi Takamoto[4], Hisao Nishijyo[4], Naotaka Nitta[2]

[1]Department of Radiological Science, Graduate School of Human Health Science, Tokyo Metropolitan University, [2]National Institute of Advanced Industri al Science and Technology, Health Research Institute, [3]TOKYO DENKI UNIVERSITY, [4]University of Toyama

【要旨】本研究ではGradient-echo type Multi-echo MREシーケンスによって,大腰筋の弾性率(硬さ)を測定した．腰痛の原因として,大腰筋の緊張状態による影響が示唆されているが,大腰筋の硬さを測定した報告は決して多くない．今回は,深層に位置し,振動が伝播しにくいと考えられる大腰筋に,効率的に振動を加える方法について検討した．

Purpose
Low back pain (LBP) is a very common health problem. Stiffness of psoas major muscle (PM) is considered one of the potential source of LBP. However, there is little research on stiffness of the PM because inner muscle cannot be measured by muscle hardness tester. From this back ground, we have measured stiffness of the PM using MR Elastography (MRE) technique. In MRE, shear waves must be propagated in the tissue. Meanwhile, PM is inner muscle. Therefore, it is considered that to propagate shear waves to the PM is difficult. However, in MRE volunteer-study performed by us, PM were vibrated sufficiently. We speculated that the vibration transferred from lumbar spine (L-spine) to the PM. In this study we conduct verification experiments for our speculation, and investigate the method to propagate efficiently shear waves to the PM.
Method
All MRE experiments were performed on 3.0-T clinical imager by using a gradient-echo type multi-echo sequence. We obtained wave images and elastograms of the axial images of the PM with the volunteer in face-down position. A vibration pad was placed on center of low back in order to vibrate L-spine. The vibration sensitivity of our MRE sequence depends on a readout gradient. We acquired both A-P and L-R readout direction.
Result
Both of the PM, the oscillation intensity of A-P readout direction was higher than L-R readout direction. In addition, shear waves looked like propagating symmetrically to the PM from the L-spine in wave image of A-P readout direction. From the above, it is considered that L-spine was vibrated A-P direction by external vibration, as it turned out, the PM was vibrated A-P direction along with L-spine. Therefore, shear waves were propagated efficiently to the PM by using shear waves generated by vibrated L-spine.

O-1-084　棘上筋MR Elastographyにおける撮像位置の最適化
Optimization of imaging planes for MR elastography of the supraspinatus muscle

伊東　大輝（首都大学東京大学院 人間健康科学研究科 放射線科学域）
Daiki Ito[1,2], Tomokazu Numano[1,2], Takaaki Onishi[1], Kazuyuki Mizuhara[3], Koichi Takamoto[4], Hisao Nishijyo[4], Masaki Misawa[2]

[1]Department of Radiological Science, Graduate School of Human Health Science, Tokyo Metropolitan University, [2]Health Research Institute, National Institute of Advanced Industrial Science and Technology, [3]TOKYO DENKI UNIVERSITY, [4]University of Toyama

【要旨】MREは振動を加えながら撮像するため,撮像位置が変わると可視化できる伝播波の形状が変化する．撮像対象は棘上筋で,棘上筋の上部・下部の２種類の位置でMREを行った．上部を選択した場合は明瞭,下部を選択した場合には不明瞭な伝播波となった．棘上筋のMREにおける撮像位置は,棘上筋の上部に設定すべきことが示唆された．

[Objective] The supraspinatus (SSP) muscle is one of the rotator cuff muscles, which help stabilizing the humeral head. Tissue palpation is a standard diagnostic tool to detect abnormal stiffness changes in soft tissues. However, it is difficult to palpate the SSP muscle because the trapezius muscle covers the SSP muscle. MR elastography (MRE) enables to quantitatively measure stiffness of both superficial and deep tissues. In MRE, changes of the imaging planes induce changes of the patterns of wave propagation (wave image). We investigated optimal imaging planes for MRE of the SSP muscle.
[Material & Method] All MRI and MRE experiments were performed on a 3.0-T clinical imager while using a shoulder coil. MRE acquisitions were performed with a gradient-echo type multi-echo MR sequence at 100Hz phenumatic vibrations and axial images of the SSP muscle were obtained. A custom-designed vibration pad was used as a pneumatic transducer in order to adapt to individual shoulder shapes. Motion sensitized direction was perpendicular to the long axis of the SSP muscle. We conducted MRE at two different imaging planes (superior and inferior position of the SSP muscle).
[Results] When the imaging planes were set at the superior position of the SSP muscle, the wave images represented clear wave propagation. When the imaging planes were set at the inferior position of the SSP muscle, the wave images represented unclear wave propagation.
[Conclusion] The SSP muscle is located in the supraspinous fossa. Therefore, the inferior position of the SSP muscle could be affected by the reflection from the boundaries of the supraspinous fossa compared with that of the superior position. Our results indicated that the imaging plane should be selected the superior position of the SSP muscle in MRE.

O-1-085　MR elastographyと 脂肪/水 画像の同時収集
Simultaneous MR elastography and Fat/Water Imaging acquisitions

沼野　智一（首都大学東京大学院 人間健康科学研究科 放射線科学域）
Tomokazu Numano[1,2], Daiki Ito[1,2], Takaaki Onishi[1], Kazuyuki Mizuhara[3], Koichi Takamoto[4], Hisao Nishijyo[4], Masaki Misawa[2], Naotaka Nitta[2]

[1]Department of Radiological Science, Graduate School of Human Health Sciences, Tokyo Metropolitan University, [2]National Institute of Advanced Industrial Science and Technology, [3]TOKYO DENKI UNIVERSITY, [4]University of Toyama

【要旨】GRE型multiecho法を利用したMREシーケンスに[脂肪/水]画像法(Dixon法)を組み合わせた新しいMREパルスシーケンスを開発した. MRIにおいて,脂肪からの高信号や特有のアーチファクトは診断の妨げになる場合があり,脂肪抑制法の併用が必須となる場合がある. よって,MREにも何らかの脂肪抑制法が必要になると想定される.

[Objective] In this work, we developed integration a simple MR elastography (MRE) technique with a fat/water separation method (two point Dixon) based on a conventional gradient-echo type multi-echo MR sequence (GRE-multiecho-MRE). Fat is often a source of problems in MR imaging. It tends to have high signal intensity at all contrasts, and that can mask pathologies. It also causes two types of artifact due to its structure, known as a chemical shift artefact and a phase cancellation artifact. As these artifacts affect in a similar fashion on the MRE, a fat suppression technique is required in all MRE sequence. This present work can be obtained both of the elastogram and the fat/water image simultaneously.
[Material and Method] All MRI and MRE experiments were performed on a 3.0-T clinical imager. The GRE-multiecho-MRE that does not need a built-in motion encoding gradient (MEG). Readout gradient lobes of the GRE-multiecho-MRE have a similar function to MEG effect. In a built-in MEG MRE sequence, the vibration phase offset is controlled by MEG directions, polarities, and offsets at each imaging. In the GRE-multiecho MRE, the vibration phase offset is controlled by a self-made pneumatic waveform generator. The 1st echo time (TE) parameter of the GRE-multiecho MRE was two types, in-phase TE and opposed-phase TE. Two types 1st TE images are then added together to get water image and subtracted to get fat image.
[Result and Conclusion] This present work can deliver up to fat/water images and elastogram in a series of MRE acquisition. Because the GRE-multiecho MRE is MEG-less MRE sequence, the 1st TE is able to select shortest in- / opposed-phase TE. Therefore, the GRE-multiecho MRE have the opportunity to increase signal-to-noise ratio of fat/water images.

O-1-086　子宮筋腫に対するMRエラストグラフィ
Magnetic resonance elastography for uterine fibroids

大宮　慶惠（山梨大学 医学部 放射線科）
Yoshie Omiya[1], Shintaro Ichikawa[1], Utaroh Motosugi[1], Tetsuya Wakayama[2], Takashi Kakegawa[1], Hiroshi Kumagai[1], Hiroshi Onishi[1]

[1]Department of Radiology, University of Yamanashi, [2]GE Healthcare Japan

【要旨】MRエラストグラフィ（MRE）で子宮筋腫の弾性率測定を行った．2種類の撮像シーケンス（spin-echo echo-planar imaging (SE-EPI)法，gradient-echo (GRE)法）を用いた．対象は22症例23筋腫で、2人の放射線科医が測定し、一致率を求めた.どの撮像法でも一致率は良好であり，SE-EPI法はGRE法よりも弾性率が高めに算出された.

Purpose: To evaluate the feasibility of MR elastography (MRE) for uterine fibroids and the effect of imaging sequences (i.e., spin-echo echo-planar imaging [SE-EPI] and gradient-echo [GRE]) on stiffness measurements. Materials and Methods: Twenty-two patients with 23 fibroids were enrolled. The mean size of the fibroids was 90.1 ± 23.1 mm. Location of the fibroids was intramural (n = 19), submucosal (n = 3), or subserosal (n = 1). All patients underwent MRE examinations via two methods (SE-EPI and GRE) using a pneumatic vibrator which was placed on the lower abdominal wall and fixed with an elastic band. All MRE were performed in two cross-sectional planes (i.e., axial and sagittal). A two-dimensional postprocessing method was used for GE-MRE, while a three-dimensional postprocessing method was used for SE-EPI-MRE. Two radiologists measured the stiffness of fibroids. We manually placed as large a region of interest as possible to exclude crosshatching of areas inadequate for measurement on the stiffness map. Central slices were selected for SE-EPI-MRE. We used the intraclass correlation coefficient (ICC) to analyze inter-observer agreement in measurements.Result: The mean stiffness values of the fibroids were as follows: GREaxial, 4.43 ± 1.48 kPa; GREsagittal, 4.32 ± 1.78 kPa; SE-EPIaxial, 5.44 ± 2.10 kPa; and SE-EPIsagittal, 5.58 ± 2.33 kPa. The ICC between the 2 observers was excellent for all methods (ρ = 0.903-0.981).Conclusion: SE-EPI-MRE showed lower fibroid stiffness values than GRE-MRE. Each MRE method is a valid and reliable technique for measuring the stiffness of uterine fibroids.

O-1-087　アルコール性肝障害の線維化ステージングにおけるMRエラストグラフィの有用性
Vlidity and Reliability of Magnetic Resonance Elastography for Staging Hepatic Fibrosis in Patients with Alcoholic Hepatitis

佐々木　優（山梨大学 医学部 放射線科）
Yu Sasaki[1], Shintaro Ichikawa[1], Utaroh Motosugi[1], Tetsuya Wakayama[2], Takashi Kakegawa[1], Hiroshi Kumagai[1], Hiroshi Onishi[1]

[1]Department of Radiology, Universtiy of Yamanashi, [2]GE Healthcare Japan

【要旨】アルコール性肝障害患者52名に対してMRエラストグラフィ（MRE）で肝弾性率を測定した。線維化スコアの診断能を血液学的線維化マーカーと比較し、測定の再現性を検討した。1.5T MRIを使用し撮像シークエンスは2D-GRE法を用いた。MREは血液学的線維化マーカーと比較して有意に優れた診断能を有し、再現性も非常に良好だった。

Purpose: We evaluated the validity and reliability of magnetic resonance elastography (MRE) for staging hepatic fibrosis in patients with alcoholic hepatitis.
Methods: The study included 52 patients with alcoholic hepatitis　confirmed stages of pathological fibrosis (fibrosis stage 1 [F1], n = 11; F2, n = 8; F3, n = 7; and F4, n = 26　). All patients underwent MRE using a 1.5- or 3-tesla MR system and pneumatic driver system . Two radiologists measured liver stiffness in a circular region of interest placed on elastograms. We compared the area under the receiver operating characteristic (ROC) curve (AZ) for distinguishing stages of fibrosis compared with MRE and serum fibrosis markers. We used interclass correlation coefficients (ICC) to analyze interobserver agreement for measurements of liver stiffness.
Results: The mean stiffness values　of the liver increased with stage of fibrosis: F1, 3.01 ±　0.74 kPa; F2-3, 4.15 ±　0.98 kPa; and F4, 7.73 ±　2.69 kPa. ROC analyses revealed the significantly superior discrimination abilities of MRE for staging hepatic fibrosis (Az =　0.931 and 0.955) to those of serum fibrosis markers (0.594 to 0.803) ($P < 0.0047$) except for F1 vs F2-4 on APRI. The inter-reader ICC v alues between the 2 observers was excellent (ρ=0.966 (0.941-0.981)).
Conclusion: MRE is a valid and reliable technique for discriminating the stage of hepatic fibrosis in patients with alcoholic hepatitis.

O-1-088　第1法　MRIにおける市販電磁波遮蔽材を用いたRF遮蔽効果の検討
Part.1 Examination of the effect of RF shielding, using an electromagnetic wave shield material offered commercially in MRI

谷口　正成（一般財団法人 住友病院 放射線技術科）
Masanari Taniguchi[1,2], Toshihiko Nishida[1], Hidekazu Niikawa[1], Daichi Shimokawa[1], Tatsuya Kuwagaki[1], Kota Uematsu[1], Akira Tamada[1,2], Hideki Matsui[2]

[1]General Foundation Corporation Sumitomo Hospital Department of Radiological Technology, [2]MEDICAL-AID CO., LTD

【要旨】市販の電磁波遮蔽材であるカーボン繊維製と銀繊維製についてRF遮蔽効果を検討した。各繊維をファントムに巻きつけ、冠状断と矢状断像を得た。ImageJで感度分布とSNR解析を実施した。カーボン繊維に比べて銀繊維のRF遮蔽効果は非常に高く、取扱いも簡便であった。MRI検査の安全管理に最適な素材である。

Purpose:In recent years, various kinds of electromagnetic shielding products including carbon fiber are offered in market. We examined the effect of RF shielding intended to select the material for nearly complete RF shielding. Material:MRI;GE Co.SignaHDxt1.5T,SIEMENS Co.MagnetomSkyra3.0T Coil;GE Co.HD Body Array Coil,SIEMENS Co.Body18,Spine 32Phantom;GE Co.SNR Phantom SquareElectromagnetic wave shielding material;manufactured by Toray Industries,Inc.Torayca Cross(CO6343),MEDICAL-AID,Inc.EMC sheet(ES100) size:1m*1m/sheets Method:Each fiber was wound around Phantom.It was placed in the center of the top surface portion.Using a T1 weighted fast SE method,it was taken sagittal and coronal phantom center.It was taken at each MRI unit under the same conditions.It was measured SNR and sensitivity distribution using by image analysis software. Results:Compared to carbon fiber,silver fiber showed uniformly decrease in sensitivity distribution and SNR. Also,resonant frequency showed the same result in the comparison between 1.5T and 3.0T device that resonant frequency is different.Conclusions:We have to use sealed carbon fiber in plastic bags because of prevention of scatter of carbon fiber.Carbon fiber has a negative impact on the human body through direct contact,such as itch and rash.Therefore,care should be taken when handling carbon fiber.In contrast,silver fiber has a strong affinity for the human body,and offers great flexibility.　Also,there is no risk of scattering.Therefore,it is safe and easy for us to handle silver fiber.Silver fiber is suitable for use in an electromagnetic wave shield material in MRI.For the reasons set forth below.High heat dissipation because of its honeycomb structure,and diamagnet.

O-1-089　第２報　頭部領域におけるカプセル内視鏡用電磁波防護服の応用
Part.2 Application experiment of electromagnetic wave protective clothing for capsule endoscopy in MRI head area scans

谷口　正成（一般財団法人 住友病院 放射線技術科）
Masanari Taniguchi[1,2], Toshihiko Nishida[1], Hidekazu Niikawa[1], Daichi Shimokawa[1], Tatsuya Kuwagaki[1], Kota Uematsu[1], Akira Tamada[2], Hideki Matsui[2]

[1]General Foundation Corporation Sumitomo Hospital Department of Radiological Technology, [2]MEDICAL-AID CO., LTD

【要旨】カプセル内視鏡用電磁波防護服は、高周波遮蔽効果が36dBに達する。防護服と頭頸部ファントムを用いて、頭部以外の高周波遮蔽効果を検討した。ImageJで感度分布とSNRについて分析し、加えて、電磁波減衰効果判定テストを依頼した。防護服を２重に着用した場合、RFを59dB遮蔽する結果となった。

Purpose:We examined high-frequency shielding effect on body parts other than the head in both the case of wearing one electromagnetic wave protective clothing for capsule endoscopy and the case of wearing two protective clothing.Material:MRI;GE Co.SignaHDxt1.5T,SIEMENS Co.MagnetomSkyra3T Coil;GE Co.HD HeadNeckSpineArray,SIEMENS Co.HEAD/NECK20 Phantom;GE Co.8chNVA Phantom,SNR Phantom Square Electromagnetic wave shielding material;MEDICAL-AID Inc.capsule endoscope electromagnetic wave protective clothing.Method:We covered the phantom with protective clothing and put it on the head and neck coil.Sagittal and Coronal in the center of the phantom was imaged,using a T1 Weighted Fast SE method.The same examination was performed under the same conditions with layering two protective clothing.SNR and sensitivity distribution was measured by using by image analysis software.We confirmed the correlation between the results of electromagnetic wave attenuation effect judgment test and the results of image analysis.Result:In case of wearing one protective clothing,high-frequency shielding effect in body parts except head and neck uniformly decreased in sensitivity distribution and SNR.In case of layering two protective clothing,we could not obtain images by rapid RF shielding effect.The results of image analysis agreed with the results of electromagnetic wave attenuation effect judgment test.RF showed the same result in the comparison between 1.5T and 3T device.Conclusion:Patients who embedded heart devices have various concerns physically and mentally,therefore electromagnetic wave protective clothing for capsule endoscopy is helpful for them to relieve concerns.We believe that continuous improvements will make it possible to protect pace maker and ICD from the electromagnetic wave.

O-1-090　1.5T MRI装置における条件付きMRI対応人工内耳の安全性
The Safety of MR Conditional Cochlear Implant at the 1.5 Tesla Magnetic Resonance Imaging System

高橋　大輔（北福島医療センター 放射線技術科）
Daisuke Takahashi[1], Akio Ogura[2], Norio Hayashi[2], Shinya Seino[3], Ryosuke Kawai[4], Tsuyoshi Matsuda[5], Tsukasa Doi[6], Toshio Tsuchihashi[7]

[1]Northern Fukushima Medical Center, [2]Gunma Prefectural College of Health Sciences, [3]Fukushima Medical University Hospital, [4]Med-EL Japan, [5]GE Healthcare Japan, [6]Osaka University Hospital, [7]Nippon Medical School Hospital

【要旨】条件付きMRI対応人工内耳装着者の検査において，吸引力とトルクはISOやEN規格に比べて十分小さいため身体的影響は小さいと言えるが，人工内耳内のインプラント磁石の減磁量は静磁場とインプラント磁石の磁力の方向に依存して大きくなるため，検査時は患者の頭部の角度や位置に最も注意を払わなければならないと考える．

For magnetic resonance imaging (MRI) examination of patients with a cochlea implant, little safety information is provided in the manufacturer's manual. Because of that lack of detailed information, MRI examinations might affect the quality of life of patients. Therefore, operators require more precise and detailed safety information.
We performed the following detailed examinations for a cochlear implant at the 1.5 tesla MRI system based on American Society for Testing and Materials (ASTM) standard.
1. Displacement force
2. Torque
3. Demagnetization
Results show that the displacement force and torque were less than the numerical values presented in the manual. Therefore, these have almost no effect on the body. Furthermore, demagnetization of the implant magnet occur because of changes in the magnetic field depending on the direction of the magnetic lines of the static magnetic field and the implant magnet.
Operators must be careful about the patient head position during induction in the magnet chamber.

Subject	Deflection angle	Displacement force	Torque
PULSAR	37.3°	0.206±0.001 N	4.66±0.01 N
CONCERTO	45.8°	0.261±0.003 N	4.30±0.03 N

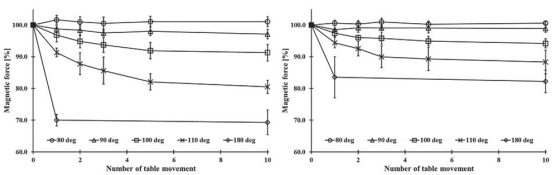

PULSAR　CONCERTO

O-1-091　Ti合金材料の静磁場中でのトルク異常性：磁化率異方性効果
Torque abnormality of the Ti alloy material in a static magnetic field: magnetic susceptibility anisotropy effect

川平　慎悟（北海道大学大学院 保健科学院）
Shingo Kawahira[1], Minghui Tang[1], Takahiko Kaneda[1], Toru Yamamoto[2]
[1]Graduate School of Health Sciences, Hokkaido Univ., [2]Faculty of Health Sciences, Hokkaido Univ.

【要旨】磁場中で同一形状試料にはたらく理論的トルクは材料磁化率に比例するが、Co-Cr-Ni合金の1/10以下の磁化率であるTi合金棒状試料には同程度のトルクがはたらき、その値は理論値の約150倍であった。インプラント素材として多用されているTi合金のこのトルク異常性は磁化率異方性を考慮することで解釈できた。

[Purpose] The Co-Cr-Ni alloy (Elgiloy) has long been used for MR-safe implantable medical devices, the Ti alloy has also been introduced for those devices to reduce MR artifact because of its low magnetic susceptibility: approx. 1/10 of that of Elgiloy. The torque that works on metallic materials in a static magnetic field theoretically increases with an increase in magnetic susceptibility of the material. However, comparable values of the torque of cerebral aneurysm clips made of Ti alloy and Elgiloy have been reported. To clarify this controversial evidence we accurately measured the torque that works on the Ti alloy and Elgiloy rods with the same shape and size. [Materials and Methods]The torque of Elgiloy and Ti alloy (Ti-4Al-6V) rods (diameter of 3 mm, length of 20 mm) was measured by a torque measurement device (PT7000, PROTECH) which was placed in the center of a 3T MRI scanner (MAGNETOM Prisma, Siemens). The value of torque was accurately obtained by analyzing the influence of the rotating friction of the device.[Results and Discussion] The maximum torque of the Elgiloy rod was 0.7 μNm which almost agreed with the theoretical value. On the other hand, that of the Ti alloy rod was 1.2 μNm which was about 150 times larger than the theoretical value. The conventional theory of the torque is based on shape magnetic anisotropy. We theoretically introduced the influence of susceptibility anisotropy on the torque, and the larger torque of Ti alloy was explained by 1% difference of the directional susceptibility between long and short axis of a rod. [Conclusion] The Ti alloy rod showed extraordinary larger torque than that predicted by the conventional torque theory. This abnormality can be explained by introducing susceptibility anisotropy effect to the theory.

O-1-092　RF熱傷事故例の電磁界シミュレーション解析
Analysis of RF burning by electromagnetic simulation

菊地　　侑（北海道大学 大学院 保健科学院）
Yu Kikuchi[1], Takuya Haruyama[2], Minghui Tang[1], Toru Yamamoto[3]
[1]Graduate School of Health Sciences, Hokkaido Univ., [2]Department of Health Sciences, School of Medicine, Hokkaido Univ., [3]Faculty of Health Sciences, Hokkaido Univ.

【要旨】右親指と大腿部の近接部位に発生したRF熱傷事故例を電磁界シミュレーション上でモデル化し、熱傷に至るSARを確認した。また、この姿勢を保ち、スキャナー内での患者位置を体軸方向に移動させることで、近接部位のSARが大きく変化した。さらに、近接部位にわずかに間隙を設けることで、その部位のSARが増加した。

[Purpose] RF heating causes most of injuries during MRI examinations. To prove high SARs in the actual RF burn injuries by simulation, we modeled a RF burn injury case in the in silico phantom and simulated the peak SAR at the injured location. Changes in this peak SAR value were also investigated by changing the patient position in an MR scanner.[Methods] Simulation software (Sim4Life) was used to map SAR. An RF burn injury case that occurred at the contact point of the right thumb on the right thigh was modeled in the in silico phantom (Duke). We modeled two types of the contact point: tight contact and close contact spaced by 2 mm. Moreover, the phantom position in the MR scanner was changed; the contact point was set at the center of the MR scanner (1), 53 cm (2) and 85 cm (3) along z-direction from the center. The generic MRI birdcage model operating at 64 MHz was used as a transmission RF coil.[Results and Discussion] Both tight and close contact models showed the peak SAR at the contact position as well as the actual RF injury case. All peak SARs in the close contact model were higher than those in the tight contact model, indicating the effect of the resonant-like capacitance of the gap between the thumb and the thigh. The maximum value of the peak SAR was observed in (2) when the contact point position was almost at the edge of the transmission RF coil: 181 and 648 W/kg for the tight and close contact model, respectively. The peak SAR was lowered to less than half in (1) and to 1-2% in (3). In particular, the patient position like (3) is the position for the head imaging. [Conclusions] The high heat generation at an RF burning position was confirmed by simulation. This heat value depends on the patient position in an MR scanner.

O-1-093　日本における体内留置インプラントのMRI検査の適合性検索システムの開発
Web-based searchable magnetic resonance imaging safety information system for medical implant compatibility in Japan

藤原　康博（熊本大学 大学院 生命科学研究部）
Yasuhiro Fujiwara[1], Hitoshi Fujioka[2], Tomoko Watanabe[2], Maiko Sekiguchi[2], Ryuji Murakami[1]
[1]Department of Medical Imaging, Faculty of Life Sciences, Kumamoto University, [2]MEDIE Co., Ltd.

【要旨】体内インプラント留置患者に対するMRI検査の適合性の調査方法は限られており，時間も要する．我々は，国内に流通するインプラントを調査し，データベース化して適合性検索システムを作成した．本システムは，インターネットを通じて医療現場で簡便で適合性に特化した情報提供ができることから，有用性が示唆された．

Purpose: It is necessary to confirm the compatibility of medical devices implanted in patients before conducting MRI examinations. However, in Japan, there are very few confirmation methods, and these methods are time consuming. We hypothesize that offering MRI safety information related to medical implants will improve the safety of MRI examinations for patients and will reduce the time required for confirmation. The purpose of this study was to develop a web-based searchable MRI safety information system for confirming medical implant compatibility. Methods: First, MR safety information for intravascular stents and stent-grafts sold in Japan were investigated by interviewing 20 manufactures. These implants were categorized as MR Safe, MR Conditional, MR Unsafe, and having no safety information, based on the descriptions on their medical packaging inserts. An MR safety information database for the implants was created considering the previously proposed item lists. Finally, a web-based searchable system was developed using this database. A questionnaire was given to medical personnel in Japan to evaluate the usefulness of this system. Results and Discussion: Seventy-nine datasets were collected using information provided by 12 manufacturers and by investigating the medical packaging of the devices. The safety statuses of 62 devices were MR Conditional, which implies that there are restrictions on performing MRI examinations on patients with these devices. The medical packaging of the other devices did not mention their safety statuses. Although the datasets need to be updated by collecting data from other manufactures, this system makes it possible to obtain MRI safety information for medical implants more easily and quickly and to improve safety.

O-1-094　絶対値画像と単板ファントムを用いたPSFおよびMTF計測
PSF and MTF measurement with MR magnitude images using single thin-plate phantom method

吉田　　礼（栗原市立栗原中央病院）
Rei Yoshida[1,2], Takeo Hikichi[1], Yoshio Machida[2]
[1]Kurihara Central Hospital, [2]Tohoku University Graduate School of Medicine

【要旨】我々は先行研究として、単板ファントムを用い複素画像データを取得することで正確なMTFが可能であることを示したが、今回は、すべての装置で取得可能である絶対値画像を用いてPSFとMTFを計測し、解像特性の評価が可能か検討した。その結果、PSFは評価が可能であったものの、MTFは評価には不適切であった。

[Purpose]Evaluation of resolution characteristics of MR images is extremely difficult. No correct measurement method has yet been established. For more precise measurement, we have proposed a newly developed "single thin-plate phantom method". Using this method, the point spread function (PSF) and modulation transfer function (MTF) can be evaluated more precisely when complex image data are available. However, complex image data were not necessarily obtained from all scanners.This study was conducted to investigate and revisit the PSF and MTF measurements using magnitude images that are obtainable in all scanners.[Methods]T1-weighted and T2-weighted magnitude images were obtained from turbo spin echo sequences. Then the PSFs and MTFs in phase-encoding directions of the images were compared with those of complex images.[Results and Conclusion]For the PSFs of T1-weighted images, the full width at half maximum (FWHM) of the main lobe was increased. The side lobes became smaller as the echo train length increased. The side lobe shape became larger in the PSFs of T2-weighted images. In contrast, measured MTFs calculated from magnitude images were incapable of representing the theoretically expected MTF such as a cutoff frequency or an echo-train-dependent shape.In conclusion, PSF measurement with magnitude images is useful to evaluate the resolution characteristics, although MTF measurement is inappropriate for evaluation.

O-1-095　トレンド補正を用いた同一関心領域法によるSignal to Noise Ratio測定の検討
Signal-to-noise ratio measurement using the identical region of interest method by trend correction

石川　和希（独立行政法人 国立病院機構 四国こどもとおとなの医療センター 放射線科）
Kazuki Ishikawa

Department of Radiology, National Hospital Organization Shikoku Medical Center for Children and Adults

【要旨】同一関心領域法によるSNR測定では信号ムラに起因しノイズを過大評価する。そこで信号ムラをトレンド成分として多項近似によって抽出し除去する。これによりノイズの過大評価を防ぎ、正確なSNR測定が可能か差分法との比較によって検討した。トレンド補正によって差分法と同等な精度でSNR測定が可能であった。

Purpose
In signal-to-noise ratio (SNR) measurement using the identical region of interest method, noise is overestimated due to signal distortion. Therefore, signal distortion is extracted as a trend by polynomial approximation and removed from the image. This study examines whether trend correction prevents overestimation of noise, thereby resulting in improved accuracy of SNR measurements.
Method
We used uniform phantom images taken on a MAGNETOM Aera 1.5 T (SIEMENS).Extraction of the trend elements was performed using Polynomial Fit, which is a plugin for ImageJ.The SNR of images was obtained by varying NEX from one to five and comparing it with the subtraction method and trend-corrected identical region of interest method. The SNR was also measured by changing the Polynomial Fit orders to 2 × 2, 4 × 4, 6 × 6, 8 × 8, and 10 × 10 and comparing the SNR with that obtained using the subtraction method.The Mann-Whitney U test was performed to compare the two methods so as to estimate the significant difference between the two.This was performed on sensitivity-corrected images as well as non-sensitivity-corrected images.
Results
The SNR of images obtained without applying sensitivity correction showed no significant difference between the subtraction method and trend-corrected identical region of interest method, whereas the SNR of images obtained with the application of sensitivity correction showed a significant difference of $p < 0.01$ when the polynomial approximation order was 2 × 2 however, there was no significant difference at other orders.
Conclusion
It was possible to measure the SNR with the trend-corrected identical region of interest method with the same accuracy as that using the subtraction method.

O-1-096　VSRAD advence2 を用いた頭部放射線治療後萎縮計測のための基礎的検討
Evaluation of Brain atrophy after radiotherapy using Voxel Based Morphometry (VSRAD advance2); Fundamental Assessment

伊藤　猛（長岡赤十字病院 放射線治療科）
Takeshi Ito[1], Tadatoshi Iihama[2], Naoki Kawamoto[2]

[1]Japanese Red Cross Society Nagaoka Hospital, Department of Radiotherapy, [2]Japanese Red Cross Society Nagaoka Hospital, Department of Radiology

【要旨】転移性脳腫瘍の放射線治療後脳萎縮を評価する目的でVBMを適応するための基礎的検討を行った。病期評価や経過観察のため撮影されている造影後T1強調画像をVSRADで解析するにあたり組織分離の妥当性や同一症例の計時変化を検討した。

In management of metastatic brain tumor, it is generally considered that standard therapy is whole brain irradiation . But it is sometimes observed cognitive decline or mental disturbance as adverse effect on irradiated patients. To estimate this problem several examination is administrated to patients , as an example MMSE(mini-mental state examination).Recently , hippocampus spared whole brain irradiation is applied to prevent cognitive disorder. We attempt to estimate the usefulness of this new radiation technique by using Voxel-Based Morphometry(VBM) for measuring medial temporal robe volume , as similarity to Alzheimer's disease. But it is not established method . The purpose of this presentation is to confirm the validity of VBM on using Image of post Gadlinium-enhanced T1-weighted images. VSRAD advance2 was used for VBM tools. In our hospital, Brain MRI protocol for cancer patients is as below :1.5T MRI scanner (Siemens Avant or GE SignaHDx), T1 and T2 weighted axial image as 6mm slice thickness on multiple spin-echo sequence, and Gd-enhanced Image was obtained by 3D-T1 spin echo sequence 0.9mm sagittal slice using variable flip-angle. The last image-set satisfied the requirements of VSRAD analysis. Tissue segmentation was almost accurate by default setting, But edema accompanied by radiation or tumor is visualized as low intensity area, this region segmented to CSF. Vessels and flow artifact were not severe problem. Further investigation is needed about tissue signal intensity change after Gd-enhancement.

O-1-097　Wall Motion Tracking(WMT)を用いた左室心筋ストレイン解析におけるTemporal filterの検討
Evaluation of Temporal Filter for LV Myocardial Strain Analysis in Wall Motion Tracking

佐野雄一郎（東芝メディカルシステムズ株式会社 MRI営業部）
Yuichiro Sano, Tatsuya Ohkubo, Yuichi Yamashita, Shuhei Takemoto, Seiya Kai
Toshiba Medical Systems Corporation MRI sales department

【要旨】シネMRIでストレイン解析が可能なソフトウェアを用い、ノイズ低減フィルターであるTemporal filterの有無により、ストレイン値に差が生じるか検討した。Temporalfilterの有無により、解析結果に有意差が認められ、シネMRIの視認性を改善するとともに、左室輪郭の自動トラッキング精度を向上させることが示唆された。

[Introduction & Purpose]
LV myocardial strain analysis has mainly been performed by speckle tracking in echocardiography and by tagging MRI, but cine MRI has recently been used to measure strain values without tagging. Previous studies have reported that myocardial strain values differ depending on the type of reconstruction filter used. The appropriate reconstruction filter must be selected. We have developed the "Temporal filter" to reduce noise in stationary areas with no deterioration of sharpness in moving areas in cine MRI.
We investigated the differences in the myocardial strain values obtained with and without the Temporal filter in Vitrea 7.1 MR WMT for myocardial strain analysis by cine MRI.
[Methods]Cine MR images of healthy adult volunteers were obtained using a 1.5-T MRI scanner (Vantage Titan, Toshiba Medical Systems). Informed consent was obtained. The SSFP imaging parameters were TR: 4.2 ms, TE: 2.1 ms, FA: 77, slice thickness: 8 mm, FOV: 380 × 380 mm, matrix size: 208 × 192, and phase: 20 phases/R-R. The strain values in cine MRI of the left ventricular short axis were analyzed automatically with and without the Temporal filter, and the results of both types of automatic analysis were then compared against the results of manual analysis by experts in cardiac function analysis.
[Results & Discussion]The difference between the results of automatic analysis and manual analysis by the experts was significantly reduced when the Temporal filter was used ($p<0.05$), indicating that the Temporal filter improved the accuracy of automatic tracking.
[Conclusion]A significant difference was observed in LV myocardial strain values with and without the Temporal filter, suggesting that the Temporal filter improves visualization in cine MRI and accuracy in automatic tracking.

O-1-098　MRCAにおける冠動脈芯線の自動追跡法を用いたワークフロー軽減の検討
Workflow Improvement Using the Automatic Tracking Method for MRCA

竹本　周平（東芝メディカルシステムズ株式会社 営業本部 MRI営業部）
Shuhei Takemoto[1], Tatsuya Ohkubo[1], Yuichi Yamashita[1], Seiya Kai[1], Yoichirou Sano[1], Yoshimori Kassai[2], Nobuyasu Ichinose[2], Shuhei Bannae[3], Takuma Igarashi[3]
[1]TOSHIBA Medical Systems Co., Ltd., [2]TOSHIBA Medical Systems Co., Ltd. MRI Development, [3]TOSHIBA Medical Systems Co., Ltd. Clinical Application Development

【要旨】3Tと1.5T MRI装置によるMRCAデータでは撮像条件は異なり画像コントラストに差が生じる。我々はどちらのシステムにも対応した冠動脈の芯線自動追跡法（MR Coronary Tracking）を開発した。MRCAデータの後処理に要した作業時間と作業数を提案法と手動法で計測し、ワークフローの軽減効果を検討し報告する。

Background: Time cost of post-processing on MR Coronary Artery (MRCA) Examination is huge. Also, it is difficult that one workstation runs the post-process compatibile with 3T and 1.5T-MRCA data because of the image contrast difference depending on sequence or pre-pulse. Purpose: We developed new post-processing application which is compatible with 3T and 1.5T-MRCA. We report a study of the improvement of the workflow of the centerline drawing analysis of the MRCA.Method: We used Vantage Galan 3T (M-Power V4.0) and Vantage Titan 1.5T (V3.6) to acquire Whole Heart MRCA which was obtained by aligning the spatial resolution in the same conditions for one healthy volunteer. MR Coronary Tracking in Vitrea workstation (W.I.P.) was performed post-processing for drawing the centerlines of 3 major coronary arteries with using automatic tracking(proposed method) and manual drawing. We defined the processing workflow is drawing the centerlines of 3 major coronary arteries, labeling each branch, and saving CPR and SPR rotated images. We measured and compared the users' operating time and the number of operations for both proposed method and manual drawing.Result: Compared with proposed method and manual drawing, user's operating time was improved by 50%, and the number of operations was improved by 70%.Conclusions: MR Coronary Tracking which has compatibility with 3T and 1.5T-MRCA improves the post-processing workflow by using automatic tracking(proposed method).

O-1-099　Feature Tracking Cine MRIによる心室の捻れ運動の評価
Evaluation of Ventricular Torsion by Feature Tracking Cine MRI

河窪　正照（帝京大学 福岡医療技術学部）
Masateru Kawakubo[1], Yuzo Yamasaki[2], Junji Morishita[3], Michinobu Nagao[4]
[1]Faculty of Fukuoka Medical Technology, Teikyo University, [2]Department of Clinical Radiology, Graduate School of Medical Sciences, Kyushu University, [3]Faculty of Medical Sciences, Kyushu University, [4]Department of Diagnostic Imaging & Nuclear Medicine, Tokyo Womens Medical University

【要旨】本研究は、feature tracking cine magnetic resonance imaging (FT-MRI) により左心室の捻れ運動を解析した。その結果、FT-MRIは心基部の時計回りの回転と、心尖部の反時計回りの回転を自動的に追跡し、左心室の捻れ運動を定量的に算出することができた。

Purpose
Left ventricular (LV) torsion plays an important role for cardiac pump, and means counterclockwise rotation of LV apex and clockwise rotation of LV base during systole. Feature tracking cine magnetic resonance imaging (FT-MRI) can analyze LV deformation throughout a cardiac cycle. The present study evaluated LV torsion using FT-MRI and investigated the ability in clinical application.
Methods
Data sets of basal and apical short-axis LV cine images in 33 subjects from York University were analyzed. First, coordinates of LV endocardium were manually defined at end-diastole, the following coordinates were automatically tracked throughout a cardiac cycle using FT-MRI. Clockwise rotation angle against to end-diastole was measured at each cardiac phase. The maximum basal rotation angle (R_{base}), the minimum apical rotation angle (R_{apex}) were calculated. Finally, the absolute difference (T_{rot}) between R_{base} and R_{apex} was defined as LV torsion.
Results
R_{base}, R_{apex} and T_{rot} were 1.80 ± 1.52, −2.62 ± 2.50, 4.42 ± 3.43, respectively. Figure 1 indicates time curves of R_{base}, R_{apex} and T_{rot}.
Conclusion
FT-MRI can quantify semi-automatically LV torsion and expected to apply for clinical use.

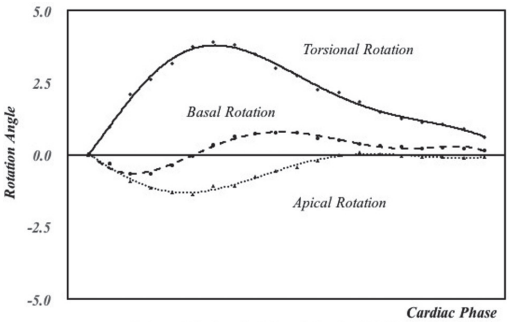

Figure 1. Left ventricular rotation by FT-MRI.

O-1-100　ボーラストラッキングにおける2次元MRA画像の自動位置決めの検討
Automated planning of 2D MRA in bolus tracking

後藤　隆男（GEヘルスケアジャパン株式会社）
Takao Goto, Mirai Araki
GE Healthcare Japan Coporation

【要旨】造影MRにおいて、ボーラス追跡のため大動脈を通るMRA画像を計画するのは難しい作業である。我々はこの画像を自動で設定するため、スカウト画像から画像の分類の後、機械学習による識別器により大動脈の位置を検出した。結果から自動化できることを示し、操作者のワークフロー改善に寄与できることを示した。

INTRODUCTION
In bolus tracking techniques monitoring the arrival of the bolus, the operator prescribes the 2D plane of MRA passing through the aorta in dynamic contrast-enhanced (DCE) scan. The prescription of the 2D plane is a complex process and its accuracy highly depends on the skill of the operator. Our goal is to position the 2D MRA plane automatically, thus resulting in the improvement of operator workflow.
METHODS
2D SSFSE scout images are analyzed for the detection of the aorta not to prolong the total study time. In our algorithm, axial images are classified into 4 classes by Laplacian eigenmaps. And then, the corresponding atlas is applied to the axial image to narrow down the searching area of the aorta. To detect the aorta, we used the Hough Forests classifier that utilizes the feature value in the neighboring patches of objects, and creates a map of votes from each feature patch. The Hough map is weighted by the atlas and the location of the maximum value in the map shows the aorta location. The oblique plane is positioned by the line passing through the center of the detected aortas using the regression method. The oblique plane was reformatted from 3D datasets of DCE liver images acquired in the aortic phase to simulate an oblique MRA plane. We tested 40 patients after informed consent was obtained under institutional review and approval.
DISCUSSION AND RESULTS
The error of the detected center position of the aorta was 6 mm average and 8 mm standard deviation. In the resulting reformatted oblique images, 35 of 40 datasets showed a sufficient delineation of the aorta. We demonstrated that our algorithm was able to plan the 2D scan plane for MRA. This automation will help the operator and decrease the total study time.

O-1-101　CAIPIRINHAを用いたdixon vibeの基礎的検討
A pilot study of dixon vibe with Controlled aliasing in parallel imaging results in higher acceleration (CAIPIRINHA)

香川　福宏（医療法人 高松画像診断クリニック）
Fukuhiro Kagawa[1], Tomoko Takaichi[1], Hiroaki Yasuda[1], Yoshihito Matsumoto[1,2], Kei Yokomine[3], Junpei Yamaguchi[3], Hiroki Ogura[3]
[1]Takamatsu Gazo Shindan Clinic, [2]Nishi Takamatsu Neurosurgical Clinic, [3]NHO Shikoku Medical Center for Children and Adults

【要旨】3.0TにおいてControl Aliasing in parallel imaging results in higher acceleration(CAIPIRINHA)併用dixon vibeが使用可能となった。ファントム実験でFAとTRをそれぞれ変化させSNR、CNRの測定を行った。また、最適と思われた条件下で健常ボランティアの撮像を行い、CNRの比較を行い最適条件の検討を行ったので報告する。

[Purpose] Since Controlled Aliasing in parallel imaging results in higher acceleration (CAIPIRINHA) combination dixon vibe imaging was enabled, a pilot study was conducted. This is a report on that study. [Method] SEIMENS Co. Magnetom Skyra 3.0T, Body Matrix Coil, Spine Coil, Nikko Fiennes phantom (90-401) was used, and basic imaging conditions were fixed. We changed the Flip Angle (FA) to 1-15 (degrees) using self-made phantom which were mocked as liver, muscle and fat, and compared Signal Noise Ratio (SNR), Signal Intensity (S.I.) and Contrast Noise Ratio (CNR). TR was changed to 4.0-20.0msec in the FA by which it seemed most suitable and was compared equally. Under the conditions that were considered optimum from the discussion above, CNR was compared by changing the FA to 7, 9 and 11 using three healthy volunteers that have consented to the experiment. In addition, a comparison was made with the vibe that was normally imaged.[Result] In Phantom, when FA was increased, the liver of both SNR and CNR were on an upward tendency to FA9, and was on a downward tendency thereafter. On the other hand, SNR muscle and fat were plateaued. When fixed with FA9 and TR was increased, the liver SNR was on a downward tendency, the muscle SNR was on an upward tendency and the fat plateaued. The CNR was at the maximum value at FA9 in volunteer imaging.[Conclusion] There is no fat suppression with dixon vibe so we can conclude that it is a useful sequence.

O-1-102　IVIM-DWIの計算法の比較：肝細胞癌の悪性度診断
Comparing the results of intravoxel incoherent motion diffusion-weighted imaging calculated by different estimation methods

市川新太郎（山梨大学 医学部 放射線科）
Shintaro Ichikawa[1], Utaroh Motosugi[1], Hernando Diego[2], Hiroyuki Morisaka[3], Hiroshi Onishi[1]
[1]Department of Radiology, University of Yamanashi, [2]Department of Radiology, University of Wisconsin, [3]Department of Diagnostic Radiology, Saitama International Medical Center, Saitama Medical University

【要旨】IVIMのfitting modelを3種類設定し、high grade肝細胞癌の診断能を比較した。また、2名の計測の一致率（級内相関係数）を求めた。
結果：非線形フィットを用いない方法は計測の一致率は高かったが、診断能は線形フィットを用いた手法よりも低かった。

Purpose: To compare the measurement repeatability of intravoxel incoherent motion (IVIM) imaging using 3 different approximation methods for discriminating the histological grade of hepatocellular carcinoma (HCC).
Materials and Methods: Fifty-eight patients (60 HCCs) underwent IVIM imaging with 11 b-values (0-1000 s/mm2). Slow (D) and fast diffusion coefficients (D*) and the perfusion fraction (f) were calculated for HCCs using regions of interest placed individually by two radiologists. The following approximation methods were used during calculation. First, all 3 parameters were obtained simultaneously, using non-linear fitting (method A). Second, D was first obtained using linear fitting (b = 500 and 1000), followed by non-linear fitting for D* and f (method B). Third, D was obtained by linear fitting, after which, f was obtained using the regression line intersection and signals (b = 0) and non-linear fitting was used for D* only (method C). A receiver operating characteristic analysis was performed to discriminate high-grade from low-to-moderate-grade HCCs. Inter-reader agreements were assessed using intraclass correlation coefficients (ICC).
Results: Methods B and C (Az value, 0.707-0.881) yielded better HCC grade discrimination ability, compared with method A (Az value, 0.537-0.583). The ICCs of D and f were good-to-excellent (0.639-0.835) with all methods. The ICCs of D* were moderate with method B (0.580) and C (0.463), and good with method A (0.705).
Conclusion: Compared with partial linear fitting, complete non-linear fitting, although reproducible, exhibited a worse discrimination ability.

O-1-103　腹部MRIにおけるComputed DWIの有用性
Computed Diffusion-Weighted Image for Abdominal MRI

吉川　武（神戸大学大学院 医学研究科 先端生体医用画像研究センター）
Takeshi Yoshikawa[1,2], Yoshiharu Ohno[1,2], Katsusuke Kyotani[3], Yoshimori Kassai[4], Koya Nishiyama[3], Yuji Kishida[2], Kazuro Sugimura[2]

[1]Advanced Biomedical Imaging Research Center, Kobe University Graduate School of Medicine, [2]Department of Radiology, Kobe University Graduate School of Medicine, [3]Center of Radiology and Radiation Oncology, Kobe University Hospital, [4]Toshiba Medical Systems Corporation

【要旨】Computed DWIは腹部において画質および悪性病変のコントラスト・検出能・質的診断能を向上する。

[PURPOSE] To assess capability of cDWI in abdominal MRI [METHODS AND MATERIALS] 102 patients (52 men & 50 women, mean: 67.3years), who were suspected to have hepato-biliary-pancreatic malignancy and underwent 3T-MRI, were retrospectively analyzed. DWIs were obtained with SE-EPI (b: 0 & 1000, DWI0 & DWI1000). cDWI images at b values of 200, 400, 600, 800, 1200, 1400, 1600, 1800, and 2000 were reconstructed (cDWI200-2000). 65 malignant lesions and 68 benign lesions were confirmed. Signal-to-noise ratio of each organ ($SNR=SI_{organ}/SD_{organ}$) and lesion contrasts ($C_M=SI_{lesion}-SI_{organ}/SI_{lesion}+SI_{organ}$) were compared among the images. Two readers assessed recorded b values with best quality and with complete gallbladder signal suppression, and assessed lesion conspicuity on DWI1000 and cDWIs. Malignant lesion detection and accuracy of lesion characterization were assessed on DWI0+1000 and +cDWIs sets and compared. ROC analysis was used for detections and accuracies. [RESULTS] SNRs were significantly highest on cDWI800 in the liver and on cDWI600 in the pancreas and spleen ($P<0.0001$). Malignant lesions contrasts were significantly increased (0.026) and benign ones were significantly decreased (<0.0001) in proportion to increase of b value. Image quality was best on cDWI800 followed by DWI1000 (b: 835 ± 176). GB signal was completely suppressed on cDWI1200 or higher (b: 1777 ± 266). Conspicuity of malignant lesion was significantly highest (0.005) and that of benign lesion was significantly lowest (<0.0001) on cDWI2000. Malignant lesion detection was significantly higher (Az: 0.728 vs 0.798, 0.033) and accuracy of lesion characterization was significantly higher (Az: 0.662 & 0.904, <0.0001) on +cDWIs set. [CONCLUSION] Computed DWI is a useful post-processing tool for abdominal MRI.

O-1-104　腹部FASE-DWI
Abdominal Fast Advanced Spin Echo Diffusion-Weighted Imaging

吉川　武（神戸大学大学院 医学研究科 先端生体医用画像研究センター）
Takeshi Yoshikawa[1,2], Katsusuke Kyotani[3], Yoshiharu Ohno[1,2], Yoshimori Kassai[4], Koya Nishiyama[3], Shinichiro Seki[1,2], Yuji Kishida[2], Kazuro Sugimura[2]

[1]Advanced Biomedical Imaging Research Center, Kobe University Graduate School of Medicine, [2]Department of Radiology, Kobe University Graduate School of Medicine, [3]Center of Radiology and Radiation Oncology, Kobe University Hospital, [4]Toshiba Medical Systems Co.

【要旨】FASE-DWIは腹部において病変検出能およびADCによる評価に影響することなく画像の歪みを抑制し画質を向上する。

[PURPOSE] To assess FASE-DWI in evaluation of abdominal diseases [METHODS AND MATERIALS] 70 patients (44 men and 26 women, mean: 68.4 years), who were suspected to have hepato-biliary-pancreatic malignancy and underwent 3T-MRI, were enrolled. FSE-T2WI, SE-EPI-DWI (b=0,1000), and FASE-DWI (0,600) were obtained. Amount of abdominal gas and ascites on images were recorded. AP and RL abdominal diameters were measured on the slice with most severe image distortion, and correlation analyses were performed among the sequences. Overall image quality and severity of distortion were visually assessed on EPI and FASE, and compared. Regression analyses were done to estimate factors for low image quality and severe distortion. Malignant lesion detection and lesion conspicuity was separately assessed on EPI and FASE and compared. ROC analysis was used for lesion detection. ADCs in malignant lesions and background organs were measured on FASE and compared. [RESULTS] Correlation coefficient was the highest between T2WI and FASE for both the diameters. Coefficient was lowest in AP direction on EPI. There was no significant difference between overall image qualities. Image distortion was significantly more severe on EPI. Sex and gas were found to be significant factors for image quality and distortion on EPI, and sex was a significant factor for image quality on FASE. There was no significant difference in malignant lesion detection (Az-EPI: 0.859, Az-FASE: 0.845, $p=0.298$) and conspicuity (Az-EPI: 4.24, Az-FASE: 4.20, 0.689). Mean ADC in lesions was significantly lower than that in backgrounds(1.63 vs 2.17×10^{-6}, <0.0001). [CONCLUSION] Abdominal FASE-DWI can improve image quality and decrease image distortion without hampering lesion detection and ADC measurement.

O-1-105　位相情報を用いた肝線維症の非侵襲的評価
Noninvasive assessment of liver fibrosis by using phase information

三尾　素平（福岡大学筑紫病院 放射線部）
Motohira Mio[1], Tetsuya Yoneda[2], Kazuki Tani[1], Tatsuo Toyofuku[1], Toshihiro Maeda[1], Masatoshi Matsushima[1], Syoichi Morimoto[3]
[1]Fukuoka University Chikushi Hospital, [2]Kumamoto University, [3]Fukuoka University Hospital

【要旨】肝癌発症リスクと関連する肝線維症の診断は重要である．そこで本研究では，PADREから得られる位相画像より肝臓の位相値を測定し，線維化マーカーとの相関関係を検討した．その結果，PLTとAPRIおよびFIB-4 indexと相関を示した．よって，位相値を用いて肝線維症の程度を評価できる可能性がある．

Accurate assessment of liver fibrosis is important for its prognosis, since the risk of hepatocarcinogenesis becomes higher as liver fibrosis progressed. Recently, several MRI methods to assess liver fibrosis were developed and already worked on clinical MRI. Among them, SWI technique was improved to depict a signal changing due to fibrosis. This meant that phase information might directly detect the fibrosis and assess it quantitatively. The purpose of this study was to come out a correlation between phase signal and serum biomarkers of liver in order to further clinical application to noninvasive assess liver fibrosis by MRI.
Subjects of this study were 50 patients with liver MRI (28males, 22females; 66.75 ± 12.29, 35-82years). All studies were performed on a 3.0T-MR system (Ingenia, Philips Healthcare). T2*-weighted images were acquired to obtain phase images. The imaging parameters were as follows: TR, 150ms; TE, 10ms; FOV, 350 × 300mm; matrix, 300 × 300; slice thickness, 8mm; FA, 20° . We used PADRE to obtain phase image and measured average phase value in ROI located on the right hepatic lobe. The serum biomarkers of fibrosis and cirrhosis (PLT, AAR, APRI, FIB-4index) vs. phase value were plotted and correlation were statistically examined.
The phase values of liver obtained in this study showed significant correlations with PLT, APRI and FIB-4index (r=0.70, r=-0.69, r=-0.75, P<0.001). There was no significant correlations between the phase values and AAR (r=-0.02, P=0.81). Furthermore, the phase values of the liver decreased as liver fibrosis progressing.
The phase values of liver were significantly correlated to PLT, APRI, FIB-4index used as the fibrosis marker. Therefore, MRI-phase information may be used for noninvasive assessment of liver fibrosis and its progression.

O-1-106　Crohn病のMR EnterographyにおけるDISCO法を用いた自由呼吸下Gd造影撮像の検討
Initial experience of MR Enterography using DISCO technique

鈴木　達也（慶應義塾大学 医学部 放射線診断科）
Tatsuya Suzuki[1], Shigeo Okuda[1], Shunsuke Matsumoto[1], Hirokazu Fujiwara[1], Akihiro Tanimoto[1], Masahiro Jinzaki[1], Yoshinobu Nunokawa[2], Sari Motomatsu[2], Rikiya Fujishiro[2], Yasutomi Shimada[2], Atsushi Nozaki[3]
[1]Department of Diagnostic Radiology, Keio University School of Medicine, [2]Department of Central Radiology, Keio University Hospital, [3]GE Healthcare Japan

【要旨】6例のMRエンテログラフィーにおいて、高速3DFsT1強調画像である DISCO dynamic法を用いて自由呼吸下でGd造影撮像を行い、有用性について検討した（撮像装置：Pioneer 3T, GE Healthcare)。過去の呼吸停止LAVA-Flex法で撮像した画像を対照とし、画質を5ポイントで比較した。DISCO法では臨床評価として十分な画質が得られた。

[Background] MR Enterography (MRE) has been used for evaluating Crohn's disease. Gd-dynamic study using 3D-FsT1WI is a key technique for evaluating the activity of inflammatory process in the alimentary tract. Differential Subsampling with Cartesian Ordering (DISCO) is recently available with the advantage of high spatio-temporal resolution. **[Purpose]** To evaluate the diagnostic value of DISCO technique for MRE. **[Material and Methods]** A total of six patients was enrolled. The images were acquired in 3T clinical scanner (Pioneer, GE Healthcare) with 32-channel coil. Patients were instructed to take polyethylene glycol solution (1-1.5 L) two hours before starting examination. Image protocol included SSFSE, FsFIESTA and Gd-dynamic study for the entire abdomen. In the current study, the dynamic study was replaced from LAVA-Flex to DISCO with following parameters: TR/TE = 4/1.7 msec, flip angle = 12, slice thickness/gap = 3 mm/ -1.5 mm, matrices 260x200, reconstructed diameter = 42x34 cm, NEX = 0.7, temporal resolution = 4.5 sec/phase. Image acquisition was continuously repeated 20 times, the total imaging time was 90 sec under mildly-free breathing. The DISCO images were independently scored in 5-point scale (blurring, contrast, noise, total image quality; 5=excellent) by two experienced radiologist. The images of LAVA-Flex dynamic study for MRE using the previous protocol were retrieved from PACS and they were scored as same as the DISCO method. Images of different patients were utilized as reference in two cases. **[Results and Discussions]** The average scores were 3.42, 3.92, 4.08, 4.08 by LAVA-Flex and 3.58, 4.00, 4.08, 3.83 by DISCO. The image quality of DISCO MRE was acceptable even under free-breathing. **[Conclusion]** DISCO is feasible for dynamic study in MRE.

O-1-107　ガドリニウム造影剤により皮膚は造影されるのか？
Can dermal tissue be enhancing with Gadolinium-chelate contrast material?

山本　憲（京都大学大学院 医学研究科 放射線医学講座（画像診断学・核医学））
Akira Yamamoto, Yasutaka Fushimi, Tsutomu Okada, Tomohisa Okada, Kaori Togashi
Department of Diagnostic Imaging and Nuclear Medicine, Graduate School of Medicine, Kyoto University

【要旨】ガドリニウム造影剤注入前後の頭部3D-T1強調画像のサブトラクション画像を作成し、病変の造影効果について詳細な評価を行おうとしたところ、常に皮膚に一層の信号上昇が造影後に認められている。皮膚組織に認めるこの信号上昇はGdによる増強効果なのか、位置ズレによるアーチファクトなのか？

[PURPOSE] To evaluate the contrast enhancement of the dermal tissue due to Gadolinium contrast material. [MATERIALS AND METHODS] Subtraction image between postcontrast and precontrast 3D-T1 weighted image of the brain was calculated. Image registration was performed before the calculation of subtraction. On these subtraction images, dermal tissue signal was evaluated by visual inspection, intensity profile curve analysis and ROI measurements. [RESULTS] Postcontrast 3-D T1WI shows signal intensity increase of the dermal tissue. Also, subtraction image shows the same high-signal intensity in the skin. 3-D volume rendering image and thick slab MIP image shows various enhancement pattern of the dermal tissue. [CONCLUSION] The cranial dermal tissue shows enhancement due to Gadolinium contrast material.

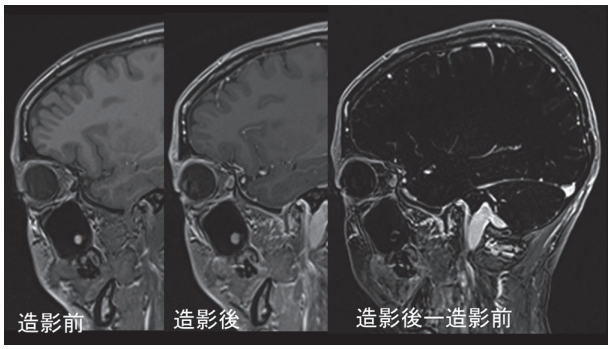

O-1-108　海馬構造の描出について
Visualizing the Structure of the Hippocampus

宮武　祐士（おさか脳神経外科病院 放射線部）
Yuji Miyatake[1], Sunao Nakata[1], Yasuaki Kamada[1], Yuko Takahashi[1], Naomi Honjo[2]
[1]Radiation Department, Osaka Neurosurgical Hospital, [2]Department of Radiology, Osaka Neurosurgical Hospital

【要旨】海馬は微細な構造であり、内部構造を描出するのは困難である。高磁場MRI装置の普及により、高分解能画像による海馬内部構造描出能の向上が期待できる。日常的に使用されるT2WI, PDWI, FLAIRを用いて、海馬構造の描出について検討を行い、高分解能T2WIが最も安定して海馬構造を描出できることを確認した。

Background: Evaluation of the hippocampal structure is often needed in diseases such as dementia and hippocampal sclerosis, but visualizing the fine internal architecture of areas such as Ammon's horn is difficult. The growing use of high-field-strength MRI promises improvement in visualizing the hippocampus in thin slices and at high resolution.Objective: To compare T2WI, PDWI, and FLAIR for visualizing the structure of the hippocampus. Methods: We used a Siemens Magnetom Verio B19. For 5 healthy volunteers, we scanned the hippocampus with each sequence optimized for high resolution. Coronal cross-sections perpendicular to the long axis of the hippocampus were evaluated visually by a radiologist and radiological technician, and scored on a 4-point scale for each of 6 areas: parahippocampal gyrus, subiculum, Ammon's horn, dentate gyrus, hippocampal sulcus, and superficial medullary lamina.Results: T2WI and PDWI yielded high scores for each area, but visualization of the corticomedullary junction was worse with PWDI than with T2WI. FLAIR yielded variable scores for each area, and motion-induced artifacts were seen.Discussion: T2WI is superior for both signal to noise ratio (SNR) and tissue contrast, and is suited to obtaining anatomical information. PDWI is high SNR, but the tissue contrast is inferior than T2WI and FLAIR, and differences in tissue contrast were reflected in the evaluations. FLAIR is superior in tissue contrast, but scan time and motion artifacts is a disadvantage.Conclusion: High resolution T2WI is useful for understanding the structure of the hippocampus.

O-1-109　人体における局所磁場不均一補正用パットの最適な塩化マンガン濃度について
Local Magnetic Field Inhomogeneity Correction Pad; Utlity for Improvement of B0 Inhomogeneity on MR System as Compared with $MnCl_2$ concentration

京谷　勉輔（神戸大学医学部附属病院 医療技術部 放射線部門）
Katsusuke Kyotani[1], Hideaki Kawamitsu[1], Kazuya Sato[2], Satoru Takahashi[1,3], Kazuro Sugimura[3]
[1]Division of Radiology, Kobe University Hospital, [2]Kobe BioMedix Co.,Ltd, [3]Department of Radiology, Kobe University Graduate School of Medicine

【要旨】新素材として検証している塩化マンガンを含んだ局所磁場不均一補正用パットを使用することにより、従来の塩化第二鉄を含んだパットよりも局所磁場不均一の改善傾向を示した。さらに、人体の導電率、比誘電率に応じた最適な塩化マンガン濃度を模索するために、異なるマンガン含有量のパットを試作し、ボランティアで検証した

Introduction:To correct static magnetic field (B0) inhomogeneity, which can cause inhomogeneous fat suppression in complex region; such as neck, breasts, hip joint, "local magnetic field inhomogeneity correction pad" with $FeCl_3$ has been developed and used in clinical practices. We have reported in JSMRM2015 that $MnCl_2$ impregnated beads showed better B0 inhomogeneity correction than those with $FeCl_2$. Our aim of this investigation was to optimize the concentration of $MnCl_2$ in local B0 inhomogeneity correction pad.Material and Method:Four sets of B0 correction pad with different concentration of $MnCl_2$ (1, 2, 3, 4 g/L) were developed. Five volunteers were scanned with 1.5T clinical MR scanner (HITACHI, ECHELON Vega) using 8-channel neuro-vascular coil. Reference B0 measurement was performed with gradient echo method and seven ROIs were placed on B0 map. Relative evaluated standard deviation (RSD) for seven ROIs were compared with and without B0 correction pad. Result:Mean ± SD of RSD was -105.4% ± 11.7% without correction pad, while those with different concentration of $MnCl_2$ pad (1, 2, 3, 4 g/L) were -14.5% ± 16.3%, 19.4% ± 17. 2%, -24.1% ± 68.7%, 32.2% ± 80.2%, respectively. Conclusion:Local magnetic field inhomogeneity correcting pad with 1 g/L of $MnCl_2$ showed optimal improvement of B0 inhomogeneity.

O-1-110　1.0M Gd造影剤を用いたDCE-MRDSA-DSC 3連続撮像とMRDSA-DSC 2連続撮像の比較検討
Comparison between two consecutive acquisition methods (DCE-MRDSA-DSC vs. MRDSA-DSC) using a 1.0-M Gd-based contrast agent

五明　美穂（杏林大学 医学部 放射線医学教室）
Miho Gomyo[1], Kazuhiro Tsuchiya[1,2], Arisa Ohara[1], Shichirou Katase[1], Masanaka Watanabe[1], Toshiaki Nitatori[1]
[1]Department of Radiology, Kyorin University Faculty of Medicine, [2]Department of Radiology, Tokyo Teishin Hospital

【要旨】高濃度造影剤1.0-M Gd（GBCA, Gadobutrol）を用い、DCE-MRDSA-DSC法の3連続撮像8例とMRDSA-DSC法の2連続撮像8例とで、MRDSAとDSCの結果を統計学的に比較検討した。結果は両者間で有意差はなく3連続撮像が可能である結論が得られた。

[Object] As a recently introduced 1.0-M Gd-based contrast agent (GBCA, Gadobutrol) has high concentration, it is expected to have good bolus property. Therefore we evaluated the feasibility of consecutive acquisition of time-resolved enhanced MR angiography (MRDSA) and perfusion imaging by dynamic contrast enhanced method (DCE) and dynamic susceptibility contrast method (DSC) using the GBCA.
[Materials and Methods] Our study group comprised 16 patients with a preoperative intra-axial brain tumor. On a 3-T imager, consecutive acquisition of MRDSA and DSC was performed in 8 patients (group 1). Meanwhile, consecutive acquisition of DCE, MRDSA, and DSC was performed in 8 patients (group 2). In group 1, each scan was performed using a half dose, while each scan in group 2 was performed using a one third dose of the GBCA determined by patient's body weight. For MRDSA, we set a region of interest in a siphon of internal carotid artery and a superior sagittal sinus and the peak value was obtained from the signal intensity curve. For DSC method, we calculated the cerebral blood volume (CBV), cerebral blood flow (CBF), and mean transit time (MTT) ratios by dividing the CBV, CBF, and MTT values of the solid components by those of the contralateral normal white matter in patients with high-grade glioma (n=5 in group 1 and n=7 in group 2). The peak values of MRDSA and each parameter of DSC were assessed between the two groups.
[Result] Between group 1 and group 2, significant difference was found in neither MRDSA nor DSC.
[Conclusion] It is possible to consecutively acquire DCE and MRDSA and DSC using one third of the standard dose of the 1.0-M GBCA for each.

O-1-111　実験動物としての海洋生物III：MRI法と赤外プレチスモグラフィー法による心拍測定
Heart rate measurement by T_{1w}-MRI and infrared photoplethysmography of *Mytilus galloprovincialis*

瀬尾　芳輝（獨協医大 医学部 生理学（生体制御））
Yoshiteru Seo[1], Toshiyuki Sazi[2], Morio Togawa[2], Osamu Nagata[2], Mika Yokoi-Hayakawa[1], Yoshie Imaizumi-Ohashi[1], Masataka Murakami[2]

[1]Dept. of Regul. Physiol. Dokkyo Med. Univ. Schl of Med., [2]Niatl. Inst. Physiol. Sci.

【要旨】我々は、深海性二枚貝をモデル動物として、内皮細胞性血管弛緩因子(EDRF)の研究を進めている。心拍動の非侵襲的連続測定のため、赤外線光プレチスモグラフ法の導入を試みた。T_{1w}-MRIにより心周期との対応を検証し、ムラサキイガイでは5-35 bpmの範囲で心拍数を測定できることを明らかにした。

We have picked up *Bathymodiolus* mussels live in deep-sea as an experimental animal model for studying H_2S function as endothelium-derived relaxing factor (EDRF). Due to a little knowledge of cardiac physiology of *Bathymodiolus*, we have developed noninvasive techniques for analyzing cardiovascular system using *Mytilus galloprovincialis*. By using cine T_1-weighted gradient-echo imaging (T_{1w}-MRI), we could depict inflow of hemolymph through the auriculoventricular valves and also pulsatile flow in the aorta as higher signal intensity (inflow effect). From the beat-to-beat interval, we could calculate heart rate up to 30 beat/min. In order to measure heartbeat continuously, we have introduced infrared photoplethysmograph (IR-PP). In principle, the intensity of IR reflection from the object increased when the volume of the object increased. However, the trace of infrared photoprethysmogram (IR-PPG) of the heart of *Mytilus* varied from a single peak to a multiple peak. Until this study, the relationship between the trace of IR-PPG and the actual heartbeat has not been confirmed in bivalves. At a higher heart rate (35-20 beat/min), the IR-PPG usually consisted of a single sharp peak (peak *v*). The upward and downward slopes of the peak *v* corresponded to the filling and contraction of the ventricle, respectively. A double-peak IR-PPG was observed in a wide range of heart rates from 35 to 5 beats/min, and a multiple-peak IR-PPG often observed at lower heart rate. The origin of the second and later peaks varied heart rate dependently, but initial peak *v* corresponded to the filling of the ventricle. Therefore, we can calculate the heart rate from the *v-v* interval. Thus, IR-PP is a real-time, noninvasive, and economical method useful to monitor the heartbeat of the mussel.

O-2-001　EEG-fMRI同時計測による意味記憶課題中のサブセカンドレベルでの連続的な脳活動の検出
Detecting sequential activation in sub-second resolution during semantic memory test using simultaneous EEG-fMRI measurement

水野　健吾（名古屋大学大学院 医学系研究科 医療技術学専攻 医用量子科学分野）
Kengo Mizuno[1], Epifanio Bagarinao[2], Satoshi Maesawa[2], Saea Tohira[3], Hirohisa Watanabe[2], Toshiharu Nakai[4], Haruo Isoda[1,2]

[1]Department of Radiological and Medical Laboratory Sciences, Nagoya University Graduate School of Medicine, [2]Brain & Mind Research Center, Nagoya University, [3]Center for General Education, Aichi Institute of Technology, [4]National Center for Geriatrics & Gerontology, Ohbu

【要旨】EEG-fMRI同時計測を用いて、意味記憶課題中の連続的な脳活動の変化を検出するため、EEGにより取得した信号をregressorとしてfMRIのGLM解析に組み込んだ。その結果、サブセカンドレベルでの連続的な脳活動のパターンの変化を捉えることができたことから、EEG-fMRIにより経時的な脳活動を検出可能であると考えられた。

Introduction: EEG-fMRI has received substantial attention as a method for assessing brain activity with high spatiotemporal resolution. The purpose of this study was to utilize simultaneous EEG-fMRI to detect sequential activation changes in the brain in sub-second range during a Pyramids and Palm Trees Test (PPT), which evaluate semantic memory. **Methods:** This study involved 10 healthy volunteers from whom we obtained informed consent. We used a 3.0T MR scanner and a 32-channel EEG equipment. For each participant, we acquired functional MR images and EEG data using simultaneous EEG-fMRI during PPT task (Fig. 1a).Preprocessing fMRI data was carried out using SPM8. Correlation series obtained from EEG signal was convolved with the canonical HRF, and used as a regressor in the succeeding GLM analysis. **Results:** Results using only fMRI data (Fig. 1b) showed significant activations in several regions related to PPT. Activation maps using EEG-fMRI data (Fig. 1c) also showed several dynamically changing activation patterns within the sub-second range. **Conclusions:** The present results suggested that EEG-fMRI might detect the sequential brain activations processed in a very short time.

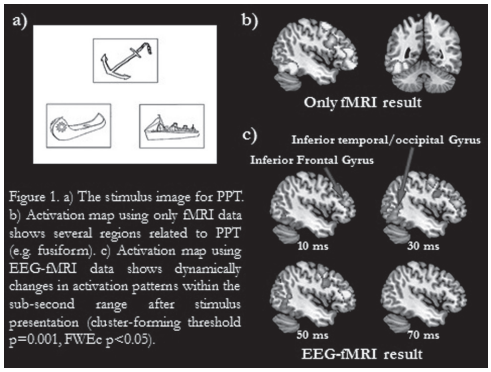

Figure 1. a) The stimulus image for PPT. b) Activation map using only fMRI data shows several regions related to PPT (e.g. fusiform). c) Activation map using EEG-fMRI data shows dynamically changes in activation patterns within the sub-second range after stimulus presentation (cluster-forming threshold p=0.001, FWEc p<0.05).

O-2-002　白内障術後の一過性脳接続性変化　－安静時fMRIによる検討－
Transiently altered brain connectivity after cataract surgery -resting fMRI study-

吉田　正樹（東急病院眼科）
Masaki Yoshida[1], Masahiro Ida[2], Yuri Masaoka[3], Nobuyoshi Koiwa[4], Akira Yoshikawa[3], Keiko Watanabe[3]

[1]Department of Ophthalmology, Tokyu Railway Company, Tokyu Hospital, [2]Department of Radiology, Tokyo Metropolitan Health and Medical Treatment Corporation, Ebara Hospital, [3]Department of Physiology, Showa University School of Medicine, [4]Department of Health and Science, University of Human Arts and Sciences

【要旨】白内障手術が脳接続性に与える影響を安静時fMRIで検討した。両眼白内障手術を施行し、術後早期から矯正視力1.0以上が観察された20名に、術前、術後1ヶ月、3ヶ月の時点で撮像を施行した。グラフ理論による解析で、術後1ヶ月にsmall worldnessの一過性上昇を認めた。術後網膜像の変化により、脳接続性の再構成が示唆された。

IntroductionCataract surgery is one of a most frequent operation in ophthalmology field. A majority shows recovered visual acuity at early postoperative period. On the other hand, complaint of patients is varied and it is not necessarily consistent with outcome of visual acuity. Brain connectivity pre- and post-cataract surgery was explored by using resting state fMRI.Material and MethodsTwenty patients, having cataract surgery for both eyes within 14 days, were scanned with 3T clinical MR (SIEMENS, MAGNETOM A Trio Tim). Resting state fMRI was acquired prior to, following one and three month of cataract surgery with 10-min multi-band accelerated (MB=6) echo planar imaging. 3D T1 weighted images were also acquired as 1mm isotropic special resolution to determine 90 cortical regions with automated anatomical labeling (AAL). Functional brain connectivity matrix for each period of subject was calculated by using DPERSF software. Matrices of each three period were statistically compared applying graph theory by means GraphVar software.ResultsAll subject show post-operative corrected visual acuity (1.0) or more prior to post-one month fMRI acquisition. Post-one month fMRI series had increased small worldness comparing with pre- and post-three month period.　Discussion and ConclusionIt was suggested that transiently increased small worldness at post-one month support some need of re-modelling of brain network for abrupt change of retinal image quality caused by cataract surgery.

O-2-003　急性期脳卒中における運動機能ネットワークの回復：経頭蓋磁気刺激と安静時機能的MRI所見の関係
Recovery of motor network in acute stroke: Transcranial magnetic stimulation motor evoked potential and resting state functional MRI

松下　　明（茨城県立医療大学付属病院脳神経外科）
Akira Matsushita[1,2], Hada Hada[4], Kousaku Saotome[3], Tomohiko Masumoto[5], Aiki Marushima[2], Kei Nakai[1,2], Yoshiyuki Sankai[3], Masashi Yamazaki[6], Akira Matsumura[2]

[1]Dept. of Neurosurgery, Ibaraki Prefectural University of Health Sciences, [2]Dept. of Neurosurgery, University of Tsukuba, [3]Center for Cybernics Research, [4]Dept. of Rehabilitation, [5]Dept. of Radiology, [6]Dept. of Orthopedic Surgery

【要旨】右被殻出血46歳男性にロボットスーツHALを用いた臨床研究において，複数回の機能的MRI(rsfMRI)および経頭蓋磁気刺激による誘発電位(MEP)を測定した。MEPとrsfMRIの対比から，患側はネットワークの規則性が振幅を高くし，健側はネットワークの複雑さが不規則な波形を招いたと考えられた。

Introduction: We have used robot suit HAL (hybrid assistive limbs) as novel therapy for patients with impairment of gait. In addition, we explorer the neural system changes using functional images and electrophysiological examination.
Case presentation: Forty-six y/o male with hemiparesis had been admitted. CT showed right putaminal hemorrhage. He had participated in the clinical study of HAL therapy after informed consent. Totally, seven sessions of HAL therapy were done. Resting state functional MRIs were acquired 3 times on 3rd, 4th, and 5th week. The functional connectivity (FC) of motor execute network was calculated in connectivity toolbox (CONN) on SPM12. The two properties of graph theory were used; average path length (APL) and clustering coefficiency (CC) of primary motor area. The transcranial magnetic stimulation motor evoked potentials (TMS-MEPs) were obtained 2 times on 4th and 5th week. It seems that the increasing amplitude in TMS-MEP of affected side is related to lattice network of FC and the larger variance and the lower amplitude in unaffected side are related to longer APL.
Conclusion: This is the first report to show the neural reorganization in both TMS-MEPs and FC of acute stroke patient. Both data commonly showed rapid shift of network characteristics during acute phase.

O-2-004　脳賦活タイミングの違いを描出するための新しいfMRI解析法
A New fMRI analysis method to visualize the difference of the brain activation timing

丸山　純人（国際医療福祉大学 保健医療学部 放射線・情報科学科）
Sumito Maruyama

Department of Radiological Sciences, School of Health Science,International University of Health and Welfare

【要旨】fMRI解析時の統計モデルのタスクオンセットタイムを実際の刺激タイミングからずらしながら解析することによって、局所賦活領域の賦活タイミングの違いを可視化できるか検討した。右手利き健常人の右手掌握運動課題において一次運動野が小脳や補足運動野よりも先に賦活する傾向にあることが示唆された。

[Purpose] The task onset time of a statistical model in fMRI analysis is typically set according to the timing of stimulation. In this study, using a high temporal resolution fMRI data, we examined the way of dynamically visualizing the difference of the activation timing between the brain activation areas by analyzing the task onset time of the statistical model shifted from the actual stimulation timing. [Method] High temporal resolution fMRI data were obtained using PRESTO-SENSE sequence on 3T MRI with right handed healthy volunteers. Task paradigm was block design to carry out two sets of the rest and right hand grasp task. The analysis of the fMRI was used SPM12. After the preprocessing, statistical analyzes were performed by shifting the onset time of the statistical model by about one second back and forth from the actual stimulation timing. [Result] Activations were found to the left of the primary motor cortex and the right of the cerebellum and supplementary motor area in FWE ($P = 0.05$). In the right hand grasp motion, it was found that there is a tendency that the primary motor cortex is activated earlier than the cerebellum or supplementary motor area. [Conclusions] By using this new analysis method, it was suggested that it is possible to visualize the difference of the activation timing between the activation areas.

O-2-005　Serial Autocorrelations and Multiband fMRI

Allen Waggoner（理化学研究所 脳科学総合研究センター）
Allen Waggoner, Topi Tanskanen, Keiji Tanaka, Kang Cheng
RIKEN - Brain Science Institute

【要旨】Serial Autocorrelations and Multiband fMRI

Multiband EPI offers much faster sampling rates for fMRI experiments than were previously available and this enables a better characterization of the hemodynamic response, especially in event-related fMRI. The faster sampling rates also lead to increased serial autocorrelations. This raises the question of whether the increased extents of activation observed with the short Tr values permitted by multiband EPI are solely the result of increased autocorrelations or also a result of the improved sampling of the hemodynamic response. We have performed whole brain event-related fMRI studies, employing various levels of in-plane and slice acceleration, to achieve Tr values ranging from 3.25s down to 0.5s, at both 3T and 4T. A flickering checkerboard paradigm was used with 1s events separated by 14s rest periods. Serial autocorrelations were corrected using an AR(10) model. For sub-second Tr values the use of the AR(10) model reduced the observed extents of activation by more than 50%. After the AR(10) correction, the extents of activation observed for sub-second Tr values were still as much as 3 times larger than the observed extents at traditional Tr values. These results demonstrate that while using the shorter Tr values allowed with multiband EPI is highly advantageous, it is increasingly important to properly account for serial autocorrelations with using very short Tr values.

O-2-006　広帯域双極子場を用いた定量的磁化率マッピングによる脳血管の視認性の向上
Improved Visualization of Cerebral Blood Vessels by Using Wider Band Dipole Inversion in Quantitative Susceptibility Mapping

梅本　勇哉（京都大学 大学院医学研究科 人間健康科学系専攻）
Yuya Umemoto[1], Tomohiro Ueno[1], Shin-ichi Urayama[2], Toshihiko Aso[2], Hidenao Fukuyama[2], Naozo Sugimoto[1]
[1]Human Health Sciences, Graduate School of Medicine, Kyoto University, [2]Human Brain Research Center, Graduate School of Medicine, Kyoto University

【要旨】定量的磁化率マッピングにおいて、広帯域の双極子場を用いて逆問題を解く方法を提案し、磁化率マップの質が向上することをシミュレーションとファントム実験で示した。本研究では、提案手法を健常被験者の脳組織に応用し、MIP画像での脳血管の視認性が向上することを確認した。

(Introduction) Quantitative Susceptibility Mapping (QSM) enables us to calculate iron accumulation in a brain tissue and cerebral venous oxygen saturation. To obtain more precise local susceptibility mapping, we have proposed a new QSM method, High Resolution QSM, that utilizes wider band dipole inversion. The High Resolution QSM improves quality of a susceptibility map in numerical simulations and phantom experiments. In this study, we examined the High Resolution QSM by comparing a MIP of cerebral blood vessels. (Materials & Methods) A healthy volunteer was imaged using a 3T whole body MRI scanner (Tim Trio, Siemens Medical Solutions) and a 12 channel head coil. A 3D flow compensated gradient echo sequence was used to obtain phase data with two different voxel sizes: 1.2 mm^3, 0.6 mm^3. We employed the COSMOS and the SHARP to calculate the susceptibility distribution. In the High Resolution QSM, we employed a dipole field with twice wider band width to obtain twice smaller voxel size than that of the input data. We compared MIP of the High Resolution QSM image with that of a conventional QSM image that was tricubically interpolated to have the twice smaller voxel size. As a ground truth, we used a conventional QSM image that was calculated from higher resolution input data (0.6 mm^3). (Results&Discussions) Susceptibility values of sub-structures of the basal ganglia were consistent with previously reported values. Degraded appearances of small vessels in the tricubically interpolated conventional QSM image were recovered in the High Resolution QSM image. This improvement can show that the High Resolution QSM reduces partial volume effects due to the finite voxel size. (Conclusions) We can improve the visibility of a susceptibility map of a human brain.

O-2-007　前立腺定量的磁化率マッピングにおけるムラ低減および脂肪内精度改善手法
Quantitative Susceptibility Mapping with Reduced Inhomogeneity and Improved Accuracy of Fat Susceptibility for Prostate Imaging

佐藤　良太（株式会社日立製作所 研究開発グループ）
Ryota Sato[1], Toru Shirai[1], Yo Taniguchi[1], Takenori Murase[2], Atsushi Kuratani[2], Taisei Ueda[2], Takashi Tsuneki[2], Yoshitaka Bito[2], Hisaaki Ochi[1], Yoshihisa Soutome[1]

[1]Research and Development Group, Hitachi, Ltd., Tokyo, Japan., [2]Healthcare Business Unit, Hitachi, Ltd., Tokyo, Japan.

【要旨】体幹部における定量的磁化率マッピング法の実現を目的として、脂肪と脂肪以外の領域の磁化率を別々に算出して統合する手法を提案し、数値シミュレーションおよびヒト前立腺画像を用いて提案手法の有効性を評価した。その結果、提案手法により皮下脂肪周辺のムラおよび脂肪内の算出誤差が低減し、その有効性が示された。

Introduction: Quantitative susceptibility mapping (QSM) is well studied for application to diagnosis of brain diseases, but also expected to be applied to body diseases, such as iron overload or prostate cancer. In body QSM, the presence of fat sometimes causes inhomogeneity and calculation error due to magnetic resonance signal losses in bone or air around fat. In this study, in order to reduce inhomogeneity and improve accuracy in body QSM, we have proposed a new calculation method and evaluated its effect in prostate imaging.
Methods: In the proposed method, susceptibilities in fat and non-fat regions are calculated separately, and then combined. In fat region, to improve accuracy, susceptibility is calculated by setting constraints that susceptibility in non-fat region is zero. In non-fat region, to reduce inhomogeneity, background field removal is performed regarding fat region as background susceptibility source. Numerical simulation and human volunteer's prostate imaging are used to compare the proposed method with the conventional method. Data from volunteer were obtained according to the regulations of internal review board on Central Research Laboratory, Hitachi, Ltd., following receipt of written informed consent.
Results: In simulation, inhomogeneity in non-fat region reduced in susceptibility map obtained by the proposed method. The calculation error in fat region obtained by the proposed method is decreased compared to the conventional method. In prostate imaging, inhomogeneity in non-fat region reduced and mean fat susceptibility obtained by the proposed method got close to the standard value compared to the conventional method. These results suggest that the proposed method reduces inhomogeneity and improves accuracy of fat susceptibility.

O-2-008　適応的エッジ保存フィルタを用いた定量的磁化率マッピング法：ヒト複数エコー画像によるCOSMOSとの比較
Quantitative Susceptibility Mapping using Adaptive Edge-preserving Filtering: Comparison with COSMOS in Multi-echo data of Human Brain

白猪　亨（株式会社 日立製作所 研究開発グループ）
Toru Shirai[1], Ryota Sato[1], Yo Taniguchi[1], Takenori Murase[2], Atsushi Kuratani[2], Taisei Ueda[2], Takashi Tsuneki[2], Yoshitaka Bito[2], Yoshihisa Soutome[1], Hisaaki Ochi[1]

[1]Research and Development Group, Hitachi, Ltd., [2]Healthcare Business Unit, Hitachi, Ltd.

【要旨】適応的エッジ保存フィルタを用いた定量的磁化率マッピング(QSM)再構成法を提案し，複数のエコー時間のグラディエントエコー画像を用いて磁化率分布を算出した。定量性が検証されているCOSMOS法と提案法を定量比較し，両手法の推定磁化率に強い相関があることを確認した。

[Purpose]
Quantitative susceptibility mapping (QSM) is very useful for obtaining biological information. Determination of a susceptibility map is known as ill-conditioned inverse problem caused by zero-cone region of dipole function in k-space. To solve the problem, a calculation of susceptibility through multiple-orientation sampling (COSMOS) was proposed, but it is clinically impractical to carry out on human subjects in clinically acceptable scan time. We proposed a QSM reconstruction of single orientation sampling method which combined an iterative least-square minimization and an adaptive edge-preserving filtering. In this study, we demonstrate qualitative and quantitative comparison between susceptibility calculated by the proposed method and COSMOS in multi-echo data of healthy volunteers.
[Methods]Three healthy volunteers recruited to perform on a 3T MRI (Hitachi, Ltd.) with 15-channel head coil. Data from volunteer were obtained according to the regulations of internal review board on Central Research Laboratory, Hitachi, Ltd., following receipt of written informed consent. A 3D RF-spoiled gradient-echo sequence was used, TR = 37 ms, TEs = 5.5 / 11 / 16.5 /22 / 27.5 / 33 ms, FA = 15deg, FOV: 240 x 240 x 144 mm, matrix: 200 x 200 x 120 (zero filled to 480 x 480 x 240). For the quantitative evaluation of susceptibility between the proposed method and COSMOS, we performed a region of interest-based and voxel-based quantitative comparison.
[Results and Discussion]The results show that signal to noise ratio of susceptibility map calculated by the proposed method is improved by using multi-echo data, and a high degree of agreement between the proposed method and COSMOS. The proposed method is useful for generating a high-quality susceptibility map in human brain.

O-2-009　Ill-Conditioned Point Weighted Dipole Inversionを利用したQuantitaive susceptibility mapping再構成法
Quantitative Susceptibility Mapping Reconstruction Using Ill-Conditioned Points Weighted Dipole Inversion

菅　　博人（名古屋市立大学病院 中央放射線部）
Hirohito Kan[1], Nobuyuki Arai[1], Harumasa Kasai[1], Masahiro Takizawa[2], Yoshimasa Matsuda[2], Kazuyoshi Omori[2], Yasujiro Hirose[1]

[1]Department of Radiology, Nagoya City University Hospital, [2]Healthcare Business Unit, Hitachi, Ltd.

【要旨】Ill-conditioned points weighted dipole inversion（ICPDI)法を開発し，ボランティアの頭部で評価を行った．ICPDIはストリークアーチファクトの発生するポイント付近にL1ノルムの最小化を行う．両手法の磁化率は相関した．アーチファクトはICPDIはTVに比べて減少した．さらにICPDIは詳細な構造を保っていた．

Purpose: Quantitative susceptibility mapping (QSM) reconstructed from single-orientation dataset is desired to decrease streaking artifact along magic angle without a loss of structural detail. We developed an Ill-Conditioned Points weighted Dipole Inversion method (ICPDI) and evaluated it in human brain experiment. Method: The susceptibility map in ICPDI was reconstructed by minimizing the L1-norm of the gradient along magic angle to avoid large streaking artifacts. The loss of edge detail was minimized, because the other k-space points were estimated with no influence of regularization. The optimal regularization parameter was investigated by L-curve method. The 1 mm isovoxel phase dataset on healthy volunteer was obtained using 3D spoiled gradient echo sequence on 3.0 T scanner. Background field removal method was used regularization enabled sophisticated harmonic artifact reduction with varying kernel sizes with 5-9 mm kernel sizes. We determined the relationship between susceptibility values in ICPDI and QSM with total variation penalty (TV).Result: The optimal regularization parameters were 0.043 and 0.00062 in ICPDI and TV, respectively. There was a significant correlation between susceptibility values in ICPDI and TV. The susceptibility map estimated by ICPDI was effectively suppressed streaking artifacts related to magic angle with minimal loss of edge detail, compared with TV. Conclusion: The proposed ICPDI method was more accurate and effective method for reduction of streaking artifact with the loss of structural detail and provided excellent image quality.

O-2-010　パーキンソン病診断における定量的磁化率マッピングと神経メラニンを用いた背外側黒質領域評価の有用性
Clinical application of QSM and neuromelanin imaging of the dorsolateral substantia nigra in the diagnosis of Parkinson's disease

高橋　洋人（Osaka University Graduate School of Medicine）
Hiroto Takahashi[1], Yoshiyuki Watanabe[1], Hisashi Tanaka[1], Masahito Mihara[1], Hideki Mochizuki[1], Tian Liu[2], Yi Wang[2], Noriyuki Tomiyama[1]

[1]Osaka University Graduate School of Medicine, [2]Cornell University

【要旨】14名のパーキンソン病患者と健常者の背外側黒質領域の鉄沈着とドパミン神経変性を定量的磁化率マッピングと神経メラニンを用いて評価した。健常者に比してパーキンソン病患者における有意な鉄沈着の亢進とドパミン神経の減少が見られた。パーキンソン病診断において背外側黒質領域の評価は有用である。

Purpose;To assess dopaminergic neurodegeneration and iron overload in the dorsolateral substantia nigra <SN> in patients with Parkinson's disease <PD> in a quantitative and reproducible manner.Materials and Methods;This study included 14 patients with PD <Group A> and 14 normal controls <Group B> who underwent quantitative susceptibility mapping <QSM>, neuromelanin <NM> imaging and 3D-T1W imaging on a 3T MR imager. Both QSM and NM values of the dorsolateral SN were calculated using an ROI based automated segmentation system with the voxel-based morphometric technique. Images were preprocessed as follows: All QSM and NM images were co-registered with 3D T1-weighted structural images and were spatially normalized using SPM, thus allowing voxel-based measurement with automatic setting of the ROI encompassing the dorsolateral SN. The spatially normalized images of all subjects were smoothed. Finally, the ROI was set on the QSM-NM fused image. SNR of the dorsolateral SN in the NM images was calculated on the basis of mean value of the automatically segmented background region <tegmentum>. The significance of intergroup differences in each QSM value and higher SNR NM area than that of the background region was tested using Mann-Whitney's U test.Results;When comparing the 95th percentile QSM values in each group, the mean in Group A was significantly larger than that in Group B <Group A/B: mean value <ppb> = 140.18/97.87, SD = 37.16/33.39> <P < 0.01>. The NM area of higher SNR in Group A was significantly less than that in Group B <Group A/B: mean value <pixel> = 871.21/1098.43, SD = 108.63/41.21> <P < 0.01>.Conclusion;A voxel-based automatic measurement system for dopaminergic neurodegeneration and iron overload in the dorsolateral SN is useful in the diagnosis of PD.

O-2-011　定量的磁化率マッピングを用いた小児期の磁化率変化の検討
Susceptibility changes from neonate to childhood on quantitative susceptibility mapping

日野田卓也（京都大学 大学院医学研究科 放射線医学講座（画像診断学・核医学））
Takuya Hinoda[1], Yasutaka Fushimi[1], Tomohisa Okada[1,2], Akira Yamamoto[1], Tsutomu Okada[1], Kaori Togashi[1]

[1]Department of Diagnostic Imaging and Nuclear Medicine, Graduate school of Medicine, Kyoto University, [2]Human Brain Research Center, Graduate School of Medicine, Kyoto University

【要旨】定量的磁化率マッピングを用い小児期の磁化率の変化を検討した。8人の小児（0ヶ月～44ヶ月）を対象に行った。撮影した画像から定量的磁化率マッピングを作成し、関心領域（被殻・淡蒼球・尾状核・内包後脚）の磁化率変化を分析した。結果は、被殻・淡蒼球・尾状核で磁化率は正の相関を示し、内包後脚は負の相関を示した。

Purpose The Quantitative susceptibility mapping (QSM) provides us voxel-based susceptibility values. In early childhood, brain development rapidly progresses and the process is observed as mainly myelination on white matter structures and iron-deposition on deep gray matters. The purpose of this study is to observe the susceptibility changes in the deep gray structures and white matter structures. **Materials and Methods** 8 children (0M-44M) without any abnormalities in brain MR images were enrolled to this study. A 2D gradient-echo T2* weighted was acquired on a 3.0T MR scanner (Skyra, Siemens). TR=55ms, number of echoes=4, TE=20~50ms, FA=15°, slice/gap=2mm /0.4mm, FOV=24 × 24cm2, matrix=256 × 256. QSM was calculated with STIsuite, using the sophisticated harmonic artifact reduction for phase data with a variable radius of the spherical kernel at the brain boundary (V-SHARP) and the algorithm for sparse linear equations and sparse least squares (iLSQR method). Regions of interest (ROIs) were outlined manually in caudate nucleus (CN), putamen (PUT), globus pallidus (GP), and posterior limb of internal capsule (IC). Susceptibility changes were evaluated, using linear regression analysis. **Results** Susceptibility values in the CN, PUT and GP showed positive correlation with subject's age. Susceptibility values in the IC showed negative correlation. The R^2 values were 0.88 (CN), 0.80 (PUT), 0.67 (GP), 0.40 (IC). **Discussion and conclusion** Brain development is assessed with T1 weighted and T2 images. QSM could provide us more quantitative evaluation during early childhood.

O-2-012　基底核血管周囲腔造影効果と内リンパ水腫の関係
Relationship between contrast enhancement of basal ganglia perivascular space and endolymphatic hydrops

大橋　俊夫（総合上飯田第一病院 放射線科）
Toshio Ohashi[1], Toshio Katagiri[1], Kayao Kuno[2], Shinji Naganawa[3]

[1]Department of Radiology, Kamiiida Daiichi General Hospital, [2]Department of Otolaryngology, Kamiiida Daiichi General Hospital, [3]Department of Radiology, Nagoya University Hospital

【要旨】我々の施設では、内リンパ水腫の体積測定による評価を行っている。その経験から、血管周囲腔の造影効果は内リンパ水腫の程度と関連があるように思われた。そこで、全リンパ腔に対する内リンパ腔が占める体積比と血管周囲腔の造影効果との関係を検討した。その結果、蝸牛において両者の間に強い相関が認められた。

Purpose
Heavily T2-weighted 3D-FLAIR (hT2-3D-FLAIR) after IV-Gd has been used for the evaluation of endolymphatic hydrops (EH). In our hospital, we obtain EH image 4 hours after IV of single-dose Gd-based contrast material (IV-SD-GBCM) and measure the endolymphatic volume ratio (%EL_{volume}) semi-quantitatively. From our experience, we speculated that contrast enhancement of the perivascular space (PVS) might be related to degree of EH.
Therefore the purpose of this study was to investigate the relationship between %EL_{volume} and signal intensity of PVS (SI-PVS).
Method
We evaluated 20 patients suspected with EH (median: 64-year-old).
MR imaging was performed on 3T MR unit (MAGNETOM Skyra, Siemens) using 32ch array head coil.
We obtained two kinds of following images 4 hours after IV-SD-GBCM.
(1) MR cisternography (MRC): hT2-3D-turbo spin echo, TR/TE = 4400/544ms.
(2) Positive perilymph image (PPI): hT2-3D-FLAIR, TR/TE = 9000/544ms, TI2250ms.
We generated HYDROPS2-Mi2 by the processing shown below, and measured %EL_{volume} of cochlea and vestibule on HYDROPS2-Mi2.

(PPI - 0.04 × MRC) = HYDROPS2, (HYDROPS2 × MRC) = HYDROPS2-Mi2, according to the previously reported study.

Then we segmented PVS of basal ganglia on all slices of MRC using region growing method. We pasted the segmented PVS region onto PPI, and measured SI-PVS.
We evaluated the relationship between %EL_{volume} and SI-PVS using Pearson's correlation coefficient, then the larger %EL_{volume} out of right and left ears was employed for this evaluation.
Result
There was a strong negative correlation between cochlear %EL_{volume} and SI-PVS (r = -0.740).
Conclusion
It was found that there is a strong negative correlation between cochlear %EL_{volume} and SI-PVS.
There might be a co-factor for the EH and PVS function.

O-2-013　安静時脳機能磁気共鳴画像を用いた機械学習による自閉スペクトラム症の神経基盤研究
A small number of abnormal functional connections in the brain predicts adult autism spectrum disorder

八幡　憲明（放射線医学総合研究所）
Noriaki Yahata[1,2,3], Giuseppe Lisi[3], Ryuichiro Hashimoto[3,4], Jun Morimoto[3], Kazuhisa Shibata[3,5], Yuki Kawakubo[2], Hitoshi Kuwabara[2], Miho Kuroda[2], Takashi Yamada[3,4], Megumi Fukuda[6], Hiroshi Imamizu[3], Hidehiko Takahashi[7], Yasumasa Okamoto[8], Kiyoto Kasai[2], Nobumasa Kato[4], Yuka Sasaki[3,5], Takeo Watanabe[3,5], Mitsuo Kawato[3]
[1]NIRS, [2]Univ Tokyo, [3]ATR, [4]Showa Univ, [5]Brown Univ, [6]UCL, [7]Kyoto Univ, [8]Hiroshima Univ

【要旨】自閉スペクトラム症（ASD）当事者および定型発達者（TD）の安静時脳機能磁気共鳴画像に機械学習技術を適用することでASD特異的な脳機能結合が少数発見され、これにより国と人種を超えたASD/TD群の高精度判別に成功した。更にこの手法を他の精神疾患データ（統合失調症等）に適用し、複数疾患間のスペクトル構造を検討した。

Autism spectrum disorder (ASD) is a major developmental disorder characterized by deficits in reciprocal social interactions and communication, and by repetitive and restricted behaviors. Despite the significance of this disorder, its underlying neural mechanism remains unclear. Recently, using resting-state functional-connectivity MRI (rs-fcMRI) techniques, attempts have been made to develop classifiers of ASD and typically developed (TD) individuals, and thereby to identify the abnormality of functional connections (FCs) in ASD. However, none of the previous classifiers has ever been successfully validated for an independent cohort because of overfitting and the interferential effects of nuisance variables such as measurement conditions and demographic distributions. Here, using a multiple-site data set from Japan, we developed an ASD classifier by focusing on abnormal FCs in ASD as revealed by rs-fcMRI. To overcome the above difficulties, we developed a novel machine-learning algorithm that automatically identified a small number of abnormal FCs in ASD (0.2% of all FCs). The resultant classifier attained high accuracy for a Japanese discovery cohort, and furthermore, demonstrated a remarkable degree of generalization for two independent cohorts in the US and Japan. We also examined the extent to which the ASD classifier was specific to ASD or extendable to other psychiatric disorders. We found that the developed classifier did not distinguish individuals with major depressive disorder and attention-deficit hyperactivity disorder from their controls but moderately distinguished patients with schizophrenia from their controls. These results leave open the viable possibility of exploring neuroimaging-based dimensions that quantify the multiple-disorder spectrum.

O-2-014　胎児標本MRIにおける下垂体、後蝶形骨化中心の画像所見
Pituitary Gland and Postsphenoid Ossification in Fetal Specimens

伏見　育崇（京都大学大学院医学研究科 放射線医学講座（画像診断学・核医学））
Yasutaka Fushimi[1], Tomohisa Okada[2], Mitsunori Kanagaki[3], Akira Yamamoto[1], Tsutomu Okada[1], Kaori Togashi[1]
[1]Department of Diagnostic Imaging and Nuclear Medicine, Kyoto University Graduate School of Medicine, [2]Human Brain Research Center, Kyoto University Graduate School of Medicine, [3]Department of Radiology, Hyogo Prefectural Amagasaki General Medical Center

【要旨】12～31週の胎児標本MRIのT1強調画像において下垂体信号、postsphenoidの骨化中心の画像所見、下垂体/橋の信号比、postsphenoidの骨化中心/蝶形骨の信号比を在胎週数と対比した。下垂体は高信号で、下垂体/橋比は在胎週数と弱い相関を示した。postsphenoidの骨化中心のサイズは在胎週数にともなって増大した。

Background and Purpose: A thorough understanding of fetal growth and development is key to understanding both normal and abnormal fetal MRI findings. We investigated the size and signal intensity of normal pituitary gland and the intrasphenoidal ossification around Rathke's pouch in formalin-fixed fetuses on MRI.
Materials and Methods: A total of 32 fetuses with undamaged brains were included in this study (mean age, 19.93 weeks; age range, 12-31 weeks). Visual inspection of pituitary and the ossification around Rathke's pouch in the sphenoid bone (SP), or the postshenoid ossification, was conducted. The extent of pituitary and postsphenoid ossification, pituitary/pons signal ratio and postsphenoid ossification/SP signal ratio were compared according to gestational age.
Results: Pituitary gland was identified as a hyperintense intrasellar structure in all cases, and postsphenoid ossification was identified as an intrasphenoidal hyperintense area in 27 of the 32 cases (84%). Pituitary/pons signal ratio was 1.13 ± 0.18 and correlated weakly with gestational age (R2=0.243), while postsphenoid ossification/SP signal ratio was 2.14 ± 0.56 and did not show any increase with gestational age (R2=0.05). No apparent change in size of pituitary hyperintensity was seen with gestational age (R2=0.001). Postsphenoid ossification showed an increase in size with gestational age (R2=0.307).
Conclusion: Fetal pituitary was hyperintense on T1-weighted images and pituitary/pons ratio and extent of postsphenoid ossification correlated weakly with gestational age.

O-2-015　Quiet DWIによる静音効果と画質への影響
Influence on Sound effect and Image quality with Quiet DWI

市場　義人（シーメンスヘルスケア株式会社 カスタマーサービス事業本部 アプリケーション部）
Yoshito Ichiba, Takasi Ueda, Terumasa Takemaru, Tsubasa Kaji, Kanae Yamamoto
Siemens Healthcare K.K., Customer Service Division, Application Department

【要旨】2015年、弊社は静音技術を搭載したが、臨床において広く活用されている拡散強調画像には対応していなかった。今回、新たな静音化技術としてQuiet DWIを開発し、静音の効果と画質への影響を従来法と比較した。Quiet DWIは、従来のss-EPI法と比較して画質の劣化なく静音化された拡散強調画像の提供が可能となる。

BACKGRAUND AND PURPOSE: The diffusion weighted image (following DWI) is used in an examination of MRI in cerebral infarction or a malignant tumor widely for the immediate nature period. In 2015, Acoustic noise reduction techniques called Quiet X and PETRA were equipped, but did not support for DWI imaging.Then, Quiet DWI is developed as a new acoustic noise reduction technique. We inspect the influence on Sound effect and Image quality with Quiet DWI.METHODS: 5 healthy volunteers were scanned with Quiet DWI of the head at a Siemens Skyra 3T- MRI (Magnetom Skyra; Siemens Healthcare, Erlangen, Germany). I changed the echo space (following ES) with 0.5msec,0.7msec,1.0msec,1.5msec and measured with a sound-level meter. And we evaluated visually with Quiet DWI and conventional DWI (ss-EPI). At that time, the ES on Quiet DWI was set with 0.7msec. RESULTS AND DISCUSSION: The Acoustic noise decreased as the ES extended with 0.5 msec, 0.7 msec, 1.0 msec, 1.5 msec. But The Image Quality also decreased from the viewpoint of distortion. The Image quality of Quiet DWI which ES set with 0.7msec had a equivalence or more in comparison with conventional DWI (ss-EPI). Conclusion: we can offer the diffusion weighted image of more few acoustic noise without deterioration of image quality by development of Quiet DWI.

O-2-016　FASE法DWIを用いた静音化シーケンスの開発とVariable Refocusing Flip Angleパターンの最適化
The Quiet Fast Advanced Spin Echo DWI Sequence with Optimized Variable Refocusing Flip Angle

近藤　大貴（東芝メディカルシステムズ株式会社 MRI事業部）
Hiroki Kondo, Nobuyasu Ichinose, Masaaki Umeda, Yoshimori Kassai, Kota Watanabe, Ayumi Katsunuma, Keiichiro Ishi
MRI systems Division, Toshiba Medical Systems Corporation

【要旨】FASE DWIを用いた静音化シーケンスを開発し、騒音測定とVFAパターンの検討を行った。騒音測定の結果、SEEPIや従来のFASEDWIシーケンスと比較し、約15dBAの騒音低減を実現した。また、VFAパターンの検討としてシミュレーション及びボランティア評価を行った結果、FASE DWIで問題となる、SARやT2 blurringの改善を認めた。

Purpose: The acoustic noise reduction in DWI protocol is indispensable for quiet examination because the sound intensity of DWI protocol using single shot echo planar imaging (SSEPI) is obviously louder than other protocols. We optimize fast advanced spin echo DWI (FASE DWI) as quiet DWI sequence by controlling the rise time of gradient waveform. In addition, we investigate variable refocusing flip angle (VFA) patterns for reducing SAR and T2 blurring.
Method: We used 3T scanner(Toshiba Medical Systems). First, the acoustic noise was measured at the isocenter of the magnet using following three sequences, (1)SSEPI, (2)Conventional FASE DWI and (3)Quiet FASE DWI. Second, the following two VFA patterns were evaluated by Bloch simulation and healthy volunteer images. The VFA pattern:A has higher flop angles in the center of k space with gradually reduced flop angles for the high frequency part of k space. The VFA pattern:B has lower flop angles in the center of k space with gradually increased flop angles for the high frequency part of k space to reduce the apparent T2 decay.
Result: As a result of the acoustic noise measurement, the noise level of Quiet FASE DWI was reduced approximately 15dBA compared to others. As a result of the VFA evaluation, the images with pattern A were equivalent to the images with constant flop angle pattern. The images with pattern B had the low SNR but were much clearer than other patterns. In both pattern A and B, TR was so reduced due to lower SAR that shorter scan time was achieved.
Conclusion: We developed the quiet DWI sequence with VFA. This sequence significantly reduces acoustic noise compared with other sequences. Moreover, the issues of FASE DWI, T2 blurring and SAR, were improved by the VFA pattern:B.

O-2-017　脳腫瘍周囲の異常信号について：NODDIの初期経験
Evaluation of peritumoral signal change: Initial experience with neurite orientation dispersion and density imaging (NODDI)

門田　善仁（宮崎大学 医学部 放射線診断学講座）
Yoshihito Kadota[1], Minako Azuma[1], Takanori Yano[1], Masahiro Enzaki[1], Toshiya Azuma[1], Toshinori Hirai[1], Masaaki Hori[2], Shigeki Aoki[2]

[1]Department of Radiology, Faculty of Medicine, University of Miyazaki, [2]Department of Radiology, Juntendo University School of Medicine

【要旨】我々はNODDIを脳腫瘍に応用し、脳腫瘍周囲の異常信号範囲についてNODDIとT2WI、FLAIRでの違いについて比較した。グリオーマ患者ではICVFで脳腫瘍周囲の異常信号範囲がT2WI、FLAIRより広かった。リンパ腫や脳転移の症例ではほぼ一致した。NODDIとT2WI、FLAIRでの脳腫瘍周囲の異常信号範囲は腫瘍によって異なる可能性がある。

<PURPOSE> To compare the extent of peritumoral signal change in various brain tumors on T2 weighted and FLAIR images and the recent developed technique of diffusion weighted imaging, neurite orientation dispersion and density imaging (NODDI).<METHODS> This study included 5 brain tumors of 5 patients. At 3T MRI unit (Philips), diffusion weighted imaging data were acquired with b values of 0, 1000, 2000 sec/mm2 and 32 motion probing gradient axes. Intracellular volume fraction (ICVF) and orientation dispersion index (ODI) of the whole brain were calculated by using MATLAB R2015b. Compared with contralateral brain to the tumor, two radiologists assessed the extent of peritumoral signal change (EPSC) on T2 weighted, FLAIR and NODDI images.<RESULTS> In 3 patients with glioma, the EPSC was larger for ICVF than T2WI and FLAIR images. By contrast, in 2 patients with malignant lymphoma or metastatic brain tumor, the EPSC on ICVF images nearly corresponded with that on T2WI and FLAIR images. The reviewers were not able to identify the EPSC on ODI images. <CONCLUSION> Although this study is our initial experience, the extent of peritumoral signal change between NODDI and T2WI/FLAIR may differ in the types of brain tumors.

O-2-018　小児期胎児性腫瘍に対する放射線治療後の海綿状血管腫検出におけるT2*強調画像の有用性
The usefulness of T2*WI for the detection of cavernous angioma in long-term survivors of childhood embryonal tumors treated by cranial irradiation

山崎　文之（広島大学病院 脳神経外科）
Fumiyuki Yamasaki[1], Takeshi Takayasu[1], Ryo Nosaka[1], Yuji Akiyama[3], Taiichi Saito[1], Fusao Ikawa[1], Kazuhiko Sugiyama[2], Kaoru Kurisu[1]

[1]Department of Neurosurgery, Hiroshima University Hospital, [2]Department of Clinical Oncology & Neuro-oncology Program, Hiroshima University Hospital, [3]Department of Clinical Radiology, Hiroshima University Hospital

【要旨】胎児性腫瘍は治療方法の進歩に伴い長期生存後のQOL にも注目が集まっている。6歳未満で放射線治療を受けた患者は有意に早く脳海綿状血管腫が発生し (P=0.0242)、大脳の胎児性腫瘍患者は髄芽腫患者に比べてより早期に Zabramski type 1&2 の海綿状血管腫が出現した (P=0.0007)。T2*WIは経過観察のプロトコールに必要である。

PURPOSE: The purpose of this study is to investigate the incidence of cavernous angioma (CVA) in long-term survivors of childhood embryonal tumors treated by cranial irradiation. MATERIALS AND METHODS: Between 1990 and 2015, we treated 32 pediatric patients (13 males, 12 females) with embryonal tumors (23 medulloblastomas, 6 primitive neuroectodermal tumors (PNET), 3 pineoblastomas) with craniospinal irradiation. Follow-up ranged from 9.1 to 308.5 months (medain 77.8mos, mean 99.8mos), the irradiation dose to the whole neural axis from 18 to 36 Gy, and the total local dose from 49.6 to 60 Gy. All patients underwent follow-up magnetic resonance imaging (MRI) studies at least once a year, and the diagnosis of posttreatment CVA was based solely on MRI findings. RESULTS: At the time of this writing, 24 were alive and free of the event of the original disease recurrence or the development of secondary neoplasms other than CVA; another 1 was alive with diffuse astrocytoma. Post-treatment, 16 patients developed CVAs in the course of a median of 82.3 months; 15 of these presented with multiple CVAs. Patients who underwent radiation therapy (RT) at an age younger than 6 years developed CVA significantly earlier than those treated at a later age (P = 0.0242). Patients with cerebral embryonal tumors developed Zabramski type 1 and 2 CVA significantly earlier than did medulloblastoma patients (P = 0.0007). CONCLUSION: We attribute the high rate of post-RT CVA in our long-term follow-up study of pediatric patients to the delivery of cranial irradiation for embryonal tumors, especially cerebral embryonal tumors, and recommend the regular, long-term follow-up of patients whose embryonal tumors were treated by cranial irradiation.

O-2-019　造影MRIのSURF特徴量を用いた膠芽腫と原発性中枢神経悪性リンパ腫の鑑別：診断困難例への応用可能性
Differentiation of glioblastoma and primary central nervous system lymphoma by using MR image-based speeded up robust features

國松　聡（東京大学大学院 医学系研究科 放射線医学講座）

Akira Kunimatsu[1], Kouhei Kamiya[2], Yuichi Suzuki[3], Yasushi Watanabe[3], Natsuko Kunimatsu[4], Kaoru Sumida[1], Akifumi Hagiwara[1], Harushi Mori[1]

[1]Department of Radiology, Graduate School of Medicine, The University of Tokyo, [2]Department of Radiology, The University of Tokyo Hospital, [3]Imaging Center, The University of Tokyo Hospital, [4]Department of Radiology, IUHW Mita Hospital

【要旨】病理学的に診断された膠芽腫と中枢神経悪性リンパ腫の頭部造影T1強調画像からspeeded up robust features (SURF) 特徴量を抽出し、両腫瘍の機械学習による判別を行った。典型的画像からなる教師データでは平均判別精度は0.98 [0.93-1.00] であったが、同じ識別器による非典型例の平均判別精度は0.34 [0.14-0.71] であった。

[Objective] To evaluate accuracy of a machine learning technique in differentiation between glioblastoma (GBM) and primary central nervous system lymphoma (PCNSL) by using MR-based speeded up robust features (SURF). [Materials and Methods] This was an IRB-approved, retrospective study and informed consent was waived. Forty-five cases of GBM and 16 cases of PCNSL were included. Contrast-enhanced, trans-axial, 2D spin-echo T1-weighted MR images (TR/TE (ms) = 400/minimum, FOV = 21.0 cm, matrix = 256 × 256, slice thickness = 5 mm) were used from among preoperative brain MR images acquired on a 3T system. Through a radiology report search, initial imaging diagnosis suggested PCNSL for five cases of GBM and GBM for two cases of PCNSL, and images of these seven atypical cases were designated as the test set. Out of the other 40 GBM cases kept for training, 14 cases were randomly chosen so that the number of images was balanced between GBM and PCNSL. As a result, 14 GBM cases and 14 PCNSL cases constituted the training set. SURF statistics were extracted on the largest enhanced area on post-contrast MR images of each case. K-means clustering and support vector machine algorithms were adopted to obtain a classifier between GBM and PCNSL with the training set. Finally, the test data were categorized with the classifier. [Results] The classifiers showed the average accuracy of 0.98 [0.93-1.00] in classifying the training set. However, the classifiers categorized the test set with the average accuracy of 0.34 [0.14-0.71]. [Conclusion] SURF-based classification may be feasible for differentiating GBM from PCNSL in typical cases but may offer limited accuracy in diagnosing atypical cases.

O-2-020　MRIを用いた膠芽腫患者におけるTERT遺伝子変異の予測
MR imaging for the prediction of TERT promoter mutations in patients with wild-type IDH1 Glioblastoma

山下　孝二（九州大学 臨床放射線科学分野）

Koji Yamashita[1], Akio Hiwatashi[1], Osamu Togao[1], Kazufumi Kikuchi[1], Ryo Somehara[1], Ryotaro Kamei[1], Ryusuke Hatae[2], Hiroshi Honda[1]

[1]Department of Clinical Radiology, Graduate School of Medical Sciences, Kyushu University, [2]Departments of Neurosurgery, Graduate School of Medical Sciences, Kyushu University

【要旨】TERT遺伝子変異を持つ膠芽腫患者は予後不良であり、MR画像にて遺伝子変異の有無を予測可能であるか検討。104名の膠芽腫患者に対して、拡散強調像および造影前後のT1強調像を用いパラメータを設定、また発生部位の違いをVBM解析にて比較した。遺伝子変異群は左島領域発生が多く画像診断の有用性が期待される。

Purpose: GBM patients with telomerase reverse transcriptase (TERT) mutations have a poor clinical outcome. Our purpose was to investigate whether TERT mutation status in GBM patients can be predicted using MR imaging.Materials and Methods: We retrospectively studied 38 patients with wild-type IDH1/wild-type TERT (IDHw/TERTw), and 66 patients with wild-type IDH1/mutant TERT (IDHw/TERTm). The mean (ADCmean) and 10th percentile (ADC10) ADCs within the enhancing portion of each tumor were measured using DWI data. The maximum necrosis area (NECarea) and percentage necrosis (%NEC) were obtained from with and without contrast-enhanced T1-weighted images. Each of the four parameters was compared between the two groups using the Kruskal-Warris test. In addition, voxel-based morphometry (VBM) analysis was performed to compare with the location of GBM occurrence. Results: NECarea was significantly higher in IDHw/TERTm than in IDHw/TERTw patients. VBM analysis showed significantly higher frequency of occurrence in the left insular region in IDHw/TERTm than in IDHw/TERTw patients ($p < 0.001$ uncorrected). Conclusion: Distribution analysis of GBM may be useful for predicting TERT mutation status.

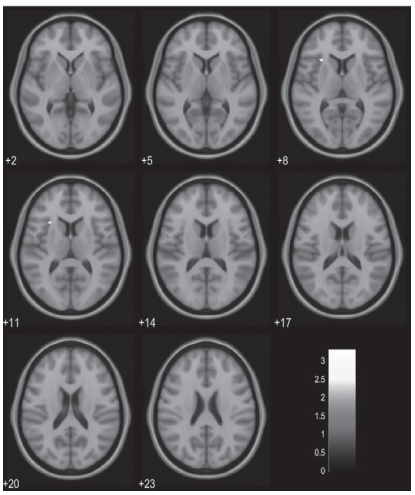

O-2-021　NSsaFe: Observational study on the incidence of Nephrogenic Systemic Fibrosis in patients with renal impairment following gadoterate meglumine administration

Bodo Kress, Andreas Gottschalk

Department of Neuroradiology, Krankenhaus Nordwest, Germany

Purpose: To determine the incidence of Nephrogenic Systemic Fibrosis (NSF) in patients with renal impairment after gadoterate meglumine (DOTAREM,Guerbet,France)administration.
Material and methods: Worldwide post-marketing study including hundreds of patients with at least moderate renal impairment scheduled to undergo a routine contrast-enhanced Magnetic Resonance Imaging (MRI) using gadoterate meglumine.At inclusion visit, medical history and indications for MRI were recorded for each patient.Adverse Events (AEs) occurring during MRI examination or usual follow-up period post-contrast agent administration were recorded. Patients were followed up over 2 years with 3 visits separated by at least 3 months in order to detect any signs of NSF.
Results:As of 16 March 2016, data of 540 patients were analyzed (mean age: 69.6 +- 12.7 years [min-max: 21-95]; male: 58.5%). Renal impairment was evaluated as moderate for 69.3% of patients, severe for 16.1% and end-stage for 12.0%; 2.6% of patients had undergone a previous kidney transplant. The mean (+-SD) estimated Glomerular Filtration Rate (eGFR) was 37.6 ± 15.7 ml/min/1.73 m2 [4.0-74.2].Main MRI indication was to assess suspected abnormalities of the central nervous system (34.6%). A total of 407 patients (97.4%) attended the first follow-up visit, 308 (73.7%) attended the second, and 222 (53.1%) attended the third. No AEs considered to be related to the administration of gadoterate meglumine were reported. No cases of NSF have been observed.
Conclusion: Intermediate data of the NSsaFe study show no cases of NSF after gadoterate meglumine administration in patients with at least moderate renal impairment. Data collected so far confirm the good safety profile of gadoterate meglumine in this high risk population.

O-2-022　Seronegative neuromyelitis opticaの一例
A case of seronegative neuromyelitis optica

森本　伶美（社会医療法人 仁生会 細木病院）
Remi Morimoto[1], Shino Kousaki[1], Kazuo Kitaoka[1], Tadashi Horimi[1], Masahiko Ikeuti[2], Naoto Oosawa[2], Hirokazu Furutani[2]

[1]Hosogi Hospital, [2]Kochi Medical School Hospital

【要旨】視神経脊髄炎の確定診断の根拠となる抗アクアポリン４抗体は約２割で陰性となり、seronegative NMOが存在することが知られている。確定診断にMRIが非常に有用であった、seronegative NMOの一例を経験したので、文献的考察を加えて報告する。

Neuromyelitis optica (NMO) typically occurs in middle- and old-aged women. It is an intractable neurological disease characterized by repeated patterns of spatiotemporal recurrence, remission, and exacerbation. In the past, NMO was considered a subtype of multiple sclerosis; however, the discovery of specific anti-aquaporin-4 antibodies has led to NMO being treated as a different pathology than typical multiple sclerosis. However, approximately 20% of cases are seronegative NMO, meaning that they are negative for the anti-aquaporin-4 antibodies that typically serve as the basis of a definite diagnosis. We experienced a case of seronegative NMO in which magnetic resonance imaging was extremely useful in providing a definite diagnosis. We report this case along with a review of the literature.

O-2-023　パーキンソン病および認知症を伴うパーキンソン病/レビー小体型認知症における海馬の磁化率変化: QSMの検討
Hippocampal susceptibility changes in Parkinson disease and Parkinson disease with dementia/Lewy body dementia: QSM assessment

宮田　真里（産業医科大学 放射線科）
Mari Miyata[1], Shingo Kakeda[1], Jyunji Moriya[1], Hidekuni Narimatsu[1], Toru Sato[1], Hiroaki Adachi[2], Yi Wang[3], Yukunori Korogi[1]

[1]department of radiology, university of occupational and environmental health, [2]department of neurology, university of occupational and environmental health, [3]department of biomedical engineering, Cornell university

【要旨】PD41例、PDD/DLB群17例、正常群14例を対象に、定量的磁化率マッピング (QSM) 冠状断像を用いて、海馬の3領域（内側、中間、外側）における磁化率値を測定した。結果、PD群と正常群に比べ、PDD/DLB群のQSM値は、海馬内側において有意に高値を示した。臨床所見との比較において、海馬内側の高いQSM値は幻視の存在に関連した。

PURPOSE: In a previous postmortem study, iron-containing microglia was present in hippocampal specimens in patients with Alzheimer disease. Therefore, we hypothesized that hippocampal iron deposition may also relate to developing dementia in patients with Parkinson disease (PD). We compared quantitative susceptibility mapping (QSM) values in the hippocampi among PD and patients with Parkinson disease with dementia (PDD)/ Lewy body dementia (DLB) and healthy controls (HC), and assessed clinical significance of hippocampal iron deposition in the PD and PDD/DLB.　MATERIALS AND METHODS: For 41 PD, 17 PDD/DLB, and 14 age/sex-matched HC, two radiologists independently evaluated the mean QSM values in the hippocampi, which were subdivided into three parts: external, middle, and internal parts on the coronal QSM images. The QSM values in each part were compared among three groups. In the PD and PDD/DLB, the correlations between the QSM values and the clinical characteristics (e.g., age, presence of dementia and hallucinaiton, Hoehn and Yahr scale) were evaluated using a binary logistics regression analysis.RESULTS: The QSM values in the middle and internal parts of hippocampi were signifucantly higher in PDD/DLB than in both PD ($p<.005$) and HC ($p<.001$), whereas there were no significant differences between PD and HC for QSM values in any parts. The multivariate analyses showed that high QSM values (>123: optimal cut-off value for QSM from receiver operator characteristic analysis) in the internal part of hippocampi were associated with the presence of hallucination in the PD and PDD/DLB ($p<.001$). CONCLUSION: The internal part of hippocampi in PDD/DLB, compared with that in PD, showed higher QSM values, which may be associated with the presence of hallucination.

O-2-024　進行性核上性麻痺の診断における定量的磁化率マップの有用性
Differentiation of Progressive Supranuclear Palsy from Parkinson Disease by Quantitative Susceptibility Mapping

東　美菜子（宮崎大学 医学部 放射線科）
Minako Azuma[1], Mika Kitajima[2], Kazumichi Yamada[3], Satoshi Yamashita[4], Mamoru Hashimoto[5], Manabu Ikeda[5], Yasuhiko Iryo[2], Yoshihito Kadota[1], Takanori Yano[1], Yasuyuki Yamashita[2], Toshinori Hirai[1]

[1]Department of Diagnostic Radiology, Miyazaki University, [2]Department of Diagnostic Radiology,Kumamoto University, [3]Department of Neurosurgery, [4]Department of Neurology, [5]Department of Neuropsychiatry

【要旨】定量的磁化率マップ（QSM）を用いて進行性核上性麻痺（PSP），パーキンソン病（PD）と健常者の脳内の鉄分布の定量評価を行い、PSPの診断におけるQSMの有用性を検討した。淡蒼球・黒質・赤核の磁化率において、PSPは、PD、健常者と比較し有意に高値を示した。QSMはPSPとPDの鑑別に有用と考えられ、診断の一助となり得る。

Purpose: The differentiation between progressive supranuclear palsy (PSP) and Parkinson's disease (PD) on conventional MR images is challenging, especially in the early stage of the disease. Quantitative Susceptibility Mapping (QSM) is a useful tool to assess the brain iron levels in patients with neurodegenerative diseases, particularly PD. We compared the susceptibility of the deep gray matters among PSP and PD patients and healthy controls (HC) to determine whether QSM can differentiate PSP from PD and HC.
Materials and Methods: With a 3T MR unit, QSM data were obtained from 9 patients with PSP, 18 patients with PD, and 18 age-matched HC. The clinical diagnoses were made by a neurologist and a psychiatrist based on the established consensus criteria for PSP and unified Parkinson disease rating scale for PD. We measured the mean susceptibility values (MSVs) in the bilateral deep gray matter including the globus pallidus (GP), red nucleus (RN), substantia nigra (SN), putamen (PT), and caudate nucleus (CN) in all participants. Measurement differences were assessed with one-way ANOVA and the post hoc test.
Results: The mean MSVs of GP, RN and SN were higher in PSP (300.3 ± 84.8 ppb, GP; 199.8 ± 113.5 ppb, RN; 238.4 ± 75.0 ppb, SN) than PD (160.4 ± 34.0 ppb, GP; 132.7 ± 41.4 ppb, RN; 151.6 ± 44.9 ppb, SN) and HC (183.5 ± 62.3 ppb, GP; 109.1 ± 20.7 ppb, RN; 109.0 ± 36.3 ppb, SN) ($p<0.05$). We found no statistically significant difference in the MSVs of the PT between PSP (122.7 ± 65.7 ppb) and HC (96.7 ± 16.1 ppb), and the CN among PSP (88.5 ± 46.7 ppb), PD (69.9 ± 25.9 ppb), and HC (72.0 ± 16.6 ppb).
Conclusion: QSM of the GP, RN, and SN may help to differentiate PSP from PD and HC.

O-2-025　瘤壁造影効果の定量評価：破裂-未破裂脳動脈瘤の比較
Quantitative assessment of intracranial aneurysm wall enhancement using magnetic resonance imaging

面高　俊介（白河厚生総合病院 脳神経外科）
Shunsuke Omodaka[1], Hidenori Endo[2], Kuniyasu Niizuma[3], Miki Fujimura[3], Takashi Inoue[4], Teiji Tominaga[3]

[1]Department of Neurosurgery, Shirakawa Kosei General Hospital, [2]Department of Neurosurgery, Kohnan Hospital, [3]Department of Neurosurgery, Tohoku University Graduate School of Medicine, [4]Department of Neurosurgery, Sendai Medical Center

【要旨】MRIにおける動脈瘤壁造影効果の定量評価を行った。造影性の指標となるWEIを算出し破裂瘤 (n=28) と未破裂瘤 (n=76) で比較した。WEI高値は有意に破裂瘤と関連していた。瘤壁造影効果を定量評価することで破裂瘤と未破裂瘤を識別できる可能性がある。

Background and Purpose: The incidence of wall enhancement of the cerebral aneurysms on MR vessel wall imaging has been described to be higher in ruptured intracranial aneurysms than in unruptured intracranial aneurysms, but the difference in the degree of enhancement between ruptured and unruptured aneurysms is unknown. We compared the degree of enhancement between ruptured and unruptured intracranial aneurysms using MR quantitative measures.Materials and Methods: We performed quantitative analyses of circumferential enhancement along the wall of the cerebral aneurysms in 28 ruptured and 76 unruptured consecutive cases using MR vessel wall imaging. A 3-dimensional T1-weighted fast spin-echo sequence was obtained before and after contrast media injection, and the wall enhancement index (WEI) was calculated. We then compared characteristics between ruptured and unruptured aneurysms.Results: The WEI was significantly higher in ruptured than in unruptured aneurysms (1.70 ± 1.06 versus 0.89 ± 0.88, respectively; P=0.0001). The receiver-operating characteristic curve analysis found that the most reliable cutoff value of the WEI to differentiate ruptured from unruptured aneurysms was 0.53 (sensitivity, 0.96; specificity, 0.47). The WEI remained significant in the multivariate logistic regression analysis (P<0.0001). Conclusions: Greater circumferential enhancement along the wall of the cerebral aneurysm correlates with the ruptured state. A quantitative evaluation of circumferential enhancement using MR vessel wall imaging could be useful in differentiating ruptured from unruptured intracranial aneurysms.

O-2-026　硬膜動静脈瘻経静脈的塞栓術前における造影 3D SPGRと3D time-resolved MRAの有用性
Usefulness of CE 3D SPGR and TRICKS in the estimation of occluded dural sinus for transvenous embolization of dural arteriovenous fistulas

森川　　実（長崎大学病院 放射線科）
Minoru Morikawa[1], Hideki Ishimaru[1], Reiko Ideguchi[1], Nobutaka Horie[2], Takayuki Matsuo[2], Masataka Uetani[1]

[1]Nagasaki University Hospital, Department of Radiology, [2]Nagasaki University Hospital, Department of Neurosurgery

【要旨】横洞-S状静脈洞部硬膜動静脈瘻14例中9例で静脈洞が閉塞か殆ど閉塞し、閉塞部を介した経静脈的塞栓術を要した。造影3D SPGRでは閉塞部位に増強効果認めたが、増強不良部位が混在した4例はカテーテル誘導困難で、その予測に有用と考えられた。造影3D time-resolved MRAは閉塞部の描出に優れていた。

PURPOSE: This study aimed to evaluate the usefulness of contrast-enhanced 3D SPGR (CE SPGR) and 3D dynamic time-resolved CE MRA (TRICKS) in the estimation of transverse-sigmoid (TS) sinus with complete or near occlusion for the endovascular treatment using transvenous embolization (TVE). METHOD AND MATERIALS: Between January 2008 and Dec 2015, we treated 14 patients of TS-dAVF. We retrospectively evaluated the MR imaging findings in 24 occluded venous segments of the 14 patients with T1WI, T2WI, TOF MRA, CE SPGR and TRICKS. RESULTS: 9 of the 14 patients were performed TVE via occluded or near occluded sinuses. Venous access via these sinuses was easy in 5 of the 9 patients, and was difficult in the remaining 4 patients. Most occluded segments were enhanced equal to or greater than normal venous sinuses. Heterogeneous enhancement including poorly enhancing portion were observed in 12 segments on CE SPGR, and these findings were correlated with the venous access difficulty in the 4 patients. TRICKS clearly demonstrated thrombosed segment in comparison with other MR sequences. CONCLUSION: Occluded sinuses filled with chronic thrombosis have a characteristic appearance on CE SPGR, and TRICKS. Poorly enhancing portion in occluded sinuses on CE SPGR may represent organized fibrotic thrombus, and can be helpful for estimating difficulty of passing venous access route. Combined CE SPGR and TRICKS findings are useful for searching the route to shunting point of TS-dAVF.

O-2-027　脳梗塞急性期症例におけるMRSによる脳温経時的評価
Serial change of brain temperature measured using magnetic resonance spectroscopy in patients with ischemic stroke

石田　朋久（さいたま赤十字病院 脳外科）
Tomohisa Ishida[1], Takashi Inoue[2], Hidenori Endo[3], Ryo Itabashi[4], Nobuo Noshita[1], Toshie Takahashi[1], Kuniyasu Niizuma[5], Miki Fujimura[5], Teiji Tominaga[5]

[1]Department of Neurosurgery, Saitama Red Cross hospital, [2]Department of Neurosurgery, Sendai Medical Center, [3]Department of Neurosurgery, Kohnan Hospital, [4]Department of Stroke Neurology, Kohnan Hospital, [5]Department of Neurosurgery, Tohoku University

【要旨】脳温は脳循環代謝を反映する。脳梗塞急性期5症例においてMRSで経時的に脳温を測定した。脳温の経時的変化と脳浮腫増悪には関連が見られた。今後MRSにて脳温を測定することにより、臨床転帰改善がはかれる可能性が示唆された。

Object. The brain temperature at rest is determined by the balance between heat produced by cerebral energy turnover, which is identical to cerebral metabolism, and heat that is removed, primarily by cerebral blood flow. The present study investigated that serial change of brain temperature measured by proton magnetic resonance (MR) spectroscopy in patients with ischemic stroke. The relationship between the brain temperature and the edema were also estimated. Methods. Brain temperature was measured using proton MR spectroscopy in five patients with major cerebral artery occlusion at least twice (first MR spectroscopy was done within 24 hours). Regions of interest were selected in infarct area and in the corresponding contralateral region. Single voxel MR spectroscopy was performed with the following parameters: TR 2000 ms, TE 136 ms, and 128 excitations. The brain temperature was calculated from the chemical shift between NAA/Cho/Cre and water using original software.Results. Brain temperature in ischemic lesion within 48 hours was decreased compared with contralateral region in three patients, and increased in the other two patients. The brain edema was aggravated in two patients, and their brain temperature was serially decreased. Three patients who did not decreased brain temperature did not show severe brain edema.Conclusion. The serial brain temperature change measured by proton MR spectroscopy can be related with the brain edema in patients with major cerebral artery occlusive disease. Large number of investigations regarding the relationships between brain temperature and clinical feature in patients with ischemic stroke is needed.

O-2-028　定量的磁化率マッピング（QSM）を用いた乳児軸索ジストロフィの評価
Quantitative susceptibility mapping (QSM) evaluation of Infantile neuroaxonal dystrophy: a case report

藤原　拓也（大阪大学大学院 医学系研究科 放射線統合医学講座 放射線医学教室）
Takuya Fujiwara[1], Yoshiyuki Watanabe[1], Hisashi Tanaka[1], Hiroto Takahashi[1], Atsuko Arisawa[1], Shin Nabatame[2], Yi Wang[3], Noriyuki Tomiyama[1]

[1]Diagnostic and Interventional Radiology, Osaka University Graduate School of Medicine, [2]Pediatrics, Osaka University Graduate School of Medicine, [3]Biomedical Engineering, Cornell University

【要旨】乳児軸索ジストロフィ (INAD) は淡蒼球、黒質への鉄沈着を認めることが特徴である。今回QSMで鉄沈着を評価した双胎児のINAD2例を経験したので報告する。症例は6歳の男児 (双胎児)。MRI T2*強調像で淡蒼球、黒質に低信号域を認めた。淡蒼球、黒質のQSM値の平均はでそれぞれ0.19, 0.29ppmであった。弟もほぼ同様の所見であった。

(Background and Purpose)Infantile neuroaxonal dystrophy (INAD) is a neurodegenaration with brain iron accumulation (NBIA) disorder, and inherited as an autosomal recessive trait. Most patients with INAD have a mutation in the PLA2G6 gene. The symptoms such as psychomotor regression, ataxia, hypotonia, optic atrophy, and seizure appear between the ages of 6 months and 2 years. The characteristic MRI findings are low intensity areas in globus pallidus (GP) and substantia nigra (SN) on T2* weighted image. To the best of our knowledge, evaluation of INAD using quantitative susceptibility mapping (QSM) has never been reported. We present the first case of twin patients with INAD evaluated using QSM.(Case)A 6-year-old boy who was normal at birth had psychomotor regression and hypotonia at 2 years old. Conventional MRI showed slight cerebellar atrophy with normal signal intensity, and low intensity areas in GP and SN on T2* weighted image. QSM values of GP and SN were 0.19 and 0.29 ppm, respectively. His twin brother showed almost the same symptoms and imaging findings. QSM values were the same (GP is 0.19, SN is 0.29 ppm). PLA2G6 gene mutation was identified from the patients and their parents, which confirmed the diagnosis of INAD. In healthy control children, QSM values of GP and SN were 0.10 and 0.10 ppm, respectively.(Conclusion)QSM suggests marked iron deposition in globus pallidus and substantia nigra.

O-2-029　パーキンソン病の黒質線条体神経線維の神経突起イメージングによる評価
Neurite Orientation Dispersion and Density Imaging (NODDI) of Nigrostriatal Pathway in Parkinson Disease

中澤　美咲（首都大学東京人間健康科学研究科放射線科学域）
Misaki Nakazawa[1,2], Christina Andica[2], Koji Kamagata[2], Ryo Ueda[1,2], Sho Murata[2], Taku Hatano[2], Ayami Okuzumi[2], Osamu Abe[3], Michimasa Suzuki[2], Masaaki Hori[2], Kanako Kumamaru[2], Nobutaka Hattori[2], Shigeki Aoki[2]

[1]Department of Radiological Sciences, Graduate School of Human Health Sciences, Tokyo Metropolitan University, [2]Juntendo University School of Medicine, [3]Department of Radiology, Nihon University School of Medicine

【要旨】本研究ではパーキンソン病（PD）の黒質線条体神経線維を神経突起イメージングにより評価を行い、健常群と比較した。その結果、PD群で有意にIntracellular volume fraction（神経線維の密度を反映する）が有意に低下しており、PD診断に有用な可能性が示された。

Background: Parkinson disease (PD) is a movement disorder caused by the degeneration of dopaminergic neurons of the substantia nigra pars compacta (SNc) projecting to the corpus striatum, called nigrostriatal tract. Previous studies had used diffusion tensor imaging (DTI) to examine nigrostriatal degeneration, but they were unable to attain sufficient diagnostic accuracy and reliability to justify DTI in clinical practice. We applied neurite orientation dispersion and density imaging (NODDI) in PD patients to examine the nigrostriatal tract compared with healthy individuals.
Methods: This study involved 5 PD patients and 5 age and sex-matched healthy controls. MR Scanning was performed on a 3.0T Philips Achieva system. NODDI DWI protocol: TR: 9810ms, TE: 100ms, resolution: 2mm × 2mm, slice thickness: 2mm, b-value: 0, 1000, 2000[s/mm^2], MPG: 32 directions. DWI analysis: NODDI fitting was performed with the NODDI Matlab Toolbox. Maps of Vic (intra cellular volume fraction), ODI (orientation dispersion index) were generated. For comparison standard DTI parameter map of FA was derived from the same dataset, using only the b=0 and b=1000s mm2 acquisitions. Tractography of the nigrostriatal tract was performed using Diffusion Toolkit. Unpaired t-test was used to compare mean FA, Vic, and OD values of nigrostriatal tract from PD group and control group. All resulting P values were corrected with the Bonferroni method.
Results: Vic in the nigrostriatal tract was significantly lower in PD patients than in healthy controls (P=0.0053). There were no significant FA (P=0.11) and OD (P=0.78) differences among the groups.
Conclusion: NODDI can detect alterations of the nigrostriatal tract in PD patients more sensitively and specifically than conventional diffusion tensor imaging.

O-2-030　NODDIを用いた視神経脊髄炎におけるNormal-appearing White Matterの検討
Application of Neurite Orientation Dispersion and Density Imaging for Normal-appearing White Matter in Neuromyelitis Optica

高村　朋宏（山梨大学医学部放射線科）
Takamura Tomohiro[1], Shou Murata[2], Koji Kamagata[2], Masaaki Hori[2], Michimasa Suzuki[2], Shigeki Aoki[2]

[1]Department of Radiology, University of Yamanashi, [2]Department of Radiology, Juntendo University School of Medicine

【要旨】NODDIとDTIで得られる従来の拡散指標を用いて、NMOにおけるwhite matter lesion, perilesion, normal appearing white matterの微細構造変化を評価した。NODDIを用いて従来の拡散指標に加えたさらなる白質障害の詳細な解釈ができると考えられる。

(Purpose)To investigate the microstructural disruption in neuromyelitis optica (NMO) in lesional tissue, perilesional tissue and normal appearing white matter (NAWM) compared to healthy controls by applying NODDI and standard DTI images. (Materials and Methods)Nineteen NMO patients and 19 age- and sex- matched controls were included in this study. Diffusion data were acquired on a clinical 3T-MRI scanner (Philips Medical systems). NODDI image were computed by applying diffusion-weighted images with b = 0, 1000, 2000 sec/mm2. Standard DTI parameter maps were derived from the same dataset, using only the b = 0 and b = 1000 sec/mm2. White matter was segmented on the T1WI by using SPM12 software. ROIs of lesion were automatically marked with LST software which is based on a lesion growth algorithm, using FLAIR and T1WI. To create ROIs of perilesion, the lesion was dilated 12 mm, then dilated lesion was subtracted from the diameter of the original lesion. ROIs of NAWM was generated by subtracting the lesion and perilesion masks from the whole WM masks. Finally, created ROIs were non-linearly registered from T1WI to b0-image of each subject with SPM12. Steel-Dwass test was employed for statistics.(Result)Lesions and perilesions showed significantly increased AD, RD, MD compared with HCWM and NAWM. Significant lower FA of perilesions were also observed compared with that of HCWM and NAWM. In NODDI, ICVF and ODI were significantly reduced in lesions compared to HCWM and NAWM. ICVF of perilesion was also significantly lower than NAWM, whereas ODI of perilesion was significantly higher. Moreover, only ODI detects significant differences between HCWM and NAWM. (Conclusion)NODDI provides additional value by disentangling neurite density and orientation dispersion in NMO pathology.

O-2-031　Machado-Joseph 病の神経メラニンイメージング
Neuromelanin-sensitive MR imaging of Machado-Joseph disease

越智　誠（長崎北病院 放射線科）
Makoto Ochi[1], Yoko Nakao[2], Akira Satoh[2], Makiko Seto[2], Mitsuhiro Tsujihata[2]
[1]Department of Radiology, Nagasaki Kita Hospital, [2]Division fo Neurology, Department of Internal Medicine, Nagasaki Kita Hospital

【要旨】Machado-Joseph 病(MJD)8例の神経メラニンイメージングを撮像し，黒質緻密部の信号強度を測定し，上小脳脚交叉とのコントラスト比を算出した．MJD群のコントラスト比は 0.154±0.018，コントロール群は 0.240±0.025 で，MJD群では有意に低下していた．

Objective: To evaluate efficacy of neuromelanin-sensitive MR imaging in the diagnosis of Machado-Joseph disease (MJD).
Materials and Methods: We obtained neuromelanin-sensitive T1-weighted MR images using 3.0 T clinical MR system (GE Signa HDx 3.0T). The following sequence was used to obtain neuromelanin-sensitive image: T1-weighted fast SE: repetition time/effective echo time, 600/14; slice thickness, 2.4 mm; intersection gap, 1.0 mm; acquisition matrix, 512 x 320; field of view, 220 mm; number of excitation, 8; and acquisition time, 2 min 51 sec. We examined 8 patients with MJD, 3 women and 5 men, age range 25-55 years. All of them were diagnosed genetically or patients in families with genetically confirmed MJD. Control subjects included 8 women and 2 men, age 49-86, whose dopamine transporter SPECT and cardiac Iodine-123 MIBG imaging were normal. The signal intensities of the area corresponding to the substantia nigra pars compacta were measured and the contrast ratios to the adjacent decussation of superior cerebellar peduncles were calculated.
Results: Contrast ratio of patients with MJD and control subjects were 0.154±0.018 and 0.240±0.025, respectively. Contrast ratio of patients with MJD was significantly lower than that of control subjects (P<0.001).
Conclusions: Neuromelanin-sensitive MR imaging demonstrated a significant decrease in contrast ratio of substantia nigra in patients with MJD. Neuromelanin-senetive MR imaging might have potential clinical efficacy in the detection of pathological lesions in MJD.

O-2-032　髄鞘と浮腫の状態を評価するマルチパラメトリック定量MRIによる多発性硬化症患者における白質障害の評価
A multi-parametric quantitative MRI model that assesses myelin and edema for evaluating white-matter damage in patients with multiple sclerosis

萩原　彰文（東京大学大学院 医学系研究科 放射線医学講座）
Akifumi Hagiwara[1,2], Masaaki Hori[2], Misaki Nakazawa[2,3], Christina Andica[2], Mariko Yoshida[2], Michimasa Suzuki[2], Nao Takano[2], Hideo Kawasaki[2], Nozomi Hamasaki[2], Shuji Sato[2], Shigeki Aoki[2]
[1]Department of Radiology, Graduate School of Medicine, The University of Tokyo, [2]Department of Radiology, Juntendo University School of Medicine, [3]Department of Radiological Sciences, Tokyo Metropolitan University

【要旨】ミエリン（V_{MY}）と浮腫（V_{EPW}）の状態を評価するマルチパラメトリック定量MRIを用いて、多発性硬化症患者におけるプラーク、ペリプラーク、正常に見える白質（NAWM）を測定した。マルチパラメトリック定量MRIは白質の損傷状態を評価するのに有用であり、V_{MY}とV_{EPW}はR1・R2・プロトン密度（PD）よりもその感度は高かった。

OBJECTIVES: To evaluate a multi-parametric quantitative MRI model that assesses myelin and edema for characterizing plaques, periplaque white matter (PWM), and normal-appearing white matter (NAWM) in patients with multiple sclerosis (MS).
METHODS: We examined 3.0-T quantitative MRI data from 21 MS patients. The myelin partial volume (V_{MY}), excess parenchymal water partial volume (V_{EPW}), R1, R2, and proton density (PD) were compared among plaques, PWM, and NAWM (Fig).
RESULTS: All metrics differed significantly across the three groups ($p < 0.001$). Those in plaques differed most from those in NAWM. The percentage changes of the metrics in plaques and PWM relative to NAWM were significantly more different from zero for V_{MY} (-61.59 ± 20.28% (mean ± SD) [plaque relative to NAWM] and -10.51 ± 11.41% [PWM relative to NAWM]) and V_{EPW} (13.82 × 10^3 ± 49.47 × 10^3% and 51.33 × 10^2 ± 155.31 × 10^2%) than for R1 (-35.23 ± 13.93% and -6.08 ± 8.66%), R2 (-21.06 ± 11.39% and -4.79 ± 6.79%), and PD (23.37 ± 10.30% and 3.37 ± 4.24%).
CONCLUSION: Multi-parametric quantitative MRI captures white-matter damage in MS. V_{MY} and V_{EPW} are more sensitive to the MS disease process than are R1, R2, and PD.

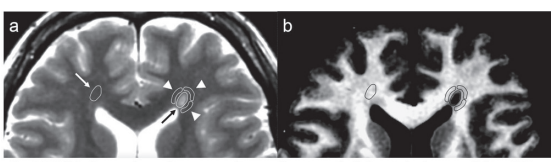

Fig. A ROI (black arrow) was drawn on a plaque adjacent to the left anterior horn, and three ROIs (arrowheads) were placed on periplaque white matter (PWM) to encircle the plaque on T2-weighted image (a). The ROI of the plaque was copied and pasted onto the contralateral normal-appearing white matter (NAWM) (white arrow). These ROIs were then copied and pasted onto each quantification map. A map of the corresponding myelin partial volume V_{MY} (b) is shown as an example.

O-2-033　Simultaneous Multi-Slice (SMS) を使用したEPIシーケンスの時間分解能向上
Improvement of time resolution with EPI sequence using Simultaneous Multi-Slice (SMS)

竹丸　輝政（シーメンスヘルスケア株式会社 カスタマーサービス事業本部 アプリケーション部）
Terumasa Takemaru, Takashi Ueda, Yoshito Ichiba, Tsubasa Kaji, Kanae Yamamoto
Siemens Healthcare K.K., Customer Service Division, Application Department

【要旨】EPIシーケンスにおいて複数スライスを同時に励起するSimultaneous Multi-Slice (SMS)を開発し製品化した。SMS技術を使用することでTRが短縮し時間分解能が向上する。fMRIとDTIでg-factorの増加が見られたが、視覚的には劣化はなく高い画質が得られた。時間分解能が向上しfMRI解析においてBOLD効果の向上が見られた。

BACKGRAUND AND PURPOSE:To acquire whole brain images with high spatialresolution in functional MRI (fMRI) and Diffusion Tensor Imaging (DTI) using EPI sequence, number of slice must be increased. Increment of number of slice causes increase of TR, prolong scan time and decrease time resolution. We developed Simultaneous Multi-Slice (SMS) that enable to excite multi-slice simultaneous, and released product version. SMS can decrease TR and increase time resolution. We report fMRI and DTI using SMS with product version in this study.METHODS: We evaluated image quality of fMRI and DTI with SMS and without SMS in phantom scan and healthy volunteer scan at MAGNETOM Skyra 3T- MRI (Siemens Healthcare, Erlangen, Germany). SMS factor is changed from 0 to 2, GRAPPA factor is changed from 0 to 2. In each combination, we evaluate g-factor and visual image quality. Also, we do fMRI post processing and DTI post processing to EPI image with short TR using SMS, and then compared it from no-SMS data.RESULTS AND DISCUSSIONg-factor was increased but not deteriorated visual image quality in EPI image with SMS. By using SMS, time resolution was increased in fMRI and we confirmed improvement of BOLD effect. Scan time can be shot by decrease TR in DTI.

O-2-034　人工知能を用いた脳形状画像解析：Alzheimer's disease scoreの開発
Brain morphometric analysis using artificial intelligence: Development of Alzheimer's disease score

椎野　顯彦（滋賀医科大学 神経難病センター）
Akihiko Shiino[1], Yutaro Iwamoto[2], Chen Yen-Wei[2]
[1]Shiga University of Medical Science, Molecular Neuroscience Research Center, [2]Ritsumeikan University, College of Information Science and Engineering

【要旨】Voxel-based morphometryを用いた脳の形状解析でsupport vector machineを用いた人工知能による診断補助プログラムを開発した。学習には北米のADNIのデータを用い、オーストラリアのAIBLでの予測制度を検討した。結果、ADの予測精度は86.2%、感度88.0%、特異度85.9%、オッズ44.6であった。

We studied an availability of artificial intelligence (AI) based on support vector machine (RBF kernel) for diagnosis of Alzheimer's disease (AD).
VBM was performed by CAT12 and spm12, and z values of the AAL ROIs were calculated by BAAD software. Data on 331 patients with AD and 372 normal subjects, who had undergone structural MRI (sMRI) in ADNI study at North America, were used as training set. Data on 131 AD patients and 404 normal subjects in Australian AIBL study were used as application set. In machine learning, we used radial basis function (RBF) kernel and compute optimal cost parameter "C" and slack variable in discrimination of AD and normal subjects using z values of the AAL ROIs. For the efficient tuning was done by a procedures based on minimization of radius/margin and span bound for leave-one-out errors.
In the training phase, the accuracy, sensitivity, and specificity were 88.6%, 86.4% and 90.8%, respectively. In the application phase, those results were 86.2%, 88.0% and 85.9%, respectively, which was showing very nice ability of AD discrimination from sMRI.
We applied an AI program to BAAD software, and showed the availability of diagnostic tool for AD patients.

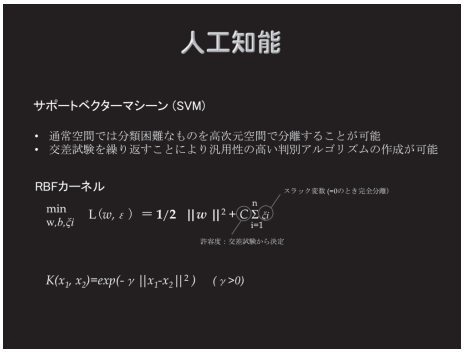

O-2-035　DBS患者に対するSARを考慮した頭部および頸髄MR撮像プロトコルの検討
Evaluation of Cerebral and Cervical MR Scan Designs for DBS Patients within SAR Limits

鈴木　智明（名古屋セントラル病院 中央放射線室）
Tomoaki Suzuki[1], Tomoki Nishihata[1], Teruhisa Ohno[1], Tsutomu Minoura[1], Takumi Kuwahara[1], Shigenori Takebayashi[2]

[1]Department of Radiological Technology, Nagoya Central Hospital, [2]Division of Neurosurgery, Nagoya Central Hospital

【要旨】B_{1+RMS}非表示の1.5テスラMR装置で脳深部刺激療法（DBS）患者のMR検査を行う場合、平均SARが0.1W/kg以下の設定で撮像する必要がある。我々は上記MR装置における脳および頸髄MR撮像プロトコル（各々撮像時間は30分を超えない）を検討した。

Purpose: In case of a magnetic resonance (MR) system did not display B_{1+RMS}, it is necessary to create a protocol for patients with deep brain stimulators (DBS) within specific absorption rate (SAR) limits of 0.1W/kg. The purpose of our study is to evaluate cerebral and cervical MR scan designs for DBS patients in the system.
Methods: Several preliminary scans were performed as follows: One healthy volunteer (man, 70.0kg) was imaged using a receive head coil and spine coil at 1.5 Tesla MR System (Signa HDxt Optima Edition, GE Healthcare, Milwaukee, WI, USA). MR scanning time was set to less than 30 minutes in total by adjusting TR and flip angles within the limits. Thick-slice coronal sequences utilizing fast spin-echo (FSE) T_2-weighted and T_2 fast fluid-attenuated inversion recovery (T_2 FLAIR)-weighted were modified from 3D-Cube (GE Healthcare, Milwaukee, WI, USA) sequence. One DBS patient who had undergone cervical MR scan was evaluated by expert neurosurgeon in DBS surgeries.
Results: Multi-slice FSE technique was almost all over the limits. T_2-star (T_2^*) sequence was substantially low SAR. Therefore, T_2-weighted images were replaced by T_2^*-weighted images except for Cube images. The designs were as follows: Cerebral MR Scan; diffusion-weighted imaging (DWI), 3D vascular time-of-flight (TOF) imaging, T_1-weighted imaging, and Cube (-T_2-weighted or -T_2 FLAIR-weighted) imaging: Cervical MR Scan; T_1-weighted imaging, and T_2^*-weighted imaging. Replaced T_2^*-weighted images had adequate contrast to identify structures of hernia.
Conclusion: We demonstrated diagnostic quality of cerebral and cervical MR scan designs for DBS patients within SAR limits.

O-2-036　Variable refocusing flip angleを用いた3D FSE法の撮像パラメータがT1強調画像コントラストに与える影響
Effect of three-dimensional fast spin-echo method imaging parameters using variable refocusing flip angle on T1-weighted image contrast

塚本　一真（独立行政法人国立病院機構 四国こどもとおとなの医療センター 放射線科）
Kazuma Tsukamoto[1], Fukuhiro Kagawa[2], Yusaku Yamaguchi[1]

[1]Department of Radiology , National Hospital Organization Shikoku Medical Center for Children and Adults, [2]Takamatsu Gazo Shindan Clinic

【要旨】VRFAを用いた3D FSEの撮像パラメータによるT1コントラストの変化について検討を行った。MAGNETOM Aera 1.5Tにて自作ファントムを撮像し、コントラストを求めた。検討項目はTR、TE、Tarbo Facter、Exitation、Magn. preparetion。SE法、FSE法で一般的に知られているものとは異なる知見が得られたため考察を行った。

Purpose:
Sampling perfection with application optimized contrast using different flip angle evolution (SPACE) is a three-dimensional fast spin-echo imaging sequence that uses a variable refocusing flip angle (VRFA) and is capable of imaging thin slices. While SPACE is considered effective for detecting small lesions in the pituitary and other glands, it is inadequate for verifying the contrast of T1-wieghted images. The purpose of this report was to verify the effects of the imaging parameters on the contrast of T1-weighted SPACE images.
Equipment Used:
MAGNETOM Aera 1.5T (SIEMENS), Head/Neck 20 Coil, self-made phantom (white-matter phantom: T1 value 760 ms, grey-matter phantom: T1 value 980 ms, saline-filled phantom)
Method:
In the flip angle mode, SPACE was set in T1var, and the self-made phantom was imaged while measuring the contrast of the white-matter and gray-matter phantoms, the white-matter and saline filled phantoms, and the gray-matter and saline-filled phantoms. TR, TE, Turbo Factor (TF), Excitation, Magn. preparation were used, and images were obtained for each by changing the basic criteria of each item individually. The resulting contrast measurement results were evaluated using a t-test as a significant difference check.
Results:
As TR increased, the contrast also increased, and a significant difference of $p < 0.01$ was confirmed. However, with TE, no significant difference in contrast was confirmed within the limits of this test. In addition, as TF increased, the contrast decreased, and a significant difference of $p < 0.01$ was confirmed. For Excitation, slab-sel. was $p < 0.01$, and the contrast was significantly high. For Magn. preparation, $p < 0.01$, and None had the highest contrast of all.

O-2-037　FBI法における超音波検査用ゼリーを用いたB1不均一の改善および画質改善の試み
Improvement of B1 inhomogeneity in the arterial visualization of FBI using ultrasound gel

的場　博輝（社会医療法人 共愛会 戸畑共立病院）
Hiroki Matoba[1], Akiyoshi Yamamoto[1], Yuuya Kuroki[1], Daiji Uchiyama[1], Seigo Yoshida[1], Katsumi Nakamura[1], Mitsue Miyazaki[2]

[1]Tobatakyouritsu hospital, [2]Toshiba Medical Research Institute USA

【要旨】3T装置を用いたFBI法では、しばしば被験者の体型によってB1の不均一性が主な原因と思われる画質の劣化が発生することがある。この問題に対処するために超音波検査用ジェルを用いた誘電パッドを作成して撮像に用いた。それらの画質を評価した結果、B1不均一性の改善による画質改善の可能性が示唆された。

[PURPOSE] To evaluate efficacy of a homemade ultrasound-gel (US-gel) dielectric pad to adjust the B1 inhomogeneity, causing the image degradation of peripheral non-contrast FBI MRA at 3T.[MATERIALS and METHODS] The effect of US gel pad for improvement in the visualization of femoral arteries was evaluated in six healthy volunteers using a 4-point grading subjective evaluation by four technologists, and contrast ratio index (CRI) of femoral artery to vastus medialis muscle was calculated as follows; CRI=(rFSI)-(lFSI)/(mSI). Acquisition parameters of FBI using 3D FASE were as follows; TR 3-4RR,TE 60ms, slice thickness 3mm, FOV 37cmX37cm, matrix 256X256, and parallel imaging 2. US-pad thickness was 20 x 15 cm with 2 thickness.[RESULTS] CRI of femoral arteries was 142 with no pad, 0.77 with one pad, and 0.52 with two pads. Subjective score was 1.7 ± 0.5 with no pad, 2.7 ± 0.5 with one pad, 3.2 ± 0.4 with two pads. The signal difference between the left and right femoral arteries was smallest and the visualization of the left femoral artery improved using two US-gel pads. However, it has to consider the size and thickness of pad, and the position of pad according to patient's body size and shape. [CONCLUSION] The US-gel pad improves the RF power penetration under the condition of B1 inhomogeneity and thus further advances the visualization of the left femoral artery in the FBI peripheral examination at 3T.

O-2-038　閾値ベース磁気共鳴セグメンテーション・アルゴリズムによる肉柱構造が肺、体及び単右心室容量に及ぼす影響
Impacts of the pulmonary, systemic and single right ventricular trabeculations on volume assessed by threshold-based segmentation MR algorithm

稲毛　章郎（榊原記念病院小児循環器科）
Akio Inage[1], Naokazu Mizuno[2], Jun Matsuda[2]

[1]Division of Pediatric Cardiology, Sakakibara Heart Institute, [2]Department of Radiology, Sakakibara Heart Institute

【要旨】右室心筋は緻密な左室に比し緻密性に欠き、特殊な肉柱と乳頭筋構造を有している。そのため右室の容量解析をする際、これらの構造物の取扱いにより計測値にかなりの差異を生じてしまう。今回、閾値ベースの磁気共鳴セグメンテーション・アルゴリズムを使用し、肺右心室、体右心室及び単右心室の真の容量について検討した。

Objective: To assess impacts of the right ventricular (RV) trabeculae and papillary muscles on measured function and blood flow in pulmonary, systemic and single right ventricle by cardiac magnetic resonance imaging (CMR) using new algorithm excludes trabeculations from the blood pool.
Method: We retrospectively examined three groups of patients. Those in group 1 included pulmonary right ventricle (TOF), group 2 included systemic right ventricle (ccTGA, dTGA following atrial switch procedure), and group 3 included systemic single right ventricle (Fontan circulation). We measured RV myocardial mass (RV mass), end-diastolic and end-systolic volume (RVEDV and RVESV) and stroke volume (RVSV) by CMR using standard approach and segmentation algorithm. Also, we measured net pulmonary artery forward flow volume (PAFV) as RVSV in group 1 and net ascending aorta forward flow volume (AoFV) as RVSV in group 2 and 3 using phase contrast MR imaging.
Results: There were 15 cases each of group and the mean age was 25+/-13 years. The systemic RV mass in group 2 and 3 were more hypertrophied than pulmonary RV mass in group 1 ($p<0.05$). By excluding trabeculations in the RV blood volume, RVEDV, RVESV and RVSV in group 2 and 3 were more decreased than it in group 1 ($p<0.005$). RVSV by PAFV in group 1 and AoFV in group 2 and 3 were more related ($r=0.58$ to 0.72) with value measured by segmentation algorithm rather than standard approach.
Conclusion: Excluding trabeculae and papillary muscle significantly affect measured pulmonary, systemic and single RV volumes. We highly recommended this novel method for measurement of true RV function and blood volume.

O-2-039　PAD患者のFBIと血管造影の比較
Can sufficient pretreatment information of peripheral artery disease be obtained by Non-contrast MR Angiography Fresh Blood Imaging ?

沖川　隆志（済生会熊本病院 中央放射線部）
Takashi Okigawa[1], Akira Sasao[2], Takeshi Ohta[1], Satomi Tajiri[1], Miho Kitamura[3], Masahiro Kosaka[3], Mitsue Miyazaki[3], Hiroyuki Hazeyama[1], Suguru Kawamura[1], Daisuke Masuda[1], Megumi Katayama[1], Hirofumi Wada[1]

[1]Department of Radiology, Saiseikai Kumamoto Hospital, [2]Department of Radiology, Tamana Central Hospital, [3]Toshiba Medical Systems Corporation

【要旨】末梢血管疾患の狭窄部をFBIと血管造影の血管描出能を比較検討した。対象患者はPADが疑われた20例。(平均年齢74歳、期間 2006年8月から2015年8月)を対象とした。使用機器東芝製1.5テスラMRI装置、血管狭窄部の描出能のは両者で同等であり、FBIはPAD患者の評価において有用な撮像法である。

PURPOSE: Contrast Enhancement Angiography is used as a technique in peripheral artery disease imaging. However, it requires chelated contrast material, which associates with some risk and cost. The aim of this study is to evaluate the Non-contrast MRA Fresh Blood Imaging (FBI) sequences on the patients with peripheral artery disease (PAD) as compared to conventional Angiography. MATERIALS AND METHODS: FBI studies were performed at 1.5T-MRI(EXCELART Vantage XGV; Toshiba Medical ,Japan) , in 20 consecutive patients with PAD; (mean age 74 years) were enrolled between August 2006 and August 2015. Before 3D acquisition, ECG preparation images were acquired to determine the appropriate diastolic and systolic ECG delay times. Both diastolic and systolic ECG-triggered 3D data were acquired with the same conditions. All patients were diagnosed PAD with conventional Angiography and trans catheter angioplasty after the MRI study. Two radiologists independently evaluated the degree of artery stenosis on FBI and conventional Angiography. Inter observer agreement was determined by κstatistics.RESULTS: In overall quality of FBI and conventional Angiography, no images interfered with interpretation. The inter observer agreement of FBI was good agreement. CONCLUSION: The FBI method of PAD is feasible; the vascular information it provides is nearly equal to conventional Angiography. CLINICAL RELEVANCE/APPLICATION: FBI can provide information on the PAD without the use of contrast material.

O-2-040　Motion Probe自動設定機能を用いた3T冠動脈MRA初期経験 -1.5T従来法との比較-
Early Experience With 3-T WH MRCA Using an Automatic Motion Probe Setting Function: Comparison Against Conventional Balanced SSFP 1.5-T WH MRCA

石村理英子（杏林大学医学部放射線医学教室）
Rieko Ishimura[1], Toshiya Kariyasu[1], Kenichi Yokoyama[1], Toshiaki Nitatori[1], Tatsuya Yoshioka[2], Isao Miyazaki[2], Shigehide Kuhara[3], Nobuyasu Ichinose[4], Shuhei Bannae[4]

[1]Department of Radiology, Kyorin University School of Medicine, [2]Department of Radiology, Kyorin University Hospital, [3]Department of Medical Radiological Technology, Faculty of Health Science, Kyorin University, [4]Toshiba Medical Systems Corporation

【要旨】Motion probe自動設定機能を用いたFFE法3T冠動脈MRAを試み、従来法の1.5T冠動脈MRAと比較した。冠動脈描出長、冠動脈-心筋間コントラスト比において従来法と同等の画質を得た。本法により非造影3T冠動脈MRAにおける安定した精度の高い検査が可能になるものと期待される。

[Purpose]Non-contrast-enhanced whole-heart magnetic resonance coronary angiography (WH MRCA) using free-breathing navigator gating (FBNG) is an efficient method for evaluating coronary artery disease. In FBNG, setting of the respiratory motion probe (MP) is a complex procedure. We have proposed a new automatic MP setting function to simplify FBNG. In this study, we evaluated the clinical usefulness of 3-T WH MRCA with the automatic MP setting function as compared to conventional 1.5-T WH MRCA.[Methods]Five healthy male volunteers (25-51 years) underwent WH MRCA using 3-T and 1.5-T scanners (Toshiba Medical Systems). At 3 T, a fast field echo sequence with optimized T2 preparation and fat suppression was used with the automatic MP setting function. At 1.5 T, a conventional steady state free precision sequence was used. Image quality was assessed by measuring the visible coronary artery length with image processing and the contrast ratio (CR) between the blood pool and myocardium. [Results]The visible coronary artery lengths at 3 T and 1.5 T were 149.2 ± 47.4 vs 137 ± 41.4 for RCA (p= 0.134), 107.4 ± 10.9 vs 128.2 ± 32.6 for LAD (p=0.237), and 103.3 ± 24.9 vs 82.2 ± 30.1 for LCX (p= 0.389). The CR between the distal LMT lumen and basal anterior wall were 2.09 ± 0.2 at 3T and 2.19 ± 0.5 at 1.5T (p= 0.05), and the CR between mean signal in the coronary lumen and in myocardium were 1.89 ± 0.3 at 3T and 1.81 ± 0.3 at 1.5T (p=0. 182). The differences in coronary artery length and CR were not significant.[Conclusion]3-T WH MRCA with automatic MP setting provides image quality comparable to conventional methods and can be used for clinical diagnosis with fewer and simpler operations.

O-2-041　3T　MRI計測による冠血流速度予備能の冠動脈病変診断能評価
Coronary flow velocity reserve on left main trunk using 3T-MRI can predict coronary artery disease as ^{15}O-labeled Water PET

菊池　穏香（北海道大学病院 放射線診断科）
Yasuka Kikuchi[1], Noriko Oyama-Manabe[1], Fumi Kato[1], Rie Mimura[1], Keita Sakamoto[1], Satoshi Yabusaki[1], Kohsuke Kudo[1], Hiroki Shirato[2]

[1]Hokkaido University Hospital, Department of Diagnostic and Interventional Radiology, [2]Department of Radiation Medicine, Hokkaido University Graduate School of Medicine

【要旨】3T　MRIで得た左主管部の冠血流速度予備能は^{15}O標識水PETから得た同領域の冠血流予備能とよい相関を示した。また、冠動脈疾患の検出能にも両者には有意差を認めず、冠血流速度予備能は高い感度で冠動脈疾患患者を検出できることが示された。

Purpose: To estimate coronary flow reserve (CFR) by using fast velocity-encoded cine imaging (CFVR) on 3T-MRI in comparison with ^{15}O-labeled water PET (CFR_PET) and to compare CFVR in healthy volunteers to patients with coronary artery disease (CAD) in order to evaluate feasibility of CFVR by MRI for identifying CAD. Methods: Ten patients with CAD who underwent diagnostic coronary angiography (age; 64.9 ± 13.5 year, 8 male) and 6 healthy male volunteers (age; 24.3 ± 4.2 year) who underwent MRI and PET with adenosine triphosphate (ATP) infusion (160μg/kg/min) and at rest were evaluated. CFVR was measured with breath-hold velocity-encoded cine MRI during ATP stress and at rest. CFVR was calculated by dividing peak-velocity during that at rest. CFR_PET was calculated of the left main trunk. Linear regression and Bland-Altman analyses were used to assess the relationship between CFVR and CFR_PET. Receiver operating characteristics (ROC) analysis for detection of CAD was conducted in both CFVR and CFR_PET. Results: Pearson's correlation coefficients from linear regression showed good correlations (R=0.64, P=0.0039) between CFVR and CFR_PET. There was a small bias on the Bland-Altman plot suggesting that CFVR tended to be lower than CFR_PET. CFVR (1.91 ± 0.67) in CAD patients was significantly lower than that in volunteers (2.85 ± 0.83, P=0.0257). In the ROC analysis of CFVR and CFR_PET for the detection of CAD, the area under the curve (AUC) was 0.8167 (P=0.0204) and 0.9333 (P=0.0005), respectively. There was no significant difference between AUCs of CFVR and CFR_PET (P=0.2401). Using CFVR, the sensitivity was 0.90 and specificity was 0.67, when a cutoff of 2.38 was used for the detection of CAD. Conclusion: CFVR can detect CAD patients with high sensitivity.

O-2-042　3T MRIにおける可変再収束フリップアングル法を用いたFBI法の臨床的有用性-従来法によるFBI法との比較-
Clinical usefulness of FBI using with variable refocusing flip angle at 3T MRI - comparison with conventional FBI in peripheral arteries -

山本　晃義（社会医療法人 共愛会 戸畑共立病院）
Akiyoshi Yamamoto[1], Hiroki Matoba[1], Yuuya Kuroki[1], Daiji Uchiyama[1], Seigo Yoshida[1], Katsumi Nakamura[1], Mitsue Miyazaki[2], Keiichirou Ishi[3]

[1]Tobatakyouritsu hospital, [2]Toshiba Medical Research Institute USA, [3]Toshiba Medical Systems

【要旨】3T装置を用いたFBI法において、可変再収束フリップアングル法と従来法であるフリップ角度を使用して得られたボランティア画像の画質を評価した。その結果、可変再収束フリップアングル法を使用した方では、画質を維持しつつ撮像時間をおよそ30％短縮することが可能であった。

[PURPOSE]To compare FBI using variable refocusing flip angle (vFA-FBI) with FBI using constant flop angle (cFA-FBI) for the visualization of peripheral arteries and the examination time.[MATERIALS and METHODS]vFA-FBI was applied to high refocusing flip angles at the center of k space and gradually decreased to lower flip angles in order to reduce SAR as compared to use the constant high refocusing flip angles. Both vFA-FBI and cFA-FBI were performed on 6 healthy volunteers (age 26-38, mean 29). The visualization of lower extremity arteries was evaluated with a 4-point grade in comparison with cFA-FBI as a gold standard. The CNR of the arteries to muscle was also calculated. An average examination time was compared in both methods.The acquisition parameters were as follows; vFA-FBI; 3D SSFSE, TR 1-2RR, TEeff 60ms, ETS 5ms, high/low refocusing flip of vFA pattern 200°/30°, thickness 3mm, FOV 37cmX37cm, and matrix 256X256. cFA-FBI: 3D SSFSE, same parameters as vFA-FBI except TR 3-4RR and constant refocusing flip angle 180°. [RESULTS]The average scores of cFA-FBI and vFA-FBI were 2.8 ± 0.41 for popliteal artery, 2.7 ± 0.52 for anterior tibial artery, 2.5 ± 0.55 for peroneal artery, and 2.7 ± 0.52 for posterior tibial artery. CNR of cFA-FBI and vFA-FBI were 305.4 ± 67.5 and260.1 ± 64.1, respectively (p <0.05). The average examination times were 3:22 ± 24sec for cFA-FBI and 2:13 ± 13sec for vFA-FBI. [DISCUSSION]SAR of vFA-FBI was lower than that of cFA-FBI because of lowering refocusing flip angles in vFA-FBI. Shorter TR could be used in vFA-FBI, therefore, the acquisition time was reduced with appropriate image quality despite a little decrease of CNR.[CONCLUSION]The vFA-FBI technique can reduce the acquisition time of the cFA-FBI with maintaining good image quality.

O-2-043　心臓MRI検査の撮像アシスト機能のユーザビリティ評価
Usability Evaluation of Cardiac MRI Assist applications

篠田　健輔（東芝メディカルシステムズ株式会社 MRI事業部）
Kensuke Shinoda[1], Shuhei Takemoto[1], Shuhei Nitta[2]

[1]MRI Systems Division, Toshiba Medical Systems Corporation, [2]Corporate Research & Development Center, Toshiba Corporation

【要旨】心臓MRI検査アシスト機能を用いると、位置決め操作数や操作時間は、熟練者5名と非熟練者6名ともに平均して約25%に減った。また、熟練者5名における、冠動脈撮像時間を補正した平均検査時間は約80%に減った。また、操作者間の検査時間の差が約3分に減った。心臓MRI検査を計画しやすくなることが期待される。

[Purpose] We have developed two Cardiac MRI assist applications such as CardioLine+ and SURE VOI Cardiac which detects planes and regions of CMRI protocol. In this study, we evaluated how the two assist applications could reduce operation steps and time of CMRI.[Methods] CMRI protocols including left ventricular structure and function module and coronary arteries evaluation module were acquired for a healthy volunteer by 2 kinds of operators: 5 experts who have experience of CMRI as well, and 6 non-experts who are not familiar with CMRI. Usability was assessed through measuring (1) total number of operation steps, (2) operation time for slice positioning and (3) elapsed time until completing CMRI with and without the assist applications. Time until completing CMRI is corrected with mean time of coronary artery acquisitions because the acquisition time depends on stability of respiratory motion.[Results] On using the CMRI assist application, the average number of operation steps was reduced from 291.4 to 77.0 for the experts and from 282.4 to 62.7 for the non-experts. The average operation time was reduced from 14m7s to 3m31s for the experts and from 23m40s to 5m59s for the non-experts. (Max., min., mean) of the elapsed time until completing CMRI was reduced from (48m29s, 38m16s, 42m17s) to (34m54, 32m33s, 32m46s) for the experts.[Conclusion] The operation steps and the operation time were reduced to about 25% for both experts and non-experts. The time to complete slice positioning was reduced to about 60%. The time until completing CMRI was reduced to about 80%, and its variation was reduced from about 10 minutes to about 3 minutes. Using the CMRI assist applications, everyone can perform CMRI with fewer operation steps and in stably shorter time.

O-2-044　Polarity Corrected TI prep法を用いた1.5Tと3TでのT1値測定精度の基礎的検討
Basic Study on the Accuracy of T1 Values Obtained Using the Polarity Corrected TI Prep Method in Both 1.5-T and 3-T MRI Systems

安達　卓哉（杏林大学医学部付属病院 放射線部）
Takuya Adachi[1], Isao Miyazaki[1], Toshiaki Nitatori[2], Kenichi Yokoyama[2], Shigehide Kuhara[3], shuhei Bannae[4], Yoshimori Kassai[4]

[1]Radiation Department Kyorin University Hospital, [2]Department of Radiology Faculty of Medicine Kyorin University, [3]Department of Medical Radiological Technology Faculty of Health Sciences Kyorin University, [4]TOSHIBA MEDICAL SYSTEMS CORPORATION

【要旨】新しい心筋T1map用シーケンスPolarity corrected TI prep 法に関してファントムを用いて基礎的な検討を行った。実験では3Tと1.5T装置を使用し、心拍数を変えてT1値の測定を行った。今回の結果から、心拍数や静磁場強度を変えても、精度よく安定したT1値を測定できることが確認された。

<Purpose>A cardiac T1 mapping sequence employing the Polarity Corrected TI prep method was installed in both 1.5-T and 3-T MRI systems at our hospital. We evaluated the accuracy of the T1 mapping values and the effects of the static magnetic field strength using a dedicated T1 mapping phantom.
<Methods>Studies were performed with 1.5-T and 3-T MRI systems (EXCELART Vantage and Vantage Titan 3T; Toshiba Medical Systems) using Atlas SPEEDER Body and Atlas SPEEDER Spine coils. A dedicated T1 mapping phantom including the T1 values of myocardium and blood pre/post Gd enhancement was used. For the Polarity Corrected TI prep method with a Fast Field Echo sequence, the parameters were TR 5.0 ms, TE 2.0 ms, FA 10 deg, FOV 35.0×36.0 cm, matrix 128×256, and slice thickness 10 mm.Some different TI points were obtained. ECG gating was performed using a pseudo waveform generator at various heart rate settings (50, 60, 75, and 100 bpm). The T1 values for each cavity of the phantom at each heart rate were calculated using the Polarity Corrected TI prep method, and the T1 values were compared against those obtained using the Standard IR method.
<Results & Discussion>In the 1.5T and 3T MRI systems, only slight variation in the T1 values was observed even when the heart rate was changed. The T1 values obtained using the Polarity Corrected TI prep method were slightly shorter than those obtained using the Standard IR method at both 1.5T and 3T.
<Conclusion>The Polarity Corrected TI prep method could measure the T1 values of the dedicated T1 mapping phantom in MRI systems with static magnetic field strengths of 1.5T and 3T. This sequence will be clinically applied in the near future to conduct further research on the effects of ECV and arrhythmias.

O-2-045　専用プロトコルを用いないコンソール上での心筋T1マップ作成
Creating Myocardial T1-map on the MRI Scanner without the Use of a Dedicated Protocol

畠山　憲重（長野中央病院）
Norishige Hatakeyama[1], Kazuki Sakata[1], Yuuya Ishizawa[1], Megumi Sakurai[1], Kouta Ishizaka[1], Hiroshi Imai[2]

[1]Nagano chuo hospital, [2]Siemens Healthcare

【要旨】ライセンス購入不要の方法で心筋T1マップを作成した。飽和回復法に基づき元画像は既存のプロトコルを連続させて1回の息止めで取得可能な範囲とした。T1値推測はカーブフィッティングに変えて四則演算で近似し、一連を装置上で処理可能とした。本法で算出されたT1値はリファレンスと近い値を得ることが可能であった。

Background Recently, there have been some reports of myocardial T1mapping technique such as MOLLI and SASHA. To use them it requires purchasing a license. The SASHA acquires several ECG-triggered single-shot images of a non-saturated (NS) and multiple saturation recovery time (TS). T1 value estimation is performed using pixel-wise curve fitting. It has been reported that approximately equivalent T1 map could be acquired from single TS point. Based on this method, we can obtained similar image set using two separated single shot protocols, and a T1map can be calculated using imageJ. However, the calculated T1map is not DICOM. **Purpose** To create a myocardial T1map on a MRI scanner without dedicated protocol. **Theory** Our proposal is based on the Bloch equation; $dM_Z/dt=(M_0-M_Z)/T1$. If the recovery of longitudinal magnetization between the origin and TS_A can be approximated as linear the T1-value can be written by the following; $T1=(M_0-M_Z)/(dM_Z/dt)=\{S_{NS}-(S_A/2)\}/(S_A/TS_A)$. **Methods** Phantom Experiments: The reference phantom contained 9 different concentration of dextrin solution. Range of T1 value was 419 to 3343 ms. This phantom was scanned by a single-shot ECG-triggered gradient echo protocol on a clinical 3T MRI scanner (SIEMENS, MAGNETOM Skyra). Post processing: T1map was calculated by 2 methods. One was our proposal. Another one was calculated by offline curve fitting on ImageJ. Average and SD of T1 value and coefficient variation ($CV=SD/T1_{reference}$) for each solution were measured. **Results** Strong correlation of T1 value between the proposal method and the curve fitting method were shown. CV of the proposal method was slightly higher than the curve fitting method. **Conclusions** Our proposal method makes it possible to create the T1-map on console without dedicated protocol.

O-2-046　SMART1Mapping法を用いた心筋T1値計測：1.5Tおよび3T装置における正常値の検討
Myocardial T1 values of healthy volunteers measured with SMART1Mapping on 1.5T and 3T scanners

松本　俊亮（慶應義塾大学医学部放射線診断科）
Shunsuke Matsumoto[1], Shigeo Okuda[1], Tatsuya Suzuki[1], Hirokazu Fujiwara[1], Akihiro Tanimoto[1], Masahiro Jinzaki[1], Yoshinobu Nunokawa[2], Sari Motomatsu[2], Rikiya Fujishiro[2], Yasutomi Shimada[2], Atsushi Nozaki[3]

[1]Department of Diagnostic Radiology Keio University School of Medicine, [2]Department of Central Radiological Technology Keio University Hospital, [3]GE healthcare Japan

【要旨】SMART1Mapping法(S法)の心筋T1値計測による正常値を知るため、健常者23名を対照にMOLLI法(M法)とともに計測を行った。S法、M法による計測値の平均は、それぞれ1277.7msecと1024.0msec(1.5T)、1518.7msecと1213.1msec(3T）であり、過去の文献値とおおむね一致した。

[Purpose] To reveal the normal range of myocardial T1 values measured with SMART1Mapping in healthy people. [Material and Methods] A total of 23 health volunteers (12 male, 11 female; mean age 27.5 y.o., range between 21 and 35) was enrolled in this study with written informed consent under the approval of the local ethical committee. We used 1.5T (N = 12) and 3T (N = 21) MR scanners for data acquisition (Discovery MR450w and MR750, GE Healthcare) with 32-channel cardiac coils. Images of ten people were obtained on both of 1.5T and 3T scanners. In the three locations (apex, mid and base) on the short axis of the left ventricle, the T1 mapping was acquired with both of SMART1Mapping and MOLLI. The values acquired with MOLLI were corrected using Deichmann's method. The T1 map was divided into AHA 17 segment model excluding segment 17 (the apex). The values were measured and compared between the methods.[Results] In 3 segments of SMART1Mapping on 3T, measurements were not available due to the presence of banding artifact. Averaged myocardial T1 value was measured to be 1277.7 msec and 1024.0 msec using SMART1Mapping and MOLLI on 1.5T, and 1518.7 msec and 1213.1 msec on 3T scanners. [Discussion and Conclusion] Myocardial T1 values are reported to be different depending on the measurement technique. The normal range of myocardial T1 was previously reported to be 950-1050 msec, 1200-1300 msec with MOLLI on 1.5T and 3T, respectively. The T1 value obtained from another saturation-recovery technique (SAHSA) was revealed to be around 1200 msec on 1.5T scanners. The results of the current study were compatible with the previous reports using other imaging techniques, and can be referred as normal range of myocardial T1 values with SMART1Mapping.

O-2-047　Polarity Corrected Variable TI Prep Toolを用いたECV算出を目的としたT1値測定精度の検討
Evaluation of T1 Value Measurement for ECV Mapping Using the Polarity Corrected Variable TI Prep Tool

高済　英彰（福島県立医科大学附属病院 放射線部）
Hideaki Takasumi[1], Shinya Seino[1], Hironobu Ishikawa[1], Takashi Kanezawa[1], Naoki Watanabe[1], Takanori Sato[1], Shuhei Bannae[2]

[1]Fukushima Medical University Hospital Department of Radiology, [2]TOSHIBA MEDICAL SYSTEMS CORPORATION

【要旨】ECVは、心筋線維化の定量評価法の一つとして注目され、造影前後の心筋と血液のT1値及びヘマトクリット値を用いて算出される。ECVの算出精度は、T1値測定精度に依存すると考えられる。特に血液は、心拍変動やflowなどの影響により、信号変化が大きいことが予想されるため、より安定した測定精度が求められる。

PurposeExtracellular volume fraction (ECV) mapping is a widely employed method for the quantitative evaluation of myocardial fibrosis. ECV values can be calculated from the T1 values of myocardium and blood before/after Gd enhancement. At the 43rd JSMRM, we reported the T1 values obtained using PC Constant TI prep for blood before Gd enhancement fluctuated widely. As an upgrade, PC Variable TI prep was installed in our MRI system last year. We evaluated the accuracy of T1 measurement using PC Variable TI prep for blood before Gd enhancement.MethodsStudies were performed using a 1.5-T MRI system (EXCELART Vantage; Toshiba Medical Systems). A Fast Field Echo sequence with ECG gating was used (TR 5.0 ms, TE 2.0 ms, FA 12 deg, trigger interval 3000 ms, number of TI points 5). We scanned a T1 mapping phantom including the T1 value of blood before Gd enhancement (T1 value 1520 ms) and 3 healthy male volunteers (age 27 ± 3 years, HR 55-65 bpm). Blood T1 values were measured in the mid LV.Results and DiscussionIn the phantom study, no differences were observed between the variable and constant TI methods. In the volunteer study, the T1 values were as follows: variable TI method 1458 ± 22.4 ms, constant TI method 1888 ± 51 ms, and reference 1580 ± 130 ms.*The variable TI method provided T1 values close to the reference values, with less variance than the constant TI method. Blood signals may be affected by various factors such as blood flow, but optimizing the different TI intervals during the triggering period is effective in suppressing the influence of these factors and improving the fitting accuracy. ConclusionPC Variable TI prep, in which the TI intervals are optimized, can accurately measure T1 values before/after Gd enhancement.*Sharma et al. J Magn Reson Imaging 2006;23:323-330

O-2-048　MOLLI法を使用したT1値測定における心拍数変化の影響の検討
Evaluation of the influence of heart rate on T1 value determined from MOLLI method in Phantom

持木　瑞規（群馬県立心臓血管センター 放射線課）
Mizunori Mochiki, Satoshi Tomioka, Toshihiko Ino, Hatsuo Kigure

Division of Radiology, Gunma Prefectural Cardiovascular Center

【要旨】Ingenia 1.5TにおいてMOLLI法が撮像可能になったため、コントラスト評価ファントムを使用し、MOLLI法にて心拍数を変化させて撮像しT1値を計測した。SE－IR法より求めたT1値と比較したところ、各試料における誤差は最大20％以内であった。

[Background] Modified Look-Locker Inversion Recovery (MOLLI) method is known as a method for measurement of T1 value in myocardium. Replacement of the MR equipment in our facility brought us a chance to investigate of T1 map using the Ingina 1.5T.
[Purpose]We estimated the influence of heart rate on T1 value determined from MOLLI method in the phantom.
[Methods]The phantom ordered for contrast evaluation was scanned by Ingina 1.5T. The acrylic coil frame was located between the phantom and front coil. Samples we evaluated were seven (moisture laden PVA gel 75, 77, 79, mixed with Gd^{3+} of PVA gel 0.1, 0.2, 0.3 mmol and pure water).We used the SE-IR method and MOLLI method for imaging. In MOLLI method, two types of parameters were arranged, *native* for pre-contrast and *enhanced* for post-contrast. T1 value obtained from MOLLI method was compared to that from SE-IR method. Setting of simulated ECG generator was from 30 to 100 BPM.
[Results]The difference of T1 value derived from SE-IR method and that from MOLLI method was within 20% in each sample and heart rate.
[Conclusions] In the phantom study, range of change in T1 value was within 20% in sequence of heart rate. In the future, further evaluation will be needed to estimate the influence of heart rate on T1 value in clinical fields.

O-2-049　肺野MRIにおける呼吸停止下T2W-BLADE法の有用性
The usefulness of the BLADE application in breath-hold lung MRI

山下　達也（明成会 塩川医院）
Tatsuya Yamashita
Meiseikai shiokawa-clinic

【要旨】肺MRIの撮影には、心電図同期撮影、横隔膜下同期撮影がよく用いられるが、不整脈等により安定しない場合、呼気での撮影では肺野が広く描出できない等の問題がある。そこで今回、呼吸停止下BLADE法を用いて、フローの影響を抑え、さらに吸気での撮影により肺野を広く描出できるか検討を行ったので報告する。

[Purpose]The purpose of this study was to investigate the usefulness of the BLADE application in breath-hold lung MRI.[Methods]We obtained consent from the volunteers prior to the commencement of the study.Lung MRI was performed using a 1.5 Tesla imager and included a respiratory-triggered T2-weighted BLADE sequence, a breath-hold T2-weighted BLADE sequence, and a HASTE sequence.We performed a visual evaluation of the artifacts and image quality in the respiratory-triggered T2-weighted BLADE sequence, the breath-hold T2-weighted BLADE sequence and the HASTE sequence (N=3).[Results]The HASTE sequence was inferior to the respiratory-triggered T2-weighted BLADE sequence, the breath-hold T2-weighted BLADE sequence for artifacts. The respiratory-triggered T2-weighted BLADE sequence, the breath-hold T2-weighted BLADE sequence had no significant impact on artifacts . However, the breath-hold T2-weighted BLADE sequence was superior in terms of the presence of mage quality.[Conclusions]The breath-hold T2-weighted BLADE sequence would be useful for lung MRI.

O-2-050　肺血管におけるUltrashort TE(UTE)の1.5Tと3Tの比較
Comparison between 1.5T and 3T of UTE in the optical evaluation of the pulmonary vascular

太田　　雄（済生会熊本病院 中央放射線部）
Takeshi Ohta[1], Takashi Okigawa[1], Satomi Tajiri[1], Hiroyuki Hazeyama[1], Suguru Kawamura[1], Daisuke Masuda[1], Megumi Katayama[1], Hirofumi Wada[1], Masahiro Kosaka[2], Kenntaro Haraoka[2], Miho Kitamura[2], Mitsue Miyazaki[2], Masato Ikedo[2]

[1]Department of Radiology, Saiseikai Kumamoto Hospital, Kumamoto, Japan, [2]Toshiba Medical Systems Corporation, Japan

【要旨】1.5T装置でも3T装置と同等の肺血管の描出が可能であると示唆された。

Purpose: There is a report of 3T in pulmonary vascular, but there are few reports of 1.5T. The visualization of the pulmonary vascular was compared at 1.5T and 3T under various conditions.Materials and Methods:UTE studies were performed at 1.5T MRI and 3T MRI (Vantage Titan 3T,Vantage Titan 1.5T;Toshiba Medical,JAPAN). Coronal UTE images were acquired in five volunteers(age range 34-43 years,mean age 38.2) at 1.5T and 3T. Imaging parameters were changed with and without respiratory gating and the visualization of the pulmonary vascular was compared. Image evaluation was performed through consultation among five technologists.Result: Imaging with respiratory gating on 3T had better SNR and could even visualize peripheral blood vessel more clearly than 1.5T.Imaging without respiratory gating on 1.5T had could even visualize peripheral blood vessel than 3T.However, visualization of peripheral blood vessels near the diaphragm degraded.Conclusion : Visualization of the pulmonary vascular is possible with UTE at 1.5T-MRI.

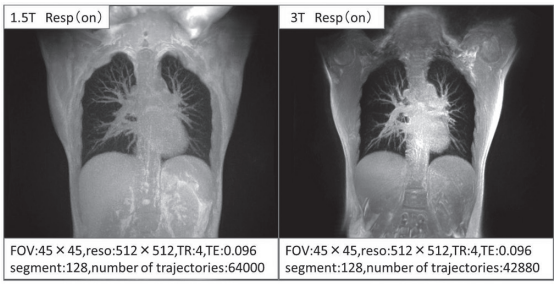

O-2-051　Dynamic CE-MRIおよびADCTとPET/CTにおける非小細胞肺癌患者における保存的治療効果予測能の比較
Comparison of the Capability for Therapeutic Outcome Prediction among Dynamic CE-Perfusion MRI and ADCT and PET/CT in NSCLC Patients

大野　良治（神戸大学大学院医学研究科内科系講座放射線医学分野 機能・画像診断学部門）
Yoshiharu Ohno[1,2], Yuji Kishida[1], Shinichiro Seki[1], Takeshi Yoshikawa[1,2], Yoshiko Ueno[1], Yasuko Fujisawa[3], Masao Yui[3], Shigeharu Ohyu[3], Kouya Nishiyama[4], Katsusuke Kyotani[4], Kazuro Sugimura[1]

[1]Dept. of Radiology, Kobe Univ., [2]ABIRC, Kobe Univ., [3]TMSC, [4]Kobe Univ. Hosp.

【要旨】Dynamic CE-perfusion ADCTおよびMRIとPET/CTにて非小細胞肺癌患者の保存的治療後の予後予測能を43名のStage IIIBの非小細胞肺癌患者にて統計学的に比較検討した。そして，両手法にて求めた灌流指標は$_{max}$と同等の予後予測能を有していることが示唆された。

Purpose: To directly compare the capability for therapeutic outcome prediction between dynamic CE-perfusion ADCT and MRIand FDG-PET/CT in non-small cell lung cancer (NSCLC) patients treated with chemoradiotherapy. METHOD AND MATERIALS: 43 Stage IIIB NSCLC patients underwent PET/CT, dynamic CE-perfusion ADCT and MRI, chemoradiotherapy, and follow-up examination. According to RECIST guideline, all patients were divided into two groups as follows: 1) CR+PR (n=23) and 2) SD+PD (n=20) groups. In each patient, total perfusion (TP) and tumor perfusions from pulmonary (TPP) and systemic (TPS) circulations calculated by dual-input maximum slope method on dynamic ADCT and MRI and SUV_{max} on PET/CT were assessed at each targeted lesion, and averaged to determine final values. To compare the capability for distinguishing two groups, ROC analyses were performed. Then, disease free and overall survivals between responders and non-responders assessed by each index were compared by Kaplan-Meier method followed by log-rank test. RESULTS: Area under the curves (Azs) of TP (MRI: Az=0.90, ADCT: Az=0.87) and TPS (MRI: Az=0.84, ADCT: Az=0.84) were significantly larger than that of TPP (MRI: Az=0.72, $p<0.05$; ADCT: Az=0.72, $p<0.05$). Disease free survivals of responder were significantly longer than that of non-responder by TP (MRI: p=0.01, ADCT: p=0.03) and TPS (MRI: p=0.01, ADCT: p=0.001). Overall survivals of responder were also significantly longer than that of non-responder by TP (MRI: p=0.007, ADCT: p=0.004), TPP (ADCT: p=0.008), TPS (MRI: p=0.001; ADCT: p=0.0001) and SUV_{max} (p=0.04). CONCLUSION: Dynamic CE-perfusion ADCT and MRI has equal to or better potential to predict therapeutic outcome than PET/CT in NSCLC patients with chemoradiotherapy.

O-2-052　3T 造影Perfusion MRIにおける至適造影法の検討：造影Perfusion ADCTとの比較
Dynamic Perfusion MRI at 3T System: Appropriate Contrast Media Injection Protocol for Perfusion Measurement as Compared with Dynamic Perfusion ADCT

大野　良治（神戸大学大学院医学研究科 内科系講座 放射線医学分野 機能・画像診断学部門）
Yoshiharu Ohno[1,2], Yuji Kishida[1], Shinichiro Seki[1], Takeshi Yoshikawa[1,2], Shigeharu Ohyu[3], Masao Yui[3], Yoshimori Kassai[3], Kazuro Sugimura[1]

[1]Dept. of Radiology, Kobe Univ., [2]ABIRC, Kobe Univ., [3]TMSC

【要旨】3T MR装置における造影Perfusion MRIの至適造影剤量を明らかにするために，異なる2種類の造影剤量にて造影Perfusion MRIを施行し，造影Perfusion ADCTと同一手法で求めた肺血流量を比較した。

Purpose: To determine the influence of gadolinium (Gd) contrast media volume for quantitative perfusion and functional assessments on dynamic CE-perfusion MRI, when compared with dynamic CE-perfusion ADCT. Materials and Methods: 17 consecutive patients with suspicious of small pulmonary nodule and pulmonary emphysema (11 males, 6 females; mean age 72 years) underwent dynamic CE- perfusion ADCT, dynamic CE-perfusion MRI evaluated by contrast media volume as 1.5 (MRI1.5ml) and 3.5 (MRI1.5ml) ml at a 3T system and %FEV1 measurement. From perfusion ADCT and MR data, regional perfusion maps were computationally generated by dual-input maximum slope method. For capabilities of regional perfusion and disease severity assessments, region of interests (ROIs) were placed over each lung field, and mean perfusion was also determined from all ROI measurements. To access the influence of Gd contrast media volume for regional perfusion assessment, correlation and mean difference of each perfusion parameter between ADCT and MRI were statistically evaluated. To evaluate the capability for functional assessment, each perfusion parameter was also correlated with %FEV1. Results: Total ($r=0.37$, $p < 0.0001$) and pulmonary arterial ($r=0.35$, $p < 0.0001$) perfusions of MRI1.5ml had significant correlations with those of ADCT. Mean differences on MRI1.5ml was significantly smaller than those on MRI3.5ml ($p < 0.05$). In addition, total and pulmonary arterial perfusions assessed by MRI1.5ml had significant and moderate correlations with %FEV1 ($0.57 < r < 0.62$, $p < 0.05$). Conclusion: Contrast media volume has significant influence to the capability of perfusion MRI for quantitative perfusion and functional assessments in patients with pulmonary emphysema, when compared with perfusion ADCT.

O-2-053　CEST Imagingにおける良・悪性肺病変鑑別能診断能のDWIおよびPET/CTとの対比
CEST Imaging: Comparison of the Capability for Differentiation of Malignant from Benign Pulmonary Lesions with DWI and FDG-PET/CT

大野　良治（神戸大学大学院医学研究科内科系講座放射線医学分野 機能・画像診断学部門）
Yoshiharu Ohno[1,2], Yuji Kishida[1], Shinichiro Seki[1], Masao Yui[3], Takeshi Yoshikawa[1,2], Yoshiko Ueno[1], Kouya Nishiyama[4], Katsusuke Kyotani[4], Mitsue Miyazaki[5], Kazuro Sugimura[1]

[1]Dept. of Radiology, Kobe Univ., [2]ABIRC, Kobe Univ., [3]TMSC, [4]Kobe Univ. Hosp., [5]TAMS

【要旨】CEST imagingとPET/CTにおける肺結節の良・悪性鑑別診断能を88名の肺結節を有する患者にて統計学的に比較検討した。そして，MTR_{asym}とSUV_{amax}は良・悪性鑑別診断能において有意差はなく，両手法は同等の肺結節の良・悪性鑑別診断能を有していることが示唆された。

PURPOSE: To directly and prospectively compare the capability for differentiation of malignant from benign pulmonary nodules and/ or masses among chemical exchange saturation transfer (CEST) imaging, diffusion-weighted MR imaging (DWI) and FDG-PET/CT. MATERIALS AND METHODS: 88 consecutive patients with pulmonary nodules and/ or masses underwent CEST imaging and DWI at a 3T MR system, FDG-PET/CT and pathological and/or follow-up examinations. According to final diagnoses, all lesions were divided into malignant (n=49) and benign (n=39) groups. Then, magnetization transfer ratio asymmetry (MTR_{asym}) was calculated from z-spectra at 3.5ppm in each pixel, and MTR_{asym} map was computationally generated. To evaluate the capability for differentiation between two groups at each lesion, MT_{asym}, ADC and SUV_{max}x were assessed by ROI measurements. To compare each index between two groups, Student's t-test was performed. Then, ROC analysis was performed to determine each feasible threshold value for differentiation of two groups. Finally, diagnostic performance was compared each other by McNemar's test. RESULTS: Mean MTR_{asym} (1.97 ± 6.38%), ADC (1.17 ± 0.25 × 10-3mm2/sec) and SUV_{max} (3. ± 1.60) of malignant group had significant difference with those of benign group (MTR_{asym}: -2.9 ± 4.9%, p=0.0002; ADC: $1.33 \pm 0.18 \times 10^{-3}$ mm^2/sec, p=0.0024, SUV_{max}: 2.27 ± 0.48, p=0.0008). Results of ROC analysis showed that there were no significant differences of area under the curve (Az) among all indexes ($p > 0.05$). When applied feasible threshold values, there were no significant differences of diagnostic performance among all indexes ($p > 0.05$). CONCLUSION: CEST imaging is considered at least as valuable as DWI and FDG-PET/CT for differentiation of malignant from benign pulmonary lesions.

O-2-054　PET/MRI，全身MRI，PET/CTおよび通常画像検査における胸腺上皮性腫瘍の病気診断能の比較
Comparison of the Capability for the IASLC/ ITMIG Thymic Epithelial Tumor Staging among PET/MRI, Whole-Body MRI, PET/CT and Conventional Examination

大野　良治（神戸大学大学院医学研究科内科系講座放射線医学分野 機能・画像診断学部門）
Yoshiharu Ohno[1,2], Yuji Kishida[1], Shinnichiro Seki[1], Takeshi Yoshikawa[1,2], Yoshiko Ueno[1], Kota Aoyagi[3], Masao Yui[3], Yoshimori Kassai[3], Hitoshi Yamagata[3], Koya Nishiyama[4], Katsusuke Kyotani[4], Kazuro Sugimura[1]

[1]Dept. of Radiology, Kobe Univ., [2]ABIRC, Kobe Univ., [3]TMSC, [4]Kobe Univ. Hosp.

【要旨】胸腺上皮性腫瘍の病期診断能を64名の胸腺上皮性腫瘍患者において全身PET/MRI，MRIおよびPET/CTとガイドラインに沿った通常画像検査にて統計学的に比較検討し，PET/MRIおよびMRIは通常画像検査に比して有意に高い診断能を有し，PET/CTと同様に有用であることが示唆された。

PURPOSE: To compare the diagnostic capability for the IASLC/ ITMIG thymic epithelial tumor staging among whole-body FDG-PET/MRI, MRI, FDG-PET/CT and conventional radiological examinations based on guidelines. MATERIALS AND METHODS: 64 consecutive thymic epithelial tumor patients (30 men, 34 women; mean age 56 years) prospectively underwent whole-body MRI, integrated PET/CTs, conventional radiological, pathological and follow-up examinations. Then, TNM staging in each patient was determined based on tumor board reviewing all examination results. All co-registered PET/MRIs were generated by means of our proprietary software. Then, TNM staging was evaluated by four different reader groups based on the IASLC/ ITMIG thymic epithelial tumor staging system. To evaluate agreements of all factors between each method and final diagnosis, kappa statistics were performed. Finally, diagnostic accuracy of each factor and clinical stage was statistically compared each other by using McNemar's test. RESULTS: Agreements of all factors between each method and final diagnosis were also assessed as fair, moderate, or substantial (0.27<kappa value<0.81). Accuracies of N factor and staging on PET/MRI (N factor: 93.8 [60/64] %, staging: 84.4 [54/64] %) and MRI (N factor: 93.8 [60/64] %, staging: 84.4 [54/64] %) were significantly higher than those on conventional radiological examinations (N factor: 81.3 [52/64] %, p=0.008; staging: 71.9 [46/64] %, p=0.008). CONCLUSIONS: Whole-body PET/MRI and MRI have better potential for the IASLC/ ITMIG thymic epithelial tumor staging than conventional radiological examination, and are considered at least as valuable as PET/CT in this setting.

O-2-055　3T-MR装置を用いた腹部のComputed DWIにおける画質改善法の比較
Comparison of method that image quality improvement. In Computed DWI of Abdominal region using 3T-MR scanner

白勢　竜二（株式会社 日立製作所 ヘルスケアビジネスユニット）
Ryuji Shirase, Yasuo Kawata, Kuniaki Harada, Masahiro Takizawa, Hiroyuki Itagaki, Yoshitaka Bito
Healthcare Business Unit, Hitachi, Ltd.

【要旨】cDWIにおけるADC計算時の輝点ノイズ低減アルゴリズムを開発し、3T-MR装置における腹部cDWIに応用した。従来法と比較しcDWI画像に生じた黒点が低減した。

[Background & Objective]
Diffusion weighted imaging (DWI) with high b-value is useful in detecting malignant lesion. Computed DWI (cDWI) is possible to make high b-value images by using apparent diffusion coefficient (ADC) value calculated from low b-value images. However, bright spot noises were usually observed during calculation of ADC map, and this causes dark spots in the resulting cDWI images. We developed modified cDWI algorithm that reduces these bright spot noises for 0.4T open MRI system. In this study, we applied our algorithm to abdominal DWI using 3T MRI, and compared visualization of trace image between our algorithm and conventional algorithm.
[Method]
3T MRI (Hitachi, Ltd., Tokyo, Japan) was used for volunteer imaging after obtaining written informed consent in accordance with our institutional review board guidelines. Scan parameters were; FOV=400mm, TE/TR=55ms/7500ms, slice thickness=8mm, matrix=96x128, b=800s/mm^2. STIR was used for suppressing fat signals. cDWI image with b=2000s/mm^2 was made from acquired DWI image (b=800s/mm^2). In calculating ADC value during cDWI process, two different methods were applied.(a) Detect abnormal ADC value and correct them before calculating cDWI image (our algorithm).(b) Cutoff abnormal ADC value (conventional algorithm).
[Result & Discussion]
Abnormal ADC values frequently occurred due to pixel shift or signal loss by body motion during data acquisition. Even if cDWI images calculated by conventional algorithm had much dark spots, our algorithm reduces these dark spots drastically, and thus visualization of cDWI images was improved.
[Conclusion]
Our cDWI algorithm reduced abnormal ADC value and improved visualization of cDWI abdominal images using 3T MRI.

O-2-056　乳癌に於けるcomputed DWIの最適なb値の検討
Optimal b-value in computed diffusion-weighted imaging for detecting breast cancer

田島　　祐（東京医科大学病院 放射線科）
Yu Tajima, Kazuhiro Saito, Taiyo Harada, Natsuhiko Shirota, Yoichi Araki, Noriko Kobayashi, Nobutaka Yoshimura, Koichi Tokuuye
Tokyo medical university hospital

【要旨】術前に撮像した乳癌の拡散強調画像よりcomputed DWIを作成し、2名による評点付けによって感度・特異度を求め、ROCから求めたAz値による統計学的検討を行った。b値0-500で得たcomputed DWIではb値800および1100で最も診断能が高かった。

PurposeTo investigate optimal b-value in computed diffusion-weighted imaging (cDWI) for detecting breast cancer.Materials and methodsThis retrospective study included consecutive 30 patients who underwent MRI and had surgically proven breast cancer. All MRI examinations were performed with a 1.5 T superconductive MRI system (Avanto, Siemens) with a two-channel breast coil. DWI was performed using a single-shot echo-planar imaging sequence. The parameters as follows: TR/TE, 8500/96; b-value, 0, 500 and 1000 s/mm^2; FOV, 340 × 380 mm; matrix, 160 × 144; NEX, 3; section thickness, 4mm; intersection gap, 2mm. In this study b-values of 0 and 500 s/mm^2 were used for cDWI. The cDWI of b-values of 800, 1100, 1400, 1700 and 2000 s/mm^2 were generated on DICOM imaging platform (OsiriX MD 7.5) by using mono-exponential model. Blind reading was performed to evaluate 60 breasts including normal contralateral breast by 2 radiologists (observer A and B). Observers pointed out the lesions freely and the conspicuity of the lesions classified into the following 4 categories, 1, obscure or faint; 2, weak; 3, indeterminate; 3, not strong but distinguishable; 4, clear. The score 2 or more was defined as a positive. Receiver operating characteristic (ROC) analysis was performed. ResultsThe inter-observer agreement was good (κ=0.76). The Az values on b-values of 500, 800, 1100, 1400, 1700 and 2000 s/mm2 was 0.75, 0.87, 0.87, 0.78, 0.80 and 0.77 in observer A and 0.80, 0.88, 0.88, 0.83, 0.81, 0.72 in observer B, respectively. Those of the lesion which size was less than 1 cm was 0.76, 0.89, 0.90, 0.78, 0.73 and 0.69 in observer A and 0.68, 0.82, 0.79, 0.75, 0.61 and 0.52 in observer B, respectively.ConclusionThe optimal b-value of cDWI for detecting breast cancer was between 800 and 1100 s/mm^2.

O-2-057　cDWIにおいて信号が消失してしまう非浸潤性乳管癌とその悪性度の関係について
Shrinking phenomenon of ductal carcinoma in situ on cDWI; Is it depend on pathological grade?

那須　克宏（筑波大学大学院 人間総合医学研究科 疾患制御医学専攻 応用放射線医学分野）
Katsuhiro Nasu, Hiroaki Takahashi, Manabu Minami

University of Tsukuba, Faculty of Medicine, Department of Diagnostic Radiology

【要旨】b=3000を用いたcDWIは高濃度乳腺における偽病変のみならず、非浸潤癌の信号も抑制し腫瘍の範囲が狭く描出されることがある（縮小現象）。縮小現象は腫瘍の悪性度とは関係なく発生する。

Purpose: In the last JSMRM meeting, we had reported that computed DWI (cDWI) could eliminate the pseudo-lesions in dense breasts but it also suppressed the signals of DCISs occasionally (hereinafter we call this finding shrinking phenomenon). In this study, we investigated the pathological characteristics of DCISs showing shrinking phenomenon.
Methods: 40 DCISs in 39 females who had dense breasts were evaluated (1 patients had two cancers in bilateral breasts). All patients had MR examinations including DWI and underwent surgical resection without any adjuvant therapies. We induced cDWI (b=3000) from DWIs having b-factors of 0 and 1000. Two trained radiologists reviewed all imaging examinations including MMG, US and dynamic MRI with full-knowledge of pathological results and confirmed the cancer extent on MR images. Then we classified cDWI findings in each cancer in into two groups (Group A: The cancers did not show shrinking phenomenon and Group B: The cancers showed shrinking phenomenon). Finally, we evaluated the incidence of pathological grades (low/intermediate/high) in each group.
Results: Among 40 cancers, 13 were classified into Group A and the remaining 27 were classified into Group B. Group A included 6 low, 2 intermediate and 5 high grade tumors. Group B included 11 low, 13 intermediate and 3 high grade tumors.
Conclusion: The shrinking phenomenon does not have correlation with pathological grades. It was assumed to be determined by the size of cancer foci in each tumor.

O-2-058　超高速撮像法(KWIC撮像法)を用いた造影超早期のMSによる診断能の評価
Diagnostic Performance of Maximum Slope in High Resolution Ultrafast Dynamic Contrast Enhanced Breast MRI using KWIC

大橋　茜（京都大学 医学部付属病院 放射線診断科）
Akane Ohashi[1], Masako Kataoka[1], Shotaro Kanao[1], Mami Iima[1], Natsuko Onishi[1], Makiko Kawai[1], Rena Sakaguchi[1], Ayami Oono[1], Masakazu Toi[2], Weiland Elizabeth[3], Kaori Togashi[1]

[1]Department of Diagnostic Imaging and Nuclear Medicine Kyoto University Graduate School of Medicine, [2]Department of Breast Surgery Medicine Kyoto University Graduate School of Medicine, [3]Siemens Healthcare GmbH, Erlangen, Germany

【要旨】高速撮像法であるKWIC撮像における造影超早期のMaximum Slope(MS)の診断能を、標準DCEMRIのパラメーターであるWashout index(WI)やBI-RADSカテゴリーと比較した。MSの診断能はWIより良好であったがBI-RADS Categoryには及ばなかった。

Purpose: Maximum slope (MS) is a novel parameter obtained from the initial slope of the dynamic curve in ultrafast dynamic contrast enhanced (DCE) MRI. This parameter requires breast DCE MRI with high temporal (3.75 sec) and spatial resolution (1.0x1.0x2.5mm3), that can be achieved using K-space weighted Imaging Contrast (KWIC). This study aimed to evaluate diagnostic performance of MS obtained by ultrafast DCE MRI using KWIC acquisition compared to washout index (WI) obtained by standard DCE-MRI, and to BI-RADS category scored in reporting in breast lesions. Materials and Methods: Breast MRI were performed with a 3T scanner (MAGNETOM Trio, A Tim System, Siemens AG) with 16ch dedicated bilateral breast coil. T2WI, T1WI, DWI and three fat-suppressed T1WI DCE images (pre, post 1-2min early, 5-6min delayed), and high resolution T1WI CE images were obtained. KWIC sequence was obtained 0-1 min after gadolinium injection. MS was evaluated using dedicated software (TWIST Breast Viewer prototype) and calculated as percentage relative enhancement/ second [%/s]. MS were compared to washout Index (WI) and to BIRADS categories incorporating both kinetic and morphological information. The WI is defined as 100 x (SI delay-SI early)/ SI pre (%). Diagnostic performance was compared using ROC analysis and area under the ROC curve (AUC). Results: In total 94 patients with 106 enhancing lesions (60 malignant / 46 benign lesions) were included. MS shows significantly higher AUC than WI (0.91 vs 0.80; P=0.03), however lower AUC than BIRADS lexicon (0.91 vs 0.98; P=0.03). This result suggested that, although MS is a promising kinetic parameter, the morphological characteristics are still important to diagnose lesions.

O-2-059　授乳期・非授乳期乳腺におけるIVIM・非ガウス拡散MRIの検討
the investigation of IVIM and non-Gaussian diffusion MRI in the lactating and non-lactating breasts

飯間　麻美（京都大学 大学院 医学研究科 放射線医学講座）
Mami Iima[1,2], Masako Kataoka[1], Shotaro Kanao[1], Makiko Kawai[1], Natsuko Onishi[1], Akane Ohashi[1], Rena Sakaguchi[1], Ayami Oono[1], Kaori Togashi[1]

[1]Department of Diagnostic Imaging and Nuclear Medicine, Kyoto University School of Medicine, [2]Hakubi Center, Kyoto University

【要旨】7名の授乳期乳腺・13名の非授乳期乳腺ボランティアに対し、0-2500 sec/mm^2 のb値を用い拡散強調MRIを撮影し、IVIM・非ガウス拡散MRIの有用性を検討した。授乳期乳腺においては非授乳期乳腺に比し有意に高いIVIM, K値, 低いADCo, ADC200-1500値を示し、乳腺組織の評価に有用である可能性が示唆された。

Introduction: Non-Gaussianity for water diffusion can be quantified by using diffusion kurtosis model beyond ADC, and we have investigated the usefulness of non-Gaussian DWI parameter estimates according to the lactating status. Material and Methods: 7 lactating and 13 non-lactating volunteers were recruited in this prospective study. Breast MRI was performed using a 3-T system. DWI was acquired with 16 b values of 0-2500 sec/mm^2 with a scan time of 3min 55sec. Images processing was performed comprising the IVIM and Kurtosis model with noise correction. Additionally a synthetic ADC,encompassing both Gaussian and non-Gaussian diffusion effects, ADC200-1500, was defined. Results: ADCo and ADC200-1500 values significantly decreased in lactating volunteers ($p<0.01$,$p<0.01$). Significantly higher K and fIVIM were observed in lactating volunteers($p<0.01$,$p<0.01$). Discussion&Conclusion: Interestingly significant difference of non-Gaussian diffusion and IVIM parameters was observed with lactation status, and there will be a need for the consideration of lactation status when assessing breast DWI data.

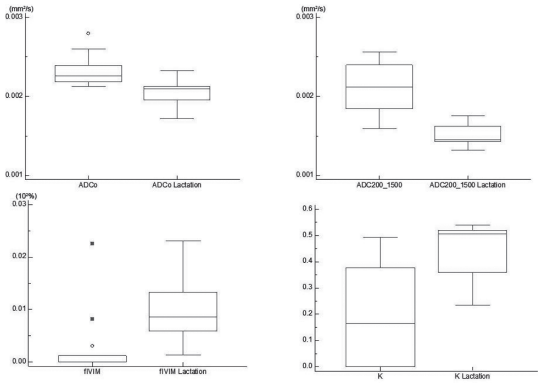

Diffusion and IVIM MRI parameters of non-lactating and lactating volunteers

O-2-060　ナノ磁性体を内包した糖PEG修飾リポソームの材料設計
Material design of sugar -PEG-modified liposome encapsulating the nano magnetic material

八木　一夫（首都大学東京 大学院人間健康科学研究科）
Kazuo Yagi[1,2], Daichi Mizutani[2], Yoshihiro Yazu[2], Hiroyuki Kawabata[3], Seiichi Sugimoto[4], Masataka Kubo[2], Tadashi Inaba[2]

[1]Graduate School of Human Health Sciences, Tokyo Metropolitan University, [2]Graduate School of Engineering, Mie University, [3]Faculty of Engineering, Mie University, [4]Tokyo Metropolitan College of Industrial Technology

【要旨】RES回避リポソームをモデルとした糖被膜型磁性流体を作製する為，多糖であるコンドロイチン硫酸とポリエチレングリコール(PEG)をエステル結合およびアミド結合により合成させたPEG化コンドロイチン硫酸の作成。PEG化とはメトキシPEG末端水酸基のアミノ化によるPEGの結合で、それを分散剤として糖被膜型磁性流体の作製した。

Background: Research and development of Reticuloendothelial system (RES) avoidance liposomes were modified closed vesicle called a liposome approximate lipid bilayer having a recognition is slow nature from the immune system as foreign is being performed.[Purpose] In order to produce a RES avoid liposome the model and the sugar coating type magnetic fluid, chondroitin sulfate(CS) and polyethylene glycol (PEG) is a polysaccharide to produce a PEG of CS, which was synthesized by the ester bond. In addition, it was carried out the production of the sugar coating type magnetic fluid using as a dispersing agent.[Method] in order to produce a composite 1, PEG sugar coating type MF, it is necessary to PEG the sugar. By the amide bond PEG was binding of amination of methoxy PEG terminal hydroxyl groups.The CS C and amides PEG of CS by hydroxyl bonded to prepare a sugar coating type MF (PEG / CS / MF) was used for the dispersant.The prepared samples were measured saturation magnetization value using a vibrating magnetometer (VSM), particle size by light scattering measuring instrument (DSL), and that were carried out the sample identification by 7T- NMR analysis.[Result] saturation magnetization value of the sample, composition, core particle diameter, and by comparing the colloid size in the presence or absence of PEG-modified, it was to investigate the impact on the sugar coating type magnetic fluid. For confirmation of the synthesis of PEG CS, a sample analysis obtained by the PEG methyl ether and synthesized in the 1H-NMR spectroscopy and IR method.It was identified substance contained in a sample to compare with the NMR spectrum of the sample synthesized with the NMR spectrum of the CS and PEG methyl ether.

O-2-061　液相合成法によるフェライト磁性ナノ粒子の生成とコロイドマテリアル法による糖被膜型磁性体の磁気特性評価
Evaluation of the sugar coating type material due to the formation of ferrite nanoparticles by liquid phase synthesis and colloidal material method

八木　一夫（首都大東京 大学院人間健康科学研究科）
Kazuo Yagi[1,2], Daichi Mizutani[2], Hiroyuki Kawabata[3], Takanori Tanaka[3], Yoshihiro Yazu[2], Yujiro Harada[2], Seiichi Sugimoto[2,4], Masataka Kubo[2], Tadashi Inaba[2]

[1]Graduate School of Human Health Sciences, Tokyo Metropolitan University, [2]Graduate School of Engineering, Mie University, [3]Faculty of Engineering, Mie University, [4]Tokyo Metropolitan College of Industrial Technology

【要旨】優れた磁気特性を有する微粒子の創製を目指し，MxMyO・Fe2O3の組み合わせにより種々のフェライト微粒子を作製した．Mx，Myのモル比率を変化させ，飽和磁化値と組成比率の関係は、Co2+とZn2+とFe2+とFe3+の組み合わせが良好な磁気特性を示し最大飽和磁化値はZnFeO・Fe2O3で78.1，CoZnFeO・Fe2O3で83.1[emu/g]であった．

Aiming to creation of new magnetic microparticles having more excellent magnetic properties, to produce a variety of fine ferrite particles by a combination of MxMyO・Fe2O3, their characteristics were evaluated. It shows a specific manufacturing process of MxMyO・Fe2O3 magnetic fine particles.(1)By changing the molar ratio of M2 +, Fe2 + and Fe3 + metal ions to the total sample 14 mmol, it is dissolved Ar gas for preventing oxidation through the added distilled water (100ml).Thus, to obtain a mixed solution of the M2 +, Fe2 +, Fe3 + three kinds metal ions is mixed.The mixed solution is heated and maintained with stirring to 363 [K]. (2) To adjust the pH to an appropriate amount of the 3 provisions of the aqueous NaOH solution to this mixed solution. It is the pH of at this time and during the synthesis pH.(3) After cooling and centrifuged 15 min at 3000 [rpm] by a centrifugal separator to obtain a precipitate. (4)The precipitate was washed twice, frozen immersed in liquid nitrogen to obtain a fine powder sample by lyophilizer.In this study, by changing the molar ratio of the Mx and My, that were examined for relation between saturation magnetization value, composition ratio and the particle diameter.From the inverse spinel structure ferrite, the ratio of divalent and trivalent metal by 1: 2, high saturation magnetization values can be expected.Therefore, the divalent: trivalent = 1: 2 is set to. Ferrite Mx, investigated the effect on the magnetic properties by changing the combination of My. The combination of Co2 + and Zn2 + and Fe2 + and Fe3 + exhibited good magnetic properties.

O-2-062　高分解 2D ^{1}H定時間MRSの開発 〜 時間領域データの共有再構成法を用いたグルタミン酸、GABAの絶対定量化 〜
Absolute quantitation of glutamate and γ-aminobutyric acid on highly resolved 2D constant time ^{1}H spectra using 2D FT with shared time domain data

渡邉　英宏（国立環境研究所 環境計測研究センター 画像・スペクトル計測研究室）
Hidehiro Watanabe, Nobuhiro Takaya

Environmental Imaging and Spectrum Measurement Section, Center for Environmental Measurement and Analysis, National Institute for Environmental Studies

【要旨】ヒト脳内の主要な神経伝達物質のグルタミン酸とGABAは、ピークオーバーラップのため通常の^{1}Hスペクトルでは検出が難しい。今回、これらのピークを分離検出可能な2D定時間PRESS法を用いた絶対定量化法を提案、開発し、4.7 Tヒト用MR装置を用いて、ファントム実験により定量化が可能であることを実証した。

Introduction: While peaks of glutamate (Glu) and γ-aminobutyric acid (GABA) of major neurotransmitters are heavily overlapped on the conventional ^{1}H spectra of human brain, these peaks can be clearly resolved on 2D constant time (CT) PRESS spectra with ^{1}H decoupling along F_1. In this work, we will measure concentration of Glu and GABA in phantom experiments by our proposed quantitation method of 2D FT with shared time domain (TD) data.

Methods: Figure 1 shows a schematic of our proposed quantitation method. Reconstruction of a partial TD data generates a CT-PRESS spectrum weighted by $\exp(-T_{ct}/T_2)$. T_2 correction can be done by series of ^{1}H decoupled spectra.

Results: All experiments were performed using a 4.7 T whole-body MR system (INOVA, Agilent). In phantom experiments with a mixture of brain metabolites including 9.0 mM Glu and 2.6 mM GABA, concentrations were calculated as 9.5 mM of Glu, 2.5 mM of GABA.

Conclusions: Our proposed method is useful to measure concentrations of Glu and GABA. This method will also be applied in human brain CT-PRESS spectra with the internal water reference method.

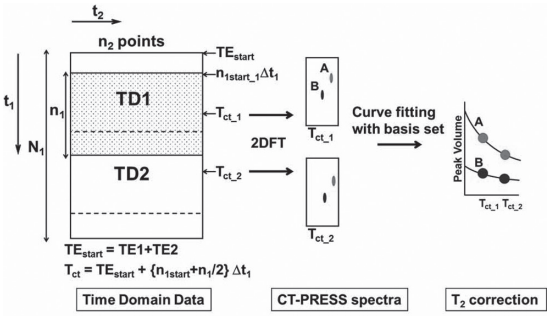

Fig. 1. A schematic of a proposed quantitation method on highly resolved CT-PRESS spectra

O-2-063　マウス脳内REDOXイメージング用theranosticプローブの開発
Development of nitroxide-based theranostic probes for septic mouse brain

藤井　博匡（札幌医科大学 医療人育成センター）
Hirotada Fujii[1], Miho Emoto[1], Shingo Sato[2]

[1]Sapporo Medical University Center for Medical Education, [2]Yamagata Univeristy

【要旨】血液脳関門を通過しうるナイトロオキシド化合物は、脳内の酸化還元状態に依存してその常磁性を消失するため、脳内レドックス状態を非侵襲的に視覚化可能な分子プローブとして着目されている。本研究は、治療薬と分子プローブの機能を併せ持ったセラノスティク分子プローブの合成及びその応用研究を実施した。

Theranostic probes provide both therapeutic and diagnostic imaging capabilities in one molecule. Recently, we synthesized a probe by connecting nitroxide T1 contrast agents to anti-inflammatory drugs. In this study, these synthesized theranostic probes were applied to brain disease model mice for diagnostic and therapy. We examined their detail distribution and kinetics in mouse heads. Additionally, the therapeutic effects of these probes were evaluated in septic mouse brains. [Methods] Theranostic probes were synthesized by connecting ibuprofen or ketoprofen to 3-hydroxymethyl-2,2,5,5-tetramethylprrolidine-1-oxyl (3-hydroxymethyl-PROXYL). Septic mice were prepared by the injection of lipopolysaccharide into mice. The amount of nitric oxide (NO) generated in septic mouse brains was quantitated through a fluorescence method. MRI of mouse heads was acquired using an MRmini (MRT). [RESULTS AND DISCUSSION] To examine if nitroxide-based theranostic probes can act as T1 contrast agents for MRI in mouse brains, MRI of mouse heads was taken. Difference MRI obtained from images before and after administration of probes clearly indicated that both probes entered the brains by passing through the blood brain barrier. Time-course MRI of mouse heads was examined after injection of both probes, and their half-lives were evaluated. To examine if both probes have anti-inflammatory effects, the amount of NO produced in septic mouse brains was measured. Percent inhibition of NO generation in septic mouse brains by the administration of the probes was more than 80% (n=3) for both probes. These results suggest that ibuprofen-PROXYL and ketoprofen-PROXYL can act both as anti-inflammatory drugs and as T1 contrast agents in MRI.

O-2-064　ゲルファントムにおけるSPIO標識骨髄間質細胞の磁化率・R2*定量解析
Quantitative measurement of susceptibility/R2* values of SPIO-labeled bone marrow stromal cells in gel phantom

原田太以佑（北海道大学病院 放射線診断科）
Taisuke Harada[1], Kohsuke Kudo[1], Toru Shirai[2], Yoshitaka Bito[3], Hideo Shichinohe[4], Chengbo Tan[4], Ziefeng Wang[4,5], Kiyohiro Houkin[4], Hiroki Shirato[5]

[1]Diagnostic and Interventional Radiology, Hokkaido University Hospital, [2]Research and Development Group, Hitachi, Ltd., [3]Healthcare Business Unit, Hitachi, Ltd., [4]Neurosurgery, Hokkaido University, [5]Radiation Medicine, Hokkaido University

【要旨】様々な細胞数のSPIO標識骨髄間質細胞（BMSC）をゲルファントムに注入し、磁化率とR2*の定量測定を行った。いずれの値もBMSC細胞数と高い相関が見られ、再現性も良好であり、臨床研究において移植されたBMSCの細胞数推定や細胞トラッキングに応用可能であると考えられた。

[PURPOSE] In the bone marrow stromal cell (BMSC) therapy for stroke patients, it would be desirable to monitor the distribution and number of BMSC. As those cells are labeled by super paramagnetic iron oxide (SPIO), quantitative susceptibility mapping (QSM) can be used for the cell tracking. The purpose of this study was to evaluate the relationship between the amount of SPIO-labeled BMSC and susceptibility/R2* value in gel phantom. [MATERIAL and METHOD] The various amount of SPIO-labelled BMSCs (50000, 25000, 12500, 6250, 3300, 1560, 780, and 0 cells/μl, each 0.1 ml) were injected into a polyvinyl alcohol gel. This phantom was repeatedly scanned for 16 times in every 30 min with 3T MRI (Hitachi, Ltd.), using 3D multi-echo gradient echo sequence. QSM images were reconstructed using iterative reconstruction using edge-preserving filtering. Spherical ROIs were manually placed on each cell cluster in QSM images to measure the susceptibility/R2* values. Linear regression analysis was performed between the amount of BMSC and susceptibility/R2* value. The reproducibility were also evaluated by the coefficient of variation (CV) of repeated scans for each cell cluster.[RESULT] The regression line and correlation coefficients were $y = 0.0081x - 4.55$ ($r = 0.998 \pm 0.0002$) and $y = 0.0021x + 0.51$ ($r = 0.998 \pm 0.0002$) for susceptibility and R2* values, respectively. The CV values were smaller in R2* (0.032-0.040) than QSM (0.066-0.068) in the low amount (1560 and 780 cells/μl), and smaller in QSM (0.017-0.050) than R2* (0.030-0.054) in the middle-high amount (over 1560 cells/μl) of BMSC.[CONCLUSION]The amount of BMSCs can be accurately estimated by both susceptibility and R2* values in gel phantom. This result can facilitate the monitoring of BMSC in vivo in clinical studies.

O-2-065　^{13}C MRS を用いた急速減量と回復による筋グリコーゲン動態の描出
^{13}C MRS reveals changes in muscle glycogen content during rapid weight loss and recovery

高橋　英幸（国立スポーツ科学センター）
Hideyuki Takahashi[1], Emi Kondo[1], Keisuke Shiose[1], Takuya Osawa[2], Keiko Motonaga[1], Shiori Ouchi[1], Akiko Kamei[1], Kohei Nakajima[1], Katsuya Maruyama[3]
[1]Japan Institute of Sports Sciences, [2]Juntendo University, [3]Siemens Healthcare K.K.

【要旨】^{13}C MRSを用いて、レスリング選手の急速減量(53時間で体重の6%低下)とその後の高炭水化物摂取が大腿部筋グリコーゲン(Gly)に及ぼす影響を調べた。その結果、急速減量中に筋Glyは64.6%まで低下し、高炭水化物食摂取を含む13時間の回復でも83.3%までしか回復しないことが明らかとなった。

Many athletes who are engaged in weight restrictions-related sports events experience frequent rapid weight loss (RWL). However, there is little information regarding the changes in the content of muscle glycogen (Gly) during RWL and the recovery period. The purpose of this study was to investigate changes in the muscle Gly content of wrestlers during RWL and recovery phase by using ^{13}C MRS. Ten male collegiate wrestlers participated in this study. The subjects lost 6 % of body mass over the course of 53 hours by using their own methods. Further, they took recovery meals with a large amount of carbohydrate (7.1 ± 0.2 g/kg BM) for a period of 13 hours. The Gly concentration measurements of the thigh muscle by using ^{13}C MRS were performed before and after RWL as well as after the recovery phase. ^{13}C MRS was performed by using a clinical 3T-MR scanner (Magnetom Verio, Siemens). The ^{13}C MRS spectra were collected with a ^{13}C -^{1}H double-tuned surface coil (Takashima seisakusho). The measurement parameters were TR = 200 ms, data points = 2,048, sweep width = 20,000 Hz, and averages = 4,500. Furthermore, we applied proton decoupling and nuclear Overhauser enhancement. The muscle Gly concentrations were determined by comparison with an external standard solution. Body mass decreased by 4.6 ± 0.6 kg (6.3 ± 0.5 %) during RWL and did not recover completely after the recovery phase. The muscle Gly decreased to 64.6 ± 9.5 % after RWL, and after the recovery phase, it recovered to only 83.3 ± 11.4 % of the basal value. The ^{13}C MRS revealed that the muscle Gly concentration decreased largely during RWL and did not recover completely after 13 h of recovery phase. The noninvasive evaluation of the muscle Gly concentration will contribute to design nutritional strategies for athletes.

O-2-066　ヒト脳内におけるグルタチオン測定の検討
Examination of the glutathione measurement in the human brain

村瀬　智一（明治国際医療大学 医療情報学ユニット）
Tomokazu Murase[1], Masahiro Umeda[1], Yuko Kawai[1], Ayako Mandai[2], Toshihiro Higuchi[2]
[1]Meiji University of Integrative Medicine Dept. of Medical Informatics, [2]Meiji University of Integrative Medicine Dept. of Neurosurgery

【要旨】今回我々は生体内で生成される抗酸化物質であるGSHの測定条件を検討した。健常成人5名(23-48歳)を対象にMEGA-PRESS によるGSH測定を行い、全例で差分スペクトルの2.95ppm2.95ppm付近のピークを観察できた。

Background and Purpose:GSH (glutathione) is an anti-oxidants that are generated in vivo. GSH is has been attracting attention as the measurement target of the MRS, the peak of the signal is like the GABA or lactate, in order to overlap with the other of the spectrum peak, MEGAPRESS method is required. Therefore, we investigated the measurement conditions of GSHMethods:Healthy adult five subjects gave their consent to the experiment (23-48 years old) . The experiments were carried out in a 3.0T Trio system and 32ch head array coil. Single voxel MRS (MEGA-PRESS) was used to measure GSH levels with the following parameters: TR/TE = 3,000 ms/68 ms, NEX = 128 (*2), VOI = 20 mm *30 mm *20 mm, selective excitation pulse = 7.5 ppm /4.56 ppm, measurement time = 13 min 18 s. The analysis of MRS data was used by [ramo1D4] (ISBN: 9784782705971) Results and Discussion:The difference spectrum was able to observe a peak in the vicinity of 2.95ppm in all cases, in Figure. The ratio of GSH / Cr concentration was 0.11 ± 0.03. Than this result, it is considered to be able to measure the GSH.

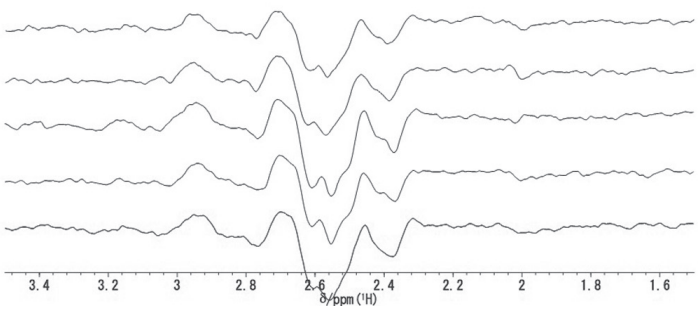

O-2-067　APT-CEST imagingのCEST効果の定量値とMT及びNOE指標との関連
Correlation between quantitative values depending on CEST effect and indices of MT and NOE for APT-CEST imaging

原田　雅史（徳島大学大学院 放射線医学分野）
Masafumi Harada[1], Sonoka Hisaoka[1], Maki Ohtomo[1], Mitsuhiro Kinoshita[1], Saho Irahara[1], Mitsuharu Miyoshi[2], Yuki Kanazawa[3]

[1]Departement of Radiology, Tokushima University, [2]Global MR Applications and Workflow, GE Healthcare Japan, [3]Institute of Biomedical Sciences, Tokushima University

【要旨】APT-CEST imagingのZ spectrumをCPE解析することによりMT及びNOE指標を定量し、APTの定量値と併せて検討した。対象は脳腫瘍患者12症例で、腫瘍を中心とする一断面を撮像した。Z spectrumのasymmetry ratioは、CPE解析で得られたAPT rateと高い相関を有したが、MT効果やNOEと逆相関が認められた。

Purposes: The new fitting program using multiple pools model for APT-CEST imaging can separate several quantitative values depending on CEST effect and indices of Magnetization Transfer (MT) of water and Nuclear Overhauser Effect (NOE). The purpose of this study was to evaluate the correlation between APT-CEST effect and MT or NOE indices on the subjects of brain tumors.Subjects: Twelve patients of brain tumor (6 gliomas, 2 malignant lymphomas, 4 metastases) were recruited in this study. This study was approved by the ethical committee of Tokushima University Hospital. A single slice measurement for APT-CEST imaging was conducted using phase cycled rectangular RF preparation pulse with the offset frequency equivalent to ±7ppm in 32 steps for CEST effect. Two minuets' 20 sec scan was conducted before the enhanced study. The curve fitting for the obtained Z-spectrum depending on the CEST Peak Extraction (CPE) method was conducted and the several parameters including APT, MT and NOE rates in addition to the asymmetry ratio of Z-spectrum.Results: The indices of NOE were not extracted from the data of 5 subjects, whose NOE data were excluded from the NOE comparison. The most significant correlation was found between the asymmetry ratio and APT rates ($r=0.74$, $p<0.01$), and the negative correlations between APT rate and MT or NOE rates were also seen respectively (MT: $r=-0.67$, $p<0.01$, NOE: $r=-0.60$, $p<0.01$). The asymmetry ratio showed higher correlation with NOE rates ($r=-0.73$) than APT rates, suggesting additional influence of NOE to the asymmetry ratio. Conclusion: The negative correlations with APT-CEST and MT or NOE effects was suggested on the subjects with brain tumors using CPE method, and these effects may be analyzed separately for the evaluation of APT-CEST imaging.

O-2-068　pH強調APTイメージングにおける飽和パルスの持続時間と強度の影響
Dependence of the duration and power of saturation pulse on chemical exchange saturation transfer in pH sensitive amide proton transfer imaging

徳永　千晶（九州大学病院 医療技術部 放射線部門）
Chiaki Tokunaga[1], Tatsuhiro Wada[1], Osamu Togao[2], Yasuo Yamashita[1], Kouji Kobayashi[1]

[1]Division of Radiology, Department of Medical Technology, Kyushu University Hospital, [2]Department of Clinical Radiology, Graduate School of Medical Sciences, Kyushu University

【要旨】APT イメージングのpH依存性と飽和パルスの持続時間と強度の影響を自作の卵白アルブミンファントムを用いて評価した．APTイメージングにおけるCEST効果はpHと正の相関を示した。飽和パルスの印加時間を長くかつ強くすることで，pH変化をより鋭敏に反映したAPTイメージングを得ることができた．

[Purpose] Amide proton transfer (APT) imaging has the potential to detect changes in tissue pH based on the chemical exchange saturation transfer (CEST) phenomenon, and thus may be useful in the identification of penumbra in ischemic stroke. The purpose of our study was to investigate the dependence of the duration and power of saturation pulse on the CEST effect in pH-phantoms.
[Methods] Five samples were prepared from egg white albumin at the concentration of 10% diluted with phosphate buffer solution at different pH of 6.72, 6.91, 7.08, 7.42, and 7.63. Experiments were performed on a 3.0-T clinical MR scanner with use of a body coil for two-channel parallel radiofrequency transmission. The CEST effects was defined as asymmetry of the magnetization transfer ratio at 3.5 ppm. We measured the CEST effects in the egg white albumin samples with different pH at saturation pulse duration of 0.5, 1.0, 2.0, and 3.0 s, and power of 0.5, 1.5, and 2.5 μT. The increase ratio of the CEST effect to pH concentration was defined as the slope of the linear regression.
[Results] The CEST effect was significantly increased with the pH when the duration was longer and power was stronger unless duration was $\geq$ 2.0 s at pH 7.63. The CEST effect was highly correlated with the pH at all saturation pulse durations and powers, and its increase ratio was higher at longer durations and stronger powers for the saturation pulses.
[Conclusions] The saturation pulse which have long duration and strong power was useful for the sensitive detection of the changes in CEST effects in the egg white albumin samples with different pH.

O-2-069　脳腫瘍患者でのCEST Peak Extraction Spectrumを用いたMultiple pools model fitting map
Multiple pools model fitting map with CEST Peak Extraction Spectrum in brain tumor patients

三好　光晴（GEヘルスケア・ジャパン研究開発部）
Mitsuharu Miyoshi[1], Masafumi Harada[2], Yuki Kanazawa[2], Hiroyuki Kabasawa[1]
[1]Global MR Applications and Workflow, GE Healthcare Japan, [2]Department of Radiology, Institute of Health Biosciences, The University of Tokushima Graduate School

【要旨】CEST Peak Extraction Spectrumを用いてMultiple pools model fittingを行い、脳腫瘍患者でAPT, MT, Free water pool mapを作成した。脳腫瘍とwhite matterは各mapで異なるコントラストを持つことが示された。

[Purpose] CEST, Magnetization Transfer (MT) and Free water maps of brain tumor were calculated by using multiple pools model.
[Methods] Patient study: Seven brain tumor patients were scanned under IRB approval and written informed consent. Investigational version Phase Cycle RF preparation pulse (ref.1) was used for CEST contrast with the offset frequency equivalent to ± 7ppm in 32 steps. Mean B1 was 2μT. Total RF irradiation time was 3.5sec before EPI data acquisition. Scan time was 2:20 for one slice. Levenberg-Marquardt algorism was used for non-linear Lorentzian fitting. Matlab was used for calculation. Field strength was 3T (MR750, GE Healthcare).
CEST Peak Extraction (CPE) spectrum: Approximation solution of CPE-spectrum (ref.2) could separate multiple pools (Free water, binding water MT, and several CEST pools) as a fitting coefficient. The width of Z-spectrum at 0ppm is visualized as a Free water T2/T1 map. The height of Z-spectrum at off-resonance is visualized as an MT map. The +3.5ppm peak area of CPE-spectrum was visualized as an APT map. MTR asymmetry (MTR_asym) map at ± 3.5ppm was calculated as a reference.
[Results and Discussions] Brain tumor had inhomogeneous signal in APT and Free water map. If tumor signal was high in Free water map, it was low in APT map. If it was mid in free water, it was high in APT. Tumor signal was low in MT map in general. APT map had less noise than MTR_asym map because fitting algorism reduces the influence of noise in the spectrum. White matter was high in MT map, low in Free water and APT maps.
[Conclusion] CPE-spectrum fitting was performed in patient. Tumor and white matter signal had different contrast in APT, MT and Free water maps.
[References] (1)Miyoshi M. et al., ISMRM 2014, #3299, (2)Miyoshi M. et al., ISMRM 2015, #3346

O-2-070　Readout RFパルスが脳腫瘍のamide proton transferイメージングに及ぼす影響
Effect of the readout RF pulse on amide proton transfer imaging contrast in brain tumor: comparison between single-shot and multi-shot turbo spin echo

和田　達弘（九州大学病院 医療技術部 放射線部門）
Tatsuhiro Wada[1], Osamu Togao[2], Chiaki Tokunaga[1], Yasuo Yamashita[1], Kouji Kobayashi[1]
[1]Division of Radiology, Department of Medical Technology, Kyushu University Hospital, [2]Department of Clinical Radiology, Graduate School of Medical Sciences, Kyushu University

【要旨】Readout RFパルスの違いによる脳腫瘍のAPTイメージングの変化を検討した．正常白質においては2つのRFパルスの間（SS-TSE、MS-TSE）で信号の違いが見られたが，腫瘍の信号および腫瘍と正常白質の信号差には違いが見られなかった．脳腫瘍のAPTイメージングにおいてreadout RFパルスによる信号変化は僅かであった．

[Purpose] Amide proton transfer (APT) imaging is one subset of the endogenous chemical exchange saturation transfer (CEST) imaging. The purpose of this study was to investigate the effect of readout RF pulses on APT imaging contrast in brain tumors.[Methods] Twelve patients (meningioma=5, metastasis=3, low-grade glioma=2, high-grade glioma=2) were examined in this study. The examination was performed on a 3T MR scanner using an 8-channel head coil. APT images were acquired with the two different readout RF pulses. One is the single-shot turbo spin-echo (SS-TSE) and the other is multi-shot TSE (MS-TSE). Saturation pulses with duration of 2.0 s and power of 2.0 μT were irradiated at 31 frequency offsets (ω=-12..12 ppm and ω=-1650 ppm). Other parameters of SS-TSE were as follows: TR/TE=5215 ms/6.2 ms, FOV=230x230 mm^2, matrix=128x128, SENSE=none, acquisition time = 2 m32 s. Other parameters of MS-TSE were as follows: TR/TE=4000 ms/6.2 ms, FOV=230x230 mm^2, matrix=128x128, TSE factor=32, SENSE factor=2, acquisition time = 4 m24 s. ROIs were placed in normal appearing white matter (NAWM) and tumor. Mean and 90th percentile values of APT signal values were measured, and δAPT signal (tumor-NAWM) were calculated.[Results] In NAWM, the mean value of APT signal obtained with MS-TSE was significantly lower than that with SS-TSE (p=0.01), while the 90th percentile values of APT signal obtained with both readout pulses were not significantly different. In tumors, the mean and 90th percentile values of APT signal were not significantly different between SS-TSE and MS-TSE. The δAPT signal also did not differ between the both readout pulses.[Conclusion] The Variation of APT signal measured with different readout RF pulses might be negligible in brain tumors.

O-2-071　部分空間高密度サンプリングを使用したMR圧縮センシング
Magnetic Resonance Compressed Sensing using Higher-density Sampling in Restricted Signal Space

松本　知之（宇都宮大学 大学院工学研究科 情報システム科学専攻）
Tomoyuki Matsumoto, Mone Shibuya, Satoshi Ito

Information Systems Sciences, Utsunomiya University

【要旨】本研究では圧縮センシング応用における画質改善を目的とし，信号量を同量とする条件で制限された信号空間内で信号を間引く方の検討を行った．再構成シミュレーションを行った結果，信号量を30%から50%の範囲では，制限された空間を間引く方が信号空間全域から間引く場合より高い信号対雑音比が得られる結果となった．

Introduction
Variable density random sampling (VDS) selecting more low frequencies than high frequencies is often adopted in compressed sensing (CS) MRI. Structures or details of images may be lost by the loss of higher frequency. We consider a combined partial signal-space sampling and CS reconstruction to improve the quality of reconstructed images.
Method
In general, partial signal space sampling results in the decrease of image quality, however, it has the advantage of higher density signal sampling when it is combined with CS scheme. Partial signal sampling like half Fourier imaging is combined with CS reconstruction. To meet the phase variation on the image, we used the multi-scale eFREBAS transform based CS [1] scheme in which estimation of phase variation is not required in image reconstruction.
Results and Discussions
Simulation studies using phase-varied images shows that higher signal-to-noise ratio can be obtained by proposed partial signal-space sampling than standard full-space under-sampling method when the amount of acquired signal is the same, which ranges from 30% to 50%. In addition, obtained images has much more structures of image with sharpened edges.
Conclusion
Partial signal-space under-sampling is promising method in CS, since it provides higher density signal sampling.

[1] S. Ito et al., ISMRM2015, 2459, 2015

O-2-072　信号の非ランダムサンプリングを利用した圧縮センシング画像再構成
Compressed Sensing Image Reconstruction using Non-randomly Sampled Signa

伊藤　聡志（宇都宮大学 大学院工学研究科 情報システム科学専攻）
Satoshi Ito, Kazuki Sekine

Information Systems Sciences, Utsunomiya University

【要旨】本研究では再生像の画質安定化を図る一手法として信号の収集を規則的かつ可変密度とする新たな方法について検討を行った．スパース化関数にマルチスケール・カーブレット変換を利用した結果，ランダム収集に比肩する信号対雑音比の画像を得ることができた．

Introduction
Image quality obtained in compressed sensing (CS) reconstruction depends on the randomness or sampling density in k-space. We propose a novel image reconstruction scheme in which nonrandomly sampled signal is adopted in reconstruction scheme.
Methods
Curvelet transform[1] was designed to represent edges and other singularities along curves much more efficiently than traditional transforms. Since the curvelet transform is a multiscale pyramid with many directions, it has a high ability to reduce the aliasing artifact. To enhance the incoherency with the sampling matrix, we introduce multi-scale Curvelet transform in which scale of image decomposition varies in each iteration step.
Results
Averaged PSNRs of multi-curvelet with random sampling, single-scale curvelet, proposed multi-scale and wavelet with nonrandom sampling using 35% of signal.are 32.3, 31.0, 31.8 and 28.0 (dB), respectively. Figure 1 shows the reconstructed images and error images.
Conclusion
Curvelet regularized CS reconstruction method using nonrandom sampling is proposed and demonstrated. Almost the same PSNRs were obtained with small artifacts.

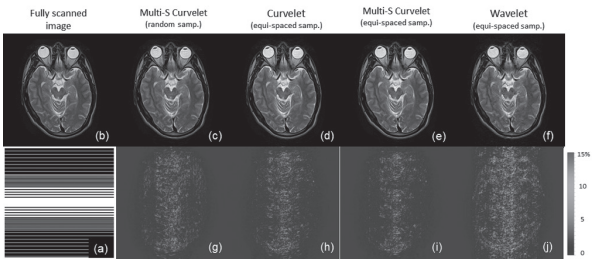

References
1. Candes EJ wt al. Pure Appl. Math. 2004:219--266

O-2-073　SMSTSE法による膝関節MRI検査の撮像時間短縮
Simultaneous multi slice turbo spin echo imaging of the knee joint for examination time reduction

采澤　大志（埼玉医科大学病院 中央放射線部）
Taishi Unezawa[1], Takahiro Watanabe[1], Atushi Kondou[1], Takashi Ogino[1], Shinichi Watanabe[1], Tomio Yamasaki[1], Masashi Suzuki[1], Hiroshi Imai[2], Mayuko Haraikawa[1], Iichiro Osawa[1], Kaiji Inoue[1], Eito Kozawa[1], Mamoru Niitsu[1]
[1]Saitama Medical University Hospital, [2]SIEMENS Healthcare K.K

【要旨】膝関節MRIでは軟骨や靭帯の評価をするため高分解能の画像が必要であり、撮影時間が延長しがちである。SMSは同時に数枚の画像を励起取得する事で撮像時間の短縮が可能となる。PD画像においてパラメータの最適化を行った。患者撮影において撮像時間は25％程度短縮できた。SMSは撮像時間を短縮できると考えられる。

IntroductionThin slice, high-resolution imaging are mandatory for the knee joint MRI to evaluate cartilage, menisci and ligaments. To preserve SNR, the examination time tends to be prolonged. The SMS, activating several slices simultaneously, enables the examination time reduction. We optimized the parameters in PD weighted imaging. MethodUsing MAGNETOM Skyra 3T and TxRx15ch knee coil (Siemens), we imaged a pig knee joint with SMS factors(off, 2, 3), FOV shifts (off,1/2,1/3,1/5) to improve of slice grappa precision on the PDWI. Then, ten patients with IRB approval were examined with optimized SMS sequence and compared with the conventional PDWI. Results and DiscussionSNR were altered by the excitation slice numbers and the in-plane shifts. The artifact from SMS was not observed. Compared to the conventional imaging, SMS was evaluated with similar imaging quality and the examination time was reduced by approximately 25%.ConclusionSMS sequence can reduce the examination time preserving the imaging qualities of thin slice, high-resolution imaging of the knee joint.

O-2-074　3DTOF パラレルイメージと圧縮センシング併用におけるアクセラレーションファクター選択の検討
Selection of Mixed Acceleration Factors in Combined Parallel imaging and Compressed Sensing in 3D Time of Flight

竹井　直行（GE ヘルスケア・ジャパン 研究開発部 MR研究室）
Naoyuki Takei[1], Masayuki Kanamoto[2], Tatsuya Yamamoto[3], Hirohiko Kimura[3], Hiroyuki Kabasawa[1]
[1]GE Healthcare Applications and Workflow, [2]Department of Radiology, University of Fukui Hospital,
[3]Radiological Center, University of Fukui Hospital

【要旨】並列に処理する圧縮センシング(CS)とパラレルイメージング(PI)を用いた撮像高速化法において、CSファクターとPIファクターの組み合わせがどのように画質に影響するか検討した。g-factorによる影響を避けるため、PIファクターよりCSファクターを相対的に上げたほうが有利であることがわかった。

INTRODUCTION:
Compressed sensing (CS) has shown great promise on acceleration technique in research as well as in clinical. Compressible image of MRI is favorable to CS due to having inherent sparsity characteristic. Parallel imaging (PI) is another acceleration technique to utilize redundancy of multiple coil data. These techniques can be combined to give further more acceleration than each is applied. Serial combination of PI and CS[(1)] is one of the methods to give choice of freedom in acceleration of PI and CS separately. In this work, we will investigate impact on image quality for selection of PI and CS acceleration using 3D Time of Flight (TOF).
MATERIALS and METHODS:
Healthy volunteer were scanned under an approved IRB study using 3D TOF with HNS Coil on 3T MRI (GE MR750) to collect Gaussian random undersampled dataset on k-space (Ky,Kz) changing acceleration factor of PI and CS. In reconstruction, firstly CS was processed to fill random missing samples and then data-driven PI was followed. We compared images of combined PI and CS to PI only image as reference.
RESULTS:
Image quality is degraded as PI acceleration is increased much more than CS acceleration at the same total acceleration. High accelerated image such as reduction factor = 3 by only PI suffers from noise amplification with unfolded aliasing artifact comes from coil geometry factor (g-factor). On the contrary, additional CS gives consistent image quality in acceleration with PI factor that is not damaged by g-factor.
DISCUSSIONS and CONCLUSIONS:
We have shown that the choice of combination between PI and CS is important in image quality. CS is complement to PI where it suffers from g-factor. Appropriate mixing of PI and CS gives robust acceleration strategy.
REFERENCE
1) King et al, ISMRM.2008, 1488

O-2-075　数値ファントムを用いたTotal Variationによる圧縮センシングMRアンギオグラフィにおける血管描出能の検討
Evaluating Vessel Depictability in Total Variation Compressed Sensing MR Angiography Using Numerical Phantom

三浦　洋亮（東北大学 大学院 医学系研究科）
Yousuke Miura[1,2], Toshiki Saito[3], Yoshio Machida[1]

[1]Tohoku University Graduate School of Medicine, [2]Sendai Medical Centor, [3]Tokai University Hospital

【要旨】我々は、数値ファントムを用いてTotal Variation（TV）による圧縮センシングMRアンギオグラフィー（CS-MRA）の画質をwavelet変換によるCS再構成法と比較することで評価を行った。今回用いた数値ファントムモデルにおいては、TVによるCS再構成の方が、血管径のボケ、信号値の低下が抑えられていた。

[Purpose]Our previous study evaluated image quality in compressed sensing MR Angiography (CS-MRA) using a numerical phantom model. The image was CS reconstructed using wavelet transform as a sparsifying transform. (CS_wl). For this study, we used the Total Variation (TV) penalty in CS reconstruction (CS_TV). Then we compared CS_TV images with CS_wl images for image quality evaluation.[Methods]With the numerical model mimicking cerebral arteries, we reconstructed CS_wl, CS_TV, and zero-fill-interpolated images (ZF) from randomly undersampled k-space data. For comparison, we also reconstructed a complete Nyquist sampled image (Full). As indices of vessel signal intensity and vessel blurring, we measured the peak value and full width at half maximum (FWHM) of the profile along phase and frequency encoding directions in a vessel. The undersampling ratios were set to 50, 33, 25, and 20%. No noise was added to reconstructed images for this study.[Results and Discussion]Both CS_wl and CS_TV images had higher vessel signal intensities than that of ZF along the phase encoding direction. Vessel blurring observed in ZF image was suppressed. Moreover, the vessel signal intensity of CS_TV showed a higher value than that of CS_wl. Therefore, CS_TV has better vessel detectability than CS_wl in the case of the numerical phantom model that simply mimics vessels. Although the clinical images have more complex structures, dependence of CS reconstructed images on sparse transform condition shown in this study might be helpful for elucidating clinical CS image quality.

O-2-076　MR指紋法によるNMRマイクロスコピーの高速化
NMR microscopy accelerated by MR Fingerprinting

寺田　康彦（筑波大学 数理物質系 物理工学域）
Yasuhiko Terada

Institute of Applied Physics, University of Tsukuba

【要旨】NMR マイクロスコピーは様々な画像コントラストを高い分解能で供給する手法である。しかし緩和時間などの定量計測は、膨大な撮像時間により現実的には難しい。一方、MR指紋法(MRF)は高速に定量画像を取得できる手法である。そこで、MRFをNMRマイクロスコピーに導入し、短時間での物理量の定量化が可能であることを示した。

NMR microscopy is a technique that provides a variety of image contrasts at high resolutions. However, the long scan time often complicates the quantification of tissue physical parameters (T_1, T_2, etc). Meanwhile, MR fingerprinting (MRF) is a rapid method for quantifying multiple tissue parameters. In this study, we introduced MRF to NMR microscopy and verified the feasibility of multi-parameter mapping.We used an 88 mm vertical bore SCM (Oxford Instruments, 4.74 T), an RF coil, shielded gradients, and a digital transceiver (DDRX6, MRTechnology, Tsukuba) that has the flexibility of designing sequences. The MRF data were acquired from CuSO4-doped water phantoms with varied concentrations and fruits. The 3D MRF acquisition was developed from a 3D IR-FISP sequence (100 data points; varying FA and TR; 256 x 256 x 64 matrices; voxel size, 100 μm x 100 μm x 625 μm; scan time, 22 h 45 m). T_1, T_2, and PD maps were calculated using the MRF dictionary (715400 entries).Figure 1 shows T_1, T_2, and PD maps for a tomato fruit. The vascular bundles were visible in the peripheral region. In short, the MRF-based microscopy is useful for quantifying tissue parameters within short scan times.

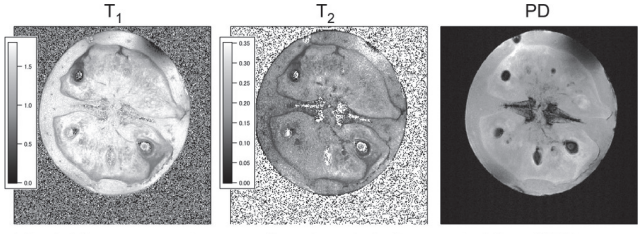

Fig. 1: Tissue parameter maps for a tomato fruit generated from MRF-FISP. MRF, magnetic resonance fingerprinting; FISP, fast imaging with steady-state precession; PD, proton density.

O-2-077　Quiet sequenceによる騒音軽減効果
Effect of scanner noise reduction at Quiet sequence

中井　浩大（名古屋大学医学部付属病院 医療技術部 放射線部門）
Kodai Nakai[1], Shinji Naganawa[2], Toshiaki Taoka[3], Hisashi Kawai[3], Kazusige Ichikawa[1], Yasuo Sakurai[1], Minako Kawamura[1], Katsuhiro Sakakibara[1], Yutaka Katou[1], Yasuo Andou[1], Kiminori Bokura[1], Isami Konishi[1]

[1]Radiological technology department of medical technique Nagoya university hospital, [2]Department of Radiology, Nagoya University Graduate School of Medicine, [3]Department of Radiology, Nagoya university hospital

【要旨】Quiet sequenceに よる騒音低減効果を、SE法T1WI、TSE法T1WI、T2WI、SWI、FLASHで実測した。いずれも騒音低減効果（-4.48 ~ -17.96dB）が確認できたが、中でもSE法T1WI(-17.96dB)とFLASH(-16.19dB)での騒音低減効果が顕著であった。

<Purpose>
Quiet sequence with acoustic noise reduction reduces scanning noise by applying the best possible gradient trajectory and reduction of slew rates. The purpose of our research is to measure and compare the scanner noise with and without acoustic noise reduction for the conventional imaging sequences.
<Methods>
Experiments were performed on 1.5T MR scanner (MAGNETOM Aera, Siemens AG, Erlangen, Germany). A microphone was set in the scanner at the same position of the ear, and connected to a sound level meter (NL-18, RION Co. Ltd. Tokyo). For measuring scanning noise, frequency weighting characteristic of the level meter was set to the subjective sound level impression of human's hearing.
The imaging sequences that we measured the scanning noise level were as follows; (1)Spin Echo T1 Weighted Imaging (SE-T1WI), (2) T2 Weighted Imaging (T2WI), (3) Susceptibility Weighted Imaging (SWI), (4) Fast Low Angel Shot (FLASH), and (5)Pointwise Encoding Time reduction with Radial Acquisition (PETRA). We measured the scanning noise with and without application of acoustic noise reduction for five sequences, while, only quiet sequence mode was available for PETRA.
<Results>
The measured scanner noise level (dB) without and with application of the acoustic noise reduction were as follows, for SE-T1WI, the noise level was reduced from 88.91 to 70.95, for T2WI; from 88.52 to 80.33, for SWI; from 80.12 to 75.64, for FLASH; from 92.08 to 75.89, and for PETRA, it was 68.95.
<Conclusion>
When the acoustic noise reduction was applied, the scanner noise was reduced in all imaging sequences. Especially, noise reduction was most prominent in SE-T1WI followed by FLASH.

O-2-078　時間軸方向のフェーズアンラップを用いた水脂肪分離法によるダイナミック撮像の基礎検討
Phase unwrapping method considering phase variance between dynamic phases for dynamic fat-water separation imaging

中井　則正（株式会社日立製作所 ヘルスケアビジネスユニット）
Norimasa Nakai, Hiroyuki Itagaki, Masahiro Takizawa

Healthcare Business Unit, Hitachi, Ltd.

【要旨】水脂肪分離法を用いたダイナミック撮像において、体動の影響を低減するために静磁場不均一マップを時間方向へフェーズアンラップする新たな領域拡張法を開発した。造影剤未使用の健常ボランティアのデータを用いて評価した結果、従来の空間的なフェーズアンラップする方法に比べ、水と脂肪の分離の安定性を向上できた。

[Purpose] Phase unwrapping process on a B0 map is necessary to separate fat and water signals for fat-water separation imaging. To prevent undesired fat-water swapping on the resulting image caused by body motion during a dynamic scan, we developed a new region-growing method of phase unwrapping process which uses phase information on dynamic phase (time) domain of B0 map.[Methods] Two different phase unwrapping methods were compared. The first method puts multiple start (seed) points of region-growing on each dynamic phases, and the phase unwrapping is performed for statial domain separately for each dynamic phase (conventional method). The second method puts only one seed point in the whole dynamic phases, and the phase unwrapping is performed for both spatial and time domain (new method). The evaluation data were acquired on a 1.5T MRI scannar. A healthy volunteer was scanned without contrast media after informed written consent was obtained in accordance with our institutional review board guidelines.[Results] No fat-water swapping over whole dynamic phases was observed on new method. In contrast, some fat-water swapping on dynamic phases due to phase differences of B0 map between seed points caused by body motion were observed on conventional method. [Conclusions] In dynamic fat-water separation imaging, the phase unwrapping method which uses only one seed point and region-growing for both statial and time domain well worked.

O-2-079　Fast BLADEシーケンスの腹部T2WIへの応用
Improving T2 weighted imaging of the Abdomen: Using fast BLADE Sequences

植田　隆史（シーメンスヘルスケア株式会社 カスタマーサービス事業本部 アプリケーション部）
Takashi Ueda, Terumasa Takemaru, Yoshito Ichiba, Tsubasa Kaji, Kanae Yamamoto
Siemens Healthcare K.K. Customer Service Division Application Department

【要旨】BLADEは体動による画質低下が少なく、頭部や腹部など多くの部位で使用されている。しかし、通常のTSEと比較して撮像時間延長等が問題となる。今回、RFパルスを改良したfastBLADEを開発し、従来法との比較を行った。fast BLADEは従来法と比較して撮像時間短縮が可能であった。

BACKGRAUND AND PURPOSE: BLADE reduces motion artifacts and can obtain better image quality. However, BLADE has some limitations: Firstly, parts of the k-space are under-sampled and T2 decay along the phase encoding direction of each BLADE results in blurring. Secondly, BLADE scan time is longer than conventional TSE. We developed new fast TSE sequence (fast BLADE) as a completely redesigned pulse sequence. The purpose of this study was compare to image quality of fast BLADE with standard BLADE. METHODS: Five healthy adult volunteers underwent upper abdominal MRI with a 3T scanner (Magnetom Skyra; Siemens Healthcare, Erlangen, Germany).First, for each subject, fat-saturated T2WI with respiratory compensation were performed with fast BLADE and standard BLADE. Next, standard SPAIR and optimized SPAIR were performed with fast BLADE. Each Image quality and scan time were evaluated.RESULTS AND DISCUSSION: In the fast BLADE, scan time and radial artifacts were reduced, and fat saturation was improved. These results were regarded as an effect of the improvement of RF pulse and SPAIR pulse. Conclusion: Fast BLADE technique could provide reduced scan time and provide better image quality.

O-2-080　2ポイントDixon水脂肪分離法におけるTE柔軟性の検討
How Flexible Can TEs Be in Two-Point Dixon with Out-Of-Phase and In-Phase Model?

岩舘　雄治（GEヘルスケア・ジャパン 研究開発部）
Yuji Iwadate[1], Kang Wang[2], Aya Shiobara[3], Yasuo Adachi[3], Akira Yamada[4], Yoshihiro Kito[3], Yasunari Fujinaga[3], Atsushi Nozaki[1], Masumi Kadoya[4], Horoyuki Kabasawa[1]
[1]Global MR Applications and Workflow, GE Healthcare Japan, [2]Global MR Applications and Workflow, GE Healthcare, [3]Division of Radiology, Shinshu University Hospital, [4]Department of Radiology, Shinshu University School of Medicine

【要旨】2ポイントDixon水脂肪分離法において、TEがout-of-phaseとin-phaseの条件から外れていても水もしくは脂肪信号が支配的であれば良好な水脂肪分離が行えることが分かっている。本研究では、水と脂肪が1ピクセル内に混在しても問題とならないTEの範囲をシミュレーションによって検証した。

Purpose: It has been shown that robust 2-pt Dixon water-fat separation is achieved with the out-of-phase (OOP) and in-phase (IP) model even when the TEs deviate from the ideal OOP/IP with a single species domination assumption. The purpose of this work was to examine the TE ranges for getting reasonable signals in the final image when water-fat mixture occurs with the OOP/IP model.

Methods: Simulation was performed by calculating the dual-echo SPGR signals with the cosine theorem, followed by the calculation of the dominant component signal *D* (water or fat). These calculations were repeated by changing dephasing angle of fat with respect to water in the first echo (θ_1) and dephasing angle difference between the two echoes ($\Delta\theta$). Finally, the appropriate combination of the two angles was determined with which the calculated *D* was within the allowance of 20% from the original value.

Results and Discussion: The white region in the figure shows the combination of the two angles whose calculated signal was in the allowance range with the *D* fraction from 0.5 to 1.0. So, TEs determined from hardware/safety limitations can be used if they result in the two angles in this region.

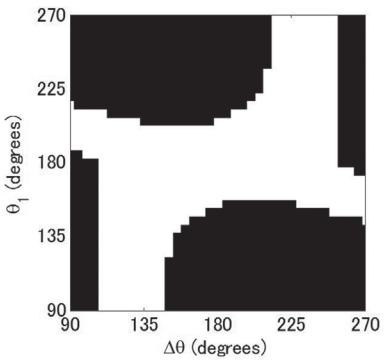

O-2-081　Dual echo法を用いたin/out-of-phase画像信号強度の機種依存性について
Variation among scanners in signal intensity of in/out-of-phase images using dual echo sequences

茂木　俊一（城西クリニック 放射線科）
Shunichi Motegi[1,2], Yasuo Takatsu[3,4], Kouichi Ujita[5], Norio Hayashi[6], Mitsuomi Matsumoto[1], Yoshito Tsushima[2]

[1]Josai Clinic, [2]Gunma University Graduate School of Medicine, [3]Osaka Red Cross Hospital, [4]Graduate School of Medical Sciences, Kanazawa University, [5]Gunma University Hospital, [6]Gunma Prefectural College of Health Sciences

【要旨】脂肪含有ファントムを用いて、Dual echo法によるin/out-of-phase (IP/OP) 画像の信号強度比測定に対する種々の影響を検討した。信号強度比は磁場強度と使用装置に依存し、有意に低値を示す機種があった。腫瘤脂肪含有量評価の際には本結果を考慮する必要がある。

Purpose: Quantitative fat content evaluation by the signal intensity ratio of the in/out-of-phase (IP/OP) images using dual echo sequences has been reported to be very useful in diagnosing adrenal masses and fatty liver. But the extent of the influence of equipment used, parameters, and magnetic field strength on signal intensity ratio using this method is unknown. The purpose of this research is to evaluate the influence of these factors on signal intensity ratio using a fat containing phantom.
Methods: We made an original phantom (fat content 5%, 10%, 20%). Imaging was performed in multiple institutions (35models: 25 1.5T and 10 3T units; 18models from company A, 10models from company B, 7models from company C). Imaging was performed using the parameters used clinically in each institution. Signal intensity index: SII (=[SI(IP)-SI(OP)/ SI(IP)] × 100%) was calculated from the signal intensity of the phantom.
Results: In SII according to the magnetic field strength, SII when fat content was 5% were 1.5T, 26.5 ± 5.0% (mean ± SD) and 3T, 21.3 ± 7.7 %. SII of 3T was significantly lower ($p<0.05$) compared to those of 1.5T (t-test). The SII of 3T was also significantly lower when fat content was 10% and 20% ($p<0.05$). In SII according to the company, SII when fat content was 5% were company A, 25.3 ± 5.1 % and company B, 29.0 ± 4.6 % and company C, 18.8 ± 5.2 %. SII of company C was significantly lower ($p<0.05$) compared to those of company A and B (one-way ANOVA). The SII of company C was also significantly lower when fat content was 10% and 20% ($p<0.05$).
Conclusion: SII depended on magnetic field strength and equipment used, with some models showing significantly lower values. These points should be taken into consideration when evaluating fat content of tumors using SII.

O-2-082　6point-Dixon法を用いたスライス厚の違いによる脂肪含有率測定の基礎的検討
Basic study of fat fraction measurement by difference of slice thickness using 6point-Dixon method

神岡　尚吾（広島大学病院 診療支援部 画像診断部門）
Shogo Kamioka[1], Yuji Akiyama[1], Takayuki Tamura[1], Kazushi Yokomachi[1], Yuuji Takahashi[1], Yoshiko Iwakado[1], ryuji Akita[1], Kazuo Awai[2]

[1]Hiroshima University Hospital department of radiology, [2]Diagnostic Radiology, Institute of Biomedical and Health Sciences, Hiroshima University

【要旨】6point-Dixon法を用いた脂肪含有率測定において、薄いスライス厚での撮像ではsignal-to-noise ratioの低下により定量値に影響を与えることが懸念されるためファントム実験でこれを明らかにした。スライス厚が1.5 mm以上の撮像では高い精度を示し、薄いスライス厚による脂肪含有率測定が可能であることが示唆された。

Purpose:
Measurement of fat fraction (FF) using 6point-Dixon method has higher accuracy than traditional 2point-Dixon method because it can correct effect of T2* relaxation. It is important to identify fat component in adrenal tumor for diagnosis of adrenal adenoma. However, quantification of fat may be affected by decrease of signal-to-noise ratio because it is necessary to use thinner slice thickness for diagnosis of the adrenal tumor. Our purpose is to investigate the effect of slice thickness on measurement of FF using 6point-Dixon method.
Methods:
We evaluated water and lard by using emulsifier, created phantom that has known FF from 0% to 100%, and imaged the phantom by a MRI scanner(Ingenia3.0 T; Philips). Changing the slice thickness from 1.0 to 7.0 mm. We calculated the FF in each imaging, and correlated them with known FF.
Results:
The slice thickness became thinner, difference between value of FF and true values, became larger and its accuracy drastically decreased below 1.5 mm thickness. R^2 values decreased below 1.5 mm (Fig 1).
Conclusions:
In the measurement of FF with 6point-DIXON method, accuracy of FF measurement could be maintained at slice thickness of 1.5 mm of more.

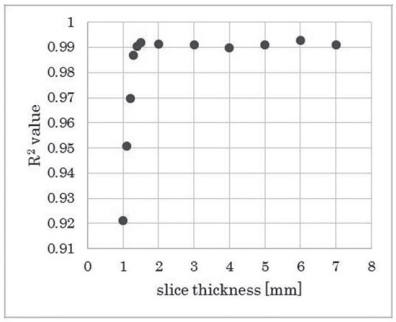

Figure 1. Relationship of slice thickness and R^2 value

O-2-083　非造影MRA向けスライス選択スピンラベリング用2次元局所励起パルスの検討
Study on two-dimensional spatial selective pulse for non-enhanced MRA slice selective spin labeling

瀬川　陽子（株式会社 東芝 研究開発センター）
Yoko Segawa[1], Koji Akita[1], Masao Yui[2], Kazuya Okamoto[2]
[1]Toshiba Corporation Corporate Research and Development Center, [2]Toshiba Medical Systems Corporation

【要旨】非造影の血管撮像技術であるスピンラベリング法向けの2次元選択断熱パルスの開発を行った。シミュレーションによる検証で2次元選択範囲内の均一なスピンの反転を確認した。B1不均一性が問題となる高磁場の撮像において、均一かつ詳細な血液描写が期待される。

Purpose: Spin labeling angiography such as ASL and Time-Spatial Labeling Inversion Pulse (Time-SLIP) has been used for selective visualization of the blood vessels without the contrast medium. Since the technique relies on the tagged blood inflow which replaces the spins in the arteries of interest, the volume of tagged blood greatly controls the selectivity of the vascular visualization. Thus selectivity of the tagging pulse is important to obtain the desired image. Furthermore, B1 inhomogeneity is the sever problem especially for the high field MRI. We have designed the two-dimensional selective tagging pulse to depict the fine structure of the individual arteries, which is suitable for the flow territory mapping.
Methods: We designed the two-dimensional spatial selective adiabatic pulse. The pulse is designed using separable k-space excitation method with successive subpulses. The Bloch equation simulation was performed to examine the inversion profile of spins after the two-dimensional spatial selective pulse applied. We calculated the average magnitude and inhomogeneity of the magnetization in the target region.
Results: The designed pulse could achieve more than 70% inversion of longitudinal magnetization in average and less than 10% inhomogeneity with the more than 270 degrees equivalent pulse power, under the condition of T1 = 1000 ms, T2 = 100 ms. The inhomogeneity decrease when the number of subpulse increases.
Discussion: Employing two-dimensional spatial selective adiabatic pulse, the magnetization in the region of interest can be inverted homogeneously under the inhomogeneous B1 condition. Designed two-dimensional selective inversion can be effectively applied for spin labeling angiography sequence.

O-2-084　非同期位相コントラスト法に基づく心拍動性及び呼吸性脳脊髄液運動の方向の解析
Analysis of Directions of Cardiac- and Respiratory-driven Cerebrospinal Fluid Motions using Asynchronous Phase Contrast Technique

春原紗依子（東海大学 工学研究科 電気電子工学専攻）
Saeko Sunohara[1], Satoshi Yatsushiro[2], Toru Yamada[1], Ken Takizawa[3], Mitsunori Matsumae[3], Nao Kajiwara[4], Kagayaki Kuroda[2]
[1]Graduate School of Engineering, Tokai University., [2]Graduate School of Science and Technology, Tokai University., [3]Department of Neurosurgery, Tokai University School of Medicine., [4]Department of Radiology, Tokai University Hospital.

【要旨】心拍動及び呼吸性CSF運動の特性を解析するために，非同期PC法に基づくパワー・周波数マッピングを提案した．パワーマップでは両運動の占める周波数帯におけるパワーの，周波数マップでは最大パワーを有する周波数の空間分布を可視化した．これらにより両運動のパワーが方向に依存して変わることが分かった．

Introduction
This study was conducted to characterize the cardiac- and respiratory-driven cerebrospinal fluid (CSF) motions in 3 spatial directions.
Methods
Asynchronous 2D-PC with a 217-ms temporal resolution was performed at 3T for 5 healthy subjects (male, 28 ± 6 yo) under controlled 6-sec cycle respiration. Number of time-points was 256 per direction resulting in 167-sec observation. The cardiac- and respiratory-driven motions were separated by Fourier-transforming the time series of the velocities voxel-by-voxel. The power-map (P-map) visualized the power of the velocity spectra over 0.3 Hz bandwidth, whereas the frequency-map (F-map) depicts the maximum peak frequency.
Results
A significant difference between the two motion components was recognized ($p<0.01$) in the FH direction.
Conclusion
The present results exhibited that the power ratio of the cardiac- and respiratory-driven motions were different in the 3 directions. In the present velocity analysis, the motion fractions were significantly different in the FH-direction.
Figure
Fig. 1 P-maps of the motions in the 3 directions. The values denote the relative power fraction in the ROIs placed at the spinal subarachnoid space.

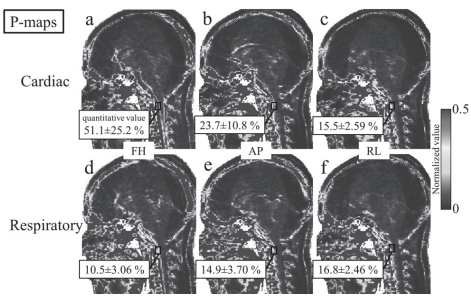

O-2-085　位相コントラスト法とTime-SLIP法の観測方法の違いの影響
Effect of Difference between Phase Contrast and Time-SLIP Techniques in View of Observation

八ツ代　諭（東海大学大学院 総合理工学研究科 総合理工学専攻）
Satoshi Yatsushiro[1], Saeko Sunohara[2], Toru Yamada[2], ken Takizawa[3], Mitsunori Matsumae[3], Nao Kajiwara[3,4], Kagayaki Kuroda[2]

[1]Graduate School of Science and Technology, Tokai University, [2]Graduate School of Engineering, Tokai University, [3]Department of Neurosurgery, Tokai University School of Medicine, [4]Department of Radiology, Tokai University Hospital

【要旨】PC法とTime-SLIP法の観測方法の違いによる影響を確かめるために非同期PC法に基づく周波数解析で心拍動性，呼吸性運動を分離し，両成分のCSF変位量を先行研究と比較した．PC法においては心拍動性変位量が2倍ほど大きくなった．PC法により観測できる呼吸性変位量は過小評価されている可能性がある．

Background
Techniques to visualize cerebrospinal fluid (CSF) motion are PC and Time-SLIP. The techniques are different in the observation of spin traveling and spin phase change. A research based on Time-SLIP has shown that the respiratory-driven CSF motion is larger than the cardiac-driven motion. Our result based on asynchronous PC has indicated the opposed observation. To reveal the cause of the difference, we compared the cardiac- and respiratory-driven CSF displacement obtained by PC and Time-SLIP techniques.
Methods
To separate the cardiac- and respiratory-driven CSF motion, frequency analysis of velocity waveform based on asynchronous 2D-PC with a temporal resolution of 217 ms (4.7 frames/sec) was performed for 7 subjects. To compare PC with Time-SLIP of previous research directly, velocity waveform in prepontine was integrated over the sampling time (56-sec). In addition, the cardiac- and respiratory-driven CSF displacements were compared.
Results
The figure shows the cardiac- and respiratory-driven CSF waveforms. Integrated value of the cardiac waveform is larger about 2-fold.
Conclusions
There is a possibility of underestimation of respiratory-driven CSF velocity.

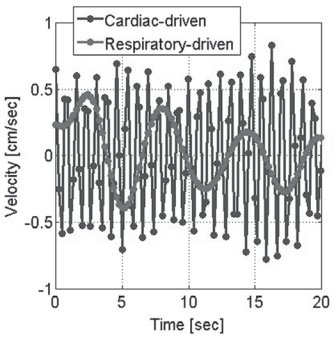

O-2-086　腹部大動脈瘤における嚢状瘤と紡錘状瘤の壁剪断応力および異常血行動態の解析
Abnormal Hemodynamics and Wall Shear Stress within the Saccular Aneurysm in Contrast to Fusiform Aneurysm in the Abdominal Aorta

杉山　将隆（浜松医科大学 放射線科）
Masataka Sugiyama[1], Yasuo Takehara[2], Naoki Ooishi[2], Marcus Alley[3], Tetsuya Wakayama[4], Hatsuko Nasu[1], Mika Kamiya[1], Shuhei Yamashita[1], Yohei Ito[1], Harumi Sakahara[1]

[1]Hamamatsu University School of Medicine Departmet of Radiology, [2]Hamamatsu University Hospital Radiology Department, [3]Stanford University School of Medicine Department of Radiology, [4]Applied Science Laboratory Asia Pacific GE Healthcare

【要旨】嚢状(n=8)と紡錘状(n=13)の腹部大動脈瘤患者に対し3Dシネ位相コントラストMRI(4DFlow)を撮影し、血行力学的計測と流形の解析をおこなった。嚢状瘤において収縮期の有意な壁剪断応力(WSS)の低下と、瘤内の螺旋流が観察され、嚢状瘤がatherogenic driveにより危険な経過をたどる要因となっている可能性がある。

Purpose
Saccular aortic aneurysm is believed to have more ominous natural history than the typical fusiform aneurysm. The purpose of our study is to characterize the flow abnormalities within the saccular aneurysm of the abdominal aorta as compared to the fusiform aneurysm.
Methods
8 patients with abdominal saccular aneurysm and 13 patients with abdominal fusiform aneurysm (62-90 y.o.) underwent 3D cine PC MR imaging (4D-Flow). 1.5T (Signa Twinspeed) or a 3.0T MR scanner (Discovery 750) with torso-array coil were used. Gd3DMRA was performed for determination of aortic boundary. The acquired data was post-processed with flow analysis software. The wall shear stress (WSS) of whole cardiac phase within the aortic wall were measured. Streamlines of the abdominal aorta were depicted for streamline analysis. The peak systolic and diastolic WSS within saccular and fusiform aneurysms was compared using Mann-Whitney test.
Result
The peak systolic WSS of saccular aneurysm was significantly lower than that of fusiform aneurysm (p= 0.006). The streamline analysis showed vortex flow within the saccular aneurysm, which is isolated from the mainstream of the aorta. This trend was not observed within the fusiform aneurysm. The separated turbulent flow within the saccular aneurysm may be the reason for lower WSS.
Conclusion
Majorities of physiological evidences indicate that the decline of WSS produces an expression of pro-atherogenic genes. The separated vortex flow and consequent low WSS within the saccular aneurysm may be reflecting the continuing risk of atherogenic changes compared to fusiform aneurysm.

O-2-087　頸動脈ステント前後のfast-cine位相画像による脳動脈血流量測定
Serial blood flow measurements of the brain arteries before and after carotid artery stenting

田中　　壽（大阪大学 医学部 放射線科）
Hisashi Tanaka[1], Hajime Nakamura[2], Yoshiyuki Watanabe[1], Hiroto Takahashi[1], Atsuko Arisawa[1], Takuya Fujiwara[1], Noriyuki Tomiyama[1]

[1]Osaka University Graduate School of Medicine, Department of Radiology, [2]Osaka University Graduate School of Medicine, Department of Neurosurgery

【要旨】7名の頸動脈ステント患者の両側内頚動脈、脳底動脈の血流量をfast-cine phase contrast 画像で術前、1日後、1週間後、3か月後に測定した。内頚動脈と脳底動脈の血流量の合計は、術後増加するがその後減少する傾向が見られた。

Purpose: To measure blood flow volume rates of the internal carotid arteries and the basilar artery before and after carotid artery stenting and to elucidate time trend of blood flow rates. Materials and Methods: Seven patients who were planned to undergo carotid artery stenting constitute a cohort of this prospective study. Each patient had MRI examinations four times, namely, before, one day after, one week after and three months after carotid artery stenting. MR blood flow measurement was done with fast-cine phase-contrast imaging, whose parameters were TR:7.2 TE:3.8 FA:20 FOV:120 Matrix:192x192 Encoding Velocity:150cm/sec Slice thickness: 3mm Number of cardiac phase 16. Results: The volume flow rate of stented internal carotid artery had significantly increased after carotid artery stenting. The volume flow rates of contralateral internal carotid artery and the basilar artery decreased after carotid artery stenting. The sum of volume flow rates of the bilateral internal carotid arteries and the basilar artery was 9.1+/- 2.8 (ml/sec average +/- standard deviation of six patients), 11.0 +/- 2.3, 10.4 +/- 2.4 and 9.6 +/- 1.8 for before, one day after, one week after and three month after the procedure, respectively. Two-factor analysis of variance revealed significant difference for timing of the examination. The one-sided uncorrected probabilities calculated with paired t-test were 0.009 (before vs one day after), 0.009 (one day vs three month after), 0.030 (one week vs three month after). In conclusion, sum of blood flow rates, once increases after carotid artery stenting, declines over three months.

O-2-088　In vivoでの造影前後の4D flowの精度検証
The effects of the gadolinium-based contrast agent injection on 4D flow

松本　卓弥（総合病院 聖隷三方原病院 画像診断部）
Takuya Matsumoto[1], Tomoyasu Amano[1], Mutsuki Tanaka[1], Mamoru Takahashi[2], Tomoyuki Okuaki[3], Hideo Yamamoto[1]

[1]Seirei Mikatahara General Hospital The department of Radiological Technology, [2]Seirei Mikatahara General Hospital The department of Radiology, [3]Philips Healthcare AsiaPacific

【要旨】造影剤の使用により、phase-contrast MRAのSNRや画質が向上すると報告されている。今回我々は造影剤投与前後でIn-vivo の4D flowでの定量の精度を検証比較した。造影剤を使用することで、定量精度を保ったままreduction factorを上げることが可能であることが確認できた。

[Purpose]
The latest MR systems can perform 3D cine PCA (4D flow) even in clinical mode, though the imaging time is still not short enough. Using parallel imaging techniques can shorten the time, but sacrifices SNR and the quality. Gadolinium-based contrast agent has been reported to improve SNR and the quality of PCA. In this study we tested the effects of gadolinium-based contrast agent injections on in-vivo 4D flow.
[Material and Methods]
Patients underwent routine examinations together with additional 4D flow and 2D cine PCA (as gold standard) on a 3.0T MR scanner. Written informed consent was provided in all cases for this IRB approved study. 4D flow and 2D cine PCA were obtained both before and after injection of the contrast agent. 4D PCA was obtained using the following parameters: TR(ms) / TE(ms) / FA(degree) of 4 / 2 / 10, VENC 120 cm/sec, 1mm iso pixel, reduction factor of 3, 4 and 5, 20 phases/cardiac cycle. The flow rates of bilateral common carotid arteries were calculated on each 4D flow examination and compared with those on 2D cine PCA.
[Results]
The mean values of flow rates calculated on 4D flow were lower than those on 2D cine PCA. As the reduction factor was high, this tendency became more apparent. The mean relative error of flow rate on contrast enhanced 4D flow of sense factor 3 compared to 2D PCA was 12.5%, which was the lowest value in this study. The mean relative error on contrasted 4D flow of sense factor 4 was 22.2%, which was between that of non-contrast 4D flow sense factor 3 (18.8%) and sense factor 4 (26.2%).
[Conclusion]
The application of contrast agent improved accuracy of flow measurements on 4D flow.

O-2-089　4D-PCA と MRFD による肝血管の血行力学的評価
Hemodynamic Assessments of Hepatic Vasculatures using 4D-PCA and MRFD

吉川　武（神戸大学大学院 医学研究科 先端生体医用画像研究センター）
Takeshi Yoshikawa[1,2], Katsusuke Kyotani[3], Yoshiharu Ohno[1,2], Yuji Kishida[2], Shinichiro Seki[1,2], Koya Nishiyama[3], Kazuro Sugimura[2]

[1]Advanced Biomedical Imaging Research Center, Kobe University Graduate School of Medicine, [2]Department of Radiology, Kobe University Graduate School of Medicine, [3]Center of Radiology and Radiation Oncology, Kobe University Hospital

【要旨】4D-PCA 法と MRFD 解析により肝血管の詳細な血行力学的評価が可能であり、肝疾患診断への応用の可能性が示された。

[PURPOSE] To evaluate the capability of four-dimensional phase-contrast angiography (4D-PCA) and magnetic resonance fluid dynamics (MRFD) for assessment of hepatic vasculatures [METHODS AND MATERIALS] 33 patients (21 men, 12 women, mean 64.1 years), who were suspected to have hepato-biliary-pancreatic malignancy and underwent 3T-MRI, were enrolled. 4D-PCA (TR/TE/FA: 4.1/2.4/10, matrix: 240 × 191, 10 aqs/cardiac cycle, scan time: 6-10min, pulse gating, VENC: 30, 80cm/s) was obtained. Hemodynamic assessment of abdominal aorta, celiac, common and proper hepatic, superior mesenteric, splenic arteries, main, right, left portal, superior mesenteric, splenic, hepatic veins, and inferior vena cava was performed on MRFD software (FLOVA, R'Tech). Blood flow, velocity, and shear stresses to vessel wall such as wall shear stress (WSS), oscillatory shear gradient (OSI), spatial WSS gradient (SWSSG), and gradient oscillatory number (GON), were measured. The values were compared among vessel types, arteries, portal veins, and systemic veins, and between liver disease (n=15) and non-liver disease groups (n=10). [RESULTS] Hemodynamic assessment could be done in all the vessels except for proper hepatic arteries with diameters < 4mm. Significant differences were found in flow and all 4 shear stresses in comparisons of vessel types ($P<0.007$), all parameters in comparisons of arteries (<0.004), flow and GON in comparisons of portal veins (<0.011), flow, WSS, and SWSSG in comparisons of systemic veins (<0.042), and systemic vein flow, portal velocity, arterial and portal WSSs, portal SWSSG, systemic vein OSI and GON in comparisons between the groups (<0.042). [CONCLUSION] 4D-PCA and MRFD enables detailed hemodynamic assessment and has the potential to be used for liver disease assessments.

O-2-090　頸動脈を対象とした３次元シネ位相コントラスト磁気共鳴法の血流動態解析の再現性
Reproducibility of the carotid arterial hemodynamic analysis using 3D cine phase contrast MRI

七条　来夢（名古屋大学 医学部 保健学科 放射線技術科学専攻）
Raimu Shichijou[1], Atsushi Fukuyama[2], Tomoya Watanabe[2], Kenta Ishiguro[2], Haruo Isoda[2,3]

[1]Department of Radiological Technology, School of Health Sciences, Faculty of Medicine, Nagoya University, [2]Department of Radiological and Medical Laboratory Sciences, Graduate School of Medicine, Nagoya University, [3]Brain & Mind Research Center, Nagoya University

【要旨】3D cine PC MRI を用いた頸動脈の血流動態解析の再現性を検証するために健常者 10 名の右頸動脈を 2 回ずつ 3T MR 装置で撮像し、総頸動脈、内頸動脈、外頸動脈の一心拍中の空間的平均流速及び最高流速、収縮期壁剪断応力を算出した。1 回目と 2 回目の結果は、良い再現性を示した。

Purpose: The purpose of this study was to assess the reproducibility of the carotid arterial hemodynamic analysis using the 3D cine phase contrast (PC) MRI.
Methods: This study involved 10 healthy volunteers (10 male; mean age, 23.2 years) from whom informed consents were obtained. For each participant, we performed 3D time-of-flight (TOF) MR angiography (MRA) followed by 3D cine PC MR imaging for 10 right carotid arteries using a 3T MR scanner (MAGNETOM Verio, Siemens) and did the second set of scans within 60 minutes. We created vascular wall from 3D TOF MRA data and input velocity information acquired from 3D cine PC MR images using flow visualization and analysis software (Flova). The analysis plane of the common carotid artery (CCA) was 20 mm upstream from the carotid bifurcation, and those of the internal carotid artery (ICA) and the external carotid artery (ECA) were 12 mm and 10 mm downstream from the carotid bifurcation, respectively. We calculated the velocity-time curves of spatially averaged velocity, maximum velocity during one cardiac cycle on each plane and obtained the contours maps of peak systolic wall shear stress (WSS). We compared these results between the first scan set and the second scan set.
Results: Reproducibility of the velocity-time curves of spatially averaged and maximum velocity were good in CCA, ICA and ECA during one cardiac cycle. Reproducibility in CCA and ICA was better than ECA, because their diameter were bigger than that of ECA. Reproducibility of the distribution of WSS was not so good due to differences in the process of creating vascular wall.
Conclusion: Carotid arterial hemodynamic analysis using 3D cine PC MRI showed good reproducibility.

O-2-091　3T MRIを用いた非造影下肢FBIにおけるVariable Refocusing Flip Angle パターンの最適化
Application of Variable Refocusing Flip Angle (vFA) in FBI for 6-min Three-Station Peripheral MRA at 3T

宮崎美津恵（TOSHIBA MEDICAL RESEARCH INSTITUTE）
Mitsue Miyazaki[1,2], Keiichiro Ishi[2], Xiangzhi Zhou[1], Masaaki Umeda[2], Nobuyasu Ichinose[2], Akiyoshi Yamamoto[3], Katsumi Nakamura[3]

[1]TOSHIBA MEDICAL RESEARCH INSTITUTE, [2]Toshiba Medical Systems, [3]Kyoritsu Tobata Hospital

【要旨】3T MRIを用いた非造影下肢MRAにおいてVFAパターンの検討を行った。VFAパターンの最適化により、画像のボケを抑えつつSARを低減できることを確認した。これによって、従来3～4心拍を要した下肢FBIが2心拍で撮像可能となり、骨盤部、大腿部、下腿から成る3-stationを約6分の撮像時間に収めることに成功した。

Purpose: To investigate variable refocusing flip angle (vFA) in FBI for scan reduction in peripheral MRA at 3T. Methods: Seven volunteers were enrolled in the 3-station experiment, pelvic, thigh and calf using FBI with vFA, having higher refocusing flip (or flop) angles in the center of k space with gradually reduced at the peripheral part of k space. The vFA with high flop angles was controlled as number of lines (NumTE) in TEeff, e.g., echo train spacing (ETS) of 5 ms with TEeff of 60 ms with NumTE of 1 is 12 lines. We evaluated NumTE of 1 (12 lines), 2 (24 lines), 3 (36 lines), 4 (48 lines), and 5 (60 lines) with high flop angles. With the proposed vFA method, SAR can be significantly reduced, allowing shorter TR or RR interval. The vFA with low flop ware also evaluated using high/low flop of 200/90 deg. 200/60 deg, 200/30 deg, and 200/0 deg. Results: Using constant high flop angles, TR of 4RR interval was required in FBI at 3T, which led to about a 4 min scan time per station. By applying NumTE of 1 or 2 (only 12 or 24 PE lines with high flop), the resulting images were blurred. The images with NumTE of 3, 4, and 5 are clear and show comparable arterial image quality. NumTE of 3 (36 lines) was selected due to less SAR. The vFA with high/low flop of 200/90 deg. reduces to TR=3RR. The vFA with high/low flop of 200/60 deg., 200/30 deg., and 200/0 deg. patterns further reduces to TR=2RR. Image quality was similar between them. However, the 200/0deg. pattern allows less SAR and more flexibility and gaining brighter blood signal. In a result, the 3-station peripheral non-contrast MRA scan was able to perform in about 6 mins. Conclusion: Peripheral FBI with vFA permits a 6-min 3-station scan with good image quality.

O-2-092　Multiple Phase Silent MRAの基礎的検討
Evaluation of Multiple Phases Silent MRA

坂下　尚孝（東芝メディカルシステムズ株式会社 医用システム研究開発センター）
Naotaka Sakashita[1], Masaaki Umeda[2], Yoshimori Kassai[2], Masao Yui[1], Seiji Nozaki[2], Andrew Wheaton[3], Deepak Bhat[3], Aiming Lu[3]

[1]Center for Medical Research and Development, Toshiba Medical Systems Corporation, [2]MRI systems Division, Toshiba Medical Systems Corporation, [3]Toshiba Medical Research Institute USA

【要旨】Multiple Phase Silent MRAを開発し、基礎検討を行った。ファントム実験より1時相目のフリップ角及びNspが信号値に影響することが分かった。また、頭部MRA撮影より、本シーケンスを用いることで、静音を実現したMRA画像が得られることができた。

Purpose: The acoustic noise reduction in MRA protocol is indispensable for quiet examination. Zero-TE based radial sequence has been developed as a silent sequence recent years. Wide bandwidth RF pulse is used for the sequence, which leads to large volume excitation. With such reason, Time-of-Flight effect cannot be efficient and ASL-based technique is used for MRA with the sequence. However, conventional single phase ASL is affected by delay effect which resulted in limited coverage of artery. Here, Multiple Phase Silent MRA is developed for overcoming the problem and image quality is evaluated.
Method: The experiment was conducted using 3T scanner. 1) Phantom experiment (2phase): Firstly, relationship between Flip Angle (FA) of first phase and the signal of each phase was evaluated. Secondary, the relationship between the number of spokes per phase (Nsp) and signal intensity of each phase was evaluated. 2) Brain MRA (4phase): Multiple Phase Silent MRA was acquired from healthy volunteers with optimal scan parameter based on phantom experiment. Image quality and acoustic noise were evaluated.
Result: 1) The signal of first phase was increased and that of second phase was decreased with increasing FA of first phase. The signals of both phases were increased with decreasing Nsp. 2) The dynamic MRA images were obtained and combined image provided large coverage which was equivalent to TOF. Acoustic noise of the sequence was 62.8dB and that of TOF was 94.1dB.
Conclusion: Multiple Phase Silent MRA was developed and evaluated. It was found that FA of the first phase and Nsp affected the image quality and resulted image depicted the large coverage of brain artery. The sequence enabled MRA with significantly reduced acoustic noise.

O-2-093　Beam IRパルスを用いた選択的肝動脈撮像
Selective Hepatic Artery Imaging Using VASC-ASL with Beam IR Sequence

西原　崇（株式会社日立製作所 ヘルスケアビジネスユニット）
Takashi Nishihara, Kuniaki Harada, Ryuji Shirase, Noriko Itabashi, Kuniharu Oka, Hiroyuki Itagaki
Healthcare Business Unit, Hitachi, Ltd.

【要旨】前回の検討では、2次元選択励起を用いたプリサチパルス(Beam Satパルス)を肝動脈の描出に適用したが、右肝動脈が不明瞭であった。今回、2次元選択励起をIRパルスに適用し(Beam IR パルス)、肝動脈の描出を試みた。本手法により、静脈を描出することなく選択的に肝動脈を明瞭に描出できたので報告する。

Introduction
In previous study, 2-dimentional presaturation pulses (Beam Sat pulse) were applied to the hepatic arteriography, but the right hepatic artery (RHA) was unclear. The objective of this study was to visualize the RHA clearly and selectively using Beam IR.
Materials and Methods
Sequence: VASC-ASL is non-CE MRA sequence. The Beam IR is added immediately after the non-slice selective IR to recover the inflow signal (Fig.1).
Volunteer study: We optimized the position of Beam IR and TI, and evaluated the visibility of arteries. We explained the purpose and significance of this study to healthy volunteers and obtained written consent.
Results and Discussion
The RHA and abdominal arteries were visualized clearly in the subtracted image (Fig.2) without veins when Beam IR overlapped with the descending aorta and TI is 800ms. The more peripheral arteries than RHA were not visualized. It is supposed that the signal loss is caused by absence of inflow blood. We assume that the visualization of peripheral arteries is improved by the increased inflow blood, when ECG gate is applied.
Conclusion
The usefulness of the developed VASC-ASL with Beam IR was demonstrated by the volunteer study.

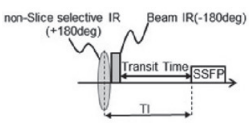

Figure 1 Beam IR VASC-ASL sequence diagram

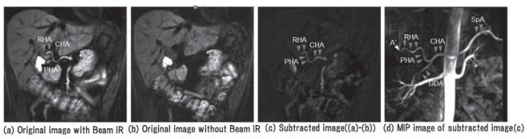

(a) Original image with Beam IR (b) Original image without Beam IR (c) Subtracted image((a)-(b)) (d) MIP image of subtracted image(c)
Figure 2 Images of VASC-ASL sequence

O-2-094　FE型マルチショット3D EPI法による短時間全脳Black Blood MRAの検討
Study of short-acquisition time imaging of whole brain Black Blood MRA imaging with 3D Gradient Echo EPI sequence

高橋沙奈江（杏林大学医学部付属病院 放射線部）
Sanae Takahashi[1], Kenji Hamada[1], Isao Miyazaki[1], Nanae Kawano[2], Hiroshi Kusahara[2]
[1]Section of Radiology, Kyorin University Hospital, [2]Toshiba Medical Systems Corporation

【要旨】FE型マルチショット3D EPIシーケンスによる短時間全脳Black Blood(BB)撮像の至適条件検討を,歪みとBB効果に注目し行った.この最適化により全脳を55秒で良好にBB撮像でき,バイパス血管の確認や異常血管網の描出など臨床での有用性を期待することができる.

(Purpose) The purpose of this study was to optimal imaging parameter in a short time, for whole brain Black blood MR Angiography with 3D Gradient Echo EPI sequence.(Method) MR imaging was performed with a 3Tesla MR system (Vantage Titan 3T; Toshiba Medical Systems Corporation. Japan) using 32channel head SPEEDER coil. Using a phantom (with Gadolinium), by varying Number of shots and SPEEDER factor, it was subjected to evaluation of image distortion. Images were acquired of healthy volunteers obtained consent to this study. It was studied of Black Blood effect from the contrast ratio of the brain parenchyma and the blood vessel. Imaging parameters ware as shown below. TR 50msec, Matrix 320 (PE) x 240 (RO), FOV 23 x 23cm, Slice thickness 2.8mm, NAQ 1. TE, Flip angle and Number of shots changed.(Result) In study of distortion of the image using the phantom, increasing number of shots and SPEEDER factor, it tended distortion of the image was to be improved. In the volunteer images, TE 16msec, Flip angles 20 degrees, Black Blood effect was higher.(Discussion) Distortion was improved by increasing the number of shots and SPEEDER factor, considering imaging time and SNR at clinical use, number of shots 18, SPEEDER 2.0 was optimal imaging parameter. TE is too was shortened, Black Blood effect was weakened by dephase effect. According TE prolongs, 16 msec was considered optimal because artifacts from magnetic susceptibility increases. Contrast of the blood vessel and parenchyma becomes better, Flip angle was considered to become good 20 degrees.(Conclusion) Parameters of 3D Gradient Echo EPI sequence that studied, Whole brain blood vessels can be imaged in 55 seconds. In clinical, such as rendering of a bypass blood vessel and abnormal blood vessels can be expected.

O-3-001　膝軟骨における定量的T1ρおよびT2同時撮影
Simultaneous Acquisition of quantitative T1ρ and T2 measurement in knee cartilage

奥秋　知幸（Philips Healthcare）
Tomoyuki Okuaki[1], Kosuke Morita[2], Seitaro Oda[3], Takeshi Nakaura[3], Makoto Obara[4], Yasuyuki Yamashita[3], Marc Van Cauteren[1]

[1]Philips Healthcare, [2]Department of Central Radiology, Kumamoto University Hospital, [3]Department of Diagnostic Radiology, Faculty of Life Sciences, Kumamoto University, [4]Philips Electronics Japan

【要旨】T1ρ値はプロテオグリカンの変化を反映し、T2値はコラーゲンおよび水分含有量を反映するといわれる。同じリードアウトシーケンスを用いることで、T1ρおよびT2を同時に撮影するシーケンスを開発し、T1ρおよびT2マッピングを作成した。ボランティアでの初期検討を行ったので報告する。

Introduction　T1ρ values is sensitive to change in proteoglycan content and T2 mapping is sensitive to change in collagen and water content. Most of clinical practice, T2 mapping is normally acquired with TSE sequence and T1ρ mapping is acquired gradient echo (or steady state) sequence followed by spin locked prepared pulse. The aim of this study is to develop the simultaneous acquisition of T1ρ and T2 mapping using same read-out sequence for investigation of the sensitivity of proteoglycan change in the knee cartilage.Material and methodsA combined T1ρ and T2 quantification sequence is designed the changeable preparation pulse, spin lock pulse for T1ρ mapping and T2 preparation for T2 mapping.　T1ρ : SLF = 500Hz, TSL = 0, 10, 20,40 ms, T2 : T2 prep = 0,10,20,40 ms, T1ρ and T2 map are generated using post-processing SW(in house).Results and conclusionThe preliminary result in healthy volunteer was mostly same comparison with the result acquired with conventional separated sequence. The simultaneous T1ρ-T2 sequence is a robust quantitative method for the relationship between T1ρ and T2 due to the change of the proteoglycan content with shortening the scanning time.

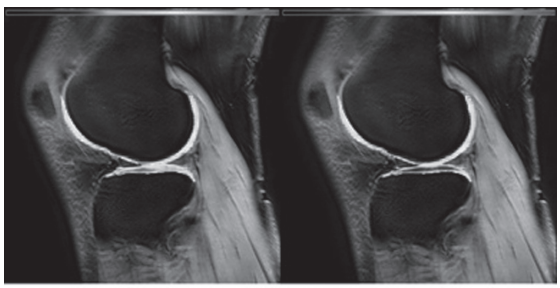

T1rho map　　T2 map

O-3-002　拡散尖度画像における神経鞘腫と軟部肉腫の鑑別の有用性
Feasibility of diffusion kurtosis imaging for differentiation between schwannomas and soft tissue sarcomas

中條　正典（鹿児島大学大学院医歯学総合研究科 放射線診断治療学分野）
Masanori Nakajo[1], Yoshihiko Fukukura[1], Kiyohisa Kamimura[1], Takashi Iwanaga[2], Tomoyuki Okuaki[3], Takashi Yoshiura[1]

[1]Department of Radiology, Kagoshima University Graduate School of Medical and Dental Sciences, Kagoshima, Japan, [2]Department of Radiological Technology, Kagoshima University Hospital, Kagoshima, Japan, [3]Philips Electronics Japan, Tokyo, Japan.

【要旨】拡散尖度画像（b=0, 500, 1000, 1500, 2000, 2500 s/mm2）の神経鞘腫と軟部肉腫の鑑別の有用性を検討した。軟部肉腫は神経鞘腫よりADCは有意に低く、尖度は有意に高かった。ADCと尖度は神経鞘腫と軟部肉腫の鑑別に有用である。

PurposeSchwannoma is one of the most frequently misdiagnosed entities as soft tissue sarcomas (STSs). No study has demonstrated the utility of DKI for characterizing soft tissue tumors. The purpose of this study was to evaluate the feasibility of DKI for differentiating schwannomas from STSs.MethodsThe study population consisted of 35 patients with soft tissue tumors including 15 schwannomas and 20 STSs. Diffusivity (D) and kurtosis (K) maps were calculated from DKI data obtained with b values of 0, 500, 1000, 1500, 2000 and 2500 s/mm2. ADC map was generated from b values of 0 and 1000 s/mm2. Regions of interest were placed in tumors avoiding bulky fat, and necrotic and cystic areas. ADC, D and K were compared between schwannomas and STSs by using the Mann-Whitney U test. Receiver operating characteristic (ROC) analyses were used to assess the ability of ADC, D and K for differentiating STSs from schwannomas.ResultsADCs of STSs were significantly lower than those of schwannomas. K was significantly higher in STSs than in schwannomas. The areas under the ROC curve of ADC and K were 0.703 and 0.707, respectively.ConclusionADC and K enable differentiation between STSs and schwannomas.

ADC, D and K compared between schwannoma and STSs

	Schwannoma (n=15)	STSs (n=20)	*P* Value[a]
ADC ($\times 10^{-3}$s/mm^2)	1.57±0.31	1.26± 0.48	0.042
D	1.84 ±0.38	1.50 ± 0.59	0.064
K	0.52 ±0.17	0.70 ± 0.25	0.039

Note-Values are mean ±SD　　a : Mann-Whitney U test

ROC analyses of ADC, D and K for diagnosing STSs

	Area under ROC curve*	Cut off value	Sensitivity (%)	Specificity (%)
ADC ($\times 10^{-3}$s/mm^2)	0.703 (0.525, 0.845)	≦1 .00	50.0	100
D	0.687 (0.508, 0.832)	≦1.13	45.0	100
K	0.707 (0.529, 0.848)	> 0.50	70.0	73.3

*Data in parentheses are 95% confidence　　a: comparison of ROC curve

O-3-003　全身MRIによる関節リウマチのスコアリング評価
Effectiveness of whole-body MRI for the evaluation of patients with rheumatoid arthritis receiving biologic agents: a retrospective study

神島　保（北大 保健科学研究院）
Tamotsu Kamishima[1], Michihito Kono[2], Shinsuke Yasuda[2], Keita Sakamoto[3], Atsushi Noguchi[2], Toshiyuki Watanabe[2], Yuka Shimizu[2], Kenji Oku[2], Toshiyuki Bohgaki[2], Olga Amengual[2], Tetsuya Horita[2], Tatsuya Atsumi[2]

[1]Faculty of Health Sciences, Hokkaido University, [2]Division of Rheumatology, Endocrinology and Nephrology, Hokkaido University Graduate School of Medicine, [3]Hokkaido University Hospital

【要旨】関節リウマチ患者30例に対し治療前後に全身MRIを施行し、スコアリングにて治療効果を評価した。手の滑膜炎の変化は全身の滑膜炎の変化と相関したが、手の骨病変の変化は全身の骨病変の評価に相関しなかった。全身MRIは手のみのMRIでは得られない情報を有しており、関節リウマチ患者評価に有用であると考えられた。

Objectives. Few studies have evaluated whole-body magnetic resonance imaging (WBMRI) in patients with rheumatoid arthritis (RA). Here we aimed to evaluate the effectiveness of WBMRI in RA patients receiving biological DMARDs (bDMARDs).Methods. Thirty consecutive RA patients receiving bDMARDs were included in this retrospective study. Contrast WBMRI was performed before and 1 year after bDMARDs initiation. Hand joints were evaluated according to RA MRI score (RAMRIS) while other joints (atlantoaxial, shoulder, hip, and knee joints) were assessed using a modified RAMRIS.Results. Twenty-one patients received tocilizumab, five etanercept, and four infliximab. Mean age was 57.1 years and mean disease duration was 3.0 years. Median disease activity score in 28 joints improved from 5.1 to 2.1 ($P < 0.001$). The treatment with bDMARDs resulted in improvements in mean whole-body synovitis score (from 31.2 to 23.2; $P = 0.02$) and median whole-body bone-oedema score (from 11 to 3; $P = 0.03$). Whole-body bone-erosion score improved in seven patients and deteriorated in 17 patients. Logistic regression analysis identified whole-body synovitis score as a poor prognostic factor for whole-body bone-erosion progression ($P = 0.04$). Bone-oedema score in individual bone was identified as a poor prognostic factor for the progression of bone-erosion in individual bones ($P < 0.001$). Changes in synovitis score of hands correlated with those of other joints, but changes in bone-oedema or erosion score of hands did not correlate with those of other joints in WBMRI.Conclusions. WBMRI can be useful for the evaluation and total care of patients with RA.

O-3-004　PET/MR装置を用いたSUVとADCのvoxel-based analysis：軟部肉腫の治療効果判定への応用
Evaluation of treatment effect in soft-tissue sarcoma with multiparametric voxel-based analysis of SUVs and ADCs in a PET/MR system

鷺山　幸二（九州大学医学研究院大学院 臨床放射線科学分野）
Koji Sagiyama[1], Yuji Watanabe[2], Ryotaro Kamei[1], Sungtak Hong[3], Satoshi Kawanami[2], Yoshihiro Matsumoto[4], Hiroshi Honda[1]

[1]Kyushu University Graduate School of Medical Sciences, Department of Clinical Radiology, [2]Kyushu University Graduate School of Medical Sciences, Department of Molecular Imaging and Diagnosis, [3]Philips Electronics Japan, [4]Kyushu University Hosp. Dept. Orthopaedics

【要旨】悪性軟部肉腫の治療前後でPET/MR装置を用いてSUVとADCのvoxel単位での解析を行い、治療効果判定への有用性を検討した。SUVとADCとの相関係数およびSUV/ADCとADCとの線形相関の傾きが治療後には有意に変化しており、腫瘍体積、SUVmax、ADCなど単独の測定値では困難であった早期の治療効果を検出できた。

Purpose: To investigate the feasibility of the voxel-by-voxel comparisons of SUVs and ADCs with a PET/MR system in the evaluation of the treatment effect in soft-tissue tumors.
Materials and Methods: Eight patients with soft-tissue tumors were examined with Ingenuity TF PET/MR system (Philips) before and after the treatment. Five patients underwent chemotherapy and 3 patients underwent heavy-particle radiotherapy. Zoomed DWI and ^{18}FDG-PET were acquired along with fat-suppressed T2WI. The ROIs were manually drawn on T2WI to include the tumor in all slices and copied and pasted on the ADC maps and PET images. The ADCs and SUVs within the tumor ROIs were recorded in a voxel-by-voxel manner, and voxel-based SUV/ADCs were calculated. The scatter plots of SUV vs. ADC and SUV/ADC vs. ADC were generated for each tumor. The indicators of SUVmax, ADCmin, tumor volume, slopes of linear regression of SUV/ADC vs. ADC and correlations between SUVs and ADCs were compared between the pre- and post-treatment.
Results: The correlation coefficient between SUV and ADC significantly increased (-0.52 ± 0.14 vs. -0.23 ± 0.21, $P < 0.01$) and the slope of linear regression of SUV/ADC vs. ADC significantly decreased (-3.42 ± 1.22 vs. -1.82 ± 1.79, $P < 0.05$) after treatment. In contrast, the conventional indicators of tumor volume, SUVmax, and ADCmin did not show significant differences between pre- and post-treatment.
Conclusion: Voxel-based analysis of SUVs and ADCs with PET/MR hybrid systems is useful for the evaluation of the treatment effect in soft-tissue tumors.

O-3-005　若年・壮年患者の良性腰椎疾患に対する「早期」MRI検査頻度と病院因子：大規模レセプトデータベース解析
Hospital factors associated with early MR imaging for low back pain in working-age subjects: a Japanese Claims Database study

佐野由起子（順天堂大学医学部 放射線診断学講座）
Yukiko Sano, Kanako Kumamaru, Michimasa Suzuki, Masaaki Hori, Ryusuke Irie, Atsushi Nakanishi, Shigeki Aoki

Juntendo Univesity, Department of Radiology

【要旨】28619人のレセプトデータ解析にて、ベッド数が300未満の病院および1.5T未満のMR機器しか有しない施設では、若年・壮年の良性腰椎疾患に対する早期のMRI検査頻度が有意に上昇していた。一部施設でのMRI検査施行閾値の低下を表している可能性があり、稼働率や放射線科医の有無との関連も含めさらなる研究が求められる。

Purpose
Evidences suggest that MR imaging of the spine in patients with acute "benign" low back pain during the early phase of symptom onset is unnecessary. The purpose of the study was to identify the characteristics of facilities where "early MR imaging" for benign lumbar conditions in working-age patients is frequently performed.
Methods
This retrospective cohort study used unlinkable anonymized claims data from the Japan Medical Data Center mainly including working-age insured people. Subjects who underwent at least one outpatient MR exam in 2013-2014 for benign lumbar conditions were included. The outcome was MR exam performed within 4 weeks of the first "benign lumbar disease" diagnosis. Patients who underwent any surgery/admission before or after the imaging and patients with malignancy were excluded. A hierarchical multivariable logistic regression model was developed to identify patient and hospital characteristics associated with frequent "early" MR imaging.
Results
A total of 28619 patients were included (mean age 43.5 ± 15.5 years); the most prevalent diagnosis was lumbar disc herniation/discopathy (41.6%). 57.3% of the patients underwent MR exam within 4 weeks of the first benign lumbar disease diagnosis. The model including age, sex, comorbidities, and related hospital characteristics showed higher odds of frequent "early" MR exam at facilities with <300 beds (OR vs >=500 beds: 2.49, p<0.0001) and facilities without >=1.5 tesla MR scanners (OR vs those with 3T: 1.63, p<0.0001).
Conclusions
Small-medium size facilities and those without >=1.5T MR scanners may have a low threshold for MR exam for benign lumbar disease in working-age patients and thus further investigation is warranted.

O-3-006　syngoWARP(VAT)を併用したBLADEによるアーチファクト低減の基礎的検討
An Experimental Investigation of Artifact Reduction by BLADE Combined with SyngoWARP(VAT)

井隈　美鶴（マツダ病院 画像診断科）
Mitsuru Ikuma, Yoshihide Asao, Akitoshi Sunada, Yoshiko Nakamura, Toshiharu Shimokawa, Kumiko Miyake

Department of Diagnostic Imaging Mazda Hospital

【要旨】BLADEにsyngoWARP(VAT)を併用することでモーションアーチファクトとメタルアーチファクトを低減することが可能である事を自作ファントムを使用して確認した。

[Purpose]SyngoWARP is the technique to reduce metal artifacts. BLADE is the technique to reduce motion artifacts based on Turbo Spin Echo(TSE) by sampling strips of date in a rotating fashion around the center of k-space. We examined that the combination of SyngoWARP and BLADE technique was useful to reduce both metal and motion artifacts.[Material]MAGNETOM Aera XJ 24ch(SIEMENS),3mm diameter Kirschner wire(Stainless wire with NI and Cr is used for fixing inside the body. MIZUHO Ltd.)Kirschner wire is embedded in agar and it was used as the phantom.[Method]The images were corrected by dynamic scan with TSE,TSE-VAT(100%),BLADE,BLADE-VAT(100%)sequence respectively. And each T2 weighted image was evaluated by visual.[Result]The image on TSE contained strong motion artifacts and on TSE-VAT(100%)contained strong motion artifacts and less metal artifacts. The image on BLADE did not contained motion artifacts but remained metal artifacts, and BLADE-VAT(100%)could reduce metal and motion artifacts mostly.[Conclusion]Both metal and motion artifacts were reduced by using BLADE combined with SyngoWARP(VAT). It was considered the sequence was useful for scanning on body parts were sensitive to motion artifacts such as shoulder joint implanted metal.

O-3-007　折り返しを利用した両手指高分解能撮像法の考案
High-resolution MRI of both hands using aliasing phenomenon

加藤　広士（国家公務員共済組合連合会 新別府病院 放射線科）
Hiroshi Kato, Kentarou Abiru, Kyouichi Misaka
Shinbeppu Hospital Radiology department

【要旨】関節リュウマチの手指MRIにおいて両側撮像は非常に有用であるが、高分解能撮像は困難である。そこで我々は補助具を作成し折り返しを利用した両側同時高分解能撮像法を考案し、画質の評価を行った。実画像と折り返し画像のSNRには有意差はなかった。STIR法、Dixon法で脂肪抑制効果が良好であった。

Background&purposeBoth sides simultaneous MR imaging is useful in the hand of rheumatoid arthritis. However high-resolution imaging is difficult and sufficient satisfactory image cannot be obtained on both sides simultaneous imaging.So we devised a both sides simultaneous high-resolution imaging using aliasing phenomenon and evaluated the image quality.MethodAll MR imaging were performed by using a 1.5T MR unit (Optima MR450w, GE Healthcare, Milwaukee, WI) with 16 channel small flex coil.1) We have created an assisting tool for a both sides simultaneous high-resolution imaging using an aliasing phenomenon.2) We have compared the signal to noise ratio (SNR) between the real image and the aliasing image using a copper sulfate phantom image acquired by whole body coil.We have visual assessment of the fat suppression effect in chess method, STIR method and Dixon method in both hands of healthy volunteers data.ResultThere was no significant difference in the SNR between the real image and the aliasing image.Chess method could insufficient fat suppression effect compare to STIR and Dixon method.ConclusionBoth sides simultaneous high-resolution imaging using aliasing phenomenon was possible.

O-3-008　Ultra-short TE（UTE）を用いた三角線維軟骨評価：回内位と正常位との比較
Ultrashort time-to-echo quantitative magnetic resonance imaging of the triangular fibrocartilage: comparison between pronation and neutral position

藤崎　瑛隆（産業医科大学 放射線科）
Akitaka Fujisaki[1], Takatoshi Aoki[1], Hidekuni Narimatsu[1], Sho Watanabe[1], Chie Kuwahara[1], Atsushi Nozaki[2], Yukunori Korogi[1]
[1]Department of Radiology, University of Occupational and Environmental Health School of Medicine, [2]MR Applications and Workflow, Asia Pacific, GE Healthcare Japan

【要旨】UTEシーケンスを用いて、前腕の回旋と三角線維軟骨の$T2^*$値との関係を評価した。前腕を回内することで三角線維軟骨の$T2^*$値は有意に低下し、UTEを用いた手関節$T2^*$マッピング画像は、三角線維軟骨の圧力分布変化の解析に使用可能と思われる。

PURPOSE:To compare $T2^*$ values of the triangular fibrocartilage (TFC) obtained by ultrashort time-to-echo (UTE) techniques at pronation and at neutral position of the forearm. MATERIALS AND METHODS:MR imaging was performed in the wrist of 6 healthy subjects with a 3T MR system by using an eight-channel wrist coil. Coronal $T2^*$ maps from three-dimensional cones UTE pulse sequence were obtained with the forearm at pronation and at normal position. $T2^*$ relaxation time maps were calculated on a pixel-by-pixel basis for all structures of the wrist visualized in the coronal planes. The entire region of interest for TFC was delineated on the $T2^*$ map, and the average $T2^*$ value was calculated. RESULTS:Quantitative wrist UTE MRI was successfully performed in vivo. Average $T2^*$ value of TFC at pronation (8.1 ± 0.9 ms) was significantly lower than that at neutral position (10.4 ± 1.3 ms; $P < 0.01$).CONCLUSION: $T2^*$ relaxation time measurement of the TFC using UTE seems feasible at 3T MRI, and may be useful for assessing the effect of loading by wrist rotation.

O-3-009　IDEAL-IQ法を用いた骨髄脂肪定量化による糖尿病患者の骨強度解析
Vertebral strength prediction in diabetic patients: quantification of bone marrow fat content obtained by IDEAL-IQ

山口　晋平（産業医科大学 放射線科）
Shinpei Yamaguchi[1], Takatoshi Aoki[1], Masami Fujii[1], Michiko Kobayashi[1], Chihiro Chihara[1], Yoshiko Hayashida[1], Yukunori Korogi[1], Yosuke Okada[2], Yoshiya Tanaka[2]

[1]Department of Radiology, University of Occupational and Environmental Health School of Medicine, [2]First department of Internal Medicine, University of Occupational and Environmental Health

【要旨】糖尿病患者は骨密度(BMD)が正常でも骨折リスクが高く、血糖降下薬のチアゾリジン誘導体は骨折リスクを増加させることが知られている。MRIのIDEAL-IQ法を用いた骨髄脂肪量の定量的評価は、糖尿病患者の骨強度予測に役立ち、特にチアゾリジン誘導体使用者で有用性が高い可能性がある。

PURPOSE: Although bone mineral density (BMD) by dual X-ray absorptiometry (DXA) has been used to predict bone strength, diabetes mellitus (DM) patients have an elevated fracture risk despite normal BMD. In addition, thiazolidinedione (TZD), which is one of the antidiabetic drugs, has been proven to increase fracture risk. The purpose of this study is to determine the value of the quantitative chemical shift-based water–fat separation method with a multiecho gradient echo sequence (known as IDEAL-IQ) of MRI to BMD in vertebral bone strength prediction of DM patients.MATERIALS AND METHODS: Sixty-six consecutive DM patients were included in this study, and 11 of them were treated with TZD. They underwent DXA, IDEAL-IQ, and CT covering the vertebral body of L1 to L4 within a week. Quantitative fat fraction (FF) using IDEAL-IQ of 4 lumbar vertebrae was analyzed. Failure load of the vertebra, determined by the CT-based finite-element method (FEM), was used as the gold standard for bone strength. A forward stepwise multiple regression analysis for evaluating the availability of the FF using IDEAL-IQ was performed. Independent variables considered in the analysis were age, disease duration, BMD, and FF using IDEAL-IQ.RESULTS: The combination of age, BMD, and the FF using IDEAL-IQ showed the highest correlation to the failure load by CT-FEM. The correlation between the failure load and the BMD with age and the FF using IDEAL-IQ (r^2=0.63) was significantly higher than that between the failure load and the BMD alone (r^2=0.53; p<.001), and the combination in patients treated with TZD showed excellent correlation with the failure load (r^2=0.82).CONCLUSION: FF using IDEAL-IQ in combination with BMD measurements can potentially be used in predicting bone strength in DM patients.

O-3-010　炎症を有する頚部痛患者へのMRIは診断に貢献するのか
Acute neck pain in patients with inflammation : Dose MRI contribute to the diagnosis?

結城　雅子（北摂総合病院 放射線科）
Masako Yuki[1], Yoshifumi Narumi[2]

[1]Department of Radiology, Hokusetsu general hospital, [2]Department of Diagnostic Radiology, Osaka medical college

【要旨】炎症を伴う頚部痛を呈する患者に対し頚椎MRIが診断に貢献するかどうかを検討した。患者14名（37-89歳）。T2WI/T1WI横断と矢状断、STIR矢状断を撮像。結果、炎症や液体の評価には脂肪抑制系T2WIが有用で、咽後を含めC1/2の撮像が必要であった。石灰化の描出にはCTが欠かせない。

Purpose: To evaluate the usefulness of cervical spine MRI to patients with acute febrile neck pain.Material and Methods: There were 14 patients, 7 men and 7 women with an age range of 37 to 89 years. CRP level was 4.8-28. Imaging diagnosis was 8 cervical spondylosis, 6 crowned dens syndrome (CDS), 3 calcific tendinitis of the longus colli, 2 amyloid deposition, one retropharyngeal abscess, one inflammatory cervical lymphadenitis, one pyogenic spondylitis and 2 normal findings. All patients presented with acute febrile neck pain and were performed cervical spine MRI with 1.5T or 3T, which included sagittal images through the entire neck and cervical spine and axial images both T1WI and T2WI. Some cases included STIR sagittal images. Evidence of capsule or perivertebral edema and joint space T2 increase were recorded. Additionally, signs of muscle edema, alignment, disc disease, were recorded. For the cases with CT was scanned, CT findings were compared. Results: In the cases of CDS, MR findings were positive (n=4/6) vs. CT findings were positive (n=6/6). In the cases of calcific tendinitis of the longus colli, MR findings were positive (n=3/3) vs. CT findings were positive (n=2/3). STIR was useful in the evaluation of fluid and edema. A calcification on CT showed no signal on MRI, the visualization of calcification of CT was superior to MRI. Some cases were observed that C1/2 of axial images was not scanned.Conclusions: Fat saturation T2WI was needed to evaluate the inflammation and fluid collection, moreover axial images included C1/2 and retropharyngeal space should be scanned. Also to detect calcification, CT scan was essential.

O-3-011　手根管症候群におけるMicroNeurographyと同時取得するT2*mapの有用性
Usefulness of simultaneous acquisition of MR MicroNeurography and T2*mapping for assessment of carpal tunnel syndrome

小澤由莉子（八重洲クリニック）
Yuriko Ozawa[1], Masami Yoneyama[2], Satoshi Tatsuno[1], Koji Fujita[4], Takashi Miyamoto[5], Yuji Inoue[1,3], Nozomu Koyama[1,3]

[1]Yaesu clinic, [2]Philips electronics Japan, [3]Tsukuba advanced imaging center, [4]Department of Orthopedic and Spinal Surgery, Tokyo Medical and Dental University, [5]Department of Functional Joint Anatomy, Tokyo Medical and Dental University

【要旨】手根管症候群にて、T2mapやT2*mapの有用性が報告されているが、T2*mapとT2mapは撮像時間に差がある。当院倫理委員会の承認を得た手根管症候群患者の手関節の正中神経を対象に、超高分解能にてT2*mapを取得し、神経浮腫部/正常部/小指外転筋にてT2mapと比較した。超高分解能T2*強調画像とT2*mapの同時取得は有用である。

[Introduction]In the carpal tunnel syndrome, T2 value rises by the edematous change of the median nerve. So usefulness of T2mapping is reported. We acquired T2* map at the same time this time by imaging the high-resolution T2* weighted image (MR MicroNeurography) of the median nerve in multi echo and weighed it against T2 map of the law conventionally.
[method]the examination object assumed it the median nerve of the wrist of the carpal tunnel syndrome patient with the approval of our local institutional review board. I got image of MicroNeurography in multi echo and acquired T2*map. I compared the T2* value which I measured with the T2 value about a nerve edematous part, a nerve normal part.
[results and discussion] as for the value of a nerve edematous part and the normal part, there was significantly a difference with T2 value and T2* value. T2*map which is the gradient echo method has a shorter imaging time than T2map which is the spin echo method. Scaning with the high resolution is possible by just that much.
[conclusion] For median nerve edema part identification in the carpal tunnel syndrome, the simultaneous income of MicroNeurography and T2*map is useful.

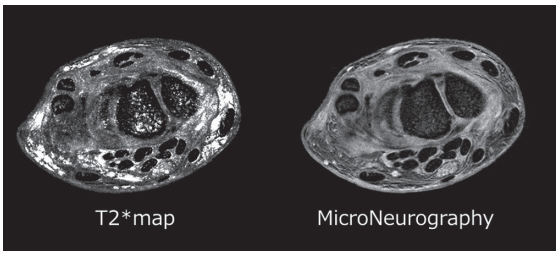

O-3-012　2-Point Dixon法による棘上筋脂肪変性の定量評価の信頼性の検討、Goutallier分類による定性評価との比較
Reliability of MR quantification of rotator cuff muscle fatty degeneration using a Two-point Dixon technique

堀内　沙矢（聖路加国際病院 放射線科）
Saya Horiuchi[1], Taiki Nozaki[1], Atsushi Tasaki[2], Akira Yamakawa[3], Yasuhito Kaneko[4], Starkey Jay[1], Takeshi Hara[5], Yasuyuki Kurihara[1], Hiroshi Yoshioka[4]

[1]Department of Radiology, St.Luke's International Hospital, [2]Department of Orthopaedic Surgery, St.Luke's International Hospital, [3]Division of Clinical Biotechnology, University of Tokyo Graduate School of Medicine, [4]Department of Radiological Sciences, University of California, [5]Department of Intelligent Image Information, Division of Regeneration and Advanced Medical Sciences, Gifu University Graduate School of Medicine

【要旨】肩痛患者200例の肩関節MRIにおいて、2-Point Dixon法を用いて棘上筋内の脂肪含有量を定量化し、modified-Goutallier分類による定性評価との信頼性/再現性について比較検討を行った。2-Point Dixon法を用いた定量評価の方が観察者間一致率、観察者内一致率ともに高かった。

Background
The objective of this study was to quantify fatty degeneration of the supraspinatus muscle using a 2-point Dixon technique at 3.0-T MRI in patients with rotator cuff tears by multiple-readers, and to evaluate the reproducibility and its clinical usefulness compared to the modified-Goutallier classification.
Methods
Two hundred patients with rotator cuff tears were selected retrospectively, who underwent MRI at 3.0-T, including 2-point Dixon sequence. Qualitative evaluations using the modified-Goutallier classification and quantitative analysis of fatty degeneration were performed by two radiologists and three orthopedic surgeons independently. The fat quantification was performed by measuring signal intensity values of in phase (S(In)) and fat image (S(Fat)), and calculating fat fraction as S(Fat)/S(In). The reproducibility of MR quantification among multiple-readers was analyzed by the intra- and inter-class correlation coefficients.
Results
The interobserver agreement of the modified-Goutallier classification among 5 readers was moderate (k=0.44), while the inter-class correlation coefficient regarding fat fraction value quantified in 2-point Dixon sequence was excellent (0.893). The intra- class correlation coefficient of the quantification was also excellent for each reader (0.893-0.956). Proposed fat fraction grading and modified- Goutallier grading showed similar frequency and distribution in severity of rotator cuff tears.
Conclusions
Fat quantification in the rotator cuff muscles using a 2-point Dixon technique at 3.0-T MRI is highly reproducible and clinically feasible in comparison with the qualitative evaluation using modified-Goutallier classification.

O-3-013　四肢領域における phase-cycling modified DSDE を用いた 3D MR Neurography の改善法の検討
Improvement of 3D MR Neurography in the extremities using phase-cycling modified diffusion-sensitized driven equilibrium (pc-mDSDE)

坂井　上之（東千葉メディカルセンター 放射線部）
Takayuki Sakai[1], Atsuya Watanabe[2,3], Masami Yoneyama[4], Kiichi Nose[1], Noriyuki Yanagawa[1]
[1]Department of radiology, Eastern Chiba Medical Center, [2]Department of general medical services, Chiba university graduate school of medicine, [3]Department of orthopedic surgery, Eastern Chiba Medical Center, [4]Philips Electronics Japan

【要旨】我々は先行研究にて pc-DSDE 法を用い，歪みの影響が少なくかつ高分解能の末梢神経描出を試みた．しかし撮像法の安定性や静脈信号の消え残りなど問題点があった．そこでプリパルスである DSDE の部分において，RF パルスの改善と MPG のタイプを印可軸により使い分けることで画質が改善するか検討を行った．

<Purpose>The role of MRI in diagnosis of peripheral neuropathy is depiction of the anatomical detail of peripheral nerves and the pathological changes related to entrapment. As a preliminary, we developed T1-TFE using phase-cycling combined with diffusion-sensitized driven equilibrium (pc-DSDE) that enables the visualization of peripheral nerves. However, pc-DSDE has several problems, such as low image stability, poor reproducibility, and partially remaining venous signal. To solve these problems, RF pulses were modified to adiabatic pulse type. Also, we combined bipolar MPG with unipolar MPG in three axes(pc-mDSDE). The purpose of this study was to evaluate the visualization of peripheral nerves by pc-mDSDE around the extremities such as wrist, elbow, and knee.
<Methods>All subjects were examined using a 1.5 T whole-body clinical system and an eight-channel coil (Ingenia, Philips Healthcare). Five healthy volunteers were included for the examination of peripheral nerves in the extremities. We assessed the detectability of peripheral nerves to compare with pc-mDSDE and pc-DSDE.
<Results & Discussion>Pc-mDSDE clearly depicted the course of peripheral nerves on the MIP images. Image uniformity of pc-mDSDE was improved, because adiabatic RF pulses were applied to reduce B0 and B1 inhomogeneity. Therefore, contrast ratio of pc-mDSDE was more increased than that of pc-DSDE. We applied weak MPGs in the direction parallel to the major nerves and vessels. Even if a weak MPG, bipolar gradient type sufficiently suppressed the vessel signals.
<Conclusion>MR neurography using pc-mDSDE enables improved visualization of peripheral nerves with more insensitive to inhomogeneous and more suppression of venous signal than those of pc-DSDE in the extremities.

O-3-014　精巣の MRS：非可逆的な虚血障害ではクレアチン信号が低下する
MR spectroscopy of the testis: The reduction in creatine signals is a potential marker of irreversible ischemic damage

山口　雅之（国立がん研究センター 先端医療開発センター 機能診断開発分野）
Masayuki Yamaguchi[1], Hidehiro Watanabe[2], Nobuhiro Takaya[2], Fumiyuki Mitsumori[2], Hirofumi Fujii[1]
[1]National Cancer Center, Exploratory Oncology Research & Clinical Trial Center, Division of Functional Imaging, [2]National Institute for Environmental Studies

【要旨】精巣にはクレアチン（Cr）が多く蓄積している。虚血が長期間持続すると、Cr が血中に逸脱し、精巣の Cr 含有量は低下すると予想される。本実験では、長期虚血状態の動物精巣において、9.4 tesla 装置を用い in vivo MRS や過塩素酸抽出物の NMR 計測を実施した。Cr 信号の低下が観測された。

Background:The testis contains high levels of creatine. Testicular tissues reportedly release creatine molecules into blood circulation after ischemic insult, thereby reduce their creatine concentration under prolonged ischemic conditions. The purpose of this experimental study was to investigate MR spectroscopy (MRS) is capable of detecting the reduction in creatine levels in the ischemic testis. Materials and Methods: Institutional Animal Care and Use Committee approved this experiment. We used four male Wistar rats and ligated their left testicular arteries to produce testicular ischemia. The right testicles served as control. On the next day, we performed single-voxel ^{1}H MRS measurements of the bilateral testicles by using a 9.4 tesla scanner and evaluated creatine/choline ratios (Cre/Cho) in 125 μL-testicular regions. After MRS examinations, we excised the testicles, extracted metabolites by using perchloric acid extraction technique, and obtained NMR spectra of the extract by using a 400 MHz NMR spectrometer. Results: Cre/Cho was 0.60 ± 0.09 and 1.03 ± 0.25 in the left and right testes ($P < 0.05$). The reduction in creatine signals in the left testis was confirmed on NMR spectra. Conclusion: The reduction in creatine levels in the testis is detectable by using MRS and it is indicative of severe testicular damage caused by circulatory disturbance. MRS of the ischemic testis may help urologists to evaluate whether ischemic damage is reversible or irreversible and to plan appropriate treatment to the ischemic testis.

O-3-015　3テスラMRIを用いた婦人科癌小線源治療患者のADC値とT2値の経時変化：放射線抵抗性予測の可能性について
Validation of Adaptive Brachytherapy using 3T MRI in Gynecological Cancer Patients: Impact of Sequential Evaluation of ADC and T2 values

京谷　勉輔（神戸大学医学部附属病院 医療技術部 放射線部門）
Katsusuke Kyotani[1], Satoru Takahashi[1,2], Kenji Yoshida[3], Ryo Nishikawa[3], Yuuichirou Somiya[1], Hideaki Kawamitsu[1], Ryohei Sasaki[3], Kazuro Sugimura[2]

[1]Department of Diagnostic Radiology, Division of Diagnostic Imaging, Kobe University Hospital, [2]Department of Radiology, Kobe University Graduate School of Medicine, [3]Division of Radiation Oncology, Kobe University Graduate School of Medicine

【要旨】3テスラMRIを用いた婦人科癌小線源治療患者のADC値とT2値の経時変化を評価した．放射線治療の効果的な群では治療と共にADC値が低値から高値変化し，T2値が高値から低値に変化したが、放射線治療が効かなかった群では，ADC値もT2値も高値のまま変化しなかった．

Introduction: To obtain the optimal radiation field, an MR image has involved that basically depends upon the higher soft tissue contrast resolution than CT image. Thus, recently it is increasing radiotherapy planning using MR image, moreover it can evaluate tissue characterization such as T2, T1 value and apparent diffusion coefficient (ADC) value. The purpose of this study was to evaluate sequential changes of ADC and T2 values during brachytherapy in patients with gynecological cancer.Material and Method: 13 patients (65y ± 14y) suffering from gynecological cancer were evaluated, who treated with external radiotherapy followed by adaptive brachytherapy using MRI (4 times for times for each patient). MR protocol including diffusion weight image (DWI) and single-shot multi-echo gradient-echo echo-planar imaging (EPI) sequence at 3T system using a phased array coil. Then, ADC and T2 values calculated by DWI and EPI. Sequential changes as for ADC and T2 values in response to brachytherapy were evaluated. Each ADC and T2 value was compared by Tukey's test.Result: The pre-treatment ADC values ($\times 10^{-3}$ mm^2/s) in those 8 patients seemed to be comparatively low (0.89 ± 0.14), and then the ADC values increased according to the frequency of the brachytherapy. One the contrary, the pretreatment T2 maps seemed to be high (46.33ms ± 4.93ms), and then gradually decreased according to the treatment. Interestingly, the tendency seemed to be different in 5 patients who recurred after the same treatment. In those 5 patients, initial ADC and T2 value was higher compared to other 8 patients ($p<0.05$).Conclusion: Sequential evaluation of ADC and T2 values using 3T MRI during brachytherapy might include important predictive information about pattern of failures after adaptive brachytherapy.

O-3-016　子宮肉腫と子宮筋腫の鑑別におけるmultiparametric MRIとPET/CTの診断能の比較
Comparison of the diagnostic accuracy of multiparametric MRI and 18F-FDG PET/CT in the differentiation between uterine sarcoma and benign leiomyoma

中川　雅貴（熊本大学 医学部 放射線診断学）
Masataka Nakagawa, Tomohiro Namimoto, Kie Shimizu, Fumi Sakamoto, Shinnya Shiraishi, Seitarou Oda, Takeshi Nakaura, Daisuke Utsunomiya, Yasuyuki Yamashita

Diagnostic Radiology, Faculty of Life Sciences, Kumamoto University

【要旨】子宮肉腫と子宮筋腫の鑑別能について、multiparametric MRIとPET/CTの比較を行った。multiparametric MRI（DWI有/無）、SUVmax、meanADCのAUC値はそれぞれ0.963、0.915、0.892、0.814であり、multiparametric MRI with DWIが最も有用であった。

PURPOSE, To compare the diagnostic accuracy of multiparametric MRI and Fluorine-18 fluorodeoxyglucose(18F-FDG) positron emission tomography combined with CT(PET/CT) in the differentiation between uterine sarcoma and benign leiomyoma.MATERIALS AND METHODS, This retrospective study was approved by the institutional review board. The requirement to obtain informed consent was waived. Eighty-nine consecutive patients diagnosed with benign leiomyoma or uterine sarcoma who underwent pelvic MRI exam at 3T and 18F-FDG PET/CT before surgery were included. Of 89 patients, 11(12.4%) patients had uterine sarcomas and 78(87.6%) patients had benign leiomyomas. Two radiologists blinded to the diagnoses of uterine tumors independently evaluated images based on MRI images(T2-weighted images, T1-weighted images, dynamic MRI, with or without DWI) and rated likelihood of the presence of malignancy on a scale of 1 to 5(1,definitely absent; 2, probably absent; 3, equivocal; 4, probably present; 5, definitely present). The apparent diffusion coefficients(ADC) values were calculated from b=0 and 1000 s/mm2. The mean ADC value was also evaluated. The maximum standardized uptake values(SUVmax) of lesions were also measured.Receiver-operating-characteristic(ROC) curve analysis was performed to compare the diagnostic performance among multiparametric MRI with/ without DWI, the ADC values and SUV max.RESULTS, The area under the curves(AUCs) of ROC for multiparametric MRI with DWI, MRI without DWI, SUVmax, and meanADC were 0.963, 0.915, 0.892, and 0.814 for differentiation uterine sarcoma from benign leiomyoma, respectively.CONCLUSION, Multiparametric MRI with DWI had highest AUC of ROC and can provide accurate information for differentiation between uterine sarcoma and benign leiomyoma.

O-3-017　演題取り下げ

O-3-018　前立腺癌のSynthetic FOCUS DWI: PIRADS version2における有用性についての検討
Evaluation of prostate cancer on synthetic FOCUS DWI by using the PI-RADS version 2.0

片山　元之（聖隷浜松病院 放射線科）
Motoyuki Katayama[1], Takayuki Masui[1], Kei Tsukamoto[1], Kenichi Mizuki[1], Yuki Baba[1], Masako Sasaki[1], Tetsuya Wakayama[1,2], Mitsuharu Miyoshi[2]

[1]Dept. of Radiology, Seirei Hamamtsu General Hospital, [2]GE Healthcare Japan

【要旨】前立腺癌に対するPIRADS verion2.0を用いたsynthetic FOCUS DWIの診断能をconventional DWIとFOCUS DWIと比較しその有用性を検討した。Synthetic FOCUS DWIは画質、診断能とも良好でありsynthetic technique はFOCUS DWIの有用性を向上させていると考えられる。

Objective: Field-of-view optimized and constrained undistorted single-shot (FOCUS) is one of the new methods. Synthetic DW Imaging (S-DWI) is a new method that can calculate DWIs for any b-value from at least two DWIs using different b-values. While the Prostate Imaging Reporting and Data System (PI-RADS) has been popular for the assessment of the prostate cancer. The purpose of this study is to compare delineation of prostate cancers in FOCUS-DWI and s-FOCUS DWI with those in conventional FOV DWI by means of PIRADS version 2.0.Materials and Methods: 31 patients with cancers in the peripheral zone of the prostate glands were included in this study, underwent MRI on a 3T unit. The b-value of FOCUS imaging was 800, and that of conventional DWI was 1500. S-DWI with b-value of 1500 calculated from FOCUS with that of 800. The scores (1, 2, 3, and 4 including 5) on PIRADS assessment of DWI without ADC maps were applied to the tumor detection on each imaging.Results; 24 of 31 patients were performed trans-rectal biopsies of the prostate glands before MRI. Correlation Coefficient (R) of calculated ADC of tumor between in FOCUS imaging and in Conventional imaging was 0.77. The PIRADS scores of each imaging were as follows: FOCUS-DWI; 3.0, conventional FOV DWI; 2.6, S-FOCUS DWI; 3.2, respectively. The SI of tumor to that of prostate tissue in FOCUS DWI was inferior to that in S-FOCUS DWI (SI tumor/SI muscle: FOCUS-DWI; 1.5, conventional FOV DWI; 2.3, S-FOCUS DWI; 2.4, respectively).Conclusion: Although FOCUS DWI was more affected by bleeding than conventional DWI, it is useful for evaluation of prostate cancer with high spatial resolution and less distortion. S-DWI is able to enhance diagnostic ability of FOCUS without image degradation, and might be one of the best combinations.

O-3-019　子宮DCEにおけるガドブトロールGd-BT-DO3Aの注入速度の変化がもたらす影響と至適条件の検討
Effect and optimization of Gadobutrol (Gd-BT-DO3A) injection speeds on uterus DCE-MRI

伊東　直博（社会医療法人愛仁会 千船病院 技術部 放射線科）
Naohiro Itou, Akira Tsubota, Ryouta Nakamura, Noriaki Kuriyama, Hiroya Tanaka, Yutaka M.D Tanaka

Chibune General Hospital.

【要旨】MRI用造影剤ガドブトロールGd-BT-DO3Aは、従来製剤より2倍の高濃度という特徴から造影剤注入速度を変化することで、コントラストの改善がみられた。また生理食塩水の後押し速度もコントラスト変化に関与してると考えられる。我々は注入速度の変更による子宮DCEのコントラスト変化を報告する。

Introduction: GadobtrolGd-BT-DO3A is a double-Gd concentration MRI contrast agent(CA). We report(1) contrast ratios,(2)changes of early-phase signal intensity(SI)in uterus DCE-MRI with different injection speeds. Methods: Fifty uterus DCE-MRIs were examined with different injection speeds (0.5, 1.0, 1.5, 2.0 mL/s)of the CA and different 20-mL saline flushing speeds.(1)Contrast ratios were calculated from time-intensity curves(TIC) drawn from mean SI values at pre-contrast and 30, 60, 90, 120s after injection in normal myometrium and rectus abdominis muscle. A contrast ratio between Tunica Intima and muscular coat was calculated at 60 s after injection in order to evaluate depiction of subendometrial enhancement (SEE). (2) Changes of early-phase SI in an endometrium with the different CA injection speeds.Results: (1)There were no significant differences among different CA injection speeds in the mean contrast ratio at 60 s after injection. The contrast ratio in SEE with 1.0-mL/s CA injection speed was significantly higher than the others($p<0.05$). The contrast ratio in SEE with 1.0-mL/s CA injection speed was improved with 1.5-mL/s saline-flushing speeds. (2)Mean signal intensities in the endometrium were in proportion to CA injection speeds.Discussion: From the results of TIC, CA arrival time is delayed with 0.5-mL/s CA injection speed. 1.0-mL or faster CA injection speed should be chosen for hypervascular lesions. The contrast ratio in SEE with 2.0-mL/s CA injection speed was low in endometrial cancer. The reason was fast CA uptake into the muscular coat, which equalized contrast in between endometrial cancer and Tunica Intima. The reason of the improvement of the contrast ratio in SEE with the 1.5-mL/s saline-flushing speeds would be shortened CA arrival time.

P-1-001　内頸動脈―前大脳動脈吻合のMRA診断
Carotid-Anterior Cerebral Artery Anastomosis Diagnosed by MR Angiography

内野　晃（埼玉医科大学 国際医療センター 画像診断科）
Akira Uchino, Naoko Saito

Department of Diagnostic Radiology, Saitama Medical University International Medical Center

【要旨】内頸動脈―前大脳動脈吻合は眼動脈分岐レベルの内頸動脈から内側へ分岐後、両側視神経の間を上行して、前大脳動脈A1-A2移行部と吻合する。我々はMRAで12例を診断した。右側7例、左側2例、両側3例であった。右側4例では同側のA1が、両側例はすべて両側のA1が欠損していた。同側の眼動脈破格の頻度も高かった。

Purpose: Carotid-anterior cerebral artery (ACA) anastomosis is rare, with reported prevalence of about 0.1%. In this variation, the ACA arises from the ophthalmic segment of the internal carotid artery, courses cranially through the space between the optic nerves, and anastomoses with the A1-A2 junction of the ACA. We evaluated its features on MR angiography.Methods: From our university hospital records, we identified 12 patients with this cerebral arterial variation that was diagnosed by MR angiography at 1.5 or 3.0 tesla machine using the standard 3D-TOF technique. We checked source images of MR angiography to confirm the variation and created partial MIP images of the carotid system to demonstrate the variations clearly.Results: Seven of the 12 cases were right-sided, two were left-sided, and three were bilateral. In the 7 right-sided cases, the A1 segment of the ipsilateral ACA was absent in four, normal in two, and tiny in one case. In all 3 bilateral cases, the bilateral A1 segments were absent. Of 14 ipsilateral ophthalmic arteries (OAs), three arose from the middle meningeal artery and two from the anastomotic artery.Conclusion: We reaffirmed the right-side predominance of this variation. There is wide spectrum in this variation. Bilateral type is considered most severe, but it may easily be overlooked because of its symmetry. Associated OA variations are frequently observed.

P-1-002　全脳撮像を対象とした3D ASLのリードアウトシーケンスの検討
Study of readout sequence for 3D whole brain ASL

吉澤　延之（株式会社 日立製作所 ヘルスケアビジネスユニット）
Nobuyuki Yoshizawa, Hiroyuki Itagaki

Healthcare Business Unit, Hitachi, Ltd.

【要旨】全脳撮像を目的とした3D ASLのリードアウトシーケンスとしてGRASEとFSEを適用した。撮像時間と画像歪みを比較し、撮像時間の点でGRASEが優位であり、画像歪みの点ではFSEが優位であった。用途に応じてリードアウトシーケンスを使い分けることが推奨される。

<Background and Purpose>
Arterial spin labeling (ASL) perfusion imaging has been widely applied to clinical for brain region. 3D Spiral FSE and 3D GRASE are well-known sequence for 3D whole brain imaging. Those sequences can achieve short scan time but have demerit like blurring (slice direction), distortion, and limitation of scan parameter. In this study, we apply GRASE and FSE as readout sequence and compare scan time and distortion.
<Method>
Experiments were conducted using 3T whole body MRI system with 4-channel RF transmit and 15-channel head coil (Hitachi Ltd. Japan). Healthy volunteers were evaluated after informed written consent was obtained in accordance with our institutional review board guidelines. PCASL labeling method was applied. For the evaluation of distortion, we used 6 slices around the frontal lobe (±24mm). Scan parameters of readout sequence are as follows.
1) 3D GRASE;AX, FOV = 250 mm, TR = 4260 ms, TE = 22 ms, Slice# = 48, E.Factor = 12, RFA = 140, Matrix = 64 × 64, Scan Time = 1:51
2) 3D FSE;AX, FOV = 250 mm, TR = 4500 ms, TE = 9.3 ms, Slice# = 48, E.Factor = 100, Variable RFA = ON, Matrix = 64 × 50, Scan Time = 4:49
<Results and Discussion>
The result of 3D GRASE ASL image had the distortion of approximately 8mm to the Anterior side, and approximately 3mm to the Posterior side. But a clinical applicable image quality was acquired in short scan time (less than two minutes). The result of 3D FSE ASL image was acquired about five minutes without distortion. 3D GRASE has an advantage in scan time. So, we consider 3D GRASE is useful for Multi PLD imaging though it has the distortion. If longer scan time is acceptable, we recommend using 3D FSE to acquire the image without distortion.

P-1-003　multiphase ASLと4DMRA の救急頭部領域における有用性
Utility of multiphase ASL and 4DMRA for evaluating patients with acute neurological disorder

田中　茂子（若草第一病院 放射線科）
Shigeko Tanaka[1], Shiromaru Ishida[2], Masayuki Fujioka[3]
[1]Department of Radiology, Wakakusa Daiichi Hospital, [2]Department of Neurosurgery, Wakakusa Daiichi Hospital, [3]Department of Neurosurgery, Senri Saiseikai Hospital

【要旨】Multiphase ASLと4DMRAの適応を探るためにtry itの40日間全ての頭部のMRIで両者を追加試用した。Single phase ASLで問題となる片側内頸動脈閉塞でのdelay効果を判別できた。DWI高信号域の血流増加を痙攣後脳症3例中3例で確認できた。特に痙攣を伴う救急頭部疾患において痙攣後脳症と梗塞巣との鑑別に本法は有用と考える。

Objective) To investigate the utility of multiphase ASL and 4DMRA in the neuroemergency setting.Material and method) We added multiphase ASL (arterial spin labeled) and 4DMRA for 193 cases with neurological deficits from 2015/10/31 to 2015/12/9 with MRI (1.5T Achieva Nova Dual R 3.2). 59 patients (30 males 40-90yo. 29 females 42-98yo.) of 193 underwent " brain emergency plan sequences " (smart brain, b0, b1000, ADC, MRA, b2000, FLAIR, BPAS, T2*), and the remaining 134 (65 males 27-90yo, 69 females 14-94yo.) underwent " brain routine plan sequences " Result) In this study, we had three patients with epileptic encephalopathies revealed an increase in cerebral blood flow. In two of the three underwent " brain emergency plan sequence " . There were 16 patients with cerebral infarction in this study. 13 of them developed BAD (branch atheromatous disease) and lacunar infarction. Multiphase ASL showed no particular findings in these 13 patients. The remaining three patients had cortical infarction in the MCA (middle cerebral artery) territory. These patients showed decreased cerebral blood flow on multiphase ASL. Unilateral internal cerebral artery was obstructive in 3 cases, and had so-called " tracer delay phenomenon " in MCA territory. In one patient with meningioma, the local cerebral blood flow was increased on multiphase ASL. The large aneurysm in one patient showed signal loss of 3DTOF-MRA, but could be detected by 4D MRA.Conclusion) Although both epileptic encephalopathy and cortical infarction showed hyper-intensity on DWI, multiphase ASL and 4DMRA without delay phenomenon were useful for the differential diagnosis between epileptic encephalopathy and cortical infarction. Multiphase ASL and 4D MRA were especially valuable for neuroemergencies with convulsion.

P-1-004　虚血性脳卒中に対する血管内治療術前検査として適応可能な基底核レベルの高速pCASL
Rapid-Basal ganglia pCASL which can be applied pre endovascular therapy protocol for acute ischemic stroke

大浦　大輔（小樽市立病院 放射線室）
Daisuke Oura, Kyohei Abe, Tomoka Kadoya, Takumi Yokohama
Otaru general hospital Department of Radiology

【要旨】基底核レベルの短時間pCASLを検討した。全脳撮像と比較してラベル距離およびpost label delyaの短縮により、T2減衰の少ない信号が取得可能であり、少ない加算回数でSNRは担保され撮像時間は短縮された。本法は2分以内で撮像可能で、虚血性脳卒中に対する血管内治療術前検査として適応可能と考えられた。

BackgroundOn acute ischemic stroke patient, penumbra is identified as perfusion-diffusion mismatch. pCASL is one of perfusion techniques without contrast medicine. However, whole brain pCASL scan time needs 4-5min. So, this technique is not suitable for pre endovascular therapy examination, because Door-to-puncture time is crucial to obtain good outcomes. Therefore, short time pCASL is required.PurposeThe aim of this study is to construct Rapid-ASL which is able to be applied for pre endvascular therapy protocol for acute Ischemic stroke.Method5 healthy volunteers were underwent 2D-EPI read out pCASL with different imaging range: Whole brain and Basal-ganglia. MRI was used Ingenia 3Tesla (PHILIPS, Netherlands). Whole brain pCASL was Scan time: 4 min 55 sec, slice thickness: 5 mm, label distance: 94.86 mm, post label delay (PLD): 1800 ms. Number of Signal average (NSA): 30. Basal-ganglia pCASL was imaged changing slice thickness: 5, 7, 10mm and NSA: 2-14. Other setting was the following: Label distance: 65 mm; PLD: 1232 ms. SNR of brain tissue was compered between two settings. On Basal ganglia pCASL, we investigated the shorter scan time setting which become an equivalent SNR with whole brain pCASL.ResultOn every slice thichness, SNR of Basal-ganglia pCASL which is spent more than 1min was equivalent to whole brain pCASL.ConsiderationOn Basal-ganglia pCASL, scan time was reduced by the shorter label distance and PLD. The shortening of label distance and PLD decrease an T2-attenuation of labeled blood signal. Therefore, NSA can be reduced, scan time is shortened while retaining SNR. ConclusionBasal-ganglia pCASL can be perform within 2 min. Therefore, it can be applied for pre endovascular therapy protocol for acute Ischemic stroke.

P-1-005　DW-ASLを用いた脳虚血領域におけるwater permeabilityの評価
Evaluation of water permeability for ischemic lesion in the brain using DW-ASL

藤間　憲幸（北海道大学病院放射線診断科）
Noriyuki Fujima[1], Tomoyuki Okuaki[2], Takuya Aoike[3], Suzuko Aoike[3], Hiroyuki Sugimori[4], Kohsuke Kudo[1]

[1]Department of diagnostic and interventional radiology, Hokkaido University Hospital, [2]Philips Electronics Japan, [3]Department of Radiological Technology, Hokkaido University Hospital, [4]Faculty of Health Sciences, Hokkaido University

【要旨】ASLに拡散傾斜磁場を併用させた技術であるDW-ASLを用いて、脳実質における虚血性病変のWater permeabilityを評価することが可能であった。この手法は大脳の虚血性病変における新たな機能的評価の指標として今後、有効に活用されうると考えられた。

Purpose; To evaluate the water permeability in ischemic lesion of the brain using diffusion weighted arterial spin labeling (DW-ASL) method.Methods; Total 65 regional water permeability was assessed from five patients who have single of multiple chronic ischemic lesions in their brain. ASL images were acquired by using pseudo-continuous labeling technique with the labeling duration of 1800 ms and post labeling delay of 1500 ms. Readout of 2D-EPI was used after the bipolar diffusion gradient in multiple b-values; total 5 scanning were performed using b-value of 0, 25, 38, 102 and 225 respectively. Water permeability was calculated from the signal intensity of ASL image in each b-value, using previously reported calculation method. In each segmented ROI in the brain, ischemic severity was divided into 3 groups (non-ischemic, moderate ischemic and severe ischemic lesion) based on the T2WI and FLAIR imaging findings. Calculated water permeability was compared between 3 groups based on the ischemic severity.Results; Water permeability in severe ischemic lesion was significantly higher than other 2 groups. In addition, increased permeability area tended to be visually larger than the ischemic lesion observed by T2WI and FLAIR. In contrast, non-significant difference was observed between non- and moderate-ischemic lesion.Conclusion; Water permeability information obtained by DW-ASL can be one of useful tool for the assessment of ischemic lesion more in detail.

P-1-006　パイプラインステントによる治療後のフォローアップに対するSilent MRAの有用性
Usefulness of silent MRA for follow-up of intracranial aneurysms treated with pipeline embolization device

高野　　直（順天堂大学大学院 医学研究科 放射線医学）
Nao Takano[1,2], Michimasa Suzuki[1,2], Ryusuke Irie[2], Munetaka Yamamoto[3], Shuji Sato[2], Nozomi Hamasaki[2], Tomoya Muroi[2], Shiori Hamagawa[2], Haruyoshi Hoshito[2], Masaaki Hori[1,2], Hidenori Oishi[3], Shigeki Aoki[1,2]

[1]Department of Radiology, Graduate School of Medicine, Juntendo University, [2]Department of Radiology, Juntendo University Hospital, [3]Department of Neurosurgery, Graduate School of Medicine, Juntendo University

【要旨】フローダイバーターステント治療後のフォローアップに対するSilent MRAの有用性を3D TOF-MRAとの比較から検討した。放射線科医師2名による血管描出のスコアはSilent MRA (3.50 ± 0.68) のほうが3D TOF-MRA (1.87 ± 0.66) よりも有意に高く ($p<0.05$、$\kappa=0.71$)、その有用性が示唆された。

PurposeThe aim of this study was to assess usefulness of silent MRA (non-contrast enhanced MRA using ultrashort echo time with arterial spin labeling) by a comparison between silent MRA and three-dimensional time-of-flight MRA (3D TOF-MRA) with treated by pipeline embolization device.Materials and MethodsBetween August 2015 and March 2016, 19 patients (1 men, 18 women; age 58.8 ± 15.5 years) treated with pipeline embolization device underwent silent MRA, 3D TOF-MRA and digital subtraction angiography (DSA). Duration between aneurysm treatment and MRA scanning were 0 day (1case), 1 day (14cases), and 2 days (4cases). The average of the interval between the latest DSA and both MRAs was 1.2 ± 0.5 days. Two types of MRA were obtained on a 3Tesla MRI unit (Discovery MR750w; GE Healthcare, Milwaukee, WI). All images were independently evaluated in random order by two neuroradiologists. Visualization of the reconstructed artery by MRA was graded by using a 4-point scale from 1 (not visible) to 4 (excellent) by referring to the DSA image as a gold standard. The scores of the two observers were averaged and a Wilcoxon signed-rank test was performed in the statistical analysis of the subjective scores for flow in stent. The level of interobserver agreement was analyzed by weighted kappa statistics. ResultsThe average scores ± SD for silent MRA was 3.50 ± 0.68, and for 3D TOF-MRA was 1.87 ± 0.66 ($p<0.05$). Interobserver agreement was substantial agreement ($\kappa=0.71$). In 17 cases (89%), both observers gave silent MRA higher scores than 3D TOF-MRA. In 2 cases (11%), both observers gave equal scores.ConclusionSilent MRA is useful follow-up method for treated with pipeline embolization device.

P-1-007　脳神経外科領域におけるMR-angiographyによる体内金属アーチファクト低減の検討
a evaluation of the metal artifact reduction by MR-angiography in neurosurgery

木村　紀行（札幌白石記念病院 放射線部）
Noriyuki Kimura, Hideyuki Osanai, Hideki Hirata, Kenta Yamanaka, Shouta Fukushima
Sapporo Shiroishi Memorial Hospital Department of Radiology

【要旨】近年、脳血管内治療において様々なコイルやステントなどの金属デバイスが使用される。患者においても体内金属を装着しているケースが増えている。これらはMRAで磁化率アーチファクトの原因となる。これらのうちstent assisted coil embolization後の血流の描出改善及び磁化率アーチファクト低減を検討した。

[Purpose]Recently, some metal devices are used in endovascular treatment of cerebral aneurysms and intracranial stenosis, also a few new metal devices has been obtainmant of pharmaceutical approval.And patients wearing body implants such as dental implant are increasing.These metal device causes the magnetic susceptibility artifact. And this artifact was defect of blood flow.With the 3D MR-angiography(MRA), we investigated the availability to diminish the susceptibility effects by the metal device and implants. [Method] (Investigation 1) We performed 3D time of flight(TOF) MRA, flowing 20% glycerine water-solution in the simulated blood vessel that the close cell type stent was detained with the injector. We changed flip angle and TE of the scan parameters then, to search the useful scan parameters. (Investigation 2) We compared 3D TOF MRA and 3D Phase Contrast(PC) MRA against the magnetic susceptibility artifact.We performed 3D TOF MRA and 3D PC MRA, flowing 20% glycerine water-solution in the simulated blood vessel with the injector in the phantom filled with the gelatin and leads was put beside this tube. [Results] (Investigation 1) The scan parameters of good flow visualization was the shortest TE and 30 degrees Flip Angle. (Investigation 2) 3D PC MRA decreased the influence of the magnetic susceptibility effect than 3D TOF MRA. [Conclusion] 3D MRA is much useful in the case of susceptibility effect by the metal devices and metal implants.

P-1-008　小児疾患におけるSynthetic MRIの臨床応用
The Advantages of Synthetic MRI in pediatric patients

アンディカ　クリスティナ（順天堂大学医学部放射線科）
Christina Andica[1], Akifumi Hagiwara[1,2], Misaki Nakazawa[1,3], Aki Hattori[1], Sho Murata[1], Nao Takano[1], Masaaki Hori[1], Shigeki Aoki[1]
[1]Department of Radiology, Juntendo University School of Medicine, [2]Department of Radiology, Graduate School of Medicine, The University of Tokyo, [3]Department of Radiological Sciences, Graduate School of Human Health Sciences, Tokyo Metropolitan University

【要旨】Synthetic MRIはT1、T2値、プロトン密度の定量により、任意のコントラスト画像を作成できる。本研究ではSynthetic MRIの基本原理とその特徴、当施設における撮像パラメータおよび小児疾患における臨床応用を示す。

Diagnostic imaging of pediatric patients sometime can be challenging. Optimal parameter settings for the developing brain and shorter examination time are needed to give the most accurate diagnosis and a better experience to children. Synthetic MRI is a method based on quantification of the longitudinal T1 and transverse T2 relaxation times, the proton density (PD), and the amplitude of the local radio frequency B1 field by a single scan. From this quantitative data, any contrast-weighted image with combination of echo time (TE), repetition time (TR), and inversion time (TI) can be created and freely adjusted retrospectively. Tailored contrast-weighted image can be applied to each patient in order to evaluate brain diseases with a significant reduction in examination time. Volumetric measurement obtained by automatic segmentation and myelin map for evaluating the presence of myelin are also features of synthetic MRI. In our institute, we applied synthetic MRI to pediatric patients and found a few interesting cases that shows the advantage of synthetic MRI in the evaluation of brain diseases.
This exhibit consists of three sections:
1. The basic principles and features of synthetic MRI.
2. The clinical settings in our institute.
3. The clinical application:
- Meningeal enhancement in Sturge-Weber syndrome and meningitis were more prominent on double inversion recovery (DIR) images for suppressing the signals of brain parenchyma and fat in the bone marrow than on T1-weighted images.
- "Accelerated myelination" in Sturge-Weber syndrome was clearly seen by using appropriate parameters setting, quantitative maps and myelin map.
- Imaging of myelination of the developing brain can be tailored by adjusting parameters after quantification.

P-1-009　自律神経訓練後のresting state functional connectivityの諸変化
Altered resting state functional connectivity after autogenic training

雫石　崇（日本大学 医学部 放射線医学系 画像診断学分野）
Takashi Shizukuishi[1], Osamu Abe[1], Takahiro Shinozaki[2], Akihiko Wada[1], Haruyasu Yamada[1], Ryutaro Kohashi[2], Yoshiki Imamura[2]
[1]Nihon University School of Medicine, Department of Radiology, [2]Nihon University School of Dentistry

【要旨】目的：自律神経訓練（AT）施行前後の安静時fMRIの諸変化について検討した。方法：7人のAT指導者において、AT前後で安静時fMRIを施行し、Conn toolboxを用いてROI解析を施行た（p<0.05 with FWE)。結果：右尾状核-扁桃体、楔前部-左淡蒼球、右上側頭回-左淡蒼球においてAT後に有意なfuntional connectivityの増加を認めた。

Background: Autogenic training (AT) is a common clinically used relaxation method. However, the evaluation of AT is almost subjective. The purpose of this study was to investigate the alterations of resting state functional connectivity after AT. Methods: Seven volunteers familiar with AT were studied with resting state functional MRI (rs-fMRI) pre and after AT. The CONN toolbox was used to conduct several ROI-to-ROI analyses. We searched for functional connectivity increases between pre and after AT.Results: FMRI revealed the significantly increase activations between right caudate and amygdala, precuneus and left pallidum, right superior temporal gyrus and left pallidum, those include a part of commonly detected resting state networks (p<0.05 with FWE).Conclusion: Resting state functional connectivity alters by performing AT, and rs-fMRI could be useful in the quantitative evaluation of AT.

P-1-010　TOF-PET/MR臨床機で用いられているsingle atlas-based methodによる頭部吸収補正
Evaluation of clincal single atlas-based attenuation correction for integrated PET/MR

関根　鉄朗（日本医科大学 放射線科）
Tetsuro Sekine[1,2], Buck Alfred[2], Delso Gaspar[2], Ter Voert Edwin[2], Huellner Martin[2], Veit-Haibach Patrick[2], Warnock Geoffrey[2]
[1]Department of Radiology, Nippon Medical School, [2]Department of nuclear medicine, University Hospital Zurich

【要旨】GE-PET/MR臨床機は頭部PET撮像の際、T1WIから、atlas-based法を用いて頭部CTを推定し吸収補正を行っている。8名の対象の脳PET画像に、それぞれ67箇所のVOIを設定し、同手法の精度検証を行った。結果、いずれのVOIにおいても、8%を超える誤差は無かったが、頭蓋底近くでは比較的誤差が大きい(3%強)事が示された。

Purpose: To evaluate clinical atlas-based attenuation correction (Atlas-AC) by comparing it with CT-AC. Methods: We enrolled 8 patients. All patients underwent both PET/CT and PET/MR (GE SIGNA PET/MR) of the head. For each patient, based on each Atlas-AC and CT-AC, PET images were reconstructed using the raw data from the PET/MRI scanner. All PET images were normalized and FDG accumulation was quantified in 67 volumes-of-interest. Relative difference (%diff) between images was calculated.Results: The range of error in all 536VOIs was -3.0% ~ 7.3%. The underestimation was most pronounced in the regions near base skull (%diff = 3.05%~3.69%).Conclusion: When compared to the gold-standard CT-AC, errors introduced using Atlas-AC did not exceed 8 % in any brain region investigated. Underestimation of FDG uptake was minor (<4 %) but significant in regions near the skull base.

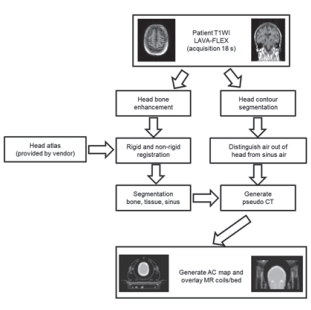

Overview of atlas-based pseudo CT and AC map processing. All computational time < 30 sec.

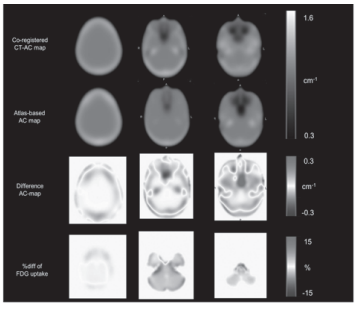

All images were averaged from 8 normalized images.
Atlas-based AC map slightly overestimated skull in superior cranium. However, the impact of this error on the PET image is small. The mixed under- and over-estimation of Atlas-based AC map on Maxillary sinus and adjacent bone was observed. The overall result is the underestimation of base of temporal lobe and cerebellum.

P-1-011　3D-FIESTAを用いた小脳橋角部近傍のVR表示：3D-SPGRとの比較も含め
VR images of the cerebellopontine angle using 3D-FIESTA: comparison with 3D-SPGR

四家　洋介（総合南東北病院 診療放射線科）
Yosuke Shike[1], Mika Kokubun[1], Takashi Konno[1], Hidekazu Yamazaki[1], Natsuru Kobiyama[1], Noriaki Tomura[2], Syunsuke Sato[3]

[1]Department of Radiology, Sothern Tohoku General Hospital, [2]Department of Neuroadiology, Sothern Tohoku General Hospital, [3]Department of Neurosurgery, Sothern Tohoku General Hospital

【要旨】小脳橋角部近傍のMRIによるVR表示は、臨床例においても、脳神経と血管の解剖学的関係の把握に有用と思われ、3D-FIESTAの方が3D-SPGRより有用と思われた。ただ、腫瘍の症例では、腫瘍近傍の脳神経の描出が不十分で、次回の研究内容として考えた。

[Purpose]For clinical feasibility of VR images in the cerebellopontine (CP) angle,3D-FIESTA was cpmpared with 3D-SPGR.
[Materials and method]In 3 patients with CP angle tumors and 3 patients with facial spasm,both 3D-FIESTA and SPGR were aquired using 3T MRI. Imaging parameters are as follows; 3D FIESTA,TR5.6/eTE2.7-12; FA37; BW62.5; NEX2; scan time3:02 min.,3D SPGR,TR35/eTE2.5; FA30; BW15.63;NEX1; scan time3:59 min.VR images fused with TOF were aquired using in Advantage Workstation ver.4.6P. A neuroradiologist and a neurosurgeon independently reviewed both images.Visibility of the cranial nerves and arteries in the CP angle was visually scored (1-5).
[Result]In visibility of the cranial nerves and arteries, 3D-FIESTA was significantly ($p<0.05$) superior to 3D-SPGR in both reviewers.However, imaging of the cranial nerves adjacent to the tumors were insufficient.
[Conclusion]VR using 3D-FIESTA is superior to VR using 3D-SPGR to image the cranial nerves and arteries in the CP-angle.Further investigation is required for clinical use.

P-1-012　Ultra-short TEシーケンス（PETRA法）におけるTI値の違いによる脳白質・灰白質コントラストの検討
Relationship of cerebral gray and white matter contrast in different inversion time using ultra-short echo time sequence (PETRA)

塩田　正和（手稲渓仁会病院）
Masakazu Shioda, Ken Masuyama, Syun Akimoto, Kazuya Akiyoshi

Teine Keijinkai Hospital

【要旨】Ultra-short TEシーケンスのPETRA法は2つTI値が設定可能だが、それらを変えることによる組織間コントラストの検討報告はまだ少ない。そこで、脳の白質と灰白質のGd造影剤希釈ファントムを作成しPETRA法を用いたT1強調画像におけるコントラスが、2つのTI値によりどのように変化するかを実験し最適なTI値を決定した。

Purpose: Pointwise-Encoding Time reduction with Radial Acquisition (PETRA) is an ultra-short echo time sequence and configurable two inversion times. It can be obtained T1-weighted imaging by varying the inversion time (TI). Few studies have reported on the relationship of cerebral gray and white matter contrast and water signal intensity by varying TI. The purpose of this study is to determine appropriate TI in T1-weighted imaging using PETRA.Materials: 1.5-T MR system (Siemens Magnetom Aera). Cerebral white matter phantom (water-gadolinium solution of 0.5mmol/l, T1=374msec). Cerebral gray matter phantom (water-gadolinium solution of 0.25mmol/l, T1=631msec). Water phantom (physiological salt water, T1=2613msec).Methods: In T1-weighted imaging with PETRA, a phantom similar to T1 value of cerebral gray and white matter, and a water phantom were imaged on different TI. Inversion time1 (TI1) = 100, 400, 800, 1200, 1600, 2000 (msec). Inversion time2 (TI2) =100, 300, 600, 900 (msec). For comparison, magnetization prepared rapid gradient echo (MPRAGE) were imaged under condition in our hospital (TI=800msec, TR/TE=2200/3.02msec). From the imaged data, each signal-to-noise ratio (SNR) was measured by difference method, and the contrast of cerebral gray matter and cerebral white matter was evaluated. We have defined as the appropriate TI to obtain good contrast; water signal intensity is lower set, compared to MPRAGE.Conclusion: The lower the TI1 and TI2, the higher contrast of cerebral gray and white matter. Water signal intensity was reduced when the TI2 was low except when TI1=100msec, and was less changed by the difference in TI1. Compared to MPRAGE, good contrast is obtained, and water signal intensity is lowered TI was TI1=800msec and TI2=300msec.

P-1-013　3次元画像マッチング手法を用いた肝MRgHIFUのターゲット追尾
Three-dimensional target tracking method for MRgHIFU using image matching technique with liver deformation volumes

熊本　悦子（神戸大学 情報基盤センター）
Etsuko Kumamoto[1,2], Daisuke Kokuryo[2], Tatsuhiko Matsumoto[2], Kagayaki Kuroda[3,4]
[1]Information Science and Technology Center, Kobe University, [2]Graduate School of System Informatics, Kobe University, [3]Graduate School of Engineering, Tokai University, [4]Center for Frontier Medical Engeeromg, Chiba University

【要旨】本研究では，呼吸性移動・変形を有する肝臓に対するMRガイド下集束超音波治療において，術前に連続撮像したマルチスライスボリューム像から，3次元画像処理手法を用いて推定した横隔膜位置および血管分岐点の推移から刊組織の移動・変形の情報を取得，これに基づいた3次元焦点追尾手法を提案し，有効性を検証した．

Purpose: MR guided High intensity focused ultrasound (HIFU) treatment of a liver requires a tracking technique to 'lock on' to the focal spot at the target tissue region during respiratory induced motion. To maintain sufficient tracking accuracy, both translation and deformation of the tissue need to be considered. In this study, we proposed target tracking method using image matching technique with liver deformation volumes obtained with time-resolved volume acquisitions.
Methods: Forty-two image sets of six interleaved sagittal images from a healthy volunteer's liver were acquired by 3.0T MRI with SSFP under natural slow breathing and a single coronal slice with breath holding. TR/TE, 4.85ms/1.98ms; FA, 90 degrees; Slice thickness, 5mm; FOV, 350x350 mm^2; Acquisition matrix, 256x256; Parallel factor, 2.0. Three dimensional image sets were re-ordered according the diaphragm profile in the coronal image. ROI's including vessel branching points and target point were set in the isotropic voxel space. Vessel branching points in each frame were estimated with 3D pattern matching method. 3D target tracing was performed using 2D projections of 3D branching position based on three branch points and maintaining relative angles and distance among the vessels.
Results: Estimation of branching vessel positions in each frame were performed quasi-real time under 600ms. Average value of gaps between target position and estimated position of AP, SI and LR directions were 0.4mm, 4.0mm and 1.4mm.
Conclusion: The feasibility of the proposed method to track target position with reconstructed 3D MR volumes was demonstrated.
References: (1) Kumamoto E, et al, Trans. Japanese Soc. Med. Bio. Eng., 53(3), 168-178, 2015. (2) Kumamoto E, et al, Proc. of 23rd ISMRM, 1647, 2015.

P-1-014　ノイズの多い環境中における遅い流れのQSI解析に対する誤差評価
Error in QSI analysis for slow flow in a noisy environment

長田　晃佳（筑波大学大学院 数理物質科学研究科 電子・物理工学専攻）
Akiyoshi Nagata, Yasuhiko Terada, Katsumi Kose
Institute of Applied Physics, University of Tsukuba

【要旨】我々は、屋外樹木用MRIシステムを開発し、樹液流のq-space imaging (QSI)を行っている。しかし屋外計測においては電磁的な外来ノイズが多いため、特に屋外樹木内のように遅い流速に対しては計算誤差が大きくなってしまう可能性がある。本研究では、体積流に対するノイズの影響をシミュレーションし、誤差率の検証を行った。

We have developed an outdoor MRI system and measured flow in a tree by q-space imaging (QSI). Large external noise coming from the outdoor environment may degrade QSI data and lead to false estimation in flow volume, especially for slow flow as in trees. Here we simulated QSI data at given noise levels, and estimated errors in the volume flow.
The QSI flow was simulated using the propagator approach. The volume flows were calculated from hypothetical propagators (80% stationary and 20% flowing water) with and without random noises (Fig.1(a); max q=14.4mm^{-1}, Δq=1.8mm^{-1}, interval between MPG pulses Δ=100 ms, 16 sampling points). This was repeated for 1000 times, and the SD of the difference between the hypothetical and calculated volume flows was estimated as an error.
Fig.1(b) shows the estimated errors in the volume flow, which increase as the volume flow decreases. The error in the volume flow per pixel (circles curve) ranges from 26 to 81 % within the typical flow range for the tree (Figs.1(c) and (d)). The error becomes smaller when the volume flow is averaged for multiple pixels (squares and triangles curves). In short, the averaging is necessary for evaluation of volume flow.

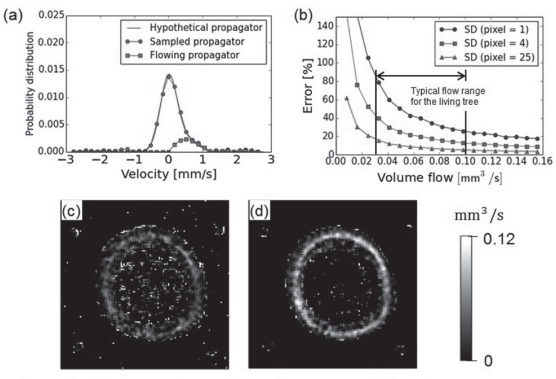

Fig. 1:(a) Probability distribution of flow velocity calculated from different propagators. (b) Estimated error in volume flow. (c), (d) Volume flow maps obtained by QSI (c) at night and (d) at midday (11/28/2015).

P-1-015　高速撮像法によるT1計測の撮像時間短縮化
Rapid T_1 Measurement using Fast imaging

俵　　紀行（日本医療大学 保健医療学部 診療放射線学科）
Noriyuki Tawara, Atsushi Nishiyama

Department of Radiological Sciences, Faculty of Health Sciences, Japan Health Care College

【要旨】 縦緩和時間(T1)は、筋線維の非侵襲的同定法として期待されるが、反転回復法を用いたスピンエコー法では撮像時間が長くなる。本研究では、TurboFLASHを用いてT1計測の撮像時間短縮に関する検討を筋のT1に近いPVAゲルファントムにより検証を行った。その結果、十分活用できることが示唆された。

It has been reported that T_1 in skeletal muscles is proportional to the percentage of type I fibers which would be a determinant for athletic performance. However, the precision of the measured T_1 values is unclear due to various pulse sequences used for the measurement. In this study, we evaluated the reliability of T_1 measured by pulse sequences with inversion recovery (IR) technique that is believed to be most accurate in T_1 measurement. Polyvinyl alcohol (PVA) gel was examined on 1.5T MR-units using an extremity coil (Ex) or a built-in body coil (Bo). Temperature was 27℃ . The protocol used an IR pulse sequence used spin echo (IR-SE), a saturation recovery used spin echo (SR-SE), and an IR technique used TurboFLASH (IR-TF). T_1 was calculated by non-linear regression. The estimation of fitting the calculating results used the parameter Q that is one of the goodness of fit. Evaluation of significant difference was used by T_1 and the parameter Q. T_1 values measured using Ex from IR-SE, SR-SE, and IR-TR was 835.0 ± 2.0 ms, 948.7 ± 23.8 ms, 879.1 ± 5.3 ms, respectively. In T_1 calculated by SR-SE, the variance of T_1 was large as compared with the other images. A T_1 comparison between IR-SE to IR-TF showed no significant differences in T_1. In regard to the parameter Q, The parameter Q of all protocols using Ex was higher than the value using Bo. In IR-SE and IR-TF, 180 degree's reverse pulse irradiates before the rf pulse, it that the effect of imperfect 180 degree's pulse is suggested less. In addition, TI of IR-SE and IR-TF are independent of the acquisition time in each measurement points. Therefore, T_1 between IR-SE and IR-TF was no significant difference. In conclusion, IR-TF can be applied for rapid T_1 measurement.

P-1-016　GPGPUを利用したMR位相画像の圧縮センシング再構成の高速化
Accelerating Imaging Reconstruction by GPGPU Computing in Magnetic Resonance Compressed Sensing for Phase-varied Images

市村　亮祐（宇都宮大学 大学院工学研究科 情報システム科学専攻）
Ryosuke Ichimura, Satoshi Ito

Information Systems Sciences, Utsunomiya University

【要旨】位相を持つMR画像の再構成に対し，圧縮センシングを適用すると画像再構成に時間がかかるという問題がある．GPUを利用し画像再構成を並列的に行うことで再構成時間を短縮することができる．圧縮センシングに関わる処理全体をGPU内で連続的に計算させることで再構成時間の大幅な短縮を達成することができた．

Introduction
We have proposed a new CS reconstruction method which is robust to spatial phase variation on the images. In that method, complex-value image transform (eFREBAS transform) is used as sparsifying transform function in which scaling parameters are varied in each iteration step. In this study, we examine to accelerate the CS reconstruction of phase-varied images using a massively parallel numerical computing of the Graphics Processing Units (GPU).
Methods
We used NVIDIA's software platform for GPUs (CUDA). CUDA uses a single-instruction multiple-thread (SIMT) model, which means that the threads running in a multiprocessor share the same code but run at possibly different states with different streams of data. CUFFT contained in CUDA library, which is optimized for GPU, is used for several time Fourier transform operations required for eFREBAS transform. In our GPU implementation, significant data transfer between the host machine and GPUs occurs only at the beginning and the end of the algorithm. Computation of threshold and total variation are carried out in GPU computation.
Results
We used voluntary images(256x256) obtained with 1.5 T MRI. GPU used in the experiment is a NVIDIA Tesla C2075. Main specifications of the Tesla C2075 is, CUDA core number 448, memory bandwidth 144GB /s, core clock frequency 1.15GHz. Reconstruction time with GPU based implementation was 1.1 seconds, while single thread CPU-based implementation took 19.7 seconds.
Conclusions
GPU implementation significantly reduces the reconstruction time in multi-scale eFREBAS based CS. Reconstruction speed will be improved using a higher performance GPUs, such as K20 or K40.
[1] Ito S, Yamada Y, IEICE Transactions, J93-D: 999-1008, 2010

P-1-017　FCSAを用いたMR画像の雑音除去法
Denoising of MR images using Fast Composite Splitting Algorithm

奥木　稜平（宇都宮大学 大学院工学研究科 情報システム科学専攻）
Ryohei Okugi, Satoshi Ito

Information System Sciences, Utsunomiya University

【要旨】画像に対してFREBAS変換を適用すると，FREBAS変換空間において，画像情報を含む信号は比較的高い振幅値をとるスパース性を呈する．この特徴を利用し，L1ノルム最小化を用いた雑音除去法を提案する．本雑音除去法により，画像の詳細構造を保存しながら雑音除去が可能となった．

Introduction
In general, images can be represented in a highly sparse manner by an adequate transform. The eFREBAS (enhanced Fresnel band split) transform has many directional feature-tracking functions, which allow higher degree of directional representation than that obtained in wavelet transform. We propose a multi-frame eFREBAS transform regularized image denoising algorithm.
Methods
We use composite splitting techniques to solve the TV, L1- and L2-norm regularization problem. Original problem was decomposed into L1- and TV norm regularization problems respectively. Then, those problems are separately solved. Finally, the denoised image is obtained from the weighted average of solutions from two problems in an iterative framework.
Results
Comparison of denoising performances were executed with anisotropic diffusion filter [1], wavelet L1-norm filter, BM3D [2] and DDID [3] filters. Evaluation of denoised images were carried out using SNR improvement ratio and SSIM. SNR improvement of proposed method is higher than anisotropic diffusion filter or wavelet filter, and lower than BM3D and DDID filter, however structures of images were much more remained in proposed method than those of BM3D and DDID filters.
Conclusion
Noises on the images were removed with remaining small structure of images by proposed method. Future study is improvement of proposed method.
References
[1] P. Perona et al, IEEE Tran on PAMI, Vol.12, No7:629-639, 1990
[2] K. Dabov et al, IEEE Tran on Image Proc, Vol.16:2080-2095, 2007
[3] C. Knaus et al., IEEE ICIP, Australia, 2013

P-1-018　Fallot四徴症術後患者における phase contrast MRI による肺血流評価
Asymmetry of pulmonary perfusion and pulmonary regurgitation in Tetralogy of Fallot after repair

小川　　遼（愛媛大学大学院 医学系研究科放射線医学）
Ryo Ogawa[1], Tomoyuki Kido[1], Masashi Nakamura[1], Teruhito Kido[1], Teruhito Mochizuki[1], Takashi Higaki[2]

[1]Ehime University Graduate School of Medicine Department of Radiology, [2]Department of Pediatrics Ehime University Graduate School of Medicine

【要旨】Phase contrast MRI を用いて14名のファロー四徴症（TOF）術後患者における肺動脈血流を評価し、右室機能との関連を検討した。肺動脈血流量には有意な左右差を認めた (p<0.05)。主肺動脈の解析では逆流や、average velocityの低下を認め、逆流率と右室駆出率には有意な相関を認めた (r= −0.67, p<0.01)。

(Introduction) Asymmetry of pulmonary perfusion and pulmonary regurgitation lead to a poor outcome in Tetralogy of Fallot (TOF) after repair. (Purpose) The purpose of this study was to examine asymmetry of pulmonary perfusion, and influence of pulmonary regurgitation on right ventricular (RV) function in TOF after repair. (Method) Fourteen patients received phase contrast MRI (PC-MRI) and RV function analysis. All cases were performed examination using a 3-Tesla MR scanner (Philips Achieva). Every patient was measured pulmonary perfusion at the main, right, and left pulmonary arteries (MPA, RPA, and LPA). (Result) PC-MRI showed that net flow (forward flow - backward flow) volume of cardiac cycle at RPA was significantly larger than that of LPA. Pulmonary regurgitation and low average velocity at MPA were observed. There was significant correlation between regurgitant fraction at MPA and RV ejection fraction (r= −0.67). (Conclusions) PC-MRI could evaluate asymmetry of pulmonary perfusion and pulmonary regurgitation in TOF after repair. This study showed the relationship between pulmonary regurgitation and RV function.

P-1-019　kat-ARC用いた4Dflow：撮像パラメータの検討
Study on scan parameters for 4Dflow using kat-ARC

藤代　力也（慶應義塾大学病院 放射線技術室）
Rikiya Fujishiro[1], Shigeo Okuda[2], Atsushi Nozaki[3], Yoshinobu Nunokawa[1], Yasutomi Shimada[1], Masahiro Jinzaki[2]

[1]Office of Radiation Technology, Keio University Hospital, [2]Department of Radiology, Keio University School of Medicine, [3]MR Applications and workflow, Asia Pacific, GE Healthcare Japan

【要旨】今回の目的は，ルーチンの心臓MRI検査時間内での遅延造影の待ち時間である５分間に撮影可能な4Dflow撮像パラメータの検討である．従来法である2DPCと相関した流速の測定結果が4DFlowでも得られ，遅延造影の待ち時間内に臨床的に有用な4Dflowイメージが得られることが確認できた．

[Purpose] To evaluate the reliability of five-minute 4D flow using kat-ARC (k-and adaptive-t auto-calibrating reconstruction for Cartesian sampling). [Methods] The subjects were five healthy volunteers. The 2D PC cine and 4D flow using kat-ARC were obtained on 1.5T and 3T scanners (Optima MR450W and Discovery MR750, GE) with 32-channel cardiac coil. The heart and aortic arch were included in a scan range. The scan parameters of 3T (*1.5T) were as follows; TR/TE=3.6/1.8msec (*5.3/2msec), FOV=380mm, Flip angle=10, matrix 180x180, slice thickness=3mm, NEX=4, RBW=125kHz, VENC=200mm/sec, Recon phases=20, Reduction Factor=katARC8x2 (7 times in speed). The maximum flow speed (Fmax) in the ascending aorta was measured using Functool (GE), and compared with Bland-Altman plot. [Results] 4D flow were successfully obtained in all subjects. The bias of Fmax were 18.4 mm/sec and -57.0 mm/sec on 1.5T and 3T, respectively. The bias in 3T (7.3%) is acceptable in the clinical setting; however, the reason should be clarified in further studies. [Conclusion] 4D flow using kat-ARC is feasible. This technique enables to perform 4D flow during waiting time for late Gd enhancement in cardiac MRI.

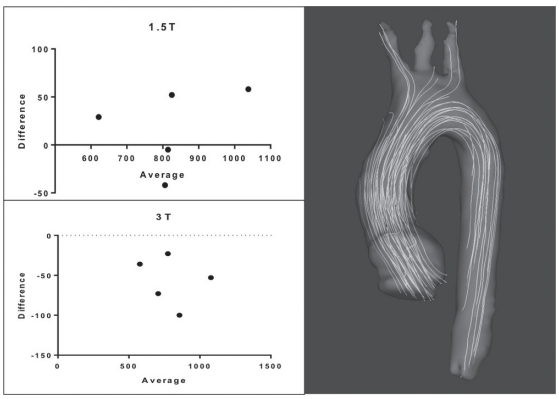

P-1-020　4D-PC MRIを用いた腸骨動脈における脂肪抑制法の比較
Four-dimensional Phase Contrast MRI Iliac Artery with Fat Suppression Techniques

福島　沙知（倉敷中央病院 放射線技術部）
Sachi Fukushima[1], Kenichi Nakagawa[1], Shohei Naruishi[1], Hiroaki Kameiyama[1], Noriyoshi Morimoto[1], Takashi Tabuchi[2]

[1]Department of Radiological Technology, Kurashiki Central Hospital, [2]Department of Medical Technology, Kurashiki Central Hospital

【要旨】近年、4D flowの有用性について多岐にわたり報告されているが、画質不良の場合、4D flowの解析が困難となってしまうケースがある。そこで骨盤領域を対象に撮像条件の検討を行った結果、脂肪抑制による有用性の知見が得られたので報告する。

Purpose:Recently, magnetic resonance fluid dynamics (MRFD) using 4D-PC MRI has been reported as a method for obtaining hemodynamic information. However, reports on 4D-PC MRI of the iliac arteries are few. The purpose of this study was to assess the usefulness of fat suppression.Methods:Five healthy volunteers participated in this study. All imaging protocols were done at 1.5T using Ingenia (Philips). Date acquisition was prospectively PPU-gated during free breathing. Imaging parameters were:reconstruction matrix,1.37*1.37*4mm; flip angle, 10, TE,2.2-4.8ms, TR,3.3-8.4ms. The study protocol compared fat suppression techniques: without fat suppression; spectral presaturation with IR (SPIR); spectral attenuated inversion recovery (SPAIR); principle of selective excitation technique (PROSET) with a binomial excitation of 1-1 (PROSET1-1), and PROSET1-2-1.We used blood flow analysis software (Gyro Tools GTFlow) for date analysis. Results:PROSET 1-2-1 provided the best definition of the iliac arteries.Conclusion:Fat suppression is useful for 4D-PC MRI and blood flow visualization of the iliac arteries. From our results, the optimal fat suppression technique was PROSET1-2-1.

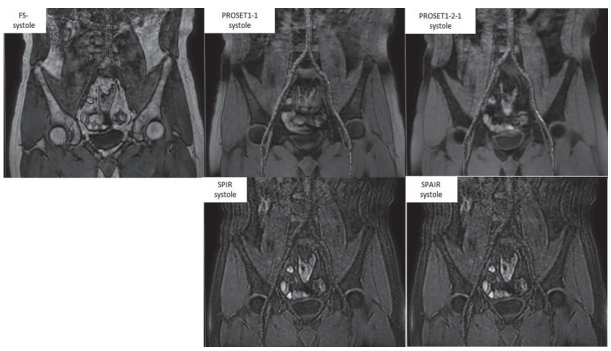

P-1-021　4D-Flow解析を用いた腎動脈血流可視化法: 脂肪抑制法のパラメータ適正化
Visualization of Blood Flow for Renal Artery using Four-dimensional Flow Analysis: Optimization of Fat Suppression Parameters

亀井山弘晃（倉敷中央病院 放射線技術部）
Hiroaki Kameiyama[1], Syohei Naruishi[1], kenichi Nakagawa[1], Sachi Fukushima[1], Noriyoshi Morimoto[1], Takashi Tabuchi[2]

[1]Department of Radiological Technology, Kurashiki Central Hospital, [2]Department of Medical Technology, Kurashiki Central Hospital

【要旨】3D Phase Contrast MRIを用いた血流可視化法（4D-flow）は、腎動脈狭窄症の診断能向上の可能性があるが、腹腔内の脂肪信号が4D-flow解析の障害となりうる。本検討では、腎動脈4D-fowにおける脂肪抑制法の有用性を視覚評価により検証したので報告する。

Purpose: Four-dimensional flow (4D-flow) Analysis using Three-dimensional phase contrast MRI has a potential to improve the diagnostic accuracy of renal artery stenosis. However, the 4D-flow sequence for renal artery (RA) are not optimized. The high signal of fat may have harmful effects for 4D-flow analysis because the RA was surrounded by intra-abdominal fat. Therefore, we devised that using fat suppression technique with the principle of selective excitation technique (PROSET) can improve the image quality of 4D-flow. The aim of this study was to evaluate the effect of PROSET and to optimize the conditions of 4D-flow sequence for the RA.Materials and Methods: We evaluated five healthy volunteers who underwent 4D-flow MRI for RA with/without PROSET (PROSET/non-PROSET) using 1.5T MRI. The conditions of PROSET with a binomial excitation were 1:1 (PROSET1:1), 1:2:1 (PROSET1:2:1) and 1:3:3:1 (PROSET1:3:3:1). The quality of 4D-flow image obtained by GT-flow software was visually evaluated by radiologic technologist. Furthermore, the contrast ratio (CR) between RA and inferior vena cava (IVC) were calculated on each magnitude images.Results and Discussion: In the visual evaluation, 4D-flow images with PROSET1:1 tended to be clearly compared with that obtained by other conditions. The CR between RA and IVC decreased in the order; non-PROSET, PROSET1:1, PROSET1:2:1 and PROSET1:3:3:1. It was considered that 4D-flow images with PROSET improved by increasing the contrast between RA and fat. However, for PROSET1:2:1 and PROSET1:3:3:1, increasing the signal of IVC decreased CR on 4D-flow images because the repetition time was extended by the division of PROSET.Conclusions: Our study suggested that PROSET1:1 is recommended to improve the image quality for 4D-flow analysis.

P-1-022　4D Flow解析を用いた腎動脈血流可視化法：スライス断面とk空間の収集方法の適正化
Visualization of Blood Flow for Renal Artery using Four-dimensional Flow Analysis : Optimization of slice orientation and k-space trajectory

成石　将平（倉敷中央病院 放射線技術部）
Syohei Naruishi[1], Hiroaki Kameiyama[1], Kenichi Nakagawa[1], Sachi Fukushima[1], Noriyoshi Morimoto[1], Takashi Tabuchi[2]

[1]Department of Radiological Technology, Kurashiki Central Hospital, [2]Department of Medical Technology, Kurashiki Central Hospital

【要旨】4D-flow解析における腎動脈血流評価に最適なスライス断面（transverse, coronal）とProfile order (Y, radial)について検討を行った．スライス断面はtransverse，Profile orderはradialが腎動脈の4D flow解析に最適であった．

[INTRODUCTION] Four-dimensional flow MR imaging is becoming a valuable tool in the blood flow evaluation which allows the evaluation of the form and kinetics of the blood vessel by utilizing the phase shift. However, the adoption of this technique in routine clinical imaging is primarily hampered by two issues: The long scan time inherent in the acquisition of the 3-dimensionality of time-resolved data including anatomy and flow information, and the resulting respiratory artifacts. Therefore, we evaluated the differences in renal artery visualization due to the differences in the slice orientation and profile order.[MATERIAL AND METHODS]Imaging was performed on the target renal artery of 5 volunteers who underwent MRI at 1.5T(Ingenia, Philips) utilizing navigator respiratory gating based on diaphragm motion and fat suppression acquisition techniques, with 4D PC imaging of flow patterns.We compared images in each sliced orientation (transverse, coronal) and profile order (Y, radial). Comparison images were magnitude images and 4D flow images obtained by GT-flow software in each of the conditions.[RESULTS]For the results of the magnitude images, respiration artifact reduction and visualization of peripheral blood vessel was better in the transverse orientation compared to the coronal orientation. There was no difference according to profile order in the transverse orientations, but in the coronal orientations, there was less motion artifact in the radial. For 4D flow analysis images, the best combination for imaging was transverse orientation and a radial profile order.[CONCLUSION]Our study suggested that transverse orientation and a radial profile order are recommended to improve the image quality for 4D-flow analysis.

P-1-023　RF-Spoiled Gradient Echoを用いた緩和時間と磁化率の高速3Dマッピング
Fast 3D Multi-Parameter Mapping of Relaxation Times and Susceptibility Using RF-Spoiled Gradient Echo

谷口　陽（株式会社日立製作所 研究開発グループ）
Yo Taniguchi, Suguru Yokosawa, Tomoki Amemiya, Toru Shirai, Ryota Sato, Hisaaki Ochi, Yoshihisa Soutome

Hitachi, Ltd. Research & Development Group

【要旨】マルチエコーの高速RF-spoiled GEを用いてT1, T2*, PD, B1の各マップを取得するマルチパラメータマッピングにおいて、磁化率マップと水/脂肪画像も同時に取得する方法を提案し、ヒト頭部へ適用した。全脳を1.1 mmの3D等方ボクセルにて12分で撮影可能であった。

Introduction

Multi-parameter mapping of relaxation times and proton density can be applied to clinical image diagnosis and is expected for disease quantification. Quantitative susceptibility mapping (QSM) is also expected for early diagnosis of brain diseases such as neurodegenerative diseases. In this work, a simultaneous quantification method of these multiple tissue parameters is presented. 3D T1, T2*, proton density (PD), B1, and susceptibility (χ) maps and fat/water images can be acquired from a whole brain scan at clinical resolution.

Method

1.1 mm-isotropic 3D images were acquired at 3 T using RF-spoiled gradient echo sequences with six scan parameter sets where TR, FA, and RF phases are varied in the range of 10-40 ms, 10-40 degrees, and 2-22 degrees, respectively. The optimal parameter sets were selected using the law of error propagation with target relaxation times of GM, WM, CSF, and fat at 3 T. The intensity function used in the optimization was formulated by computer simulations. Five multi-echo images were acquired in one of the parameter sets for QSM and fat/water imaging. TEs of the images were 4.6, 10.4, 16.2, 22.0, and 27.8 ms. The acquisition time per parameter set is a few minutes using a parallel scan, and thus the ten volume images were acquired in 12 minutes. T1, T2*, PD, and B1 maps were calculated pixel by pixel by fitting intensities to the intensity function using a least-square method. Other parameters were as follows: Fov 167x205x167 mm, matrix size 148x186x148, 32-ch head coil.

Results and Discussion

T1, T2*, PD, B1, and χ maps and fat/water images were successfully obtained. Image registration between the volume images will be expected to reduce the likelihood of motion, as the scan time for each volume is only a few minutes.

P-1-024　MR指紋法におけるB0不均一性由来の定量誤差
Quantification error due to B0 inhomogeneity in MR fingerprinting

小林　優太（筑波大学大学院 数理物質科学研究科 電子・物理工学専攻）
Yuta Kobayashi, Yasuhiko Terada

Institute of Applied Physics

【要旨】MRFは複数の組織パラメタを同時に画像化できる新しい手法である。MRFでは、B_0不均一性由来のbanding artifactを消すためにunbalance gradientを用いたFISPシーケンスを用いることが多い。しかし、磁場の不均一性が大きい場合は、banding artifactが残る可能性がある。そこでB_0の不均一性とT_1とT_2の定量誤差の関係を調べた。

MR fingerprinting (MRF) is a novel technique, which enables simultaneous mapping of multiple tissue parameters. A bSSFP sequence is originally used, but it could suffer from banding artifacts due to B_0 inhomogeneity. Thus, a FISP sequence that uses unbalanced gradient to destroy the coherence of the transverse magnetization is often used. However, for a conventional system that has large B_0 inhomogeneity, banding artifacts could remain even because of insufficient dephasing. Here we investigated the relationship between B_0 inhomogeneity and quantification error of T_1 and T_2.An MRI system consited of a 4.7 T wide vertical bore SCM (Oxford Instruments), an RF probe, shielded gradients, an digital transceiver (DTRX-6, MRTechnology), etc. MRF data of $CuSO_4$;doped water phantoms with varied concentrations were acquired with a FISP-MRF sequence with various unbalanced gradient moments, m_0. T_1 and T_2 values were estimated using an MRF dictionary (715400 entries).For $m_0 = 8\pi$, the MRF-T_1 and T_2 maps (Fig. 1a, b) showed strong banding artifacts, which led to the large variations and errors in the estimated values (Fig. 1e). This was greatly alleviated for the larger m_0 (Fig. 1c, d, and f).

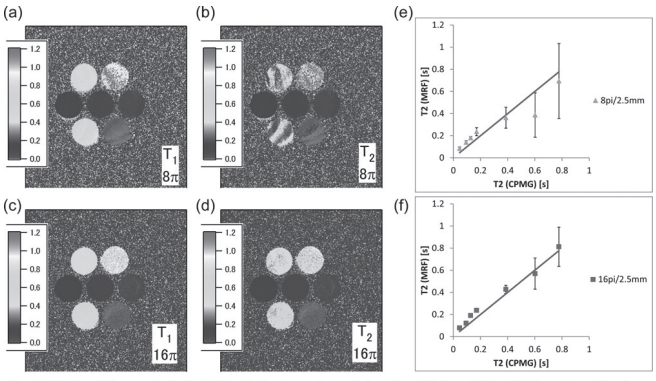

Fig. 1 (a)-(d) T_1 and T_2 maps obtained with MRF. Gradient moment $m_0 = 8\pi$ for a, b and 16π for c, d. (e) and (f) Comparison of T_2 values obtained with MRF and CPMG methods. FOV = 25.6 mm x 25.6 mm. Slice width = 2.5 mm. Matrix size = 256 x 256.

P-1-025　9.4T/54mm縦型開口径超伝導磁石におけるSpiral imagingの開発
Spiral imaging for a 9.4T/54mm vertical bore superconducting magnet

瀬戸井綾菜（筑波大学 数理物質科学研究科 電子・物理工学専攻）
Ayana Setoi, Nao Kodama, Katsumi Kose
University of Tsukuba

【要旨】9.4T/54mmの縦型開口超伝導磁石において，非シールド型（内径32mm）と自己シールド型（内径24mm）勾配磁場コイルを用いたSpiral imagingを開発した．渦電流の影響は，自己シールド型ではほとんどなく，非シールド型では顕著であったが，レファレンススキャンによる位相補正により解決した．

Introduction
Spiral imaging sequences have several unique advantages over other imaging sequences. However, they are considerably sensitive to magnetic field inhomogeneity, eddy current fields, and gradient power amplifier fidelity. In this study, we developed spiral imaging sequences for a 9.4T/54mm vertical bore superconducting magnet.
Materials and Methods
Our MRI system consisted of a vertical bore SCM, a 2nd order RT shim, unshielded and self-shielded gradient coils (Fig.1), a saddle shaped RF coil, and a digital MRI console. Multishot (2-64) spiral sequences were designed according to the Glover's paper (1999).
Results and discussion
Fig.2 shows spiral images acquired with both G coils for 64 shot sequences. Severe shading artifacts were observed for the image acquired with the unshielded G coil. Phase shift caused by spiral readout gradients were measured using pulse sequences with Gx or Gy readout gradients. Fig.3 clearly shows that the phase shift was proportional to the G current because B0 shift was proportional to its time derivative. Fig.4 shows spiral images acquired with the unshielded G coil corrected by the measured phase shift, presenting usefulness of our approach.

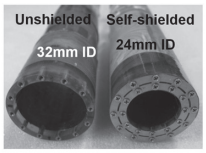

Fig. 1 Gradient coils

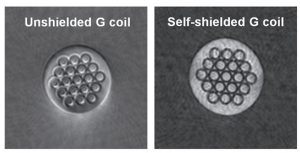

Fig.2 Images acquired with both gradient coils.

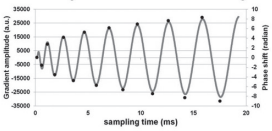

Fig.3 Phase shift proportional to Gy current

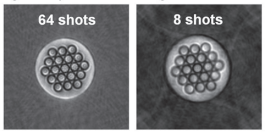

Fig.4 Corrected with the reference scan

P-1-026　1.5T/280mm水平開口超伝導磁石におけるスパイラルイメージングの開発
Development of spiral imaging for a 1.5T/280mm horizontal bore superconducting magnet

瀬戸井綾菜（筑波大学 数理物質科学研究科 電子・物理工学専攻）
Ayana Setoi, Katsumi Kose
University of Tsukuba

【要旨】1.5T/280mm水平開口超伝導磁石において、T_2の短い試料の撮像を行うためスパイラルイメージングの開発を行った。2DSEと2DGREを用い、最短のTEとして前者では4ms、後者では2msを実現し、TEによる画像コントラストの変化を確認した。今後、3D化することにより、TEを0msとする予定である。

Introduction
Spiral imaging sequences have several advantages over other pulse sequences such as higher data acquisition efficiency, flexible k-trajectory design, robustness to motion, and shorter echo time. In this study, we developed spiral imaging sequences for a 1.5 T horizontal bore superconducting magnet to image short T_2 materials.
Material and method
The MRI system consisted of a 1.5 T and 28 cm horizontal bore superconducting magnet, a second order shim coil, a gradient coil set, a 6 cm bore RF coil, and a digital MRI console. We developed spin-echo and gradient-echo multishot (2-64) spiral imaging sequences with 128 × 128 image matrix and 64 mm square FOV. The echo time was 4-20 ms and 2-20ms for the SE and GRE sequences.
Result and discussion
Figure shows cross-sectional images of kiwi fruit (slice thickness = 3 mm) acquired with the SE (upper row) and GRE (lower row) spiral imaging sequences. Clear spiral images are obtained with image contrasts depending on T_2 (SE) and T_2^* (GRE). At present, the shortest echo time is 2 ms for the GRE images but we are planning to shorten the echo time using 3D version of the spiral imaging (conical imaging).

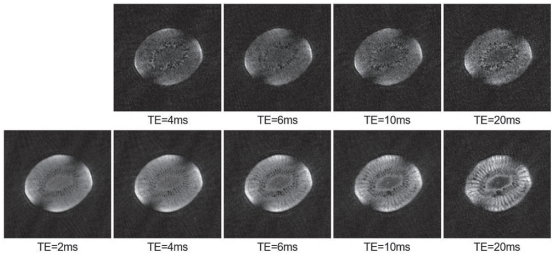

Figure　Cross-section images of kiwi fruit acquired with the SE (upper) and GRE (lower) spiral imaging sequences.

P-1-027　信号収集領域の制限による信号収集の高密度化を利用した3次元MR撮像の圧縮センシング
3D MR Compressed Sensing using Higher-density Sampling in Restricted Signal Space

松本　知之（宇都宮大学 大学院工学研究科 情報システム科学専攻）
Tomoyuki Matsumoto, Satoshi Ito

Information System Science, Utsunomiya University

【要旨】本研究では圧縮センシングを3次元フーリエ変換映像法に応用する場合に，信号量を同量とし信号を全信号空間または制限された空間から間引き収集した場合との画像再生精度の比較を行った．シミュレーションの結果，全信号空間から信号を間引く場合よりも制限された領域内で信号を間引く方が再生精度の高い画像が得られた．

Introduction
This study examines the sampling strategy of partial signal-space sampling with higher sampling density compared to standard full signal-space under-sampling when the amount of acquired signal is the same in 3D Compressed Sensing(CS) MRI.
Materials and Methods
To meet the phase variation on the image, we applied the eFREBAS transform based CS [1] to 3D image reconstruction in which estimation of phase variation is not required in image reconstruction. We use Split Bregman [2] method efficiently for solving L1-L2 minimization algorithms. 3D echo-signal was numerically made using the MR image models and signals were picked-up in the manner of variable density sampling except the central $k_y = \pm 20$, $k_z = \pm 8$ space.
Portion of sampling region is varied from 1 to k_w for k_y direction, $N/2 < k_w < N$.
Results
Simulation studies using 3D phase-varied images of healthy volunteer showed that higher signal-to-noise ratio can be obtained by proposed partial signal-space sampling CS than standard full signal space under-sampling CS when sampling ratios are 20%, 30%, 40%.
Conclusion
Partial signal-space under-sampling method can provide higher signal-to-noise ratio than standard full-space under-sampling method when the same amount of signal is given.
[1] S. Ito et al., ISMRM2015, 2459, 2015
[2] Goldstein T, et al., SIAM J Imaging Sci 2: 323-343, 2009

P-1-028　マルチスケール・スパース化変換を利用した3次元MR位相画像の圧縮センシング
Compressed Sensing of 3D MR Phase-varied Images using Multi-scale Sparsify Transform

渋谷　萌音（宇都宮大学 大学院工学研究科 情報システム科学専攻）
Mone Shibuya, Satoshi Ito

Information Systems Sciences, Utsunomiya University

【要旨】位相を持つ3次元位相画像に圧縮センシングを適用するとき，複数のスライスをまとめて3次元空間内で再構成することにより，再生誤差が3次元空間内にランダム雑音状に分布し，再生誤差を除去できる．複数のスケール係数を用いるeFREBAS変換を利用することで，より効果的に再生誤差が除去でき，高品質な再生像が得られた．

Introduction
We have proposed and demonstrated 2D image reconstruction scheme for 2D phase-varied images in which multi-scale eFREBAS transform is used as sparsifying function[1]. In this study, feasibility studies of proposed method to 3D images were carried out.
Method
Phase-varied 3D images are directly transformed to sparsified space using 3D eFREBAS transform. Scaling parameter for xy plane and Z direction varies from 3 to 8 and from 3 to 5 in each iteration step. SpaRSA [2] was used for L1 and L2 minimization problem.
Results
We used a healthy voluntary images using a 3D gradient echo sequence by Toshiba 1.5-tesla MR scanner. PSNRs of the reconstructed images of the proposed 3D reconstruction and 2D reconstruction are 29.46, 28.68. 3D reconstruction provides much more detailed structures of objects and shows fewer artifacts.
Conclusion
Multi-scale eFREBAS transform is effective to 3D images with strong phase variations and 3D reconstruction can improve the image quality compared to 2D single-slice reconstruction.
[1] S Ito et al., ISMRM2015, 2459, 2015 [2] S J Wright et al., IEEE Trans. Sig. Proc., 57:2479-2493, 2009

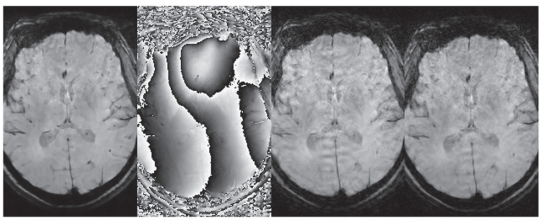

P-1-029　MR血管画像に対するマルチスケール・スパース化変換圧縮センシングの基礎検討
Study on Multi-sparsified Transform Compressed Sensing for MR Angiography

生井　勇己（宇都宮大学 大学院工学研究科 情報システム科学専攻）
Yuki Namai, Satoshi Ito

Information Systems Sciences, Utsunmiya University

【要旨】スパース性が高い血管画像に対し圧縮センシングを応用する場合，複数のスケーリング係数を用いるMulti-scale eFREBAS変換を使用することで効果的な再生誤差の除去が可能である．本研究ではTotal Variationノルムを組み込むFCAアルゴリズムを利用し良質な再生像を得た．

Introduction

We've been studying the compressed sensing (CS) MRI for relatively low sparsity images, such as proton density or T1, T2 weighted images using the multi-scale eFREBAS as a sparsifying transform function. In this study, proposed multi-scale eFREBAS based CS was applied to MR angiography and comparison with other sparsifying transform was carried out.

Method

FCSA[1] method was used to minimize the regularization term including L1, L2 and total variation norm. Scaling parameters of multi-scale eFREBAS transform was sequentially varied from 3 to 10. The basis of wavelet transform was Daubechies (N=4).

Results and Discussions

Simulation experiments were carried out using healthy voluntary images (256 × 256 pixels).

When the amount of acquired signal was 30%, the image PSNRs of Multi-scale eFREBAS transform, wavelet transform based method were 37.45 and 34.17, respectively. It should be noted that the images of vessels are much more smoothly represented compared to wavelet based method as shown in Fig.1.

Conclusion

Multi-scale eFREBAS transform based FCSA showed higher PSNR compared to wavelet one.

[1] J. Huang, et al., Medical Image Analysis, 15: 670-679, 2010.

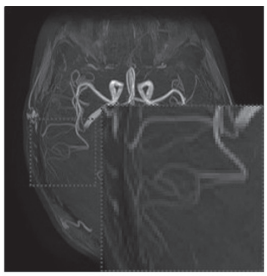

Multi-scale eFREBAS transform

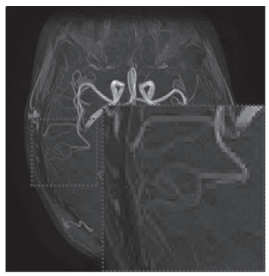

Wavelet transform

P-1-030　ASLによる肺動脈4D-flow画像の至適条件検討
Novel cardiac 4D flow imaging using arterial spin labeling with modified flow sensitive alternating radio frequency: analysis of pulmonary artery flow

後藤　康裕（東京女子医科大学病院 中央放射線部）
Yasuhiro Goto[1], Michinobu Nagao[2], Kenji Fukushima[2], Masami Yoneyama[3], Hitoshi Tadenuma[1], Mamoru Takeyama[1], Shuji Sakai[2]

[1]Tokyo Women's Medical University, Department of Radiological services, Tokyo, Japan, [2]Tokyo Women's Medical University, Department of Diagnostic imaging & Nuclear Medicine, Tokyo, Japan, [3]Philips Electronics Japan, Tokyo, Japan

【要旨】先天性心疾患の診断において肺動脈の形態及び動態画像は重要である。今回我々は、ASLを用いた肺動脈4D-flowの撮像条件であるslice selection TFE pre-pulse の厚さを変化させ、至適撮像条件の検討を行った。TFE pre-pulseの厚さを30mmにすることで、肺動脈末梢まで描出可能であった。

Aims: Non-invasive imaging for assessment of pulmonary artery (PA) flow is clinically required in adult congenital heart disease (ACHD). Here, we have proposed a novel cardiac four-dimensional (4D) flow imaging using arterial spin labeling (ASL) with modified flow sensitive alternating radio frequency (FAIR) to analyze PA flow. Methods: 4D flow imaging using 3-Teslar (Ingenia, Philips Healthcare) with breath hold FAIR was performed for healthy controls and patients with ACHD. Scan parameters were slice thickness 14mm, 3 slices, FOV 180mm, NSA 1, TR 20mmsec, SENSE-factor 1.0, and shot duration 13sec. Optimal slice section of turbo filed echo (TFE) pre-pulse (14mm, 30mm, and 50mm) to visualize PA branch flow was analyzed.Results: Use of slice section of 30mm obtains the best visualization of PA flow in the bilateral second branches. Conclusion: Novel 4D flow imaging can analyze PA flow for a short scan time without special software, and is useful for diagnosis and treatment strategy in patients with ACHD.

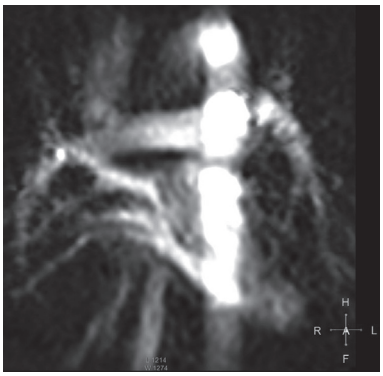

P-1-031　Free-Breathによる心臓シネMRIにおいて心機能評価の精度向上を目的とした撮影条件の検討
Study of parameter to improve the accuracy of cardiac function evaluation at free breath in cardiac cine magnetic resonance imaging

原　久美子（倉敷中央病院 放射線技術部）
Kumiko Hara[1], Kenichi Nakagawa[1], Noriyoshi Morimoto[1], Takashi Tabuchi[2]

[1]Department of Radiological Technology, Kurashiki Central Hospital, [2]Department of Medical Technology, Kurashiki Central Hospital

【要旨】心機能評価のための心臓シネMRIの撮影には息止めが必要である。息止めが困難な患者では呼吸の動きによるアーチファクトが生じ、画質の低下を招き心機能評価の精度が低下する。そこで、加算効果やパラレルイメージングなどのパラメータを利用してFree-Breathでの心臓シネMRIの最適な撮影条件の検討を行ったので報告する。

Purpose: Cardiac cine magnetic resonance imaging (MRI) is used for the accurate evaluation of cardiac function. The holding of breath by the patient is needed when undertaking cardiac cine MRI, and, motion artifacts can result from the inability of the patient to hold their breath. As a result, the image quality and accuracy of cardiac function evaluation are reduced. In order to clarify the accuracy of free-breathing cardiac cine MRI, we captured and compared images using NSA and SENSE factor.Methods: Healthy volunteer underwent MRI scanning with a 1.5T MRI scanner (Ingenia, Philips Healthcare, Best, The Netherlands). First, we undertook free-breathing MRI, by changing the NSA, and then by pair comparison method we visually evaluated for artifacts resulting from breathing and cardiac wall motion. Next, we undertook free-breathing MRI, by changing SENSE factor, and evaluated the images in the same way.Results: In the analysis, there was not a significant difference between degrees of preference in NSA 3 or greater at the artifacts and cardiac wall motion. In the second analysis, there was not a significant difference between the degree of preference up to SENSE factor 3 for artifacts and cardiac wall motion.Conclusion: In free-breathing cardiac cine MRI, once a certain NSA number was exceeded the effect was the same, and the level of artifacts increased when a certain SENSE factor number was exceeded.

P-1-032　Look-Locker法による心筋Color MAPの検討
Development of the myocardial color map by Look-Locker method

立石　敏樹（国立病院機構山形病院 放射線科）
Toshiki Tateishi[1], Atsuko Idogawa[2], Hiroya Rikimaru[2], Akihiro Satou[2], Nobuyuki Kihara[4], Hiroshi Oonishi[4], Takeshi Shinozaki[3]

[1]Department of Radiology, Yamagata National Hospital, [2]Department of Radiology, Sendai Medical Center, [3]Department of Cardiology, Sendai Medical Center, [4]TERARECON INC

【要旨】心臓の遅延画像を撮像する際に使用するLook-Locker法の画像をカラーマップ化し診断支援となるソフトを作成した。虚血性心疾患と心筋症において比較検討し良好な結果を得た。撮像シーケンスを増やすことなく、微妙な濃染への対応もできることから心筋遅延画像の診断向上に寄与できるソフトであると考える。

[Aims]The setting of optimum inversion delay time (TI) where a normal myocardium will be a null point is important in myocardial late gadolinium enhanced (LGE). But for clinical, I sometimes have trouble with setting of TI. So we considered developing adjunctive software which indicates the images of look-locker method used on the occasion of setting of null points by a color map. Using MR device was 1.5T Philips Achieva system. Using Work Station was TERARECON Aquarius iNtuition Server.　[Method]The Look-Locker MAP software indicates normal part and abnormal part signal intensity changes by a color map using nonlinear regression analysis from the look-locker method images. The Look-Locker MAP software and LGE result were compared and examined about 20 examples in patient consent.[Result]There is no extended inspection time since no sequence are added. It was possible to detect myocardial changes by a color map in comparative examination with LGE in a ischaemic heart disease and myocardial infarction. The precision improved by enabling to choose the phase.[Conclusion]Up to now, the look-locker method has been used for the sequence which just finds the myocardial null points. The Look-Locker MAP is a software that can be improved diagnostic accuracy and can be reducing patient scan time.

P-1-033　エメリードレフィス型筋ジストロフィーの管理におけるガドリニウム遅延造影を用いた磁気共鳴画像の意義。
Implication of late gadolinium enhancement magnetic resonance imaging in the management of a patient with Emery-Dreifuss muscular dystrophy

山澤　弘州（北海道大学病院 小児科）
Hirokuni Yamazawa[1], Atsuhito Takeda[1], Gaku Izumi[1], Osamu Sasaki[1], Jiro Abe[1], Daisuke Sasaki[1], Noriko Oyama-Manabe[2]

[1]Department of Pediatrics, Hokkaido University Hospital, [2]Department of Radiation Medicine, Hokkaido University Hospital

【要旨】致死的不整脈はエメリードレフィス型筋ジストロフィーの重大な合併症である。今回既存の評価でリスクは低いと考えられた症例でMRIにて遅延造影陽性及び心電図上PQ延長を認めた。新たなリスク因子とされるPQ延長の背景に、心筋性状の変化を捉えたことは、突然死予防としての植え込み型除細動器の運用に一石を投じる。

Introduction: Malignant ventricular arrhythmia (MVA) is one of the most serious complications of Emery-Dreifuss muscular dystrophy (EDMD). The previous report said that MVA occurred only in persons with at least two of four risk factors that are men, heart dysfunction, ventricular tachycardia, and non-missense mutations. Therefore, patients who have two or more risk factors are considered most likely to benefit from an implantable defibrillator (ICD). Methods: The subject is a female patient with EDMD, who underwent genetic diagnosis. We evaluated electrocardiographic changes and evaluated not only heart structure, function but also changes in the myocardial properties using magnetic resonance imaging (MRI) including late gadolinium enhancement (LGE). MRI studies were performed on a clinical 1.5-Tesla MRI system with a five-element cardiac phased-array coil. The extent of LGE was expressed as a percentage of the left ventricular mass by using the full width at half maximum method. Results: Atrioventricular conduction was delayed from 0.16 sec to 0.24 sec during four years. MRI did not demonstrate left ventricular wall thinning and reducing left ventricular ejection fraction. However, LGE became from negative to 5% positive over time. Conclusions: This case only has a non-missense mutation that is an one of risk factors as mentioned above. However, more than 0.24 seconds prolongation of PQ interval was reported of an independent risk factor recently. Positive LGE, in this case, revealed that there is myocardial damage in the background of PQ prolongation. Abnormal change of myocardial property detected by MRI gives a chance to review the adaptation of the ICD as primary prevention for MVA in the patient with EDMD.

P-1-034　頸動脈造影MRA撮像における混合専用チューブを用いた造影剤生理食塩水同時混同注入の有用性
Improvement of contrast enhancement MRA with the tube for exclusive use of injecting contrast media and saline together in carotid arteries

浜口　明巧（札幌麻生脳神経外科病院 放射線科）
Akiyoshi Hamaguchi, Naoko Hamaguchi, Tetsuji Hayashi

Sapporo Azabu neurosurgery hospital department of radiology

【要旨】本検討の目的は、造影剤生理食塩水混合注入における、混合専用チューブの有用性を明らかにすることである。従来に比べ、専用チューブは頸動脈信号の変動係数を低くすることができた (0.20 ± 0.04 vs 0.25 ± 0.05 p<.05)。これより、広範囲に、均一な造影効果が得られる専用チューブは有用であると考えられる。

[BACKGROUND] We evaluated the contrast medium – saline mixed injection for the contrast enhancement magnetic resonance angiography (ceMRA) in carotid arteries (The 43rd annual meeting of JSMRM). However the injection tube wasn't the one for exclusive use of injecting contrast media and saline together in that study.
[PURPOSE] The aim of this study is to compare the enhancement of carotid arteries using the tube for exclusive use of the mixture (mixture exclusive tube) during ceMRA.
[METHOD] From October 2015 to May 2016, 46 patients who underwent ceMRA from the aortic arch to craniovertebral junction were prospectively analyzed. The mixture exclusive tube compared with the conventional connecting tube for the coefficient of variation (CV) and the average of carotid arteries enhancement. The average of carotid arteries enhancement was normalized by the signal of the brain stem. Written informed consent was obtained from all patients, and our institutional review board approved this prospective review of patient studies.
[RESULT] The mixture exclusive tube significantly decreased the CV of carotid arteries enhancement (0.20 ± 0.04 vs 0.25 ± 0.05 p<.05). The average of carotid arteries enhancement using mixture exclusive tube and conventional connecting tube were 12.8 ± 1.8 and 11.9 ± 1.4, respectively.
[CONCLUSION] The mixture exclusive tube decreased the CV of carotid arteries enhancement in ceMRA.

P-1-035　MTC併用FE3D法における非同期四肢非造影MRAの検討
A study on asynchronous extremity non-contrast MRA by FE3D method with MTC

矢澤　真一（日本私立学校振興・共済事業団 東京臨海病院）
Shinichi Yazawa, Ichirou Iijima, Atsushi Yamaki

Tokyo Rinkai Hospital

【要旨】腰椎ミエログラフィなどに使用するFE3D法が四肢領域の非同期・非造影MRAに使用可能か検討した。MTC印可の有無とFAを可変し、血管描出良好な撮像条件を求めた。MTC印可により血管の描出は向上し、FAを最適化したMTC併用FE3D法は、四肢領域の非同期・非造影MRAに使用可能であることが示唆された。

[Purpose]There are various methods for non-contrast MRA in the extremity such as FBI and 2D TOF, but extension of imaging time at the time of synchronized imaging or poor visualization at the time of irregular pulse may cause a problem. We report whether FE3D method for lumbar myelography can be used with asynchronous/non-contrast MRA in the extremity.　[Method]The equipment and coil used in the study were Vantage Titan 3T (Toshiba) and 4ch Flex SPEEDER coil respectively. For the lower leg of the volunteer subject with the study consent, the study examined favorable imaging requirements for visualization of blood vessel while checking existence/non-existence of MTC pulse application by using FE3D method and calculating CNR/SNR for blood vessel and muscle by changing FA to 5~30°. [Result]With by MTC pulse application, SNR was decreased by 7% in artery, 8% in vein, and 25% in muscle while CNR was increased by 47% in artery/muscle and 156% in vein/muscle. When FA was changed, SNR became the highest as 10° with both artery and vein, but became lower as exceeding the value. CNR was continuously decreasing when FA was increasing. [Conclusion]It was suggested that FE3D method with FA-optimized MTC pulse may have a difficulty to separate artery and vein, but could be used for asynchronous/non-contrast MRA in the extremity.

P-1-036　3 Tesla MRIにおける非造影冠動脈描出の撮像断面の比較
Comparison of the imaging plane of the non-contrast-enhanced coronary artery visualization in 3 Tesla MRI

渡邉　城大（埼玉県済生会栗橋病院 放射線技術科）
Kunihiro Watanabe[1], Mayumi Ootani[1], Kazuihiro Maruyama[1], Nobuyasu Ichinose[2], Shinichi Kitane[2], Tomoko Miyata[2], Kouki Kurita[1]

[1]Department of Radiology, Saitama Prefecture Saiseikai Kurihashi Hospital, [2]Toshiba Medical Systems Corporation

【要旨】3Tを用い，ボランティア4名にAXとSGで撮像し，技師5名で描出能の違いを検討した．AHA分類のRCA#2.3.4, LCX#5,11,13，LAD#6,7,8を各々1~3点とした．AX像でRCA:2.55±0.60, LCX:2.45±0.69, LAD:2.1±0.79，SG像でRCA:2.6±0.60, LCX:2.35±0.75, LAD:2.35±0.49で，撮像断面による有意差は認められなかった．

BACKGROUND: Non-contrast coronary angiography using 3 Tesla MRI is difficult to visualize, and the image quality often isn't stable.
METHODS: It picked up a transverse plane image and sagittal plane image using a 3D-FFE method in normal volunteers (4 persons). Used equipment is the Vantage Titan3T (Toshiba Medical Systems Co.). Due to 5 radiologic technologists, the difference of visualization between axial and sagittal plane was investigated. The coronary artery blanches are followed by AHA classification. The evaluated blanches were RCA: # 2, 3, 4, LCX: # 5, 11, 13, LAD: # 6, 7, 8 and each of them were scored with 1 to 3 points from viaualization point of view.
RESULTS: In the transverse image was RCA: 2.55 ± 0.60, LCX: 2.45 ± 0.69, LAD: 2.1 ± 0.79. In the sagittalimage was RCA: 2.6 ± 0.60, LCX: 2.35 ± 0.75, LAD: 2.35 ± 0.49.
CONCLUSIONS: No significant difference by the imaging plane was observed in all of the coronary artery blanches.

P-1-037　モルフォロジーマッチングによるR波検出技術を用いたロバスト心電図同期法：検出性能の評価
Morphology-Matching-Based R-Wave Detection For Noise-Robust ECG Gating: Evaluation of the R-wave detection accuracy

川上　毅人（東芝メディカルシステムズ株式会社 MRI事業部 MRI開発部）
Taketo Kawakami[1], Takami Yoshida[2], Makoto Hirohata[2], Shigehide Kuhara[3], Akio Mori[1]

[1]MRI Systems Development Department MRI Systems Division, Toshiba Medical Systems Corporation, [2]Corporate Research & Development Center, Toshiba Corporation, [3]Faculty of Health Sciences, Kyorin University

【要旨】心拍同期撮像の要素技術であるR波検出について,著者らが開発したモルフォロジーマッチングによる手法の性能評価を行った.MRI検査中の被験者から収録した2チャネル（第1誘導と第2誘導）の心電波形データを用いて既存手法との比較を行い,本手法は他手法を上回る約99％の精度を達成しその優位性が確認された.

Background:
Accurate ElectroCardioGram (ECG)-gating is crucial for cardiac MRI. However, the accuracy of ECG-gating deteriorates especially in a high field MRI scanner due to the electromagnetic induction and the magnetohydrodynamic effect. To solve this issue, we proposed ECG-gating based on Morphology Matching (MM) [1]. Morphology is described by filtered ECG signal(s), and R-wave is detected by matching input ECG signal(s) and pre-stored R-wave templates, which are updated when the MRI scanner is idling. In this study, we report experimental result and comparison result to validate the effectiveness of the MM.
Methods:
We built dataset consisting of 66 ECG signals; 20 and 46 ECG signals were recorded using 1.5T and 3T MRI scanners, respectively. Each ECG signal was recorded by using a dual lead ECG monitor during 9 cardiac MRI sequences.
For comparison, we evaluated the performance of MM [1], Pan and Tompkins algorithm (PT) [2], and Planer Vectorcardiogram (PV)[3], which is a kind of ECG-gating method. PT was not designed for MR environment. However, this algorithm is famous, and thus, we used PT as a comparative method.
Results:
The accuracy was evaluated using sensitivity (Se) and positive predictive value (+P). MM showed average Se of 98.6% and +P of 99.2%, which was better than both PT (79.1%, 83.9%) and PV (94.0%, 95.0%). MM showed high noise robustness; MM achieved Se of 98.4% and +P of 99.2% in 3T MRI.
Conclusions:
Morphology-matching-based R-wave detection for dual lead ECG signal showed high accuracy in 1.5T and 3T MRI.
[1] Yoshida et al., JCMR 18(Suppl 1): P21, 2016, [2] Pan et al., IEEE Trans Biomed Eng 32(3), 230-236, 1985, [3] Fischer et al., Magn Reson Imaging 12(5), 678-688, 2000

P-1-038　Multi-shot EPIを用いた非造影冠動脈MRAの検討
Comparison of whole-heart unenhanced coronary MRA using multi-shot gradient echo EPI and TFE coronary MRA in healthy volunteers at 3T MRI

中浦　猛（熊本大学 医学部 画像診断解析学）
Takeshi Nakaura, Kosuke Morita, Seitaro Oda, Daisuke Utsunomiya, Tomohiro Namimoto, Mika Kitajima, Yasuyuki Yamashita

Kumamoto University, Diagnostic Radiology

【要旨】ボランティアにたいしてTFEとMulti-shot EPIを用いたMRAを撮影し、撮影時間と画質について検討した。Multishot-EPIを使用することにより、57%程度撮影時間の短縮、SNRの上昇が得られ、コントラストの低下もなかった。視覚評価でも同等以上の結果が得られた。

Introduction: We investigated the feasibility of whole-heart unenhanced coronary magnetic resonance angiography (MRA) using multi-shot gradient echo planar imaging (MSG-EPI) on a 3T scanner.Material and Methods: Healthy male volunteers (n=14) underwent unenhanced whole-heart coronary MRA using a standard turbo field echo (TFE)- and a MSG-EPI sequence at 3T. The acquisition time, signal to noise ratio (SNR) of the ascending aorta and cardiac muscle, and the contrast between the right coronary artery (RCA) and the cardiac muscle of the sequences were compared with the paired t-test. Two radiologists independently recorded the image contrast, -noise, and -sharpness, artifacts, and the overall image quality on a 4-point scale.Results: The acquisition time was 57% shorter for MSG-EPI than TFE (88.1 ± 10.0 vs 206.4 ± 23.1 sec, $p<0.01$). The SNR of the ascending aorta and cardiac muscle was significantly higher on MSG-EPI than TFE scans (ascending aorta: 18.7 ± 5.5 vs 11.1 ± 4.0, $p<0.01$; cardiac muscle: 14.5 ± 8.9 vs 8.3 ± 2.6, $p<0.01$). There was no significant difference in the contrast of the RCA and the cardiac muscle on MSG-EPI and TFE scans (2.0 ± 0.4 vs 1.9 ± 0.3, $p=0.83$). All qualitative scores except for sharpness were significantly higher on MSG-EPI than TFE scans ($p<0.05$). Conclusions: The MSG-EPI sequence is a promising technique for shortening the scan time and for improving the image quality of unenhanced whole heart coronary MRA on a 3T scanner.

P-1-039　3D T1強調black-blood turbo spin echoの検討：大動脈弓部の血管壁画像
Examination of Three-dimensional T1-Weighted Black- Blood Turbo Spin-Echo: The Vessel Wall Imaging in the Aortic Arch

中河　賢一（倉敷中央病院 放射線技術部）
Kenichi Nakagawa[1], Noriyoshi Morimoto[1], Sachi Fukushima[1], Takashi Tabuchi[2]
[1]Department of Radiological Technology, Kurashiki Central Hospital, [2]Department of Medical Technology, Kurashiki Central Hospital

【要旨】MRIにおけるT1強調black blood法は、血管壁やプラークの性状を評価できる有用な撮像方法である。今回われわれは、大動脈弓部を対象とした3D T1w black-blood TSEにおける撮像条件の検討を行い，明瞭な画像と臨床における有用性を得ることができたので報告する。

INTRODUCTION:Complex plaques in the aortic arch on transthoracic echocardiography (TEE) can cause aortogenic brain embolism. However, TEE, which is associated with a number of complications and contraindications, is not suitable for all patients. Therefore, we focused on contrast evaluation of magnetic resonance imaging as an adjunct to diagnosis of complex plaques in the aortic arch, which was difficult to scan in the aortic arch because of several artifacts. As a solution to these problems, we devised the scan methodology of 3D T1wBB-TSE in the aortic arch. The aim of this study is to clarify the optimal scan method for 3D T1wBB-TSE. MATERIALS and METHODS:Five healthy volunteers (mean age 33.8 years, range 25.0 to 57.0) participated in this study. All experiments were acquired by volume isotropic TSE acquisition (VISTA) with anti-DRIVE using a 1.5T unit (Ingenia, Philips Healthcare). The study protocol was divided into two parts: 1) To evaluate the combination of six patterns for phase direction, with and without ECG-gating and navigator respiratory gating, respectively, and 2) To compare the timing of ECG-gating on systole and diastole to determine the optimal trigger timing. There were evaluated by visual assessment.RESULTS:The combination of phase direction AP or FH, with ECG-gating, and using navigator respiratory gating were best scan methods. When we compared the timing of ECG-gating systole with diastole, diastole was better because movement of the vessel wall was less on diastole. However, for the patients with reduced blood flow, black blood can result in weakness. CONCLUSION:Our results suggest that 3D T1wBB-TSE in the aortic arch can reduce the amount of artifact by using the optimal trigger timing by ECG-gating and navigator respiratory gating.

P-1-040　3D-T1FFEEPIを用いた下肢MR-Venography
Non-contrast enhanced MR-Venography using 3D-T1FFEEPI in lower extremity

古牧　伸介（川崎医科大学附属川崎病院 中央放射線部）
Shinsuke Komaki[1], Katsuhiro Kida[2], Yukako Hayashi[1], Akihiko Tabuchi[1]
[1]Kawasaki Medical School, Kawasaki Hospital, [2]Okayama Red Cross Hospital

【要旨】非造影下肢MRVにおいて，浮腫性病変が血管描出の妨げとなる場合や心電図同期を併用する場合，不整脈による制限が生じることがある．そこで本検討では，これらの問題点を改善するために，心電図非同期3D-T1FFEEPIシーケンスに着目し，その撮像条件の最適化と臨床的有用性についての検討を行った．

Purpose In lower extremity non contrast enhancement magnetic resonance venography (MRV), when using the 3D-FSE sequences and Balanced SSFP, edematous lesions hinder the blood vessel visualization. In the case of using a sequence used in combination with ECG gating, patients with arrhythmia of the imaging it is difficult. The purpose of this study, in order to improve these problems, focusing on the ECG non gating 3D-T1 FFEEPI sequence, optimization of scan parameters and clinical utility of the imaging conditions.Methods All MR images were acquired on a clinical 1.5T system(Philips Achieva). The manufacturer-provided 16-channel XL Torso coil was used for image acquisition. Our subjects were healthy volunteers and patients with Venous disease obtained consent. Varying the EPI factor(3, 6, 9, 13, 15, 17, 19), fat suppression (SPIR, ProSet1-2-1), MTC pulse(on, off), SNR and image contrast was compared. Using the scan parameters optimized to scan patients with venous disease, it was verified clinical utility. The parameters of the 3D-T1 FFEEPI sequence were TE shortest(17ms), TR shortest(53ms), Flip angle 20deg, FOV 400mm, matrix 256*512(r), Slices 20/1stack, Slice thickness 2.0mm, Stacks 5, Flow compensation yes, NEX 3. Results and Conclusion Optimized scan parameters were the EPI factor : 13, fat suppression : ProSet1-2-1, MTC pulse : on. ECG non gating 3D-T1 FFEEPI was possible shorten the imaging time, In addition to the Inflow effect, low flow rate and stagnation to have blood also can be signaling. More of that organization in the perivascular receive the depahase effect, contrast rise of the blood vessels can be expected. This sequence is applicable as a method of non-contrast lower extremity MR-Venography.

P-1-041　冠動脈および末梢血管ステント挿入後の MRI検査可能時期に関するステントメーカー各社の見解の調査
Investigation to the stent makers about MRI examination start time after implanted of stent to coronary artery and peripheral arteries

蛸井　邦宏（山形県立新庄病院 放射線部）
Kunihiro Takoi[1], Shuichi Otake[2], Shintaro Saito[2], Soichi Ono[1], Toshiro Shibasaki[1], Yuitu Narasaki[1], Takatomo Itagaki[2]

[1]Department of Radiological Technologists, Yamagata Prefectural Shinjo hospital, [2]Department of Radiology, Yamagata Prefectural Shinjo hospital

【要旨】冠動脈・末梢血管ステントは、挿入後一定の期間、MR検査を避けるべきとされてきた。しかし、2016年4月現在、ほとんどの商品の添付文書に上記の記述は見られない。過去に販売されていた一部の商品で8週の経過を求めていたが、これらは販売終了していた。ステントの商品名の確認できれば、早期に検査実施可能と考えられた。

Back ground/purpose
In patient whom the stent was implanted to the coronary arteries and the peripheral artery, the Magnetic resonance imaging (MRI) were not examined for 8 weeks. However, as for the above-mentioned description, almost all the stents currently sold in Japan not be looked at by the package leaflet as of April, 2016. In the investigation which we conducted in 2014, the stopped period of the MRI was not decided and it had set a different stopped period by each medical institution. We did the questionnaire about the opinion of each stent maker company in order to consider the MRI for the patient in whom the stent was implanted.
Method
In February, 2016, we requested the questionnaire by a document from 8 companies which sell the stent in Japan. The main contents of a question
(1) In patient who implanted the stent, have to conduct the MRI after about 8 weeks. What is the reason?
(2) There is no statement of (1) in the present package leaflet. What difference do the conventional stent and the present stent have? Are there a related paper and a report?
The others
Discussion/conclusion
In 6 companies of 8 company, for the MRI of the patient who implanted the stent sold in the past that was not demand to passage 8 weeks after insert. Other 2 companies necessitated the passage of 8 weeks after stent insertion. These 2 companies showed the paper used as a reason.The summary of the paper, the implanted stent is endothelialized about 6-8 weeks. By these papers, each medical institution determined uniquely about the MRI stop period. Therefore, it is thought that variation arose about the MRI stop period. However, sale of these stents has ended. If the product name of a stent can trust it certainly, the MRI will become possible at the early stage after stent implant.

P-2-001　悪性転化した脳腫瘍のCEST APTimage
CEST APTimaging of Intracranial Tumor with anaplastic transformation

若山　季樹（東京都保健医療公社 荏原病院 放射線科）
Toshiki Wakayama[1,2], Masahiro Ida[1], Katsutoshi Murata[3], Kenji Saitou[1], Takashi Ueda[1], Fumiaki Kawakami[1], Toshiyuki Onodera[1,2], Atsushi Senoo[2], Akira Yamashita[1]

[1]Tokyo Metropolitan Health and Medical Treatment Corporation Ebara Hospital, Department of Radiology, [2]Tokyo Metropolitan University, Graduate School of Human Health Sciences, Division of Radiological Sciences, [3]Siemens Healthcare Japan, Division of Research and Collaboration

【要旨】経過観察中に悪性転化したと考えられた脳腫瘍のAPT imageは、APT imageのみが初回検査より上昇していた。APT imageは標準的なMRI検査によって良性と考えられた脳腫瘍が、後に悪性転化することをを示唆している可能性があると考えられた。

[Background]
The CEST MRI method enables to detect low concentrations of metabolites that contain residues with exchangeable protons such amide. APT imaging is technique which focuses on an amide proton pool.APT imaging has potential for imaging malignant intracranial tumors through an increase in cellular protein /peptide content of mobile protons in malignant tumor tissue with respect to normal brain tissue.
[Purpose]
The aim of this study is to evaluate usefulness of APT imaging in intracranial tumor with anaplastic transformation.
[Method]
*Patient
2 adult patients of intracranial tumor which appeared to transform into malignant tumor during follow-up.
*MRI
CEST MR was performed on 3T MRI (MAGNETOM Trio, Siemens) using a 32-channel head coil. A single-slice, 2D CEST sequence (WIP) was carried out with following parameters (matrix:128 / FOV: 220 mm/ slice thickness: 5 mm/ TR: 5.6 ms/ TE: 2.46 ms/ FA: 10 degree). The frequency offset range was ±4.5 ppm with 13 points.
For reference, several standard MRIs, including diffusion-weighted imaging, DSC perfusion study, T2WI and post contrast (CE) T1WI were acquired.
[Result]
At the initial MRI, T2WI shows hyperintense lesion with increased ADC and non-enhancing CE T1WI suggesting low grade. However, elevation of APT signal intensity (APT SI) can be seen within the tumor. In the MRI taken a few years after, a CE T1WI shows enhancement in the tumor suggesting high grade.
[Discussion]
In this case, only the APT SI had increased from the initial exam but other standard methods had not denoted malignant findings. Elevating APT SI in the benign tumor suggests the malignant transformation potential of the neoplasm.
[Conclusion]
Increasing APT SI of benign intracranial tumor suggests the possibility of anaplastic transformation.

P-2-002　脳転移へのガンマナイフ治療後の再発、壊死の鑑別における、MR-permeability imagingとMET-PETの比較
Comparison of MR-permeability imaging from MET-PET in differentiating radiation necrosis from recurrent tumors after gamma knife radiosurgery

戸村　則昭（脳神経疾患研究所附属 総合南東北病院 神経放射線診断科）
Noriaki Tomura[1], Mika Kokubun[2], Yasuhiro Kikuchi[3]

[1]Department of Neuroradiology, Southern Tohoku Research Institute for Neuroscience, Sothern Tohoku General Hospital, [2]Department of Radiology, Southern Tohoku Research Institute for Neuroscience, Sothern Tohoku General Hospital, [3]Department of Neurosurgery, Southern Tohoku Research Institute for Neuroscience, Sothern Tohoku General Hospital

【要旨】脳転移へのガンマナイフ治療後の、再発と壊死の鑑別における、MR-permeability imaging, ^{11}C-methionine PET (MET-PET), ^{18}F-FDG PET (FDG-PET)とを比較した。ROC解析では、ME-PETが最もすぐれており、FDG-PETが最も劣っていた。MR-permeability imagingではCERが最も優れていた。

Purpose: MR-permeability imaging was compared with ^{11}C methionine (MET) PET in differentiating radiation necrosis from recurrent metastatic tumors after γ knife radiosurgery (GK).
Materials and Methods: The study was performed for 18 lesions after GK. Ten lesions were identified as recurrent tumors. Eight lesions were diagnosed as radiation necrosis. Both MET-PET and FDG-PET were performed. For MR-permeability imaging, the transfer constant between intra- and extravascular and extracellular spaces (Ktrans), the extravascular extracellular space (Ve), the transfer constant from the extracellular extravascular space to plasma (Kep), initial area under the signal intensity-time curve (IAUGC), contrast enhancement ratio (CER), bolus arrival time (BAT), maximum slope of increase (Max. slope), and fractional plasma volume (fPV) were calculated, and the minimum ADC were calculated of the lesion. On PET images, the ratio of SUVmax of the lesion divided by the SUVmax of the symmetrical normal site was measured (MET-ratio and FDG ratio, respectively). ROC analysis was performed to evaluate the utility of those parameters.
Results: AUC of ROC curve for differentiating radiation necrosis from recurrent tumors was the most excellent for MET-ratio (0.90) followed by CER (0.81), Max slope (0.80), IAUGC (0.78), fPV (0.76), BAT (0.76), Ktrans (0.74), Ve (0.68), ADCmin (0.60), Kep (0.55), FDG ratio (0.53). Significant difference in MET ratio ($p<0.01$), CER ($p<0.01$), Max. slope ($p<0.05$) and IAUGC ($p<0.05$) were evident between radiation necrosis and recurrent tumor.
Conclusion: MET-PET is superior to MR-permeability imaging, ADC, and FDG-PET in differentiating radiation necrosis from recurrent tumors. In MR-permeability imaging, CER, Max. slope, and IAUGC are superior to other parameters.

P-2-003　T1ρによる髄膜腫の硬さの評価
Predicting the Consistency of Meningioma with T1ρ at 3T-MR: Preliminary Study

北島　美香（熊本大学 医学部 画像診断・治療科）
Mika Kitajima[1], Shigetoshi Yano[2], Hiroyuki Uetani[1], Tomoyuki Okuaki[3], Yasuyuki Yamashita[1]

[1]Department of Diagnostic Radiology, Graduate School of Medical Sciences, Kumamoto University, [2]Department of Neurosurgery, Graduate School of Medical Sciences, Kumamoto University, [3]Philips Healthcare AsiaPacific

【要旨】髄膜腫の硬さがT1T1ρにより評価可能であるかを検討するために、5例の髄膜腫でT1ρ値と組織標本1視野内に占める線維成分の割合を比較した。線維成分が44%以下では、線維成分が増加するとT1ρも延長した。しかし、線維化の程度がそれ以上ではT1ρは短縮した。

Purpose: T1ρ represents the spin-lattice relaxation time constant in the rotating frame. It can be used to study the macromolecular composition of and the proton exchange of collagen and proteoglycans. In meningiomas, knowing the tumor consistency comprised of fibrotic tissue is important for predicting the degree of tumor removal. We investigated whether the T1ρ predicts the consistency of meningiomas by comparing the T1ρ value with histopathologic findings.
Materials and Methods: This study included 5 patients with meningiomas who underwent preoperative 3T-MR imaging. Axial images for T1ρ weighted images were acquired using a multi-shot TFE based 2D T1ρ pulse sequence with TSL (time of spin lock) of 0, 20, 80 ms, spin lock frequency = 500 Hz, TR/TE of 5.2/1.5 ms, flip angle of 10°, acquisition matrix (frequency × phase) of 256 × 199, 250 × 250 mm field of view, and 5 mm slice thickness. Acquisition time for each TSL sequence was about 1 min 48 sec.The fibrotic fraction of the tumor was semiquantitatively determined by calculating the collagen volume fraction (CVF) in Elastica van Gieson (EVG)-stained histologic specimens. We then compared T1ρ and histologic findings.
Results: The T1ρ values ranged from 61.0 to 90.3 ms (74.3 ± 11.0 ms) and the CVF from 16.8 to 49.7% (36.18 ± 13.6%). The T1ρ values rose as the CVF increased. However, the T1ρ value decreased when CVF exceeded 44%.
Conclusion: The amount of fibrotic tissue in meningiomas was correlated with an increase of T1ρ value when the CVF was less than 44%.

P-2-004　髄膜腫と悪性神経膠腫の鑑別におけるMR灌流画像の有用性の検討
Differentiation of meningioma and high-grade glioma using dynamic susceptibility contrast and dynamic contrast-enhanced MRI

村山　和宏（藤田保健衛生大学 医学部 放射線医学）
Kazuhiro Murayama[1], Takashi Fukuba[2], Shigeharu Ohyu[3], Ayako Ninomiya[3], Masato Ikedo[3], Kazuhiro Katada[4], Hiroshi Toyama[1]

[1]Department of Radiology, Fujita Health University, [2]Department of Radiology, Fujita Health University Hospital, [3]Toshiba Medical Systems Corporation, [4]Joint Research Laboratory of Advanced Medical Imaging, Fujita Health University

【要旨】非典型的な形態や局在を呈する髄膜腫では悪性神経膠腫との鑑別が問題になることがある。髄膜腫13例と悪性神経膠腫11例、合計24例を対象に東芝製3T MRIを用いてMR灌流画像による鑑別能を評価した。Ktrans, Vp, Kep, corrected CBVは髄膜腫で悪性神経膠腫と比べ高値を示し、これらの鑑別に有用である可能性が示唆された。

[Objective] Meningiomas are the most common extra-axial tumor, so that advanced images including dynamic contrast enhanced (DCE) and dynamic susceptibility contrast (DSC) techniques aren't necessary for the diagnosis of intracranial meningioma. However, some meningiomas with atypical morphological features and in the atypical locations may resemble other brain tumors, especially high-grade glioma (HGG). The purpose of this study was to evaluate the diagnostic performance between meningioma and HGG in DCE and DSC imaging.[Materials and Methods] From January 2015 to September 2015, 24 consecutive patients who underwent preoperative MRI examination at 3T MRI (Vantage Titan 3T, Toshiba) and 13 meningiomas, 11 HGGs were enrolled in this study. Ktrans, Ve, Vp, Kep and corrected CBV were measured by manual region of interest and histogram analysis. The diagnostic performance of these parameters was assessed with the area under the curve of the receiver operating characteristic analysis.[Results] Statistically significant differences were observed between meningioma and HGG in Ktrans (p=0.0073), Vp (p=0.0073), Kep (p=0.0059), corrected CBV (p=0.0002). No statistically significant difference was observed in Ve (p=0.8645). Ktrans, Vp, Kep, corrected CBV of meningioma was significantly higher than that of HGG. In differentiating between meningioma and HGG, the area under the curve of the corrected CBV, Kep, Ktrans, Vp, Ve were 0.867, 0.825, 0.818, 0.818, 0.518, respectively. [Conclusion] Our findings suggest that DCE and DSC imagings may help to distinguishing meningioma from HGG in atypical cases. Corrected CBV can be a most sensitive and specific method of quantitative estimates for the vascular microenvironment in characterizing meningioma.

P-2-005　T2強調像での高信号域におけるテクスチャ解析による検討: gliomaと浮腫との比較
Pattern difference in the area with T2-hyperintensity: comparison between gliomas and edema by using texture analysis

川井　恒（名古屋大学 医学部附属病院 放射線科）
Hisashi Kawai, Toshiaki Taoka, Toshiki Nakane, Shinji Naganawa
Department of Radiology, Nagoya University Hspital

【要旨】T2強調像の高信号域を神経膠腫によるものと脳転移周囲の浮腫の間でテクスチャ解析を行うと、低悪性度神経膠腫と浮腫の間で4つの特徴量に明確な有意差があり、膠芽腫と浮腫の間でもこの4つで有意差が認められた。神経膠腫と転移周囲の浮腫はT2強調像の画像パターンが異なり、画像解析により区別できる可能性がある。

Purpose:T2 hyperintensity area in the glioma cases have something characteristic pattern compared to other lesion with T2 hyperintensity such as edema. In order to evaluate the characteristic imaging pattern of gliomas quantitatively, we applied texture analysis and made comparison between different grade of gliomas and peritumoral edema (PTE) of metastases.
Method:Low grade glioma (LGG; 7 cases), glioblastoma (GBM; 7cases) and metastases (7cases) which underwent 3D-T2WI as well as CE-MRI before the surgery were evaluated. Texture analysis was performed with MaZda software (Technical University of Lodz). For the LGG and GBM cases, regions of interest (ROI) were manually located on T2WI in the hyperintensity areas of the white matter in which contrast enhancement is absent. For the metastasis cases, ROI were located in PTE. Eleven texture parameters for the ROI were acquired including "angular second moment" and "contrast", and statistical analysis was performed among LGG, GBM and PTE.
Result:The significant differences ($p<0.05$) were detected in 9 parameters of texture between LGG and PTE. There were strong statistical difference ($p<0.01$) shown in the features of "contrast", "inverse difference moment", "difference variance" and "difference entropy" between LGG and PTE, and between LGG and GBM. While, no significant difference was detected between GBM and PTE for the 4 features above.
Conclusion:On texture analysis, definite differences were shown between T2 hyperintensity area in gliomas and edema. On the other hand, area with T2 hyperintensity without enhancement in low grade and high grade glioma share the texture characteristics. Quantitative analysis for T2 hyperintensity area by texture may be helpful when there is difficulty in differential diagnosis.

P-2-006　PRESTO-MRIによる腫瘍血管形態評価の試み：神経膠腫悪性度診断への応用
Morphologic features of intratumoral susceptibility signals on PRESTO for predicting the WHO grade of gliomas

李　麗（東北大学 医学系研究科 放射線診断科）
Li Li[1], Shunji Mugikura[1], Takaki Murata[1], Toshiaki Akashi[1], Shiho Sato[1], Masayuki Kanamori[2], Mika Watanabe[3], Hajime Tamura[1], Shoki Takahashi[1], kei Takase[1]
[1]Department of Diagnostic Radiology, Graduate School of Medicine, Tohoku University., [2]Department of Neurosurgery, Graduate School of Medicine, Tohoku University., [3]Department of Pathology, Tohoku University Hospital.

【要旨】PRESTO上のIntratumoral Susceptibility Signal (ITSS) の形態的評価を行い、神経膠腫のWHO gradeとの関係を検討した。ITSSはGradeの進行に伴い、点状や線状→点状集族や限局性拡張像→蛇行状となる傾向があり、病理上の腫瘍内血管構築を反映している可能性がある。

[Objective] The principles of echo-shifting with a train of observation (PRESTO) magnetic resonance (MR) imaging techniques employ MR sequences that can increase the sensitivity to susceptibility effects of microvascular structures with low-oxygen level and blood products. Therefore, this imaging technique may demonstrate brain tumor vascularity. We determined whether the morphologic features of intratumoral susceptibility signals (ITSS) on PRESTO correlated with the WHO histological grading of gliomas. [Materials and Methods] Eighty patients with histologically proved gliomas were enrolled in this retrospective study. The morphology of ITSS was classified into 5 categories: 1) scattered dots and/or fine linear, 2) aggregate of dots, 3) localized dilated linear, 4) tortuous, and 5) conglomerate structures. [Results] With an increase in tumor grade, the morphology of ITSS changed from dot-like and/or fine linear ITSS to aggregate of dots and/or localized dilated linear ITSS, and then to tortuous ITSS. Aggregate of dots and localized dilated linear ITSS were observed characteristically in patients with grade III gliomas, and tortuous ITSS were observed in patients with grade IV gliomas. [Conclusion] The morphologic pattern of ITSS could provide tumor vascularity information in different-grade gliomas.

P-2-007　SE法による3T頭部T1強調画像の画質改善
Improvement of Brain T1 Weighted Images Quality using Spin Echo Sequence at 3.0T

松下　利（岡山大学病院 医療技術部 放射線部門）
Toshi Matsushita, Seiichirou Ohno, Shunsuke Fuji, Akira Kurozumi, Takatugu Yamauchi, Naoki Nishida, Akira Nagano, Seiji Tahara
Okayama University Hospital, Division of Radiology, Department of Medical Technology

【要旨】転移性脳腫瘍症例において、造影後T1-FLAIRにて疑陰性となる症例を経験。3Tにおける頭部T1強調画像へのSE法の適用を再考する。Excitation Flip Angleを下げることが、T1コントラスト改善として最も効果が高かった。一方、pre saturation pulseの有無によるコントラストの変化が認められた。

We had an experience with false negative case of metastatic brain tumor on contrast enhanced T1-FLAIR. On the basis of the case, the aim of this study was to reconsidering the application of spin echo brain T1 weighted image at 3.0T.
We compared gray-to-white matter contrast with following parameters, (1) sequence type (se, se_15b130, se_20rb130hf and tse), (2) distant factor (10, 30, 50 and 70%), (3) excitation flip angle (90, 80, 70, 60 and 50degrees), (4) refocus flip angle (180, 160, 140 and 120degrees) and (5) RF pulse type (Fast, Normal and LowSAR).
The most effective approach to increase gray-to-white matter contrast is to reduce the excitation flip angle. On the other hand, this approach reduces SNR. To reduce the refocus flip angle and to change the RF pulse type do not have much effect on increase gray-to-white matter contrast, and to reduce the refocus flip angle increased intensity inhomogeneous. In addition, cerebrospinal fluid/ cerebral parenchyma contrast depend on the presence or absence of pre saturation pulse at pituitary imaging.
To reduce the excitation flip angle produced good contrast. In pituitary imaging, absence of pre saturation pulse increase contrast.

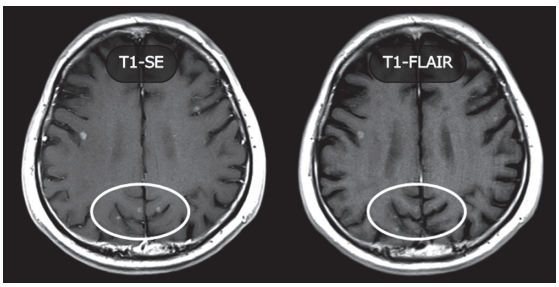

P-2-008　リンパ腫とGBMの鑑別診断：CBVとADC画像のヒストグラム解析
Differentiation among GBM, and Primary CNS Lymphoma Using Whole-Tumor Histogram Analysis of the nCBV and minimum ADC in Enhancing Lesions

包　是星（大阪大学 医学研究科 放射線医学）
Shixing Bao, Yoshiyuki Watanabe
Osaka University Department of Radiology

【要旨】Histogram method has been used to analysis PWI and DWI images for brain tumors , include high grade glioma and lymphoma. Our purpose is to demonstrate whether normalized cerebral blood volume and apparent diffusion coefficient facilitates differential di

BACKGROUND This study aimed to determine whether whole-tumor histogram analysis(WHA) of the normalized CBV(nCBV) and ADC for contrast-enhancing lesions differentiates among GBMs and primary CNS Lymphomas(PCNSLs)METHODS 25 patients, 8 with PCNSL and 17 with GBM underwent DWI and DSC-PWI imaging before surgery. The ADC and nCBV were obtained from DWI and DSC-PWI respectively, while histogram distribution of the nCBV and ADC from whole-tumor voxels in contrast-enhancing lesions. Results To WHA for contrast-enhancing lesions, most nCBV parameters of GBMs (mean 5.77 ± 4.14 , Max 17.06 ± 9.52 ,min 0.59 ± 0.59, Va50% 5.08 ± 3.53, Va97.5% 13.31 ± 9.58,SD3.27 ± 2.53 , kurtosis2.67 ± 3.34,skewness1.04 ± 0.75) were significantly larger than that of PCNSLs(mean2.68 ± 1.11,Max11.68 ± 6.58,min0.64 ± 0.59,Va50%2.70 ± 1.27, Va97.5% 4.90 ± 1.82,SD1.12 ± 0.45,kurtosis15.47 ± 15.83,skewness 2.56 ± 3.23). Whereas ADCmin parameters suspected no significant difference between GBMs(mean 145.61 ± 47.95,Max385.78 ± 142.35,min61.48 ± 28.67,Va50%136.61 ± 44.36,Va97.5%253.33 ± 106.00,SD38.15 ± 20.46,kurtosis6.36 ± 6.58,skewness1.49 ± 1.14) and PCNSLs(mean135.50 ± 41.94,Max359.69 ± 136.36,min66.10 ± 19.98,Va50%128.10 ± 41.67,Va97.5%235.06 ± 73.41,SD42.67 ± 18.30,kurtosis8.98 ± 10.00,skewness1.77 ± 1.17).To ROC analysis, nCBV value of GBM was significantly larger than that of PCNSL ,mainly in mean(area 86%,sig 0.004),SD(area 89.7%,sig 0.002)and Va97.5%(area 90.4%,sig 0.001),while no significance existed between GBM and PCNSL in ROC analysis of ADC ,except for Va25%(area 75%,Sig 0.048)Conclusion Using WHA of nCBV to show values for contrast-enhancing lesions facilitates differentiation of GBMs and PCNSLs. Compared to ADC, nCBV is found more sensitive in differential diagnosis of GBMs and PCNSLs

P-2-009　ガドビストダイナミックMRI至適注入速度の検討
Evaluation of optimal injection rate in gadovist enhanced MR dynamic study

中村　誠（三豊総合病院 診療技術部 放射線科）
Makoto Nakamura[1], Shinya Azuma[1], Masashi Kiyohara[1], Hironori Kurokawa[2]
[1]Mitoyo General Hospital medical Technology Department of Radiology, [2]Mitoyo General Hospital Department of Radiology

【要旨】ガドビストは新たな造影剤であり,ダイナミックでの至適注入速度の検討を行った。脳転移精査目的で造影MRIを施行した15症例.注入速度は3ml/sec,2ml/s,1ml/sで注入ダイナミックカーブを作成した.結果は3ml/sで最も急峻な立ち上がりを呈し3ml/sで注入することで良好な早期造影効果が期待できる.

Purpose: Gadovist is a new MRI contrast media that has been demonstrated to improve the enhancement effect. There were no reports of gadovist MR dynamic study in Japan Medical Abstracts Society. The present study was performed for determining the optimal injection rate of gadovistMR dynamic study.Materials and methods:15 patients underwent brain MRI. Gadovist enhanced MR dynamic study was performed.Gadovist was intravenously administered at injection rate of 1ml/s, 2ml/s and 3ml/s.Dynamic MRI was repeated at 20s.Signal intensity of ROI located in pituitary gland was measured and displayed in dynamic curve.Results:Dynamic curve of 1ml/s tend to increase in signal intensity during injection. Dynamic curve of 2ml/s showed peak time in 40s~60s.Dynamic curve of 3ml/s showed peak time in 20s~60s.Conclusion:Injection rate of 3ml/s was considered as the optimal injection rate for gadovist dyanamic MR.

P-2-010　コモンマーモセットの海馬体とその関連領域の形態的発達
Anatomical Development of Hippocampus and its Related Regions in Common Marmosets

植松　明子（慶應義塾大学大学院 医学研究科 生理学教室）
Akiko Uematsu[1,2,3], Junichi Hata[1,2,3], Yuji Komaki[1,3], Fumiko Seki[1,2,3], Erika Sasaki[1,2,3], Hideyuki Okano[1,2]
[1]Department of Physiology Keio University School of Medicine, [2]RIKEN Brain Science Institute, [3]Central Institute for Experimental Animals

【要旨】本研究ではコモンマーモセットのT2強調・拡散強調画像データを継時的に収集し、発達に伴う海馬体とその関連領域である帯状回、嗅内皮質の形態的発達を検討した。計測部位の体積とMean Diffusivityは月齢とともに非線形的・線形的に変化し、特に生後半年間は細胞密度の上昇や髄鞘化が急速に起こっていることが示唆された。

Hippocampus and its related limbic regions, including entorhinal and cingulate gyrus, play an important role in learning and memory functions. Their morphological and microstructures can be affected by age-related neuropsychiatric disorders and disease such as autism and schizophrenia. Thus, investigating typical development of these regions could serve not only as the key to elucidate the mechanism but also as a normal reference for these disorders or disease. Noninvasive technique, MRI, allow evaluating such developmental changes even within the same subjects.
In this study, we used a nonhuman primate species, common marmosets, as a human model. From normally developing 23 marmosets, we collected longitudinal T2-weighted and diffusion weighted brain images to see age-related changes of the volumes and diffusion tensor imaging (DTI) metrics, which include fractional anisotropy (FA), mean diffusivity(MD), and radial diffusivity (RD), of hippocampus, entorhinal cortex, and cingulate gyrus.
We found polynomial age-related trajectory for the volumes in all the regions. For the DTI metrics, either logarithmic or linear decreases were observed with age in cingulate gyrus and entorhinal cortex. However, in Hippocampus only its MD showed significant change.
Since DTI metrics are known to be correspond with cell density, myelination, and fiber integrity, statistically significant age-related changes of these values indicated the continuous neural development even after postnatal age. Such changes were intense especially during the first half year of life. For marmoset, 6 months old is as old as a human juvenile child before puberty, so this period would be sensitive for morphological and microstructural development of limbic cortex regions for primates including human beings.

P-2-011　コモンマーモセットの脳発達に伴うMagnetization Transfer Ratioの変化
Age-related changes in magnetization transfer ratio with atlas based whole brain analysis in common marmoset development

西尾　真鈴（首都大学東京 健康福祉学部 放射線学科）
Marin Nishio[1,2], Yuji Komaki[2,3], Fumiko Seki[2,3,4], Junichi Hata[2,3,4], Akiko Uematsu[2,3,4], Ryosuke Ishihara[2,3], Ryutaro Yano[2,3], Erika Sasaki[2,3], Akira Furukawa[1]

[1]Tokyo Metropolitan University, [2]Central Institute for Experimental Animals, [3]Keio University, [4]RIKEN

【要旨】Magnetization transfer ratio(MTR)は脳の髄鞘形成を反映することが分かっており発達に伴い増加する。本研究では健常な1-18ヶ月のcommon marmosetを対象にMTRを計測し、発達段階におけるMTRの変化を調べた。視床や内包、帯状束、皮質等でMTRは月齢に伴い増加したため詳細な脳発達を評価するパラメータになり得ると考える。

Magnetization transfer contrast (MTC) is based on exchange of magnetization between protons that are bound to macromolecules and protons in free water. Magnetization transfer ratio (MTR) is a value reflecting the amount of protein such as myelin of nerves in the nervous system. In human, myelination progresses rapidly during infancy and continues through the adolescent stage. A number of studies have suggested that MTR value increases in healthy human brain development.

We calculated MTR images by using non MT images and MTC images of common marmosets from 1 to 18 months. We measured MTR value in a plural region of brain parcels, and assessed the age-related changes of MTR for each region.

Among them, a logarithmic relationship existed between MTR value and age at anterior commissure, cingulum, fimbria of the hippocampus, fornix, internal capsule, superior cerebellar peduncle, and several regions of cerebral cortex.

These results indicate MTR can be a good marker to evaluate the normal brain development of common marmoset, and eventually a suitable parameter to assess brain developmental disorders for neuropathology, diagnosis, and treatments.

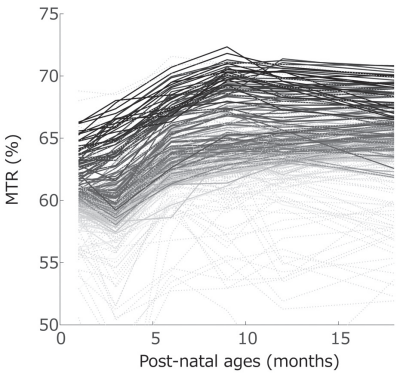

P-2-012　コモンマーモセット脳における標本固定の影響
Postmortem MRI properties of common marmoset brain during formaldehyde-fixed

羽賀　柔（首都大学東京 健康福祉学部 放射線学科）
Yawara Haga[1,2,3], Junichi Hata[2,3,4], Akiko Uematsu[2,3,4], Takaaki Kaneko[2], Yukiko Nagawa[1,2], Marin Nishio[1,3], Yuji Komaki[3,4], Fumiko Seki[3,4], Noriyuki Kishi[2,4], Erika Sasaki[3,4], Hideyuki Okano[2,4], Akira Furukawa[1]

[1]Tokyo Metropolitan University, [2]RIKEN BSI, [3]Central Institute for Experimental Animals, [4]Keio University

【要旨】標本脳MRIは高解像画像を得られるが、固定法や時間によって緩和値は変化することが知られている。本研究では、マーモセットの脳を固定して経時的に撮像し部位による緩和、拡散値の変化を観察した。新たに知見として得られた拡散値では、変化は認められなかった。よって拡散計測では、標本脳での評価も有用であるといえる。

Introduction
The postmortem brain magnetic resonance imaging (MRI) can provide high-resolution images. However, the postmortem tissue's MRI properties are known to change over time by chemical fixation and postmortem interval. Recently, the common marmoset is widely used in neuroscience research. Nonetheless the changes of its postmortem MRI properties are little known. The purpose of this study is to examine MRI properties changes that occur over time in paraformaldehyde (PFA)-fixed marmoset brain.

Method
A healthy common marmoset (adult male 4 years old) was used for this study. The animal was perfused with 4 % PFA and the brain was extracted, immersed into PFA for post-fixation.We collected both *in vivo* and *ex vivo* images using 9.4 T Bruker MRI. Regions of interest (ROI) were selected on thalamus, splenium of corpus callosum, hippocampus and the gray matter near the surface. T1, T2, T2* and the Diffusion values were calculated.

Results
The T1, T2 and T2* values of all ROIs reduced linearly over time. The T2/T1 ratio of the gray matter near the surface had little change. Conversely, that of the others logarithmically decreased. The Diffusion values remained approximately constant though they varied day by day. Comparing with *in vivo* data, the diffusivity values of all ROIs after fixation also changed.

Discussion
The constant reduction of MRI properties indicated in the process of protein cross-linking during the fixation. In addition, the way of reduction T1, T2 and T2* values didn't depend on the regions in the marmoset brain. It suggested that the process of protein cross-linking didn't depend on the distance from the surface in marmoset brain. This information could be useful for assigning acquisition sequence parameters for postmortem MRI.

P-2-013　透明化試薬の違いによるマウス脳への影響
Impacts of difference of transparency reagents on mouse brain

名川友紀子（首都大学東京大学院 人間健康科学研究科）
Yukiko Nagawa[1], Junichi Hata[2,3,4], Akiko Uematsu[2,3,4], Fumiko Seki[3,4], Yuji Komaki[4], Ryutaro Yano[3], Masakazu Sato[2], Ryousuke Ishihara[3], Hideyuki Okano[3], Kazuo Yagi[1], Norio Sekine[1]

[1]Tokyo Metropolitan University Graduate School of Human Health Sciences, [2]RIKEN Brain Science Institute, [3]Keio University Graduate School of Medicine, [4]Central Institute for Experimental Animals

【要旨】全脳の神経連絡を３次元解析する技術の１つである透明脳は注目されており、手法も複数報告されている。本研究ではMRIにて各種試薬による透明脳の特性をFA、ADC、T1、T2といった物理値により評価した。結果、試薬により脳への影響は異なることが示唆され、目的に合わせた透明脳の選択が非常に重要であるといえる。

＜ Introduction ＞
In recent years, the development of the technologies for revealing the whole brain neural networks has been prospered. A noteworthy method is lipid extraction reagent, which increases tissue transparency. There are several technics and methods to clear brain, which may affect differently on the brain tissues. In this study we evaluated the influences of transparent technics on brain with MRI.
＜ Methods ＞
Five transparent reagents Sca*l*eA2, Sca*l*eS, CUBIC, 3DISCO and SeeDB were compared in this study. First, mouse brains were fixed with 4% paraformaldehyde and replaced to phosphate-buffered saline (PBS). These were incubated in each reagent, and lastly replaced them with PBS again. T1, T2-weighted, and Diffusion-weighted MR images with each condition described above and the reagents themselves were acquired. T1 and T2 values, fractional anisotropy (FA), apparent diffusion coefficient (ADC), and lambda values were measured.
＜ Results and Discussion ＞
For the brains treated by water-soluble reagents (Sca*l*eA2, Sca*l*eS and SeeDB), which easily permeated the brain, the influence on T1 and T2 values was strong especially in grey matter (GM). The stronger effect on GM suggested the destruction of cell bodies, which may provide clear microstructural image of fibers inside of GM. Contrarily, like the diffusion metric values of brain soaked in only PBS, the ADC of the brains with organic solvent reagents (3DISCO) showed almost half and the FA was doubled in white matter compared to GM, meaning that the reagent affected uniformly the whole brains. For mixed liquor with water-soluble and organic solvent reagents (CUBIC), the ADC behaved as free water. A possible reason is destruction of cell membranes, compromised for higher degrees of transparency.

P-2-014　超高磁場MRIによる小型霊長類脳構造のマイクロイメージング
Depiction of Neural Microstructures by Ultra High Field MRI

畑　　純一（理化学研究所 脳科学総合研究センター）
Junichi Hata[1,2,3], Akiko Uematsu[1,2,3], Takaaki Kaneko[1,2], Makoto Fukushima[1,2], Fumiko Seki[1,2,3], Yuji Komaki[2,3], Yukiko Nagawa[1], Keigo Hikishima[4], Noriyuki Kishi[1,2,3], Erika Sasaki[1,2,3], Hideyuki Okano[1,2]

[1]RIKEN Brain Science Institute, [2]Keio University School of Medicine, [3]Central Institute for Experimental Animals, [4]Okinawa Institute of Science and Technology Graduate University

【要旨】近年、小型霊長類を用いた脳科学研究が注目を浴びている。本研究では顕微鏡MRI技術を用いることで、切片画像に匹敵する超高解像度イメージを取得し、脳領域の検出を試みた。結果、MRIにて詳細な脳領域を区分けすることが可能となり、今後の小型霊長類の脳科学研究の加速化が期待される。

Growing interest in viral and genetic manipulations on non-human primates brings neuroscientists' attention to marmoset (Callithrix jaccus). However, the question as to what extent the brain of marmoset shares neural architectures with that of humans still remains. To measure neural structures, we investigated and evaluated the image acquired by the MRI microscopic technique with 9.4T Superconductivity magnet to enhance NMR signal, using high slew late gradient system. We obtained the super high resolution T2-star weighted image of a whole marmoset's brain with 60[um]^3 spatial resolution as in the figure. Super high resolution diffusion weighted imaging was also acquired to evaluate the neural microstructures. These results could be substitutions for histology image. Indeed, these images provided clear laminar structures of the cortex and the borders between MT and V4T, V1 and V2. Furthermore, unlike histological sectioning, MRI is free from cutting the tissues and could acquire a 3D volume image. From these points of view, the MRI microscope technique would provide accurate and detailed neural architectures and could be applicable as in vivo histology in the future.

P-2-015　マウス生体脳内における４次元免疫細胞追跡の検討について
Four-dimensional in vivo MRI for tracking individual immune cells in mouse brain

森　　勇樹（大阪大学 免疫学フロンティア研究センター 生体機能イメージング）
Yuki Mori[1,2], Daniela Martinez de la Mora[1,2], Atsuki Tashita[3], Syoji Kobashi[3], Ikuhiro Kida[2], Yutaka Hata[3], Yoshichika Yoshioka[1,2]

[1]Biofunctional Imaging, WPI Immunology Frontier Research Center, Osaka University, [2]Center for Information and Neural Networks, NICT and Osaka University, [3]Graduate School of Engineering, University of Hyogo

【要旨】我々は、11.7T小動物用MRIと超常磁性粒子(SPIO)を用いることで、生体マウス脳内における１細胞レベルの免疫細胞動態を３次元空間＋時間軸(4次元追跡)で視覚化し、移動スピード及びパターンを定量評価することに成功した。脳虚血モデル動物における傷害側と正常側では、標識された免疫細胞の移動パターンに違いがみられた。

Improved imaging techniques are being used to broaden the scope and understanding of the intricate reactions of cells in the body. Previously, we reported that high-field MRI has a possibility to track individual monocytes/macrophages in the living mouse brain with time-lapse movies (Mori, 2014). To interrogate three-dimensional whole brain *in vivo* samples over time (four dimensional, or 4D, imaging), here, we used MRI with intravenously injected superparamagnetic iron oxide particles (SPIO) to create a 4D cellular tracking dataset of intrinsic monocytes/macrophages in the living mouse brain. In addition, we conducted quantitative analysis of individual cells using this dataset. In this procedure, we successfully monitored the dynamic migration of infiltrating monocytes/macrophages in the living mouse brain with a time resolution of 6 minutes/frame and a 3D spatial resolution of 59 μm × 59 μm × 100 μm. Moreover, we found a significant difference in velocity and migration patterns between the contralateral and the ipsilateral cortex in the mouse stroke model. Our novel MRI technique offers a new approach to understand the behavior of immune cells in the healthy and diseased brain.

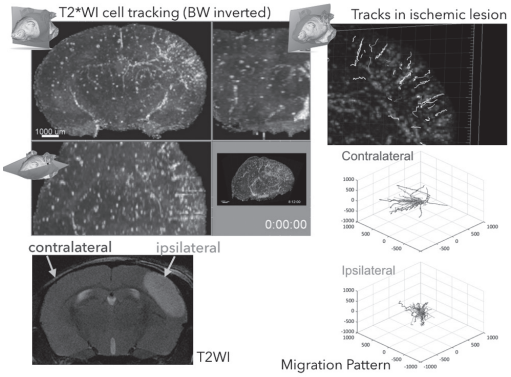

P-2-016　三次元MR組織学的評価法を用いたガドリニウム造影能のマウス系統間の違い
Gd-enhancement differences between mouse strains as shown by 3D MR histology

森　　勇樹（大阪大学 免疫学フロンティア研究センター 生体機能イメージング）
Yuki Mori[1,2], Kiyoyuki Osugi[1,2], Daniela Martinez de la Mora[1,2], Yoshichika Yoshioka[1,2]

[1]Biofunctional Imaging, WPI Immunology Frontier Research Center, Osaka University, [2]Center for Information and Neural Networks, NICT and Osaka University

【要旨】MR Histology（MRIを使った組織学的評価）では、組織標本を切り刻むことなく、多様な構造を３次元で可視化することが可能である。化学固定された標本の場合に、画像コントラストを付与することを目的に常磁性造影剤などを使用するが、同じ動物でも系統が違うことで、各構造の造影能に違いがあることがわかった。

Morphological differences between mouse strains have been studied at the two-dimensional histologic level. Microscopic MRI has a possibility for non-invasive morphological analysis, capable of producing high-resolution 3D images of *ex-vivo* brains, after fixation with an MR contrast agent. In this study, we investigated mouse strain differences in Gd-stained MR microscopy to help the studies of three-dimensional (3D) mouse histology. Three mouse strains (Hos:HR1, C57BL/6J, and Balb/c; 8 week-old, male) were obtained from Japan SLC. MRI images of fixed mouse brain were obtained using an 11.7 T Bruker AVANCE II MRI scanner with 3D-RARE (TR/TE = 80 msec/8.1 msec) and 3D-FLASH pulse sequences (TR/TE = 30 msec/1.5 msec). Spatial resolution was 50 μm × 50 μm × 50 μm. Perfusion fixation and immersion were performed with 4% PFA containing diluted gadoteridol (ProHance). Image analysis was performed using the VivoQuant software and compare the signal intensity in the individual anatomical structure of the brain between mouse strains. In this study, we observed several strain-specific contrast enhancements such as layer structures in the cortex and nuclei.

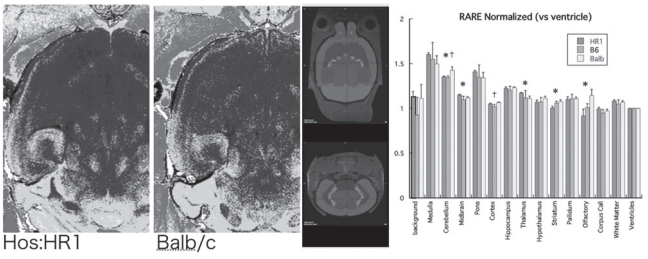

P-2-017　ホルマリン固定胎児標本蝸牛構造描出：臨床機による0.1mm等方性撮像の試み
High resolution 3-D T2-weighted imaging of human fetus

山本　憲（京都大学大学院 医学研究科 放射線医学講座（画像診断学・核医学））
Akira Yamamoto[1], Yasutaka Fushimi[1], Tsutomu Okada[1], Tomohisa Okada[1], Yutaka Yamaguchi[2], Rena Miyazaki[2], Haruyuki Makishima[2], Shigehito Yamada[2], Kaori Togashi[1]
[1]Department of Diagnostic Imaging and Nuclear Medicine, Graduate School of Medicine, Kyoto University, [2]Human Health Sciences, Kyoto University Graduate School of Medicine

【要旨】京都大学医学研究科附属先天異常標本解析センター所蔵の胎児標本を3-T臨床機を用いて、3-D T2強調画像で撮像した。蝸牛構造描出に注目し、臨床機を用いた0.1mm等方性撮像を目指した。

[PURPOSE]To evaluate the fetal development of the inner-ear structure with up to 0.1 mm isotropic 3-D T2WI by clinical 3-T MR scanner. [METHODS]Formalin-fixed fetal samples (SS 15.7 weeks) were scanned with clinical 3-T MRI with 64-ch head-neck coil. Formalin was replaced by PBS for 5 days before scanning. 3-D T2WI was obtained with resolution of 0.2 mm isotropic and also 0.1mm isotropic acquisition was challenged. [RESULTS] 0.2 mm isotropic resolution 3-D T2WI was successfully obtained. Increasing number of acquisition gave a better quality of image and enabled us to evaluate fine structure of inner ear of the developing fetus. 0.1 mm isotropic image shows some image degradation and also requires to improve various parameters to obtain good quality images. [CONCLUSION]Clinical 3-T MRI scanner was used to evaluate the fine structure of the inner ear of developing fetus.

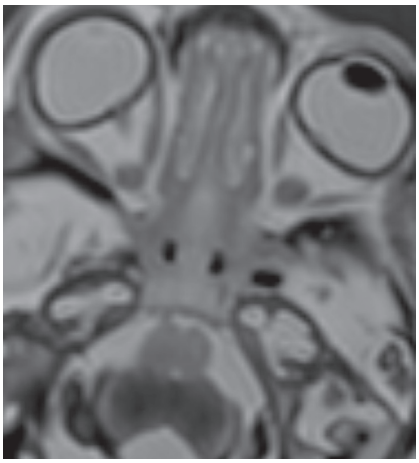

P-2-018　野球肘初期診断用ポータブルMRIの開発
Development of portable MRI for early detection of baseball elbow

田辺　亮勝（筑波大学大学院 数理物質科学研究科 電子・物理工学専攻）
Katsumasa Tanabe[1], Syuhei Oka[1], Yoshikazu Okamoto[2], Katsumi Kose[1], Yasuhiko Terada[1]
[1]Institute of Applied Physics, [2]Comprehensive Human Sciences

【要旨】近年、岡本らは関節用低磁場MRIが野球肘の初期診断に有益であることを示した。ポータブルMRIでそれが可能になれば、遠く離れた野球場でのスクリーニング検査が可能となり、被験者の対象を大幅に広げることができる。そこで本研究では、重量200 kgの0.2 T永久磁石を用いた野球肘診断用ポータブルMRIシステムを開発した。

Okamoto et al. have reported that a low-field MRI system specialized for small joints is useful for early detection of baseball elbow [1]. However, they used the stationary scanner, and the subjects were limited to nearby players. Having a potable elbow MRI would allow MRI screening at a remote baseball ground and expand the availability of the screening. In this study, we developed a portable MRI system for early detection of baseball elbow.We used a 0.2 T permanent magnet (NEOMAX Engineering, Japan; 200 kg; 16 cm gap; 44 cm x 50 cm x 36 cm) (Fig. 1(a)), a home-built RF coil, gradient, and shim coils, which is portable using a hand lift. An MRI console consisted of a digital transceiver (DDRX6, MRTechnology, Japan), a gradient driver (20 V, 10 A, DST Inc., Japan), and a transmitter (150 W, DST Inc., Japan), which were installed in a 19-inch rack (56 cm x 77 cm x 60 cm, 80 kg) (Fig. 1(b)) and portable manually.Fig. 1(c) shows an MRI elbow image of a 22-yr-old male (Fig. 1(d)). The anatomical structures are visible. The image quality is currently being improved by further correcting B0 inhomogeneity and shielding external noises.[1] Y. Okamoto et al., ISMRM2015, p1212.

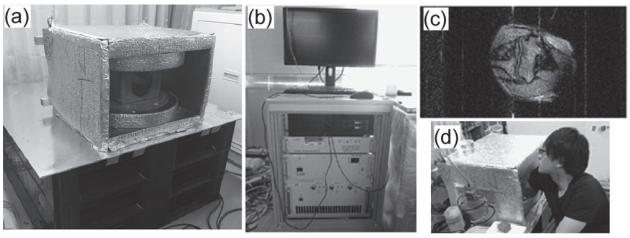

Fig. 1: (a), (b) Portable elbow MRI system. (c) MRI elbow image (Multislice gradient echo, coronal, FOV = 256 mm x 128 mm, slice thickness = 3 mm, TR = 500 ms, TE = 16 ms, FA = 75, Scan time = 2 min 4 s, Matrix size = 256 x 128.) (d) MRI examination.

P-2-019　MRI simulatorの可能性と問題点
Potential and Problems of MRI simulators

巨瀬　勝美（筑波大学 数理物質系 物理工学域）
Katsumi Kose[1], Ryoichi Kose[2]
[1]Institute of Applied Physics, University of Tsukuba, [2]MRTechnology Inc.

【要旨】GPUの進化に伴い，現実的なMR撮像プロセスの再現に不可欠な10^7個以上の核磁化の計算が実用化目前にある．このようなMRI simulatorは，MRIの研究と開発に不可欠なツールになると期待されているが，現状では，まだ問題点も多い．そこで，本研究では，その可能性と問題点についての検討を行った．

Introduction
With recent progress of high performance computing using GPUs, computation of 10^7 (~256^3) spin isochromats has become practical using a desktop PC. MRI simulators will be an indispensable tool for MRI studies and developments, but there are still many problems to be overcome.
Potential and Problems of MRI simulators
Potential of simulators is (1) any experimental conditions can be tested, (2) motion of any spin isochromats can be known, (3) calculation times are faster than that of experiments for small number (<10^7) spin systems, (4) cost of simulators is much less than that of real MRI systems.
Problems of simulators are (1) realistic digital phantoms are difficult to construct, (2) some parameters are difficult to simulate (T_2*, diffusion), (3) approximation of continuous object using a discrete matrix produce numeric errors, (4) interface between experiments and simulators is generally difficult, and so on.
Discussion and Conclusion
Because cost performance of GPUs is about two orders better than that of CPUs, a PC with one to several GPUs is sufficient for MRI simulators. If the above problems are solved, MRI simulators will accelerate MRI studies and developments.

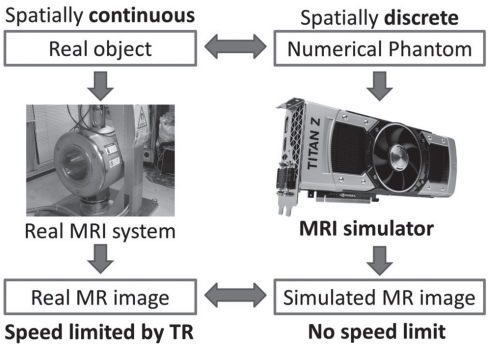

P-2-020　GPUに最適化した汎用MRIシミュレータの開発
GPU optimized general purpose MRI simulator

巨瀬　亮一（株式会社 エム・アール・テクノロジー）
Ryoichi Kose[1], Katsumi Kose[2]
[1]MRTechnolocy Inc., [2]University of Tsukuba

【要旨】MRIシステムの発展とシーケンスの高度化に伴い，撮像プロセスを正確に再現するシミュレータが渇望されている．これに関しては，多くの試みがなされ，ソースコードが公開されたものもあるが，シーケンスが限定され，計算速度が不十分であった．そこで，本研究では，これらの問題を解決するシミュレータを開発した．

Introduction
With progress of MRI hardware and pulse sequences, MRI simulators are eagerly desired. Up to now, several simulators have been proposed but available pulse sequences and system parameters were limited and the processing speeds for large image matrices were impractical. In this study, we developed an MRI simulator (TrueBlochSolver) to solve these problems.
Materials and Methods
We developed the simulator using a GPU (GTX TITAN-Z) and CUDA. For comparison, imaging experiments were performed using an MRI system with a 9.4T/54mm bore superconducting magnet.
Results and Discussion
Fig.1 shows B_0, B_1, PD, and T_1 maps of a water phantom measured and used for the calculation. Fig.2 shows cross-sections measured and calculated with the 2D multiple SE, 3D FLASH, 3D GRASS, and 3D balanced SSFP sequences. The calculated images well reproduced the measured images (matrix: 256^2 (2D) and $256^2 \times 128$ (3D)) by quadrupling the matrix size of the numerical phantom along the readout direction for the calculation ($1024 \times 256 \times 128$: 3D) with about half calculation times compared with the experiments. Image contrast can be more precisely reproduced by considering diffusion effects.

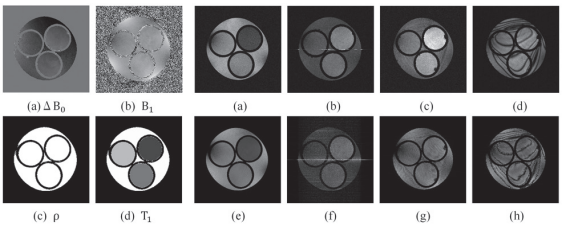

Fig.1 Numerical phantom
Fig.2 Acquired images (upper) and calculated images (lower).
(a), (e) : Multiple SE (2000/80). (b), (f) : 3D FLASH (20/10/30°).
(c), (g) : 3D GRASS (20/10/30°). (d), (h) : 3D b-SSFP (20/10/60°)

P-2-021　汎用PCで制御するNMR/MRI用デジタルトランシーバを多チャンネル化するハブユニットの開発
Development of a multi-channel hub-unit for 8 digital transceivers using a console-PC and software for NMR/MRI

拝師　智之（株式会社エム・アール・テクノロジー）
Tomoyuki Haishi[1], Seitaro Hashimoto[2], Hisao Mizukami[3], Hiroshi Hasegawa[3], Masaru Aoki[3]
[1]MRTechnology, Inc, [2]EXA Corporation, [3]Digital Signal Technology, Inc.

【要旨】NMR/MRIの送信系、受信系、およびG駆動系の多チャンネル化を目的として、2～8台の小型のデジタルトランシーバーを1台の汎用PCから同期制御するためのHUB(ハブ)-UNITを開発した。送信I/Q は2系統、受信I/Qは最大8系統、G駆動系GX/GY/GZは2系統で、TR=40msの撮像ができた。

A new MRI pulse sequence and its image reconstruction have become more complex with using medical scanners of 1.5/3T. A research MRI console to be used in such basic sciences, because it is necessary to meet both various B0 and NMR nuclei, doubling implementation of I/O hardware function are not easy. In order to accomplish a multi-channel function for TX, RX, and gradients simultaneously, we have developed an hub-unit which performs synchronized operation of eight indivisual small digital MRI transceivers.

For the connection between a control for PC (Core-i7, Win10) and up to eight of digital MRI transceivers (Ref.1, DTRX6), we have developed the hub-unit (Fig.1). Two same I/O boards (PCIe-6536, NI Inc., 25MHz) were installed in the PC. The MRI transceivers were synchronized by a 10MHz standard.

As a result, the rf transmission has become of 2 I/Q-systems (32 bit x2), the rf receiver has becomeof 2 to 8 I/Q-systems (32 bit x 2~8), the gradient driver channels has become of two GX/GY/GZ-systems (48bit x 2). With using an imaging sequence of a repetition time TR = 40 ms and simultaneously driving the DTRX6 transceiers of three, imaging experiments were succesfully performed.

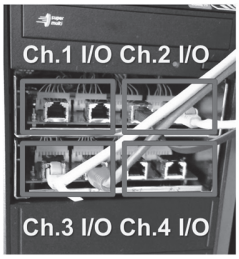

Fig.1. Multi-channel hub-unit installed at 5-inch bays of a control PC (Core-i7, Win10). Up to 8 digital transceivers are able to be connected and controlled simultaneously.

Ref.1 Hashimoto et al., Development of a pulse programmer for magnetic resonance imaging using a personal computer and a high-speed digital input–output board, Rev. Sci. Instrum. 83 (2012)

P-2-022　400MHzまでのMRI信号をアンダーサンプリングでデジタル化するAD変換ヘッドと光接続リンクの開発
Development of a fast analog-to-digital converter-haed performing rf under-sampling of MRI signals and an optical fiber link upto 400MHz

拝師　智之（株式会社エム・アール・テクノロジー）
Tomoyuki Haishi[1], Shin-ichi Morisaka[2], Hiroshi Hasegawa[3], Masaru Aoki[3]
[1]MRTechnology, Inc, [2]Morisaka lab., [3]Digital Signal Technology, Inc.

【要旨】受信コイル直下でMRI信号をデジタル化するトランシーバーを開発した。高速AD変換チップをアンダーサンプリング動作させ1GHzまで受信対応し、光ファイバー伝送によってノイズ混入を最小化した。超高速DA変換チップは600MHzまでの送信信号を生成した。9.4Tの撮像比較で従来装置以上の性能を確認できた。

Major requirements for a signal receiving subsystem in research MRI consoles are, a dynamic range, SNR, and tuning function to destinated NMR frequencies. In order to avoid degradation of receiving MR signals, it is desired to digitize MRI signals just near by a RX coil and then to transfer the signal data through an optical-fiber connection to the console as preventing a contamination with noises running on shielding metal wires. To achieve the above motivation, we have developed a high-speed AD converter head and optical fiber link.

A digital MRI transceiver (Ref.1) using a PC (Win10, Core-i7) was remodeled to have a wide frequency bandwidth with using the over-sampling ADC head. On the receiving side, the AD converter chip was AD9683 (14BIT, 250MSPS), and the optical fiber module was BR-59R5LZ (4.25GBd). On the transmittion side, the DA converter was AD9144 (16BIT, 2.8GSPS).

As a result, the lower power limit of MRI signal as an input sigal was -70dBm, and the dynamic ranges at a frequency of 64MHz, 123.5MHz, and 400MHz were about 80dB (Fig.1). It was also successful in imaging experiments of watetr phantom (Fig.2) at ^{1}H-400 MHz.

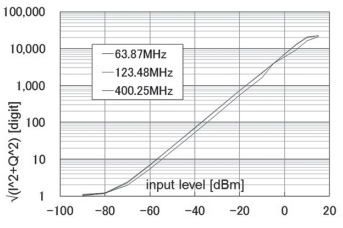

Fig.1. Dynamic range of ADC head @140MSPS

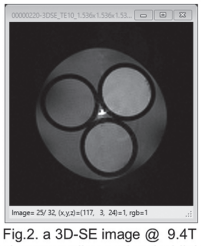

Fig.2. a 3D-SE image @ 9.4T w/ oversampling and optical-link

Ref.1 Hashimoto et al., Development of a pulse programmer for magnetic resonance imaging using a personal computer and a high-speed digital input–output board, Rev. Sci. Instrum. 83 (2012)

P-2-023　4チャンネルRFシミングを用いた，頸椎撮像での部分領域に対するB1+不均一低減効果の検討
Reduction of B1+ Inhomogeneity Using 4-channel RF Shimming for Partial Region in Cervical Spine Imaging at 3T

金子　幸生（株式会社日立製作所 研究開発グループ）
Yukio Kaneko[1], Kosuke Ito[2], Masahiro Takizawa[2], Yoshihisa Soutome[1], Hideta Habara[2], Yusuke Seki[1], Tetsuhiko Takahashi[2], Yoshitaka Bito[2], Hisaaki Ochi[1]

[1]Research & Development Group, Hitachi, Ltd., [2]Healthcare Business Unit, Hitachi, Ltd.

【要旨】3Tにおける脊椎撮像を想定し，脊椎を含む部分領域に対する4チャンネル(ch)のRFシミングの効果を明らかにすることを目的とする。4chのRF照射コイルモデルおよび人体モデルを用いて，電磁界シミュレーションを行った。結果，部分領域の設定時において，4chのRFシミングによるB_1^+不均一低減効果が大きくなることが示された。

PURPOSE
As the strength of a static magnetic field increases, the B_1^+ inhomogeneity in a human body increases. Various multi-channel RF transmission techniques for reducing B_1^+ inhomogeneity have recently been developed. One of these methods, RF shimming, is currently used in commercial MRI systems. The effect of the number of RF transmit channels (ch) has been investigated numerically and experimentally [1-5]. However, the effect for cervical spine (C-spine) imaging, especially for the partial region, has not yet been investigated. In this study, the effect of the number of RF transmit channels between 2ch and 4ch regional RF shimming for C-spine imaging was investigated.
METHODS
The spatial distributions of B_1^+ in the human model were calculated using an electromagnetic simulation tool. A four-channel coil was used for RF transmission [6]. The RF transmission mode was QD / 2ch RF shimming / 4ch RF shimming. The whole Region of Interest (ROI) covered the entire neck region, and the partial ROI covered the region where the C-spine exists. The value of B_1^+ inhomogeneity (U_{SD}) was defined as the standard deviation divided by the average of B_1^+. The U_{SD} in whole ROI / partial ROI was optimized.
RESULTS
The U_{SD} in 4ch RF shimming is about 20% smaller than that in 2ch RF shimming for the partial ROI. The U_{SD} in 4ch RF shimming for the partial ROI is about 10% smaller than that in 4ch RF shimming for the whole ROI. It is shown that 4ch RF shimming for the partial ROI can contribute to reducing the B_1^+ inhomogeneity.
REFERENCES
[1] Harvey PR.et al. ISMRM 2010; 18: 1486. [2] Childs AS. et al. MAGMA 2013; 26: 401-410. [3] Kaneko, et al. ISMRM 2013; 21: 2756. [4] Ito K, et al. ISMRM 2014; 22: 942. [5] Kaneko Y, et al. ISMRM 2016; 24: 2167. [6] Soutome, et al. ISMRM 2013; 21: 2750.

P-2-024　同一容量のリングキャパシタを用いた楕円バードケージコイルの開発
Elliptical Birdcage Coil with Identical Ring Capacitor Value

五月女悦久（株式会社日立製作所 研究開発グループ）
Yoshihisa Soutome[1], Shin-ichiro Suzuki[2], Hideta Habara[2], Takahide Shimoda[2], Yoshitaka Bito[2]

[1]Research & Development Group, Hitachi, Ltd., [2]Healthcare Business Unit, Hitachi, Ltd.

【要旨】楕円バードケージコイルが均一なB1+分布を生成するにはリングキャパシタの値を位置に応じて連続的に変化させる必要がある。しかし実際のキャパシタ値は離散的で調整が困難である。そこで同じキャパシタ値をもった楕円バードケージコイルを考案しファントム評価により均一度6%(30cm FOV)を示す均一なB1+分布を得た。

Introduction: The ring capacitor value of an elliptical birdcage coil (EBC) must be changed gradually according to the location of the capacitor in order to operate in correct oscillation mode. However, it is difficult to adjust the capacitor value precisely by using fixed capacitor value because an actual capacitor has discretized value. We have designed EBC with identical ring capacitor and evaluated it at 1.5T.
Method: The designed coil has rungs with different widths and intervals. We have found that the designed coil has the oscillation mode which generates uniform circularly polarized magnetic field by adjusting the number, width and interval of rungs.
Results: Results from electromagnetic simulation showed that the uniformity of B_1^+ field distribution was 4% in the 30 cm FOV under unloaded condition. There were no differences of transmit efficiency and B_1^+ uniformity between EBC with identical ring capacitor value and EBC with different ring capacitor values. Oil phantom studies showed that B_1^+ uniformity was 6% in the 30 cm FOV. These results demonstrated that EBC with identical ring capacitor value can generate uniform circularly-polarized magnetic field.

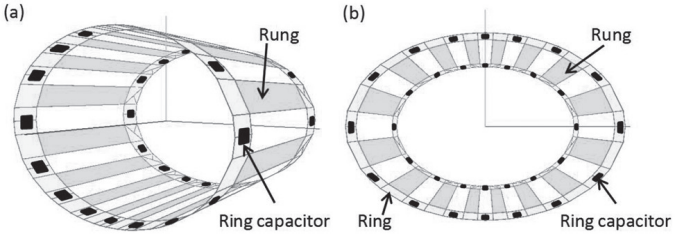

Fig. 1 Elliptical birdcage coil with identical ring capacitor value
((a) side perspective view, (b) front perspective view)

P-2-025　ワイドボアMRI向け分割型照射ボディコイルの電磁界解析
Electromagnetic Field Analysis of Split Transmit Body Coil for Wide-bore MRI

五月女悦久（株式会社日立製作所 研究開発グループ）
Yoshihisa Soutome[1], Hisaaki Ochi[1], Yoshitaka Bito[2]
[1]Research & Development Group, Hitachi, Ltd., [2]Healthcare Business Unit, Hitachi, Ltd.

【要旨】照射ボディコイルを上下に分割することで、よりワイドなMRIのボアが実現できる。そこで、バードケージコイルとTEMコイルを上下に分割して組合せた分割型照射ボディコイルを検討し電磁界解析を行った。その結果、QD照射が可能で、均一度6.5%(30cm FOV)を示す均一なB1+分布が照射できることを確認した。

Introduction: Recently, wide-bore MRI system has been developed. When a transmit body coil is split, the bore size in the horizontal direction can be increased furthermore. To realize wider bore, we have designed a split transmit body coil as shown in Fig. 1 and evaluated it at 3T using electromagnetic field simulator.
Method: The split transmit body coil is composed of split birdcage and split TEM coils as shown in Fig. 1. The split birdcage and the split TEM coil are decoupled each other because the transmit magnetic field of the split birdcage is orthogonal to that of the split TEM coil. The split transmit body coil can generate a circularly polarized magnetic field (B_1^+) when a quadrature drive signal is applied.
Results: When the quadrature drive signal is applied to the split transmit body coil, the transmit efficiency of the coil was increased by a factor of 1.4 compared to the transmit efficiency when the signal was applied to the split birdcage or the split TEM coil. NEMA uniformity of B_1^+ field distribution was 6.5% in the 30 cm FOV under unloaded condition. We have demonstrated that the split transmit body coil can generate uniform circularly-polarized magnetic field.

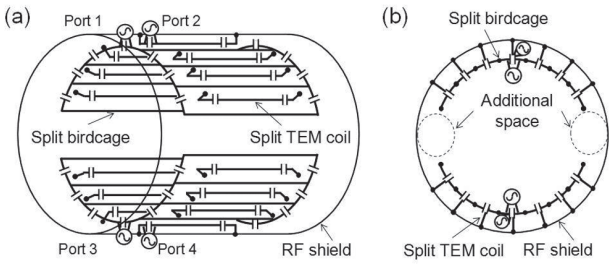

Fig. 1 Split transmit body coil ((a) side perspective view, (b) front view)

P-2-026　3T高磁場MRIにおける32ch 頭部用コイルの開発
Development of 32ch Head receiver coil for 3T high-field MRI

加藤　和之（株式会社日立製作所 ヘルスケアビジネスユニット）
Kazuyuki Kato[1], Takeshi Taniguchi[1], Takahide Shimoda[1], Koenig Steven[2], Napier Christophor[2]
[1]Healthcare Business Unit, Hitachi, Ltd., [2]Hitachi Medical Systems America, Inc.

【要旨】3T頭部撮像では、3Tの高SNRの特徴を生かし、Functional MRIや、3D高空間分解能撮像などが行われているが、撮像時間短縮や、さらなる高空間分解能撮像の要求があり、今回32ch 頭部用コイルを開発した。開発した受信コイルでは、3T 頭部用コイルに比べ均一度は低下したが、コイル周辺部最大2.5倍の感度（自社比）となった。

[Purpose]
3-tesla MRI systems are useful for functional MRI, 3D high resolution imaging and other high SNR (Signal to Noise Ratio) required imaging. Clinical sites have demanded to have more benefit of 3-tesla MRI with following challenges.
- Scan time becomes half with keeping equal image quality
- Images become high resolution with keeping same SNR and scan time

32 channel head coil is developed to satisfy these requirements.
[Methods]
The developed receiver coil is configured with 32 elements of surface coil. The target sensitivity is 1.4 times than the conventional head coil. The target coverage is between the top of head and the cerebellum for US 95% human size. The inner shape of the coil has been considered to apply a goggle and a headphone for functional MRI.The coil performance is acquired in a phantom as fundamental studies.
[Results]
The developed receiver coil obtains 1.36 times sensitivity for center and up to 2.5 times sensitivity around coil surface than the conventional head coil. On the other hand, the result indicates that the optimized sensitivity correction algorithm is required to obtain homogeneous images because of the steep sensitivity map.

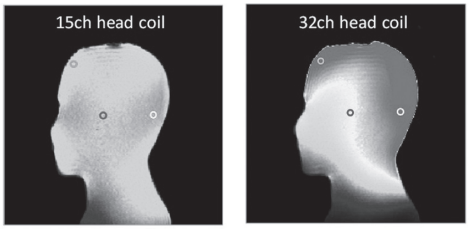

Location	Sensitivity of 15ch	Sensitivity of 32ch	32ch／15ch
○	100	136	1.36 times
○	112	192	1.71 times
○	96	240	2.5 times
The sensitivity is normalized by the value of 15ch center			

P-2-027　32チャンネル頭部用コイルにおける撮像プロトコルの最適化
Optimization of scan protocol for 32ch Head receiver coil

立花　美紀（株式会社 日立製作所 ヘルスケアビジネスユニット）
Miki Tachibana, Kuniaki Harada, Ryuji Shirase, Takeshi Taniguchi, Takahide Shimoda, Kazuyuki Kato, Yasuhiro Kamada, Chikako Moriwake
Healthcare Business Unit, Hitachi, Ltd.

【要旨】3T装置を対象とした32チャンネル頭部用コイルを開発した。受信コイルの感度向上により、健常ボランティアの頭部撮像において、当社15チャンネルコイルに比較してSNRが中心部で約1.2倍、表面部で1.5倍程度向上することを確認した。頭部ルーチン撮像プロトコルの高精細化および高速化に寄与する。

[Purpose] 32ch head coil is usually used for functional MRI etc. utilizing the high sensitivity near cortical area. We have developed new 32ch head coil to be utilized for brain routine examinations. We have optimized scan parameters and confirm 32ch head coil is able to get higher spatial resolution and/or shorter scan time compared to the conventional 15ch head coil.
[Methods] A 3T scanner (Hitachi, Ltd., Tokyo, Japan) was used. Healthy volunteers were evaluated after informed written consent was obtained in accordance with our institutional review board guidelines. 32ch and 15ch head coil were used. Sequence parameters were:
FIR T1WI AX. FOV = 220mm, Thickness = 5.0mm, 20 slices, TR/TE/TI = 3620/12/1300ms. SNR and CNR of the resulted images using both coils were calculated and compared. SNR was calculated by the identical ROI method (1) and CNR between CSF and white matter was calculated by the between tissues method by using background noise (2):
(1) SNR = SIa / SDa　(2) CNR = (Sib - Sic) / SDair
Further, sequence parameters were adjusted as:
a) Half scan time while keeping image quality of 15ch.
b) Higher spatial resolution while keeping SNR of 15ch.
c) Higher CNR while keeping scan time of 15ch.
[Results] We have confirmed that the 32ch head coil shows 1.2times higher SNR at the centre of the head, 1.5 times higher SNR at the surface and twice higher CNR compared to those of the 15ch coil. We have optimized the head routine protocol as it can achieve higher spatial resolution or shorter scan time compared with 15ch coil.
[Conclusions] The newly developed 32ch head coil will contribute to obtain higher spatial resolution, and/or shorter scan time at the conventional head routine protocol compared with the 15ch head coil.

P-2-028　7T 装置における8ch送信コイルと2ch送信コイルによるB1+分布の比較
Comparison of B1+ distribution between 8ch and 2ch RF transmit coils at 7T

松田　豪（岩手医科大学 医歯薬総合研究所 超高磁場MRI診断・病態研究部門）
Tsuyoshi Matsuda[1], Tsuyoshi Metoki[1], Yuji Iwadate[2], Hiroyuki Kameda[3], Taisuke Harada[3], Kohsuke Kudo[3], Makoto Sasaki[1]
[1]Iwate Medical University. Division of Ultrahigh Field MRI, Institute for Biomedical Sciences., [2]GE Healthcare Japan Corporation. MR Applications and Workflow., [3]Hokkaido University Hospital. Department of Diagnostic and Interventional Radiology.

【要旨】7T MRIにおいて8ch送信コイルと2ch送信コイルをもちいて、ボランティアとファントムでB1+分布を測定した。CP modeのB1+分布は8ch送信コイルと2ch送信コイルでは異なる特性であった。pTx modeでは8ch送信コイルの均一性は高かった。特性を理解して適切に使用することが必要である。

[Purpose] Multichannel RF transmit (Tx) systems are considered to optimize properties of the B1+ field at ultrahigh field such as 7T. Although 8ch and 2ch Tx coils are now available for human studies, the performances for improving B1+ fields remain unknown. Hence, we compared B1+ distributions of the phantom and human volunteers by using the two kinds of Tx coils at 7T.
[Methods] We used a 7T MRI system (Discovery MR950, GE Healthcare) and 8chTx/32chRx and 2chTx/32chRx coils (Nova Medical). After obtaining an approval of the institutional ethical committee, a GE MRS phantom and two healthy volunteers were examined by using RF-spoiled gradient-echo (SPGR) acquisitions. We calculated B1+ field maps of the phantom by the two kinds of coils on the circular polarization (CP) mode from varied TRs as well as on the parallel transmit (pTx) mode. In addition, the B1+ field maps of the volunteers on the CP mode using the actual flip-angle (AFI) method with TRs of 25ms and 125ms were obtained and were then compared between the coils.
[Results] The uniformity of the B1+ field measured by the standard deviation of the B1+ distribution in the phantom was improved by the 8ch Tx coil with the pTx mode when compared with other conditions. In the volunteers, the area of the B1+ field by the 8ch Tx coil was increased in the magnetic field direction; however, the uniformity tended to be decreased in the anteroposterior direction.
[Conclusion] The distribution of the B1+ field was different between the multichannel Tx coils and can be improved by using the pTx technique. Appropriate use with a full understanding of the characteristics of the multichannel coils can improve B1+ distributions at 7T.

P-2-029　快適性を考慮した頭部用RFコイルの開発
Development of the Head Coil with Comfort Design

今井　聡志（東芝メディカルシステムズ株式会社）
Satoshi Imai[1], Sadanori Tomiha[1], Zachary Bauer[2], Xiaoyu Yang[2], Hiroyuki Fujita[2,3,4], Shinji Mitsui[1]
[1]Toshiba Medical Systems Corporation, [2]Quality Electrodynamics, LLC, [3]Case Western Reserve University, [4]The University of Queensland

【要旨】MRIで用いられる既存の頭部用RFコイル(Atlas SPEEDER Head)に対して，患者快適性（開放感）を改善した3.0T用の頭部用RFコイルを開発し，比較評価を行った．既存のRFコイルに対して，視野角が約1.4倍、SNRが約1.2倍、SPEEDER性能も同等以上の性能となった。

[Purpose] RF coils used in MRI are specifically designed for each anatomical region of interest and are attached directly to the patients. With this background, patient comfort is important in RF coil design as it results in reducing patient motion and claustrophobia. In addition, high level of openness or visibility is required for the design of RF coil for head (head coil). Therefore, we developed a head coil for 3T (Atlas SPEEDER Head/Neck) with improved performance in terms of above mentioned characteristics. In this study, we report the evaluation result.
[Method] We evaluated the openness in comparison with the conventional head coil (Atlas SPEEDER Head) as well as SNR, and parallel imaging (SPEEDER) acceleration factor to confirm the open design does not impact the RF coil performance. Openness was evaluated by view angle of the subject being tested. Phantom images were acquired from the position corresponding to the area from head to chest. The SNR of the center of the phantom in the transaxial plane was measured. For the evaluation of SPEEDER, g-factor was calculated with the fixed SPEEDER factor (=2). The evaluation was conducted on a 3T MRI system (Toshiba Medical Systems).
[Result] The view angle is about 1.4 times wide compared to the existing head coil, which results in high level of openness. SNR is about 1.2 times better than that of the conventional head coil. The g-factor was improved in the regions from neck to chest. The reason is thought to be due to the optimization of coil element position.
[Conclusion] We developed head coil which provide patient comfort with wider view angle and same or better performance compared with conventional coil image quality. The wider view angle allows to reduce motion and claustrophobia.

P-2-030　磁石回転型Field Cycle MRIにおけるEddy Currentの効果と補正
Correction for eddy current effect of field cycle MRI using rotary magnet

小林　竜馬（九州大学 先端融合医療レドックスナビ研究拠点）
Ryoma Kobayashi[1], Hideo Utsumi[2]
[1]Innovation center for medical redox navigation, Kyushu University, [2]ReMI Co,.LTD.

【要旨】DNP-MRIのための新しいField cycle法として磁石回転型装置を提案し開発した。強弱2つの磁石を回転させることで磁場強度を変更しながらMRI撮像することに成功した。磁束密度が時間変化するため、装置内にEddy Currentが生じる。その効果の定量と補正方法について詳細を報告する。

DNP-MRI is the system with high future growth potential for imaging of free radical and redox state in vivo. The imaging method has the electron spin excitation before MRI Imaging. However the electron spin has high frequency for excitation. Because of limited penetration depth for radio frequency, there is the serious problem that is inhomogeneously excited of electron spins in vivo.Therefore the magnetic field cycle method was suggested, for example, "magnetic field switching using the electric magnet" or "sample transportation between two permanent magnets". However they have several problems for clinical application.We suggest a new field cycle method using rotation system that has 0.3T and 13.5mT magnets. The eddy current is attributed to time dependent of magnetic flux density because of magnet rotation.We report the measurement and the correction of the effect of eddy current.

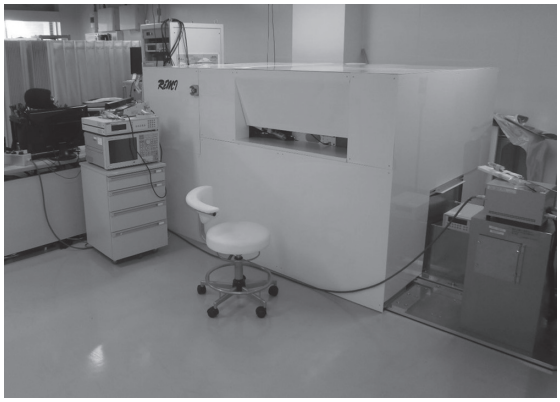

P-2-031　打ち切り特異値分解正則化計算を用いたMRI用磁石用シミング計算手法(HiSHIM)の開発
Magnetic Field Shimming Calculation (HiSHIM) Using TSVD Regularization With Descritization and Limitation of Iron Pieces Placements

阿部　充志（日立製作所 研究開発グループ エネルギーイノベーションセンタ）
Mitsushi Abe[1], Kenji Sakakibara[2]
[1]Hitachi, Ltd.,Research & Development Group, Center of Technology Innovation - Energy, [2]Hitachi, Ltd. Healthcare Business Unit

【要旨】打ち切り特異値分解による正則化演算を用いて、静磁場分布を均一化するシミング作業時に鉄片などの磁気モーメント配置を計算するシミング計算手法(HiSHIM)を開発した。鉄配置を考慮して計算した磁場分布をシミング後に実現できることを実機にて確認した。

A new shimming calculation method (HiSHIM) has been developed and the validity has been confirmed by test magnetic shimming works. The technique based on the truncated singular value decomposition (SVD) to solve a linear equation with a response matrix from iron piece volumes in shim tray pockets to magnetic fields on the volume of interest. SVD obtains eigenmodes which are numbered in descending sequence of the singular values. Low ordered eigenmodes are chosen considering the number of the main coil blocks in the magnet and their strengths are tuned. The shimming calculation treats integerizations of the number of iron plates and limitations of the iron volumes at pockets. High ordered eigenmodes, which have little magnetic field, are utilized to make the iron volumes within the limitations in each pocket using iterative calculations. HiSHIM can, not only calculate the iron piece placements but also predict the shimmed magnetic field distribution from the measured magnetic field distribution. By test shimming works, iron pieces were placed according to the calculation and well shimmed magnetic fields with good homogeneities were obtained. The shimmed magnetic fields agreed well with those that the predicted magnetic fields by the shimming calculation, showing that the shimming calculation works well.

P-2-032　MRI用磁石のシミング計算手法HiSHIMの装置適用
Applications to MRI magnets of shimming calculation method HiSHIM

榊原　健二（株式会社日立製作所 ヘルスケアビジネスユニット）
Kenji Sakakibara[1], Mitsushi Abe[2], Hikaru Hanada[1], Takuya Fujikawa[1], Akihiro Shimada[1]
[1]Hitachi, Ltd. Healthcare Business Unit, [2]Hitachi, Ltd., Research & Development Group, Center of Technology Innovation - Energy

【要旨】新シミング計算手法(HiSHIM)を、MRI装置の静磁場分布を均一化する作業に適用した。本手法は、打ち切り特異値分解による正則化演算を用いた点と複数種磁石に汎用的に適用できる特徴がある。その結果、粗調整/微調整の2つの過程でのシミングが可能になり、より少ない鉄量で目標の磁場均一度を達成した。

A new calculation technique (HiSHIM) based on the truncated singular value decomposition (SVD) is applied for the magnetic field shimming of the whole body magnetic resonance imaging (MRI) system. SVD obtains eigenmodes which are numbered in descending sequence of the singular values and this new shimming calculation technique has the characteristics below. 1) By selecting the Low ordered eigenmodes, which has the larger singular values, the shimming can be completed more effectively with less amount of the used shim irons. 2) The High ordered eigenmodes, which have little magnetic field, are utilized to make the iron volumes within the limitations in each shim pocket using iterative calculations. 3) Computational time at the shimming work is short. By utilizing the above merits, this method can divide the shimming process into two steps; "The Coarse shimming" in which the repeated magnet ramping is required and "the Fine shimming" in which the shimming can be performed with the small amount of shim irons under the magnetic field. As a result, in Hitachi whole body MRI system, this new shimming calculation technique can provide the reduction in the installation time of the MRI system by reducing the repeats of the magnet ramping and the shortened time of the shimming work. Additionally, less amount of the used shim iron can improve the image quality of the MRI system.

P-2-033　DUCASによる楕円傾斜磁場コイルパターン最適化設計手法の検討
Study of optimal design of oval shaped gradient coil pattern using DUCAS

今村　幸信（株式会社 日立製作所 研究開発グループ）
Yukinobu Imamura[1], Takeshi Kawamura[1], Tatsuhiko Kawakami[1], Mitsushi Abe[1], Akira Kurome[2], Shin Hoshino[2]

[1]Hitachi, Ltd. Research & Development Group, [2]Hitachi, Ltd. Healthcare Business Unit

【要旨】任意形状コイルパターン設計ツールDUCASを用い楕円形状の傾斜磁場コイルパターンを試設計した。本研究では多数の電流ポテンシャル分布の初期値に対してコイルパターンを計算し、磁場性能と電気性能および製作性に優れた結果を選択する。また、多数の結果より線形性とインダクタンスの関係と限界値が明らかとなった。

[Purpose]For oval shaped gradient magnetic field coil, it was examined excellent coil pattern to magnetic field and electrical performance and productivity by using the arbitrary magnetic field coil design tool DUCAS. Also, to compare the performance of coil pattern design by continuous current distribution and discretized actual production. [Methods]In DUCAS, coil pattern was obtained as current potential distribution by superposition of eigenmodes based on singular value decomposition. Current potential distribution is determined by least-square method, coil pattern is in infinite with respect to the combination of basis function and coefficient. Especially, in the design of active shield type (ASGC), eigenmodes are repeatedly superimposed until required magnetic field performance while suppressing leakage magnetic field. As excellent coil pattern was depend on initial state of current potential distribution, it was important experience of designer and trial and error in actual coil pattern design. In this study, a large number of initial current potential (approximately 5000) was generated, and coil pattern was calculated for each initial value. Moreover, the resulting current potential distribution was discretized with line or surface current model with actual conductor shape, and its magnetic field and inductance were compared with the values of current potential.[Results]As a large number of results were organized, coil's inductance was in a contradictory relation with respect to its linearity, and it was found that there is a limit value in inductance for gradient magnetic field. Also, in the discretized coil pattern for current potential, inductance was increased by approximately 8 percent. On the other hand, deterioration of the linearity was about 0.5 percent.

P-2-034　1.5T/280mm水平開口型超伝導磁石のための挿入型勾配磁場コイルの開発
Development of an insertable gradient coil for a 1.5T/280mm horizontal bore superconducting magnet

矢野　順也（筑波大学 数理物質科学研究科 電子・物理工学専攻）
Junya Yano, Yuta Kobayashi, Yasuhiko Terada, Katsumi Kose

Master's Program in Applied Physics, Graduation School of Pure and Applied S cences, University of Tsukuba

【要旨】勾配磁場コイルの性能は幾何学的サイズに大きく依存するため，撮像対象に最適なものを使用することが望ましい．そこで本研究では，マウスやラットなどの小動物を主な撮像対象とし，均一領域を直径60mm球とした勾配磁場コイルをTarget Field法で設計し，1.5T/280mmの水平開口超伝導磁石に実装してその有用性を検証した．

IntroductionBecause gradient coil performance considerably depends on the geometrical size of the gradient coil, it is desirable to use an optimum size gradient coil. In this study, we developed an insertable gradient coil for mice and rats that can be used in a 1.5T/280mm horizontal bore superconducting magnet.Materials and MethodsWe designed the gradient coil using the target field method. The designed and calculated parameters were as follows: diameter = 96, 98.7, and 101.4 mm, number of turns = 48, 48, and 40, efficiency = 4.99, 4.86, and 5.25 mT/m/A for Gx, Gy, and Gz. The gradient coils were wound over an acrylic pipe (95 mm OD) using 0.8 mm diameter PU coated Cu wire.Results and DiscussionFig.1 shows the constructed gradient coils. The efficiencies were 4.44, 4.77, and 5.04 mT/m/A. The differences between the designed and measured values were −11, −2, and −5%. Fig.2 shows 2D cross-section of a spherical phantom acquired with a 3DSE, showing the linearity of the gradient coils. Fig.3 shows cross-section of a capillary phantom acquired with 2DSE and 2DEPI sequences. These images demonstrated usefulness of the insertable gradient coil.

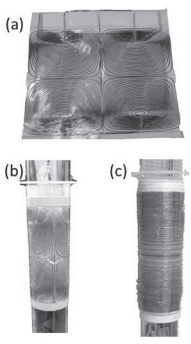

Fig.1: (a) and (b) x-gradient pattern.
(c) overview of the constructed gradient coil

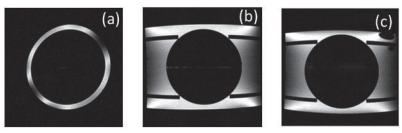

Fig.2: 2D cross-section of a spherical phantom acquired with a 3DSE
(a) xy plane, (b) xz plane, and (c) yz plane

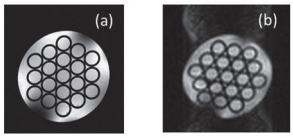

Fig.3: Cross-section of a capillary phantom acquired with
(a) 2DSE and (b) 2DEPI sequences.

P-2-035　1.5T超伝導磁石におけるField Cameraを用いた磁場モニタリングシステムの開発
Development of field monitoring system using field cameras for a 1.5 T superconducting magnet system

小林　優太（筑波大学大学院 数理物質科学研究科 電子・物理工学専攻）
Yuta Kobayashi, Katsumi Kose, Yasuhiko Terada
Institute of Applied Physics

【要旨】近年のMRIでは，EPIやSpiralをはじめとする高速撮像法が盛んに開発されている．一方で，これらの撮像法では高速な電流のスイッチングを要するため，渦電流等による画像歪み等のアーチファクトがしばしば問題になる．そこで本研究ではfield cameraを製作し，2次元のspiralシーケンスのk-trajectoryの計測を行った．

Fast imaging requires fast switching of gradients, and often suffers from image distortion, blurriness, etc. In this study, we developed a field monitoring system with a home-built field camera for a 1.5 T/280 mm SCM MRI system. We verified the performance by measuring spiral k-space trajectories.The field camera consisted of a ^{1}H-NMR probe (Fig. 1(a,b)) filled with $CuSO_4$-doped water and shielded by a 0.15 mm-thick Cu cylindrical box (39 mm ϕ x 65 mm). The MRI system consisted of shielded gradient coils, gradient driver and RF transmitter, and MRI transceiver (DTRX-6). Spin-echo spiral imaging scans were performed at four different camera positions in the imaging area. The field evolution was calculated using a first-order spherical-harmonic model with four basis function [1]. A capillary phantom was measured with the spiral and Cartesian trajectories.Figs. 1(d) and (e) show the nominal and monitored k-space trajectories, respectively. The monitored trajectory was rotated and skewed, and the rotated image reconstructed with the nominal trajectory (Fig. 1(f)) was also rotated and skewed, compared with the spin echo image (Fig. 1(g)).[1] C. Barmet et al., MRM 60 (2008) 187.

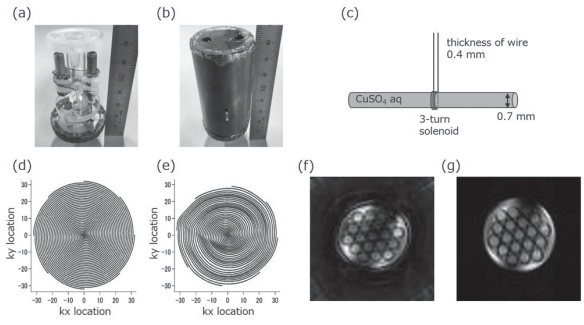

Fig. 1 (a) and (b) Home-built filed camera (a) without and (b) with a shield box. (c) Schematic of an NMR probe. (d) and (e) K-space trajectories of 8 shot spiral imaging. (d) Nominal and (e) monitored trajectories. (f) and (g) Capillary images measured and reconstructed with (f) the nominal spiral and (g) Cartesian trajectories. Matrix sizes = 64 x 64. FOV = 76.8 mm x 76.8 mm. TE/TR = 10 ms/400 ms. Acquisition time for 1 shot = 7.9 ms for spiral scan.

P-2-036　非呼吸停止下における3D radial sequenceとe-THRIVEの比較評価
Free breathing 3D radial sequence for contrast enhanced examination of the liver: comparison with e-THRIVE

吉田　学誉（財団法人自警会 東京警察病院 放射線科）
Takashige Yoshida[1,2], Yuki Furukawa[1], Kohei Yuda[1], Yuki Matsuzaka[3], Toru Sagami[3], Nobuo Kawauchi[3]
[1]Department of Radiology, Tokyo Metropolitan Police Hospital, [2]Division of Diagnostic Image Analysis, Graduate school of Medicine, Tohoku University, [3]Department of Radiodiagnosis, Tokyo Metropolitan Police Hospital

【要旨】Gd-EOBの肝細胞相は呼吸停止下で撮像されるが呼吸困難症例では画質低下が著明である。今回用いた撮像法はradial sequenceとmotion averagingを用いること非呼吸停止下で画質改善が認められた。

Purpose:
Recently, free-breathing radial 3D T1W-GRE sequence with motion averaging was performed during free breath imaging of the liver with comparable image quality to BH. However, the sequence with motion averaging using Gd-EOB has not yet been investigated.This study aimed to evaluate the independent breathing motion sequence using motion averaging ky-kz radial trajectory T1 high-resolution isotropic volume excitation (MA-Xe-THRIVE) sequence in Gd-EOB imaging and compare with breath holding enhanced-THRIVE (BH-e-THRIVE) and MA-e-THRIVE.
Methods:
Using our institutional review board-approved procedures, 10 subjects undergoing Gd-EOB were imaged using a 1.5T Philips MR system and 32ch torso cardiac coil. All sequences were set transverse using MA. The obtained image was measured signal intensity (SI) and standard deviation (SD) of hepatic, and coefficient variation (CV) was calculated by SI and SD. Overall image accuracy and quality was evaluated by two blinded reviewers.
Results:
CV of MA sequence was significantly lower Xe-THRIVE than that for other sequences ($P<0.001$). Image accuracy and quality of artifact was better for MA-Xe-THRIVE sequence than for any other sequence ($P<0.001$); however, MA-Xe-THRIVE is not superior to BH-e-THRIVE.
Discussion:
The MA-e-THRIVE is possible to decrease respiratory motion effect by motion averaging. Radial trajectory of MA-Xe-THRIVE had more an average effect on in and through-plane respiratory motion effect. However, MA-Xe-THRIVE are not completely able to eliminate the respiratory motion effect such as BH-e-THRIVE.
It is possible to provide motionless hepatic image using Xe-THRIVE of motion averaging 3D radial sequence.

P-2-037　6point-DIXON MRIにおける肝臓脂肪含有量とT2*値の関係の検討：水・脂肪・鉄ファントムによる検討
Investigating the relationship between proton density fat fraction and T2* value using six-point DIXON MRI: A fat-water-iron phantom study

福澤　圭（虎の門病院 放射線部）
Kei Fukuzawa[1], Satoshi Saito[2], Hidesato Suzuki[1], Shougo Yoda[1], Chiharu Yoshihara[1], Masakatsu Tano[1]
[1]Department of Radiology Toranomon Hospital, [2]Department of Hepatology Toranomon Hospital

【要旨】6point-DIXON法による肝脂肪定量に関してFFとT2*値の測定精度や関係をファントムを使って検討した。鉄の有無に関わらず6point-DIXON法は正確な脂肪定量が可能であった。T2*値は鉄量を増やすと短縮したが、鉄のないファントムで脂肪量を増加させた場合も短縮した。T2*値は脂肪と鉄両方の影響を受けている可能性がある。

Purpose: Six-point DIXON techniques is able to estimate proton density fat fraction (PDFF) and the T2* value of liver. PDFF are useful biomarkers of triglyceride concentration, while T2* values are reported to correlate with iron concentration. The purpose of this study was to examine the effect of T2* correction upon fat quantification with six-point DIXON MRI, and to identify the relationships between PDFF and T2* value of fat-water-iron phantom. Methods: We developed a fat-water-iron phantom (fat concentrations: 10, 20, 30, 40, and 50%, iron concentrations: 0.0, 0.05, 0.1, 0.2, and 0.4 mM SPIO). A 3.0-T MRI system (Ingenia, PHILIPS) was used for all scans six-point DIXON (DIXON-quant) using the following parameters: TR, 6.2 ms; first TE, 0.95 ms; delta TE, 0.8 ms; Flip angle, 3degree. MR Spectroscopy (MRS) was performed with a single-voxel multi-TE STEAM (TE, 10, 20, 30, 40 ms) All spectra were analyzed with the LCModel. PDFF measurements from each sequence and phantom were compared to the true PDFF using linear regression analysis. Results: PDFF by six-point DIXON and MRS at 0% iron concentration significant correlated with true PDFF (R^2=0.994 and 0.986, respectively, P<0.001) for each sequence. Furthermore, T2* value reduced as PDFF increased (12.6-39.4ms). In the phantom with 30% PDFF and iron concentration, the PDFF determined by six-point DIXON (23.4-29.0%), and T2* value (5.1-19.1ms). Conclusion: Six-point DIXON methods provide good agreement with MRS with high correlation coefficients. Furthermore, it is possible to correct for the effects of iron concentration. On the other hand, the T2* value decreased as the concentration of fat and iron increased. Our results show that six-point DIXON methods could not independently estimate the T2* value of water and fat.

P-2-038　Navigator gating法を用いた横隔膜同期併用3D fast SPGR法の画質評価－息止め3D fast SPGR法との比較－
Evaluation of the image quality on respiratory navigator-gated three-dimensional spoiled gradient-recalled echo pulse sequence (3D FSPGR)

松芳　圭吾（磐田市立総合病院 医療技術部 第1放射線診断技術科）
Keigo Matsuyoshi, Masaki Terada, Masanori Oosugi, Kenichi Ootsubo, Yukina Anzawa, Mika Koitabashi
Iwata City Hospital

【要旨】eNAV法が用いられた横隔膜同期併用LAVA法と息止め撮影BH LAVA法の画質を比較検討した。ファントムとボランティアを撮像し、SNRとCRを求めた。eNAV LAVA法ではBH LAVA法よりCRが悪かったが、FAを大きくすることで改善した。同条件ではBH LAVA法と同等のCRを得られないため、画質の向上のためFAを大きくする必要がある。

Introduction:Navigator-gated (NAV) 3D spoiled gradient-recalled echo pulse sequence(LAVA) is used in place of breath-held (BH)LAVA, when the patient can't hold breath. We can obtain high quality T1-weighted images by using NAV LAVA, even if the patient is in a state without the need of breathing effort. The method of enhanced navigator gating (eNAV) LAVA contributes to the accuracy improvement of navigator echo. But it might change the quality of images. We consider optimum conditions of flip angle and receiver bandwidth by comparing with the image on BH LAVA. Materials& Methods:Five healthy volunteers and phantom underwent magnetic resonance imaging of the liver using a BH LAVA or a eNAV LAVA. All human studies were approved by the local institutional review board. Visual evaluation and calculation of the signal-to-noise ratio (SNR) and contrast ratio (CR) were performed to compare image quality between the imaging techniques. The scan parameters for the healthy volunteer experiment on eNAV LAVA were as follows: TR/TE=4.0-7.2/1.9-2.4ms, slice thickness=3.0mm, FOV=35×35cm, matrix=384×224, NEX=1, Asset factor=2.0, receiver bandwidth=±62.5, 83.3, 100, 125kHz/FOV, flip angle=12,15, 20, 25, 30, 35, 40° .Results:The eNAV LAVA didn't provide better contrast ratio than the BH LAVA in the same conditions. The increasing the flip angle on eNAV LAVA contributed to the improvement of CR. Discussion:The type of flip angle on eNAV LAVA is variable. Also increasing the flip angle automatically changes TR and inversion recovery time. These are involved in the image quality on the eNAV LAVA.Conclusion: The eNAV LAVA didn't provide better contrast ratio than the BH LAVA in the same conditions. It's necessary to increase the flip angle on eNAV LAVA for improvement of image quality.

P-2-039　1.5T 32ch torso coilを用いたSingle breath hold Whole body 3D Balanced MRCPの検討
The evaluation of Single breath hold Whole body 3D Balanced MRCP with 32ch torso coil in 1.5T

大西　宏之（王子会神戸循環器クリニック 放射線技術科）
Hiroyuki Ohnishi[1], Hiroyuki Fukuya[2], Hiroko Yamamoto[1]
[1]Ojikai Kobecirculation Clinic Radiological Technology, [2]Ojikai Kobecirculation Clinic Department of Radiology

【要旨】4倍速(phase2×slice2)の高速化を図ったSingle breath hold Balanced MRCP(本法)の検討を行った。検討内容は20例に対してFSE系MRCP(従来法)と胆膵管の描出長と背景信号に対する胆膵管信号値とのコントラストを算出し比較した。

[Objective]Balanced MRCP (B-MRCP) is scannable sequence of 3D MRCP by breath holding. This sequence and 32ch torso coil makes it possible to scan high speed parallel imaging of SENSE factor 4 by setting slab range to whole body. In this study, we devised fast scan method of B-MRCP and compared image quality with FSE-MRCP. [Characteristics and Method]Both B-MRCP and FSE-MRCP were performed to 20 subject (6men, 14women, mean 59.5 (46-81) y) for the screening. We measured and compared scan time, representation biliary length (from papilla to intrahepatic bile duct) and background-calculated signal contrast of bile duct (BD) and pancreatic duct (PD) by workstation.[Result]Scan time of B-MRCP was shorter than FSE-MRCP (16.7+−2.4sec v.s. 318.7+−100.9sec: $p<0.001$). There was no significant difference in the visible length of left hepatic duct(HD), right anterior HD, right posterior HD and PD. Contrast of B-MRCP was lower than FSE-MRCP.[Conclusion] B-MRCP succeed to reduce scan time dramatically. Although the contrast of B-MRCP is lower than FSE-MRCP, there is no obvious difference in the depiction length. B-MRCP is useful as a substitute.

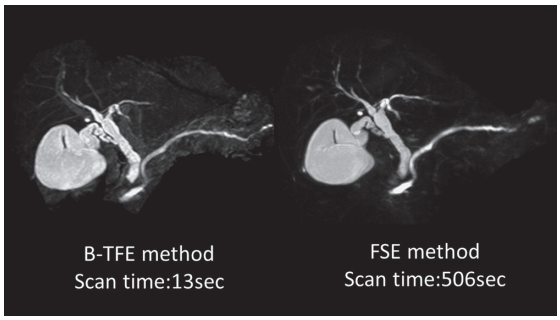

P-2-040　腹部放射線治療計画に有用なMRI撮像方法の検討
Magnetic resonance imaging for abdominal radiotherapy planning

山崎　達也（香川大学 医学部 附属病院 放射線部）
Tatsuya Yamasaki, Takuya Kobata, Akihiro Ooishi, Takashi Ishimori, Kazuo Ogawa, Yasuhiro Sasakawa
Department of Radiology, Kagawa University Hospital

【要旨】Multi Vaneの最適化を行い、Multi Vane、息止め撮像法、呼吸同期撮像法、加算効果を利用した自由呼吸下撮像法の中で、腹部領域での放射線治療計画用CTとの重ね合わせ精度について検討した。Multi Vaneの最適条件はMulti Vane percentage300、Shot Per Blade2、TSEf32であり、重ね合わせ精度はMulti Vaneが最も良かった。

Background, Purpose
Magnetic Resonance Imaging (MRI) is useful for setting gross tumor volume in abdominal radiotherapy planning. However, breathing motion artifacts cause loss of anatomical information.
The purpose of this study was to decide the best method for radiotherapy planning in 4 techniques: breath hold, free breath with high number of excitations(NEX), respiratory gating and periodically rotated overlapping parallel lines with enhanced reconstruction (PROPELLER [Multi Vane in the MR systems from Philips]).
Methods
First, we investigated optimal Multi Vane imaging parameters in phantom study, changing Multi Vane percentage, shot per blade and Turbo Spin Echo (TSE) factor. Second, 4 healthy adult volunteers with a mean age of 30 years (age range, 24-40 years) underwent upper-abdominal computed tomography (CT) and MRI (T2-weighted TSE sequences using each technique at 1.5-T scanner). Third, we superimposed MRI on CT images at radiation treatment planning systems; the accuracy of CT-MRI image fusion was evaluated visually by 5 radiologists using normalized-rank method.
Results
The Multi Vane optimal imaging parameters were 300 Multi Vane percentages, 2 shot per blade and 32 TSE factor in phantom study. Multi Vane image indicated best score in the accuracy of CT-MRI fusion images.

P-2-041　Silent Navigator の基礎的検討
Basic Study on Silent Navigator

布川　嘉信（慶應義塾大学病院 放射線技術室）
Yoshinobu Nunokawa[1], Rikiya Fujishiro[1], Yasutomi Shimada[1], Takashi Asakura[1], Shigeo Okuda[2], Hirokazu Fujiwara[2], Masahiro Jinzaki[2], Atsushi Nozaki[3], Yuji Iwadate[3]
[1]Office of Radiation Technology,Keio University Hospital, [2]Department of Ragiology,Keio University School of Medicine, [3]MR Applications and workflow, Asia Pacific, GE Health Care Japan

【要旨】呼吸同期に用いるnavigatorを静音状態にすることが可能かボランティアを用い検討を行った。検査中のノイズは、pencil-beam navigator法で81.7dB、Silent Navigator法では57.9dBであった。得られた画像に差はみられなかった。小児鎮静下の腹部呼吸同期検査など臨床での有用性が期待できる。

Purpose: Conventional pencil-beam navigator technique uses oscillating gradient waveforms during RF excitation, producing high acoustic noise. We recently developed a silent navigator technique which has no gradient pulses during excitation. The purpose of this study was to evaluate the silent navigator technique in volunteer scans. Methods: In the silent navigator, a non-selective hard RF pulse was used for excitation without any gradient pulses for not generating high levels of acoustic noise, resulting in whole volume excitation. Frequency encoding followed the excitation for respiratory motion detection in the SI direction. All scans were performed on a GE 1.5T MR450w system. The A-weighted continuous equivalent sound pressure level (LAeq) was measured for background, the conventional pencil-beam navigator, and the silent navigator scans using an iPhone application (Sound Level Analyzer Lite). Navigator repetition time in LAeq measurement was 100 ms. Navigator-gated 3D SPGR imaging was conducted with three volunteers using the pencil-beam navigator and the silent navigator. Non-gated free-breathing and breath-hold scans were also performed for comparison. Visual evaluation of resultant 3D SPGR images was performed regarding using the following scale: 1= Failure, 2=poor; 3=acceptable; 4=good, 5=excellent.Results and Discussion: The measured LAeq values of background, the pencil-beam navigator and the silent navigator were 57.7 dB(A), 81.7 dB(A) and 57.9 dB(A), respectively. Visual evaluation results did not show significant difference between the pencil-beam and silent navigators. The silent navigator integration into the silent imaging sequence should be examined in the next step.

P-2-042　2D SPGR法における横隔膜同期技術の比較
Comparison of respiratory navigator-gating techniques in 2D SPGR imaging of the liver

秦　　博文（北里大学病院 放射線部）
Hirofumi Hata[1], Yusuke Inoue[2], Ai Nakajima[1], Shotaro Komi[1], Yutaka Abe[1], Keiji Matsunaga[2], Hiroki Miyatake[1]
[1]Department of Radiology, Kitasato University Hospital, [2]Department of Diagnostic Radiology, Kitasato University School of Medicine

【要旨】2D dual-echo SPGR法による肝MRIにおいて様々なナビゲーター法を比較した。12名のボランティアを撮像し、撮像時間、ナビゲーター波形、画質の評価を行った。ナビゲーター法によりアーチファクトが減少し、異なるナビゲーター法間での有効性の違いが明らかになった。

Purpose: Our aim was to compare respiratory navigator-gating techniques for free-breathing T1-weighted 2D SPGR imaging of the liver using at 3T. Methods: Twelve healthy volunteers underwent 2D dual-echo SPGR imaging of the liver during free breathing using two conventional-navigator (CN) techniques (CN-SC and CN-DC) and two self-navigator (SN) techniques (SN-Pre and SN-Post) on a 3T scanner. In CN, the navigator and imaging were repeated alternatively. The navigators after imaging were used in CN-SC, and those before and after imaging in CN-DC. In SN, navigator signals were acquired using imaging RF pulse. Self-navigator echo was acquired before and after the imaging read-out in SN-Pre and SN-Post, respectively. Simple free-breathing (FB) and breath-hold (BH) scans were also performed. We evaluated scan time, visual waveform quality, quantitative ghost level, and visual image quality. Results: SNs took longer than CNs; the scan time was almost doubled in SN-Post compared to CNs. CNs generated better visual waveform qualities than SNs, and SN-Pre was better than SN-Post. Quantitative ghost levels were higher for all navigator methods than for BH and lower than for FB. Among the navigator techniques, they were lower for CN-DC and SN-Post than for CN-SC and SN-Pre. Visual image qualities for all navigator methods were worse than for BH and better than for FB. Among the navigator methods, visual qualities for CN-DC and SN-Post were better than for CN-SC and SN-Pre. Conclusion: The navigator techniques reduced motion artifacts and improved image qualities, and CN-DC and SN-Post were more effective than the others. Considering the scan time, CN-DC should be the best among the techniques tested in this study.

P-2-043　膵管分枝の描出能に関する研究、3種類のMRCPの比較検討
Evaluation of the numbers of pancreatic peripheral branches identified by 3D MRCP; Comparison of 3D TSE, 3D T2 SPACE and 3D T2 SPACE ZOOMit

堀　郁子（松江市立病院 放射線科）
Ikuko Hori[1], Yoshiko Kanasaki[1], Motoki Ametani[1], Masahiro Moriyama[1], Atsuya Kawaguchi[1], Toshihide Ogawa[2]

[1]Department of radiology, Matsue City Hospital, [2]Department of radiology, Tottori University School of Medicine

【要旨】1.5T 3D TFS　MRCP（A群：76)、3T 3D　SPACE　MRCP(B群：25)とBにZOOMit併用（C群：66）で膵管分枝の描出程度を比較検討した。 嚢胞のない膵管分枝は、A；0.824、B；1.577、C；2.348であった。嚢胞を含む膵管分枝は、A；2.041、B；2.160、C；3.615であった。膵管分枝の描出は、A群よりB・C群が良好であった。

(Object) It is known that cysts of IPMN are connected to the main pancreatic duct by peripheral branches. These branches can be observed by MRCP. We evaluated numbers of pancreatic branches identified by three different types of MRCP. (Material and Method) We investigated retrospectively 138 MRCP studies examined at our hospital from Nov. 2014 to April 2015. Fifteen patients with malignancy were excluded. Fifty six following studies by other types of MRCP were found. Therefore we added 46 MRCP studies to 122 studies. 168 MRCP studies contained following three groups, TSE 3D T2 weighted MRCP at 1.5 T MRI (group A) ; 76, 3D T2 weighted SPACE(sampling perfect with application optimized contrasts by using different flip angle evolution) MRCP at 3T MRI(group B) ;25, and ZOOMit T2 SPACE 3D MRCP at 3TMRI(group C) ;66. Oral contrast materials were administered to a total of 155 patients. Anticholinergic agents were injected in a total of 141 patients. We evaluated number of branches of the pancreas, dilatation of main pancreatic duct more than 5mm in diameter and numbers of multilocular cysts or monolocular cysts. (Result) Ten main pancreatic ducts were shown to be 5 to 9 mm in diameter. Mean numbers of identified pancreatic branches without cyst were 0.824 in group A, 1.577 in group B, 2.348 in group C. Statistical differences were found between A -B, and A -C. Mean numbers of all identified branches with or without cysts were 2.041 in group A, 2.160 in group B and 3.615 in group C. The mean number of branches identified in the group C was significantly larger than that in group A. (Conclusion) T2 SPACE MRCPs (group B, C) detected larger numbers of pancreatic branches than 3D TSE MRCP. But no significant difference was found between with or without ZOOMit (group B, C).

P-2-044　three dimensional ultra-short echo time imagingを用いたin vivoでの胆石の評価
In vivo MR evaluation of gallstones using three dimensional ultra-short echo time imaging

高橋　護（聖隷三方原病院 放射線科）
Mamoru Takahashi[1], Yasuo Takehara[2], Norihiro Tooyama[1], Katsutoshi Ichijo[1], Tomoyasu Amano[1], Takuya Matsumoto[1], Tomoyuki Okuaki[3], Yukiko Fukuma[3], Harumi Sakahara[4]

[1]Seirei Mikatahara General Hospital, [2]Hamamatsu University Hospital, [3]Philips Electronics Japan, Ltd., [4]Hamamatsu University School of Medicine

【要旨】In vivoで胆石の3D dual echo UTEを撮影した。UTEでは、胆石を周囲の胆汁や肝実質と比較し陽性信号として描出ができた。これは、MRIのpitfallである肝内結石や胆管に嵌頓した結石の診断に役立つと考えられた。

[Purpose]We demonstrated that using UTE sequence all gallstones were able to be detected as positive signal in-vitro. It may indicate that UTE has an added value of depicting impacted stones or hepatolithiasis. To test whether UTE can help depict gallstones as positive signals in-vivo.[Material and Method]Patients, who had suspected of having gallstone, were examined using MRI before the cholecystectomy. T1WI and UTE were performed. For UTE imaging, 3D radial dual-echo sequence with first echo (TE of 70 msec) (: UTE) and the second echo (2.24 msec). To selectively visualize only short-T2 components, subtraction images (: Subtraction) were processed.This study was approved by IRB, and all patients gave written informed consent. For a semi-quantitative assessment, CNRs for gallstone to the surrounding bile and liver parenchyma were calculated on images. Statistical evaluation was performed with non-parametric test. [Results]Averages (±SD) of CNRs to the surrounding bile on T1WI, UTE and Subtraction imaged were -16.0 (±19.4), -8.0 (±21.8), 10.1 (±7.1), respectively. Statistically significant difference between T1WI and Subtraction ($p < 0.01$) was measured. On subtraction images, all values were positive signal as compared to background bile or the liver. Averages of CNRs to liver parenchyma were -18.1 (±17.7), -7.1(±20.6), 5.8(±11.4), respectively. Statistically significant difference between T1WI and UTE ($p < 0.05$), T1WI and Subtraction ($p < 0.01$) were measured. CNRs of Subtraction were significantly highest in others; nevertheless four out of 14 stones had negative value. [Conclusion]By using dual echo UTE sequence all gallstones could be detected as higher CNRs than T1WI, which suggested an added value in depicting impacted stone in the biliary system.

P-2-045　食事摂取による肝IVIM, T2*緩和時間への影響
Effect of food intake for Intravoxel incoherent motion and T2* in the healthy liver

齋藤　和博（東京医科大学 放射線医学分野）
Kazuhiro Saito, Yoichi Araki, Yu Tajima, Taiyo L Harada, Takahiro Shimizu, Koichi Tokuuye
Department of Radiology, Tokyo Medical University

【要旨】食事摂取による門脈血流の増加のIVIM、T2*緩和時間への影響を健常ボランティア15人を対象に検討した。ADC, D, T2*緩和時間は食事による影響は少なく、再現性が認められた。D*, Fも食事による変動は認められなかったが、再現性に乏しかった。門脈血流も再現性が乏しく、D*, Fを評価するときは禁食が好ましいと考えられる。

PurposeThe purpose of this study is to evaluate the effect of portal flow increasing due to food intake for the parameters of intravoxel incoherent motion (IVIM) and T2* relaxation time in healthy liver. Materials and methodsThe subjects were consisted of 15 healthy volunteers. We used 1.5T MRI system (Avanto, Siemens). All subjects were performed MRI 3 times as follows; overnight fasting, 30 minutes and 4 hours after food intake. MRI was performed twice at more than 1 week interval. All subjects had 800 kcal of Calorie mate and 500 mL of water. The diffusion-weighted imaging was performed under free breathing and 10 b-values (0, 10, 20, 30, 50, 80, 100, 200, 400, 800 s/mm^2) were obtained. T2*-weighted imaging was performed with Map It. The portal flow measurement was performed with phase contrast sequence. The parameters of IVIM including ADC, D, D* and F were calculated and T2 * relaxation time was obtained using Map It. The statistical analysis was performed using repeated measures ANOVA. Bland-Altman plot was used to evaluate the reproducibility. P<0.05 was considered as significant.Results　The portal blood flow increased significantly 30 minutes after food intake. All IVIM parameters did not show significant differences after food intake. T2* relaxation time also did not show significant difference. The reproducibility of D* and F was found to be poor. The reproducibility of portal blood flow also showed poor.Conclusion　We supposed that the effect of food intake for ADC, D and T2* relaxation time were weak. The reproducibility of D* and F was poor. However, the reproducibility of the measurement of portal blood flow was also poor. We recommend the fasting when the perfusion related parameters such as D* and F will be evaluate.

P-2-046　レジスタンス運動と低糖質食による脂肪肝改善効果ー mDIXON法による定量的評価
Improvement of fatty liver with resistance training and low carbon diet - Quantitative evaluation with mDIXON method

高原　太郎（東海大学 工学部 医用生体工学科）
Taro Takahara[1], Toshiki Kazama[2], Munetaka Haida[3], Seism Sawano[4], Satoshi Tatsuno[4], Yuriko Ozawa[4], Yoshio Umezaki[4]
[1]Dept. of Biomedical Engineering, Tokai University School of Engineering, [2]Department of Radiology, Tokai University School of Medicine, [3]Tokai University Junior College of Nursing and Medical Technology, [4]Yeas Clinic

【要旨】肥満度1以上の被験者13名に対し、低糖質食とレジスタンス運動による2ヶ月間のダイエットを行った。mDXION法を用いて脂肪肝群と非脂肪肝群に分けて脂肪率の変化を観察した。1) 脂肪肝群（n=7）において、肝脂肪率は14.7%→5.2%と減少しダイエット前後に有意差を認めた。2)非脂肪肝群（n=6）では有意な変化を認めなかった。

[Purpose] To evaluate the improvement of fatty liver by quantitative method (mDIXON) during two month dieting consists of resistance training and low carbon meal.
[Materials and Methods] This volunteer study was approved by local IRB and written IC was obtained. 13 volunteers [8 men and 5 women, mean age, 42 years] with obesity class 1 (approx. 10 to 20kg overweight than standard range) were recruited. All volunteers had two month dieting consists of resistance training (2x/week, 50 min each) and low carbon meal (approx. 50g /day), and underwent pre/post MRI with mDIXON sequence for evaluation of fatty infiltration % of the liver (LF%). Statistical significance in differences in pre and post LF% was evaluated by paired t test and considered significant when P values were less than 0.05.
[Results] Fatty liver group (n=7) showed significant decrease of LF% from 14.7 to 5.2% (61% decrease). 4 volunteers went into normal range of LF% after dieting. On the other hand, non-fatty liver group (n=6) did not show significant difference.
[Conclusion] Two month dieting with resistance training and low carbon meal seems very effective to improve fatty liver.

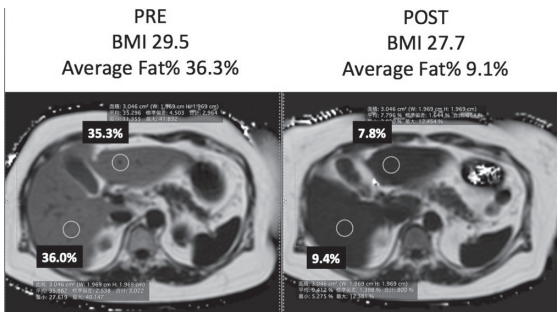

P-2-047　肝臓MRI検査の動脈相における撮像時間の短縮とリファレンススキャンの影響の検討
Scan Time Shortening of the Hepatic Arterial Phase of Liver Magnetic Resonance Imaging and the Influence of Reference Scan

辻　　良憲（国家公務員共済組合連合会 虎の門病院 放射線部）
Yoshinori Tsuji[1], Satoshi Saitoh[2], Junji Takahashi[1], Naomi Tagaya[1], Mariko Hiramoto[1], Chisato Abe[1], Yasutaka Tanuma[1], Akira Sawayama[1]

[1]Department of Radiological Technology, Toranomon Hospital, [2]Department of Hepatology, Toranomon Hospital

【要旨】肝臓の動脈相にCAIPIRINHAを併用し撮像時間の短縮を行なった。ファントムをリファレンススキャン時に動かし、モーションアーチファクトは依存しない事を確認した。アーチファクトはCAIPI-routine＝15秒＝2.5 %、CAIPI-short＝10秒＝0.5 %となり、CAIPI-shortとリファレンススキャンを使用する事で5秒で動脈相を撮像できる。

Purpose: Dynamic magnetic resonance imaging (MRI) of the liver is a parallel imaging technique. The use of controlled aliasing in parallel imaging results in higher acceleration (CAIPIRINHA) and shortens the imaging time. With respect to CAIPIRINHA, reference scan is performed first. The purpose of the present study was to focus on this reference scan and examine the influence of holding breath on the shortening of imaging time.Methods: The acceleration factor was set to 2.0 with an imaging time of 20 s using the generalized autocalibrating partially parallel acquisition (GRAPPA) method, and the acceleration factor was set to 3.0 so that the imaging time of the routine method (CAIPI-routine) could be set to 15 s. The short scanning method (CAIPI-short) had a imaging time of 10 s, and the reference scan was for 5 s. Phantom was used to compare the appearance of artifacts moved by the motor at the time of the reference scan. The phantom was moved so the scan end 5 s before for comparison. In clinical cases suspected of various chronic liver diseases, MRI of the liver was performed, while breathing at the time of the reference scan for a patient had been enforced. The motion artifact was compared by each method. Result: When the phantom was moved in the first 5 s using the GRAPPA method, there was an artifact under the influence of motion. However, artifacts were reduced in the first 5 s of the CAIPIRINHA method. Motion artifacts as a result of the failure to hold breath due to the influence of the reference scan did not make image evaluation difficult. Moreover, the motion artifact for each sequence was as follows: GRAPPA, 5.6%; CAIPI-routine, 2.5 %; and CAIPI-short, 0.5 %.Conclusion: The arterial phase can be scanned in 5 s using CAIPI-short and reference scan techniques.

P-2-048　3T MRI 超高b値(b=2000)を用いたADCによる肝腫瘍鑑別能の従来法との比較
High and ultra-high b-value diffusion-weighted MRI for the evaluation of hepatic focal lesions with 3-T MRI

浪本　智弘（熊本大学 医学部 放射線診断科）
Tomohiro Namimoto, Masataka Nakagawa, Kie Shimizu, Masafumi Kidoh, Seitaro Oda, Takeshi Nakaura, Daisuke Utsunomiya, Yasuyuki Yamashita

Dept. of Diagnostic Radiology, Faculty of Life Sciences, Kumamoto University

【要旨】3T MRI拡散強調画像による肝腫瘍鑑別において超高b値(2000)によるADC(ADC2000)と通常のb値(800)によるADC(ADC800)と鑑別能の比較を行う。対象は81症例で良悪性の鑑別能についてROC解析を行った。AUCはADC800で0.982、ADC2000で0.991となり、有意差を認めなかった。ADC2000による肝腫瘍鑑別の診断能はADC800と同等であった。

Purpose: To determine whether the apparent diffusion coefficient (ADC) obtained using b = 2000 s/mm^2 upon 3 Tesla (T) diffusion-weighted MRI is superior to b = 1000 s/mm^2 for discriminating malignant from benign focal liver lesions (FLL).Materials and Methods: Our Institutional Review Board approved this retrospective study and informed consent was waived. Eighty-one focal liver lesions in 81 patients (36 HCCs, 18 metastases, 6 CCCs, 10 hemangiomas and 11 cysts) underwent 3T MRI including diffusion weighted imaging with b-values of 0/ 800, and 0/ 2000 s/mm^2. ADCs were measured for focal hepatic lesions and normal liver parenchyma on two sets of ADC maps calculated with monoexponential fitting between b = 0 and 800 (ADC800), 0 and 2000 (ADC2000), respectively. Receiver operating characteristic (ROC) analysis was used to evaluate the diagnostic accuracy of ADC for differentiating between benign and malignant lesions. The relationship between the ADC and lesion characterization was also evaluated.Results: The areas under the ROC curves (AUCs) of ADC800 and ADC2000 were 0.982 and 0.991 for differentiating between benign and malignant lesions, respectively. No significant differences were found between ADC800 and ADC2000 (P=0.35). The mean ADC800 and ADC2000 (x10^{-3} mm^2/second) were HCCs 1.10/ 0.84, metastases 1.21/ 0.85, CCCs 1.43/ 1.08, hemangiomas 1.95/ 1.44 and cysts 3.00/ 2.30, respectively. The difference between benign (hemangiomas, cysts) and malignant (HCCs, metastases, CCCs) was significant in both ADC800 and ADC2000 except for between CCCs and hemangiomas in ADC800. Conclusion: The use of b = 2000 s/mm2 for ADC with 3-T MRI is diagnostically comparable to that of b =1000 s/mm^2 for characterization of benign and malignant hepatic lesions.

P-2-049　Bi-ExponentialモデルおよびMono-Exponentialモデルに基づくcDWIの基礎的検討
Comparative evaluation of computed diffusion weighted imaging based on the mono-exponential and bi-exponential model

甲斐　征八（東芝メディカルシステムズ株式会社）
Seiya Kai, Yuichi Yamashita, Tatsuya Ohkubo, Syuhei Takemoto, Yuichiro Sano
Toshiba Medical Systems Corporation

【要旨】肝臓においてcDWI算出時のモデルの違いによる画像の比較検討を実施し、IVIM解析を用いたBi-exponential modelの有用性が示唆された。

[Purpose]Computed diffusion weighted image (cDWI), which can reconstruct diffusion weighted image (DWI) at any b-value as a post-processing from actual DWI (aDWI), is used to get more clinical information with no additional imaging time. Although apparent diffusion coefficient (ADC) is used for calculate the cDWI by assumption that the signal decay as mono-exponential usually, there is perfusion effect at lower b values and often becomes problem which b-value sets and fitting algorithm should be used for calculation. Bi-exponential model takes in account the perfusion effect and cDWI can be calculate by using a diffusion coefficient D. The purpose of this study was to evaluate the cDWI calculated by the mono-exponential and bi-exponential model with Bayesian fitting algorithm.[Methods]aDWI and cDWIs based on mono-exponential model (cDWI_m) and bi-exponential model (cDWI_b) at Liver were compared at b-value of 1000. Actual DWIs were obtained with Single shot EPI sequence (TR/TE/FA=3086/80/90, b values: 0, 2, 5, 10, 15, 20, 30, 50, 100, 130, 160, 200, 300, 700, 1000, matrix:256*256, slice thickness: 10mm, 5slices, NAQ: 1, scan time: 4min28sec, PASTA+SPAIR, PI: 2.2(PE), MPG: PE, SL). cDWIs were reconstructed using workstation Vitrea (Toshiba Medical Systems Corporation) Version 7.1.1. SNR and CNR were used for comparative evaluation.[Result]Comparing the aDWI, cDWI_b and cDWI_m, cDWI_b was shown good contrast at visual qualitative evaluation and SNR cDWI_b and cDWI_m percent to aDWI was 120% and 94%, respectively.[Conclusion]cDWI_b was suggested that it has equivalent contrast of aDWI and good SNR compared with aDWI and cDWI_m.

P-2-050　化学放射線療法後局所進行食道癌の切除の可否を縦隔MRIは予測可能である。
Mediastinal MRI can predict respectability of a locally advanced esophageal cancer after chemoradiation therapy

小野寺祐也（社会医療法人 恵佑会札幌病院 放射線診断科）
Yuya Onodera[1], Taisuke Harada[2], Osamu Manabe[4], Hiroaki Takahashi[3], Toshinao Takenouchi[1], Masao Hosokawa[1]
[1]Keiyukai Sapporo Hospital, [2]Hokkaido University Hospital, [3]Keiyukai Second Hospital, [4]Otaru City Hospital

【要旨】縦隔内繊維化の評価をMRIで行うことが、画像的に化学放射線療法後の食道癌が切除可能か否かを予測するに重要な因子である。

Purpose; the aim of this study is to detect useful findings on mediastinal MRI that decides to resect an esophageal cancer after chemoradiation.Materials and Methods; Patients with a locally advanced esophageal cancer were performed chemoradiation therapy prior to operation. All patients were performed salvage operation. Mediastinal MRI of esophageal cancer cases were investigated retrospectively. Two board-certified diagnostic radiologists performed image interpretation with consensus reading. Intraoperative and histopathological findings were as a gold standard and compared with the results of MRI. Thin slice axial images on T2 weighted image (T2WI) and Short TI inversion recovery (STIR) were used for the assessment. Results of the comparison were statistically analyzed, and there was statistical significant difference, if P value was under 0.05. We calculated sensitivity, specificity, accuracy, positive predictive value, and negative predictive value for statistically significant results.Results; Post chemoradiation images showed three important factors to decide a tumor resection that are prevalence of wall structure, prevalence of fat border, and dense of fibrous tissue.There was statistically significant on each result to compare the finding with postoperative tumor depth. Except one case, T4 cases showed disappearance of border fat layer caused by fibrous tissues. Based on this finding, postoperative T4 or not were analyzed. Sensitivity was 91.7%, Specificity was, 67.2%, Positive predictive value was 36.7%, and Negative predictive value was 97.5%.Conclusion. Fibrous tissues surrounding esophagus after chemoradiation, which showed irregular low intensity band on T2WI or STIR, were important factor to find out a resectable tumor case.

P-2-051　ZOOMIT T2 SPACE 3Dの直腸癌に対する術前3T MRI：T2Wとの比較研究
Preoperative 3T MR imaging for rectal cancer of ZOOMit T2 SPACE 3D: A comparative study with T2W

井藤　千里（香川大学 医学部 放射線医学講座）
Senri Ito, Yuko Fukuda, Kenichi Tanaka, Akihiro Oishi, Kazuo Ogawa, Yoshihiro Nishiyama
Dep. Radiology, Kagawa University

【要旨】直腸癌患者6症例の術前MRIの深達度診断等における ZOOMit T2 SPACE 3D の実用性につき既存のT2W 2D-TSE sequenceと対比し検討した。放射線科医2名の読影結果と病理結果の統計的解析からZOOMit T2 SPACE 3D sequenceの実用の可能性が示唆された。

Purpose: The purpose of this study was to evaluate the ZOOMit T2 SPACE 3D sequence for rectal cancer images. Materials and Methods: Sex patients with diagnosed rectal cancer were retrospectively examined by 3T scanner using ZOOMit T2 SPACE 3D sequence (TR/TE/FA=1600ms/104ms/135°, FOV=250x156.3mm2 (phase 62.5%)) and T2-weighted (T2W) 2D-TSE sequence (axial: TR/TE/FA=4500ms/78ms/125°, coronal: TR/TE/FA=4500ms/95ms/160°, sagittal: TR/TE/FA=4500ms/104ms/160°, FOV=320x320mm2). Two radiologists independently assessed the radiologic findings for T and N category lesions in ZOOMit T2 SPACE 3D and T2W data. The conspicuity of tumor margin, and image quality were performed with 4- point scale.Wilcoxon signed rank test was performed to compare the tumor conspicuity and image quality.Results: T category lesion staging accuracy values for the ZOOMit T2 SPACE 3D and T2W data, respectively, were 75% and 100% for reviewer 1 and 50% and 75% for reviewer 2. N category lesion staging accuracy values for the ZOOMit T2 SPACE 3D images and T2W, respectively, were 50% and 75% for reviewer 1 and 75% and 50% for reviewer 2. Tumor conspicuity and image quality were p=0.35 and p=0.32, which were better for T2W, but no significant difference in image quality were observed.Conclusion: These preliminary results indicate that the ZOOMit T2 SPACE 3D may be useful for the detection of rectal cancer and tumor staging.

P-2-052　大腸癌のQSIによるEx Vivoでの評価：組織学的分化度とリンパ節転移の検討
q-Space MR Imaging of Colorectal Carcinoma Ex Vivo: Evaluation of Histologic Grades and Lymph Node Metastasis

山田　一郎（東京医科歯科大学 大学院医歯学総合研究科 画像診断・核医学分野）
Ichiro Yamada[1], Keigo Hikishima[2], Norio Yoshino[1], Naoyuki Miyasaka[1], Shinichi Yamauchi[1], Hiroyuki Uetake[1], Masamichi Yasuno[1], Yukihisa Saida[1], Ukihide Tateishi[1], Daisuke Kobayashi[1], Yoshinobu Eishi[1]
[1]Department of Diagnostic Radiology and Nuclear Medicine, Graduate School, Tokyo Medical and Dental University, [2]Okinawa Institute of Science and Technology Graduate University

【要旨】大腸癌20症例の手術材料及び摘出リンパ節について3T-MRIを用いてq-Space Imaging（QSI）による検討を行った。QSIパラメーター（mean displacement, zero-displacement probability及びkurtosis）は大腸癌の組織学的分化度との間に統計学的に有意な相関を示し、転移リンパ節と非転移リンパ節の鑑別においても有用であった。

PURPOSE: To determine the feasibility of q-space MR imaging as means of evaluating the histologic grades of colorectal carcinomas and lymph node metastasis by colorectal carcinomas.MATERIALS AND METHODS: Twenty colorectal specimens each containing a carcinoma and their resected lymph nodes were imaged with a 3-T MR imaging system equipped with a 4-channel phased-array surface coil. q-Space MR images were obtained with repetition time, 10000 ms; echo time, 216 ms; field of view, 113 mm x 73.45 mm; matrix, 120 x 78; section thickness, 4 mm without intersection gaps; eleven b values ranging from 0 to 9000 s/mm^2; and motion-probing gradients perpendicular to the colorectal wall. Three q-space imaging parameters were calculated from the displacement distribution profiles, and ADC was also calculated from two b values (b = 0 and 500 s/mm^2). The MR images were then compared with the histopathologic findings.RESULTS: In all 20 carcinomas, the mean displacement was calculated as 8.83 ± 0.42 μm, zero-displacement probability 82.9 ± 8.8 (arbitrary unit [a.u.]), kurtosis 74.9 ± 3.5 (a.u.), and ADC 0.206 ± 0.057 x 10^{-3} mm^2/s. The mean displacement ($r = -0.810$; $P < 0.05$), zero-displacement probability ($r = 0.926$; $P < 0.01$), and kurtosis ($r = 0.926$; $P < 0.01$) were statistically significantly correlated with the histologic grades of colorectal carcinomas, while the ADC ($r = -0.116$; $P = 0.805$) showed no significant correlation with their histologic grades. The q-space imaging parameters made it possible to differentiate between metastatic lymph nodes and nonmetastatic lymph nodes (all $P < 0.01$).CONCLUSION: q-Space MR imaging provides useful diagnostic information for evaluating the histologic grades of colorectal carcinomas and lymph node metastasis by colorectal carcinomas.

P-2-053　腎盂癌におけるMR拡散強調像の有用性について：他撮影条件との比較
A pictorial review of the impact of adding diffusion-weighted MR imaging to other MR sequences for assessment of renal pelvic carcinoma

吉田　理佳（島根大学 医学部 放射線科）
Rika Yoshida, Takeshi Yoshizako, Kazumi Araki, Megumi Nakamura, Shinji Andou, Takashi Katsube, Nobuko Yamamoto, Hajime Kitagaki

Department of Radiology, Shimane University Faculty of Medicine

【要旨】腎盂癌MR診断における拡散強調像（DWI）の付加価値を他条件と比較し検討する。DWI付加により病巣検出率、病期診断能、読影者間一致率、若年読影者診断率の改善が認められた。Apparent diffusion coefficient valueによる悪性度、転移の有無の予測についても、症例を提示し、我々のデータとこれまでの報告を解説する。

PURPOSEThe purpose of this article is to review the utility of diffusion-weighted MR imaging (DWI) findings in renal pelvic carcinoma compared to other sequences, and to become familiar with the wide useful points of DWI findings of this entity.**CONTENTS**1:To present several examples of DWI in renal pelvic carcinoma compared to T2-weighted MR imaging (T2WI) and contrast enhanced MR imaging (CEI).2:To review the tumor detection rate, the diagnosis ability and the inter-observer agreements for T categorization of DWI in renal pelvic carcinoma compared to T2WI and CEI.3:To assess the feasibility of DWI for predicting the histopathologic grade of renal pelvic carcinoma.4:Discussion of the utility and limitation of DWI for renal pelvic carcinoma compared to T2WI and CEI.**CONCLUSION**1: The use of DWI improved the detection rate of renal pelvic carcinoma for the inexperienced reader.2: The consensus detection rate using T2WI plus DWI was the same as for T2WI plus CEI, but that both were marginally higher than when using T2WI alone. 3: The mean apparent diffusion coefficient (ADC) value of the high-grade tumors was significantly lower than that of the low-grade tumors. 4: The mean ADC values of the tumors with metastasis were lower than those without metastasis, with a significant difference.

P-2-054　mUTE 4D-MRAを用いた非造影頭部MRA描出の試み
Investigation of the Non-contrast Head Magnetic Resonance Angiography using mUTE 4D-MRA

山内智恵美（東芝メディカルシステムズ株式会社 MRI営業部）
Chiemi Yamauchi[1], Hisae Chiba[1], Shin Takamatu[1], Yoshihito Miyamoto[2], Tsutomu Katou[2]
[1]TOSHIBA MEDICAL SYSTEMS CORPORATION, [2]SUMITOMO BESSHI HOSPITAL

【要旨】mUTE 4D-MRAを用いて頭部MRA描出に対する基礎検討を実施した。同意の得られたボランティアにてタグスラブ厚、Shot Interval, FAを可変させ視覚評価を行った。タグスラブ厚は厚く、shot Intervalは長く、FAは深いほど頭部MRAの描出能は向上した。

PurposeRecently, several studies has been reported on Magnetic Resonance Angiography (MRA) using ultra short TE (UTE) and Multi Phase Arterial Spin Labeling (ASL).We became available using mUTE 4D-MRA, which is UTE and Multi Phase ASL.In this study, we investigated the Head MRA using mUTE 4D-MRA.
MethodsMore than one volunteers were enrolled and scanned by Vantage Titan3T scanner equipped with Atlas SPEEDER Head coil.Parameters were : TR / TE, 3.0ms / 0.1ms ; resolution, 0.5mm isotropic; slice thickness, 0.5mm. We visually evaluated the mUTE 4D-MRA images by changing Size of tag slab, inversion time (TI), shot Interval, and Flip Angle (FA).
ResultsThe characterized of Head artery were visualized better thick tag slab than thin.In particular, at thick tag slab and long TI, the characterized of them was decreased.Internal carotid artery, vertebral artery, basilar artery was characterized in TI of 200-1000ms, 600-1200ms, 600-1200ms, respectively.At long shot Interval and high FA, the characterized of them was improved.
ConclusionWe can visualize the Non-contrast Head MRA using mUTE 4D-MRA by using investigating sequence.

P-2-055　Ultra short TEを用いた頸動脈描出における基礎的検討
A functional study of the description in carotid artery using Ultra short TE

宮本　良仁（医療法人 住友別子病院 放射線部）
Yoshihito Miyamoto[1], Tsutomu Katou[1], Shin Takamatsu[2], Chiemi Yamauchi[2], Tomonari Ishida[2], Hisae Chiba[2]

[1]Department of Radiology,Medical corporation Sumitomobesshi Hospital, [2]Toshiba Medical Systems Corporation

【要旨】頸動脈描出に関してUltra short TEを用いた頸動脈描出の基礎的検討を行った。TagSlab、TI値、shotInterval、FAを変化させ視覚評価を行うことで、頸動脈の描出が可能であった。

PurposeTo diagnose of carotid stenosis, time-of-flight(TOF) was offen used in magnetic resonance imaging, but the depiction of the image becomes poor because disorder of the bloodstream happens in the carotid divergence department.We study the benefits or feasibility of Multi phase ASL- MRA using Ultra short TE(mUTE 4D-MRA) in carotid artery becauseMethodsWe used Vantage Titan3T.We visually evaluated images by changing the size of TagSlab,invertion time(TI),shotinterval and flip angle(FA) in the signal targeting alternating radiofrequency with asymmetric inversion slab (ASTAR) sequence of volunteer.ResultsThe characterization of carotid artery were visualized better the large size of Tag Slab than small,but The characterization were decreased by too large size of Tagslab.Signal noise ratio(SNR) is higher in long shotinterval than in short shotinterval, but in long interval,scan time is extend.SNR is higher at high FA than at low FA.The carotid artery was not characterized in short TI of 200ms.In TI of 400-600ms, The carotid artery was characterized clearly.At the same TI, The carotid artery was characterized better in the first-phase than the second phase.DiscussionWe thought that the small size of Tag Slab cause decreasing the size of labeled and the signal of the internal carotid artery depending on TI, on the other hand, the large size of TagSlab made the recovery of signal, but SNR decreses if the large size of Tagslab includes in the heart.We thought that the signal recovers by long shotinterval, and SNR improved.In volunteers, we found that the peripheral vessels of the head describe good in long TI, but the characterizes decrease because SNR decreases.ConclutionWe can visualize the carotid artery using mUTE 4D-MRA.

P-2-056　ultra-short echo time 位相画像のノイズ推定．
Noise estimation of phantom phase image in ultra-short echo time imaging

松元　友暉（徳島大学 大学院 保健科学教育部）
Yuki Matsumoto[1], Yuki Kanazawa[2], Natsuki Ikemitsu[3], Toshiaki Sasaki[3], Hiroaki Hayashi[2], Mitsuharu Miyoshi[4], Masafumi Harada[5], Hideki Otsuka[2]

[1]Tokushima University, Graduate school, [2]Institute of Biomedical Sciences, Tokushima University, [3]Tokushima University, [4]GE Healthcare Japan, [5]Department of Radiology and Radiation Oncology, Tokushima University Graduate School

【要旨】位相画像のノイズを推定するために，我々はultra-short echo time (UTE)で得た位相画像を評価した．方法として，Gd-DTPAとHydroxyapatiteをサンプルチューブに入れたファントムを撮像し，サンプルチューブ内に関心領域を設定して解析を行った．

Purpose: To estimate accurately noise of phase rotation, we evaluated a signal phase of ultra-short echo time (UTE) imaging. **Materials and Methods:** On 3.0T MR system, we performed a phantom experiment using a dual-echo UTE imaging. The imaging parameters were TE, 0.032 ms (first-echo) and 3.3 ms (second-echo); matrix sizes, 256 ×256; slice, 16. The phantom consisted of Gd-DTPA and hydroxyapatite samples, which were made using three different concentrations of each material; Gd-DTPA, 0.5, 1.0, and 2.5 mmol/L; hydroxyapatite, 100, 200, and 350 mg/mL. Then, region of interest analysis was performed on two phase images, e.g., first-echo, and second-echo phase images. **Results:** The mean first-echo phase values on each Gd-DTPA (0.5, 1.0, and 2.5 mmol/L) and hydroxyapatite (100, 200, and 350 mg/mL) sample were 32.4 ± 0.04, 32.2 ± 0.04, 32.0 ± 0.01, 32.4 ± 0.02, 43.6 ± 0.03, and 60.0 ± 0.01 degree, respectively. The mean second-echo phase values on each Gd-DTPA (0.5, 1.0, and 2.5 mmol/L) and hydroxyapatite (100, 200, and 350 mg/mL) sample were 39.1 ± 0.04, 36.0 ± 0.04, 35.5 ± 0.05, 137.9 ± 0.06, 83.4 ± 0.06, and 88.02 ± 0.06 degree, respectively. The mean background phase value first-echo, and second-echo were 33.5 ± 0.11 and 87.1 ± 0.12 degree, respectively. **Discussion & Conclusion:** The phase rotation of hydroxyapatite occurred difference of phase value in each sample, i.e., this leads good contrast in UTE image. In contrast, the phase rotation of Gd-DTPA at TE 0.032 ms is small enough to estimate noise because the Gd-DTPA phase values were almost equal. Thus, UTE imaging may lead to noise derived from a phase rotation. Noise estimation using UTE imaging may render it possible to obtain more detailed information of paramagnetic materials, e.g., Gd-DTPA.

P-2-057　Ultra-short TEによる乾燥木材の年輪年代計測の試み
Feasibility study of visualizing tree-ring structures of dried wood with Ultra-short Echo Time (UTE) MR-imaging for chronological measurements

森　美加（杏林大学 保健学部 診療放射線技術学科）
Mika Mori[1,2], Shigehide Kuhara[1], Kuninori Kobayashi[1], Masahisa Yamada[3], Atsushi Senoo[2]
[1]Kyorin University Department of Medical Radiological Technology Faculty of Health Sciences, [2]Tokyo Metropolitan Univetsity Graduate School of Human Health Sciences Department of Radiological Sciences, [3]Tokyo Metropolitan Univetsity Graduate School of Humainities

【要旨】臨床用MR装置により、乾燥木材試料の年輪構造の描出が可能か検討した。含水量の異なる出土木材模擬試料を従来の撮像シーケンス、ならびにUTEシーケンスにて撮像、描出能の差について検討した。その結果、通常シーケンスでは描出困難であった乾燥木材試料に対しても、UTEを用いることにより年輪構造が描出可能であった。

<Background> As one of the non-destructive inspection methods for archaeology, a diagnostic MRI was used to visualize the tree-ring structure for water-exposed and polyethylene glycol (PEG) treated wooden boards [1]. However, it is expected to be difficult if it's applied to dried wood or PEG treated wooden boards with a very low water content.
<Purpose> To perform the feasibility study of visualizing the tree-ring structure of dried or very low water content wood using a diagnostic MRI for chronological measurements.
<Method> Several samples with different water contents were made from the same conifer or broad-leaf tree wood. Conventional field echo (FE) and spin echo (SE) sequences were used to obtain T1 and T2 weighted images on a diagnostic 3T MRI (Vantage Titan 3T; Toshiba Medical Systems Corporation). A UTE (Ultra-short TE) sequence (TE=0.096ms) was also used to visualize the tree-ring structure in the case when the visualization of tree-rings was difficult using conventional sequences. Images were compared and evaluated from the point of view of visualization of the tree-ring structure.
<Results and Discussion> In the case of conventional sequences, the visualization of the tree-ring structure of dried wood was difficult. On the other hand, The UTE sequence could visualize the structure of dried wood successfully, though several numbers of averaging were needed, even in the case when the conventional sequences could not visualize anything.
<Conclusions> It is suggested that dried wood or very low water content wood articles would be also available as objects for chronological measurements with diagnostic MRI and it is expected that this method will be more widely used in the archaeology field.
[1] Senoo, A., et al. JSMRM2014, P-3-215.

P-2-058　香りによる自伝的記憶の想起　－帯状回後部領域賦活の検討－
Odor induced autographical memory associated with activity in the posterior parts of the brain as well as limbic olfactory areas

渡辺　慶子（昭和大学 医学部 内科学講座神経内科学部門）
Keiko Watanabe[1,2], Yuri Masaoka[2], Masaki Yoshida[3], Nobuyoshi Koiwa[4], Akira Yoshikawa[2], Masahiro Ida[5], Mitsuru Kawamura[1], Kenjiro Ono[1], Masahiko Izumizaki[2]
[1]Dept of Neurol, Showa Univ Sch Med, [2]Dept of Physiol, Showa Univ Sch Med, [3]Dept of Ophthal, Jikei Med Univ, [4]Dept of Health and Sci, Uni Human Arts and Sci, [5]Dept of Radiol, Stroke Center, Ebara Tokyo Hospital

【要旨】本研究は、香りにより自伝的記憶を想起させ、それに伴う情動に関連する脳領域をfMRIを用いて検討したものである。香りによる記憶想起と情動は扁桃体、海馬、眼窩前頭部を含む嗅覚辺縁系領域を賦活させ、またエピソード記憶や視空間認知に関連する脳梁膨大後部皮質や楔前部の賦活もみられた。

Memories induced by odors enable individuals to mentally travel back into their personal past. In this study, we used functional Magnetic Resonance Imaging (fMRI) to analyze brain areas related to odor-induced Autobiographical Memory (AM) and emotions in healthy subjects. Odor stimuli were used one of three choices, Tatami, Baby Powder or Osmanthust, which elicited a specific, pleasant and AM. Subjects were instructed to breathe normally with nose mask for delivering odors and for measurement of respiratory flow. AM odor increase tidal volume and decrease respiratory frequency with activations of the olfactory limbic areas including amygdala, hippocampus and orbitofrontal cortex. AM odor also activated posterior parts of the brain including retrosplenial cortex and medial area of the superior parietal cortex of the precuneus. Those areas had been reported roles of episodic memory retrieval and visuospatial processing, respectively. AM odor induced specific emotions with strong feeling back to the past and with retrieving of the vividness of the spatial and episodic memories and these feelings may link to retrosplenial cortex and precuneus activations.

P-2-059　安静時、嗅覚刺激時の呼吸に同期した辺縁系、延髄の脳活動
Respiratory-related neural activities in medulla and limbic system during resting and olfactory states -fMRI study-

政岡　ゆり（昭和大学 医学部 生体調節機能学）
Yuri Masaoka[1], Masahiro Ida[2], Masaki Yoshida[3], Nobuyoshi Koiwa[4], Keiko Watanabe[1], Akira Yoshikawa[1], Ikuo Homma[5], Masahiko Izumizaki[1]

[1]Department of Physiology, Showa University School of Medicine, [2]Ebara Tokyo Hospital, [3]Jikei Medical University, [4]University of Human Arts and Sciences, [5]Tokyo Ariake University of Medical and Health Sciences

【要旨】本研究では嗅覚刺激による呼吸の変化と延髄での呼吸の関係をみるため、fMRIを用いて嗅覚刺激時と安静時での呼吸に同期した辺縁系と延髄の活動を捉えた。安静時では呼吸に同期して延髄背側部、腹側部の活動が捉えられ、嗅覚刺激時では情動、呼吸の変化とともに、延髄背側部、傍小脳脚核、扁桃体、海馬の賦活が認められた。

Respiratory center in the medulla generates the basic respiratory rhythm, however the respiratory rhythm is modulated by olfactory stimuli. In this study, we performed simultaneous recordings of respiration and brain activities using functional Magnetic Resonance Imaging (fMRI) during resting state and olfactory stimuli to investigate on limbic and brainstem circuitry synchronized with the respiratory cycles. Respiratory flow and cardiac signal were simultaneously recorded during scan to retrospectively remove physiological noises from fMRI-BOLD signals. During resting state, activations of dorsal and ventral medulla were synchronized with inspiration cycles, and the amygdala, hippocampus and parabrachial nucleus in addition to dorsal medulla were associated with spontaneous breathing during olfactory state. The limbic, parabrachial nucleus and -dorsal medulla circuitry may play a role for odor-induced emotions and respiratory changes.

P-2-060　クライオプローブを用いたマウス全脳の匂い応答の検出
Detecting the olfactory responses in the mouse whole brain using a cryogenic probe

舩津　大嗣（熊本大学大学院生命科学研究部 構造生命イメージング分野）
Hirotsugu Funatsu, Sosuke Yoshinaga, Naoya Yuzuriha, Shunsuke Kusanagi, Mitsuhiro Takeda, Hiroaki Terasawa

Department of Structural BioImaging, Faculty of Life Sciences, Kumamoto University, Kumamoto, Japan

【要旨】マウスの嗅覚fMRIでは、脳が小さく血流の影響を受けやすいため、脳の活性化を示す信号を得にくい。我々は高感度な極低温プローブを用いてマウス全脳を撮像した。ラット嗅球の知見と一致する嗅球外側に加え、嗅覚伝導路に含まれる梨状皮質、情動や認知機能に関与する前帯状皮質・線条体の活性化の検出に成功した。

Rodent fMRI is frequently used for olfactory studies since rodents have well-developed olfactory systems. Mice have smaller brains and are more susceptible to hemodynamic changes than rats, which makes it harder to obtain sufficient fMRI signals [1]. Thus, a robust procedure is required to detect odor responses in mice. The aim of this study is to detect odor responses in not only the olfactory bulbs (OBs) but also the whole brains of mice, by using a high-performance cryogenic probe.

Experiments were performed on a 7 T Bruker scanner with a cryogenic surface probe. Mice were anesthetized with urethane, and stimulated by isoamyl acetate (IAA) in the middle of the GRE-EPI scans.

The signals in the piriform cortex (Pir) and the dorsolateral OB rapidly increased upon the stimulation and quickly decreased upon the stimulation suspension. The Pir, which belongs to a general olfactory pathway, was actually activated. The dorsolateral OB activation sites corresponded to the sites identified in the rat study [2], which seem to be specific to IAA responses. The activation of the dorsal striatum, involved in emotion and cognitive function, suggested that the repetitive stimulation with IAA may induce appetite or addiction [3].

We successfully revealed the OB and brain responses of mice with the cryogenic probe. However, GRE-EPI suffers from distortion in the regions distant from the surface coil, and thus it is difficult to evaluate signal changes in the base of the brain. Therefore, we plan to use the CBV method, which has higher sensitivity, and the FLASH sequence, which induces less distortion.

[1] Ielacqua, G.D. et al., Proc. Intl. Soc. Mag. Reson. Med. (2015), [2] Martin, C. et al., NeuroImage (2007), [3] Everitt, B.J. et al., Ann. N. Y. Acad. Sci. (1999)

P-2-061　アロディニア特異的な痛みに対する鎮痛薬評価系に関する fMRI 研究
An fMRI study of the evaluation system for analgesic agents on allodynia-specific pain

杠　直哉（熊本大学大学院 生命科学研究部 構造生命イメージング分野）
Naoya Yuzuriha[1], Sosuke Yoshinaga[1], Hiroshi Sato[2], Sokichi Honda[3], Keisuke Tamaki[3], Toshihiro Sekizawa[3], Akihiko Fujikawa[3], Mitsuhiro Takeda[1], Hiroaki Terasawa[1]
[1]Department of Structural BioImaging, Faculty of Life Sciences, Kumamoto University, Kumamoto, Japan, [2]Bruker Biospin K.K., Yokohama, Japan, [3]Drug Discovery Research, Astellas Pharma Inc., Ibaraki, Japan

【要旨】線維筋痛症モデルラットにおけるアロディニア特異的な痛み応答に対する鎮痛薬作用の評価を行った。グリーンレーザーによって生じる脳内応答を BOLD 法により調べた結果、鎮痛薬投与依存的にアロディニア特異的な痛み応答が抑制された。我々の開発した評価系は、アロディニア発症機序の解明に貢献できると考える。

Fibromyalgia and neuropathic disorders characterized by chronic pain induce the pathological condition allodynia. The aim of this study is to elucidate the allodynia-specific neural circuits activated by green laser stimulation in the reserpine-induced myalgia (RIM) rat, an animal model of fibromyalgia [1], using the BOLD technique. We previously reported the allodynia-specific pain responses evoked by the green laser stimulation [2]. In this study, we monitored the effects of analgesic agents on allodynia-specific pain using the evaluation system.

The RIM rats were converted according to the reported method [1]. The rats were treated with analgesic agents, and later the BOLD experiments were then performed. MRI experiments were performed with a 7.0 Tesla scanner (Bruker BioSpec). Functional data were acquired with a 4-shot GRE-EPI sequence. The green laser was used to irradiate the left hind paws.

When the rats were treated with saline, the signal intensities in the primary somatosensory cortex, insular cortex, and thalamus were increased upon the laser stimulation. In contrast, when the rats were treated with analgesic, no BOLD responses were observed in the three brain regions. It is conceivable that the pain signals were inhibited by analgesic agents, and thus the stimulation-induced BOLD responses were not detected.

We successfully observed the analgesic effect on allodynia-specific pain, with the evaluation system using the RIM rats, a green laser, and BOLD-fMRI. We will compare the activation suppressing effects caused by other analgesic agents with different mechanisms, in order to clarify the underlying mechanism of allodynia.

References
[1] Yuzuriha N. et al., Proc. Intl. Soc. Mag. Reson. Med. 22, 3036 (2014)
[2] Nagakura Y. et al., PAIN 146, 26-33 (2009)

P-2-062　Awake mouse MRI 測定法における極低温プローブに適応可能なマウス服の最適化
Optimization of the awake mouse MRI method using mouse clothes for a cryogenic coil system

中田　悦史（熊本大学大学院 生命科学研究部 構造生命イメージング分野）
Etsushi Nakata[1], Shunsuke Kusanagi[1], Kazunari Kimura[1], Rikita Araki[2], Mitsuhiro Takeda[1], Sosuke Yoshinaga[1], Hiroaki Terasawa[1]
[1]Department of Structural BioImaging, Faculty of Life Sciences, Kumamoto University, Kumamoto, Japan, [2]Bruker Biospin K.K., Yokohama, Japan

【要旨】手術や訓練をせずに実施できるマウス服を用いた awake MRI 法の開発を行った。以前発表した極低温プローブ用マウス服のデザインを改良することで、EPI 撮像において画像分解能程度まで脳の動きを抑制し、SNR も改善することに今回成功した。本手法の fMRI 実験への適用を電気刺激実験に基づいて検証している。

In the current awake mouse MRI, fixing apparatuses implanted in the brain by surgery [1] and acclimation procedures by training [2] have been explored. However, these methods require technical proficiency and days of training. At the last JSMRM annual meeting, we reported an awake MRI method using mouse clothes designed for a cryogenic coil system, without surgery and training [3]. Although the previous clothes suppressed the mouse brain movement to an extent, the MR image quality was lower than that of anesthetized mice without clothes. The aim of this study is to optimize the mouse clothes for awake MRI.

MRI experiments were performed with a 7 T Bruker BioSpec scanner and a mouse brain cryogenic surface coil. C57BL/6 mice were anesthetized, clothed, and fixed in the MRI cradle. At 60 minutes after cessation of the anesthesia, MR images were acquired. Standard deviations of the mouse brain movements were calculated using SPM8.

Better brain immobilization effects and higher SNR MR images were obtained using the newly designed clothes. As compared to the MR images of anesthetized mice without clothes, a similar level of blurring suppression but lower SNR images were obtained. Reduction of the hood cover material on the mouse head will lead to higher SNR images comparable to those acquired with anesthetized mice.

We succeeded in optimizing the awake mouse MRI method, using newly designed mouse clothes for the cryogenic coil system. We are attempting to detect BOLD responses from awake mice evoked by electrical stimuli, using our MRI method. Our method will greatly facilitate the acquisition of awake-specific neuronal responses.

[1] Desai, M. et al., J. Neurophysiol. (2011), [2] King, J.A. et al., J. Neurosci. Methods (2005), [3] Kusanagi, S. et al., JSMRM (2015)

P-2-063　神経因性疼痛モデルマウスのグラフ理論に基づいた全脳網羅的解析
Atlas based whole brain analysis with the graph theoretical approach in resting state functional connectivity MRI of neuropathic pain model mice

小牧　裕司（慶應義塾大学 医学部 生理学教室）
Yuji Komaki[1,2], Fumiko Seki[1,2], Keigo Hikishima[3], Masaya Nakamura[4], Hideyuki Okano[1]

[1]Department of Physiology, Keio University School of Medicine, [2]Central Institute for Experimental Animals, [3]Okinawa Institute of Science and Technology Graduate University, [4]Department of orthopaedic surgery, Keio University School of Medicine

【要旨】神経因性疼痛のひとつであるアロディニアは通常では疼痛をもたらさない微小刺激がすべて疼痛として認識される感覚異常と定義されるが、その脳内機序は未だ明らかでない。本研究は神経因性疼痛モデルマウスを対象として、安静時機能的MRIにより脳内ネットワークを可視化し、グラフ理論に基づいて領域間相互作用を評価した。

Allodynia, a type of neuropathic pain, is defined as pain in response to a non-nociceptive stimulus. Recent research in brain imaging, which involves the integration of resting state functional connectivity MRI (rs-fc MRI) and graph theory, has revealed some fundamental aspects of brain-network organization in neurological disorders. rs-fc MRI is a novel approach that examines spontaneous brain function by using BOLD contrast in the absence of a task. Brain connectivity in a mouse model of neuropathic pain is not yet fully clear.
In this study, rs-fc fMRI analysis was conducted in allodynia model mice. Both degree and eigenvector centrality were significantly decreased in the contralateral S1, clustering coefficient and local efficiency were significantly increased in the ACA, and betweenness centrality was significantly higher in the ventral posterolateral nucleus of the thalamus.
These results indicate that the sensory information that reaches to S1 through the VPL is reduced, and a pain matrix that includes the ACA and VPL may form a complicated circuit network. The objective approach with fMRI can improve our understanding of pathophysiological mechanisms.

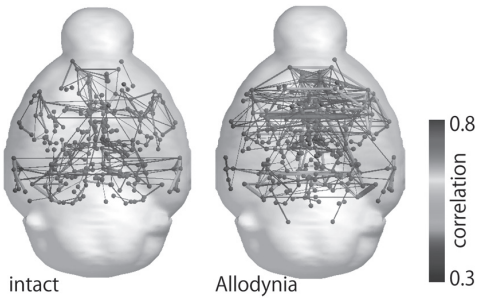

P-2-064　オペラント学習fMRI
Operant Learning fMRI

久恒　辰博（東京大学 大学院新領域創成科学研究科）
Tatsuhiro Hisatsune, Keisuke Sakurai, Naohiro Jomura, Jun Kaneko

GSFS, The University of Tokyo

【要旨】14Tを発生するボアサイズ46.5 mmの超電導磁石ならびに画像取得に必要な全コイル類（傾斜磁場コイル、室温シムコイル、RFコイル）を国内技術で製造し、マウスの機能MRI計測に適したMRI装置を開発した。機能MRI計測にはSE-EPIを用い、オペラント学習遂行中のマウス脳活動を一撮像あたり1.5秒で取得する実験系をくみ上げた。

Functional MRI (fMRI) is the most popular brain imaging to monitor neural activity, but the clinical application of fMRI has been still limited. One possible reason for this circumstance is the scarcity of fMRI data from mouse, the most popular experimental animals with the large numbers of genetic mutants, which include all kinds of neuropsychiatric as well as neurodegenerative disorder models. In this study, to overcome this condition, we have developed a mouse fMRI system which consisted of a horizontal bore ultra-high field superconductor magnet (14T, 46.5 mm: manufactured by JASTEC, Kobelco group) and high resolution MR imaging coils: a hybrid of 6 layer gradient coil and 10 layer room temperature shim coil (designed by Tesla Engineering Ltd. UK, and manufactured by Tecno Electric Industry Co., Ltd), and surface type RF coil suitable for mouse awake fMRI (Takashima Seisakusho Co., Ltd.). These coils are operated by Bruker's Paravision 5 system. For the mouse awake fMRI, we also manufactured a head-fixed operant conditioning learning apparatus (O'hara & Co., Ltd.), which consisted of fiber optics, a tube for water, and detector for licking behavior. All apparatus are non-magnetic, and are fitted in the inner diameter of 30 mm. For the functional MRI of awake mouse during operant learning task, we utilized Spin Echo EPI sequence (TE/TR=20/1500 ms, FA=90, FOV=12x12 mm, 0.125x0.125x0.5 mm). We set up to acquire functional MRI data set from mouse in 1.5 seconds per one imaging. The fMRI data acquisition timing was controlled by the cue from operant learning task. Operant learning mouse fMRI will offer unexperienced data to basic as well as clinical fMRI research fields.

P-2-065　iMSDE併用STIR3DTSE法を用いた神経叢描出における脂肪抑制効果
Fat suppression effect STIRon 3D-TSE with improved motion-sensitized driven equilibrium (iMSDE) for MR neurography

梶原　直（東海大学 医学部附属病院 診療技術部 放射線技術科）
Nao Kajihara[1], Kouki Hayasaka[1], Susumu Takano[1], Syuhei Shibukawa[1], Makoto Obara[3], Masami Yoneyama[3], Tetsu Niwa[2], Tomohiko Horie[1]

[1]Department of Radiology Tokai University Hospital, [2]Radiology Tokai University Hospital, [3]Healthcare Department Philips Electronics Japan

【要旨】我々は脂肪抑制効果において再現性の高い画像の取得を目的とし、STIR法を用いたiMSDE併用3DTSE法におけるNeurographyの撮像条件の検討を行った。腕神経叢の描出においても良好な脂肪抑制効果を示し本法の有用性が示唆された。

Purpose:Image reproducibility is an important factor when assessing the therapeutic response of peripheral nervous system disease such as chronic inflammatory demyelinating polyneuropathy (CIDP). This is also the case with recently introduced 3D nerve-SHeath signal increased with INKed rest-tissue RARE Imaging (3D SHINKEI). This new technique uses a combination of improved motion sensitized driven equilibrium (iMSDE), SPAIR, and volume isotropic turbo spin-echo acquisition (VISTA), achieving excellent-quality images. However, a use of SPAIR technique often causes inadequate fat suppression. We sought a use of STIR might achieve more stable fat suppression effect in neurography. In this study, we aimed to evaluate reproducibility of fat suppression effect of STIRon 3D-TSE with iMSDE for brachial and lumbosacral plexus regions. Method:We scanned eight healthy volunteers at a 1.5T-MRI unit (Ingenia; Philips). Basic parameters were TR/TE=2775/85 ms. We assessed following three issues 1) relationship between T2prep time and null point of fat tissue; 2) fat suppression effect with and without iMSDE setted to null point of fat on T2prep time; 3) homogeneity of fat suppression effect at the cervical region scanned with the optimized parameters. Results:Null point became short according to extension T2prep time. The intra-abdominal visceral fat showed high signal intensity with increasing gradient-strength. Well fat suppression effect was obtained with iMSDE when using T2 prep time more than 50ms on STIR. Homogeneous signal suppression for fat tissue was obtained using optimized parameters. Conclusion:A use of STIR provides homogeneous fat suppression on 3D TSE with iMSDE for the brachial plexus and lumbosacral plexus regions.

P-2-066　頚髄MR Myelographyにおける3point DIXON法併用Fast Spoiled Gradient Echo法の有用性
Usefulness of Fast Spoiled Gradient Echo with three point DIXON method in the cervical spinal cord MR Myelography

上薗　博史（東海大学 医学部付属 大磯病院 放射線技術科）
Hiroshi Uezono, Yuhei Otsuka, Shiho Sakamura, Yumiko Iida

Tokay University Oiso Hospital Radiation technology department

【要旨】3point DIXON法併用FSPGR法を用いた頚髄MR Myelographyの撮像を試み、ファントムにおいてフリップ角を変化させたCNR、健常人ボランティアを対象として受信バンド幅、撮像方向について神経根の描出を比較した。その結果、神経根を明瞭に描出することができ、有用性が示唆された。

[Purpose]It has been reported with Gradient Echo to anatomy grasp of the nerve roots in the spinal cord MR Myelography and Steady State Coherent Gradient Echo method is useful. However, at the time of cervical spinal cord MR Myelography imaging, significantly influenced by the magnetic field inhomogeneity, there is a case to be a failure rendered by the fat suppression failure or banding artifact.We will report that examined the usefulness of the cervical spinal cord MR Myelography imaging using Fast Spoiled Gradient Echo (FSPGR) with 3point DIXON method.[Materials and Methods]All MR imaging was performed on a 1.5 Tesla Scanner (GE Health Care) using 8ch CTL Spine Array Coil and QD Head Coil, water phantom and nerve root model phantom (PVA gel water content of 79%). We calculated contrast-to-noise ratio (CNR) at multiple flip angles using water phantom and nerve root model phantom. We compared nerve root visualization at multiple received bandwidth (rBW) and difference of scan direction.[Results and Discussion]CNR has become a high value in 10 degrees flip angle. No significant difference was found between high and low rBW in nerve root visualization, however banding artifact was found in low rBW because of the shortest TR extending. Nerve root visualization was the most intelligible in the Coronal direction.[Conclusion]FSPGR with 3point DIXON method was useful for visualizing cervical spinal cord.

P-2-067　Low-RFA STIR-PROPELLER法とT2FSE IDEAL法における腕神経叢描出の比較検討
Depiction of brachial plexus in MRI: Low-RFA STIR-PROPELLER method vs T2FSE-IDEAL method

小野浩二郎（千葉県こども病院 検査部 放射線科）
Kojiro Ono[1,2], Takayuki Sakai[3], Yasuhiro Oikawa[4], Akira Shirayama[1], Atsushi Senoo[2]
[1]Department of Radiology, Chiba Children's Hospital, [2]Department of Radiological Science, Graduate School of Human Health Science, Tokyo Metropolitan University, [3]Department of Radiology, Eastern Chiba medical center, [4]Department of Orthopedics, Chiba Children's Hospital

【要旨】腕神経叢の描出は血管内信号，脂肪信号の抑制と高い空間分解能が必要となる．我々は低いリフォーカスアングルの信号をPROPELLER法でk-spaceに充填した2D STIR-PROPELLER法による腕神経叢描出法を試みた．本検討ではLow-RFA STIR-PROPELLER法とIDEAL法における腕神経叢描出能の比較検討を行った．

[Background] The Low-RFA STIR-PROPELLER method is combinations of STIR (Short-TI Inversion Recovery) suppressing fat signal homogenously and low refocus flip angle (Low-RFA) PROPELLER for flow signal suppression. Furthermore, the PROPELLER is able to reduce ghost generated by flow and motion, and to maintain high resolution by averaging of k-space. Consequently, Low-RFA STIR-PROPELLER method will be expected to make clear brachial plexus imaging. In this study, we compare this new scheme (Low-RFA STIR-PROPELLER) with traditional method (T2FSE- IDEAL) in the depiction of brachial plexus. [Purpose] To compare the Low-RFA STIR-PROPELLER method with the T2FSE-IDEAL method in the depiction of brachial plexus. [Method] All subjects were scanned by 1.5T (tesla) MRI (Signa HDxt Ver.23, GE Healthcare) with HNS BrachPlx coil as receiver. This study was approved by our institutional review board. Five healthy volunteers were the subjects of this study. We evaluated 1) the effect of signal suppression from blood vessels, and 2) the signal differences between muscles and brachial plexus. The former was examined by 3 trained radiologists with visual 5 point scale, and the latter was evaluated by contrast ratio (CR) between muscle and nerves. [Result and Discussion] The PROPELLER method was better both for the signal suppression and for the contrast than the IDEAL method. The PROPELLER method could reduce signals from subclavicular vessels, that was not able to suppress by IDEAL method. Moreover, it suppressed CSF flow signals, which could lead better to visualize nerve roots than IDEAL method. [Conclusion] The Low-RFA STIR-PROPELLER method was more useful than the T2FSE-IDEA method in the depiction of brachial plexus.

P-2-068　呼吸同期併用頸椎MRIの検討
MR imaging of the cervical spine with respiratory gating

小玉　亮一（長崎北病院 放射線科）
Ryoichi Kodama, Takeshi Ideguchi, Satoru Koura, Toshimasa Fujishita, Makoto Ochi
Department of Radiology, Nagasaki Kita Hospital

【要旨】頸椎疾患の診断ではMRIの撮像は重要な役割を果たしているが、頸部領域のMRIは呼吸の影響を受けやすい。今回、我々はボランティアの頸椎MRIを従来の撮像法と呼吸同期法とを比較検討し、呼吸同期を用いることで脳脊髄液の動きと呼吸によるアーチファクトを低減できることが確認できた。

(Purpose) To evaluate the impact of respiratory gating on reduction of flow related artifact in T2-weighted axial image of the cervical spine. (Materials and Methods) We compared contrast to noise ratio (CNR) of T2-weighted axial MR images with and without respiratory gating. MR imaging was performed on a 3.0T clinical MR system (GE Signa HDx 3.0T) with Head Neck Spine CTL coil. We obtained axial T2-weighted images with and without respiratory gating. Seven volunteers,5 women and 2 men, age range 27 to 61 years, were examined. We placed ROI in subarachnoid spaces around cervical cord and outside of the body at the levels of intervertebral disks and calculated CNR using the air signal and air noise methods.(Result) On visual evaluation, images with respiratory gating were superior to those without respiratory gating. The averages of the CNRs using air noise method with and without respiratory gating were 19.59 and 8.2, respectively. The averages of the CNRs using air signal method with and without respiratory gating were 8.62and 3.59, respectively. CNRs of images with respiratory gating were significantly higher than those without respiratory gating in both air signal method and air noise methods. (Conclusion) Although scan time of imaging with respiratory gating was longer than that of without gating, MR imaging with respiratory gating appeared to be effective tool to reduce flow related artifact and motion artifact caused by respiration.

P-2-069　Variable refocus flip angle 3D FSE (Cube) における撮像断面による画質の影響
Impact of image quality due to the imaging section in Variable refocus flip angle 3D FSE (Cube)

小泉　百未（聖隷佐倉市民病院 放射線科）
Yumi Koizumi, Masaru Sonoda, Hideki Nagatomo
Seirei Sakura Citizen Hospital Division of Radiology

【要旨】Cubeの撮像断面が画質に与える影響について頚椎のT2強調画像を用いて比較した．ビーズを入れた自作ファントムを作成しビーズのプロファイルカーブを作成し，原画像と再構成画像，撮像断面を比較した．ボランティアの冠状断像，矢状断像，横断像の視覚評価を行った． Cubeは撮像断面によって画質評価に差を生じた．

Purpose
To compare image qualities of T2WI depending on imaging planes of Cube in cervical spine MRI.
Materials and methods
1.Experimental assessment
A phantom with various beads was made and imaged for assessing spatial resolution in transverse, sagittal, and coronal planes of Cube. MPR images were also generated from the transverse, sagittal, and coronal original images. The diameters of beads were measured on the original and reconstructed images and the profile curves of the diameters of beads on the all images were made. The differences of diameters of the beads on original and reconstructed images were compared.
2.Image assessment
A total of three healthy volunteers were enrolled. T2WI of the cervical spine by Cube was obtained in transverse, sagittal, and coronal planes. In addition to transverse, sagittal, and coronal MPR images, oblique sagittal MPR images along with the neural foramen in the cervical spine were also generated. Sharpness of the vertebral body, spinal cord, and nerve roots was assessed according three grading system (excellent, good, and poor).
Result
In the experimental assessment, the profile curves of diameters of beads were same on original and reconstructed images. In the image assessment, original and reconstructed images from transverse planes in Cube had an excellent sharpness of the vertebral body, spinal cord, and nerve roots compared to the other image planes.
Discussion
Since effects of flow compensation depend on image planes in Cube, the sharpness of the vertebral body, spinal cord, and nerve roots was thought to be reduced by motion artifacts.
Conclusion
Image qualities in transverse planes in cervical spine MRI by Cube were better than those in sagittal and coronal planes.

P-2-070　MR neurography/T2 mapping同時収集シーケンス (SHINKEI Quant) を用いた慢性炎症性脱髄性多発神経炎の評価
Evaluation of chronic inflammatory demyelinating polyradiculoneuropathy with MR neurography/T2 mapping (SHINKEI Quant)

樋渡　昭雄（九州大学 臨床放射線科学）
Akio Hiwatashi[1], Osamu Togao[1], Koji Yamashita[1], Kazufumi Kikuchi[1], Ryo Somehara[1], Ryotaro Kamei[1], Masami Yoneyama[2], Hiroshi Honda[1]
[1]Department of Clinical Radiology, [2]Philips Medical Systems Japan

【要旨】SHINKEI Quant により、慢性炎症性脱髄性多発神経炎 (CIDP) 患者と健常者を比較した。C5-T1 神経節及び神経根の大きさ及びT2値を測定した。神経節と神経根の大きさ、T2値はCIDP患者群が健常者群よりも大きかった (P <0.05)。SHINKEI Quantを用いて頸部神経節および神経根の評価が可能で、CIDP患者の評価に有用である。

Purpose: We have developed the new T2 mapping method called SHINKEI Quant using three-dimensional nerve-sheath signal increased with inked rest-tissue rapid acquisition of relaxation imaging (1). The purpose of this study is to discriminate the patients with CIDP from normal subjects using SHINKEI Quant.
Methods: Fine male patients with CIDP (age range 52-80 year old; median 61 year) and 5 normal male subjects (age range 25 - 43 year old; median 29 year) were studied. MRI was conducted on a 3T clinical scanner (Ingenia CX, Philips Healthcare, NL) using dS TotalSpine coil. Typical imaging parameters were as follows; TR = 2400ms, TEequiv = 60ms, TSE factor = 100, Resolution = 1 ×1 ×1 mm^3, 90 slices, Fat suppression: SPAIR with Image-based shimming, iMSDE: 36ms and 72ms, Venc=1cm/s (FH, AP and RL), TA = 6 min 19s. T2 values and size of the ganglions and the root of the brachial plexus at C5-T1 were evaluated. Statistical analysis was performed with Mann-Whitney U test. A p-value less than 0.05 was considered significant.
Results: The size of the ganglions (6.10 ± 1.22 mm vs. 5.59 ± 1.08 mm; P <0.05) and roots (4.66 ± 1.44 mm vs. 3.50 ± 0.61 mm; P < 0.0001) was larger in patients with CIDP than in the normal subjects. T2 of the ganglions (111.52 ± 43.65 ms vs. 90.42 ± 14.70 ms; P < 0.05) and roots (96.73 ± 29.89 ms vs. 83.69 ± 11.96 ms; P < 0.05) was also larger in patients with CIDP than in the normal subjects.
Conclusion: Patients with CIDP could be distinguished from normal patients in size and T2 value of the brachial plexus with SHINKEI Quant.

P-2-071　腰椎冠状断面における3D-MERGEの検討
Investigation of the Coronal Lumbar 3D-MERGE Imaging

二階堂　剛（社会医療法人孝仁会 釧路脳神経外科 診療放射線科）
Tsuyoshi Nikaidou[1], Kenji Furukawa[2], Kouki Yamamoto[2]
[1]Department of Radiology, Social Medical Coporation Kojinkai Kushiro Neurosurgery, [2]Department of Radiology, Kushiro Kojinkai Memorial Hospital

【要旨】腰椎冠状断面の神経・神経根の描出を3D-MERGEで検討した。健常ボランティアに対し、撮像条件を変化し至適条件を決定。3D-MERGE と3D-FIESTA・3D-COSMICを視覚評価し比較を行った。3D-MERGEは硬膜内・周辺組織の評価が高く、神経・神経根を明瞭に描出でき有用性が高かった。

Introduction:To obtain additional lumbar coronal images, it is desirable to use some pulse sequences that could depict spinal cord and nerve roots in a short time.Purpose:The purpose of this study was to determine optimal conditions to delineate lumber spine and its nerve roots using 3D-MERGE which can construct T2* image with high SNR and CNR.Materials and Methods:We obtained informed consents from 3 healthy male volunteers aged 26-32 years. We used a 1.5T MR unit (SIGNA HDxt, GE) equipped with a standard NV array coil to obtain the lumbar MRI. We tested various combinations of the following scan parameters for 3D-MERGE: 1) TE (min Full, in-phase and out-of-phase), 2) FA (2-12°), 3) BW (31.25-83.33 kHz). Optimal combination of the scan parameters was determined by calculating contrast ratios in the lumbar nerve roots, muscles and vertebrae. Using the optimal combination of scan parameters determined by the method described above, we compared the image quality of 3D-MERGE with those of conventional 3D-FIESTA and 3D-COSMIC. Two spinal surgeons and 1 radiologist evaluated the images by visual inspection and scored them into 3 grades regarding sharpness of the lumbar regions described above. Delineation of anatomic detail was also visually evaluated.Results:he optimal combination of the scan parameters was determined as follows: TE: out-of-phase, FA: 8° , BW: 31.25 kHz. By visual inspection of the image sharpness, 3D-COSMIC was suitable for imaging the spinal cord, and 3D-MERGE was suitable for nerve roots and surrounding tissues. Taken altogether, including delineation of anatomic detail, 3D-MERGE was thought to be the best sequence.Conclusion:Coronal lumbar 3D-MERGE imaging was useful to delineate lumbar nerve roots and surrounding tissues.

P-2-072　ボクセル単位のADC値の再現性は十分でない
Is repeatability of voxel-wise ADC value satisfactory?

小野寺耕一（札幌医科大学 医学部 放射線診断学）
Koichi Onodera[1], Naoya Yama[1], Mitsuhiro Nakanishi[2], Masamitsu Hatakenaka[1]
[1]Department of Diagnostic Radiology, School of Medicine, Sapporo Medical University, [2]Division of Radiology, Sapporo Medical University Hospital

【要旨】ADC値の再現性を評価するために臨床用3T MRI装置を用いて同一条件で連続して2回ファントムのT2値、EPI法によるADC値およびTSE法によるADC値を計測した。T2値は計測値間に有意差を認めなかったがADC-EPI値およびADC-TSE値では有意差を認めた。ADC値の再現性が高いとは言えない。

Purpose: To evaluate repeatability of voxel-wise ADC. **Methods:** ADC and T2 of phantom containing 0.2 mM gadolinium and 80% polyvinyl alcohol (Nikkofines (90-401)) was measured in a 3T clinical MRI system (Ingenia, Philips and Signa HDx, GE). The examinations were performed twice in an identical positioning for both T2WI and DWI with single shot EPI (DWI-EPI) and multi-shot TSE (DWI-TSE). The sequence parameters for T2, DWI-EPI, and DWI-TSE were as follows: FOV=220 mm, slice thickness=4 mm, acquisition matrix=112×110-112, NEX/acquisition time(s)=1/226 for T2WI, 16-18/260-292 for DWI-EPI, and 18/288 for DWI-TSE, TR/TE(ms)=2000/10-80 for T2, 4000/85 for DWI-EPI, 4000/87.4 for DWI-TSE, b-factor=0 and 1000 s/mm^2. Voxel-wise T2 and ADC were compared between examinations using Wilcoxon signed rank test. $p<0.05$ was considered statistically significant. **Results:** T2 did not show significance. ADC showed significance both for ADC-EPI (p=0.0023 for Ignenia and p=0.006 for Signa) and ADC-TSE ($p<0.0001$). 3 clinical ADC-EPI data showed different results (p=0.0002, 0.065, 0.33). **Conclusion:** The repeatability of voxel-wise ADC is not high enough.

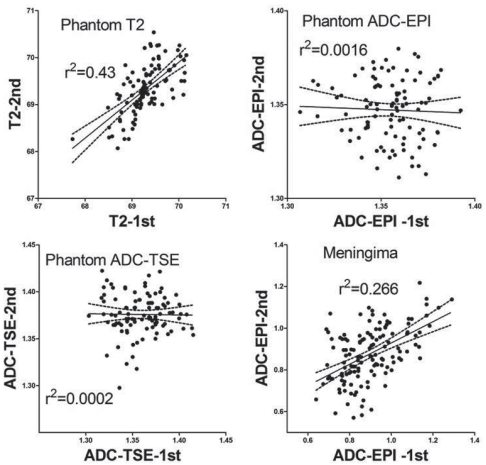

P-2-073　前立腺癌診断における改良後Computed DWIの有用性の検討
The clinical assessment of upgraded Computed Diffusion-Weighted MR Imaging for prostatic cancer

黒川　浩典（三豊総合病院 放射線診断・IVR科）
Hironori Kurokawa, Atsushi Okamura, Shumiyo Iwata
Mitoyo General Hospital, Department of Radiology

【要旨】Computed　DWIは機種によることなく、高B値画像を得ることができるが欠点としてバックノイズがあった。今回CDWIがバージョンアップされ，バックノイズの低減も期待できるため検討した。症例はMRIを施行され生検で前立腺癌を診断された10症例。高信号の位置の一致の有無、サイズ、最大信号とバックノイズを評価した。

Purpose: High b value Diffusion Weighted Imaging (DWI) is useful in detecting prostatic cancer. High b value DWI have limitation on MRI hardware.Computed DWI (CDWI) is calculated image, therefore we can get high b value DWI regardless MRI hardware. In our last examination CDWI and DWI were about the same. CDWI was useful but CDWI had a background noise as a fault. Recently CDWI was upgraded and we can expect the reduction of background noise on CDWI. The purpose of this study was to compare the efficacy of CDWI and real DWI. Materials and Methods: 10 patients who were pathologically confirmed prostatic cancer underwent MRI. CDWI (b value 2000mm2) using the two b values (0 and 1000s/mm2) were obtained. We compared real DWI and CDWI. We evaluated signal size, background noise, signal max and signal location. Results: Image qualities of CDWI and real DWI were about the same. The signal of normal prostate on CDWI was lower than real DWI. Therefore CDWI was useful in detecting prostatic cancer. Conclusions: We can easily get high b value CDWI regardless MRI hardware.Upgrade CDWI is available enough in substitution for real DWI.

P-2-074　前立腺WDS(weighted diffusion subtraction)における至適b値
Optimum b-value for WDS (weighted diffusion subtraction) in prostate cancer imaging

押尾　晃一（慶應義塾大学 医学部 放射線診断科）
Koichi Oshio[1], Hiroshi Shinmoto[2]
[1]Department of Diagnostic Radiology, Keio University School of Medicine, [2]Department of Radiology, National Defense Medical College

【要旨】拡散MRIにおいて組織の性状に関する情報は高b値の画像により多く含まれるが、b値を上げるに従って周囲の解剖学的な情報が得られなくなるというジレンマがあった。WDSを用いることによりこの問題は基本的に解消されるため、WDSを使うことを前提とした時の至適b値を検討した。

Introduction
In diffusion MRI, information on tumor tissue increases as larger b value is used, while anatomical information in the surrounding tissue decreases. This situation sometimes makes max b value selection difficult. Using WDS (weighted diffusion subtraction), this dilemma is largely resolved, since both tumor tissue information and surrounding anatomical features are both available in the single combined image. We investigated the optimum b value used with the WDS technique in prostate cancer imaging.
Methods
WDS is a technique to make a weighted subtraction image from a low- and high-b value image pair by applying following formula for each pixel,
$S = \exp(-\Delta b\ D_{thres})\ S_0 - S_1$
where S is the result, S_0 and S_1 are signal intensity for low- and high-b images, Δb is the difference between two b values, D_{thres} is the ADC threshold.
WDS images are calculated for b = 0, 1000, b = 0, 2000, and b = 0, 3000 pairs, and the result were visually inspected.
Also, a simulation was carried out to calculate expected contrast to noise ratio (CNR) between the cancer and surrounding normal tissue using using a bi-exponential model.
Results
Typical WDS images are shown on the figure.

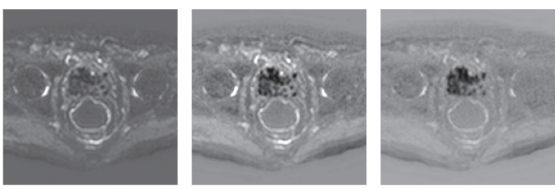

P-2-075　computed DWIを併用したFOCUSによる撮像条件の検討
Examination of imaging parameters by field-of-view optimized and constrained undistorted single-shot using computed diffusion weighted image

五十嵐太郎（一般財団法人神奈川県警友会 けいゆう病院）
Taro Igarashi[1], Mitsuyuki Takahashi[2], Hiroki Hori[3], Tetsuichi Hondera[4]
[1]Keiyu Hospital, [2]Yokohama Sakae Kyousai Hospital, [3]SHIN-YURIGAOKA General Hospita, [4]Showa University Fujigaoka Hospital

【要旨】FOCUS はphase FOV (pFOV)を減少させるで、歪が少ない画像を得ることが出来ます。しかし減少したpFOVは、SNRを低下させます。今回我々は、FOCUSとcomputed DWIを併用することで、SNRが保たれた歪の少ない高いb値の拡散強調画像を得るための撮像条件の検討を行った。

Purpose The field-of-view optimized and constrained undistorted single-shot (FOCUS) technique is Diffusion weighted image (DWI) that used a 2-dimensional spatially selective echo-planar radio frequency excitation pulse. High spatial-resolution and few distortion images will be obtained by small Field of view (FOV) or the reduced phase FOV (pFOV). However small FOV or the reduced phase FOV decreases the signal to noise ratio (SNR), therefore diagnosis will be difficult. Computed DWI (cDWI) can obtain differ b-value image from actual DWI (aDWI). Thereby, it is possible to calculate the high b-value DWI, poor SNR image may be avoided. In this study, the combined use of FOCUS and cDWI, consider possible to obtain a high b-value DWI of high resolution and few distortion images.Materials and methodsPhantom was filled with water or detergent or oil in the bottle, and fixed around in the polyvinyl alcohol. Experiments were performed on a SIGNA Explorer MRI system with 12ch body array coils. aDWIs were obtained in spin-echo echo planer imaging (SE-EPI), and excitation mode were normal excitation or FOCUS. FOCUS was performed by varying b-value or pFOV or FOV. Qualitative evaluations were performed with SNR or contrast ratio (CR) or distortion ratio (DR).ResultFOCUS was reduced image distortion by reducing the FOV or pFOV , though SNR was decreased. However the combined use of FOCUS and cDWI, we were able to acquire a good SNR and reduced distortion image of high b-value DWI.

P-2-076　等方的組織内水拡散モデル：拡散尖度と組織微細構造との関係
A model of water diffusion in isotropic tissue: a relationship between diffusion kurtosis and tissue microstructure

田村　元（東北大学大学院医学系研究科医用物理学分野）
Hajime Tamura[1], Akiko Shimauchi[2], Naoko Mori[3], Tatsuo Nagasaka[4], Hideki Ota[3]
[1]Division of Medical Physics, Tohoku University Graduate School of Medicine, [2]Kameda Kyobashi Clinic, [3]Diagnostic Radiology, Tohoku University Graduate School of Medicine, [4]Radiology, Tohoku University Hospital

【要旨】拡散係数 (ADC) は、これまで組織の「細胞密度」を、また、拡散尖度 (*K*) は、「複雑性」を表すとされてきた。本研究で、等方的組織内水拡散モデルを考えることにより、ADCは、主に、組織中で細胞の占める「体積」を、*K*は、その細胞の体積をある一定の値に固定して考えた場合、細胞の「大きさ」を反映することが示された。

Magnetic resonance diffusion weighted imaging (DWI) has been shown to provide information of tissue microstructure, especially by considering non-Gaussianity of diffusion. A simple and approximate form of the non-Gaussianity caused by restricted diffusion is the diffusion kurtosis model: $\exp[-D\,b + D^2\,b^2\,K/6]$, where b is the b-value of DWI, D is the apparent diffusion coefficient (ADC) and K is the diffusion kurtosis coefficient. Herein, we show that DWI signals obtained with multiple b-values may provide the information of cell radius (r_C) and volume fraction (V_C) of the cells in living tissue non-invasively.

Methods

We considered a simple model that mimics an isotropic tissue containing spherical cells with partially permeable membrane. We assumed appropriate self-diffusion coefficients and transverse relaxivity, and membrane permeability. Under these assumptions, the relationships between diffusion parameters (D, K) and tissue characteristics (r_C, V_C) were obtained by solving Bloch equations.

We retrospectively obtained DWI data of patients with breast cancer, where tumor specimens were available. Imaging parameters of DWI were $\delta = 7.7$ ms, DELTA = 36.8 ms, TE = 74 ms, b-values of 0, 0.05, 0.1, 0.3, 0.55, 0.85, 1 ms/μm^2. We performed IVIM analysis to obtain D and K and estimated r_C and V_C using the relationship between (D, K) and (r_C, V_C) obtained above.

Results and discussion

This study showed the relationship between diffusion measures and characteristics of tissue microstructure based on a simple mathematical model. Although ADC has been considered to be an indicator of cellular density, we have shown that ADC reflects V_C. Although K has been attributed to a tissue complexity, it was shown that K is larger for smaller radius of the cells at a fixed volume fraction.

P-2-077　ガンマナイフ治療患者におけるQ-ball imaging tractographyの有用性検討
The usefulness of Q-ball imaging tractography versus diffusion tensor tractography in gamma knife radiosurgery

鈴木　雄一（東京大学 医学部 附属病院 放射線部）
Yuichi Suzuki[1], Hirotaka Hasegawa[2], Minoru Mitsuda[1], Akihiro Kasahara[1], Kanako Matsuda[1], Takeo Sarashina[1], Yasushi Watanabe[1], Kenji Ino[1], Masahiro Shin[2], Jiro Sato[1], Keiichi Yano[1], Nobuto Saito[2], Akira Kunimatsu[1]

[1]The University of Tokyo Hospital, Department of Radiology, [2]The University of Tokyo Hospital, Department of Neurosurgery

【要旨】ガンマナイフ治療患者に対して、拡散テンソルtractography (DTT)とQ-ball imaging tractography (QBT)を用いて両側錐体路を描出し、QBTの有用性を検討した。全例においてQBTの描出容積が優れていた。特に患側で、DTTの描出容積の92.3%がQBTでも描出された。撮像時間が数分延長するが、QBTの有用性はあると考えられた。

Purpose: To minimize the morbidity associated with radiosurgery for critically located lesions, diffusion tensor tractography (DTT) was integrated into the treatment planning for gamma knife surgery (GKS). However, it is difficult to depict complicated fibers, using DTT. The aim of this study was to compare the tractography depictions of the pyramidal tract obtained using DTT and QBT and to examine the usefulness of QBT before GKS.
Materials and methods: Diffusion data were acquired in from 7 patients (4 with arteriovenous malformation; 2, with cavernous angioma; and 1, brain tumor metastasized from breast cancer) using the Siemens Magnetom Avanto 1.5T. The following conditions were compared. DTT: TR/TE = 7200/87 ms; MPG = 64; b-value = 1000 s/mm^2; and acquisition time = 491 s. QBI: TR/TE = 8500/109 ms; MPG = 64; b-value = 3000 s/mm^2; and acquisition time = 580 s. The bilateral pyramidal tract was reconstructed using the seed and target regions were located in the cerebral peduncle and the motor cortex, respectively. The volumes of the depicted tractographies were compared, and the overlap rate (the volume percentage of DTT covered by QBT) was calculated.
Results: In all cases, the volume depicted with QBT was superior to that detected with DTT. The overlap rate was 85.0% for the normal hemisphere and 92.3% for the abnormal hemisphere.
Discussion: The depiction volume was increased by QBT, primarily in the area of the corticobulbar tract. These findings suggest that QBI has an advantage over DTI in terms of a high overlap rate and the addition of pyramidal tract information. However, the acquisition time was extended by several minutes.
Conclusion: A comparison of depictions using DTT and QBT before GKS suggested the usefulness of QBT for depicting the pyramidal tract.

P-2-078　拡散強調MRIのbi-exponentialパラメーターと低酸素イメージングパラメーターとの関連性
Correlation between DWI bi-exponential estimates and PET hypoxia imaging activities in head and neck carcinoma

今泉　晶子（放射線医学総合研究所 医工連携画像研究チーム）
Akiko Imaizumi[1], Takayuki Obata[1], Masayuki Inubushi[2], Mitsuru Koizumi[3], Kyosan Yoshikawa[4], Ming-Rong Zhang[4], Katsuyuki Tanimoto[4], Rintaro Harada[5], Takashi Uno[5], Tsuneo Saga[6]

[1]Applied MRI Research, National Institute of Radiological Sciences, [2]Kawasaki Medical School, [3]Japanese Foundation for Cancer Research, [4]National Institute of Radiological Sciences, [5]Chiba University, [6]Kyoto University

【要旨】頭頚部癌の低酸素イメージング法として、拡散強調MRIの有用性を検討するため、bi-exponentialパラメーターとFAZA-PETのパラメーターの相関を評価したところ、Dslowは正の相関がみられ、低酸素の指標となる可能性が示された。

Objective
Hypoxic tumor has highly malignant property and resistance to radiotherapy and chemotherapy. Assessment of hypoxia is important for selection of treatment method, including hypoxia-targeting therapy, and prediction of treatment effect. ^{18}F-fluoroazomycin arabinoside (FAZA) positron emission tomography (PET) has been reported to be useful for hypoxia imaging, but it will take some time to become prevalent in clinical practice. Under hypoxia, alteration of cell structure leads to change in water diffusion. This change may be detected by diffusion-weighted magnetic resonance imaging (DWI) by bi-exponential model. The purpose of this study was to evaluate the correlation between DWI bi-exponential estimates and FAZA-PET activities and to investigate the usefulness of MRI for hypoxia imaging of head and neck carcinoma.
Materials and Methods
Eleven patients with head and neck carcinoma (8 primary tumors and 5 lymph nodes without necrosis) were included. They were the subjects that had this MRI protocol in the previous FAZA study [1]. By bi-exponential model, the diffusion coefficients of fast and slow components (Dfast, Dslow) and their fractions were obtained. Apparent diffusion coefficient (ADC) was also obtained at low and high b-value ranges (lowbADC, highbADC). On FAZA-PET images, tumor-muscle ratios (T/M) were measured for comparison between DWI bi-exponential and FAZA-PET estimates using Spearman's rank correlation coefficient.
Results
There was a positive correlation between Dslow and T/M (rs=0.63, p=0.022). Dfast, fraction, lowbADC, or highbADC did not correlate with T/M.
Conclusion
Among bi-exponential estimates of DWI, only Dslow correlated with FAZA-PET parameter. Dslow might be useful as an indicator of hypoxia.
Reference
1. Saga, T., et al. ANN 30, 217-224.

P-2-079　Fontan循環肝臓のIntravoxel incoherent motion(IVIM)-DWI：正常循環との比較
Intravoxel incoherent motion diffusion imaging of the liver in Fontan circulation: Comparison with the liver in normal circulation

小野浩二郎（千葉県こども病院 検査部 放射線科）
Kojiro Ono[1,2], Kazuhiro Shiraga[3,4], Takumi Okubo[1], Hirofumi Watanabe[1], Hiromichi Nakajima[4], Atsushi Senoo[2], Akira Shirayama[1]

[1]Department of Radiology, Chiba Children's Hospital, [2]Graduate School of Human Health Science, Tokyo Metropolitan University, [3]Department of Pediatrics, The University of Tokyo Hospital, [4]Department of Cardiology, Chiba Children's Hospital

【要旨】IVIMはvoxel内の(一貫性のない)ランダムな動きである．近年，IVIM-DWIから肝内灌流量をある程度定量的に評価が可能と報告があがっている．我々はこのIVIM-DWIを利用してFontan循環肝臓の線維化，うっ血肝の評価が可能ではないかと考えた．本検討は，Fontan循環肝と正常循環肝におけるIVIM-DWIのパラメータの比較を行った．

[Purpose] To compare the intravoxel incoherent motion diffusion imaging (IVIM DWI) of the liver between Fontan circulation and normal circulation. [Subjects] The subjects of this study are 5 patients with the Fontan circulation (M/F; 3/2, mean age; 12.8 ± 1.5 years, body weight; 40.0 ± 11.1 kg, body height; 144.7 ± 12.4 cm), 4 volunteers with the normal circulation (M/F; 4/0, mean age; 10.0 ± 1.9 years, body weight; 32.4 ± 9.6 kg, body height; 137.5 ± 11.7 cm). [Methods] All subjects were scanned by 1.5T (tesla) MRI (Signa HDxt 1.5T Ver.23, GE Healthcare) using the 8ch Cardiac coil as a receiver. The IVIM-DWI is acquired with respiratory triggered SE-EPI sequence. IVIM parameters were estimated with the bi-exponential model curve by the method of a using a non-linear least square fit. The IVIM parameters (D*; pseudo diffusion f; perfusion fraction, and D; true diffusion) were calculated at the 4 circular region of interest (ROIs) manually placed in the right lobe of the liver. We compared these parameters between 2 groups. [Results] Liver IVIM parameters of 5 patients with Fontan circulation showed D* value of 30.83 ± 24.82 10-3mm2/s, f value of 13.15 ± 3.07 % and D value of 1.07 ± 0.042 10-3mm2/s. And those of 4 volunteers with the normal circulation showed mean D* value of 113.20 ± 25.58 10-3mm2/s, f value of 22.44 ± 2.40 % and D value of 1.25 ± 0.158 10-3mm2/s, respectively. There were significant differences between the Fontan and normal circulation in D* (p=0.002) and f values (p=0.001), but there were no significant differences in D values (p=0.11). [Conclusion] Liver IVIM parameters (D*and f) of the Fontan circulation are significantly lower than normal circulation.

P-2-080　3T-MRIにおける直接冠状断TSE-DWIBSとEPI-DWIBSのアーチファクトの比較
Comparison of image artifacts between DWIBS using single-shot TSE (TSE-DWIBS) and DWIBS using echo-planner imaging (EPI-DWIBS) at 3T MRI scanner

鈴木　真（東京女子医科大学病院 中央放射線部）
Makoto Suzuki[1], Yuki Hachiman[1], Masami Yoneyama[2], Yu Nishina[2,3], Satoru Morita[3]

[1]Tokyo Women's Medical University Hospital, Department of Radiological Services., [2]Philips Healthcare Japan, [3]Tokyo Women's Medical University Hospital, Department of Diagnostic Imaging and Nuclear Medicine

【要旨】3T-MRIで健常ボランティアの冠状断TSE-DWIBS，冠状断と軸位断のEPI-DWIBSを撮像し，アーチファクトを比較した．定量評価として脊髄の幅を計測し，T2強調画像と各々のDWIBSの差を算出した．加えて，歪みとアーチファクトについて視覚評価を行った．TSE-DWIBSはEPI-DWIBSよりも歪みとアーチファクトが少なかった．

<Purpose>To compare the image artifacts between direct-coronal TSE-DWIBS and EPI-DWIBS.
<Methods>Direct-coronal TSE-DWIBS, direct-coronal EPI-DWIBS (cEPI-DWIBS), axial EPI-DWIBS (aEPI-DWIBS), and T2 weighted imaging (T2WI) of the neck to pelvis in 4 healthy volunteers were obtained using a 3T MRI scanner (Ingenia, Philips). The acquisition times of TSE-DWIBS, cEPI-DWIBS, and aEPI-DWIBS of each section were 3min 30s, 2min 13s and 4min 47s, respectively. The differences between the width of the spinal code on each DWIBS sequence and that on T2WI on the frontal and lateral images of MIP were calculated for an index of image distortion. All images were assessed by consensus of two radiologists. Image distortion, fat-saturation homogeneity, and overall image quality for artifacts were qualitatively assessed on the MIP images using 5 point-scale.
<Results>The difference between the width of spinal code on each DWIBS sequences (TSE-DWIBS, cEPI-DWIBS and aEPI-DWIBS) and that on T2WI in frontal image was 0.96 ± 0.5mm, 21.09 ± 9.0mm and 2.09 ± 1.7mm. The difference between the width of spinal code on each DWIBS sequences (TSE-DWIBS, cEPI-DWIBS and aEPI-DWIBS) and that on T2WI in lateral image was 2.36 ± 1.2mm, 2.00 ± 1.3mm and 11.70 ± 4.7mm.The average score of image distortion of TSE-DWIBS (4.25 ± 0.4) was better than that of cEPI-DWIBS (1.50 ± 0.5) and aEPI-DWIBS (2.25 ± 0.8).The average score of fat saturation homogeneity of TSE-DWIBS (4.25 ± 0.4) was better than that of cEPI-DWIBS (1.25 ± 0.4) and aEPI-DWIBS (2.75 ± 0.4).The average score of overall artifacts of TSE-DWIBS (4.25 ± 0.4) was better than that of cEPI-DWIBS (1.50 ± 0.50) and aEPI-DWIBS (2.50 ± 0.5).
<Conclusion>TSE-DWIBS has less image artifacts including distortion compared to EPI-DWIBS.

P-2-081　SENSEを用いないDirect Coronal DWIBSにおける撮像条件の基礎的検討
Basic study on Parameters of Direct Coronal Diffusion-weighted Whole Body Imaging with Background Body Signal Suppression without SENSE

佐藤　広崇（草加市立病院 医療技術部 放射線科）
Hirotaka Sato, Hirokazu Kato, Mamoru Okubo, Junrou Yamamoto, Tsuneaki Nakagawa, Namiko Matsui

Department of Radiological Technology, Soka municipal Hosptal

【要旨】位相方向をRLに設定すると歪みが大きいため位相方向を頭尾(SI)方向とした。また折り返しアーチファクト軽減のため、体軸方向の感度を狭めるため設定coilを1chとした。1chではSENSEが使用不可であるため、SENSE無し位相方向SIの短時間で撮像可能なdirect cornal DWIBSの基礎検討を行った。

purposeDWIBS is a useful sequence in search of bone metastases throughout the body.We are trying to add scanning of DWIBS for screening of bone metastases at the time of prostate cancer examination.As a basic condition, Phase encoding direction was craniocaudal direction(SI). Right and left direction(RL) could not be used because of large distortion.And the coil channel of the body axis direction was the smallest 1ch. Since it reduced aliasing artifacts.Generally SENSE technique cannot be used with 1 channel coil.We performed the basic study of direct DWIBS with both setting of without SENSE and phase encoding SI.Materials and MethodA self-made phantom and five healthy volunteers (3 males and 2 females) underwent the whole body (neck to pelvis) DWIBS with 1.5T MRI Equipment (Titan, TOSHIBA).Sensitivity range of the 1channel coil was about 16cm. Acquisition time was within 90 seconds.We examined the changes in the following parameters:1)Phase encoding direction(SI and RL), 2)phase matrix(48,56,64,72,80,96), 3)frequency matrix(64.80.96.112.128), and 4)Phase FOV(16,18,20,22cm).Visual assessment of the five stages of overall image quality was performed by 3 radiologic technologists.Result and DiscussionIn a setting with FOV of 48cm × 20cm, distortion reflected frequency matrix. Regarding phase matrix, no difference was observed in distortion. Adding interpretation of resolution and SNR, appropriate number of matrix was 96 × 72. In condition of same pixel size but different FOV and matrix number, distortion was not changed. However SNR was changed with matrix.In this study, appropriate condition was FOV of 48cm × 20cm and matrix of 96 × 72.ConclusionIn this study low resolution but less distorted image was collected with this snap shot in these short minutes.

P-2-082　Whole Body Coronal DWIにおけるFOCUSと従来撮像法における画像の比較
FOCUS(Fov Optimized and Constrained Undistorted Single-shot) for the whole body DWI: A comparison of image quality between FOCUS and conventional DWI

松永　奈美（GEヘルスケア・ジャパン株式会社 MRマーケティング）
Nami Matsunaga[1], Masanori Ozaki[2]

[1]GE Healthcare Japan MR Marketing, [2]GE Healthcare Japan MR Engineering

【要旨】【目的】本研究はFOCUS DWIを用いたWhole body Direct corona DWIの有用性について検討を行った.【結果】Coronal FOCUS DWIでは折り返しアーチファクトのないWhole body Coronal DWIを得ることができた.

[Introduction] FOCUS technique allows to acquire small FOV in the phase direction without wraparound artifact by using a 2D RF excitation method. It can be excited a selected region in the two directions which are phase encoding and slice encoding. Therefore, FOCUS DWI can obtain coronal DWI applying S/I phase encoding direction without wraparound artifact even if there is a subject outside the FOV. The aim of this study is to compare image quality of the whole body DW image with direct coronal plane between conventional DWI and FOCUS DWI technique.[Method] This study was performed by GE 3.0T MR scanner. We compared image quality including image distortion, wraparound artifact on coronal DWI between conventional DWI and FOCUS DWI. In phantom study, we used image distortion phantom to compare image distortion between conventional DWI and FOCUS DWI. Imaging parameter are following; FOV 40, Phase FOV 0.4, 0.5, 0.6 (FOCUS DWI), Acceleration factor 1.5, 2.0, 3.0 (conventional DWI). In volunteer study, we performed 3 stations conventional DWI and FOCUS DWI to obtain scan area from chest to pelvis. Imaging parameter are following; FOV 40, Phase FOV 0.5, 0.6 (FOCUS DWI), Acceleration factor 2.0, 3.0 (conventional DWI). This study was performed by the Internal Review Board and performed informed consent from 1 volunteer. [Result] FOCUS DWI was able to reduce wraparound artifact on direct coronal DW images with S/I phase direction and it can obtain approximately similar image distortion compared to conventional DWI with parallel imaging.This study demonstrates FOCUS DWI raise the possibility to obtain better image quality without wraparound artifacts from outside FOV than conventional DWI.

P-2-083　Intravoxel incoherent motion imagingにおいて撮像対象がb値の最適化に与える影響
Effect of imaging object on optimal b-value sampling for intravoxel incoherent motion imaging

横沢　俊（株式会社 日立製作所 研究開発グループ）
Suguru Yokosawa[1], Hisaaki Ochi[1], Yoshihisa Soutome[1], Yoshitaka Bito[2]
[1]Research & Development Group, Hitachi, Ltd., [2]Healthcare Business Unit, Hitachi, Ltd.

【要旨】本研究では，誤差伝搬法によるIVIMイメージングのb値の組合せ最適化において，撮像対象となるIVIMパラメータやその範囲が最適なb値の組合せに与える影響を検討した。その結果，最適なb値の組合せは撮像対象やパラメータの範囲に影響を受けるが，最適なb値の計測点は4点に収束することを示した。

Introduction
Intravoxel incoherent motion (IVIM) is widely used in clinical examination of various organs. Although the diffusion property varies with the organ, a fixed set of b-values, which is 10 to 16 different b-values including more number of low b-values, are generally used regardless of examination sites. Previously, we proposed a method for optimizing b-value sampling using error propagation methods for IVIM imaging. In this study, we investigated the effect of target diffusion property on an optimal set of b-values.
Methods
A set of b-values was optimized by minimizing the standard deviation (SD) of IVIM parameters estimated using error propagation methods. The optimal set of b-values was explored using the typical IVIM parameters of three organs (liver, kidney, and prostrate). Furthermore, the range of IVIM parameters was considered for liver. The calculation conditions were as follows: maximal b-value, 1000 s/mm^2; and the number of sampling points of the b-value, 10 (at least one sampling point at b = 0).
Results
The results of the optimized sets of b-values were as follows: b = 0[1], 20[4], 131[3], 1000[2] s/mm^2 for liver; b = 0[1], 34[3], 187[3], 767[3] s/mm^2 for kidney, b = 0[1], 39[4], 220[3], 1000[2] s/mm^2 for prostate. The number in square bracket is number of signal average. In each case, the optimal b-values were divided into four b-values. However, the combination of b-values varied with the organ. The result of the optimized set of b-values with considering the range of IVIM parameter was as follows: b = 0[1], 20[4], 134[3], 1000[2] s/mm^2 for liver. Although the combination of b-values was affected by the range of parameters, the optimal b-value was divided into four b-values regardless.

P-2-084　LPシャント術前後のiNPHの脳室体積測定と拡散テンソルトラクトグラフィ解析
Ventricular volumetry and anterior thalamic radiation on DTI of idiopathic normal pressure hydrocephalus after a lumboperitoneal shunt

齊藤　麻美（横浜市立大学）
Asami Saito[1,2], Koji Kamagata[2], Ryo Ueda[3], Misaki Nakazawa[3], Andica Christina[2], Sho Murata[3], Madoka Nakajima[2], Masakazu Miyajima[2], Kouhei Kamiya[2,4], Masaaki Hori[2], Kanako Kumamaru[2], Michimasa Suzuki[2], Hajime Arai[2], Shigeki Aoki[2]
[1]Yokohama City University, [2]Juntendo University School of Medecine, [3]Tokyo Metroporitan University, [4]The University of Tokyo

【要旨】iNPHにおいて、LPシャント術前後での認知機能の改善は、第三脳室の大きさと負の相関を示し、前視床放線のFAと正の相関を示した。これは、視床や視床から前頭葉への線維である前視床放線がiNPHでの認知機能障害に関連する可能性を示唆する。

Background: Idiopathic normal pressure hydrocephalus (iNPH) is a syndrome which consists of three major symptoms including cognitive deterioration, gait disturbance, and urinary incontinence. INPH is a potentially treatable syndrome by shunt surgery. It has been suggested that the destruction of neural tracts associated with ventricular enlargement can precipitate the deficits of cognitive function. Anterior thalamic radiation (ATR), carrying nerve fibers between thalamus and prefrontal cortex, has a possible link with cognitive abnormalities.
Methods: 10 patients (mean age: 75 ± 4.89) were selected from those who was admitted and had lumboperitoneal (LP) shunt surgery in our hospital. Volumetry of brain ventricles by using FreeSurfer software version 5.3 and fractional anisotropy (FA) of ATR were measured and compared between pre and post LP shunt. After that we compared the volumetry and FA results with the cognitive scores, Mini-Mental State Examination (MMSE), and Frontal Assessment Battery (FAB). The data were analyzed with paired t-test, Wilcoxon signed-rank test, and Pearson's product-moment correlation by SPSS 21.0.
Results: Compared to before shunt, the third ventricle volume after shunt was significantly decreased in all patients. We found that improvement of third ventricular volume correlated increased MMSE score ($p<0.05$), and FA change of ATR before and after LP shunt correlated with increased FAB scores ($P<0.05$).
Conclusions: Cognitive deterioration in iNPH may have a close relation to the changes of the third ventricle volume and the ATR.

P-2-085　皮質-皮質下構造間コネクティビティに着目した統合失調症の白質神経回路異常の検討
Cortico-subcortical white matter connectivity disruption in schizophrenia

奥畑　志帆（京都大学大学院 工学研究科）
Shiho Okuhata[1], Satoki Yoda[1], Naohiro Okada[2], Noriaki Yahata[3], Kiyoto Kasai[2], Tetsuo Kobayashi[1]
[1]Graduate School of Engineering, Kyoto University, [2]Department of Neuropsychiatry, The University of Tokyo Hospital, [3]National Institute of Radiological Sciences

【要旨】皮質－皮質下構造間コネクティビティに着目したDTI 神経線維追跡により、統合失調症における白質神経回路異常の検討を行った。線維追跡開始領域として線条体・側坐核・淡蒼球・被核を設定し、皮質まで到達した線維群を解析した結果、淡蒼球からの追跡線維群に統合失調症患者における有意なFA値の低下がみとめられた。

The MR-DTI fiber tracking is one of the brain mapping methods to obtain the structural information about the cerebral white matter in vivo. In order to analyze disruption of white matter connectivity in schizophrenia, we applied ROI-based fiber-tracking. Diffusion and T1 images were obtained by 3T MR scanner (PHILIPS) from age- and IQ- matched 18 healthy controls and 18 patients with schizophrenia. Starting ROIs were set at the nucleus accumbens, pallidum, caudate, and putamen based on the previous studies that reported sub-cortical volumetric alteration in patients with schizophrenia. The ROIs were individually segmented from T1 MRIs using Freesurfer. In order to set terminating point of fiber-tracking, cortices of both hemispheres were also segmented. By utilizing both starting (sub-cortical) and terminating (cortices) ROIs, we focused on the white matter cortico-subcortical network. DTIs were processed using Brain Voyager. Fiber-tracking was carried out by modified TEND method (FA ＞ 0.25, angle ＜ 50°, step size = 0.5 mm) from the 8 starting sub-cortical ROIs. Only the fiber bundles that reached to the cortex were further processed. Mean FA and MD were calculated from each tracked fiber bundles. Statistical analyses were done by 2-way ANOVA (hemisphere / groups) using SPSS. For FA, there were significant left - right main effects in the caudate, putamen and pallidum. In addition, significant FA reduction was found in SZ only in the pallidum. MD indicated significant left - right main effect in the caudate, putamen and pallidum. Group difference did not reach the significance. Our findings suggest the possibility of disruption of cortico-subcortical white matter network related to the pallidum in schizophrenia.

P-2-086　MUSE法を用いたDWIの検討
Investigation of DWI by multiplexed sensitivity encoding (MUSE)

野崎　　敦（GEヘルスケア・ジャパン 研究開発部）
Atsushi Nozaki[1], Hiroyuki Kabasawa[1], Yoshinobu Nunokawa[2], Rikiya Fujishiro[2], Shigeo Okuda[3], Hirokazu Fujiwara[3], Masahiro Jinzaki[3]
[1]MR Applications and workflow, Asia Pacific, GE Healthcare Japan, [2]Office of Radiation Technology, Keio University Hospital, [3]Department of Radiology, Keio University School of Medicine

【要旨】Sensitivity encoding を用いたmulti shot-DWIでデータ収集を行い、DWIの画質の検討を行った。Shot数を多くするほど、ボケが少なくなり画質の改善が確認できた。

[Purpose] With higher spatial resolution, the image quality of single shot-DWI poor image quality due to longer echo train. In this study, we evaluated the image quality of multi shot-DWI with MUSE. [Methods] We used GE 3.0T Discovery MR750 with 32-channel Head Coil. Enrolled one healthy volunteer with informed consent to participate and scanned head by single shot-DWI and MUSE-DWI. Scan parameters were as follows : FOV=24cm, Slice Thickness=5mm, TR=4000ms, b=800s/mm2, NEX=2, RBW=250kHz, Scan Matrix=256x256, Two setting of MUSE shot=2 and 4, Single shot-DWI TE=69.3msec, 2shot MUSE-DWI TE=56.3msec, 4shot MUSE-DWI TE=50.9msec. Images quality were visually evaluated by two radiologists. [Results] By using MUSE, the echo train was shortened and the image quality of MUSE-DWI was improved without blurring compared to single shot-DWI. [Conclusion] Scan time is longer with MUSE-DWI. However, with shorter echo train, the image quality was improved without blurring. MUSE-DWI is effective for high resolution DWI scanning.

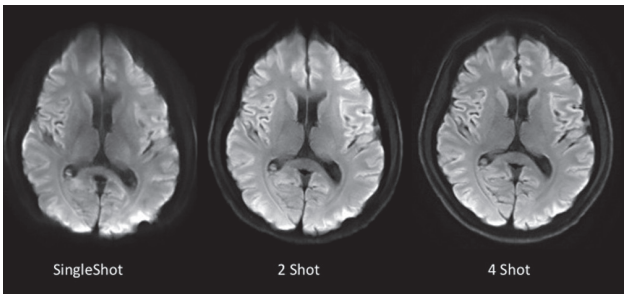

P-2-087　脳卒中後上肢片麻痺患者を対象としたrTMS・集中的OT併用療法前後の機能と構造の再編成
Functional and structural reorganization before and after repetitive transcranial magnetic stimulation plus intensive occupational therapy

上田　亮（首都大学東京大学院 人間健康科学研究科 放射線科学域）
Ryo Ueda[1], Naoki Yamada[2], Masahiro Abo[2], Atsushi Senoo[1]

[1]Department of Radiological Sciences, Graduate School of Human Health Sciences, Tokyo Metropolitan University Graduate School, [2]Department of Rehabilitation Medicine, Jikei University School of Medicine

【要旨】脳卒中後上肢片麻痺患者を対象にrTMS・集中的OT併用療法によって有意な運動機能改善が報告されているが、大脳皮質の可塑性や機能的再構築への影響ははっきりと分かっていない。本研究では50名の患者の3D-T1WI、DTI、fMRIを解析することで本介入における大脳機能と構造の再編成を明らかにした。

Background: Repetitive transcranial magnetic stimulation (rTMS) plus intensive occupational therapy (OT) is a useful intervention for poststroke patients with upper limb hemiparesis. However, few reports on the underlying mechanism of motor function with this combination treatment are available.
Aim: To clarify the recovery mechanism associated with rTMS plus OT treatment using 3D-T1-weighted imaging (3D-T1WI), functional magnetic resonance imaging (fMRI), and diffusion tensor imaging (DTI).
Methods: A total of 50 poststroke hemiparetic patients received 12 sessions of low-frequency rTMS over the non-lesional hemisphere and daily OT for 15 days. Motor function was evaluated using the Fugl-Meyer Assessment (FMA) and Wolf Motor Function Test (WMFT). fMRI was performed at admission and discharge to calculate the laterality index (LI) from the number of activated voxels. The capacity in Brodmann areas (BA) 4 and 6 and the injury ratio for the cerebral capacity were calculated using 3D-T1WI. Fractional anisotropy (FA) in the white matter of BA4 and 6 were calculated using DTI.
Results: This treatment significantly improved FMA and WMFT scores ($P<0.01$). A significant negative correlation was found between the volume of healthy side BA4 or 6 of the pretreatment and treatment volume change of the affected side BA6 ($P<0.05$). Significant negative correlations were found between FA change due to treatment of the affected side BA6 and injury rate ($P<0.05$) and between LI of the pre-treatment and LI change due to the treatment ($P<0.05$).
Conclusions: Functional reorganization caused by this treatment is related to the balance of functions between hemispheres before treatment. The brain's structure prior to treatment affects its structural reorganization with this treatment.

P-2-088　拡散テンソル・拡散尖度画像におけるSMS-RESOLVEの有用性の検討
Simultaneous Multi-Slice RESOLVE DWI: comparison of single shot technique by Diffusion tensor and Kurtosis tractography

福永　一星（順天堂大学医学部附属 順天堂医院 放射線科・部）
Issei Fukunaga[1], Masaaki Hori[1], Nozomi Hamasaki[1], Shuji Sato[1], Ryo Ueda[1,2], Hideo Kawasaki[1], Nao Takano[1], Syo Murata[1], Kouhei Tsuruta[1], Haruyosi Hoshito[1], Katsutoshi Murata[3], Shigeki Aoki[1]

[1]Department of Radiology, School of Medicine, Juntendo University, [2]Department of Health Science, Graduate School of Human Health Sciences, Tokyo Metropolitan University, [3]SIEMENS Healthcare

【要旨】SMSはblipped CAIPIRINHAを用いて複数断面を同時収集し、multishotのRESOLVEと組み合わせて、歪みの少ない高分解能のthin slice全脳撮影が容易となる。本研究では、Diffusion Tensor およびKurtosis Imagingにおける有用性をDKI tractographyにて検討した。

Introduction: The simultaneous multi-slice (SMS) with blipped-CAIPIRIHNIA technique has emerged as a powerful tool to reduce scan time. In this study, we compared Diffusion Tensor and Kurtosis Imaging Analysis with SMS-RESOLVE and multi-band (MB) single shot EPI.Methods: Three normal healthy young subjects participated in the study. DKI data sets were acquired on a clinical 3T-MRI scanner (MAGNETOM Skyra, SIEMENS healthcare) with 64ch phased array coils. 1. SMS-Resolve: 3 b values (0, 1000, and 2000 s/mm2); MPG 30; TR/TE 5430/92, 126 ms; voxel size 1.5*1.5*1.5 mm; SMS acceleration 3; GRAPPA 2; readout segment 5; Echospace 0.36 ms; NEX 2. 2. MB ss EPI: TR/TE 5430/97.2 ms; Echospace 0.94 ms. We calculated all diffusion metric maps with DKE, DKE ft, and, TrackVis (freesoft). Results and Discussions: SMS-RESOLVE techniques were effective to reduce the distortion and blurring artifacts in comparison to MB ss EPI. The clinical use of RESOLVE in combination with SMS may be a solution to reduce the scan time. Conclusion: Diffusion Tensor and Kurtosis Imaging Analysis with SMS-RESOLVE enables improved visualization of the tracts, for example, pontine crossing tract, compared with MB ss EPI.

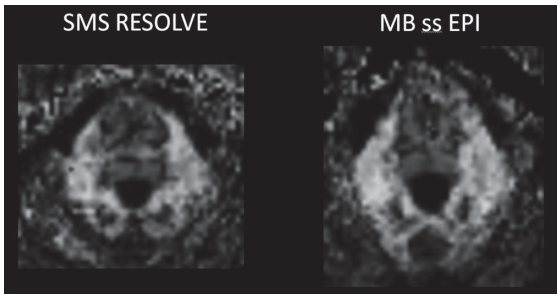

P-2-089　加速度補正型DWIによる脳温度測定
Optimal strategy for measuring intraventricular temperature using acceleration motion compensation DWI

渋川　周平（東海大学 医学部 付属病院 放射線技術科）
Shuhei Shibukawa[1,2], Naoki Ohno[2], Toshiaki Miyati[2], Susumu Takano[1], Tetsu Niwa[3], Tetsuo Ogino[4], Tomohiko Horie[1], Nao Kajihara[1]

[1]Department. of Radiology, Tokai University Hospital, [2]Division of Health Sciences, Graduate School of Medical Sciences, Kanazawa University, [3]Radiology, Tokai University, [4]Healthcare department, Philips Electronics Japan

【要旨】DWIを用いてCSFの脳室温度を測定する方法が報告されているが，CSFの拍動の影響による測定誤差があること，そして適正なb値の検討は報告されていない．そこで我々は加速度補正型DWIによる脳室温度測定を検討し，より正確な測定が可能であることを実証した．

INTRODUCTION:With MRI, it has been reported a method for monitoring the intraventricular cerebrospinal fluid (CSF) temperature calculated from the diffusion weighted image (DWI). However, this method induces a measurement temperature error due to the CSF pulsation affect. Moreover, it has been suggested that DWI should be obtained by suitable b value in consideration of the diffusion coefficient of measuring tissues. Therefore, we applied the acceleration-motion compensation DWI to the determination of the intraventricular temperature (IVT).
METHODS and MATERIALS:At a 3.0 T MR system, DWI images of the lateral ventricle (LV) and third ventricle (TV) were obtained in eight healthy volunteers. To assess the effect of the CSF pulsation on the IVT using DWI, we compared among three types diffusion gradients, ie., (1) conventional DWI (c-DWI), (2) motion compensation DWI (MC-DWI), and (3) acceleration-motion compensation DWI (aMC-DWI). We applied suitable b value of 400 s/mm^2 on the basis of the literature value of diffusion coefficient of free water at 37C° (D = 3.0 x 10^{-3} mm^2/s). Diffusion coefficient was calculated from the signal of DWI with b value 0 and 400 s/mm^2 in each ventricle. The IVT for each ventricle was assessed using Friedman test. To compare the CSF flow velocities in ventricles, we determined with PPU-synchronized phase-contrast(PC) cine MRI.
RESULTS and DISCUSSION:With b value of 400 s/mm^2, the IVT with c-DWI and MC-DWI in TV were significantly higher than that in LV. The two DWI methods were affected by the CSF flow velocity. However, with aMC-DWI, there was no significant difference in the IVT between the two ventricles. CONCLUSION:The aMC-DWI is optimal strategy for measuring accurately the IVT.

P-2-090　脳内ネットワークとNEO-FFI性格検査の５因子との関係：正常成人における検討
Brain structural connectivity and five-factor personality measures in healthy adults

上田　一生（産業医科大学 医学部 放射線科）
Issei Ueda[1], Shingo Kakeda[1], Keita Watanabe[1], Koichiro Sugimoto[1], Natsuki Igata[1], Asuka Katsuki[2], Junji Moriya[1], Reiji Yoshimura[2], Osamu Abe[3], Yukunori Korogi[1]

[1]Department of Radiology, University of Occupational and Environmental Health, Fukuoka, [2]Department of Psychiatry, University of Occupational and Environmental Health, Fukuoka, [3]Department of Radiology, Nihon University School of Medicine, Tokyo

【要旨】正常被験者51名を対象に、NEO-FFI 人格検査における５因子(神経症傾向、外向性、開放性、調和性、誠実性)と脳内ネットワークの関係について調べた。全例に拡散テンソルを撮像し、グラフ理論を用いて脳内ネットワークを解析した。結果、神経症傾向と右上側頭領域における脳内コネクティビティに負の相関関係を認めた。

PURPOSE: The five-factor model organizes personality traits into five factors: Neuroticism, Extraversion, Openness to Experience, Agreeableness, and Conscientiousness. Measures of these personality traits predict people's behaviors and important outcomes of their lives. Therefore, understanding the neural correlates of these personality traits is important. In this study, we examined a correlation between scores of NEO Five-Factor Inventory (NEO-FFI) and brain structural networks.
MATERIALS AND METHODS: Fifty-one healthy participants (18 women, 33 men; mean age, 38.5 ± 11.7 years) underwent the NEO-FFI and MRI including diffusion tensor imaging (DTI) and 3D T1WI (3D-FSPGR). Using MRI data, we constructed whole brain inter-regional connectivity matrices for each participant, and calculated graph theoretical network measures in various brain regions (83 regions from "aparc + aseg" segmentation in FreeSurfer).
RESULTS: Neuroticism negatively correlated with nodal clustering coefficient in right superior temporal regions ($p=0.00067$, FDR<0.05). Other factors of the NEO-FFI did not show significant correlation with any graph theoretical network measures of the brain regions.
CONCLUSION: Our result suggests that greater Neuroticism associates with lowered structural connectivity in the superior temporal regions. The whole brain structural connectome with DTI represents an important technique in further understanding the neural mechanisms underpinning behaviors and mental health conditions related to personality types.

P-2-091　BDNF遺伝子Val166Met多型におけるうつ病患者の脳内ネットワーク変容：テンソル画像を用いたコネクトーム解析
Relationship between a BDNF gene polymorphism and the brain structural networks in major depressive disorder patients: a connectome analysis with DTI

杉本康一郎（産業医科大学 医学部 放射線科）
Koichiro Sugimoto[1], Shinzo Kakeda[1], Keita Watanabe[1], Issei Ueda[1], Natsuki Igata[1], Asuka Katsuki[2], Junji Moriya[1], Reiji Yoshimura[2], Osamu Abe[3], Yukunori Korogi[1]

[1]Department of Radiology, University of Occupational and Environmental Health, Fukuoka, [2]Department of Psychiatry, University of Occpational and Enviromental Health, Fukuoka, [3]Department of Radiology, Nihon University School of Medicine, Tokyo

【要旨】うつ病患者群29例と正常者48例群を対象に、脳内ネットワークにおけるBDNF遺伝子の影響について調べた。両群をBDNF遺伝子多型（Met群とVal/Val群）により更に分類し、群間比較を行った。結果、うつ病群、かつVal/Val群であることが、右下前頭回眼窩部における脳内コネクティビティの低下に関連した。

PURPOSE: Brain-derived neurotrophic factor (BDNF) relates to the basic neuronal functions, such as cell survival, axonal outgrowth, and dendritic growth. The Val66Met polymorphism of BDNF gene may affect genetic susceptibility to major depressive disorder (MDD). We investigated the relationship between the Val66Met BDNF genotype and brain structural networks of first episode and drug-naive MDD patients and healthy subjects (HS). MATERIALS AND METHODS: Twenty-nine MDD patients and 48 HS matched for age and gender, who underwent MRI including diffusion tensor imaging (DTI) and 3D T1WI (3D-FSPGR), were divided into two groups based on their BDNF genotype. Using MRI data, we constructed a whole brain structural connectome for each participant, and calculated graph theoretical network measures (CC: clustering coefficient and CPL: characteristic path length). The diagnosis effects of the BDNF genotype and the genotype-diagnosis interaction in relation to CC and CPL in various brain regions (83 regions from"aparc + aseg" segmentation in FreeSurfer) were evaluated. RESULTS: Among the Val/Val-carriers, the CC in the right orbital part of inferior frontal gyrus was significantly decreased for MDD patients than for the HS, which means that there was a significant genotype-diagnosis interaction effect on brain structural connectivity. On the other hand, among the Val/Val-carriers, the CC in the left cingulate gyrus and supramarginal gyrus were significantly increased for MDD patients than for the HS, and the CPL in right nucleus accumbens and globus pallidus were significantly decreased for MDD patients than for the HS. CONCLUSION: The polymorphism of BDNF gene was associated with brain structural networks in MDD patients, which may be related to the manifestation of MDD.

P-2-092　脳NODDI解析：線形化・凸最適化による高速法と原法との解析結果の対比
Quantitative comparison between conventional and accelerated NODDI maps of the brain

上口　貴志（情報通信研究機構 脳情報通信融合研究センター）
Takashi Ueguchi[1,2,3], Ikuhiro Kida[1,2], Yasushi Kobayashi[2], Ken-ichi Okada[2], Yoshinori Kadono[3], Sachiko Yamada[4], Guoxiang Liu[1,2]

[1]CiNet, National Institute of Information and Communications Technology, [2]Graduate School of Frontier Biosciences, Osaka University, [3]Osaka University Graduate School of Medicine, [4]Osaka University Hospital

【要旨】NODDIは軸索・樹状突起の密度や方向のばらつきを推定する新しい脳拡散画像法である．ただし，この原法は非線形なモデルの当てはめに伴う計算コストの高さが実用上の課題であり，線形化によって大幅に計算時間を短縮する高速法が提案されている．本研究ではヒトおよびサルにて原法と高速法でのNODDI画像を定量的に対比した．

Neurite Orientation Dispersion and Density Imaging (NODDI) is regarded as a promising tool to estimate the microstructural information of brain tissue from MR images. NODDI fits a three-compartment tissue model to diffusion data, resulting in the following three NODDI maps: neurite intracellular volume fraction, neurite orientation dispersion index, and isotropic diffusion volume fraction. Despite its applicability, the use of this technique is often limited owing to the high computational cost of its non-linear fitting procedures. Recently, an algorithm has been proposed to drastically reduce the computation time by formulating the NODDI model as a linear system that can be solved efficiently using convex optimization. The algorithm renders NODDI more practical; however, the extent to which the accelerated NODDI maps correlate with the conventional ones is unclear. This study, therefore, aims to quantitatively compare accelerated and conventional NODDI maps obtained from images of a human subject and a Japanese monkey at 7 T, which were sourced from susceptibility and eddy-current-corrected dataset, using the NODDI MATLAB Toolbox and the AMICO framework. Two-shell (b = 1000 and 2000 s/mm^2; 30 directions each) diffusion images and b = 0 images were acquired using a spin-echo diffusion EPI sequence provided by the University of Minnesota. Quantitative comparison between accelerated and conventional NODDI maps was performed by using structural similarity (SSIM) index and region-of-interest correlational analysis. Our dataset showed that although simple correlational analysis provided high correlation coefficients, SSIM indices for two of the three NODDI maps varied across different regions.

P-2-093　卵巣ののう胞性腫瘤の鑑別診断における 6-point Dixon の有用性に関する検討
Value of automated quantitative 6-point Dixon MR imaging in distinguishing for cystic ovarian lesions

清水　紀恵（熊本大学医学部附属病院 中央放射線部）
Kie Shimizu[1,2], Tomohiro Namimoto[3], Masataka Nakagawa[2,3], Masahumi Kidou[3], Takeshi Nakaura[3], Seitaro Oda[3], Daisuke Utsunomiya[3], Yasuyuki Yamashita[3]

[1]Department of Cntral Radiology, Kumamoto University Hospital, [2]Department of Diagnostic Radiology,Graduate School of Medical Sciences, Kumamoto University, [3]Department of Diagnostic Radiology, Faculty of Life Sciences, Kumamoto University

【要旨】卵巣ののう胞性腫瘤において血液と脂肪の区別は、成熟嚢胞性奇形腫、子宮内膜およびその他の嚢胞性腫瘤の鑑別診断をする上で重要となってくる。本研究では、MRIの6-point Dixon法で算出される脂肪比率とR2＊値が、上記の卵巣ののう胞性腫瘤に対する鑑別診断において有用であるか臨床例を用いて評価した。

Purpose : The distinction between blood and lipid in ovarian cystic lesions on magnetic resonance (MR) imaging is important in the differential diagnosis among cystic teratomas, endometriomas and other tumors. This study aim is to evaluate the diagnostic utility of automated 6-point Dixon MR imaging for ovarian cystic lesions.Materials and Methods : twenty lesions from 16 patients (11 endometriomas, 3 cystic teratomas and 6 other miscellaneous cysts) were included. An automatically calculated fat fraction (FF) image with quantification algorithm correcting for T1 and T2* relaxation time effects of fat and water was developed with a 6-point Dixon on a 3.0-T MR system. The following MR imaging protocol was used: 6-point Dixon with automated reconstruction (fat- and water-image, FF image and R2*/ T2* image). For each patients, FF and R2* values measurements were obtained from the region of interest (ROI) in cystic part of the ovarian lesion. We quantitatively analyzed differences in FF, R2* values among ovarian lesions using Steel-Dwass test.Result : Cystic teratomas showed significantly higher FF than endometriomas and other miscellaneous cysts (FFteratoma=97.1 ± 1.4, FFendometriomas=1.4 ± 1.2, FFother=0.8 ± 0.5). Endometriomas and cystic teratomas showed significantly higher R2* values than other cysts (R2* endometriomas =47.3 ± 31.4, R2* teratoma =29.8 ± 5.5, R2*other=10.8 ± 2.0). Conclusions : The FF and R2* in ovarian cystic lesion is sufficiently different on 6-point Dixon MR imaging to allow an accurate distinction among endometriomas, cystic teratomas and other miscellaneous cysts. 6-point Dixon MR imaging was suggested to be effective in the diagnostic of cystic ovarian tumor.

P-2-094　子宮体癌における筋層浸潤の評価：Reduced FOV DWI および DCE-MRI による検討
Evaluation of depth of myometrial invasion in endometrial cancer: Comparison of reduced FOV DWI and DCE-MRI

竹内麻由美（徳島大学 医学部 放射線科）
Mayumi Takeuchi[1], Kenji Matsuzaki[1,2], Masafumi Harada[1]

[1]Tokushima University, [2]Tokushima Bunri University

【要旨】Reduced FOV DWIを用いて子宮体癌の筋層浸潤の評価(S:<1/2, D:1/2<=)を行い、T2WIおよびDCE-MRIと比較検討を行った。正診率は各々95%、62%、90%であり、特に腺筋症の合併症例で有用性が示唆され、相補的な読影で正診率は100%に向上した。

DWI demonstrates endometrial cancer (EC) as a high intensity mass, however, detailed evaluation of the depth of myometrial invasion (DMI) on DWI is occasionally difficult due to low spatial resolution and distortion. Reduced phase direction FOV (rFOV) technique can offer high quality DWI with improved spatial resolution, without associated phase wrap round artifact, and with probably less susceptibility artifacts. The purpose of this study is to compare the diagnostic performance of rFOV-DWI with those of T2WI and DCE-MRI in evaluating DMI in patients with EC. 21 women with EC included 12 stage S (no or superficial invasion: <1/2) and 9 stage D (deep invasion: 1/2<=) tumors underwent preoperative MRI with 3T unit (Discovery MR750, GE). DMI was evaluated at T2WI, rFOV-DWI (FOV:200*80-240*120mm, matrix:160*80, b = 800) and DCE-MRI (3D FSPGR). DMI was evaluated on both sagittal, and oblique axial or coronal images. DMI was not able to estimate on T2WI in 8 stage D tumors due to poor tumor-to-myometrium contrast, or due to poor tumor-to-coexisting adenomyosis contrast, and also not able to estimate on DCE-MRI in 2 stage D tumors due to poor tumor-to-coexisting adenomyosis contrast. DMI was overestimated on rFOV-DWI in one stage S tumor due to distortion caused by susceptibility artifact. The staging accuracy was 62% for T2WI, 90% for DCE-MRI, and 95% for rFOV-DWI. Combination of DCE-MRI and rFOV-DWI reading together with T2WI improved the assessment of DMI with a diagnostic accuracy of up to 100%.

P-2-095　卵巣のEndometrioid Carcinoma Resembling Sex-Cord Stromal TumorのMR所見の評価検討
MR Imaging Characteristics of Ovarian Endometrioid Carcinoma Resembling Sex-Cord Stromal Tumor

小澤　栄人（埼玉医科大学 放射線科）
Eito Kozawa[1], Iichirou Oosawa[1], Kaiji Inoue[1], Tomomi Katou[2], Masanori Yasuda[2], Kousei Hasegawa[3], Tomoaki Ichikawa[4], Mamoru Niitsu[1]

[1]Saitama Medical University, Department of radiology, [2]Saitama Medical University, International Medical Center (IMC), Diagnostic pathology, [3]Saitama Medical University, IMC, Gynecology and Oncology, [4]Saitama Medical University, IMC, Diagnostic Imaging

【要旨】卵巣腫瘍の内膜癌は、時に性索間質腫瘍に類似した組織像をバリエーションの一つとして呈することがあり、endometrioid carcinoma resembling sex cord-stromal tumorと診断される。この腫瘍は、高齢者でエストロゲンを産生しユニークなMR画像を呈する。今回我々は、これらの腫瘍6例についてMR所見の評価検討を行った。

Purpose: Endometrioid carcinoma resembling sex cord-stromal tumor (ECST) is an uncommon endometrioid carcinoma of the ovary appearing large solid mass. ECST should be differentiated from sex cord-stromal tumors. The purpose of our case series is to evaluate magnetic resonance (MR) characteristics of ovarian ECST for the diagnosis. Material and Methods: Six cases with surgically confirmed ECST, four large solid masses and two cystic masses with solid components, were evaluated. MR imaging findings were retrospectively reviewed. We also defined the signal intensity ratio (SIR) = the ovarian tumor's solid portion on dynamic MR imaging after 120 s DCE-MR image / the ovarian tumor's solid portion on dynamic MR imaging on pre DCE-MR image for semi-quantitative assessment. Results: All six lesions exhibited thickened myometrium and iso-intensity compared with myometrium. All six lesions showed iso-intensity compared with myometrium on T2-weighted images, and showed gradually increase and SIR values were 2.5-8.8 (mean =5.2). Conclusions: In postmenopausal women with endometrium thickness, large solid masses showing iso intensity compared with myometrium on T2-weighted images, and showing gradually increase and intense contrast enhancement on dynamic study may be suggestive for ECST.

P-2-096　子宮病変の良悪性診断における拡散尖度MR画像の有用性の検討
Feasibility of diffusion kurtosis imaging as a tool for differentiation between benign and malignant uterine lesions

熊谷　雄一（鹿児島大学 医学部歯学部付属病院 放射線科）
Yuichi Kumagae[1], Yoshihiko Fukukura[1], Koji Takumi[1], Hiroto Hakamada[1], Takashi Iwanaga[2], Masashi Sasaki[2], Takuro Fujisaki[2], Tomoyuki Okuaki[3], Takashi Yoshiura[1]

[1]Department of Radiology, Kagoshima University Graduate School of Medical and Dental Sciences, Kagoshima, Japan, [2]Departments of Radiological Technology, Kagoshima University Hospital, Kagoshima, Japan, [3]Philips Electronics Japan, Tokyo, Japan.

【要旨】子宮病変の良悪性診断における拡散尖度MR画像（DKI）の有用性を検討した．悪性腫瘍のDは良性病変（内膜増殖症，筋腫）より有意に低値を示し，Kは良性病変（内膜増殖症，筋腫）よりも有意に高値を示した．DKIは子宮病変の良悪性診断に有用である可能性が示された．

PurposeTo evaluate the feasibility of diffusion kurtosis imaging (DKI) for differentiating benign from malignant uterine lesions.MethodsOur study population comprised 118 patients with uterine lesions including 87 malignant tumors (MT), 7 endometrial hyperplasias (EH), and 24 uterine fibroids (UF). Diffusivity (D) and kurtosis (K) maps were calculated from DKI data obtained with b values of 0, 500, 1000, 1500, and 2000 s/mm^2. ADC map was generated from b values of 0 and 1000 s/mm^2. ADC, D, and K of MT were compared with those of EH, UF, normal endometrium (NE), and myometrium (NM). Receiver operating characteristic (ROC) analysis was used to assess the ability of the ADC, D, and K for differentiating MT from benign lesions and normal uterine tissues.ResultsADC and D of MT were significantly lower than those of EH, UF, NE, and NM. K was significantly higher in MT than in EH, UF, NE, and NM. The areas under the ROC curve of D and K were 0.877 and 0.883 for differentiation from EH, 0.926 and 0.823 for UF, 0.955 and 0.969 for NE, and 0.976 and 0.942 for NM, respectively.ConclusionK enables differentiation between benign from malignant uterine lesions.

Median Values of Measured Parameters (ADC, D, and K) for MT, EH, UF, NE and NM

	ADC	Diffusivity (D)	Kurtosis (K)
MT	0.90 ± 0.24	1.11 ± 0.31	1.10 ± 0.22
EH	1.30 ± 0.34	1.69 ± 0.41	0.73 ± 0.23
UF	1.28 ± 0.17	1.66 ± 0.28	0.85 ± 0.15
NE	1.42 ± 0.20	1.89 ± 0.40	0.61 ± 0.12
NM	1.51 ± 0.18	2.04 ± 0.34	0.69 ± 0.11

Note.- Data are mean ± standard deviations

ROC analysis in differentiating benign from malignant lesions

	ADC	Diffusivity (D)	Kurtosis (K)
MT vs EH	0.869	0.877	0.883
MT vs UF	0.911	0.926	0.823
MT vs NE	0.956	0.955	0.969
MT vs NM	0.975	0.976	0.942

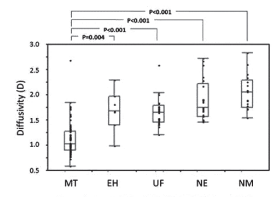

Box plots of D for MT, EH, UF, NE and NM

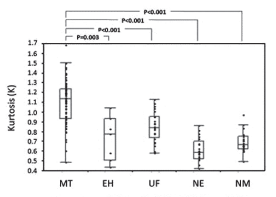

Box plots of K for MT, EH, UF, NE and NM

P-2-097　造影早期の 3D isotropic VIBE 画像による子宮内膜癌の筋層浸潤評価
Post contrast 3D isotropic VIBE images at earlier phase for diagnosis of myometrial invasion of uterine endometrial cancer

高畑　暁子（京都府立医科大学 放射線科）
Akiko Takahata, Kouji Sakai, Mariko Goto, Sachimi Yamada, Kei Yamada
Kyoto Prefectural University of Medicine

【要旨】目的：子宮内膜癌の造影早期 isotropic 撮像による筋層浸潤の診断能を調べる。方法：2013年10月～2016年4月に造影MRIを施行した32例の画像所見を術後病理と対比する。結果：1/2を超える筋層浸潤の診断能は感度90%、特異度95%、正診率93%と、ダイナミック撮像に遜色なかった。

Background: Deep myometrial invasion is one of the important prognostic factors of uterine endometrial cancer. Preoperative diagnosis is crucial in determining the operative procedure. Dynamic contrast enhanced MR examination is usually recommended because of its high tissue contrast, especially in the early phase. To perform dynamic MR study, we have to set up the most appropriate slice direction according to tumor location before injection, although this is often difficult. To overcome this problem, we applied three-dimensional (3D) isotropic data acquisition in post contrast earlier phase to avoid miss-setting of the slice direction. This will also enables making multi-planar reconstruction (MPR) image. Purpose: to assess the ability of 3D isotropic post contrast MR diagnosis for myometrial invasion of uterine endometrial cancer. Materials and Methods: Thirty-one women (45-86 years) with endometrial cancer underwent 3T MR examination including post contrast 3D isotropic T1W gradient echo sequence (VIBE) from October 2013 to April 2016. The parameters of 3D-VIBE were as follows; amount of contrast: 2ml/kg, injection speed: 2ml/sec, time to k-space center: 90sec, acquisition time: 90-110 sec, matrix: 256, FOV: 256mm, slice thickness: 1mm. One radiologist assessed MR images about the presence or absence of deep myometrial invasion and correlated the MR findings with pathological diagnosis. Result: 20 cases were G1/G2 endometrioid adenocarcinoma and 11 cases were G3, serous or clear adenocarcinoma. Sensitivity, specificity and accuracy of MR findings were respectively 90%, 95% and 93%. Conclusion: MR diagnosis of deep endometrial invasion of endometrial cancer using post contrast 3D-VIBE in earlier phase is not inferior to previously published dynamic studies.

P-2-098　骨盤部撮像でのreadout segmented echo-planer imagingの体動による影響の評価
Evaluation of motion artifact using readout segmented echo-planer imaging in pelvic imaging

斉藤　宏明（新潟大学医歯学総合病院 診療支援部 放射線部門）
Hiroaki Saito, Tatsuya Kondo, Tsutomu Kanazawa
Division of Radiology, Department of Clinical Support, Niigata University Medical and Dental Hospital

【要旨】RS-EPIはSS-EPIに比べ，体動の影響を強く受ける．motion artifactは周波数読み取り方向へ現れる．骨盤部で動きの影響を抑えた撮像にするには，readout partial fourierを併用しsegment数を抑制すること，加算回数を適切に決定することが必要である．

[Purpose]Readout segmented echo-planar imaging (RS-EPI) is used in diffusion-weighted imaging of brain as well as single-shot echo-planar imaging (SS-EPI). However, RS-EPI is likely to cause artifacts due to body motion at pelvic imaging. The purpose of this study is to clarify relationship of readout segments and motion-induced artifact in RS-EPI.
[Material and Methods]At Magnetom Prisma 3.0 T, moving phantom was performed scan using RS-EPI and SS-EPI sequences. Investigating number of readout segments were 3, 5 and 7. For each case, number of signal averages (NSA) were set 1, 2, and 4. Furthermore, readout partial fourier factor was set 5/8 and 6/8 for readout segments of 5 and 7, respectively. All schemes were used minimum echo space. A motion artifacts and image distortion were evaluated quantitatively.
[Results]Motion artifact appeared along readout direction severely comparing with SS-EPI. More severe motion artifacts were caused by increasing readout segments. Setting readout segments above 3, image distortion was approximately equivalent. In all conditions, increasing NSA led averaging motion artifacts. As adjusting read partial fourier factor 5/8 and 6/8, motion artifacts and image distortion were similarly for readout segments of 5 and 7, respectively. In addition, acquisition time was shortened by read partial fourier.
[Conclusions]RS-EPI was more sensitive for motion effects compared with SS-EPI. For mitigating motion artifacts in pelvic imaging, readout segments were set under five with read partial fourier, furthermore, increasing NSA was determined by considering motion artifacts, scan time and signal to noise ratio.

P-2-099　腎所見が異なる結節性硬化症のMRIによる出生前診断
Prenatal diagnosis of tuberous sclerosis complex with different renal appearance using MRI

桑島　成子（獨協医大 放射線医学教室）
Shigeko Kuwashima
Dept. of Radiology, Dokkyo Medical University

【要旨】超音波検査では1所見のみが指摘されMRIで診断した胎児 2例を報告する。2例とも脳と心臓と腎に本症の特徴的所見を認めた。脳と心臓所見は同じであったが腎所見は異なった。1 例目はangiomyolipoma。2例目は多嚢胞腎であり、TSC2/PKD1 contiguous gene 症候群の可能性がある。

Introduction Tuberous sclerosis complex (TSC) is an autosomal dominant disorder caused by mutations in either the TSC1 or TSC2 genes. With recent advances in both fetal US and MRI, an increasing number of cases can be diagnosed during the prenatal period. We report two cases of the prenatal diagnosis of TSC on fetal MRI, because US could not make the diagnosis. MethodCase 1: US suggested cardiac rhabdomyoma. MRI was performed at 35weeks of gestation. Case2: US suggested congenital pulmonary airway malformation. MRI was performed at 35weeks of gestation.The prenatal MR findings were compared with the postnatal radiological findings.Results Fetal MRI revealed subependymal nodules and renal abnormality (angiomyolipoma or polycystic kidney), as well as cardiac rhabdomyoma. Fetal MRI demonstrated findings consistent with TSC, which was confirmed on postnatal US, CT, and MRI. DiscussionIn this study, we evaluated areas in addition to the abnormality identified on fetal US. Using this method, we reached the correct diagnosis. Some anomalies of brain, lung, and kidney may directly influence survival or therapy plans at birth. When performing fetal MRI, we have to look at theses critical areas. The findings of cardiac and cerebral lesions were similar on both fetal MRI. In contrast, the renal appearance was different. In our second fetus, bilateral kidney showed variable sized cysts. The renal cystic disease associated with TSC suggested TSC2/PKD1 contiguous gene syndrome. Conclusion TSC have a wide variety of radiological manifestations, including those of the heart, cerebrum, and kidney. Fetal MRI is useful for the prenatal diagnosis of TSC, even when they are unsuspected on US. Renal cystic disease associated with TSC may be due to gene mutation.

P-2-100　ダイナミック造影MRIにおける参照領域法を用いた前立腺腫瘍の循環動態の定量評価
Quantitative analysis of circulatory function for prostate tumors using reference tissue model in DCE-MRI studies

生駒　洋子（量子科学技術研究開発機構 放射線医学総合研究所）
Yoko Ikoma, Takayuki Obata, Yasuhiko Tachibana, Tokuhiko Omatsu, Riwa Kishimoto, Hiroshi Tsuji
National Institute of Radiological Sciences

【要旨】ダイナミック造影MRIにおける薬物動態モデルを用いた循環動態の定量評価法として、血液入力関数を要しない簡便な参照領域法を提案した。本手法を前立腺腫瘍の造影MRI画像に応用した結果、移行速度定数は腫瘍部位で健常部位よりも高値を示し、健常、腫瘍部位の弁別能は、血液入力関数を用いた従来法と同等以上であった。

Objectives: In dynamic contrast-enhanced MRI (DCE-MRI) studies, a time-concentration curve of injected contrast agent is obtained from dynamically acquired T1-weighted images, and circulatory function around tumors is evaluated quantitatively by compartmental analysis with an arterial input function (AIF). However, it is difficult to obtain AIF individually, and AIF errors deteriorate the reliability of quantitative outcomes. In this study, we developed a quantitative analysis method using reference tissue, and applied it to DCE-MRI of prostate tumors.
Methods: The reference tissue model, providing the ratio of transfer rate constants between the target and reference regions without AIF, was derived from a conventional one-tissue compartment model. In the DCE-MRI images of patients with prostate tumors, the model parameters in normal parts (transitional zone and peripheral zone) and tumor parts were estimated by the reference tissue model using the gluteus muscle as reference region. The differences between normal and tumor parts were evaluated using paired t-test with 0.05 as significance level, and compared with those by the conventional method with AIF.
Results: The reference tissue model showed higher efflux rate constants in the tumors compared with normal parts, and the ability to discriminate between normal and tumor parts was better than that of the conventional method.
Conclusion: The proposed method can provide reliable parameters related to circulatory function by a simple analysis, and it should be useful for the diagnosis of prostate tumors.

P-2-101　Echo SpaceがT2コントラストに及ぼす影響
The influence Echo Space exerts on T2 contrast

園田　優（聖隷佐倉市民病院 放射線科）
Masaru Sonoda, Yumi Koizumi

Seirei Sakura Civilian Hospital Radiology department

【要旨】ボアのon-centerとoff-centerでecho spaceを変化さえたときのT2コントラストについて調べた。Gradient modeはWhole modeにし、Tailored RFは使用せず、バンド幅を低くすることでecho spaceが広くなり、T2コントラスト改善した。また、on-centerはoff-centerよりT2コントラストが高くなった。

[Background]
In late years the MRI of the orthopedics domain needs much Slice in Thin slice.In order to get a lot of T2-weighted image at the time of the same shooting,a lot of echo train,shorten the echospace,shorten the TR.However, T2 contrast will decrease.
[Purpose]
The present study, examined the T2 contrast when change the echospace in the on-center and off-center of the bore.
[Method]
Phantom stady;
Using manufactured MRI device (HDxt Twin) by GE, Was the arrangement of the self-made phantom in the on-center and off-center(90mm) of the bore. It changes the band width (10.42-100kHz) and Gradient mode (Zoom mode or Whole mode) and Tailored RF (on or off) in order to change the echospace.Using the 3 times captured image,it measured the SNR and CNR.
Clinical stady;
To cases of shoulder rotator cuff injury, it was to change the imaging method to Zoom mode(Tailored RF on) and Whole mode(Tailored RF on) and Whole mode(Tailored RF off) inspection. Measurement of effusion and FAT from the photographed image, and to calculate the CNR.
[Results]
Phantom stady;
The gradient mode is better Whole mode than the Zoom mode, SNR and CNR is higherTailored RF is increased in both the SNR and CNR in that it do not use.When the band width is high, SNR and CNR was smaller.Those of off-center(90mm) than on-center is, SNR and CNR was smaller.
Clinical stady;
When you do not use the Tailored RF in Whole mode, CNR of effusion and FAT became the largest.
[Consideration]
Increased CNR at imaging conditions that increase the echo space. it is considered to hold the J-coupling of the fat signal, To J-coupling fat signal are met is considered that signal is reduced.
[Conclusion]
on center and off center both can improve the T2 contrast by lengthening the echo space.

P-2-102　静磁場不均一を考慮した上肢撮像体位の検討
Study of upper limb imaging Positions in consideration of the static magnetic field inhomogeneity

岡田　敦彦（国立病院機構 大阪医療センター 医療技術部 放射線科）
Atsuhiko Okada

National Hospital Organization Osaka National Hospital department of radiology

【要旨】3T装置導入に先立ち,オフセンターの検査における B_0 不均一の影響を測定し,その影響の少ない領域での上肢撮像体位を検討する．装置内を9つに区分し,領域間のSNRと磁場均一性の比較評価及び物体間の距離による影響を比較した.寝台の中心にて上肢を8cm以上体から離すことで, B_0 不均一の影響が少ない撮像が可能であった.

objective
With the 3TMRI introduction, it is concerned about the influence of the B_0 inhomogeneity of off-center. Checking the influence of the B_0 inhomogeneity in the gantry and examined the positioning of patients within the less influence in the examination of upper extremities.
method
Using PHILIPS Achieva1.5T and Q-body coil.
1.Checking the influence of B_0 inhomogeneity by the location using a CuSO4 phantom. 9 areas were set (fig1). Compared the evaluation of SNR and uniformity from obtained images.
2.Using homemade agar Phantom (α, β) to measure the distance that a noise influenced to an object next to each other. Only scanning to α, and scanning by β in the distance of the α 2, 4, 6, 8cm.
3. From result 1.2, consider the scan physique of the patient in the B_0 inhomogeneity.
result
1.SNR and the uniformity indicate a high value in the area H.E.
2.Distance 8cm to reduce the influence of B_0 inhomogeneity.
3.It was possible to scan in the B_0 uniformity area.
Discussion
By separating the imaging region more than 8cm from the body in area H.E, we can reduce the B_0 inhomogeneity.
Conclusion
We could devise the patient position in consideration of influence of B_0 inhomogeneity in the gantry.

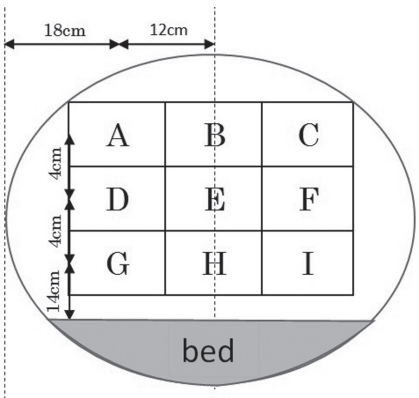

Fig1, Area of the gantry

P-2-103　T2強調画像とT2緩和時間による手関節屈曲漸増抵抗運動の活動筋分析
Analysis of muscle activity using T2 relaxation time and T2w-MRI by progressive resistance exercise on wrist flexion

秋山　純和（人間総合科学大学 保健医療学部 リハビリテーション学科）
Sumikazu Akiyama[1,2], Masayoshi Takamori[2,3], Kazuya Yoshida[1,2], Hayato Ishizaka[5], Tomoyuki Haishi[4], Hiroshi Otsuka[1], Yoshiteru Seo[2]

[1]Rehabilitation, Faculty of Health Sciences, University of Human Arts and Sciences, [2]Regulatory Physiology, Dokkyo Medical University, [3]Physical Therapy, Aoi Medical Academy, [4]MRTechnology, Inc, [5]Rehabilitation, Dokkyo Medical University

【要旨】T2w-MRIとT2緩和時間により手関節掌屈運動の筋活動を分析した。15％ Max負荷30回を1セットとし、セット数により運動負荷を漸増した。3セット運動後に尺側手根屈筋に有意な緩和時間の延長を認めた。協同筋の運動検出には5セットが必要と考えられた。

[Purpose] Muscle activities under progressive resistance exercise (PRE) were analyzed by T2w-MRI and T2 at 0.2 T. One set of exercise consisted of 30 or 50 times of wrist flexion against 15% of isometric maximum contraction (15%Max). [Method] Eight healthy adults were participated. T2w-MRI of forearm in probe was measured by multi-slice spin-echo method (TR/RE = 2000/39 ms), and T2 was measured by the CPMG multi-echo method (TR = 2000 ms, TE = 10 to 80 ms). Seven muscles were measured: the short radial extensor, digital extensor, the supinator, extensor carpi ulnaris, flexor carpi ulnaris (FCU), radial flexor and palmaris longus muscles. iPlus was used for analysis of ROI. The statistical analysis was performed by the repetitive ANOVA and Tukey test by SPSS21.0. This study was supported by scientific research fund KAKEN(C) 2400609. [Result & Discussion] As shown in Fig, T2 values of FCU increase by the progressive resistance exercise, and T2 increased significantly after the 3rd set of the exercise compared with the resting T2 value. In order to detect T2 increase in all muscles, 5 sets of exercise were needed.

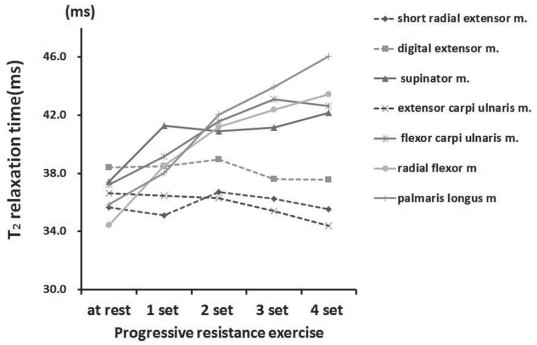

Fig

P-2-104　MRI法による示指伸筋と小指伸筋の筋活動分析
Muscle activity analysis of the Extensor digiti minimi muscle and Extensor indicis muscle by MRI method

吉田　一也（獨協医科大学 生理学（生体制御））
Kazuya Yoshida[1,2], Sumikazu Akiyama[1,2], Masayoshi Takamori[1,3], Hiroshi Otsuka[2], Yoshiteru Seo[1]

[1]Department of Regulatory Physiology, Dokkyo Medical University, [2]Department of Rehabilitation, Faculty of Health Sciences, University of Human Arts and Sciences, [3]Department of Physical Therapy, Aoi Medical Academy

【要旨】T2強調像から示指伸筋と小指伸筋の筋活動分析を行った。撮像はマルチスライススピンエコー法とし、等尺性徒手抵抗運動（40回）前後の画像信号強度変化からT検定を行った。結果より2筋ともに有意差を認めた（p=0.032, p=0.027）。40回の抵抗運動は筋力の弱い筋には最適な抵抗強度となると推察した。

[Purpose] Using a 0.2 T compact MRI system, muscle activity was detected by T2-weighted images of the extensor digiti minimi muscle and extensor indicis muscle. [Methods] Subjects were left forearm of 3 adult males. T2-weighted multi-slice spin-echo images were measured by FOV 200mm, TR 2000ms, TE 39ms, slice thickness 9.5mm, 11 slices and NA 1. T2-weighted image of resting condition was measured at first. Then, manipulative isometric contraction exercise (5 sec duration) was performed for 40 times in the MR probe. T2-weighted image was measured immediately after the exercise. Image analysis was performed using ImageJ 1.46r. Changes is signal intensity was tested by paired-t test using SPSS. The significance level was 0.05. [Results & Discussion] Image intensities were increased significantly in both the extensor digiti minimi muscle and extensor indicis muscle after the exercise (Fig1; p=0.032, p=0.027). In a previous study, we thought that 80 times the resistance movement require to detect increase of signal intensity of the extensor digitorum muscle. But, in this study, we could reduce until 40 times of the resistance movement of the muscle for detecting muscle activities.

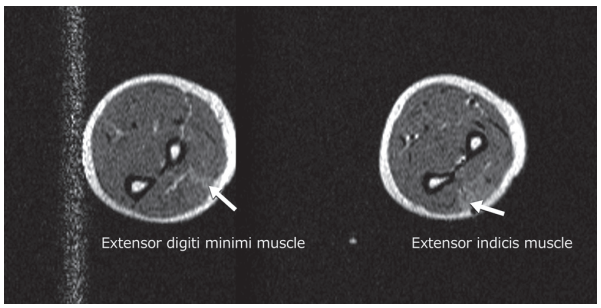

P-2-105　Fat Sat Variable Refocusing Flip Angle 3D-T2-FSE法を用いた肩関節MR Arthrographyの基礎的検討
Optimization of MR Arthrography Protocol of the Shoulder using 3D-FSE Sequence with Variable Refocusing Flip Angle

本寺　哲一（昭和大学 藤が丘病院 放射線室）
Tetsuichi Hondera[1,3], Junya Nakashima[1,3], Toshiyuki Takahashi[1,2], Ken Shinohara[1], Kyoichi Kato[1,3], Yasuo Nakazawa[1,3]

[1]Department of Radiological Technology, Showa University Fujigaoka Hospital, Yokohama, Japan, [2]Department of Radiological Technology, Showa University Koto Toyosu Hospital, Tokyo, Japan, [3]Graduate School of Health Sciences, Showa University, Tokyo, Japan

【要旨】当院の肩関節MR Arthrography検査では，透視下において生理食塩水で希釈させたヨード造影剤の関節腔への注入を確認後，T2 FSE法/FS T2 FSE法を関節窩に対して3方向撮像している．今回、Fat Sat Variable Refocusing Flip Angle 3D-T2-FSE法による画像提供を目的とし、至適撮像条件の比較検討を行った。

Background:For shoulder joint MR Arthrography inspection,iodinated contrast agent diluted with saline was injected into the joint space under fluoroscopic guidance.We employed three-way imaging T2 FSE and FS T2 FSE methods independently for the glenoid.
Purpose:We were examined the optimal imaging with Fat Sat Variable Refocusing Flip Angle 3D-T2-FSE (FS T2 CUBE)
Materials:MR imaging was performed using a 1.5T scanner (Signa HDxt Ver.15,) with an 8-channel shoulder array coil. We created a phantom assuming the following conditions:iodine/Fat/Muscle/Glenoid.
Methods:TR ranged from 2500~5500ms,TE from 50~150ms,and ETL from 20~150,showing variability,and the calculated SIR values were compared.
Results & Discussion:Greater emphasis can be placed on the impact of T2-weighted images by setting a long TR,i.e.of T2 relaxation.Therefore,in this study,all of the samples had TR 4500 ms or more in the long TR setting,and thereby revealed the optimal SIR.In shoulder joint MR Arthrography inspection, glenoid depiction is important and should focus on the SIR of the glenoid and iodine.When obtaining T2 weighted images,by setting a longer TE,and similarly considering TR,the impact of T2 relaxation can be enhanced.Our observations suggest the SIR of the glenoid and iodine to be increased when a longer TE is set.The CUBE technique employs RF pulses with a variable flip angle,while ETL allows change to a graph of approximately 80,and a high signal strength is thus gained by increasing the flip angle. Therefore,the glenoid T2 value is longer because the signal strength is high.We thus consider ETL,80 Glenoid/Iodine to be the optimal SIR.
Conclusions:The Fat Sat T2 CUBE optimal imaging conditions for MR Arthrography inspection of the shoulder joint are:TR,4500 ms or more;TE,120ms;ETL,80.

P-2-106　乳腺造影MRIでのauto scale subtractionの有用性
Usefulness of auto scale subtraction in the Contrast-enhanced breast MRI

千嶋　昭夫（メディカルスキャニング新宿）
Akio Chishima[1], Keiichi Doutanuki[2], Tatsuya Miyazaki[3], Yuu Katou[4]

[1]Medicalscanning Shinjuku, [2]Medicalscanning Shibuya, [3]Medicalscanning Ochanomizu, [4]Nagoya University School of Medicine Hospital Medical Engineering Department radiology department

【要旨】乳腺造影MRIで斑に染まる腫瘍のダイナミックカーブは撮影者間での差が大きい。そこで差分画像が漸減性腫瘍を鑑別できるか検討した。差分画像は0以下の信号は全て0として表示してしまうが、auto scale差分画像はマイナスの信号値を画像表示することができるため、漸増性、漸減性腫瘍の鑑別ができた。

porposeWe do dynamic imaging in the Contrast-enhanced breast MRI make a time signal intensity curve of the tumor.However, a setup of the region of interest when creating a time signal intensity curve depend on a photography person. Therefore we considered whether subtraction was useful.methods and materals3T-MAGNETOM spectra(Siemens Co) Target is 20 patients suspected of breast disease.Dynamic imaging captures a pre before contrast,1 minute the 1phase,2minute the 2phase,was the 3phase and 5minutes later.Time signal intensity curve is 20cases was analyzed separately by three radiological technologists. We compared it with the image which auto scale subtraction made 2phase from 3phase.results and considerationGradual decrease of the tumor which a signal becomes minus when a subtraction is done becomes equal to a background signals. Therefore we were able to display the signal which was lower than a background signal with an image by putting auto scale, and doing subtraction.The auto scale subtraction image was based on a background and was able to evaluate visually, if it's high signal, be a tumor of gradual increase, if it's low signal, be a tumor of wash out. Gradual increase was indicated all 3 people by the time signal strength curve, and there was 5 examples of tumor which indicates wash out visually with auto subtraction image.The setting of the region of interest is considered as a cause.Region of interest such as to surround the whole of Tumor which was stained with an irregularity is scarce in the reliability. conclusionThe auto scale subtraction image in the contrast-enhanced breast MRI seems that it becomes an aid of diagnosis by adding to the dynamic image and the time signal strength curve.

P-2-107　3point-DIXON法を用いたシリコンイメージの検討
An evaluation of silicon imaging using the 3-point DIXON method

坪内　隆将（木沢記念病院 放射線技術課）
Takamasa Tsubouchi[1], Saki Yoshimura[1], Kenji Sakou[1], Rikiya Syouji[1], Hiroki Nishibori[2], Mika Takagi[3]
[1]kizawa memorial hospital department of radiological technology, [2]kizawa memorial hospital department of radiology, [3]kizawa memorial hospital plastic and reconstructive surgery

【要旨】シリコンイメージはSTIR水抑制法が用いることが多いが、今回3point-DIXON法にて得たT2水抑制画像からT1水抑制画像を差分処理するシリコンイメージを考案しその特徴を確認した。本手法はSTIR水抑制法に比し低信号となるが安定した信号が得られ、乳癌術後のシリコン挿入例などアーチファクトが発生しやすい場合有効となる。

[Purpose]Continuing evaluation for the presence of tissue damage by MRI is recommended for patients who have had silicone breast implants. Generally, when imaging patients with silicone implants, the STIR water suppression method (STIR WS) is used. Here we report the results of a new method of imaging silicone which we have created using the 3-point DIXON method. [Silicon imaging]Our silicone image was obtained by subtracting the T1 water-suppression (T1WS) image from the T2 water-suppressed (T2WS) image obtained with the 3-point DIXON method (IDEAL sub). [Method]Using silicone, water, olive oil and a mammary gland QA phantom we took the following images using the IDEAL sub method: T1FS, T2FS, T1WS, T1WI, T2WS, T2WI. Next we compared SNR of each tissue sample. Finally we compared STIR WS silicone imaging to our new IDEAL sub method imaging. [Results]T2WS of silicone always has higher signal level than T1WS. Conversely, signal level is always lower when imaging olive oil with T2WS relative to T1WS. We suppressed water at equal levels in both T2WS and T1WS. By subtracting T1WS from T2WS, the silicone image can be amplified. When we compared the results of IDEAL sub and STIR WS, we found that while STIR WS produces a higher SNR, the signal is less stable than IDEAL sub. [Discussion]The IDEAL sub method produces images with lower overall signal strength than STIR WS. However, since IDEAL sub is less affected by unevenness in the local magnetic field, a more stable signal can be obtained. This suggests that IDEAL sub might be useful in imaging breast cancer survivors who have silicone implants, which are known to have uneven local magnetic fields.

P-2-108　T1値測定に脂肪抑制法は影響を与えるか？：油-水-エマルジョンファントムによる検討
Does fat suppression method Influence on T1 measurement?: Oil-in-water emulsion phantom study

池野　寛康（京都府立医科大学附属病院 放射線部）
Hiroyasu Ikeno[1], Koji Sakai[2], Hiroshi Imai[3], Toshiaki Nakagawa[1], Mariko Goto[2], Tsunao Kishida[4], Osamu Mazda[4], Kei Yamada[2]
[1]Department of Radiology, University Hospital, Kyoto Prefectural University of Medicine, [2]Graduate School of Medical Science, Kyoto Prefectural University of Medicine, [3]Siemens Healthcare K.K., [4]Department of Immunology, Kyoto Prefectural University of Medicine

【要旨】DCE-MRIでは造影dynamic撮像前にmulti flip angle法によるT1map作成を行う.乳腺腫瘍に対して行う場合には, dynamic撮像に脂肪抑制法が用いられているためT1map作成においても脂肪抑制が必要である.本報では各脂肪抑制法によって測定T1値に影響を与えることを示した.

DCE-MRI with pharmacokinetic model has been utilized for the classification of tumors. Breast DCE-MRI usually performed with fat suppression (FS). This work investigated the influence of several FS methods on T1 measurement using oil-in-water emulsion phantoms. The phantoms (50 mL) were created by homogenizing the mixture of soybean oil (0, 10, 20 vol.%), contrast agent (0, 0.3, 0.96, 2.0 vol.%), sodium dodecyl sulfate (15 mmoL/L), and 1.25g agar-water solution at 90 ℃. All MR imaging was performed on a SIEMENS Skyra and 20ch Headcoil. 3D FLASH images with several flip angles (FA) and with FS methods (Chess, SPAIR, water excitation, and DIXON water) were obtained, and each T1 map was generated based on the variable FA approaches. Scan parameters were TE/TR=1.23, 2.46/20ms and FA=5, 10, 15 for DIXON, and 4.92/20 and 5, 12, 19, 26 for the others. As a reference, T1 value of water component was evaluated from SVS with variable TRs (600-15000ms). The results showed different T1 values by FS methods on each fat fraction. There was a prominent difference on phantoms that has long T1 values. T1-Dixon had the minimum and T1-SPAIR had the maximum differences from reference values.

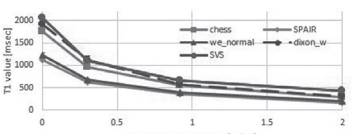

Fig1. Relationship between T1 value and content of contrast agent (fat content 0vol.%)

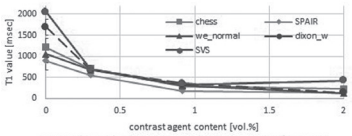

Fig2. Relationship between T1 value and content of contrast agent (fat content 10vol.%)

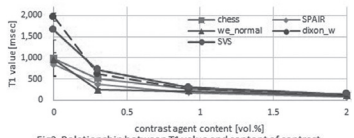

Fig3. Relationship between T1 value and content of contrast agent (fat content 20vol.%)

P-2-109　乳腺MRIにおける造影剤注入条件に関する後方視的検討
Retrospective Study of Injection Condition in Breast MRI

小塚　雪乃（東京都保健医療公社 豊島病院 放射線科）
Yukino Kozuka[1], Satoshi Honda[1], Yoichi Okada[1], Toshiyuki Onodera[2], Masanori Yamamoto[1], Kikuo Fujinami[1], Akira Yamashita[2]

[1]Department of Radiology, Tokyo Metropolitan Health and Medical Treatment Corporation Toshima Hospital,
[2]Department of Radiology, Tokyo Metropolitan Health and Medical Treatment Corporation Ebara Hospital

【要旨】乳腺dynamic MRIにおいてTIC解析は良悪性診断の所見として重要である。一方、造影の注入条件に関する検討は数少ない。そこで、造影剤注入条件や種類による信号強度変化について検討を行った。結果、TICにバラつきがみられた。超早期相に造強ピークを得るには、注入時間一定とし体重に合った造影剤量を注入する必要がある。

[Introduction]
TIC (Time Intensity Curve) analysis is useful to evaluate breast lesion on MRI. Fast-Washout pattern is particularly related to a malignant lesion. Both high partial resolution and high time resolution are needed for that analysis. 3D sequence of k-space sharing with high speed imaging technique (TWIST-VIVE) enables above conditions on a 1.5T MRI. There is an issue in the quantitative analysis on the initial slope and delayed slope. Because the appropriate infection of contrast media is not significantly investigated. We discussed the difference of TIC after bolus injection of 2 kinds of media.
[Method]
We selected 30 patients who performed Breast MRI in our hospital, using 18ch AI-breast coil on a 1.5T MRI (MAGNETOME AERA). 6 phases of a dynamic sequence with 60sec time resolution and 0.8mm iso-voxel were obtained with 3D DIXON TWIST-VIVE. Contrast media (Magnescope or Gadovist) ware injected from the cubital vein at the rate of 2.0 ml/sec.
TIC was analysis from the images retrospectively on the ROI of Ascending and Descending Aorta, ITA(Internal Thoracic Arteries), and the Mammary Gland.
[Results]
TIC analysis was variable for each ROI, regardless of the kind of media. Most patients had peak intensity at early phase than super-early phase of the ROI of Aorta, ITA.
[Discussion]
Many patients had variable peak time and the broad peak because body weight was variable. Injection time was longer under the constant rate because the heavy-weight patients needed the large amount of media. It resulted that peak became broad and peak time was valuable. It was necessary to obtain a peak in the super-early phase that injection time was constant and change the rate for body weight similar to the dynamic CT study.

P-2-110　MRガイド下凍結治療支援ロボットシステムの基礎的評価
Evaluation of an MRI-Powered Robotic Sysytem for Cryoablation

五月女康作（筑波大学 サイバニクス研究センター）
Kousaku Saotome[1], Ryutaro Ouchi[2], Akira Matsushita[1], Mitsuhiro Tozaki[4], Kenji Suzuki[1,3], Yoshiyuki Sankai[1]

[1]Center for Cybernics Research, University of Tsukuba, Japan, [2]Graduate School of Systems and Information Engineering, University of Tsukuba, Japan, [3]Japan Science and Technology Agency, Japan, [4]Department of Radiology, Sagara Hospital Affiliated Breast Center, Japan

【要旨】MRI装置のスライス選択傾斜磁場を動力とし，MRガイド下凍結治療支援を目的としたロボットシステムの開発を試み，システム内に搭載されているアクチュエータの基本的性能を評価した。出力された力は微力であったがこれを複数個使用することで目的の動力を得ることができると考える。

[Introduction]
We have developed a novel MRI-compatible robotic system including MRI-powered actuator units realizing multiaxial movement and spherical positioning mechanism. Also, we set the goal of making a robotic system for needle tip positioning in cryoablation for breast cancer.
[Methods]
Fig. 1 shows the view of the actuator unit. In the actuator unit, pendulum movement of the rotor is converted to the one way rotation and it will bet the output. We conducted three experiments to evaluate using 3.0T: area affected by the ferromagnetic sphere, activation area of the actuator unit inside the gantry of the MRI, and power output to verify the performance of the developed MRI-powered actuator unit.
[Results & Disscusion]
The area affected by the ferromagnetic sphere is linearly increasing according to the diameter of the sphere. We decided to use 8 mm sphere as a power source. The activation area of 25 cm in z -axis and 20 cm in x -axis was confirmed. The force generated by the ferromagnetic sphere is about 0.21 N and the torque is 6.17×10^{-3} Nm. Although the generated force and torque are not so strong, increasing the number of rotor will overcome the power problem.

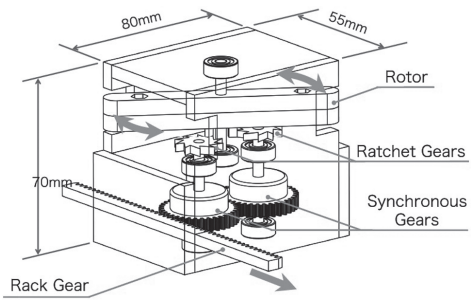

P-3-001　下垂体領域における矢状断Turbo Spin Echo-DWIの撮像条件の最適化
Optimization of the imaging of sagittal section Turbo Spin Echo-DWI in the pituitary region

圓崎　将大（宮崎大学医学部附属病院 放射線部）
Masahiro Enzaki, Toshiya Azuma, Tomomi Sumiyoshi, Takanori Yano, Yoshihito Kadota, Minako Azuma, Toshinori Hirai

Department of Radiology1, Faculty of Medicine, University of Miyazaki, Miyazaki, Japan

【要旨】歪みの低減を望めるTurbo Spin Echo-DWI(TSE-DWI)の下垂体領域における最適撮像条件を検討する。ファントム、ボランティア画像から、SENSE factor(SF)、profile order、ETLを変化させたときの歪み、SNR、blurを評価した。下垂体領域における矢状断TSE-DWIの最適撮像条件はSF：2、profile order；liner、ETL：55だった。

<PURPOSE>Diffusion-weighted image (DWI) in the sellar region is affected by the susceptibility effect of the paranasal sinus. Compared with conventional echo-planner imaging DWI (EPI-DWI), turbo spin-echo DWI (TSE-DWI) can reduce image distortion from susceptibility effect. The purpose of this study was to assess the optimized imaging conditions of TSE-DWI in the pituitary region.
<METHODS>Using a MR phantom, we evaluated distortion rate, signal noise ratio (SNR), and blurring artifact of EPI- and TSE-DW images under the various imaging conditions: profile order, liner or low-high; SENSE factor (SF), 2-3; echo train length (ETL), 30-60. We also evaluated DW images of 5 volunteers in whom written informed consent was obtained. All imaging studies were performed on a 3.0-tesla system and 32ch head coil (Ingenia 3.0T CX; PHILIPS). The parameters of TSE-DWI sequence were as follows TR/TE, 7000/56-197ms; b-factor, 0,1000s/mm^2; FA, 90°, RFA, 60°, field of view, 170mm x 170mm; slice thickness, 2.5mm with a 0.5mm gap; matrix size, 108 x 108; band width, 521.3Hz-531.2Hz; and acquisition time, 5:50.
<RESULTS>In phantom studies, the difference of SNR between liner and low-high order was small, and the distortion decreased with liner. As the number of SENSE factor increased, the distortion and SNR decreased. As the ETL increased, the distortion and SNR improved greatly although the blurring artifacts increased. Volunteer studies showed a trend like the phantom studies, but the SNR in a SF of 3 was insufficient.
<CONCLUSION>In our institution, the optimized imaging parameters in the pituitary region for TSE-DWI were a SF of 2, profile order of liner, and ETL of 55.

P-3-002　慢性炎症性脱髄性多発神経障害における腕神経叢肥厚解析のための領域分割法
Semi-automated segmentation to evaluate hypertrophy of the brachial plexus in chronic inflammatory demyelinating polyneuropathy

川口　拓之（産業技術総合研究所 人間情報研究部門）
Hiroshi Kawaguchi[1], Hajime Yokota[2,3], Hiroki Mukai[2], Kazumoto Shibuya[4], Hitoshi Shimada[4,5], Shoichi Ito[2,6], Tetsuya Suhara[5], Takashi Uno[2], Satoshi Kuwabara[4]

[1]HIRI, AIST, [2]Dept of Radiol., Chiba Univ., [3]Dept of Neurol., Chiba Univ., [4]Dept of Radiol. Sci., UCLA, [5]Dept of Func. Brain Imaging Res., NIRS, QST, [6]Office of Med. Education, Chiba Univ.

【要旨】慢性炎症性脱髄性多発神経障害において上腕神経の肥厚パターンがサブタイプに依存することが報告されている。本研究では肥厚の定量解析が病態解明や臨床応用に繋がることを目指し、STIR画像を用いた上腕神経叢の領域分割法を提案した。提案法による抽出結果は放射線科医師2名による抽出結果と同等であった。

The spatial patterns of brachial nerve hypertrophy presumably reflect the different pathophysiology of chronic inflammatory demyelinating polyneuropathy (CIDP) subtype. We proposed and evaluated the semi-automated segmentation method to extract the brachial plexus of the CIDP patients from the three-dimensional short tau inversion recovery (STIR) image for investigation of the morphological change. We studied retrospectively 6 typical CIDP patients who visited Chiba University Hospital. A 1.5T MRI scanner (Achieva; Philips) was used. MR images were acquired with STIR sequences in the coronal planes. The parameters of STIR were as follows: TR/TE/TI = 1600/200/180 ms, FOV = 380 mm, matrix = 320 x 250, slice thickness = 2.4 mm, slice gap = 1 to 2 mm. The proposed method utilized the intensity-based probability and the anatomical probability that would reflect the anatomical feature of the brachial nerve. The only manual operation is to determine the central points of 10 roots of the brachial nerve (bilateral C5, C6, C7, C8 and Th1), roughly. To assess the accuracy of the proposed method, two board-certified radiologists, operator 1 and 2, manually segmented the brachial nerve. The similarity between two extracted brachial nerves was measured by the Jaccard index. There were no statistically significant differences between Jaccard indices of each two segmentation methods (0.50 ± 0.05 0.47 ± 0.09 and 0.47 ± 0.05 for operator 1 vs operator 2, the proposed method vs operator 1 and the proposed method vs operator 2, respectively),which indicates that the proposed method has the same capabilities at board-certified operators to extract the brachial nerve from the STIR image.

P-3-003　Turbo-CINEMA法を用いた鎖骨下動脈領域における描出能の検討
Evaluation of new hemodynamic and structural imaging of the subclavian arteries using Turbo-CINEMA

蓼沼　仁（東京女子医科大学病院 中央放射線部）
Hitoshi Tadenuma[1], Kayoko Abe[2], Masami Yoneyama[3], Yasuhiro Goto[1], Mamoru Takeyama[1], Syuji Sakai[2]

[1]Department of Radiological Service, Tokyo Women's Medical University, Tokyo, Japan, [2]Department of Diagnostic Imaging and Nuclear Medicine, Tokyo Women's Medical University, Tokyo, Japan, [3]Philips Electronics Japan, Ltd.

【要旨】鎖骨下動脈の形態評価と血行動態評価を同時に評価できる撮影法のTurbo-CINEMA法の検討を行った。Turbo-CINEMA法は、TOFや4D-PCAよりも良好な画像を得ることが出来た。鎖骨下動脈の末梢では4D-PCAよりも良好だった。本法は他法よりも短い時間で同等の画像を得ることが出来た。

PurposeWe investigated the optimization of Turbo-CINEMA (ACTRESS method) protocols for new hemodynamic and structural imaging of subclavian arteries.MethodThis study consists of two parts:(1) Optimization of thickness of both labeling slab and labeling gap on Turbo-CINEMA in 5 healthy volunteers.(2) Estimation of visualization of subclavian arteries, comparing among Turbo-CINEMA, TOF-MRA, and 4D-PCA in 5 healthy volunteers. All studies were examined using 3T MR unit (Ingenia 3T, Philips Healthcare R5.1.7).Results(1) The labeling slab thickness should be as high as possible, not covering the Aortic valve. The labeling gap thickness should be set to the minimum.(2) Image quality of Turbo-CINEMA was higher than TOF-MRA, and is similar to 4D-PCA. Visualization of distal of subclavian arteries and branches on Turbo-CINEMA is superior to 4D-PCA. Acquisition time of Turbo-CINEMA is shorter than the others.ConclusionTurbo-CINEMA is a potential technique that can provide new hemodynamic and structural imaging for subclavian arteries.

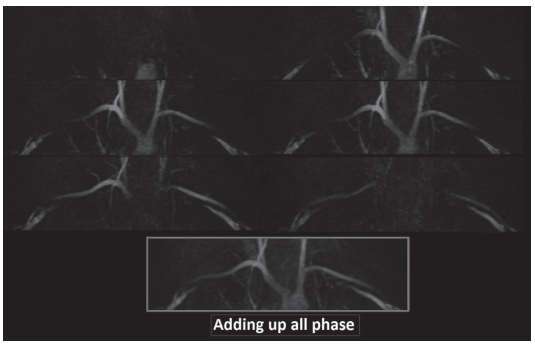

P-3-004　初発頭頸部癌ステージングに対するPET/CTとPET/MRの診断能比較; PET/CT/MR機での検討
PET/MR versus PET/CT in the Initial Staging of Head and Neck Cancer

関根　鉄朗（日本医科大学 放射線科）
Tetsuro Sekine[1,2], Barbosa Felipe[2], Kuhn Felix[2], Burger Irene[2], Delso Gaspar[2], Ter Voert Edwin[2], Veit-Haibach Patrick[2], Huellner Martin W[2]

[1]Department of Radiology, Nippon Medical School, [2]Department of nuclear medicine, University Hospital Zurich

【要旨】初発頭頸部癌に対するTNM stagingに対し、造影PET/CT及び造影PET/MRの正診率を比較した。27名の初発頭頸部癌患者に対し、shuttle type PET/CT/MRを用いた。T staging及びN stagingとも、PET/CT及びPET/MR間で正診率に有意差を認めず、PET/MRはPET/CTと比較し、少なくとも同等以上の正診率があると考えられた。

Purpose; To compare the diagnostic accuracy of PET/MR with PET/CT in the initial staging of head and neck cancer.Methods; Sequential contrast-enhanced PET/CT/MR was performed in 27 patients (median age 66, 16 males) with newly diagnosed head and neck cancer. MR sequences were: LAVA-Flex (whole body); axial T2-weighted, axial T1-weighted with and without contrast, sagittal and coronal T1-weighted with contrast, and DWI (head and neck). PET/CT and PET/MR were evaluated separately, and the TNM stage were assessed. Wilcoxon signed-ranks test was used.Results;The TNM staging by PET/MR was comparable to PET/CT (T: p = 0.331, N: p = 0.453).Conclusions; Whole-body staging with PET/MR yields at least equal diagnostic accuracy as PET/CT in determining the stage of head and neck cancer.

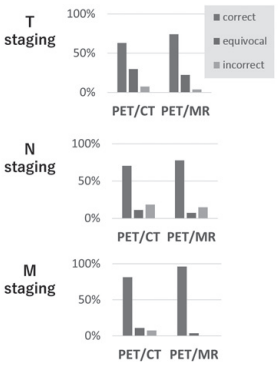

Whole-body staging with PET/MR yields equal diagnostic accuracy as PET/CT in determining the TNM staging of head and neck cancer.

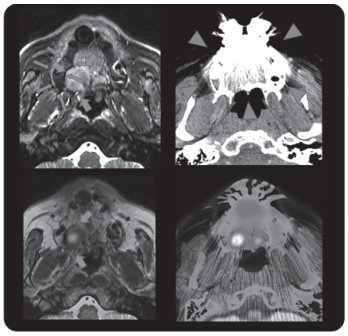

67-year-old male with mucoepidermoid carcinoma of the hard palate.
The margin of the tumor is hard to detect on CT and PET/CT because of the artifact from dental implants and low soft tissue contrast. A precise detection of the local tumor extent is mandatory for surgical planning.

P-3-005　頭頸部癌の切除可能性評価に対するPET/CTとPET/MRの診断能比較
Local resectability assessment of head and neck cancer, PET/MR versus PET/CT

関根　鉄朗（日本医科大学 放射線科）
Tetsuro Sekine[1,2], Barbosa Felipe[2], Delso Gaspar[2], Ter Voert Edwin[2], Veit-Haibach Patrick[2], Huellner Martin W[2]

[1]Department of Radiology, Nippon Medical School, [2]Department of nuclear medicine, University Hospital Zurich

【要旨】頭頸部癌における切除可能性評価について、造影PET/CTと造影PET/MRの比較を行った。対象は58名の頭頸部癌患者、shuttle type PET/CT/MR機を用いた。結果、両modalityとも、切除可能性評価に対し、90%を超える正診率を認め、有意差は存在しなかった。造影PET/MRは造影PET/CTと比較して、同等の診断能があると考えられた。

Purpose:To compare the diagnostic accuracy of PET/MR with PET/CT for local resectability of head and neck cancer.Methods: Sequential contrast-enhanced PET/CT-MR was performed in 58 patients referred for the staging or re-staging of head and neck cancer. Tumors were assessed with PET/CT and PET/MR for the presence of resectability-defining factors: T4b status and another eight findings that would imply obstacles for surgical cure.Results: The sensitivity/specificity/accuracy of local resectability-defining factors of PET/CT and PET/MR was 0.92/0.99/0.98 and 0.98/0.99/0.99 (p = 0.727), respectively, per lesion, and 0.96/0.87/0.91 and 0.96/0.90/0.93 (p = 0.687), respectively, per patient. Conclusion: Both contrast-enhanced PET/MR and contrast-enhanced PET/CT can serve as reliable examinations for defining local resectability of head and neck cancer.

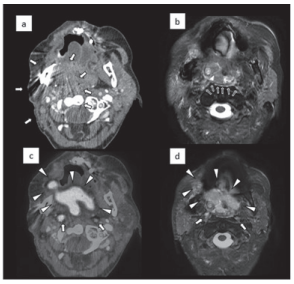

59y female with recurrent SCC of the floor of the mouth. The severe artifacts from dental implants on CT limit the interpretation of tumor extension (arrows on a). In contrast, onT2WI, an almost continuously defined thin hyperintense line between the tumor and the prevertebral muscles is seen (thin arrows on b). The lesion was correctly diagnosed as resectable on PET/MR, being confirmed by clinical examination.

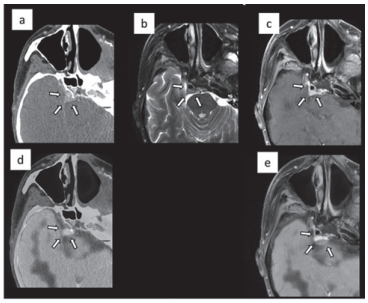

82y male after surgery and CRT of an adenocarcinoma of the hard palate. The slightly enhancing lesion around the right cavernous sinus is depicted on CT (arrows on a) and this is clearer on T2WI and ce-T1WI (arrows on b and c). It was diagnosed as perineural spread and carotid artery invasion. In this lesion, FDG uptake is observed but difficult to distinguish from brain FDG uptake(arrows on d and e).

P-3-006　口腔領域でのturbo spin echo (TSE) DWIとecho-planar imaging (EPI) DWIの比較検討
Comparison of the image quality of turbo spin echo- and echo-planar diffusion-weighted images of the oral cavity region

平田健一郎（熊本大学 医学部 画像診断科）
Kenichiro Hirata[1], Takeshi Nakaura[1], Tomoyuki Okuaki[2], Masafumi Kidoh[1], Seitaro Oda[1], Daisuke Utsunomiya[1], Tomohiro Namimoto[1], Mika Kitajima[1], Hideki Nakayama[3], Yasuyuki Yamashita[1]

[1]Diagnostic Radiology, Kumamoto University, [2]Philips Healthcare, [3]Oral surgery, Kumamoto University

【要旨】口腔領域3TMRI撮影でのturbo spin echo (TSE) DWIとecho-planar imaging (EPI) DWIの画質比較を行った。TSE-DWIとEPI-を撮影された26人が対象で歪みの比較、舌、耳下腺、神経のSNR、コントラスト、ADC値を測定し、質的評価も行った。結果、TSE-DWIはEPI-に比べ歪みが有意に少なく、質的評価でもTSE-DWIの評価が高かった。

Purpose:To compare the image quality of turbo spin echo (TSE) diffusion-weighted images (DWI) and echo-planar imaging (EPI) DWI on 3T magnetic resonance images (MRI) of the oral cavity.Materials and Methods:This retrospective study included 26 patients who had undergone both TSE- and EPI-DWI. Misregistration of DW images with T2-TSE images was assessed in the oral cavity. We also compared geometric distortion, the signal-to-noise ratio (SNR), contrast, and the apparent diffusion coefficient (ADC) for the tongue parotid gland, and spinal cord. On a 5-point scale, 2 radiologists scored the TSE- and EPI-DWI scans of each patient for ghost artifacts, image contrast, and overall image quality.Results:Distortion in the phase-encoded direction was significantly lower on TSE- than EPI-DWI scans (1.0% ± 3.9 vs. 12.0% ± 5.2, p < 0.01). The SNR of the tongue and parotid gland was significantly higher on TSE-than EPI-DWI scans except spinal cord (tongue: 7.3 ± 2.8 vs. 5.7 ± 1.9, parotid gland: 9.1 ± 3.0 vs. 5.3 ± 2.3) (p < 0.01). No significant difference was found in contrast and ADC values (except for the ADC of tongue). TSE-DWI yielded significantly higher qualitative scores for all parameters except image contrast (ghost artifacts 3.3 ± 0.9 vs. 2.5 ± 1.1, overall image quality 3.4 ± 0.8 vs. 2.7 ± 1.1, all p < 0.01). Conclusion:For imaging of the oral cavity region, TSE- was superior to EPI-DWI with respect to distortion-free images and superior image quality.

P-3-007　頭頸部領域におけるPROPELLER DWIの有用性
Utility of PROPELLER DWI in head and neck region

嶋田　　諭（国保直営総合病院 君津中央病院）
Satoshi Shimada, Hazuki Watanabe, Takashi Tsukaya, Ryu Emura, Hironori Yamamoto
Department of Radiotechnorogy, Kimitsu Central Hospital

【要旨】頭頸部領域でT2WIとDWIの融合画像作成のため、ファントム実験でPROPELLER DWIの最適化、及び臨床画像でT2WIでの病変を基準にPROPELLER　DWIとEPI　DWIでの病変の位置ズレの距離とADC値を比較した。PROPELLER DWIは位置ズレが少なく、ADC値は高くなった。

Objective: The aim of this study was to compare geometric distortions occured in T2 weighted image (T2WI) with the ones in 2 sequences diffusion weighted image (DWI) which are single shot echo-planer DWI (E-DWI) and periodically rotated overlapping parallel lines with enhanced reconstruction DWI (P-DWI) for T2WI and DWI fusion images and also to compare apparent diffusion coefficient (ADC) values of P-DWI with E-DWI.
Method: Using a 3.0-T MRI (Discovery 750w, GEHC), we optimized the parameters of P-DWI for fusing with T2WI by self-produced phantom. We adjusted those parameters shown in the following: matrix (96, 128, 160, and 192), echo train length (16, 24, 32 and 36), bandwidth (16, 31, 63, and 83 kHz), parallel imaging factor (non, 2, and 3). We measured distances of artifacts by the phantom and drew a profile curve. Then, we evaluated 7 lesions in clinical studies of 4 patients which were done by the optimized parameters. We measured the distances from the centers of each 7 lesions in T2WI to the ones in the other 2 sequences and compared the distances by using the Mann-Whitney U test. Furthermore, we compared the ADC values in P-DWI with the ones in E-DWI which obtained from 10 lesions in clinical studies of 5 patients by using the Wilcoxon signed-rank test.
Result: In the phantom study, the increase of the bandwidth decreased the distances of artifacts and the use of parallel imaging changed the profile curve. In the clinical studies, the distances of the lesions in T2WI and P-DWI were decreased more than the distances of the lesions in T2WI and E-DWI ($p<0.05$) and the ADC values of P-DWI were higher compared to E-DWI ($p<0.05$).
Conclusion: In the head and neck region, the optimized P-DWI is suitable for the fusion with T2WI and shows higher ADC values than E-DWI.

P-3-008　内リンパ体積比の定量（用手法と Region growing 法の比較）
Endolymphatic volume ratio measurement using region growing method

小川絵莉子（総合上飯田第一病院 放射線科）
Eriko Ogawa[1], Toshio Ohashi[1], Toshio Katagiri[1], Kayao Kuno[2], Shinji Naganawa[3]
[1]Department of Radiology, Kamiiida Daiichi General Hospital, [2]Department of Otolaryngology, Kamiiida Daiichi General Hospital, [3]Department of Radiology, Nagoya University Hospital

【要旨】我々の施設では用手的に蝸牛と前庭の ROI を描くことで、内リンパ腔体積を測定しているが、この方法では測定者間において結果に差が生じる可能性がある。
そこで我々は半自動的手法を考え、それによる測定値と用手的手法での測定値との整合性を検討した。
その結果、内リンパ腔体積比について両者の間に強い相関がみられた。

Purpose
In our hospital, we routinely obtain endolymphatic hydrops (EH) image 4 hours after IV of single-dose Gd-based contrast material (IV-SD-GBCM) and measure the endolymphatic volume ratio ($\%EL_{volume}$) manually. This measurement is performed by time consuming manual ROIs drawing, that is susceptible to observers' bias. Therefore we propose the semi-automatic method.
The purpose of this study was to investigate the consistency of both methods.
Method
We evaluated 20 patients suspected with EH (median: 64-year-old).
MRI was performed on 3T MR unit (MAGNETOM Skyra, Siemens) using 32ch array head coil.
We obtained two kinds of following images 4 hours after IV-SD-GBCM.
(1) MR cisternography (MRC): heavily T2-weighted 3D-turbo spin echo, TR/TE = 4400/544ms.
(2) Positive perilymph image (PPI): heavily T2-weighted 3D-FLAIR, TR/TE = 9000/544ms, TI2250ms.
We generated HYDROPS2-Mi2 by the processing shown below.

(PPI-0.04 × MRC) = HYDROPS2, (HYDROPS2 × MRC) = HYDROPS2-Mi2, according to the previously reported study.

In the preparation, we manually set two boundaries, between cochlea and vestibule, and between cochlea and internal auditory meatus on MRC.
Then we segmented cochlea and vestibule using region growing function of OsiriX and measured the entire lymphatic volume on MRC. We pasted the segmented regions onto HYDROPS2-Mi2, and measured the endolymphatic volume for cochlea and vestibule, respectively.
We evaluated the correlation of $\%EL_{volume}$ between manual method and semi-automatic method using Pearson's correlation coefficient.
Result
There was a strong positive linear correlation between both methods ($r = 0.993$ for cochlea, 0.924 for vestibule).
Conclusion
There is a strong positive correlation between two methods. The semi-automatic method is feasible and can replace manual methods.

P-3-009　Variable Flip Angle 3DT1WI（MPV：Multi Planer Voxel）の頭頸部での最適化
Optimization of Variable Flip Angle 3D T1WI MPV (Multi Planar Voxel) in Head and Neck Imaging

河野奈々恵（東芝メディカルシステムズ株式会社）
Nanae Kawano[1], Ayako Ninomiya[1], Miho Kitamura[1], Hiroshi Kusahara[2]
[1]Toshiba Medical Systems Corporation, [2]Toshiba Medical Systems Corporation MRI Systems Development Department

【要旨】Variable Flip Angle法の一つであるMulti Planar Voxel撮像を用い、3D T1WIに合わせた最適撮像条件を検討した。TRとFlop Angleの最適化によりT1コントラストを向上させることが可能であり、頚部においては、Flop Angleを浅くすることでBlack Blood効果が向上することが期待された。

Purpose:The Multi Planar Voxel (MPV) method is one of the variable flip angle methods that has been widely employed for 3D T2WI. It has also been increasingly employed for 3D T1WI. However, few studies have evaluated the imaging conditions for 3D T1WI, and the optimal imaging conditions have therefore not yet been firmly established. The purpose of the present study was to optimize the imaging parameters of 3D T1WI MPV in terms of SNR, CR, and the Black Blood effect on vascular structures in order to obtain well-balanced image quality in the head and neck.Methods:All studies were performed on a 3-T MRI system (Vantage Titan 3T; Toshiba Medical Systems) equipped with a 16-ch Atlas SPEEDER Head/Neck coil. Both phantom and volunteer studies were conducted. Informed consent was obtained from all five volunteers. In the phantom experiments, the number of shots, TR, TE, and flop angle were varied, and the SNR and CR values were compared. In the volunteer experiments, the SNR of brain parenchyma (white matter, gray matter), CR, and vascular Black Blood effect were evaluated to determine the optimal imaging parameters.Results:No differences in CR were observed when the number of shots was changed. As TR increased, SNR increased but CR decreased. CR was decreased with longer TE values. As the flop angle increased, SNR increased but CR decreased. It was possible to improve the T1 contrast of images acquired in a given scan time by setting the optimal TR and flop angle. In the neck, the Black Blood effect was expected to be improved by decreasing the flop angle.Conclusion:The optimal imaging conditions for 3D T1WI MPV in the head and neck were determined. The visualization of lesions such as plaque should also be evaluated.

P-3-010　信念伝播法を用いたベイズ推定による脳画像の自動ラベリング手法の検討
Anatomical labeling with belief propagation in Bayes estimation for human brain

山本　詩子（京都大学 情報学研究科 システム科学専攻）
Utako Yamamoto[1], Masayuki Ohzeki[1], Tomoyuki Hiroyasu[2], Megumi Nakao[1], Tetsuya Matsuda[1]
[1]Department of System Science, Graduate School of Informatics, Kyoto University, [2]Department of Biomedical Information, Faculty of Life and Medical Sciences, Doshisha University

【要旨】確率的推論を用いて脳画像の自動的な領域ラベリング手法の検討を行った。学習および推論には平均場近似法による高速計算手法を用いたベイズ推定を用いた。健常者18名分の拡散テンソル画像法による複数の画像を学習して自動領域ラベリングを行った。学習データが非常に少ないものの良好な結果を得た。

[Objective]
The anatomical labeling is an effective approach for the image analysis to detect abnormalities automatically. In the present study, we propose an automatic anatomical labeling method for human brain with probabilistic inference using the MR-DTI.
[Methods]
We propose a probabilistic inference on the anatomical labeling by use of the belief propagation in Bayes estimation. We construct a simple multi-variable Gaussian model for the assignment of the anatomical labeling by preparing several images obtained from MR-DTI of the normal human brains. Their mean and covariance are estimated from signal values in voxels on each anatomical label, which is assigned by the previous method.In addition, extraction of the spatial information from those labels by considering the adjacent labels on each voxel enables us to perform the anatomical labeling by single voxel.
[Results]
We obtain the attached figure. The inferred labels were assigned near the correct labels. Its precision is not in a satisfactory level, but its improvement is straightforward by introduction of the other quantities and those morphologically deformed images in our probabilistic model.

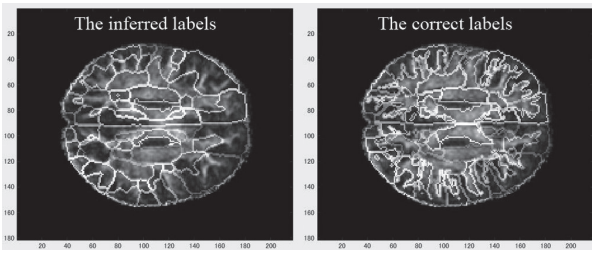

P-3-011　脳灌流MRIにおけるガドブトロールの組織信号強度の検討
Tissue time intensity curve behavior of gadobutrol bolus injection

山田　将大（トヨタ記念病院 放射線科）
Masahiro Yamada[1], Toshiaki Taoka[2], Yasushi Niinomi[1], Ai Kawaguchi[1], Kenji Yasuda[1], Yoichi Ohashi[1], Takahito Okuda[1], Shinji Naganawa[2]

[1]Department of Radiology, TOYOTA Memorial Hospital, [2]Department of Radiology, Nagoya University Hospital

【要旨】脳灌流MRIにおいて組織信号強度の時間経過と注入速度との関係をガドブトロールとガドテリドールで測定した。注入時間が2秒以内では、両者の時間信号曲線の急峻さ（ピーク値/半値幅）に有意差は無かったが、2秒以上ではガドブトロールで有意に急峻となった。

Purpose: Gadobutrol is a gadolinium based contrast agent (GBCA) approved at 1.0 mol/L Gd. Our study is to elucidate the tissue time intensity curve (TIC) of gadobutrol in various injection speed and compare with a GBCA of 0.5 mol/L.
Materials and methods: Perfusion MRI were made in 30 cases. Gadobutrol (18 cases) and gadoteridol (12 cases) were injected at variable speeds (2, 3, 4 ml/s) followed by 20 ml saline flush. TIC were analyzed in basal ganglia for the maximum signal change ratio (MCR) and bolus width (full width at half maximum: FWHM) to obtain the MCR/FWHM ratio. We correlated them with injection duration (sec) and compared them for long (2 sec<) and short injection duration group (<2 sec).
Results: MCR/FWHM ratios and injection durations are shown on the graph. In the long injection duration group, gadobutrol showed statistically significant ($p<0.001$) high ratio (mean 1.08) than that of gadteridol (mean 0.74). While, in short injection duration group, the ratio of gadobutrol (mean 0.99) and gadoteridol (mean 0.86) did not showed significant difference.
Conclusion: When the injection duration is long, Gadobutrol showed higher MCR/FWHM ratios indicating steeper flow profile.

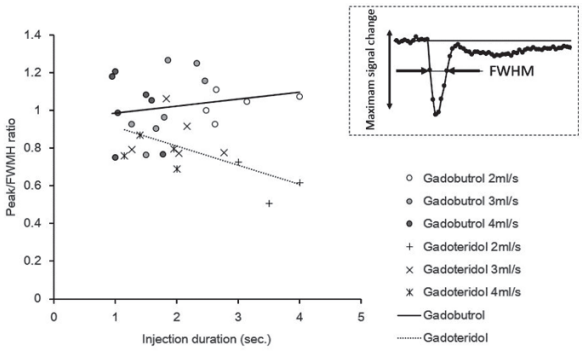

P-3-012　透明脳マウスにおける次世代拡散MRI(DKI)と共焦点顕微鏡による神経線維密度の関係
The relationship between diffusional kurtosis imaging with the neurite density in a confocal microscopy of the cleared mouse brain

入江　隆介（順天堂大学 医学部 放射線科）
Ryusuke Irie[1], Koji Kamagata[1], Aurelien Kerever[2], Suguru Yokosawa[3], Yosuke Otake[3], Hisaaki Ochi[3], Kazuhiko Tagawa[4], Hitoshi Okazawa[4], Kohske Takahashi[5,6], Kanako Sato[1], Masaaki Hori[1], Eri Arikawa-Hirasawa[2], Shigeki Aoki[1]

[1]Department of Radiology, Juntendo University School of Medicine, [2]Juntendo University School of Medicine, [3]Hitachi Ltd., [4]Tokyo Medical and Dental University, [5]Chukyo University, [6]Araya Brain Imaging

【要旨】Diffusional kurtosis imaging (DKI)の定量値と組織構造との関連を検討するため，MKおよびMD，FAなどの拡散MRI定量値と，透明脳マウスの共焦点顕微鏡画像データから算出される神経線維密度を比較した結果，MKが神経線維密度と最もよく相関していた．

[Purpose] Diffusional kurtosis imaging (DKI) provides a sensitive measure of tissue microstructure by quantifying non-Gaussian diffusion. Although DKI is applied widely in many clinical situations, there is no histological foundation in the analysis result of DKI. The purpose of this study was to determine a relationship between the metrics of DKI with the neurite density measured by a confocal microscopy of the cleared mouse brain. [Materials and methods] One thy-1 yellow fluorescent protein mouse was deeply anesthetized and perfusion fixation was performed. The brain was carefully dissected and whole brain MRI was acquired with a 7-T animal MRI system. DKI and diffusion tensor imaging (DTI) data were obtained. After scanning MRI, brain sections were prepared and then cleared by using the clear, unobstructed brain imaging cocktails and computational analysis (CUBIC) method. Confocal microscopy acquisition was performed with a Carl Zeiss LSM 780 two-photon microscope. Forty-eight regions of interest (ROIs) were set on the caudate nucleus and putamen in a confocal microscopy and a MR image. In each ROI, neurite density was calculated using Imaris Interactive Microscopy Image Analysis software. The metrics of DKI and DTI such as mean kurtosis (MK), fractional anisotropy (FA) and mean diffusivity (MD) were also calculated. The correlations between the diffusion metrics and neurite density were analyzed by Pearson correlation coefficients. [Results] There was a strongly positive correlation between MK and neurite density ($P<0.001$, $r=0.726$). There was a strongly negative correlation between MD and neurite density ($P<0.001$, $r=-0.676$). The correlation between FA and neurite density was moderate ($P=0.003$, $r=0.420$). [Conclusion] MK was strongly correlated with neurite density.

P-3-013　Diffusional kurtosis imaging を用いた intravoxel incoherent motion 解析: シミュレーションによる検討
Intravoxel incoherent motion analysis using diffusional kurtosis imaging: a simulation study

梅沢　栄三（藤田保健衛生大学 医療科学部 放射線学科）
Eizou Umezawa[1], Masahiro Kawasaki[2], Masayuki Yamada[1], Takashi Fukuba[3], Kazuhiro Murayama[4]

[1]School of Health Sciences, Fujita Health University, [2]Graduate School of Health Sciences, Fujita Health University, [3]Department of Radiology, Fujita Health University Hospital, [4]School of Medicine, Fujita Health University

【要旨】DKI で求められる拡散尖度と拡散係数を使って IVIM の灌流比率と擬拡散係数を計算する方法を、シミュレーションにより検討した。本方法によれば、従来の IVIM 法より灌流比率を確度、精度良く求めることができた。擬拡散係数の確度は、本方法で求める方が従来の IVIM 法で求めるより低くなり、精度は同程度であった。

Purpose:
Intravoxel incoherent motion analysis (IVIM) can reveal the property of perfusion in living system. Parameter estimations in IVIM tend to be unstable due to the bi-exponential (exp) fitting. We propose a method to calculate the IVIM parameters using diffusional kurtosis imaging (DKI) to improve the estimation.
Methods:The following relations were used: $f=[1+(K/3)\{D/(D-Dt)\}^2]^{-1}$, $Dp=D\{1+(K/3)D/(D-Dt)\}$, where f, Dp, Dt, D, K are the perfusion fraction, pseudodiffusion coefficient, pure diffusion coefficient, diffusivity and kurtosis, respectively. We estimated D, K and Dt using DKI, and substituted in the relations. Used b-values were 0, 10, 20, 35, 50, 100, 200, 300, 350, 400, 450, 500, 600, 800, 1000 s/mm^2. Signals at $b \leq 400$ s/mm^2 were used to estimate D and K. To estimate Dt, we implemented DKI analysis with signals at $b \geq 350$ s/mm^2. We also calculated f and Dp using conventional IVIM for comparison, in which Dt and f were obtained from mono-exp fitting with signals at $b \geq 350$ s/mm^2, and Dp was estimated from bi-exp fitting with the full signals. Simulated signal set for brain white matter (10^4) were used. Tri-exp model with Rician noises (SNR=25) was used to the simulation. The characteristic function method with a calibration procedure was used for DKI.
Results:
When the true values of f/Dp[10^{-3}mm^2/s] were 0.06/12.0, the estimated medians were 0.071(0.054-0.087)/21.6(16.4-26.8) for DKI, and 0.132(0.106-0.159)/9.8(7.1-17.6) for conventional IVIM (data in parentheses are interquartile ranges). In general, accuracy and precision of f were improved in DKI. Accuracy of Dp was degraded in DKI, and precision of that was comparable between DKI and conventional IVIM.
Conclusion:
DKI based IVIM analysis increases accuracy and precision of the perfusion fraction estimation.

P-3-014　MRI神経メラニン画像の定量評価に向けた初期検討 -DaTSCANとの比較-
Initial examination for the quantitative evaluation of MR-NM image -with DatSCAN-

小野寺聡之（東京都保健医療公社 荏原病院 放射線科）
Toshiyuki Onodera, Toshiki Wakayama, Miwa Sasaki, Ken Yashiro, Takashi Ueda, Kenji Saito, Akira Yamashita, Masahiro Ida

Department of Radiology, Tokyo Metropolitan Health and Medical Treatment Corporation Ebara Hospital

【要旨】パーキンソン病患者やレビー小体型認知症患者では、3.0T MRIによる神経メラニン画像も有用とされているが、定量的評価はあまり行われていない。DaTSCAN SPECTによるSBRと比較することによって定量評価への検討を行った。

[Introduction]
It is known that the quantity of Dopamine transporters; DAT and Neuromelanin; NM decreases in PD and DLB and the quantitative evaluation by Bolt Specific Binding Ratio; SBR and Asymmetry Index; AI from DaTSCAN SPECT using ^{123}I-FP-CIT which reflects the distribution of DAT is progressing in such diagnosis. On the other hand, although MR-NM image is also recognized to be useful and the clinical application is progressing, the diagnosis by visual evaluation is general. Therefore, the examination for the quantitative evaluation of MR-NM image was carried out by the comparison of MR-NM image and DaTSCAN SPECT.
[Method]
We selected 100 patients who performed MR-NM image and DaTSCAN SPECT in our hospital. MR-NM image was imaged by 3.0T MRI (Siemens MAGNETOM Trio) and the high intensity volume of Substantia Nigra pars Compacta; SNC was carried out using ImageJ. SBR and AI analysis of DaTSCAN SPECT was carried out by DaTView ver.3.0(AZE VirtualPlace). The correlation between the volume of SNC and SBR was examined.
[Result]
Good correlation was shown between the volume of SNC in MR-NM image and SBR and AI from DaTSCAN SPECT. In addition, good correlation was also shown between the volume of SNC, SBR and AI from DaTSCAN SPECT and the clinical severity.
[conclusion]
By the measurement and quantitative evaluation of SNC volume of MR-NM image, the diagnosing ability for PD and DLB equal to DaTSCAN SPECT was recognized. We wish to fully utilize the high resolution of MRI and examine the standardization and the population analysis, and develop the quantitative evaluation tool of MR-NM image and proceed with the examination about the usefulness.

P-3-015　黒質神経メラニンイメージングの撮像条件最適化
Optimization of MR Imaging Parameters for Neuromelanin Imaging of the Substantia Nigra

中田　直（おさか脳神経外科病院 放射線部）
Sunao Nakata[1], Yuji Miyatake[1], Yasuaki Kamada[1], Yuko Takahashi[1], Naomi Honjo[2]
[1]Radiation Department, Osaka Neurosurgical Hospital, [2]Department of Radiology, Osaka Neurosurgical Hospital

【要旨】T1-FSE法を用いた黒質神経メラニン信号の描出は3T MRIを用い、高信号強度、高分解能での撮像が必要であり、当院でも撮像条件の最適化を行った。また、MT pulseを付加することで高いコントラストを持った黒質神経メラニン信号の描出が可能となった。

Background and Objective: Visualization of the neuromelanin signal (melanin signal) in the substantia nigra with T1-FSE has been reported to be useful for the diagnosis of Parkinson's disease. Visualization of the melanin signal on 3 T MRI requires scanning with high signal intensity and spatial resolution. We optimized the imaging parameters and compared the visualization with and without an added magnetization transfer pulse (MT pulse). Equipment: Siemens Magnetom Verio B17 3.0 T system with 32-ch head coil.Subjects and Methods: For one healthy volunteer who gave consent, the signal intensity, area, and contrast ratio of the substantia nigra versus normal midbrain were determined for varying values of the T1-FSE parameters TR, TE, and TSE factor. Under optimized imaging conditions, we compared the scans obtained with and without an added MT pulse.Results and Discussion: Signal intensity ratio increased with longer TR. Contrast ratio was at maximum at TR 650 ms, and decreased with longer TE. Contrast ratio increased with higher TSE factor; taking into account of the number of slices and imaging time, the optimal sequence parameters were TR 650 ms, TE 11 ms, TSE factor 3. Adding an MT pulse to the sequence yielded a higher melanin signal and contrast ratio for normal midbrain. This may be due to suppression of the protein-bound water signal, leading to a lower normal midbrain signal. However, because the protons of free water and protein-bound water are usually interchangeable, the addition of an MT pulse might also have a slight effect on the melanin signal. Further research is needed, including studies in clinical cases. Conclusion: We optimized the imaging parameters for T1-FSE and visualized the melanin signal of the substantia nigra with high contrast.

P-3-016　ADCで補正した新たな定量的指標computed SUV：概念、技術、臨床応用
ADC-corrected SUV derived from voxel-based SUV-ADC scatter plots in FDG-PET/MR hybrid imaging: Concept, techniques, and clinical applications

渡邊　祐司（九州大学大学院 医学研究院 分子イメージング診断学）
Yuji Watanabe[1], Koji Sagiyama[2], Ryotaro Kamei[2], Sungtak Hong[3], Satoshi Kawanami[2], Yoshihiro Matsumoto[4], Hiroshi Honda[2]
[1]Kyushu University Graduate School of Medical Sciences, Dept. Molecular imaging and Diagnosis, [2]Kyushu University Graduate School of Medical Sciences, Dept. Clinical Radiology, [3]Philips Electronics Japan, [4]Kyushu University Hospital, Dept.Orthopedics

【要旨】PET/MRイメージングの新しい定量的指標としてADCで補正したc-SUV を開発した。方法はADCmapとPET画像で作成したSUV-ADC分散図から回帰直線を基に算出した。軟部腫瘍の悪性度評価では、c-SUVと回帰直線の傾きはともにSUVmaxと同等の診断能を示し、治療効果判定ではSUVmaxやADCminと比べより明瞭に治療後の変化を検出できた。

Purpose: To investigate the usefulness of newly-developed parameters derived from voxel-based SUV-ADC scatter plots in the evaluation of soft-tissue tumor malignancy and treatment effect with a hybrid PET/MR system. Materials and Methods: Thirty-five patients with soft-tissue tumors (25 high-grade and 10 low-grade tumors) were examined with Ingenuity TF PET/MR system. Zoomed DWI (b = 0 and 800) and ^{18}FDG-PET were acquired along with fat-suppressed T2WI. Tumor ROIs were manually drawn along the border of the tumor in all slices on T2WI, and were copied and pasted onto the ADC maps and PET images. The ADCs and SUVs inside the ROIs were recorded along with x-y coordinates in a voxel-wise manner. The regression line was generated from the scatter plot of SUV/ADC vs. ADC. A new parameter named computed-SUV (c-SUV) was calculated by using the SUV/ADC value on the regression line where ADC was 0.5×10^{-6} mm^2/sec. The c-SUV along with the slope of the regression line was compared with the conventional parameters of SUVmax and ADCmin to assess diagnostic performance for differentiating high-grade tumor and determining treatment effect. Results: The linear regression analysis between SUV/ADC and ADC showed a significant linearity ($P < 0.05$) in all the cases. In differentiating high grade from low/intermediate grade tumors, the area under curve of c-SUV (0.70) and slope (0.71) was similar to that of SUVmax (0.71), and were superior to that of ADCmin (0.51). Both the c-SUV and slope clearly demonstrated interval change between pre and post-treatment. Conclusion: The newly-developed computed-SUV (ADC-corrected SUV derived from voxel-based SUV-ADC scatter plots) could be a useful parameter in the evaluation of tumor malignancy grade and treatment effect.

P-3-017　原発不明癌に対するPET/CTとPET/MR診断能比較
PET/MR outperforms PET/CT in suspected occult tumors

関根　鉄朗（日本医科大学 放射線科）
Tetsuro Sekine[1,2], Barbosa Felipe[2], Sah Bert-Ram[2], Cacilia Mader[2], Delso Gaspar[2], Ter Voert Edwin[2], Veit-Haibach Patrick[2], Huellner Martin W[2]

[1]Department of Radiology, Nippon Medical School, [2]Department of nuclear medicine, University Hospital Zurich

【要旨】原発不明癌に対するPET/CTとPET/MRの診断能比較を行った。対象は原発不明癌が疑われた43名。原発巣、リンパ節転移、遠隔転移の3つのカテゴリーでの正診率比較を行った。結果、原発巣に対してPET/MRが有意に高い正診率を示した(0.97 vs. 0.73)。PET/MRは原発不明癌疑い患者に対するwork-upに有用と考えられた。

PURPOSE: To compare the diagnostic accuracy of PET/MR and PET/CT in patients with suspected occult primary tumors.METHODS: Sequential PET/CT-MR was performed in 43 patients referred for suspected occult primary tumors. Patients were assessed with PET/CT and PET/MR for the presence of a primary tumor, lymph node metastases and distant metastases. The diagnostic accuracy of PET/CT and PET/MR were compared.RESULTS: PET/MR was superior to PET/CT for primary tumor detection (Sensitivity/specificity 0.85/0.97 vs. 0.69/0.73; p=0.020), and comparable to PET/CT for the detection of lymph node metastases and distant metastasis (Sensitivity/specificity 0.93/1.00 vs. 0.93/0.93, p=0.157; 1.00/0.97 vs. 0.82/1.00; p=0.564). CONCLUSIONS:PET/MR outperforms PET/CT in the work-up of suspected occult malignancies. PET/MR may replace PET/CT to improve clinical workflow.

Table 3

Diagnostic accuracy of PET/CT and PET/MR for 43 patients. Numerical display.

		Primary tumor	Lymph node metastasis	Distant metastasis
PET/CT	TP	9	14	9
	TN	22	26	32
	FP	8	2	0
	FN	4	1	2
PET/MR	TP	11	14	11
	TN	29	28	31
	FP	1	0	1
	FN	2	1	0

NOTE. – TP, true positive; FP, false positive; FN, false negative; TN, true negative.

Table 5

Reasons for misdiagnosis (n = 22)

Physiologic / benign FDG uptake misdiagnosed as malignant lesion (n = 9, 40.9%)		
PET/CT	8	(2 nasopharynx, 2 larynx, oropharynx, kidney, rectum, para-aortic lymph node)
PET/MR	1	(pituitary adenoma)
Metastatic lesion with FDG uptake misdiagnosed as primary site, or vice versa (n = 7, 31.8%)		
PET/CT	5	(subcutaneous metastasis, lung metastasis, kidney metastasis, retroperitoneal Castleman's disease, primary cholangiocarcinoma)
PET/MR	2	(lung metastasis, primary retroperitoneal paraganglioma)
Malignant lesion missed due to subtle FDG uptake (n = 4, 18.2%)		
PET/CT	3	(appendix carcinoma, liver metastasis, inguinal lymph node metastasis)
PET/MR	1	(inguinal lymph node metastasis)
Malignant lesion with FDG uptake misdiagnosed as physiologic / benign (n = 2, 9.0%)		
PET/CT	1	(lung metastasis)
PET/MR	1	(nasopharyngeal carcinoma)

P-3-018　Zero-echo-TEによる頭蓋骨推定を用いた頭部PET/MR吸収補正法の検討
Clinical evaluation of ZTE attenuation correction for brain FDG-PET/MR imaging, comparison with atlas attenuation correction

関根　鉄朗（日本医科大学 放射線科）
Tetsuro Sekine[1,2], Ter Voert Edwin[2], Warnock Geoffrey[2], Buck Alfred[2], Huellner Martin[2], Veit-Haibach Patrick[2], Delso Gaspar[2]

[1]Department of Radiology, Nippon Medical School, [2]Department of nuclear medicine, University Hospital Zurich

【要旨】PET/MR機において、Zero-echo-TE (ZTE) MRIを用いて頭蓋骨吸収値の推定を用い、現行の臨床機で用いられているsingle-atlas法やgold standardであるCT吸収補正法と比較した。結果、ZTE法を用いたPET吸収補正では、single-atlas法と比較して、誤差が25%程度軽減する事が示された。

Purpose:To evaluate the zero-echo-time (ZTE) attenuation correction (AC) which will be implemented on the next version of GE-PET/MR scanner. Methods: We recruited 10 pt. A head PET/MR scan (GE SIGNA PET/MR) was performed. Based on clinical atlas-AC, ZTE-AC and CT-AC, PET images were reconstructed from identical raw data on the PET/MR scanner. All PET images were normalized, and quantified in 67 VOIs. Relative differences (%diff) and absolute relative differences (|%diff|) were calculated. Results:Qualitative analysis shows that ZTE-AC was robust to patient variability. The |%diff| of all 670 VOIs on ZTE was improved by approximately 25% compared to Atlas-AC (ZTE-AC vs. Atlas-AC; 1.77 ± 1.41% vs. 2.44 ± 1.63%, p<0.01). Conclusion: The ZTE-AC could provide more accurate AC than clinical Atlas-AC by improving the estimation of head skull attenuation.

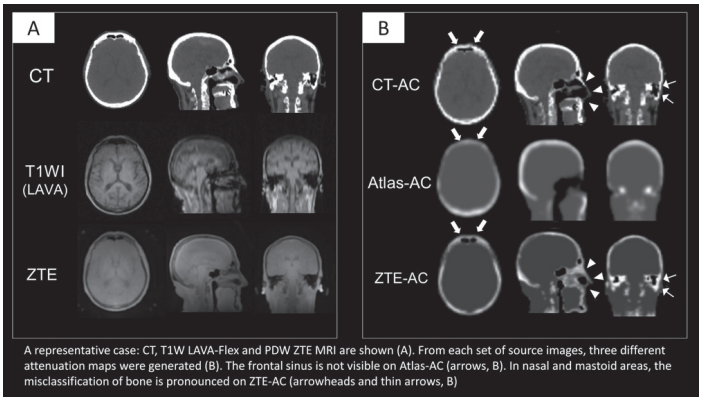

A representative case: CT, T1W LAVA-Flex and PDW ZTE MRI are shown (A). From each set of source images, three different attenuation maps were generated (B). The frontal sinus is not visible on Atlas-AC (arrows, B). In nasal and mastoid areas, the misclassification of bone is pronounced on ZTE-AC (arrowheads and thin arrows, B)

P-3-019　PET/MR頭部吸収補正における臨床用single-Atlas法とMulti-Atlas法の比較
Multi atlas-based attenuation correction for brain FDG-PET imaging

関根　鉄朗（日本医科大学 放射線科）
Tetsuro Sekine[1,2], Burgos Ninon[3], Warnock Geoffrey[2], Huellner Martin[2], Buck Alfred[2], Ter Voert Edwin[2], Ourselin Sebastien[3], Hutton Brian[3], Veit-Haibach Patrick[2], Delso Gaspar[2]
[1]Department of Radiology, Nippon Medical School, [2]Department of nuclear medicine, University Hospital Zurich, [3]Translational Imaging Group, University College London

【要旨】GE-PET/MR臨床機では単一のatlasを用いたsingle-atlas based法による吸収補正が行われる。同手法と、複数のatlasを用いたmulti-atlas based法を比較した。対象は15名、input画像にはlow resolution T1WI(scan time 18sec)を用いた。結果、multi-atlas法では誤差が20%程度、低減した。

Purpose: To assess the feasibility of attenuation correction (AC) based on a multi atlas-based method (m-Atlas) by comparing it with a clinical AC method (single atlas-based method (s-Atlas)).Methods: We enrolled 15 patients. All patients underwent brain PET/CT and PET/MRI (GE SIGNA PET/MRI). Based on s-atlas, m-atlas and CT-AC, PET images were reconstructed from raw data on the TOF-PET/MRI scanner. All PET images were normalized and FDG accumulation was quantified in 67 volumes-of-interest. Relative (%diff) and absolute differences (|%diff|) between images were calculated.Results: The range of error on m-Atlas in all 1005 VOIs was -4.99%~4.09%. The |%diff| on m-Atlas was improved by about 20% compared to s-Atlas (s-Atlas vs. m-Atlas;1.49 ± 1.06% vs.1.21 ± 0.89%,p<0.01).Conclusion: The errors introduced using either s-Atlas or m-Atlas did not exceed 5% in any brain region investigated.

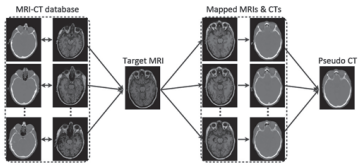

CT synthesis diagram using multi-atlas method for a given MRI image. All the MRIs in the atlas database are registered to the target MRI. The CTs in the atlas database are then mapped using the same transformation to the target MRI. A local image similarity measure between the mapped and target MRIs is converted to weights to reconstruct the target CT.

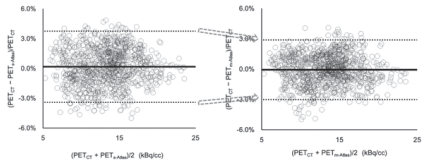

Bland-Altman plots of CT-AC and s-Atlas (left), and CT-AC and m-Atlas (right) for 67 VOIs * 15 patients.
The m-Atlas has no bias and no undere or overestimation (-0.06 ± 1.50%; range -4.99% - 4.09%).
These results are superior to the result of s-Atlas (0.17 ± 1.82%; range -5.00 – 4.84%).

P-3-020　Black-blood 脂肪抑制T2強調像を用いた限局性肺すりガラス影検出能の検討
Detection of ground-glass opacity lesions using breath-hold black-blood magnetic resonance imaging of the lungs

亀井僚太郎（九州大学大学院 医学研究院 臨床放射線科学分野）
Ryotaro Kamei[1], Yuji Watanabe[2], Koji Sagiyama[1], Satoshi Kawanami[2], Hiroshi Honda[1]
[1]Department of Clinical Radiology, Graduate School of Medical Sciences, Kyushu University, [2]Department of Molecular Imaging and Diagnosis, Graduate School of Medical Sciences, Kyushu University

【要旨】肺MRでは血管信号がアーチファクト源となり、すりガラス影のような淡い病変の検出は困難である。発表者らは病変コントラストの改善を目的としてBlack-blood法、脂肪抑制法を併用した呼吸停止下・短時間撮像のT2強調像を開発した。すりガラス結節を有する患者への適用では病変検出とサイズ評価における有用性が示唆された。

[Purpose] To investigate the feasibility and usefulness of breath-hold black-blood T2-weighted (BBT2W) turbo spin echo magnetic resonance imaging (TSE MRI) of the lungs in the detection of focal ground-glass opacity (GGO) lesions.[Materials and Methods]We included 44 consecutive patients who underwent high-resolution computed tomography (HRCT) and 3.0-T MR imaging of the whole lungs. BBT2W imaging was performed using the variable refocusing flip-angle technique. Breath-hold T1-weighted imaging (T1WI) with a 3D mDixon sequence was also performed.HRCT images were used as the reference standards. The location, number, size, and characterization (pure or mixed) of the GGO lesions were recorded. Two radiologists performed interpretation of the MR images. For the focal GGOs, lesion-based detection rates were calculated and compared between BBT2WI and T1WI scans. Statistical analyses were performed using the McNemar test, correlation analysis and the Bland-Altman plot.[Results]HRCT revealed 24 GGO lesions in 12 patients. Upon MRI interpretation, lesion-based detection rates of focal GGOs were 79.2% (19/24) for BBT2WI and 54.2% (13/24) for T1WI. T1WI detected only 1 of 10 pure GGOs and 12 of 14 mixed GGOs, while BBT2WI detected 5 of 10 pure GGOs and all the mixed GGOs. The GGO size on BBT2WI had a strong correlation with that of HRCT ($r = 0.9425$, $p < 0.0001$), and the mean difference was small (0.7095 mm). Although there was a significant correlation between the sizes detected on T1WI and HRCT ($r = 0.6868$, $p = 0.0118$), the GGOs tended to appear smaller on T1WI than on HRCT, with a mean difference of 6.694 mm.[Conclusion] Breath-hold black-blood T2-weighted MRI of the lungs with PPU gating is feasible and could provide acceptable diagnostic quality for detecting GGO lesions.

P-3-021　Balanced steady state free precession sequenceにおける脂肪抑制効果の装置間の比較-多施設評価-
Comparison of fat suppression images by using balanced steady-state free precession sequences: a multi-vendor study

上山　毅（彩都友紘会病院 放射線部）
Tsuyoshi Ueyama[1], Hiroyuki Tarewaki[2], Yuya Yamatani[3], Masaaki Kajisako[4], Kenichirou Yamamura[5]
[1]Department of Radiology, Saito-Yukoukai Hospital, [2]Department of Medical Technology, Osaka University Hospital, [3]Central Division of Radiology, Nara Medical University Hospital, [4]Department of Radiology, Kyoto University Hospital, [5]Department of Radiology, Osaka Medical College Hospital

【要旨】日本磁気共鳴専門技術者認定機構の班研究として装置間のSSFPシーケンスにおける脂肪抑制効果を比較した。自作ファントムを作成。統一条件ものと脂肪抑制パルスの有り無しで脂肪信号の変化を計算し、多重検定によって有意差を検証した。検定の結果、全ての装置間で脂肪抑制効果に有意差を認めた。

Purpose:
The available fat suppression parameters of balanced steady-state free precession (SSFP) sequence differ between magnetic resonance imaging (MRI) devices. The purpose of this study was to compare fat suppression effect by using balanced SSFP sequence images obtained from various multi-vendor MRI machines.
Materials and methods:
In this study, we performed a phantom experiment to evaluate the fat suppression effect of balanced SSFP sequences with and without the use of fat suppression pulse. The home-built phantom components were multiple syringes, including fat and liquid elements. Phantom images were acquired by using three 1.5-tesla scanners and six 3.0-tesla scanners. Scan parameters (repetition time or echo time, flip angle, matrix size, band width, and field of view) were unified as much as possible. Chemical shift selective and spectrally attenuated inversion recovery pulses were used as fat suppression pulse. However, the available fat suppression pulses differed between the different MRI devices. We measured the ratio of fat signal intensity to the reference liquid signal intensity. The percentage change in the ratio with and without the use of fat suppression pulse was defined as the evaluation index for fat suppression. The percentage changes in each MRI device were compared by using the Student t test. Bonferroni correction was used for multiple comparisons.
Results:
The results of the multiple comparisons showed a significant difference ($p < 0.05$) between all the MRI devices. The biggest difference in percentage change of > 30% was found among the 1.5-tesla devices, followed by 22% among the 3.0-tesla devices.

P-3-022　Balanced steady-state free precession sequenceにおけるコントラストの装置間の比較-多施設評価
Comparison of contrasts by using balanced steady-state free precession sequences: a multi-vendor study

垂脇　博之（大阪大学医学部附属病院 放射線部）
Hiroyuki Tarewaki[1], Tsuyoshi Ueyama[2], Yuya Yamatani[3], Masaaki Kajisako[4], Kenichirou Yamamura[5]
[1]Division of Radiology, Osaka University Hospital, [2]Department of Radiology, Saito-Yukoukai Hospital, [3]Central Division of Radiology, Nara Medical University Hospital, [4]Department of Radiology, Kyoto University Hospital, [5]Department of Radiology, Osaka Medical College Hospital

【要旨】日本磁気共鳴専門技術者認定機構の班研究として装置間のSSFPシーケンスにおけるコントラストを比較した.自作ファントムを作成.撮像条件をそろえて撮像した.コントラストを計測し,多重検定によって有意差を検証した.検定の結果,全ての装置間でコントラストに有意差を認めた.

Purpose:Our aim was to compare the contrasts of balanced steady-state free precession (SSFP) sequence images among multi-vendor MRI devices.Materials and methods:A home-built phantom used in this study consisted of 7 syringes: a fat and 6 liquid elements those had various T1 and T2 values. The liquid element with the lowest T2 value was regarded as reference. Phantom images were acquired by using three 1.5-T and six 3.0-T scanners. We measured the T1 and T2 relaxation times of the phantom each MRI device. Scan parameters of balanced SSFP sequence (repetition time or echo time, matrix size, band width, and field of view) were unified among different MRI devices as much as possible. Flip angles were set to 90° at 1.5-T and 70 ° at 3.0-T. Each image was acquired by changing repetition time little by little. We measured the contrasts from pairs of reference element and each of the other elements as a contrast index, and compared the contrasts among each MRI device. Results and discussion:The T1 and T2 values of each element were significantly different among the MRI devices. It may be because the center frequency and transmitter gain differed among the MRI devices. In comparison of the contrasts of the same liquid element among the MRI devices, the significant differences were observed in almost all of elements. There was thought to be two reasons for this result. First, the measured T1 and T2 values of the same liquid element differed among the MRI devices. Second, the scan parameters including the shapes of excitation pulse and the k-space trajectory were not the same among the MRI devices. Conclusion:Contrast of balanced SSFP sequence images could differ among the multi-vendor MRI devices.

P-3-023　mDIXON-XDとO-MAR併用による金属アーチファクト抑制効果の検討
Consideration of the effect of metal artifact suppression with combination of mDixon-XD and O-MAR

牛島　大悟（株式会社フィリップスエレクトロニクスジャパン ISビジネスグループ）
Daigo Ushijima[1], Atsushi Takemura[1], Yasutomo Katsumata[2], Akira Suwa[1], Futoshi Nakagawa[1]
[1]Philips Electronics Japan. Ltd. BG IS, [2]Philips Healthcare

【要旨】mDIXON-XDとO-MAR併用による金属アーチファクトと脂肪抑制効果への有用性を検討した。ファントムを用いてT1W TSE SPIRとO-MAR併用 T1W TSE SPIR、mDIXON-XD と O-MAR併用T1W TSEを撮像した。歪みはO-MARにより改善し、mDIXON-XDにより脂肪抑制は改善した。脂肪抑制画像における金属周囲の評価への有用性が示唆された。

Background
Recently, the number of patient having the metal implanted device shows an increasing trend. The influence of metal implanted device in the MR system leads to magnetic field inhomogeneity. Therefore image distortion, signal loss and fat suppression failure are occurred. Since the conventional method (SPIR) leads to fat suppression failure in contrast-enhanced MRI.
Purpose
We have examined the utility of the effect of metal artifact suppression and fat suppression by the combination of mDixon XD and O-MAR.
Materials and Methods
All studies were performed by using 1.5Tesla MRI device (Ingenia ststem, Philips Electronics Japan), the dStream Torso and Spine coil. We made a phantom which was inserted several metal implant devices to make a comparison between distortion effects and fat suppression effects in T1w TSE with SPIR, T1w TSE SPIR with O-MAR and T1w TSE with combination mDixon-XD and O-MAR.
Result
It showed results of the metal artifact and fat suppression failure using T1w TSE SPIR sequence. At the same comparison, the metal artifact was suppressed by using O-MAR, also fat suppression was improved by using the combination of mDixon-XD.
Conclusion
It was improved the metal artifact suppression and fat suppression by using the combination of mDixon-XD and O-MAR. This sequence is a useful method of evaluating metal surrounding tissue in contrast-enhanced MRI of T1 fat suppression techniques.

P-3-024　頭部用シーケンスを用いた静音化パラメータの検討
Optimization of a noise reduction parameter using the Brain routine 3 sequences

川又　　渉（秋田県厚生連 かづの厚生病院）
Wataru Kawamata
Akita Prefectural Welfare Federation of Agricultural Cooperative

【要旨】当院装置付属の静音パラメータを、頭部用ルーチンシーケンスを使用し、その有用性を検討した。静音強度をあげると、SNRは下がる傾向にあるが、音圧は減少した。ボランティア画像では、静音の値を大きくしていくと画質が悪くなる傾向があった。診療に用いるためには、強度4程度が妥当と考えられる。

[Purpose]In recent years, Silent technology of MRI is beginning to be introduced. These techniques are a very small sound pressure. But since they are mounted only on expensive equipment, there is a situation that cannot be introduced in many facilities. Our hospital is also similarly, equipment update is undecided. But even MRI in use, past noise reduction techniques have been introduced. Using the silent scan technology. I have examined the effect on the general 3 sequence that is used to head MRI examination.[Method]Consider the image is the T2-weighted images and T1-weighted images and FLAIR image. Using a cylindrical phantom was scanned by varying the Silent parameter. From the obtained image was measured SNR with a software for signal intensity measurement (PI-SNR). It was measured sound pressure at the same time. And to scan the head of adult volunteers. (I have to get the consent fully described the intent of the experiment)[Result]The higher the silent scan parameters, SNR became a tendency to decrease. The sound pressure was reduced in proportion to the parameter. In the volunteer image, image quality has tended to be lowered by increasing the silent scan parameters.[Discussion]Silent technology of our hospital is to control the rise of the gradient magnetic field, it is a method to reduce the noise. Its silent technique has the effect of reducing jarring high frequency component. Therefore, the effect on contrast, such as TE and TR is considered a slight.[Conclusion]The Silent Technology "Softone" reduces the noise, and the interpretation can image is obtained, considered a valid technique. Also, this technology may be able to reduce the patient's stress, I plan to actively scan the future.

P-3-025　PHIP型の超偏極 13C MRI代謝イメージングシステムの構築
Construction of a parahydrogen-induced hyperpolarized 13C MRI system for metabolic imaging

内尾　佳貴（北海道大学大学院 情報科学研究科）
Yoshiki Uchio, Hiroshi Hirata, Shingo Matsumoto

Graduate School of Information Science and Technology, Hokkaido University.

【要旨】炭素13核への超偏極誘導は生体内代謝のリアルタイムイメージングを可能としている。現行の動的核偏極法に比べ、より安価で設置要件の緩いパラ水素誘起分極法（PHIP）による超偏極^{13}C MRI代謝イメージングシステムの構築を目指して、パラ水素変換器、PHIP型励起装置、1.5T-^{1}H/^{13}C MRI装置を作製した。

[Background]Hyperpolarization is a technique to amplify ^{13}C NMR signals more than 10,000 times. Three methods have been used to induce hyperpolarization on ^{13}C nuclei; 1) Dynamic Nuclear Polarization (DNP), 2) Brute Force, and 3) Para-Hydrogen (p-H_2) Induced Polarization (PHIP). Although DNP technique has been widely used in metabolic imaging studies, high cost and long excitation time of the DNP polarizer limits its wide spread clinical applications. We set up a hyperpolarized ^{13}C metabolic MRI system with a low cost and instantly excitable PHIP polarizer. [Experiments]Hyperpolarized MRI system consists of 1) p-H_2 converter, 2) ^{1}H/^{13}C MRI scanner and 3) PHIP hyperpolarizers. In the p-H_2 converter, H_2 gas passes through a 1/4" copper tube containing iron oxide catalyst wound on a 4K GM cryocooler. The ^{1}H/^{13}C MRI scanner consists of 1.5T permanent magnet and a double wound RF coil with an inside ^{13}C solenoid and an outside ^{1}H saddle coil. Pulsed sequences were optimized using a sodium permanganate phantom which gyromagnetic ratio is similar to ^{13}C. We developed two different type of PHIP polarizers known as ALTADENA and PASADENA, and compared polarization efficiency of them.

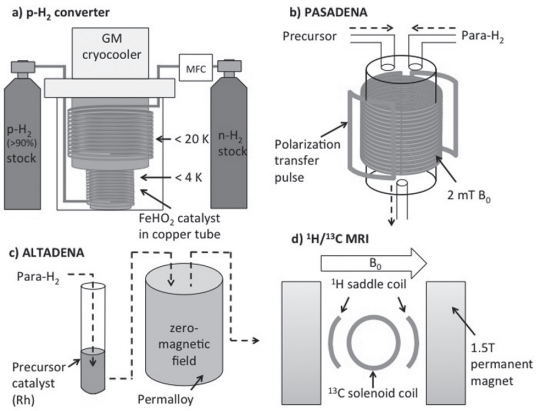

P-3-026　超偏極13C　MRI代謝イメージングのためのパラ水素誘起分極(PHIP)型13C核励起装置の開発
Development of s para-hydrogen induced polarization (PHIP) type hyperpolarizer system for hyperpolarized metabolic 13C MRI

中西沙由里（北海道大学 大学院 情報科学研究科 生命人間情報科学専攻）
Sayuri Nakanishi, Shingo Matsumoto, Hiroshi Hirata

Division of Bioengineering and Bioinfomatics, Graduate School of Information Science and Technology, Hokkaido University

【要旨】溶液中13C核への超偏極誘導技術の開発により、生体内代謝反応の可視化が可能となっている。現行の動的核偏極法に比べ、より安価で設置上の制約も少ない13C核励起装置として、パラ水素付加反応炉、主磁場、分極転移用コイル、制御システムで構成されるパラ水素誘起分極法（PHIP）型の励起装置を作製した。

Magnetic resonance spectroscopy of 13C nucleus has been used for metabolic analysis, but intrinsic low sensitivity limits its use for imaging applications. Hyperpolarization is a way to overcome the sensitivity limitation. Although dynamic nuclear polarization (DNP) is the most popular hyperpolarization technique for metabolic MRI, its high cost and installation requirements limit wide-spread clinical application of this new molecular imaging tool. Para-hydrogen induced polarization (PHIP) is an alternative hyperpolarization technique operable at low B0 field (~2mT) and room temperature. In PHIP, hyperpolarization of 13C nuclei is induced by addition of para-hydrogen into unsaturated precursor of metabolic tracer and following polarization transfer from 1H to 13C.
In this study, we developed a PASADENA type PHIP polarizer [1,2] which consists of para-hydrogenation reaction chamber, electromagnet for B0 field, saddle coil for polarization transfer, and control unit composed of 4 solenoid valves and LabVIEW / PXI system.
References
1) J.B. Hovener, et al. MAGMA 22, 123-134 (2009), 2) J.B. Hovener, et al. MAGMA 22, 111-121 (2009).

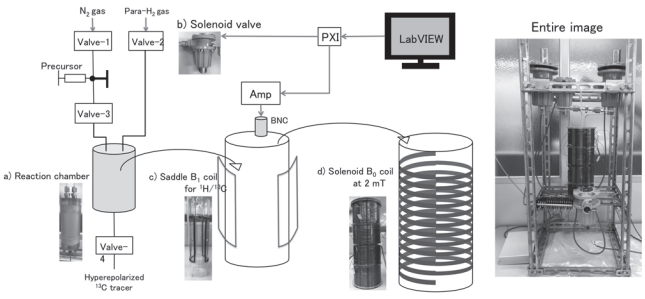

Hyperpolarization system consists of **a)** para-hydrogenation reaction chamber, **b)** solenoid valves controlled by a LabVIEW software, **c)** saddle B_1 coil for polarization transfer from ^{1}H to ^{13}C, and **d)** solenoid B_0 coil operating at 2 mT.

P-3-027　超偏極 ^{129}Xe MRIを用いた肺がんモデルマウスの病態進行評価に対する試み
An Attempt to Evaluate the Progression of Lung Cancer in Mice by means of Hyperpolarized ^{129}Xe MRI

下川　晃弘（大阪大学大学院 医学系研究科 保健学専攻 医療技術科学分野 医用物理工学講座）
Akihiro Shimokawa, Shota Hodono, Yu Ozaki, Naoto Miyazaki, Atsuomi Kimura

Department of Medical Physics and Engineering, Area of Medical Technology and Science, Division of Health Sciences, Graduate School of Medicine, Osaka University, Japan

【要旨】肺がんの早期診断を指向し、超偏極 ^{129}Xe (HPXe) MRIを用いた肺がんモデルマウスの経時的肺機能計測を試みた。病態群のガス交換能は対照群と比較して低値を示し続けた。一方、腫瘍位置の同定には至らなかった。本結果を受け、新規造影剤とHPXe MRIを組み合わせた早期腫瘍同定を計画している。

Background: Lung cancer (LC) is the leading cause of cancer mortality in the world. For early detection of lung diseases, we aimed to apply hyperpolarization technology to non-invasive assessments of pulmonary function. In this study, hyperpolarized ^{129}Xe (HPXe) MRI was exploited for longitudinally observation of the LC progression in mice.
Methods: Five male ddY mice were given intraperitoneal (i.p.) injection of an aqueous solution of ethyl carbamate to induce LC. Four healthy mice were used as a control group. For evaluating pulmonary functions, parameters of gas-exchange (f_D (%)) and fractional ventilation (r_a) were obtained using HPXe MRI. The f_D, which is defined as the fraction of HPXe diffused from gas space to blood and tissue of alveoli, was evaluated by the xenon polarization transfer contrast method. The r_a was evaluated using a series of ventilation images acquired by varying the number of breaths thereby multiple breath analyses. HPXe MRI measurements were performed before i.p. injection (month 0) and once a month for five months.
Results: The mean f_D of LC group tended to show lower values than that of control group, whilst the mean r_a values of both groups were mostly unchanged during all experimental period. On month 5, the mean f_D of LC group was significantly lower than that of the control group (f_{D_LC}=5.26 ± 1.35, $f_{D\_control}$=7.54 ± 1.24, P<0.05). HPXe images were unable to identify the region of lung tumors.
Conclusion: These results indicate that HPXe MRI measurements could demonstrate the deterioration of gas-exchange accompanied by the LC progression; regional LC identification by developing contrast agents is the next step of our investigation.

P-3-028　光ポンピング原子磁気センサ用いた超低磁場MRIの実現：超偏極 ^{129}Xeイメージング
Ultra-Low Field MRI with Optically Pumped Atomic Magnetometer: Hyperpolarized ^{129}Xe Imaging

山本　哲也（京都大学 大学院工学研究科）
Tetsuya Yamamoto, Takenori Oida, Hiroaki Natsukawa, Ingo Hilschenz, Yosuke Ito, Tetsuo Kobayashi

Graduate School of Engineering, Kyoto University

【要旨】超低磁場MRIには小型化や低コスト化等の多くの利点があるが、計測対象の核磁化やラーモア周波数が小さくなるという問題がある。本研究では、超偏極 ^{129}Xeを対象としてMR信号の増強を図ると同時に、超高感度な光ポンピング原子磁気センサを用い、850 μT（10 kHz）でのMR信号の計測と画像化に世界で初めて成功した。

Introduction
Ultra-low field (ULF) MRI has recently attracted attention because of its advantages for different scopes: miniaturization, running cost reduction, etc. However MR signal detection with conventional receiver (Rx) coils at ULFs is very hard due to the small magnetization and low Larmor frequency of samples. To overcome these problems, the present study introduced an optically pumped atomic magnetometer (OPAM) whose theoretical sensitivity is approximately 0.01 fT/Hz$^{1/2}$ and hyperpolarized ^{129}Xe (HpXe) as an MR signal detector and samples, respectively. We attempted to acquire MR signals and images at 850 μT (10 kHz).
Methods
All measurements were performed with an in-house coil system comprising a B_0 coil, Gx and Gy coils (for frequency and phase encoding), and transmission and Rx coils. The Rx coil configured a flux transformer (FT) in conjunction with an output coil to an OPAM because the OPAM is sensitive to a specific frequency band depending on a magnetic field different from B_0. HpXe gases whose polarization rate was increased up to several % were generated by Automatic Xenon Hyperpolarizer (Model HPXE2106, Toyoko Kagaku, Japan). They were packed in a gas bag with a volume of about 100 ml. The bag was put within the solenoid Rx coil.
Results and Conclusion
Due to the high sensitivity of the OPAM, MR signals of HpXe were successfully observed in each sequence for FID, SE, and GRE, though these signals were predicted less than several nT. In addition, 2-D MR images were configured with a standard GRE sequence (TR = 300 ms, TE = 90 or 110 ms, matrix size = 32 by 32, FOV = 64 or 128 mm). No averaging was done for these signals and images. By optimizing the input/output coils and resonant circuit of the FT, we plan to make B_0 further smaller in a future study.

P-3-029　超低磁場MRIにおける超偏極XeのSWIFT法による画像化
Hyperpolarized xenon imaging with SWIFT approach in ultra-low field MRI

笈田　武範（京都大学 大学院工学研究科）
Takenori Oida, Yuki Kaga, Tetsuya Yamamoto, Tetsuo Kobayashi
Graduate School of Engineering, Kyoto University

【要旨】本研究では，超低磁場MRIにおける超偏極Xeのsweep imaging with Fourier transformation (SWIFT)法を用いた画像化法についてシミュレーションによる検討を行った．シミュレーションの結果，超低磁場においても画像化が可能であり，SWIFT法の帯域を広げることにより画像再構成精度の向上が確認された．

In recent years, by using non-inductive magnetometers such as optically pumped atomic magnetometers or superconducting quantum interference devices, MR signals with lower frequency have been able to be measured in ultra-low field MRI (ULF-MRI). Meanwhile, since hyperpolarized xenon has magnetizations whose polarization rate is independent of static magnetic field in the MRI, it becomes easy to obtain the MR signals from hyperpolarized xenon even in the ULF-MRI. However, since xenon is gaseous body in room temperature, the MR signals are decayed due to rapid diffusion of the xenon in echo sequences. To reduce the decay caused by the xenon's diffusion, an imaging method using sweep imaging with Fourier transformation (SWIFT) has been proposed by Nakamura et al.
In this study, we propose the xenon imaging in ULF-MRI with the SWIFT approach. To assess the quality of signal reconstruction in the SWIFT, we simulated MR signals generated by the SWIFT pulse sequence with various bandwidth, pulse length and the oversampling in readout direction. The simulation results showed that we could obtain the hyperpolarized xenon images with the SWIFT approach in ULF-MRI. It was also confirmed that a wide bandwidth of swept transmission pulse in SWIFT approach was effective to improve the accuracy of the signal reconstruction. In addition, oversampling in readout direction was also found to reduce spike artifacts in the edge of reconstructed xenon images. Consequently, we conclude that hyperpolarized xenon images are able to be obtained by the SWIFT approach with wide bandwidth in ULF-MRI.

PDF-001　頭部外傷に対する急性期MRI,CTの比較検討
Comparison of MRI and CT for acute traumatic brain in

藏本　智士（香川県立中央病院 脳神経外科）
Satoshi Kuramoto, Hikari Matsumura, Akira Takeuchi, Atsushi Katsumata, Masamitsu Kawauchi
Department of Neurosurgery, Kagawa prefectural central hospital

【要旨】急性期頭部外傷に対する初期検査はCTが推奨されており、MRIは推奨されていない。しかしながら自験例ではMRIのほうが明らかに雄弁であり、軽症患者の予後良好を予測する因子として有用である可能性が示唆された。

Objective: CT scan is recommended for acute traumatic brain injury(TBI) on initial assessment by several guidelines. MRI studies are useful if CT scans failed to find the cause of neurological deficits. METHODS: We investigated retrospectively the 107 consecutive traumatic brain patients (aged 14-92 years, male 190, female 79) who hospitalized in our unit and received both CT and MRI scan in acute phase between January 2013 and November 2015. Result: Fifty-eight (54.2%) of all cases, especially 41 (95.3%) of 43 cases in moderate and severe TBI patients(Glasgow outcome scale <14), had abnormal signal intensity on initial MRI. MRI revealed more contusions and hemorrhages that were non-visible or underestimated on CT scan(MRI-CT mismatch)in thirty-three cases(30.1%). Prognostic factors were GCS on admission, age and d-dimer, not MRI findings with logistic regression analysis. But patients with non or small hemorrhage on CT who had no MRI-CT mismatch showed a tendency to have better outcome than the others(Odds ratio 10.36, p <0.05).Discussion: MRI provides obviously a larger amount of information than CT, but impact on the treatment strategy seemed to be less. However, the outcomes of mild TBI in who have no abnormal signals on MRI are likely to be better, we need more analysis on the future

PDF-002　Diagnostic Imaging of ASL perfusion in the grading of Non-enhancing Astrocytic Tumors

ハシバット　デルゲルダライ（徳島大学放射線科）
Delgerdalai Khashbat, Masafumi Harada, Takashi Abe, Mungunbagana Ganbold
Tokushima univeristy graduate school, Department of Radiology

【要旨】Non contrast ASL perfusion may be useful in the grading of non-enhancing astrocytic tumors.

Backgrounds: Astrocytic tumors are the most common type of glial neoplams in human. Generally, the presence of tumor contrast enhancement on MRI often indicates their high-grade malignancy. However, the malignant tumors could show no contrast enhancement sign, which leads to the misdiagnosis of tumor grade. Meantime, a novel perfusion technique Arterial spin labeling (ASL) is recommended for cerebral perfusion, which does not require contrast materials. We aimed to investigate ASL in the grading of non-enhancing astrocytic tumors.**Materials and methods:** A total of 12 patients with non-enhancing tumors were retrospectively included in the present study. The tumors were divided into high-grade astrocytoma (HGA) and low-grade astrocytoma (LGA). All patients were undergone MR imaging prior to treatments, and diagnosed as histopathologically. Maximal tumor blood flow (TBF) and normalized TBF (ratio) were measured from each of the tumors by using ASL. Independent T-test and was performed to assess the difference between tumor groups. Receiver operating characteristic (ROC) analysis was used to demonstrate the diagnostic accuracy.**Results:** TBF in HGA was showed a significantly higher value compared with LGA (118.58 ± 28.33 vs 50.7 ± 26.3, p<0.005). There was also found higher TBF ratio for HGA than for LGA (6.08 ± 1.51 vs 2.26 ± 1.09, p<0.005). The area of under ROC curve analysis for TBF and TBF ratio was 0.947 and 0.972, respectively. **Conclusion:** Non contrast ASL perfusion may be useful in the grading of non-enhancing astrocytic tumors.

PDF-003 Utility of Dynamic Contrast-Enhanced (DCE) MRI in Predicting Prognosis of Enhancing Lesions Persisting after Completion of Adjuvant Temozolomide in Glioblastoma Patients

Sung-Hye You, Roh-Eul Yoo, Seung Hong Choi

Department of Radiology, Seoul National University Department of Radiology, Korea

Purpose: To explore the value of DCE MR imaging in predicting the prognosis of enhancing lesions persisting after completion of concurrent radiation therapy and chemotherapy (CCRT) with temozolomide (TMZ) and adjuvant TMZ in patients with surgically resected glioblastoma (GBM).
Materials and Methods: This prospective study had institutional review board approval and written informed consent was obtained from all patients. 24 patients with histopathologically proven GBM, who had measurable enhancing lesions persisting after completion of CCRT and six cycles of adjuvant TMZ with TMZ after surgery or biopsy, were included. Dynamic contrast-enhanced MR imaging-derived pharmacokinetic parameters, including K^{trans}, Ve, and Vp, were calculated at the enhancing lesions. Mann-Whitney U test and multivariable stepwise logistic regression were used to compare the pharmacokinetic parameters between the progression (n = 16) and non-progression (n = 8) groups.
Results: The mean Ktrans and Ve were significantly lower in the progression group than in the non-progression group (0.08/min ± 0.05 [standard deviation] vs. 0.13/min ± 0.06, respectively; P = .037 for K^{trans}, and 0.52 ± 0.25 vs.1.04 ± 0.61, respectively; P = .037 for Ve). The 10th percentile of the cumulative K^{trans} histogram was also significantly lower in the progression group than in the non-progression group (0.03/min ± 0.03 vs. 0.05/min ± 0.02, respectively; P = .024). Multivariable analysis showed that mean Ve was the only independent predictor for progression (P = .038). Ve had a sensitivity of 100%, specificity of 63%, and an overall accuracy of 88% for prediction of progression at a threshold of 0.87.
Conclusions: Dynamic contrast enhanced MR imaging-derived pharmacokinetic parameters may help predict the prognosis of enhancing lesions persisting after completion of standard treatment in patients with surgically resected GBM, with mean Ve serving as the independent predictive factor for progression.

PDF-004 MPG併用3D-GRE(FSBB)を使用した脳神経系造影検査の有用性について Usefulness of cranial nerve system contrast ehnaced imaging using the MPG combined 3D-GRE (FSBB)

平田　恵哉（金沢医科大学病院 医療技術部 診療放射線技術部門）
Keiya Hirata, Yuuichi Murasaki, Tatsunori Kuroda, Chihiro Watari, Nanako Miyamoto, Saeko Tomida, Tomokazu Oku, Shigeo Miyazaki, Masahiro Kawashima

Divison of radiology, Kanazawa medical university

【要旨】頭部T2*WI撮像に使用されるFSBBシーケンスのパラメータを工夫し頭部造影後T1WI撮像に応用した。血管信号が抑制されるため、微小な多発脳転移、髄膜腫、硬膜下膿瘍等の脳表近くの病変の検査に特に有用であると思われる。

Background & PurposeFSBB sequence is usually used for T2*WI imaging.In FSBB sequence, vascular signal is suppressed by the effect of MPG pulses. If good use of this advantage, contrast enhanced volume image that has been the suppression of blood vessel signal can be obtained.Purpose of this study is to optimize FSBB sequence parameter for cranial nerve system contrast enhanced imaging.
Material and method Used device is Vantage Titan 1.5T.We examined the flip angle obtained optimal T1 contrast in phantom experiment.We used diluted contrast medium and fat phantom.Flip angle was changed to 5 to 70degrees.Fat suppression method was used Water Excitation Technique(WET).TR/TE is the shortest value, b value used 3sec/mm^2.
ResultOptimum contrast was obtained at a flip angle of 30 degree.
DiscussionBy a combination of FSBB and fat suppression, blood vessels and fat signals is suppressed, to distinguish from lesions adjacent to the small lesions and fat perivascular becomes easier.By using this technique, it is considered to be applicable also to volume measurement of tumor.It seems to be useful particularly in cases such as meningioma, epidural abscess, multiple brain metastasis.

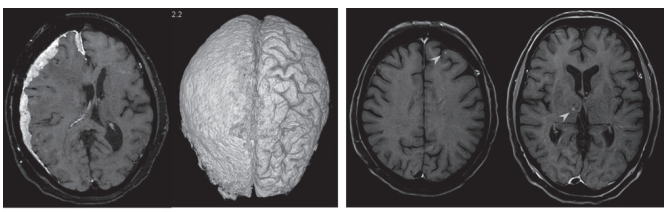

Meningioma　　Multiple brain metastasis

PDF-005　7T-MRIによる通常コントラスト画像の初期評価
Initial evaluations of conventional contrast images on a 7T-MRI system

岡田　知久（京都大学 大学院 医学研究科）
Tomohisa Okada[1], Hideto Kuribayashi[2], Yuta Urushibata[2], Junko Inoue[2]
[1]Kyoto University Graduate School of Medicine, [2]Siemens Healthineers Japan KK.

【要旨】7T-MRI装置では、1）高い信号対雑音比（SNR）を活用した高解像度化、2）組織の緩和時間変化を活用したコントラスト増加、3）化学シフトに対する感度増加が期待される。しかし同時に、4）SAR、5）静磁場・RFの不均一増強、といった課題がある。同装置導入後の、本施設での初期経験を報告する。

The 7T-MRI system is expected to improve image quality by higher SNR, different relaxation time and larger chemical shift separation. At the same time, however, it suffers from increased SAR and inhomogeneity of B0 and B1. Herein, initial evaluations of conventional contrast images are presented. Increased sensitivity to local filed inhomogeneity that is typically manifested in T2*WI can present fine structures of the medullary veins are observed in SWI at 7T. Intra-cortical veins are partly visualized, and it will contribute to close examination of cortical structures, as well as local ischemic changes. Other structures such as striate of Gennari are also identifiable. MPRAGE imaging also can be conducted in high resolution with detailed depiction of structures. However, in turbo-spin echo imaging of T2WI and FLAIR, image quality seems not much superior to 3T. There exists high need for elaboration. In TOF-MRA, elongation of T1 value plays an indispensable role, and the lenticulostriate artery is much better visualized compared to 3T. Elongation of the scan time needs shortened by applying compressed sensing. In evaluation of resting-state fMRI, default mode network was found as the primary independent component, when the patient movement was minimal. These results are still under investigation, but 7T-MRI is expected to play important roles for clinical practice in the near future.

PDF-006　improved Motion Sensitized Driven Equilibrium (iMSDE) を併用した頭部造影3D撮像法の検討
Investigation of improved Motion Sensitized Driven Equilibrium (iMSDE) for intracranial contrast-enhanced 3D black-blood imaging

岩本　勝一（函館脳神経外科病院）
Shoichi Iwamoto[1], Masaaki Ichinoseki[1], Makoto Obara[2], Takashi Namiki[2]
[1]Hakodate neuro surgical hospital, [2]philips electronics japan

【要旨】近年、improved Motion Sensitized Driven Equilibrium (iMSDE) を併用した頸動脈black bloodイメージングの有用性は報告されているが、頭部造影3D撮像においての報告は少ない。そこでiMSDEを併用した頭部造影3D撮像法について、その有用性を検討した。

[purpose]In recent years, the usefulness of the carotid artery black blood imaging using improved Motion Sensitized Driven Equilibrium (iMSDE) have been reported. However reports about intracranial contrast-enhanced 3D imaging are limited. We investigated feasibility in iMSDE with normal volunteers and patients with brain tumor. [Method]Ingenia3.0T CX (Philips) and ds Head coil (32ch) were used.In the basic study with normal volunteers, images were acquired by changing SENSE factor with 1.5, 1.7 and 2.0 in Phase (P) encoding direction and 1.5, 2.0, 2.5, 3.0 in slice (S) encoding direction while keeping velocity encoding (VENC) value 10cm/sec, and SNR was measured at white matter and gray matter . Then flow venc, 40, 20, 10, 5, 3cm/s were tested with measuring SNR at the white matter and the gray matter, and with visually assessing blood flow suppression efficacy.In clinical cases visual evaluation was conducted and compared with T1-TFE images in patients diagnosed with brain tumors.[result]In the basic study, P reduction 1.7 and S reduction 2.5 were used, considering SNR and scan time. There were no significant SNR losses observed in white matter and gray matter in tested VENCs. The maximum SNR reduction was less than 6.0%. VENC 3cm/sec demonstrated better blood flow suppression effect on visual assessment.In clinical cases, iMSDE can suppress blood flow in the vein close to brain tumor effectivelyCompared to T1-TFE, iMSDE can pose high SNR, that is useful for high -resolution 3D black-blood imaging..[Conclusion] iMSDE that can effectively suppress the blood flow while keeping sufficient SNR in intracranial region that is useful for high- resolution intracranial 3D black-blood imaging. It can be useful for brain tumor detection if it is adjacent to veins.

PDF-007　3D FIESTA-Cを用いたMRI 3D再構成頭蓋骨画像の臨床的有用性についての検討
The MR-based 3D-reconstruction image of the skull using 3D-FIESTA-C sequence; evaluation of the clinical utility

林　　哲司（札幌麻生脳神経外科病院 放射線科）
Tetsuji Hayashi[1], Akiyoshi Hamaguchi[1], Noriyuki Fujima[2]

[1]Sapporo Azabu Neuro Surgical Hospital, [2]Hokkaido Univercity Hospital

【要旨】本検討の目的は、MRIにて3D FIESTA-Cの無信号域を信号反転させ画像処理した頭蓋骨画像とMRAとのFusion画像がCTA画像との比較によって臨床上有用であるか明らかにすることである。その検討の結果、視覚評価を用いることによりMRI Fusion画像が臨床上有用であると言えた。

<Background and destination>
The internal carotid artery (ICA) – the external carotid artery (ECA) bypass surgery is one of important treatment method for several intracranial steno-occlusive diseases. Preoperative evaluation of ECA branches running skull surface was usually performed using the fusion of 3D-CTA and 3D-CT bone reconstruction image, but is invasive due to the radiation exposure and rapid injection of contrast agent. The purpose of this study was to create a MR-based 3D-reconstruction image of the skull using 3D-FIESTA sequence, and to assess the its clinical utility for the preoperative evaluation in creating the fusion image by combining the MR-based 3D skull image and TOF-MRA.
<Method>
In 17 patients, both MR scanning (including FIESTA-C and TOF-MRA) and CT angiography were performed, and then, the 3D fusion image of ECA branches and skull were created based on MR and CT image-data respectively. Visual evaluation of ECA branches were performed by experienced radiological technologists based on four segment (frontal and parietal branch in bilateral side) of superficial temporal artery (STA) using 3 point grading system (3; good, 2; moderate, 1; poor, 0; none). Kappa statistics was also performed for the assessment of interobserver agreement.
<Result>
In visual evaluation, the score of frontal branches was significantly higher in MR fusion images than CT in both right and left side. In contrast, no significant difference was observed in parietal branches. Kappa score was 0.673 on average.
<Conclusion>
MR-based 3D-reconstruction image of the skull was successfully created. The fusion of this skull 3D image and TOF-MRA can be useful for the preoperative assessment in patients with intracranial disease as non-invasive scanning.

PDF-008　静音化TSE法における画質と静音化に関する至適条件の検討
Tradeoff between image quality and acoustic noise reduction in quiet sequence of turbo spin echo

高橋　一広（秋田県立脳血管研究センター 放射線科診療部）
Kazuhiro Takahashi, Hideto Toyoshima, Kazuhiro Nakamura, Toshibumi Kinoshita

Research Institute for Brain and Blood Vessels Akita

【要旨】傾斜磁場の工夫によりMRI検査の静音化が進んでいる．静音化と画質は相反する関係にあり,我々は臨床検査における至適条件を検討した.quiet TSE法は静音効果が大きいものの,ESを150%以上とすると面内空間分解能の劣化が顕著であり,BWの増加でも画質が低下することから,条件の至適化が重要である．

[Purpose] Gradient coil activity is known to prominent source of acoustic noise in MRI. To reduce the noise, several sequence design associated with gradient activity have been developed. In the quiet sequence of turbo spin echo (TSE), we can change the echo space (ES) and band width (BW). Even though mild gradient changes as a setting of longer ES reduce the acoustic noise, image quality is deteriorated. Wider BW also reduces the acoustic noise and image quality is affected. We have evaluated the tradeoff between image quality and acoustic noise reduction in accordance with the change of ES and BW.
[Methods] Evaluation was performed on a MAGNETOM Skyla 3T Siemens scanner. Conventional TSE (cTSE), gradient mode Whisper (Whisper) and quiet TSE (qTSE) were evaluated. ES of qTSE was set between 110 % and 390 % ES of cTSE. ES of Whisper was set as same value of cTSE. Sound pressure was measured by acoustic level meter. Image quality was evaluated by spatial resolution in phantom image and contrast noise ratio (CNR) in human volunteer images. S/N was also evaluated in qTSE.
[Results] Sound pressure in TSE, Whisper, qTSE (ES:110%) and qTSE (ES:390%) are increased 60 %, 50%, 46% and 12% of the background level in the room, respectively. Acoustic noise reduction was more effective in the qTSE. Image quality of qTSE was deteriorated especially above 150 % of the ES. CNR in volunteer images were almost same in all the sequences. Sound pressure and S/N in qTSE (BW:300Hz/pixel) was reduced 6 % and 30% than the value of qTSE (BW:140Hz/pixel), respectively,.
[Discussion] Adequate ES and BW in qTSE should be selected for good image quality and acoustic noise reduction. ES and BW in qTSE should be evaluated for T2W, T2W-FLAIR and T1W FLAIR sequence.

PDF-009　MRIによる脳動脈瘤4D―FLOW解析の検討
Study of brain aneurysm 4D FLOW analysis by MRI

関根　麻生（メディカルスキャニング お茶の水）
Mau Sekine[1], Yuu Ishizaka[2], Tatsuya Miyazaki[1], Takuma Nishiwaki[2]
[1]Medical Scannig Ochanomizu, [2]Medical Scannig Tama-plaza

【要旨】3D-PC法を用いた4D-flow-MRAは脳動脈瘤の血流動態を3D＋時間軸＝4Dで観察し、脳動脈瘤の血管壁剪断応力wss(wall shearing stress)を求めることが出来る。より正確な脳動脈瘤のwssは、血流に合わせたVENC設定をすることで算出できると示唆された。正確なwssが分かれば、脳動脈瘤の治療方針決定に役立つと考えた。

<Purpose>
4D-flow-MRA offers the ability to measure and to visualize the temporal evolution of complex blood flow patterns within an acquired 3D-PC.Was considered asked to proper 4D-flow and Wss(wall shearing stress) by properly grasp the velocity of blood flow within the aneurysm of interest.
<Method>
Target:5people who from a brain aneurysmApparatus.
3T-spectra, head-coil SIEMENS
Analysis:Flova R-TEC
3D-PC:TR:32.95ms TE:5.36ms slice:16 FOV:220 NEX:1 pat:2 shim mode:standard phase:27
2D-PC:TR:34.9ms TE:5.79ms slice:1 FOV:220 NEX:1 pat:2 shim mode:standard phase:7 Venc20.40.60.80.100.120cm/sec
We imaged it using 2D-PC. The place that is parallel for the line which linked the top to the origin part of aneurysms. The flow rate in each of VENC(20.40.60.80.100.120) determined by calculation(Flow rate=SET VENC/2048*(signal value/4096/2-2048),and the fact of the aneurysm in the average value and the value of the 3D-PC.
<Result>
The 4D analysis reached without a problem by our hospital system.There were two cases that became the value that wss of the bleb point was low in.
<Consideration>
It was suggested that we could calculate wss of an accurate cerebral aneurysm by doing VENC setting to bloodstream.We thougth that exact wss helped the treatment orientation of the cerebral aneurysm.But,internal carotid artery had the exact fluid occurs phenomenon aliasing of the flow rate.Because parent atery which is the slow flow within the aneurysm is the noise level early,becouse we want to avoid as much as possible this time, the VENC setting was judged only within the aneurysm.However,We should do where influence is reflected on a value of wss to when We analyze it including internal carotid artery with future topics of discussion.

PDF-010　Simultaneous Multi-Slice Turbo Spin Echoを利用したNeuromelanin Imagingの撮像パラメータの検討
Consideration of Neuromelanin Imaging parameters using Simultaneous Multi-Slice Turbo Spin Echo

村田　　渉（順天堂大学放射線科・部）
Syo Murata[1], Koji Kamagata[1], Katsutoshi Murata[2], Misaki Nakazawa[1,3], Masaaki Hori[1], Kanako Kumamaru[1], Michimasa Suzuki[1], Issei Fukunaga[1], Asami Saito[1], Andica Christina[1], Syuji Sato[1], Nozomi Hamasaki[1], Ryo Ueda[1,3], Kohei Tsuruta[1], Haruyoshi Houshito[1], Shigeki Aoki[1]
[1]Department of Radiology, Juntendo University School of Medicine, [2]Siemens Healthcare K.K., [3]Tokyo Metropolitan University

【要旨】NMIは黒質緻密部を神経メラニン量に対応した高信号部位として描出することが可能であるが、撮像時間が長いなどの課題が存在する。本研究ではSMS-TSEシーケンスを使用することで時間を短縮してNMIが可能か検討し、若年者におけるSMS-TSEを利用したNMIの撮像パラメータを最適化した。

Introduction: Neuromelanin imaging (NMI) can visualize substantia nigra pars compacta (SNc) as high signal intensity depending on the amount of neuromelanin. NMI has a few limitations such as long imaging time. We assessed feasibility of NMI in a shorter scan time by using Simultaneous Multi-Slice Turbo Spin Echo (SMS-TSE) sequence and optimized the imaging parameters of NMI in young people by using SMS-TSE.Methods: In this study we examined 13 healthy volunteers (mean age 24 ± 3.6 years). All images were obtained using a clinical 3T MRI scanner (Skyra, SIEMENS). We scanned conventional TSE (TR=600ms, TE=12ms, NEX=2, ETL=3, in-plane resolution=0.43mm, slice thickness=3mm, Scan Time=440s) and SMS-TSE (prototype sequence, TR=600/800/1000/1200/1400/1600ms, TE=11ms, Multiband Factor=2, in-plane resolution=0.43mm, slice thickness=3mm, Scan Time=330s). We set SNc and SNc's backgrounds (cerebral peduncles and tegmentum) ROI manually for each data. We also set the ROI of Locus coeruleus (LC) and LC's background (pontine tegmentum). The contrast ratios of the SNc (CR_{SNc}) and LC (CR_{LC}), high intensity area volume of SNc (HV_{SNc}) and LC (HV_{LC}) were calculated from each ROI. To compare values of SMS-TSE with conventional TSE, correlation of CR_{SNc}, CR_{LC}, HV_{SNc}, and HV_{LC} were computed.Results: Correlation of CR_{SNc} was highest at TR=1400ms (r=0.752,p=0.005). Correlation of HV_{LC} was highest at TR=1400ms (r=0.782,p=0.003). Only TR=1400ms was significant correlation with all of the index.Conclusions: It is possible to reduce the scanning time of NMI by using SMS-TSE sequence and the optimal TR parameter for young people is 1400ms.

PDF-011　mUTE 4D-MRAを用いた頭部MRAにおけるphase数の検討
A functional study of the number of phase in the head MRA using mUTE 4D-MRA

高松　　慎（東芝メディカルシステムズ株式会社）
Shin Takamatsu[1], Chiemi Yamauchi[1], Hisae Chiba[1], Yoshihito Miyamoto[2], Tsutomu Koto[2]
[1]Toshiba Medical Systems Corporarion, [2]SUMITOMO BESSHI HOSPITAL

【要旨】mUTE 4D-MRAを用いて頭部MRA描出に対する至適phase数を検討した。同意の得られたボランティアにてTI値、phase数、TI値の間隔を変更し視覚評価を行った。描出が良好であったTI値は個人の血流速に依存し、phase数が2の場合ボランティアによってばらつきがあった。Phase数を3または4とすることで描出が良好に得られた。

Purpose
Recently, several studies have reported of arterial spin labeling-magnetic resonance angiography[ASL-MRA] using ultra short te.We became available using mUTE 4D-MRA that is Arterial Spin Labeling[ASL]in multi phase.mUTE 4D-MRA can image a stable image in various blood speed so as to increase the number of phase.In this study, we report the optimal number of phase in the form observation of head MRA.
Methods
We used Vantage Titan3T and Atlas SPEEDER Head made by Toshiba medical systems We visually evaluated images by inversion time[TI] of 200ms-1200ms, the number of phase 2-4,the interval of TI in volunteer.
Result and Discussion
In TI of 200,400,600,800,1000 and 1200, The TI that the characterization had good was various because it depended on the personal blood speed.When the number of phase was two,the characterization of peripheral blood vessel in head might not be good,so we thought that the number of phase is three or more.When the number of phase was three or four,the characterization had good in the case that the interval of TI was 200ms or more,but the scan time extended.In the the number of phase was four,the scan time was over ten minutes.
Discussion
It is desirable that the number of phase in mUTE 4D-MRA is three or more,but It is necessary to consider the scan time.

PDF-012　Synthetic MRIを用いたガドリニウム濃度マップの確度と精度についての評価
Assessment of the accuracy and precision of the gadolinium concentration map using synthetic MRI

中澤　美咲（首都大学東京人間健康科学研究科放射線科学域）
Misaki Nakazawa[1,2], Akifumi Hagiwara[2,3], Christina Andica[2], Masaaki Hori[2], Ryo Ueda[1,2], Nao Takano[2], Sho Murata[2], Shuji Sato[2], Nozomi Hamasaki[2], Hideo Kawasaki[2], Haruyoshi Houshito[2], Shigeki Aoki[2], Atsushi Senoo[1]
[1]Graduate School of Human Health Sciences, Tokyo Metropolitan University, [2]School of Medicine, Juntendo University, [3]Graduate School of Medicine, The University of Tokyo

【要旨】Synthetic MRIでは1回のスキャンからT1値、T2値、プロトン密度を定量することができる。Synthetic MRIによる定量マップ（T1値及びT2値）を用いて2種類のガドリニウム濃度マップを作成し評価したところ、T1値を用いたものの方がより正確かつ精度も高かった。

Background and Purpose:Synthetic MRI enables quantification of T1 and T2 values and proton density from one quantitative scan. The gadolinium (Gd) concentration in vivo after the contrast agent administration is not proportional to the signal intensity on T1-weighted image, so some calculations are needed to create Gd concentration map (Gd-map) with the use of quantitative values before and after Gd contrast administration. The aim of this study was to create the Gd-maps from quantitative maps and assess the accuracy and precision of them.
Materials and Methods:The phantoms of water and 6 kinds of diluted Gd solutions (0.14-0.625mmol/L) were scanned by a 3.0-T MRI system and quantitative maps were created on SyMRI software. Two types of Gd-maps (T1-Gd map and T2-Gd map) were created using T1 and T2 quantification maps each from water and diluted Gd solutions, respectively. Region of interest (ROI) analyses on these Gd-maps were performed to measure Gd concentrations and means and SDs were recorded. The size of each ROI was 23mm^2. The mean measured Gd concentrations were compared to the known values. Average SDs were compared between T1-Gd map and T2-Gd map.
Results:The means of the difference between the measured values and the known values for T1-Gd map and T2-Gd map were 0.029 and 0.072[mmol/L], respectively. The means of the SDs of the measured values for T1-Gd map and T2-Gd map were 0.0063 and 0.076[mmol/L], respectively.
Conclusion:This study showed the accuracy and precision of the Gd-maps created by synthetic MRI. T1-Gd map showed better accuracy and precision than T2-Gd map. Synthetic MRI performed on a person before and after Gd administration enables to measure the Gd concentration in a relatively short time by the same method used in this study.

PDF-013　コモンマーモセットにおける脳発達MRI解析
MRI-based characterization of lifespan development in common marmosets

関　布美子（慶應義塾大学 医学研究科）
Fumiko Seki[1,2,3], Yuji Komaki[1,2], Junichi Hata[1,2,3], Akiko Uematsu[1,2,3], Keigo Hikishima[4], Erika Sasaki[1,2], Hideyuki Okano[1,3]

[1]Keio University School of Medicine, [2]Central Institute of Experimental Animals, [3]Laboratory for Marmoset Neural Architecture RIKEN Brain Science Institute, [4]Okinawa Institute of Science and Technology Graduate University

【要旨】コモンマーモセットを用いた高次機能障害の疾患モデルの縦断評価を実施するために健常の灰白質・白質の体積評価を行った。灰白質は9か月まで増加しその後24か月まで減少、一方白質は24か月まで増加した。灰白質の減少は霊長類特有と言われる刈込が起きていると示唆される。

Common marmoset is one of the experimental animals which are especially regarded as valuable for generating various disease models for high-cognitive dysfunction, whose onset and course may range from young to age. For their longitudinal evaluation, understanding of typical brain development was crucial, yet little data of the postnatal development is available. Thus, as the fundamental data, patterns of brain development were investigated by measurements of the brain volume and white matter (WM) properties in subjects of wide-ranged age using non-invasive MRI.
MRI was performed for 23 marmosets for 7 timepoints (1 3, 6, 9, 12, 18, 24, months old and 6-7years old), as they matured by 2 years old. The same scan was performed for 30 adult marmosets. The volume of gray matter (GM),white matter (WM) and cerebral cortex were measured with T1-weighted images.
The GM volume increased and peaked at 9 months. Then gradual decrease was observed until 24 months, and the volume remained unchanged afterward. In contrast, WM increased until 24 months. Focusing on the cerebral cortex, although the decreased volume was observed to the all areas, its pattern is different at frontal, parietal, temporal, and occipital areas.
The volume changes of GM and WM of marmosets were similar to that of human data. Slight decrease of the brain volume indicated pruning might occur. Comprehensive analysis combined with structural and diffusion tensor imaging properties may help characterize these observed trends further.

PDF-014　Comparison of voxel-based morphometry (VBM) analysis and absolute T_1 value analysis

Daehun Kang, Yul-Wan Sung, Seiji Ogawa

Kansei Fukushi Research Institute, Tohoku Fukushi University, Japan

Voxel-based morphometry (VBM) has been used for the evaluation of structural changes in a grey matter in relation to disease or function. The VBM analysis has been performed based on T_1-weighted MRI images. However, it is difficult to estimate properties of tissues affected on some changes in VBM analysis because the T_1-weighted image does not carry absolute T_1 values of the brain tissues.

In this study we examined the relationship between the MR property of tissue and structural changes by measuring MRI image with absolute T_1 values and investigated it for participants with musical training experiences.

For the purpose, we used gradient echo (GRE) sequences to obtain apparent T_1 map and B_1 map. The former was derived from GRE sequences with two different TRs (0.8 & 1.6 sec.) and one FA, and the latter from GRE sequences with two different FAs (45 & 90 deg.) and long TR (about 4 times longer TR than T_1 of cerebrospinal fluid (CSF) at 3T). Absolute T_1 maps were estimated from the apparent T_1 maps after B_1 field correction.

PDF-015　3D MPVによるT1強調画像での頚部プラーク描出能の検討
Study of carotid plaque depiction performance at the T1WI using 3D MPV

福場　崇（藤田保健衛生大学病院 放射線部）
Takashi Fukuba[1], Kazuhiro Murayama[2], Ayako Ninomiya[3], Masato Ikedo[3], Akiyoshi Iwase[1], Yutaka Kinomura[1]
[1]Department of Radiology, Fujita Health University Hospital, [2]Department of Radiology, Fujita Health University, [3]Toshiba Medical Systems Corporation

【要旨】3D MPVによるT1WIでの頚部プラーク描出能の有用性について検討を行った.phantom studyとして自作ファントムを作成し，各撮像シーケンスと比較した.またClinical studyとして胸鎖乳突筋とプラーク病変のSIRを算出しプラークの描出能について検討を行なった.3DMPVがHemorrhageプラークの描出に有用であることが示唆された.

【Background】In the MRI Carotid plaque inspection, property diagnosis is important. As a feature of vulnerable plaque atheroma and hematoma have been reported to exhibit a high signal in the T1WI.【Purpose】In our facility, T1WI with black blood imaging are obtained by MPV which uses the Variable Flip Angle.In this study, we compare MPV and Spin Echo and IR-FFE with regard to the plaque depiction performance and examine the usefulness of cervical plaque depiction performance using 3D MPV in the T1IW.【Equipment】Toshiba Vantage Titan3T【Method】1), Diluted Gd-DTPA phantoms with concentrations of 1.0, 0.5, 0.25, 0.1, 0.05 , 0.025mmol / l created were acquired using 2D SpinEcho, IR-3DFFE and T1-3DMPV. The signal intensity ratio of phantom with a concentration of 0.1mmol / l (T1 value 1239ms) phantom having a similar T1 value of the muscle were calculated and compared to other phantoms with different concentrations.2), In 35 cases at the examination for plaque, we calculated the SIR of the sternocleidomastoid muscle to plaque lesions acquired using SE. We classified legions as Fibrous tissue for SIR≦1.17, Lipid / necrosis for SIR>1.17 and <1.55, Hemorrhage for SIR≧1.55, and examined the capability of visualizing plaque in each type.【Result】In the phantom experiment, the longer T1 value was, the higher SIR became in case of T1MPV. In actual clinical image, although there was not much difference in the depiction performance by the sequence in Fibrous tissue and Lipid / necrosis, visualization of 3D MPV in Hemorrhage was good.【Conclusion】This study suggested that T1WI using 3DMPV was useful to in the visualization of Hemorrhage plaque.

PDF-016　下顎運動のMRI動的撮像法における撮像パラメータの分析
Analysis of imaging parameters in dynamic imaging of mandibular movement

中井　隆介（中部大学 生命健康科学部）
Ryusuke Nakai[1,2], Takashi Azuma[2], Mariko Wakatsuki[2], Hideki Hashimoto[1], Seiji Yamaguchi[1], Hiroaki Takadama[1]
[1]College of Life and Health Sciences, Chubu University, [2]Institute for Frontier Medical Sciences, Kyoto University

【要旨】顎関節疾患の治療・診断において、顎運動状態を精度よく分析することは非常に重要である。我々はMRIを用いて顎運動状態を分析する手法を開発してきているが、今回は顎運動の分析データ取得のための最適な撮像パラメータを検討した。結果として、顎運動分析手法との適合性が最も良い撮像パラメータを見出した。

Temporomandibular joint (TMJ) disease is currently considered to be one of the therapeutic tasks in dentistry. However, the optimal methods to identify the cause and therapeutic approaches have not yet been established. This may be because TMJ disease develops as a result of multiple factors, including dysarthrosis, muscle tone, and malocclusion. These factors are related to the complex structure and extremely complex movements of the TMJ. To resolve such problems, it is important to clarify individual problems, and establish evaluation/therapeutic methods for each problem. For this, we have been discussing the imaging of mandibular movement and the articular disk using MRI. Herein, we report the results of our investigation on imaging parameters that are useful in obtaining imaging of temporomandibular movements using MRI.We used a 1.5T MRI system (Siemens MAGNETOM Sonata) with a head coil and a True FISP sequence to obtain images (4slices) of phantom and human mandibular joints while changing the bandwidth (BW(TR,TE)), flip angle (FA), etc. In addition, the subjects were requested to open and close their mouths during MRI. We extracted mandibular movements from the obtained images.As a result, the maximum signal-to-noise ratio (SNR) was confirmed when BW=130 and BW=250Hz/pixel during phantom and human mandibular movements, respectively. In addition, the maximum SNR was observed when FA=70 for the phantom and human mandibular movements. Automatic extraction with the highest accuracy was achieved when BW=250Hz/pixel and FA=70. Thus, in this study, we successfully obtained imaging parameters to improve the quality of dynamic imaging of mandibular movements. We believe that the results of this study will be useful for future investigations of mandibular movement imaging.

PDF-017　iMSDE pre-pulseを用いた定量的な3D MR Lymphography
3D Quantitative MR Lymphography using the improved Motion Sensitized Driven Equilibrium (iMSDE) pre-pulse

青池　拓哉（北海道大学病院 医療技術部 放射線部門）
Takuya Aoike[1], Noriyuki Fujima[2], Masami Yoneyama[3], Suzuko Aoike[1], Kinya Ishizaka[1], Kohsuke Kudo[2]
[1]Department of Radiological Technology, Hokkaido University Hospital, [2]Department of Diagnostic and Interventional Radiology, Hokkaido University Hospital, [3]Philips Electronics Japan

【要旨】iMSDE pre-pulse を用いて3D-MR Lymphography (MRL)を撮像し，異なるT2-prep time からT2 mapを作成した．T2-prep timeの組み合せは36-72msが最もリンパ節の描出に優れた．また，T2 mapから算出されるT2値は実際のT2値より高くなる傾向にあり，この原因についてはさらなる検討が必要である．

<Purpose>
The purpose of this study was to create the 3D-MR Lymphography (MRL) using improved motion sensitized driven equilibrium (iMSDE) pre-pulse with simultaneous acquisition of T2 map in lymph node by the use of different T2-prep time scanning within a single acquisition.
<Materials & Methods>
All healthy subjects were scanned on a 3-tesla MR scanner (Achieva TX; Philips Medical Systems, Best, The Netherlands) using a 16ch Neuro-Vascular coil. First, MRL image was obtained using three different pair of T2-prep time, and then appropriate pair of T2-prep time was determined by visual assessment. Next, T2 value of lymph node was calculated using the determined pair of T2-prep time, after that, the calculated T2 value was compared to T2 value which was calculated by the conventional measurement method.
<Result>
3D-MRL images were successfully obtained in each pair of T2-prep time, however, the most visually sufficient image was obtained with the use of pair of 36 and 72ms. In the measurement of T2 value, T2 value obtained by the MRL images and conventional method was well correlated, however, in the lymph node with the range of long T2 value (approximately > 100ms), there was the tendency of larger difference of measured T2 value between two methods.
<Conclusion>
3D-MRL based on iMSDE was successfully obtained with sufficient visualization. However, measured T2 value in the range approximately > 100ms by MRL tended to be different from that calculated by conventional method. The cause of this should be clarified by further analysis.

PDF-018　2種類の高速撮像法を併用した3D-TOF-MRAの評価
Clinical feasibility of dual acceleration 3D-TOF-MRA

金本　雅行（福井大学 医学部附属病院 放射線部）
Masayuki Kanamoto[1], Shota Ishida[1], Naoyuki Takei[2], Toshiki Adachi[1], Hiroyuki Kabasawa[2], Hirohiko Kimura[3]
[1]Radiological Center, University of Fukui Hospital, [2]GE Healthcare Applications and Workflow, [3]Department of Radiology, University of Fukui Hospital

【要旨】高速撮像法であるPIとCSを併用して3D-TOF-SPGRを取得してCS及びPIの短縮率を変化させて画質の評価を検討した。PIの短縮率を増加させれば雑音が増加し，CSの短縮率を増加させればボケの影響が増加した。PIとCSを併用することで画質低下の影響が抑えられることが分かった。

Introduction3D-time of flight magnetic resonance angiography (3D-TOF-MRA) is inherently a time-consuming technique than other sequences. Compressed sensing (CS) is a one of the rapid technique that can reconstruct images from sparse data, leading to reduction the data acquisition time. Significant scan time reduction using CS was mainly attributed to reconstruction process from fewer k-space data acquisition. The purpose of this study was to verify the feasibility of 3D-TOF-MRA combined with PI and CS, in clinical practice.MethodsMRI was performed at 3.0T (Discovery MR 750; GEHC, USA) by using a 32-element phased-array head coil. We utilized polyvinyl alcohol (PVA) gel phantom (90-40; NIKKO FINES INDUSTRIES, Japan). The reduction factor of PI varied from 1*1 (phase direction*slice direction) to 3*1. The total reduction factor of PI and CS varied from 2*1*1.5 to 2*1*2.In an IRB-approved volunteer study, 3 volunteers were included.We obtained the images of the PVA gel phantom and normal volunteers. Furthermore, we evaluated its tendency of optical spatial resolution and noise of images. The image without any acceleration technique was considered as a base line.ResultsIn the PVA gel phantom and normal volunteers, there was a tendency to increase in noise for image using PI only.Whereas, we observed a tendency to decrease in spatial resolution with an increase in the CS acceleration factor.Discussion & ConclusionThe blurring was more pronounced in the image with CS, because fewer data acquisition in the high frequency region of k-space diminished the spatial resolution. However, the noise by using CS did not exceed that with PI alone.In conclusion, it is possible to keep the high image quality of 3D-TOF-MRA by using PI with CS compared to PI alone.

PDF-019　mDIXON-XDとIR法を用いた頸動脈プラークイメージングの検討
Study of carotid artery plaque imaging using mDIXON-XD with Inversion Recovery

堀野由香梨（国家公務員共済組合連合会 熊本中央病院）
Yukari Horino[1], Seiichirou Noda[1], Nobuyuki Toyonari[1], Masami Yoneyama[2]
[1]Kumamoto Cho Hospital, [2]Philips Electronics Japan

【要旨】頸動脈プラークイメージングを鎖骨下動脈中心の広範囲に撮像することは、磁化率の違いにより均一な脂肪抑制が困難であった。脂肪抑制効果の高いmDIXON-XDとIR（Inversion Recovery）法を用いBlack　Blood画像を得る検討を試みた。

Purpose: MR plaque imaging (vessel wall imaging) is promising for characterizing atherosclerotic plaque. So far, various techniques have been proposed to assess the atherosclerotic plaque. Black blood image (BBI) is one of the most important method for evaluating the atherosclerotic plaque. Furthermore, BBI with larger FOV, from aortic artery to internal carotid artery, is clinically desirable; however, current methods often suffer from nonuniformity fat suppression because of B0 inhomogeneity. In this study we tried to use the 3D black-blood T1-weighted imaging for larger FOV (neck and chest area) with more robust fat suppression by using improved DIXON-based gradient sequence (mDIXON XD). The purpose of this study is to optimizes the scan parameters. Materials and Methods:volunteers were examined on 3.0T whole-body clinical systems (Ingenia, Philips Healthcare). The study was approved by the local IRB, and written informed consent was obtained from all subjects. The sequence we used in this study is based on inversion recovery segmented gradient echo, such as MPRAGE, with DIXON technique. That is, an adequate inversion delay (TI) for nulling blood signals should be optimized. Hence we investigated the optimal TI by changing the invert time. Results and Discussion: We found that the optimal TI of the black blood image is 1000ms. The optimized mDIXON XD BBI showed good SNR, sufficient blood suppression and robust fat suppression entire the large FOV from aortic artery to internal carotid arteries. Although further clinical investigation is needed, the optimized mDIXON XD BBI would be promising for evaluating the atherosclerotic plaque with larger FOV including head and chest area.

PDF-020　mUTEを用いた肺撮像の初期検討
Initial Evaluation of the mUTE Sequence in Lung Imaging

千葉　寿恵（東芝メディカルシステムズ株式会社 MRI営業部）
Hisae Chiba[1], Yuichi Yamashita[1], Yasutaka Sugano[1], Masaaki Umeda[2], Naotaka Sakashita[3]
[1]TOSHIBA Medical Systems Co., Ltd. MRI Sales Department, [2]TOSHIBA Medical Systems Co., Ltd. MRI Development, [3]TOSHIBA Medical Systems Co., Ltd. Clinical Application Development

【要旨】今回、UTEの静音化シーケンスmUTEを用いて肺野撮像における基礎的検討を行った。mUTEは、UTEと同様に肺野全体の画像を描出することが可能であり、STIR法により血管描出に変化をつけられ、今後の臨床応用が期待された。mUTEの高い静音性は、小児検査など患者さんの検査環境を改善できると考えられる。

Purpose
It has recently been reported that MRI lung scanning can be improved by employing the UTE sequence, and MRI lung examinations are now widely performed in order to minimize radiation exposure. The UTE sequence, which has been developed to minimize imaging noise during examinations by reducing gradient switching, was initially applied to T1WI and MRA of the head. In this study, we developed the mUTE sequence (which is a silent UTE sequence) and conducted initial evaluation of the mUTE sequence in lung imaging.
Methods
Lung imaging using the mUTE sequence was evaluated by scanning volunteers, all of whom gave informed consent. Further investigations on the applicability of STIR and selective blood pulses were also conducted. The basic scan parameters were TR: minimum, TE: 0.1 ms, flip angle: 5 degrees, matrix: 512x512 (after interpolation), and slice thickness: 1.5 mm with respiratory triggering. 3T MRI system (Toshiba Medical Systems) was used.
Results and Discussion
It was found that mUTE was able to image the lungs as well as UTE. When a STIR pulse was applied, the contrast of blood vessels was increased. However, in order to obtain the STIR effect, it was necessary to increase the number of segmentations. In addition, it was possible to select the desired blood vessel by using a tag pulse in ASL. The reason for the increase in the number of segments in STIR was the greater number of trajectories per IR pulse.
Conclusion
The mUTE sequence is useful for imaging of the lungs. In addition, mUTE with STIR allows the contrast of blood vessels to be varied, which is expected to be useful in future clinical applications.

PDF-021　3T MRI MOLLI法を用いたT1計測の心拍数の影響と補正法の検討
Evaluation of the effects of heart rate and corrections in T1 measurement using MOLLI on 3T MRI

植木　渉（国立循環器病研究センター）
Wataru Ueki[1], Yoshiaki Morita[1], Masaru Shiotani[1], Mutsumi Adachi[1], Toshiya Sano[1], Yoshiaki Komori[2]
[1]National Cerebral and Cardiovascular Center, [2]Siemens Healthcare K.K., Tokyo, Japan

【要旨】MOLLI法によるT1計測は心拍数の変化によりT1の測定値が変動することが知られている．今回，我々は、3T MRIでのMOLLI法における，心拍数の影響と補正法についてファントム実験による検討を行った．IR intervalを6500msecに固定させるようにRTを調整することで，測定誤差や心拍数によるT1値の変動を軽減できると考えられる．

Purpose: In MOLLI, measured T1 values can fluctuate depending on changes in heart rate. We performed a phantom experiment on the effects of heart rate and corrections in T1 measurement using MOLLI on 3T MRI.Methods:We used 3T clinical machine (Siemens MAGNETOM Verio). There were two IR sequences (the first had 3 images and the second had 5). SSFP (True-FISP) sequence was used for readout. Phantom contents were Gd-DTPA diluent, olive oil and saline. MOLLI was performed with a simulated ECG varied between R-R intervals of 600~1300ms and with a resting heart cycle (RT) between IR sequences that varied from 0 to 8.Results:When RT was fixed to 3, phantoms with T1 = less than 1800 produced a maximum measurement error of 20%, depending on RR. Phantoms with T1 = 1800 or higher produced a measurement error of 64% (fig 1). Adjusting the RT to fix the IR interval to 6500msec caused all phantoms to have a measurement error within 25% and reduced fluctuations due to RR interval (fig 2).Conclusions:In T1 mapping with 3T MOLLI, heart rate causes fluctuations in T1 values, resulting in measurement errors. Therefore, the IR interval needs to be corrected according to the heart rate.

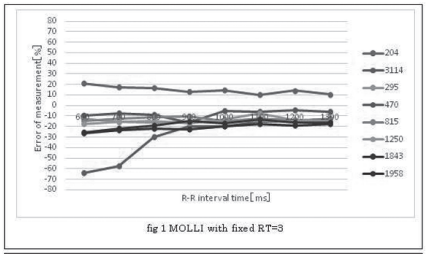

fig 1 MOLLI with fixed RT=3

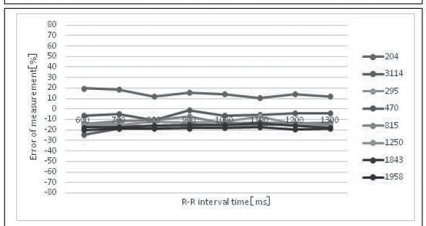

Fig 2 MOLLI adjust the IR interval (6500ms) by RT

PDF-022　3DBTFE法を用いた径カテーテル大動脈弁留置術前における末梢血管計測のための最適条件の検討
Optimum conditions to measure the peripheral vasculature using the balanced TFE technique prior to transcatheter aortic valve implantation

妹尾　大樹（埼玉医科大学国際医療センター 中央放射線部）
Taiki Senoo, Yasuo Sakurai, Masanori Morita, Kenji Abe, Kazuya Okabe, Kasumi Shiga, Yasuyuki Yoshimura

Department of Radiology, International Medical Center, Saitama Medical University

【要旨】径カテーテル大動脈弁置換術(TAVI)前における非造影での末梢血管計測用としてMulti chunk型3DBTFE法を用い、最適条件の検討を行った。Multi chunk 3DBTFEによる血管計測は造影剤、心電図同期を必要とせず簡便に検査が行えるため、造影剤の使用できないTAVI適応患者の血管計測に有用な手法と考えられる。

Background: Computed tomography is generally performed to evaluate the peripheral vasculature prior to transcatheter aortic valve implantation (TAVI), but the administration of contrast medium is contraindicated in patients with compromised renal function. Purpose: We investigated the optimal imaging conditions for non-contrast-enhanced measurement of the peripheral vasculature using fat suppression with the 3D-BTFE method and multiple 3D volumes (chunks) to suppress the influence of improving the contrast of the blood vessels and turbulence.Materials and Methods: Four volunteers underwent imaging of the pelvic region at 1.5 tesla using an Achieva imaging system (Philips Healthcare) and a 32-channel torso cardiac coil. We used the 3D-BTFE method to alter the parameters as follows and examined cross-sections to determine the settings for optimal visualization of the arteries.In a fixed imaging area, we assessed images obtained with 3D volumes of chunks, start-up echo times, and shot intervals.Results and Discussion: Increasing the number of chunks improved arterial contrast, probably by highlighting the inflow effect, which, in turn, reduced the background signal from magnetization transfer effect.Increasing the start-up echo time increased the signal from fat, and increasing the shot interval increased the signal of blood by facilitating the recovery of longitudinal magnetization to overcome the conspicuous void in the vessel resulting from blood flow. Arteries were best visualized using 10 chunks, a start-up echo time of 15 ms, and a shot interval of 1500 ms.Conclusion: The multiple-chunk 3D-BTFE technique enables convenient inspection without gating for vascular measurement in patients requiring TAVI for whom the use of contrast agents is contraindicated.

PDF-023　ECV算出における血液のT1値測定部位の検討
Evaluation of Areas for Blood T1 Value Measurement in ECV Mapping

高済　英彰（福島県立医科大学医学部附属病院 放射線部）
Hideaki Takasumi[1], Shinya Seino[1], Hironobu Ishikawa[1], Takashi Kanezawa[1], Naoki Watanabe[1], Takanori Sato[1], Shuhei Bannae[2]
[1]Fukushima Medical University Hospital Department of Radiology, [2]TOSHIBA MEDICAL SYSTEMS CORPORATION

【要旨】ECVは、造影前後の心筋と血液のT1値及びヘマトクリット値より算出される。血液のT1値測定は、左心室中部、左心房、下行大動脈などで計測している報告が多いが、部位によるT1値測定精度について検証した報告はない。今回、血液のT1値の最適な測定部位について検討を行った結果、左心室の中部が最適であると考えられる。

PurposeExtracellular volume fraction (ECV) mapping is a widely employed method for the quantitative evaluation of myocardial fibrosis. ECV values can be calculated from the T1 values of myocardium and blood before/after Gd enhancement. Various ROI positions for the measurement of blood T1 values have been described, but the influence of ROI position on T1 values has not been reported. We evaluated the accuracy of blood T1 values depending on ROI position.MethodsStudies were performed using a 1.5-T MRI system (EXCELART Vantage; Toshiba Medical Systems). A Fast Field Echo sequence with ECG gating was used (Polarity Corrected TI prep method, TR 5.0 ms, TE 2.0 ms, FA 12 deg, trigger interval 3000 ms, number of TI points 5). We scanned 3 healthy male volunteers (age 27 ± 3 years, HR 55-65 bpm). Four-chamber and short-axis planes were obtained. Blood T1 values were measured in the LV and RV (proximal, mid, apex), LA, RA, and descending aorta, and the mean and SD were calculated (excluding papillary muscle).Results and DiscussionThe T1 values of each area were as follows: for 4-chamber planes, LV (proximal 1619 ± 102, mid 1458 ± 22, apex 1324 ± 21), RV (proximal 1769 ± 204, mid 1698 ± 168, apex 1402 ± 97), LA 1595 ± 117, RA 1660 ± 230, and descending aorta 1595 ± 170; for short-axis planes, mid LV 1546 ± 41 and mid RV 1620 ± 62. The T1 values of the LA and descending aorta (4-chamber) and mid LV (short-axis) were close to the reported reference value of 1580 ± 130,* and the SD values for mid and apex LV (4-chamber) and mid LV (short-axis) were small.ConclusionThe mid LV is suitable for measurement of blood T1 values in ECV mapping.*Sharma et al. J Magn Reson Imaging 2006;23:323-330

PDF-024　3.0 T装置におけるT1-weighted turbo field echo (T1-TFE)を用いた心筋のT1マッピング
Myocardial T1 mapping using T1-weighted turbo field echo (T1-TFE) sequence at 3.0 T

木田　勝博（岡山赤十字病院 放射線科）
Katsuhiro Kida[1], Sachiko Goto[2], Takamasa Kurosaki[1], Masaki Ikeda[1], Tsutomu Kajitani[1], Yoshiharu Azuma[2]
[1]Japanese Red Cross Okayama Hospital, [2]Graduate School of Health Sciences, Okayama University

【要旨】我々は心電同期と呼吸停止下におけるT1-weighted turbo field echo (T1-TFE)を用いた心筋のT1マッピングを提案する。本法はinversion time (TI)が0と200 msecの2つの画像を用いて、フリーソフトウェアであるImageJを使用して計算する。ボランティアの心筋のT1マッピングは良好であり、心筋のT1値は1289 ± 72 msecであった。

Introduction We evaluated a method of calculating T1 mapping with only two inversion times (TIs) by using T1-weighted turbo field echo (T1-TFE) sequence for myocardial magnetic resonance imaging (MRI) with echocardiogram (ECG)-triggering and breath-hold.
Materials and methods The MRI device used in this study was Achieva 3.0T TX (Philips), and the coil used was an 8-channel SENSE head coil.To simulate various myocardial diseases, five gel phantoms were prepared from 0.025, 0.05, 0.1, 0.15, and 0.2 mmol/L gadopentetate dimeglumine (Gd) with a 2.0 wt% agar solution; lard was used as the fat component. The T1 relaxation time of each phantom was determined as the reference using the standard 2D inversion recovery spin echo (IR-SE) sequence at seven different TIs, which were 50, 200, 500, 1000, 2000, 3000, and 5000 msec. The each phantom was measured using a 2D T1-TFE sequence at TIs of 0 and 200. Six shot intervals at heart rate of 60 beats/min were investigated to determine the T1 relaxation time closest to the reference. The T1 mapping images were processed using imageJ. Furthermore, we calculated T1 mapping of the myocardium of a volunteer.
Results The T1 relaxation times obtained by using T1-TFE sequence with the shot interval of 6000 msec were close to the reference values that were obtained using 7 different TIs. However, longer T1 relaxation times were shorter than reference values. The error of the T1 relaxation time was corrected by the approximate error function. The native T1 value of the myocardium of a volunteer using our method was 1289 ± 72 msec.
Conclusion We suggest that T1 mapping for myocardial MRI can be produced using only two TIs in a T1-TFE sequence with ECG-triggering and breath-hold.

PDF-025　心室性不整脈の誘発と梗塞周囲における生存領域との関係性の評価
Inducibility of Ventricular Arrhythmia is Correlated to Viability of the Peri-Infarct Region

橘　　篤志（AIC八重洲クリニック）
Atsushi Tachibana[1], Junaid Zaman[3], Hiromi Sano[2,3], Michelle Santoso[3], Phillip Yang[3]
[1]AIC Yaesu Clinic, [2]Tokyo Metropolitan University, Graduate School of Human Health Sciences, [3]Stanford University School of Medicine, Cardiovascular Medicine

【要旨】Peri-infarct region (PIR) と心室性不整脈との関係は重要視されているが、非侵襲的方法による不整脈誘発領域を同定するのは困難である。本研究ではManganeseとGadoliniumを用いてPIRにおけるviableな領域を抽出し、心室性不整脈の発生頻度との関係性を調べた。

Introduction:
While a significant correlation between the peri-infarct region (PIR) and ventricular arrhythmia has long been established, reliable non-invasive detection of this arrhythmogenic region is difficult. Dual enhancement techniques using delayed-enhanced MRI (DEMRI) and manganese-enhanced MRI (MEMRI) identified overlapping areas in the PIR consisting of injured but viable myocardium. We hypothesized that the volume of viable myocardium in the PIR correlates with the likelihood of developing ventricular arrhythmia.
Methods:
In 12 pigs with anterior MI due to LAD ischemia-reperfusion injury (IR), we performed MEMRI, DEMRI and programmed electrical stimulation (PES) at the right ventricular apex using burst pacing and extra-stimuli. We measured baseline MEMRI indices to arrhythmia inducibility (baseline S1 – coupling interval at VT) at day 30 post-IR.
Results:
Myocardial infarctions were established using balloon catheterization in 12 pigs (LVEF 27.7 ± 8.8 %). Measurement of % infarct volume by DEMRI vs. MEMRI was 22.7 ± 10.3 % vs. 8.2 ± 3.9 % ($p<0.05$), demonstrating significant viability in the PIR by MEMRI. This discrepancy represents a possible over-estimation of the infarct scar by DEMRI. The lower threshold for burst pacing and extra-stimuli to induce VT/VF correlated strongly with increased PIR viability as shown by MEMRI ($R^2=0.469$, $p<0.05$).
Conclusion: We demonstrated a significant correlation between MEMRI measurement of PIR viability and ventricular arrhythmia inducibility by PES in a porcine IR model. These data are the first to associate the viable morphology and LV scar anatomy at high spatial resolution in the PIR with potential implications for clinical arrhythmia risk stratification in ischemic cardiomyopathy.

PDF-026　大腸癌：DKIによるEx Vivoでの組織学的分化度とリンパ節転移の検討
Colorectal Carcinoma: Diffusion Kurtosis MR Imaging Ex Vivo for Evaluation of Histologic Grades and Lymph Node Metastasis

山田　一郎（東京医科歯科大学 大学院医歯学総合研究科 画像診断・核医学分野）
Ichiro Yamada[1], Keigo Hikishima[2], Norio Yoshino[1], Shinichi Yamauchi[1], Naoyuki Miyasaka[1], Hiroyuki Uetake[1], Masamichi Yasuno[1], Yukihisa Saida[1], Ukihide Tateishi[1], Daisuke Kobayashi[1], Yoshinobu Eishi[1]
[1]Department of Diagnostic Radiology and Nuclear Medicine, Graduate School, Tokyo Medical and Dental University, [2]Okinawa Institute of Science and Technology Graduate University

【要旨】大腸癌20症例の手術材料及び摘出リンパ節について3T-MRIを用いてDiffusion Kurtosis Imaging（DKI）による検討を行った。DKIパラメーター（kurtosis及びcorrected diffusion）は大腸癌の組織学的分化度との間に統計学的に有意な相関を示し、転移リンパ節と非転移リンパ節との間にも統計学的な有意差が認められた。

PURPOSE: To determine the feasibility of diffusion kurtosis MR imaging as means of evaluating the histologic grades of colorectal carcinomas and lymph node metastasis by colorectal carcinomas.MATERIALS AND METHODS: Twenty colorectal specimens each containing a carcinoma and their resected lymph nodes were imaged with a 3-T MR imaging system equipped with a 4-channel phased-array surface coil. Diffusion kurtosis MR images were obtained with repetition time, 10000 ms; echo time, 154 ms; field of view, 113 mm × 73.45 mm; matrix, 120 × 78; section thickness, 4 mm without intersection gaps; four b values of 0, 1000, 2000, and 3000 s/mm^2; and motion-probing gradients perpendicular to the colorectal wall. Kurtosis (K) and corrected diffusion (D) were calculated by using the equation: $S = S_0 \times \exp(-b \times D + b^2 \times D^2 \times K/6)$, and standard ADC was also calculated by using the conventional monoexponential fit. The MR images were then compared with the histopathologic findings.RESULTS: In all 20 carcinomas, the kurtosis was calculated as 8.18 ± 2.01 (arbitrary unit [a.u.]), corrected diffusion 0.295 ± 0.118 x 10^{-3} mm^2/s, and ADC 0.210 ± 0.052 x 10^{-3} mm^2/s. The kurtosis ($r = 0.806$; $P < 0.001$) and corrected diffusion ($r = -0.604$; $P < 0.01$) were statistically significantly correlated with the histologic grades of colorectal carcinomas, while the ADC ($r = -0.339$; $P = 0.168$) showed no significant correlation with their histologic grades. Furthermore, the kurtosis and corrected diffusion showed statistically significant differences between metastatic lymph nodes and nonmetastatic lymph nodes (both $P < 0.01$).CONCLUSION: Diffusion kurtosis MR imaging seems to be useful for evaluating the histologic grades of colorectal carcinomas and lymph node metastasis by colorectal carcinomas.

PDF-027　CHESS法とSTIR法を併用したDWIを用いた下部消化管癌の評価
Evaluation of Lower Digestive Tract Cancer in DWI by Concurrently Using the CHESS and STIR Methods

宮崎　達也（メディカルスキャニングお茶の水）
Tatsuya Miyazaki, Akio Chishima, Yu Ishizaka, Toshihisa Miyamoto, Yuki Ito, Mau Sekine
Medicalscanning Ochanomizu

【要旨】STIR法とCHESS法を併用したDWIを用いて、大腸癌のDWI評価を行い、正常腸管組織の信号を抑制し、腫瘍を高信号領域として捉える事が出来た。脂肪抑制を併用することでSNRの低下を招くがimg.scale.Cor.を10に設定する事で改善できた。内視鏡検査では指摘出来なかった狭窄箇所より口側の病変を指摘出来た症例もあった。

ObjectiveThe DWI-MRI is known as useful to detect the presence of a cancer, however, it is still not generally recognized in a lower digestive tract examination. For these reasons, we conducted an evaluation of bowel cancer's DWI by concurrently using the STIR and CHESS methods in order to suppress the signals of normal intestinal tract tissues.MethodWe evaluated four persons who were diagnosed as bowel cancer after conducting endoscopy and two persons who are suspected as bowel cancer but cannot be examined by endoscopy due to stenosis.After performing the DWI-MRI of large bowel, one radiologist, one digestive organ surgeon and five radiological technicians evaluated the results.Equipment:MAGNETOM Spectra 3T-MRIImaging Conditions:TR:8000ms,TE66ms,EPI-factor72,slice-thickness:5mm,img.scale.Cor.: 10, fatsupression:fatsat+STIR(TI=240ms),b-factor: 50/1000,slice orientation:axialResultsUsing the DWI, we could suppress the signals of normal intestinal tract tissues and capture tumors as high signal regions.ADC value of the tumors: $1.02\times10^{-3}mm^2s$, $1.14\times10^{-3}mm^2s$, $1.04\times10^{-3}mm^2s$, $1.08\times10^{-3}mm^2s$, $1.11\times10^{-3}mm^2s$, $1.06\times10^{-3}mm^2s$, $1.21\times10^{-3}mm^2s$Among the two persons who could not be diagnosed by endoscopy due to stenosis, one person had one more bowel cancer at the entrance site. ObservationWe concurrently used the CHESS and STIR methods for fat saturation in order to suppress the normal intestinal tract tissues and fat signals in the DWI. This caused decrease of SNR, however, by configuring mg.scale.Cor.at 10 and adjusting the parameter of gray scale in the reconfiguration of images, it could be improved.This study indicated that the MRI might be useful for the cases in which a search for pathological lesion at the entrance site was difficult using endoscopy, due to the stenosis.

PDF-028　3テスラMRIを用いた非アルコール性脂肪性肝炎モデルマウスの肝内の鉄の定量に関する検討
Liver Iron Quantification in a Nonalcoholic Steatohepatitis Mouse Model by Using MR Imaging at 3.0 T: A Feasibility Study

大西　裕満（大阪大学大学院医学系研究科 放射線統合医学講座 放射線医学講座）
Hiromitsu Onishi[1], Masatoshi Hori[1], Takahiro Tsuboyama[1], Mitsuaki Tatsumi[1], Makoto Sakane[1], Yoshiyuki Watanabe[1], Noriyuki Tomiyama[1], Takashi Ueguchi[2], Guoxiang Liu[2]
[1]Department of Radiology, Osaka University Graduate School of Medicine, [2]Center for Information and Neural Networks, National Institute of Information and Communications Technology

【要旨】本研究では，非アルコール性脂肪性肝炎のモデルマウスの肝におけるMRIを用いた鉄の定量の可能性について検討した。解析の結果ではマウス肝のR2*値と鉄の病理グレードとの間にはよい相関が認められた（$r_s = 0.70$）。MRIによる鉄の定量技術は，動物モデルを用いての本疾患の病態解明に応用可能と思われた。

Purpose: To establish the feasibility of liver iron quantification in a nonalcoholic steatohepatitis mouse model by using MR imaging at 3.0 T.
Materials and Methods: All animal experiments were approved by the institutional animal experiment committee. Mice with nonalcoholic steatohepatitis were fed a standard high-fat diet, 1% iron added high-fat diet, or 2% iron added high-fat diet. MR examinations for liver iron quantification using a 3.0-T system were performed at 8-week-old or 12-week-old. At the MR imaging, both entire mouse body and extracted mouse liver were acquired. Liver specimens of all the mice were submitted to routine hematoxylin-eosin histologic analysis for the examination of the histologic appearance and Berlin blue staining for the evaluation of the liver iron. Iron was subjectively graded on a 5-point scale based on the histological findings. Spearman rank correlation coefficients (r_s) were calculated to evaluate the correlation between R2* values with MR imaging and the histologically determined iron grade.
Results: In the 13 specimens, increased liver iron was observed in nine (69%), including five (38%) with grade 1 iron overload, one (8%) with grade 2, three (23%) with grade 3, and zero (0%) with grade 4. Four of 13 samples (31%) had no increased iron identified at histologic examination (grade 0). R2* values measured by MR imaging of the extracted liver showed good correlation with histologic iron grade ($r_s = 0.70$, $P = 0.01$).
Conclusion: MR at 3.0 T enables evaluation of small amount of the liver iron deposition even in the small animal model. This technique might be useful for elucidation of the mechanism of nonalcoholic steatohepatitis with animal disease models.

PDF-029　拡散尖度画像 Diffusional Kurtosis Imaging（DKI）による肝疾患に伴う脾臓の検討
Evaluation of spleen with Diffusional Kurtosis Imaging (DKI) in patients with liver disease

濱田　雄貴（東京女子医科大学 八千代医療センター 画像検査室）
Yuhki Hamada, Daisuke Yoshimaru, Nozomi Mogi, Ayumu Funaki, Yoshihiro Ikeda
Tokyo Women's Medical University Yachiyo Medical Center

【要旨】脾臓の腫大から肝疾患が予測できるのではないかと考えた。DWIを用いて非正規分布に従う遷移確率密度分布を用いた解析法が、疾患による微細構造のわずかな変化を鋭敏にとらえられると期待されている。脾臓の腫大によって脾臓の細胞密度や内部の圧力が変化することで、拡散制限が起こっていると考えDKIを用いて調べた。

Purpose:To evaluate the relationship between Mean Diffusional Kurtosis(MDK)values and spleen size for the prediction of liver disease.MDK is defined as the average of the kurtosis over all possible diffusion directions. Materials And Methods:50 patients with liver disease and 10 healthy volunteers underwent MRI of the spleen including DKI (b values of 0, 1000, and 2000 s/mm^2).We evaluated the correlation between spleen size and MDK values of the spleen. In addition, we evaluated the statistical difference between 10 patients with splenomegaly and 10 healthy volunteers.Results:There were no significant correlations between spleen MDK values and spleen size (R^2=0.01).Moreover, there were no statistical difference in spleen MDK values between patients with splenomegaly and healthy volunteers (P>0.05).Conclusion:Spleen MDK values is not valuable analysis to predict liver disease.

PDF-030　高速画像の特徴の評価：DISCO-LAVAFLEX法と圧縮センシングとARCを併用したLAVA法の比較
Evaluation of imaging features of fast imaging technique: Comparison of DISCO-LAVAFLEX and LAVA with compressed sensing and ARC

米山　浩司（聖隷浜松病院 放射線部）
Kouji Yoneyama[1], Takayuki Masui[2], Yuji Iwadate[3], Naoyuki Takei[3], Kang Wang[4]
[1]Seirei Hamamatsu hospital radiation unit, [2]Seirei Hamamatsu hospital radiology department, [3]Global MR Applications and Workflow, GE Healthcare Japan, Hino, Tokyo, Japan, [4]Global MR Applications and Workflow, GE Healthcare, Madison, WI, United States

【要旨】造影ダイナミック検査で使用可能なview sharingを用いたDISCO-LAVAFLEX法と圧縮センシング（CS）とARC法を併用するCS-LAVA法について、ファントムと健常人を対象に画像の特徴を比較した。DISCO-LAVAFLEX法では、CS-LAVA法では見られないview sharingの影響が撮像画像全体に及ぶ可能性があり、特徴を理解する必要がある。

Recently,several faster imaging techniques have been introduced including DISCO, Which is based on LAVA FLEX with view sharing and ARC (DISCO-LAVA FLEX, GE), and LAVA with compressed sensing and ARC (CS-LAVA, GE). Both techniques can be utilized for breath-held dynamic contrast enhanced study. Accordingly, we studied influences of breathing and timing of contrast arrival on image quality of T1 weighted imaging using DISCO-LAVAFLEX and CS-LAVA.Materials and methods: All scans were performed on a 3T system (DISCOVERY750MR, GEHC). Phantom study: 1) Imaging was conducted with and without movement of the spherical phantom in the middle of the scan. 2) With tube phantom with flow, image contrast was evaluated with injection of contrast medium. Volunteer study: Abdominal imaging was obtained with two different maneuver; 1) complete breath-holding and 2) breath-holding at beginning followed by free breathing in the middle of the scan. In both sequences, imaging parameters were as follows: imaging time 25sec, 5 phases, matrix 288x192, FOV35xm, ARC 2x1 for DISCO-LAVA FLEX, ARC 2x1.8 and CS 1.3 for CS-LAVA. Results: The motion artifacts were noted in all the phase of DISCO-LAVAFLEX although they were only observed in the phases with phantom motions during the scan of CS-LAVA. The same results were observed in the volunteer study. In the tube phantom study, contamination of contrast was noted in the mages with DISCO-LAVAFLEX.Conclusions We might carefully interpret images obtained with DISCO-LAVAFLEX related to view sharing features. On the other hand, interpretation of images with CS-LAVA regarding image contrast might be more straightforward.

PDF-031　通常法MRエラストグラフィ (MRE) と局所励起技術を利用したMREとによる膵臓撮影の比較
Comparison of two MR elastography (MRE) methods for the pancreas ; conventional-MRE vs. reduced FOV MRE using local excitation technique

伊東　洋平（浜松医科大学 放射線診断学・核医学講座）
Yohei Itoh[1], Yasuo Takehara[2], Kenshi Kawamura[1], Takashi Nakajima[1], Ikumi Igarashi[1], Maho Hayashi[1], Satoshi Usami[1], Naoko Hyodo[1], Takasuke Ushio[1], Yuki Hirai[1], Nobuko Yoshizawa[1], Shuhei Yamashita[1], Hatsuko Nasu[1], Tetsuya Wakayama[3], Atsushi Nozaki[3], Hiroyuki Kabasawa[3], Harumi Sakahara[1]
[1]Hamamatsu University School of Medicine, [2]Hamamatsu University Hospital, [3]GEHCJ

【要旨】MRエラストグラフィ (MRE) では膵にクロスハッチ (CH) が出やすい。MREにFOCUSという局所励起技術を組み合わせて高空間分解能で撮影することで膵のCHが減らせるかを検討した。通常法MREもFOCUS-MREも膵の測定可能面積の割合に差はなく、BMI値が高いほど割合は低くなる傾向にあった。

Introduction: In pancreatic MR elastography (MRE), cross-hatches often covers the pancreas. To reduce this, we have tested high spatial resolution MRE through combining MRE and local excitation technique called FOCUS (FOV Optimized and Constrained Undistorted Single-shot).
Purpose: To compare the measurable area between conventional-MRE and FOCUS-MRE for the pancreatic MRE.
Materials & Methods: Consecutive 19 patients who had agreed to undergo pancreatic MRE were enrolled. All examinations were conducted on a 3.0-T MR unit (Discovery 750w) . A spin-echo based echo planar MRE utilized motion encoding gradients of 60 or 80Hz, external driver frequency/amplitude of 60Hz/50% and temporal phase of 4. The wave image and elastogram were automatically generated by MR-Touch system. Other parameters were FOV of 40x40cm, Matrix of 64x64 (conventional-MRE), variable FOV(average size 33x8cm; including both lateral side of patients body, ventral and dorsal areas of the pancreas was reduced), and Matrix of 64x64(FOCUS-MRE). Free hand ROI for pancreas was drawn on the magnitude image and copied to its elastogram. Then, avoiding cross-hatches, new ROI was drawn. The percentage of measurable areas were calculated.
Results: In both MRE method , there was no significant differences of percentage of measurable area of pancreas represented by non-cross hatched area , and the higher the body mass index (BMI) was, the smaller the measurable area became (conventional-MRE : $r = -0.61$ ($p<0.01$) , FOCUS-MRE : $r = -0.64$ ($p<0.01$)) .
Conclusion: Comparing two methods for pancreatic MRE, there was no significant differences in their percentages of measurable area of the pancreas. In both MRE, measurable areas were significantly affected by patients obesity reflected by BMI.

PDF-032　HISTO Sequenceにおける設定TEの最適化
Optimization of echo time setting in High speed T2 corrected multi echo MR spectroscopy (HISTO)

栗田　京助（埼玉医科大学病院 中央放射線部）
Kyosuke Kurita[1], Tsuyoshi Sasaki[1], Taishi Unezawa[1], Hiroshi Imai[3], Mamoru Niitsu[2]
[1]Saitama Medical University Hospital Central Radiation Department, [2]Saitama Medical University Hospital Radiology, [3]Siemens Healthcare K.K.

【要旨】呼吸停止中に複数TEのSVS撮像をするHISTO法は、T2補正された精度の高い肝臓脂肪含有率測定が可能である。しかしデフォルトTE設定のままT2の短い症例に適用すると、得られる値に誤差を生じる可能性が考えられた。我々は模擬ファントムと数値シミュレーションで肝臓T2値による設定TEの最適化を行った。

Purpose:HISTO sequence, which is used to estimate the fat fraction of liver, acquires five SVS signals with different TE repeatedly within a single breath-hold. Each of M0 value for fat and water components could be calculated by extrapolating each integrals. Thus, we could obtain the T2 corrected fat fraction. As the default TE setting is 12, 24, 36, 48 and 72ms, the calculated T2 value might be overestimated in short T2 case such as hemochromatosis or thalassemia. It has been reported that T2 of thalassemia liver was approximately 14ms. We investigated the effect of T2 and optimal TE setting by numerical simulation.Methods:The femur of pig was used as short T2 tissue phantom. It was scanned by HISTO with 12-100ms of TE on MAGNETOM Skyra (SIEMENS, Erlangen, Germany) and clinical setting of liver exam. The VOI of HISTO (3x3x3cm) was set on femoral muscle and slightly including fat layer. Then, the signal decay curve of each component and noise level were obtained. The error of fat fraction was estimated while changing the T2 value of fat and water component and scanned by the default TE setting. The error of fat fraction was also estimated with three patterns of TE which were a fixed minimum TE of 12ms and other 4 point were set with interval of 10, 8, 6ms.Results:When we make the water and fat T2 shortened more than 30% in default TE (18ms or less in fat T2), fat fraction was underestimated 15% or more it. 50% shortening (when fat T2 made 11ms) done, an error occurred in TE of the 10ms space, but an error did not occur in the 8ms space.)Discussion and Conclusion:We found that the default HISTO protocol was available with almost no error of fat fraction in case that T2 of liver was longer than 18ms. Otherwise, the TE should be shortened.

PDF-033　Multi-shot EPIを用いた腎動脈MRA
Non-contrast Renal MRA Using Multi-shot gradient echo EPI: Comparison with balanced TFE Sequence in healthy volunteers at 3-T MRI

森田　康祐（熊本大学医学部附属病院 中央放射線部）
Kosuke Morita[1], Takeshi Nakaura[2], Seitaro Oda[2], Tomohiro Namimoto[2], Makoto Goto[1], Masahiro Hashida[1], Yasuyuki Yamashita[1,2]

[1]Department of Radiology, Kumamoto University Hospital, [2]Diagnostic Radiology, Faculty of Life Sciences, Kumamoto University Hospital

【要旨】非造影腎動脈MRAは、balanced系のシーケンスが使用されることが多い。我々は、リードアウトにMulti-shot EPI(TFEPI)を用いた非造影腎動脈MRAのシーケンスを考案し、ボランティアで初期検討を行ったので報告する。

Introduction: The purpose of this study was to investigate the feasibility of non-contrast renal magnetic resonance angiography (MRA) using multi-shot gradient echo planar imaging (EPI) with a 3-T system.
Material and Methods: Experimental data was collected from phantom and 7 healthy male volunteers. Volunteers underwent non-contrast renal MRA using standard balanced turbo field echo (bTFE) sequence and multi-shot gradient echo EPI sequence. In phantom study, we evaluated the signal ratio for blood, muscle and fat phantoms at various flip angles (5, 10, 15, 20, 25 degree) and two fat suppression technique (SPAIR, Water Excitation). In volunteer study, we compared the signal ratio of renal artery and muscle between the sequences using the paired t-test.
Results and Conclusions: In phantom study, the signal intensity at 25 degree for the blood phantom was higher than the others, but the signal ratio for the blood and muscle phantoms was nearly unchanged. The signal ratio of blood and fat phantom was about three times higher with the water excitation than SPAIR (3.33 ± 0.39 vs 0.40 ± 0.07). In volunteer study, the signal ratio of renal artery and muscle was higher in multi-shot EPI than in bTFE (7.93 ± 0.88 vs 5.07 ± 0.75, $p<0.05$). The multi-shot gradient echo EPI sequence is the promising technique to shorten the scan time and to improve the image quality of the unenhanced real MRA with a 3-T system.

PDF-034　SECURE study: observational post-marketing study on the safety profile of gadoterate meglumine - Final results in 35,499 patients

Bodo Kress, Andreas Gottschalk

Department of Neuroradiology, Krankenhaus Nordwest, Germany

Purpose:To prospectively assess the safety profile of gadoterate meglumine (DOTAREM (R), Guerbet, France) and the incidence of Nephrogenic Systemic Fibrosis (NSF) in routine practice.
Materials and Methods:A worldwide observational post-marketing study was undertaken to collect safety data in adults and children with or without renal impairment, who were scheduled to undergo routine contrast-enhanced Magnetic Resonance Imaging (MRI) with gadoterate meglumine. Demography, risk factors, indication(s) for MRI and occurrence of adverse events (AE) were recorded. A 3-month follow-up period was planned for patients with at least moderate renal impairment (eGFR <60 mL/min/1.73 m2) in order to detect any suspicion of NSF.
Results:A total of 35,499 patients were analyzed (female: 53.1%; mean age: 49.5 years; range: 0-98 years). Central nervous system was the primary indication (56.8%) for contrast-enhanced MRI. The main risk factors were any stage of renal impairment (14.7%) and hypertension (11.9%). A total of 70 AEs were observed in 44 patients (0.12%), mainly urticaria (0.03% of patients), nausea (0.02%) and vomiting (0.01%). Among them, 38 AEs reported in 32 patients (0.09%) were considered as adverse drug reactions. Nine adult patients (0.03%) experienced serious AEs. Moderate to severe renal impairment was reported in 514 patients (1.4%), 92.6% of them were followed-up with no suspicion of NSF observed.
Conclusion:This final analysis in 35,499 patients of all ages confirms the excellent safety profile of gadoterate meglumine in routine practice.

PDF-035　放射線治療用の金マーカーが留置された前立腺癌に対する種々のMRIシーケンスの比較
Comparison of the MRI sequences in ideal fiducial marker-based radiotherapy for prostate cancer

広瀬　茂樹（岐阜市民病院 中央放射線部）
Shigeki Hirose, Osamu Tanaka, Mitsuyoshi Hattori, Takamasa Yokoyama, Yuko Yamada
Gifu Municipal Hospital

【要旨】前立腺癌に対して放射線治療を行う場合、治療の再現性を高めるために金マーカーを留置する。しかしCTにおいては描出が容易であるが、MRIでは撮像シーケンスによって描出能がかなり異なってくる。今回我々は種々のMRIシーケンスを試み、T2*2DおよびT2*3Dが前立腺輪郭および金マーカーが最もきれいに描出できたので報告する。

IntroductionContouring the prostate using CT alone is difficult. To overcome the uncertainty, MRI is used in registration of CT and MRI using fiducial markers. However, visualization of the marker itself can be difficult in MRI. This study was to determine the optimal MRI pulse sequence to define the marker, as well as the prostate gland, by comparing five sequences.Methods and MaterialsA total of 21 consecutive patients with prostate cancer were enrolled. Two gold fiducial markers were placed before a CT/MRI examination. We obtained five sequences of T1-weighted spin-echo ([TR]/[TE]): (400-650/8) (T1WI), T2-weighted fast spin-echo (4000/80) (T2WI), T2*-2D-weighted gradient echo (700/18) (T2*2D), T2*-3D-weighted gradient echo [TR/TE1/deltaTE] (37/14/7.3) (T2*3D), and contrast-enhanced T1-weighted spin-echo (400-650/8) (CE-T1WI). A qualitative image analysis of the sequence was also performed by three observers. These observers subjectively scored all images according to the following evaluation items: definition of the outline of the prostate and fiducial marker detection. A score of 1 to 3 (1= poor, 2= moderate, 3= good) was assigned to all items. ResultsT2WI was significantly superior to the other sequences in terms of prostate edge definition. T2*2D and T2*3D were strongly superior to other sequences and significantly superior in terms of fiducial marker definition.ConclusionT2*2D and T2*3D are superior to the other sequences for accurately determining the fiducial marker. T2WI exhibits the greatest precision in detecting the prostate outline, whereas T2*2D and T2*3D were superior to the other sequences for contouring the prostate and identifying the marker. Therefore, we recommend that T2*3D and T2*2D examinations are initially performed.

PDF-036　女性骨盤領域におけるガドビストと従来のガドリニウム造影剤の造影効果に関する対比
Intraindividual quantitative comparison of 0.5M gadolinium contrast material and 1.0M gadobutrol in female pelvic MR imaging

藤井　進也（鳥取大学 医学部 画像診断治療学分野）
Shinya Fujii, Takeru Fukunaga, Chie Inoue, Naoko Mukuda, Toshihide Ogawa
Division of Radiology, Department of Pathophysiological and Therapeutic Science, Faculty of Medicine, Tottori University

【要旨】ガドビスト及び従来のガドリニウム造影剤でダイナミック造影検査が施行された12例の患者を対象とした。注入レートは共に2.5ml/sである。内腸骨動脈にROIをとり、信号強度比を算出した。従来造影剤の信号強度比は平均2.56±0.13、ガドビストの信号強度比は2.56±0.12で有意差はなかった。

Purpose: The purpose of present study was to quantitatively examine signal intensity ratio of internal ileac artery in bolus characteristics of 1.0 (molar) M gadobutrol compared to 0.5 M gadolinium contrast materials in order to evaluate the usefulness for female pelvic magnetic resonance (MR) imaging. Materials and Methods: Twelve patients were included in this study. The patients were undertaken 3T MR imaging using 0.5 M gadolinium contrast material and 1.0M gadobutrol at different periods. Dynamic contrast enhanced imaging (DCE) was obtained before and immediately after rapid intravenous injection at a rate of 2.5 mL/sec in both contrast materials, and then repeated at 25, 60, 90, and 120 seconds during the examination. Region of interest (ROI) was placed at internal ileac artery in the proximal area and then signal intensity (SI) was obtained. Signal intensity ratio (SIR) was calculated as following formula: SIR= post contrast highest SI- pre SI/ pre SI. The paired t-test was used for statistical comparison.Results: The SIR using 0.5M contrast material was 2.56±0.13(1.56-3.21), while the SIR using 1.0M gadobutrol was 2.56±0.12(1.31-3.22). There was no significant difference between the SIRs. DiscussionThe result may be due to the rapid injection of gadobutrol and subsequent narrow time window. Further examination would be needed.

PDF-037　骨軟部悪性腫瘍の人工関節置換術後再発に対するMAVRIC-SLとSEMARを用いた金属アーチファクト低減の比較検討
Evaluate a clinical value of MAVRIC-SL and SEMAR for detecting a post operative local recurrence of soft tissue tumor around a metal implant

小黒　草太（慶應義塾大学病院 放射線診断科）
Sota Oguro[1], Shigeo Okuda[1], Hirokazu Fujiwara[1], Kuniaki Ohori[1], Kazutaka Kikuta[2], Robert Nakayama[2], Hideo Morioka[2], Masahiro Jinzaki[1]

[1]Radiology Department, School of Medicine, Keio University, [2]Department of Orthopaedic Surgery, School of Medicine, Keio University

【要旨】MRIとCTの金属アーチファクトを低減するMAVRIC-SLおよびSEMARを用いて骨軟部腫瘍術後の人工関節置換術後の再発病変を撮影し，その有用性について比較検討した．MAVRIC-SLおよびSEMARでは金属に接した部分の描出が可能であった．人工関節周囲の再発病変に対してMAVRIC-SLおよびSEMARはいずれも有用な検査と考えられた．

Purpose : To evaluate a clinical value of MAVRIC-SL (multi-acquisition with variable resonance image combination, slice encoding for metal artifact correction) and SEMAR (Single Energy Metal Artifact Reduction) for detecting a post operative local recurrence of soft tissue tumor around a metal implant.Materials and Methods : Contrast enhanced MR and CT images using MAVRIC-SL and SEMAR were obtained using 3 tesla MR scanner (Signa Pioneer, GE healthcare) and 320 multi-detector row CT (Aquilion One, Toshiba), respectively. On the MAVRIC-SL, proton density weighted image, Short tau inversion recovery (STIR), T1 weighted image were investigated. Acquisition time of each sequences of MAVRIC-SL was about 6 minutes. Contrast enhanced CT images were obtained using subtraction technique. Acquisition time of each CT scan using SEMAR was less than 10 seconds. Detectability of the recurrent tumor was evaluated by two radiologists. Tumor contour of the tumor on the images of MAVRIC-SL and SEMAR were compared with images without using those technique. The images were also compared with pathological findings. Result : All the recurrent tumors were visualized on both images using or not using MAVRIC-SL and SEMAR. However, an artifact-affected area was significantly diminished with MAVRIC-SL and SEMAR. Conclusion : The local recurrence of soft tissue tumor around a metal implant was well visualized using MAVRIC-SL and SEMAR. These technique may be incorporated into a future treatment algorithm.

PDF-038　スピン-格子緩和時間による膝関節軟骨の絶対温度分布非侵襲画像化の可能性
Feasibility of noninvasive and absolute thermometry for knee joint cartilageusing spin-lattice relaxation time

木村　智也（東海大学 工学研究科 電気電子工学専攻）
Tomoya Kimura[1], Kagayaki Kuroda[1,2], Kenji Takahashi[3]

[1]Course of Electrical and Electronic Engineering, Graduate School of Engineer ing Tokai University, [2]Center for Frontier Medical Engineering, Chiba University, [3]Department of Orthopedic Surgery, Nippon Medical School

【要旨】豚膝関節軟骨における水のT1の温度依存性を水プロトン共鳴周波数と比較により検討した．その結果，T1は温度依存性があり，温熱療法下における温度測定の好ましい指標であるとともに，T1に基づく温度分布画像化の可能性があることが分かった．

Introduction Thermal therapy for osteoarthritis is becoming one of the options for pain-relief. In order to optimize the therapeutic effect, visualization of temperature is necessary. To develop a technique tolerant to the target tissue dispacement, we have focused on the use of T_1 for mesuring absolute temperature. As a feasibility study, we have examined the temperature dependence of T_1in the porcine knee joint cartilage in vitro.Methods Proton spectra of cartilage segment samples collected from porcine knee joints were observed in a 9.4 T NMR spectrometer. Proton spectra were evaluated at various temperature ranging from room temperature to 60 oC. The sample temperature was controlled with an air blower system equipped with the spectrometer. Then a conventional IR sequence yielded T_1 in the sample.Results T_1 was in proportion to temperature with high correlation (r ~ 0.99). The temperature coefficient was 36.9 ms/oC for heating period and 36.0 ms/oC for cooling with no significant difference between as shown in Fig.1. These results support that T_1 is a strong candidate as a parameter for measuring absolute temperature in the cartilage.

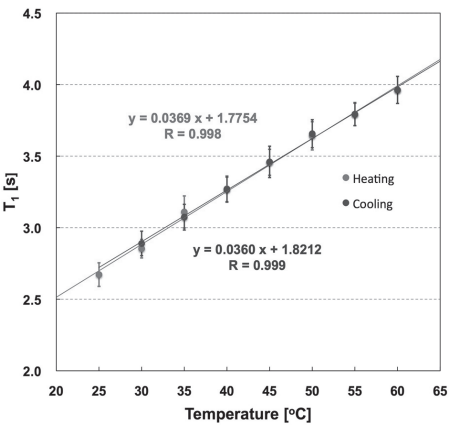

PDF-039　高分解能3T-MRIを用いた健常者での手関節軟骨のT2マッピング
Assessment of T2 values of the wrist cartilage in healthy subjects at high-resolution 3T-MRI

船田　重和（聖路加国際病院 放射線科）
Shigekazu Funada[1], Taiki Nozaki[1], Junichi Tsuchiya[1], Saya Horiuchi[1], Chiharu Osakabe[1], Yasuyo Teramura[2], Hiroshi Yoshioka[3], Hiromi Nakamura[4], Kazuhiro Umehara[4], Yasuyuki Kurihara[1]
[1]St. Luke's International Hospital, [2]National Defense Medical College Hospital, [3]Department of Radiological Sciences, University of California, Irvine, CA,USA, [4]GE Healthcare JAPAN

【要旨】T2マッピングは軟骨変性をMRIで定量する手法として関節MRIで主に用いられているが、小関節である手関節軟骨へ応用した報告は、ほとんどみられない。本研究では3T-高分解能MRIを用いて健常ボランティアでの手関節軟骨のT2値の基準値および年齢との関連について検討した。

OBJECTIVES:T2 mapping is a widely utilized MR technique for quantitative assessment of cartilage degeneration. Many reports have been published about T2 map profiles of the knee and hip joints. However, there have been few studies about T2 map profiles of the wrist joint. The purpose of this study was to create normalized T2 map profiles in wrist cartilage around the triangular fibrocartilage complex (TFCC) from healthy volunteers at high-resolution 3T-MRI. MATERIALS AND METHODS:10 healthy volunteers were enrolled in this study. The age of the healthy subjects ranged from 23 to 48 years (mean age: 32.5 ± 9.6 years, n=6 male). T2 images of each subject were acquired using a 3T MR scanner (Discovery750W, GE healthcare, USA) utilizing a 16-channel wrist coil. Wrist cartilage segmentation around the TFCC was performed by two raters. We calculated the mean T2 values at the cartilage of radius, ulna, triquetrum, lunate and disc proper of TFCC. Representative mean T2 values from these lesions were analyzed in correlation with the age. RESULTS:Mean T2 values were 31.5 ± 1.8 msec on radius, 27.6 ± 1.9 msec on ulna, 30.4 ± 2.6 msec on lunate, 28.2 ± 2.8 msec on triquetrum, and 20.3 ± 1.4 msec on disc proper of TFCC, respectively. Pearson correlation coefficients between age and T2 value were -0.121 on radius, -0.277 on ulna, -0.221 on lunate, 0.028 on triquetrum and -0.173 on disc proper of TFCC without significant differenceCONCLUSIONS: There were no significant correlations in wrist cartilage around the TFCC between age and T2 values. The potential of T2 mapping on wrist cartilage in the patients with wrist pain has to be investigated in further studies.

PDF-040　3T-MRIによるT2mappingを用いたスポーツ障害による肩関節軟骨変性の評価
Evaluation of Shoulder Joint Cartilage Degeneration by Sports disorders Using T2 Mapping at 3T MRI

伊藤　勇輝（メディカルスキャニングお茶の水）
Yuki Ito, Tatsuya Miyazaki, Akio Chishima, Yu Ishizaka, Toshihisa Miyamoto
Medicalscanning Ochanomizu

【要旨】t2mappingを用いて軟骨をエリア分類し、スポーツ障害患者の肩関節軟骨変性の評価を行った。軟骨T2値は健常ボランティアよりも有意に高値（平均20％程度高値）を示し定量的に評価できる事を示した。各スポーツ競技によりT2値が高値となるエリアが異なる特色があった。

Objective: In this study, we evaluated the shoulder joint cartilage degeneration using T2 mapping that is a sensitive evaluation method of the cartilage matrix.Methods:The evaluation was conducted for 178 patients who underwent MRI scans for their shoulder joint disorders by sports and for another 35 healthy volunteers (mean age: 26.5 years old) who had no symptoms in the shoulder joint.Cartilage T2 mapping was performed for the scapulohumeral joint using the 2D-multi-spin echo method to obtain the coronal section image and the cross section image. The cartilages on the shoulder blade side were classified into seven areas in clockwise order as follows. The cartilages on the head of the humerus side were classified into five areas as follows.Subsequently, cartilage T2 values in each ROI were measured to calculate the average value and the standard deviation. Used equipment:3T-Verio Shoulder-Coil was used for the measurement.Result:Cartilage T2 values of patients with sports injury were significantly higher than those of healthy volunteers (by 20% on average).Conclusion:The high T2 values were highly associated with the change of the cartilage degeneration and the increase of the amount of the contained water, which demonstrated the fact that cartilage degeneration that cannot be described on the images can be evaluated quantitatively using T2 mapping.The elevation of T2 values were observed in the posterior inferior area of the shoulder joint glenoid fossa (A5) of the participants who had a long experience in baseball due to Bennett's damage, while in the superior and the anterior areas (A1, A2, A3) of the rugby players, which demonstrated the characteristics that T2 values were different from one sports to another.

PDF-041　乳がんの温熱療法のための磁気共鳴による非侵襲温度分布画像化における信号処理
Signal Processing in Noninvasive Magnetic Resonance Temperature Imaging for Breast Thermotherapy

大脇　陽介（東海大学工学研究科電気電子専攻）
Yosuke Owaki[1], Kenichirou Kurihara[1], Yutaka Imai[3], Kagayaki Kuroda[1,2]
[1]Course of Electrical and Electronic Engineering, Graduate School of Engineering, Tokai University, [2]Center for Frontier Medical Engineering, Chiba University, [3]Department of Radiology, Tokai University School of Medicine

【要旨】T_1の系統誤差・ランダム誤差共に単純な2成分モデルよりも9成分モデルの方が有意に小さかった．脂肪酸成分の周波数配置ならびに密度比に関する先験情報を利用して9成分を考慮した方が、単純な2成分モデルを用いた方法よりも高い精度で温度を測定しうることがわかった．

IntroductionFor breast high intensity focused ultrasound (HIFU) therapy, we have proposed a novel thermometry technique using multiple flip angle and multiple echo time sequence to map T_1 of methylene or terminal methyl proton for fat and the resonance frequency for water. In the present work, we have examined the effect of using prior information about frequency assignments and density ratios of the fat components to reduce the complexity of signal processing as well as to maintain the accuracy of T_1 estimation. **Methods**A numerical phantom comprising SPGR signals of water and 8 components of fat including methylene chain and terminal methyl was constructed. To this phantom, two different approaches were applied; one was with a model using the full 9-component model and the prior information on the frequency assignments and density ratios for fat; the others was with a simple model using only 2-components, water and methylene chain. The estimation accuracy of the methylene T_1 was compared under SNR varied from 3.3 to 100. A phantom experiment using mayonnaise was conducted to verify the simulation results.**Results**The systematic error in T_1 estimation was significantly smaller in the 9-component approach than in the simple 2-component approach ($p < 0.01$). The random error was also smaller in the 9-component model in the present SNR range. The corresponding temperature error was about 0.3 ℃ at SNR of 10 assuming that the temperature coefficient of methylene T_1 was 1.79 %/℃ . The experimental result supported the effect of the 9-component approach.**Conclusion**The T_1 estimation technique using the prior knowledge on frequency separation and signal intensity ratio in conjunction with the full component model was superior to the technique using a simple 2-component model.

PDF-042　MRと超音波画像を併用したイメージガイド下穿刺支援のためのMR対応ロボットシステム
An MR compatible robot system using MR and ultrasound images to assist image guided puncture

森川　茂廣（滋賀医科大学 神経難病研究センター MR医学研究部門）
Shigehiro Morikawa[1], Atsushi Yamada[2], Shigeyuki Naka[3], Koichiro Murakami[3], Tohru Tani[2]
[1]Dept. Biomedical MR Science, Molecular Neuroscience Research Center, Shiga University of Medical Science, [2]Biomedical Innovation Center, Shiga University of Medical Science, [3]Dept. of Surgery, Shiga University of Medical Science

【要旨】通常のMR装置と超音波を併用した穿刺支援ロボットシステムを開発した。ロボットは常に指定したターゲットを追跡するように制御され、MR撮像後、患者テーブルを引出し、レジストレーションなしに、再構成MR画像を用いて最適の穿刺ルートを決定し、刺入される穿刺針は超音波画像でリアルタイムにモニターすることができた。

Purpose: To develop a hybrid robot system combining high resolution MR images and real-time ultrasound(US) images. We previously reported a motorized MR-compatible robot system with remote-center-of-motion (RCM) control to assist MR image-guided microwave ablation of liver tumors and successfully applied it for 23 clinical cases with a double-doughnut type open MR system. We modified this robot system to adapt it for a standard closed-bore scanner and combined US scanner. Methods: A wide bore 3T MR scanner (Siemens, Verio) and a US scanner (GE, Venue40) were combined. The magnetic parts were removed from the trolley of the US scanner. The robot system with the US scanner was located near the magnet bore and its hand piece had a needle guide and a US probe holder. A Polaris Spectra (NDI) was used as a position sensor. The RCM control automatically chased the determined target point and showed it at the center of the 3 orthogonal reformatted MR images. Overlaid image of the corresponding MR and US image was also shown based on the needle trajectory. Results and Discussion: This system enabled immediate navigation without time consuming registration process after MR image acquisition. The RCM control of the robot worked precisely and the optimal puncture route could be selected easily. Thereafter, the hand piece approached to the surface of the target while keeping its direction. A water-filled rubber bag was inserted between the surface and the US probe to observe US image. The MR images showed detailed structure along the puncture route, and US images could show the inserted needle. The combination of reformatted MR images and real-time US images was feasibloe and this hybrid robot system using them could be a promising image-guided navigation system.

PDF-043　小児鍼刺激による脳活動の変化の検討
fMRI study of clinical "shonishin" stimulation

上林紗也果（明治国際医療大学大学院 鍼灸学研究科 鍼灸学専攻 脳神経外科）
Sayaka Kanbayashi[1], Masahiro Umeda[2], Yasuharu Watanabe[2], Yuko Kawai[2], Tomokazu Murase[2], Ayako Mandai[3], Toshihiro Higuchi[3]

[1]Graduate School of Clinical Acupuncture and Moxibustion, Meiji University of Integrative Medicine, [2]Department of Medical Informatics, Meiji University of Integrative Medicine, [3]Department of Neurosurgery, Meiji University of Integrative Medicine

【要旨】鍼灸臨床で行われる小児鍼の治療効果を明らかにするため、小児鍼による治療に則った刺激、スポンジ擦過刺激、小児鍼単体刺激を fMRI を用いて比較した。ブロックデザインにて刺激を行ったところ、スポンジ擦過刺激では体性感覚野の活動が得られたが、小児鍼による刺激では観察できなかった。

Purpose: "Shonishin" is an acupuncture technique used for treating children, by stimulating wide areas, such as the back. The "shonishin" technique is a clinical complex stimulation, alternatively composed of strokes by the hands and scratches by "shonishin" tool. In this study, we focused on human brain activation induced by therapeutic "shonishin" stimulation.
Materials & Methods:All examinations were performed on a 3.0 T MRI clinical system (Trio Tim, Siemens) with gradient echo – EPI. Image processing and statistical analysis were performed using SPM12. fMRI studies used a block design in which stimulation and non-stimulation were alternated in 30 second blocks.
Study 1: The fMRI studies were performed in 11 healthy volunteers, from whom informed consent was obtained. Sponge rubbing and clinical complex stimulation were performed on the right palm and the right anterior forearm.
Study 2: The fMRI studies were performed in 9 healthy volunteers, from whom informed consent was obtained. Simple scratches using a "shonishin" tool and clinical complex stimulation were performed on the right posterior forearm and the dorsum of the hand.
Result & Discussion:Sponge rubbing stimulation of both the palm and anterior forearm activated the left somatosensory cortex 1 (S1) and 2 (S2). Clinical complex stimulation of the palm also activated the left S1 and S2. However, neither stimulation of other areas nor simple scratches by the "shonishin" tool activated S1 and S2. Further analysis may need to be carried out on sustained brain activation using clinical complex stimulation.
Reference:T. Murase et al. Magn Reson Med Sci. 2013;12(2):121-7.

PDF-044　A challenge for sub-millisecond fMRI

Yul-Wan Sung, Daehun Kang, Seiji Ogawa

Kansei Fukushi Research Institute, Tohoku Fukushi University, Japan

As advances of MRI technologies both in hardware and software, high spatial resolution imaging of hundred micrometer order came to be available. In the same way, temporal resolution also has been advanced. The acquisition of whole brain in half a second came to be available by fast imaging technologies such as the simultaneous multiple slice (SMS) imaging and inverse imaging (InI). Among them, the inverse imaging provides the shortest acquisition time up to several tenth milliseconds by obtaining the minimal number of lines on k-space though some deterioration of image quality should be tolerated. However, the conventional acquisition with temporal resolution of a few millisecond could not be realized due to the practical and essential duration of RF excitation pulses. In this study we further challenge to develop a technique for much faster imaging up to sub-millisecond by applying multiple-echo scheme into inverse imaging. The proposed imaging technique was tested with a phantom in which an additive magnetic field can be generated to give the effect of artificial activation as similar as fMRI experiment. The future goal of this ultra-fast imaging is to search for some intrinsic signals reflecting fast neuronal processing such as magnetic field or metabolite changes by neural current of field potential.

PDF-045　ASL MRIを用いた頭部外傷の脳血流評価　Tc ECD SPECTとの比較
ASL MRI in patients with traumatic brain injury as the imaging of cerebral blood flow compared with Technetium ECD SPECT

柴田　　靖（筑波大学 水戸地域医療教育センター 水戸協同病院 脳神経外科）
Yasushi Shibata, Ryota Mashiko

University of Tsukuba, Mito Medical Center, Mito Kyodo General Hospital, Department of Neurosurgery

【要旨】脳血流評価はSPECTが標準だが、高価で被ばくもあり緊急に対応できない。ASLは撮像は容易だが、頭部外傷の報告は少ない。頭部外傷21例に同時期にASLとTc ECD SPECTを撮像した。 SPECTでは定量評価が可能だが、ASLは定性画像のみでノイズが多い。硬膜下血腫、脳挫傷、高次脳機能障害の脳血流低下は両者とも同様に検出された。

Tc ECD SPECT is the standard method for evaluating CBF; however this method is associated with high cost, radiation exposure and its limited availability for emergency patients. While CBF evaluation is known to be useful in the evaluation cerebral function in traumatic brain injury, ASL perfusion MRI has not been fully evaluated. We performed ASL perfusion MRI and Tc ECD SPECT in patients with head injury and compared the imaging findings. A total of 21 patients were registered in this study. The final diagnoses were as follows contusion (n=8), ASDH (n=5), CSDH (n=3), concussion (n=3), traumatic SAH (n=2), DAI (n=2). The patients with cerebral contusion always showed low CBF with both ASL perfusion MRI and Tc ECD SPECT. In the DAI cases, low CBF were compatible with functional impairment and higher brain dysfunction. In the cases with ASDH or CSDH, cerebral compression was not revealed as a CBF change; a CBF study was therefore useful to determine the surgical indication and prognosis. SPECT was capable of providing quantitative and statistically-standardized evaluations. In contrast, ASL was only capable of providing qualitative images. SPECT is more useful than ASL for CBF studies. However, the time required for ASL imaging is very short, thus ASL can be performed in the course of a routine MRI examination. SPECT remains the gold standard of CBF evaluation. However, ASL is sufficient as a routine evaluation for the follow-up examination of patients in whom low CBF has been diagnosed and of new patients with cerebral concussion.

PDF-046　DW-ASLを用いたWater Permeabilityの算出におけるb値の最適化
Optimization of b-value Arrangement for Calculating of Water Permeability Using Diffusion-Weighted Arterial Spin Labeling

青池寿々子（北海道大学病院 医療技術部 放射線部門）
Suzuko Aoike[1], Noriyuki Fujima[2], Tomoyuki Okuaki[3], Takuya Aoike[1], Sayaka Takamori[1], Kinya Ishizaka[1], Kohsuke Kudo[2]

[1]Department of Radiological Technology, Hokkaido University Hospital, [2]Department of Diagnostic and Interventional Radiology, Hokkaido University Hospital, [3]Philips Electronics Japan

【要旨】DW-ASLを用いて脳のwater permeability(Kw)を求めるための最適なb値の組み合わせの評価を行った．5種類の組み合わせを作成し撮像を行いKwを算出した．すべてのb値を用いて算出した値を基準とし差分値を求め多重比較を行った．b値0, 26.1, 47.5, 73.6, 102.5, 188.6 s/mm^{2}の組み合わせにおいて基準との差が有意に低かった．

[Purpose]
Diffusion-weighted arterial spin labeling (DW-ASL) has become available. This technique enables to calculate water permeability non-invasively using multiple b-values acquisition. To our knowledge, there were few reports that investigated optimal b-values for calculating of water permeability, and the tendency of signal decay in multiple b-value dataset. The aim of the current study was to assess the optimum combinations of b-value for calculating of water permeability in human brain.
[Materials & Methods]
Healthy volunteers were scanned on a 3-tesla MR scanner. DW-ASL were acquired with nine b-values (b= 0, 2, 10, 18, 26.1, 47.5, 73.6, 102.5, 188.6 s/mm^2). The combination of b-value was divided into five groups. The combination of all b-value was set to control arrangement. The region of interest (ROI) selection was performed for gray matter (GM) on parietal in the flow territory of the anterior (ACA), on basal area in the flow territory ACA, middle (MCA), and posterior cerebral artery (PCA), on temporal area in the flow territory MCA, and GM in the flow territory of the cerebellum level. The signal intensities of the ROI were measured on these slices, respectively. The estimation of water permeability was performed using multiple b-value dataset.
[Result]
The measurement of water permeability using a combination of b-value: 0, 26.1, 47.5, 73.6, 102.5, 188.6 s/mm^2 was significantly lower difference from control than that using a combination of others.
[Conclusion]
The result of this study showed that the optimum combination of b-value for calculating of water permeability could be found.The results suggest that available to evaluate water permeability with less b-value and the total scan time will be expected to become shorter.

PDF-047 Pearls and Pitfalls in Arterial Spin-Labeling MR Imaging (ASL-MRI) in Various Intracranial Pathologic Condition

Aleum Lee, Chang Kee-Hyun

Department of Radiology, Soonchunhyang University Bucheon Hospital, Korea

TEACHING POINTS

The purpose of this exhibit is to present the ASL-MRI findings in various intracranial pathologic conditions 1. To review basic background and techniques of ASL-MRI 2. To illustrate the clinical applications of ASL-MRI imaging in CNS disease 3. To discuss the merits and limitations of different methods of perfusion MR imaging (ASL, DSC and DCE-MRI) in various CNS disease

TABLE OF CONTENTS/OUTLINE

1. Explanation of back ground and technique of dynamic contrast enhanced MR imaging (DCE), dynamic susceptibility contrast perfusion MR imaging (DSC) and arterial spin labeling (ASL) of CNS 2. Evaluation of different perfusion MR parameters and maps 3. Variable appearance of ASL-MRI in CNS disease

1) Congenital disease 2) Trauma 3) Vascular disease - stroke 4) Neoplasm 5) Degenerative/metabolic disorder 6) Infection 7) Other miscellaneous conditions

4. Merits and limitations of different methods for perfusion MRI

Concordant vs. discordant finding between ASL-MRI and DSC-/DCE-MRI

5. Future directions and summary.

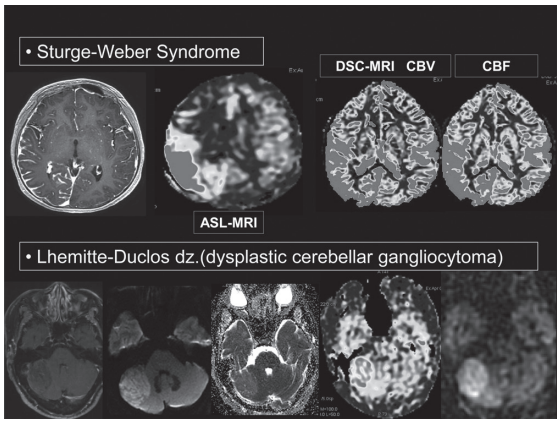

PDF-048 Diffusion Kurtosis Imaging (DKI)を使用したHCCの病態評価
Diffusion Kurtosis Imaging (DKI) for the pathophysiology of the hepatocellular carcinoma (HCC)

茂木　望（東京女子医科大学 八千代医療センター 医療技術部 画像検査室）

Nozomi Mogi, Daisuke Yoshimaru, Yuuki Hamada, Yoshihiro Ikeda, Ayumu Funaki

Tokyo woman's medical university Yachiyo medical center

【要旨】正規分布からの逸脱を定量的に評価する手法であるKurtosis解析を使用し、肝細胞癌の評価を行った。肝細胞癌から得られたKurtosis値を基に分類した結果、正常ボランティアと同様の低値を示すものから、優位に高い値へと分類された。肝細胞癌の病態によってkutosis値が変化する可能性がある。

Objectives To determine the potential of Diffusion Kurtosis Imaging (DKI) for the pathophysiology of the hepatocellular carcinoma (HCC). Methods 11 patients with HCC and 15 healthy volunteers underwent MRI of the liver including DKI (b values of 0, 1000, and 2000 s/mm2). All patients underwent MR imaging with a 3-T unit (Achieva, Philips Medical Systems, the Netherlands), equipped with a 6-channel Cardiac coil. We classified patients according to the value of kurtosis. We defined 0.5-1.0 as group A, 1.0-1.5 as group B and 1.5-2.0 as group C using each kurtosis value of the patient. Results There were 3 number of cases in group A, 6 number of cases in group B and 2 number of cases in group C. Kurtosis values of all healthy volunteers were 0.5-1.0 as well as value of group A. Conclusions We could divide the Kurtosis value obtained from HCC into some groups. Therefore, Kurtosis value can distinguish the pathophysiology of HCC.

PDF-049　3T-MRIにおけるRESOLVEを用いた骨盤部矢状断の有用性についての検討
Examination about the usefulness of the pelvis part sagittal section using RESOLVE in 3T-MRI

針生　武瑠（メディカルスキャニング 東京）
Takeru Hariu[1], Tatsuya Miyazaki[2], Akio Chishima[3], Keita Kimura[4]
[1]Medicalscanning Tokyo, [2]Medicalscanning Ochanomizu, [3]Medicalscanning Nippori, [4]Medicalscanning Tachikawa

【要旨】近年、拡散強調画像の体幹部での応用が拡く利用されているが、問題点として磁化率アーチファクトによる画像の歪みが指摘されている。そこで、当院3T-MRIに導入されたRESOLVEを使い、骨盤領域の矢状断による歪み率をSS-EPIと比較した。その結果、RESOLVEでは歪みが低減され、有用性が示唆された。

[Purpose]
The endometrial cancer and cervical cancer is depicted as a high signal in DWI. And it is useful for the grasp of position relations and the diagnosis of the progress range of the lesion by the imaging in the sagittal. But, there is the fault that is easy to produce a distortion to an image by a susceptibility arch fact with the enteric gas by the SS-EPI method. Therefore we examined clinical usefulness when we used the RESOLVE method in a pelvic domain.
[Apparatus]
3T-MRI MAGNETOM spectra(Siemens Co)
[Method]
Firstly we performed the quantitative measurement with self made phantom. We poured a detergent into the rectangular container and, on the bed, located it with the top, the center, a bottom. Distortion rate of the phantom was determined based on the length of the image taken by the SE method(DWI measured value /SE measured value). And we took the SS-EPI method and the RESOLVE method for healthy volunteers. Here, imaging was sagittal. Also in the healthy volunteer, the RESOLVE method changed the segment number and imaged it. The provided image performed a visual evaluation.
[Result/Consideration]
A distortion was improved in comparison with the SS-EPI method by the RESOLVE method. But, the big change was not seen in the distortion rate of the image when we changed the number of segment. In the healthy volunteer, although distortion was notably observed in the uterine cervix especially by the SS-EPI method, the RESOLVE method has reduced distortion compared with the SS-EPI method. In future, we want to perform the comparison with the contrasting T1 weighted image.
[Conclusion]
It was thought that the RESOLVE method had clinical usefulness in the pelvic domain.

PDF-050　小児におけるdirect coronal DWIBSの基礎検討
Basic study of the direct coronal diffusion weighted whole body imaging with background body signal suppression (DWIBS) in Children

渡邉　裕文（千葉県こども病院 検査部 放射線科）
Hirofumi Watanabe[1], Kojiro Ono[1], Takumi Ookubo[2], Miwako Suzuki[1], Akira Shirayama[1]
[1]Department of Radiology, Chiba Children's Hospital, [2]Department of Radiology, Chiba Cancer Center

【要旨】Direct Coronal DWIは歪みが出やすい。小児は体格が小さく狭い感度領域でも十分収まることから8ch cardiac Coilを使用してPhase encode方向をS-I、Wide FOVで撮影していた。さらにphase FOVを狭めることで歪みを改善した。

<Background>Children are susceptible to partial volume effects than adults.In DWIBS of children, direct coronal imaging is considered to be particularly effective.But there is issue of the distortion in direct coronal imaging, improvement of distortion is necessary.Recently, the technique using a small receiver coil and wide FOV is reported as useful resolution against the distortion of direct coronal DWIBS.In this study, we tried to make further improvement of distortion using the combination of the parameters of phase FOV and a wider FOV.<Purpose>Examined improvement of distortion using wide FOV and Phase FOV in direct coronal DWIBS, examined the efficacy in pediatric imaging.<Methods>All subjects were performed at 1.5T (Signa HDxt Ver.23,GE Healthcare) using the 8ch cardiac coil as receiver. Direct coronal DWIBS acquisition used STIR SE-EPI sequence (Imaging parameter Phase encode;S-I,TR:8000ms,TE;minimum,TI;180ms,NEX;8,BW;±250kHz,b-Values:1000s/mm2,Matrix size:192×256,Asset:2.0).We scanned the homebrew phantom by changing the FOV and Phase FOV, were studied distortion.Distortion of image was examined using sight evaluation method by 3 trained radiologists and estimating distortion ratio.<Results and Discussion>Comparing the wide FOV and a narrow FOV, distortion of the image was the same extent.Distortion of image is improved when phase FOV becomes narrower, but aliasing artifact is generated from phase FOV ratio 0.65.Wide FOV scanning are expected to improve the SNR, it is considered to be possible scanning a high-resolution DWIBS in children by combining narrow phase FOV and small matrix size.<Conclusion>Direct coronal DWIBS further can be reduced distortion without generating artifacts by about FOV 60cm and phase FOV ratio 0.7,it is effective in DWIBS in children.

PDF-051　3T拡散強調像において充分長いTRが必要な理由：MT効果とクロストークの影響
Diffusion-weighted imaging at 3T requires sufficiently long TR owing to incidental magnetization transfer and crosstalk effects

北　　美保（生長会 府中病院 放射線科）
Miho Kita[1], Kazuhiro Kawano[2], Morio Sato[3], Hideto Sakamoto[1], Seigo Ishii[1], Tetsuo Sonomura[4]
[1]Department of Radiology, Seichokai Fuchu Hospital, [2]Department of Radiological Technology, Seichokai Fuchu Hospital, [3]Department of Radiology, Hannann Municipal Hospital, [4]Department of Radiology, Wakayama Medical University

【要旨】3T躯幹部拡散強調像で通常より充分長いTRを用いた方が高画質となる理由に，我々はTR間の縦磁化のT1回復以外の要因もあると考え検証した。MT効果が乏しいと報告されてきたEPIでも、マルチスライス法でのMT効果が見られ、クロストークと共に信号低下を引き起こした。これらの影響を軽減するのに、充分長いTRが有用であった。

[Objective]
Body Diffusion-weighted (DW) images tend to have low signal intensity. Using TR sufficiently longer than usual often improves signal intensity of DW images. We investigated the reasons why DW imaging at 3T requires TR longer enough than the time necessary for T1 recovery of the longitudinal magnetization.
[Materials and Methods]
Multi-slice imaging and single-slice imaging of STIR-EPI and SPAIR-EPI sequences for body DW imaging were performed using 3T MR scanner (Magnetom Skyra; Siemens). Two types of phantoms were imaged: PVA gel phantom including bound water and free water similar to the human body (90-401 type; Nikkofines), and 0.25 mmol/l Gd-DTPA solution phantom including only free water having T1 value close to the human body. We compared the signal intensities of DW images between single-slice and multi-slice imaging using various TRs and various slice intervals.
[Results]
Signal intensities decreased by 17-26% in multi-slice imaging compared to single-slice imaging of STIR-EPI and SPAIR-EPI sequences, when using TR as long as three times of T1 value. Incidental magnetization transfer (MT) effect was observed only in gel phantom, whereas crosstalk effect was observed in both gel and solution phantoms. As the interval of slice excitation increased, signal intensities of multi-slice DW images increased and MT and crosstalk effects were reduced.
[Discussions and conclusions]
EPI sequences have been reported to have minimal MT effect. However, we observed significant MT effect in multi-slice EPI sequences used for DW imaging at 3T. The incidental MT and crosstalk effects may contribute to the reason why DW imaging requires sufficiently long TR.

PDF-052　門脈血流動態把握へのmulti-phase ASTAR（mASTAR）法の応用
Application of mASTAR to the Evaluation of Portal Vein Hemodynamics

二宮　綾子（東芝メディカルシステムズ株式会社 MRI営業部）
Ayako Ninomiya[1], Miho Kitamura[1], Naotaka Sakashita[2], Yuichi Yamashita[1]
[1]MRI Sales Department, Toshiba Medical Sysytems Corporation, [2]Center for Medical Research and Development, Toshiba Medical Systems Corpora tion

【要旨】肝臓疾患により門脈血流が逆行する場合があり、その血流動態把握は病態の把握や術前情報として重要である。一度の撮像で多時相の非造影MRA画像を得られるmASTAR法と用い、門脈血流の動態描出と撮像条件の最適化を検討したので報告する。

PurposeLiver disease may cause reverse portal vein flow, and hemodynamic evaluation is important for diagnosis and treatment planning. Time-SLIP can depict the portal vein, but hemodynamic evaluation requires a long scan time. We investigated portal vein hemodynamic evaluation using mASTAR, which provides non-contrast MRA images of multiple temporal phases in a single acquisition, and also determined the optimal scan conditions. MethodsVolunteers were examined using a Vantage Titan 3T (Toshiba Medical Systems). mASTAR is based on FFE3D in which labeling tag pulses can be set according to the target vessel. The number of temporal phases and timing increment can be freely set. Spin-labeled blood flow into the intrahepatic portal vein was observed under free breathing with respiratory gating, and the scan conditions for depicting the maximum length of the portal vein were determined. Conventional single-phase images were acquired for comparison. Tag pulses were applied to the splenic and superior mesenteric veins perpendicular to the portal vein.ResultsThe conventional method requires multiple acquisitions corresponding to the number of temporal phases. With mASTAR, multiple temporal phases are imaged in a single acquisition and spin-labeled hemodynamics can be observed. However, compared with conventional images with the same labeling wait time (BBTI), mASTAR showed lower blood flow signals, which is thought to be due to increased saturation of labeled blood in multiple temporal phase acquisition. The optimal scan conditions for depicting the portal vein, which could be assessed using the FFE3D sequence, were temporal phases = 7 and timing increment = 200 ms.ConclusionmASTAR permits hemodynamic evaluation and clearly depicts portal vein morphology in a single acquisition.

PDF-053　未破裂脳動脈瘤における 2D-Cine PC法と 3D-Cine PC法の比較検討
Comparison of 2D-Cine PC and 3D-Cine PC in unruptured cerebral aneurysm

佐藤　兼也（青森県立中央病院 放射線部）
Kenya Sato[1], Tetsuhiro Saito[1], Noriko Maeda[1], Yoko Yokoyama[1], Ryoichi Yamauchi[1], Kazuki Kudo[1], Atsushi Saito[2], Hiroshi Midorikawa[3], Tatsuya Sasaki[2], Koichi Shibutani[1], Atsushi Nozaki[4]
[1]Aomori Prefectural Central Hospital , Department of Radiology, [2]Aomori Prefectural Central Hospital , Department of Neurosurgery, [3]Aomori Prefectural Central Hospital , Department of Neuroendvascular Therapy, [4]GE Health Care Japan

【要旨】2D-Cine PCを利用した未破裂脳動脈瘤の流体解析はスライス間の時空の違いにより3D-Cine PCとの間に差異があることが懸念される。3T MRI装置で同一患者においてそれぞれを撮像し検証した。3D-PCをControlとした場合、2D-CinePCにおいても血管壁（3D-TOF MRA）との位置ずれがなければ同等であることが示唆された。

Purpose:The 2D-PC is able to analyze the direction of the flow and the speed in Cine mode. The thinness of at least approximately 1 mm is required to perform three-dimensional blood flow analysis of cerebral aneurysm. Performing the Comparison of analyzing them three-dimensionally by piling up thin 2D-Cine PC slices and 3D-Cine PC.Methods: Used MR-System was Discovery750W 3T scanner by GE Health care. And used Head24Ch Coil. Slice thickness of 2D-Cine PC is 1mm gapless. Scan range was including a cerebral aneurysm. Therefore Slice number was 17~21. Phase number 11, FOV =180mm, matrix size =256*192,spatial resolution =0.703*0.938. Imaging the 3D-TOF MRA at the same coordinates with the same spatial resolution before and after 2D-Cine PC imaging, and with the vessel wall data when analysis.3D-Cine PC is Phase number 11,FOV =180mm, matrix size =180*180,spatial resolution =0.703*0.938, slice thickness=1mm(ZIP2).The flow rate of the parent artery was the peak flow rate + 10cm / sec of the results measured by 2D-PC. Its value was VENC on the PC(2D-Cine PC and 3D-Cine PC).We transfer data provided with 2D-Cine PC and 3D-Cine PC to product made in FLOVA(R-Tech company) and analyze MR Flow Dynamic Study(MRFD).The vessel was captured by the 3D TOF MRA in 2D-PC was analyzed WSS and CSI as vessel wall.Results: 2D-PC there is no positional deviation of the blood vessel wall resulted equivalent to 3D-PC. WSS and CSI was a similar result. It showed a similar trend for except the above area.Conclusion: 2D-Cine PC and 3D-Cine PC it was considered that the difference results. The reason is because the space-time of each slice is different. Though, it can be seen from the our results it was found that the position of the vessel wall and the PC data.

PDF-054　mASTAR法を用いた末梢血管描出の検討
Evaluation of Depiction of Peripheral Arteries with mASTAR

北村　美穂（東芝メディカルシステムズ株式会社 MRI営業部）
Miho Kitamura[1], Ayako Ninomiya[1], Naotaka Sakashita[2], Yuichi Yamashita[1]
[1]MRI Sales Department, Toshiba Medical Systems Corpora tion, [2]Center for Medical Research and Development, Toshiba Medical Systems Corpora tion

【要旨】手など末梢血管描出には、TOF法、FBI法、Time-SLIP法などがあるが、これらは血管の全体像の描出が目的で動態的な観察は難しい。また、同期を併用する撮像法であり、撮像断面に依存する撮像法もある。そこで、mASTAR法を使用することで非同期で簡便にかつ血管の全体像および動態的な描出が同時に可能であったため報告する。

[Purpose]Evaluation of peripheral hemodynamics is important for clinical diagnosis. TOF and FBI are usually employed to depict peripheral arteries. Although vessels can be depicted using these methods, it is difficult to evaluate hemodynamics. Time-SLIP is suitable for evaluating hemodynamics, but it requires multiple scans. Furthermore, all these methods are affected by pulsation and suffer from limited imaging orientations. It is therefore difficult to depict vessels and evaluate hemodynamics simultaneously in a short examination time. We investigated the usefulness of dynamic depiction of peripheral arteries with mASTAR.[Methods]All studies were performed on a 3-T MRI system (Vantage Titan™3T; Toshiba Medical Systems). Images of the peripheral vessels of the hands were acquired in healthy volunteers. Informed consent was obtained from all subjects. FFE3D:mASTAR was used to image the vessels. The spatial resolution, imaging orientation, and slab thickness for optimal depiction of the vessels were investigated. The inversion time (TI), TI step, and number of steps for optimal evaluation of peripheral hemodynamics were also investigated.[Results]The imaging area and labeling position could be flexibly set because mASTAR allows imaging in any desired orientation. Optimizing the slab thickness resulted in improved depiction and shorter scan times. A scan protocol with 7 temporal phases (TI 200-1400 ms) was effective for evaluating peripheral hemodynamics. Furthermore, the peripheral arteries could be depicted by combining the images of all temporal phases.[Conclusion]mASTAR makes it possible to evaluate peripheral hemodynamics and depict peripheral arteries simultaneously in a short examination time. This method is considered to provide useful clinical information.

PDF-055　坐骨神経結紮による慢性疼痛モデルマウスの脊髄において末梢マクロファージの浸潤を確認できた
Labeled peripheral macrophages were found in the spinal cord of chronic constriction injury model mice by MRI

吉田　将太（大阪大学 免疫学フロンティア研究センター）
Shota Yoshida[1], Yuki Mori[1,2], Ting Chen[1,2], Yoshichika Yoshioka[1,2]

[1]WPI Immunology Frontier Research Center (IFReC), Osaka University, [2]Center for Information and Neural Networks (CiNet), National Institute of Information and Communications Technology (NICT) and Osaka University

【要旨】坐骨神経結紮による慢性痛モデルマウスを作り、刺激の通路である脊髄において、末梢マクロファージの関与を調べた。坐骨神経結紮による慢性疼痛モデルマウスにおいて、末梢マクロファージの浸潤が脊髄に認められた。

Purpose: Chronic constriction injury (CCI) mice have been used as a chronic pain model. Recently immune system has been reported to play an important role in the central nervous system (CNS) and to concern to a chronic pain. The spinal cord, where sensations from sciatic nerve are mediated, is important part of CCI model. Here we tried to visualize the modulation of the immune system such as macrophages' infiltration into the spinal cord of CCI model mice by MRI.Methods: C57BL6 mice and an 11.7 MRI (Bruker) scanner were used. Macrophages were labeled in vivo by intra venous administration of super paramagnetic iron oxide particles (Resovist, I'rom Pharmaceutical). CCI model mice were made by 4 times' loose constriction of sciatic nerve. For comparison, sham and non-treated control mice were also examined. CCI and sham mice were administered Resovist 8 days after operation. Mice were perfused and fixed one day after administration of Resovist. High resolution MRI of vertebras was obtained ex vivo using 2D- & 3D-FLASH sequences. Vertebras were soaked in 5mM Gd solution for one day before MRI scan.Results and Discussions: We found several labeled macrophages in the spinal cord of CCI model mice but not in sham and non-treated control mice. This shows that peripheral macrophages were recruited into the spinal cord of the CCI model mice and that the recruitment of macrophages was caused not by the scar of the surgery but by the 4 times' loose constriction of sciatic nerve. These results indicate that the CCI causes the modulation of immune system in the spinal cord.Conclusion: We could visualize several macrophages in the spinal cord of CCI chronic pain model mice using MRI.

PDF-056　位相エンコード数の低減によるMRIの高速撮像化の可能性
The possibility of high-speed imaging of MRI by the reduction of the number of phase encodes

山田　徹（東海大学大学院 工学研究科 情報理工学専攻）
Toru Yamada[1], Satoshi Yatsushiro[2], Saeko Sunohara[1], Ken Takizawa[3]

[1]Graduate School of Engineering, Tokai University, [2]Graduate School of Science and Technology, Tokai University, [3]Department of Neurosurgery, Tokai University School of Medicine

【要旨】本研究では，PC法による高速撮像化を目的として，k空間の位相エンコード数を減らすことによる速度情報への影響を検討した．位相エンコード数を18％まで減らした時のフレームレートは約40msで，設定したROI内の速度時系列の残差平方和は0.0083 cm/sであった．

Introduction
PC technique can visualize cerebrospinal fluid (CSF) motion, but it has a problem of longer acquisition time. Moreover, we have performed measuring CSF velocity by asynchronous 2D-PC. It might not fully seize cardiac-driven CSF motion since the frame rate was 217 ms. When the k-space undersampling effect on CSF velocity is sufficiently smaller, the frame rate can be shorter. In this study, the effect of undersampling of phase encoding direction on velocity was examined.
Method
In this study, we aimed for frame rate of about 80 ms. To ascertain the undersampling effect, PC technique was applied to continuous flow phantom using 1.5T-MRI. Imaging parameters are followings: matrix, 256×256; TR/TE, 18.5/8.1 ms; VENC, 5 cm/s. Figure1 shows the process of this analysis. Velocities between the original and undersampled was compared.
Result
When the number of phase encodings was 18%, residual sum of squares of the velocities of the region of interest (ROI) was 0.0083cm/s with about 40 ms/frame.
Conclusion
The undersampling effect on the velocity was little in steady flow; in addition, the frame rate was sufficiently shorter.

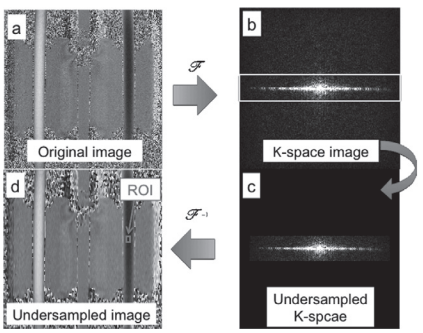

PDF-057　7T ヒト脳化学交換飽和移動 (CEST) イメージング
Chemical exchange saturation transfer imaging in human brain at 7T

栗林　秀人（シーメンスヘルスケア株式会社）
Hideto Kuribayashi[1], Yuta Urushibata[1], Tomohisa Okada[2], Benjiamin Schmitt[1], Kaori Togashi[3]
[1]Siemens Healthcare, [2]Human Brain Research Center, Kyoto University Graduate School of Medicine,
[3]Department of Diagnostic Imaging and Nuclear Medicine, Kyoto University Graduate School of Medicine

【要旨】7T 化学交換飽和移動 (CEST) イメージングは 3T と比較して アミドプロトン移動 (APT) コントラストが高いことに加えて、核オーバーハウザー効果 (NOE) コントラストが現れてくる。ヒトボランティア脳 7T CEST イメージングにおいても、NOE コントラストが APT コントラストよりも強く現れた。

Introduction: Chemical exchange saturation transfer (CEST) imaging has a potential to detect metabolic changes in vivo. CEST imaging on ultra high field may have some advantages of high sensitivity and large separation of chemical shift. For introduction of CEST imaging to clinical 7T imaging protocols, CEST imaging pulse sequence was tested both at 3T and 7T.Methods: Phantom experiments and volunteer brain scans were performed on 3T (MAGNETOM Prisma^{fit}, Siemens) and 7T (Siemens) whole-body scanners. Commercial sports nutrition (Amino Vital, Ajinomoto) with different amino acid concentrations was used as CEST phantom. A single-slice axial image (1-cm above from an AC-PC line in brains) was obtained using a prototype 2D FLASH sequence with CEST presaturation, which consisted of a series of 5 Gaussian-shaped RF pulses (100-ms duration, 100-ms gap, B1 = 1 μT) followed by spoiling gradients. Range and resolution of presaturation RF offsets were ± 6 ppm and 0.1 ppm, respectively, relative to the water resonance. This study was approved by the local ethics committee.Results: The phantoms generated CEST contrast, which correlated with amino acid concentration both at 3T and 7T. The CEST contrast around 3 ppm, i.e. amide proton transfer (APT) contrast, at 7T was clearly higher than that at 3T. In addition to the APT contrast, contrast from nuclear Overhauser effect (NOE) around -2.7 ppm was observed at 7T. Volunteer brain CEST images at 7T showed both APT and NOE contrast. NOE contrast was higher than APT in almost all of pixels in the brain.Discussion: This study showed visibility of NOE contrast at 7T. Moreover, NOE effect was much stronger than ATP effect in volunteer brain at 7T. NOE effect may give us more valuable information from 7T CEST imaging compared to APT effect.

PDF-058　スピンエコー型ナビゲータを併用した 1H-MRS において VOI とトラッカーの設定位置がコリン濃度に及ぼす影響
Measurements of choline contents by ^{1}H-MRS are affected by the position of VOI and navigator tracker in respiratory gating: A phantom study

高森　清華（北海道大学病院 医療技術部 放射線部門）
Sayaka Takamori[1], Kinya Ishizaka[1], Satoshi Yabusaki[2], Suzuko Aoike[1], Hiroyuki Hamaguchi[1], Kohsuke Kudo[2]
[1]Department of Radiological Technology, Hokkaido University Hospital, [2]Department of Diagnostic and Interventional Radiology, Hokkaido University Hospital

【要旨】スピンエコー型ナビゲータを併用した 1H-MRS において VOI とナビゲータトラッカーの設定位置がコリン濃度に及ぼす影響を調べた。ナビゲータパルスがコリン濃度を増加させるため、VOI をナビゲータパルスと近づけずに設定する事を提案する。

Introduction
Respiratory gating is necessary for ^{1}H-MRS in the upper abdomen. GE type navigator is usually used for clinical imaging; however, we found that it affected the measurement of choline contents (CC) in MRS in the previous study. The aim of this study was to evaluate the feasibility of SE type navigator for MRS using moving phantom.
Methods
The spherical MRS phantom was scanned by 3T MRI with a single voxel PRESS sequence. The phantom was mechanically moved to-and-fro in z direction. The spin echo type navigator (NV) and the respiratory bellows gating (BG) were used for the motion correction. MRS scans were conducted with nine locations of VOI, from the center to right and left with 10 mm interval (R_{40}, R_{30}, R_{20}, R_{10}, C, L_{10}, L_{20}, L_{30}, L_{40}), and the scans were repeated for 10 times for each VOI. LC model was used for the quantification of CC. The difference of CC concentration in various locations was evaluated by ANOVA, and the mean concentrations of CC between NV and BG were compared.
Results
CC concentrations in various locations were constant in BG, and no significant difference among the locations was noted ($p = 0.627$). In contrast, CC concentration was the highest in C than the other locations in NV, and significant difference among the locations was noted ($p < 0.001$). In the multiple comparison test, C, R_{10}, and L_{10} tented to be higher than the other locations. CC concentrations of NV were significantly higher than those of BG at C (NV: 2.28 ± 0.14, BG: 1.81 ± 0.16) and L_{10} (NV: 2.06 ± 0.10, BG : 1.79 ± 0.11), and there were no significant differences in the other locations.
Conclusions
CC measurement was affected by the location of SE type navigator and VOI. However, overestimation of CC concentration was only noted when the VOI was located near the navigator.

PDF-059　早産児の新生児期における脳内代謝物濃度／脳容積とその予後との関連性
Relationship between brain metabolite concentrations/volumes during neonatal period and developmental prognosis in premature birth babies

富安もよこ（量研機構 放医研）
Moyoko Tomiyasu[1,2,3], Noriko Aida[1,3], Jun Shibasaki[3], Seiichi Tomotaki[3], Masahiko Sato[1,3], Kouki Kusagiri[1,3], Yasutake Muramoto[1,3], Yuichi Suzuki[1,3], Yukako Kawasaki[4], Eiji Shimizu[2], Takayuki Obata[1]

[1]National Institutes for Quantum and Radiological Science and Technology, [2]Chiba University, [3]Kanagawa Children's Medical Center, [4]University of Toyama

【要旨】本研究は、早産児の新生児期における脳代謝物濃度／脳容積と、修正年齢1歳6ヶ月時の発達の総合指数（DQ）との関連性を調べ、早産児の予後予測の早期指標となり得るかを調査した。これら間では有意な相関は見られず、成長に伴う濃度/容積の補正や発達評価のより詳細な分類などによる検討が必要であることが示唆された。

[Purpose] It is well known that the premature birth is associated with increased risk of neurological and physical problems. The purpose of this study was to investigate whether the brain metabolite concentration (conc) and/or volumes in neonates can be an index of the prognosis for the premature birth.[Methods] Twenty-six subjects with premature birth (gestational age: 23-33 weeks) were included. At their postconceptional age of 34-40 weeks, they had brain MRI (Siemens 3T) including MRS (PRESS, TE 30ms, TR 5s). The metabolite conc were calculated using LCModel with water conc of 46.9M. Using T2W images (TE 119-123ms, TR 5s), the volumes were measured using ROI editor (John Hopkins). At a corrected age of 1.5 years, they had developmental quotient (DQ) by Kyoto Scale of Psychological Development. Correlations between the conc and DQ, and the volume and DQ were investigated using Spearman's rank correlation coefficients. The conc change with development was considered. [Results] The creatine, choline, N-acetylaspartate, myo-inositol, and glutamate/glutamine complex conc were 5.4-9.0, 1.3-2.6, 3.0-6.4, 4.8-8.8, and 3.8-11.5mM, in the basal ganglia, respectively, and 3.8-5.9, 1.5-2.3, 2.4-6.1, 5.7-9.3, and 3.9-8.9mM, in the centrum semiovale. The supratentorial, cerebellum, and intracranial volumes were 222-332, 13-22, and 352-550mL, respectively; The DQ were 44-119. No correlations were found between the metabolite conc or volumes and DQ. [Discussion] The DQ is overall index, and in this study fine classification of the DQ was not considered. Also, the volume change with development was not considered. Although we could not find any correlation, more detail studies are needed to confirm whether the MR data in neonates can be an index of the prognosis for premature birth.

PDF-060　31P MRS 計測の肝臓 3T MRI 臨床検査への導入
Introduction of 31P MR Spectroscopy measurements to clinical human liver image examination at 3T

磯田　裕義（京都大学 医学部 附属病院 先制医療・生活習慣病研究センター）
Hiroyoshi Isoda[1], Hideto Kuribayashi[2], Shun Asahina[2], Katsutoshi Murata[2], Ryutaro Nakagami[2], Yoshihiko Kawabata[3], Kaori Togashi[4]

[1]Preemptive Medicine and Lifestyle-related Disease Research Center, [2]Siemen, [3]Takashima Seisakusho, [4]Department of Diagnostic Imaging and Nuclear Medicine Kyoto University Graduate School of Medicin

【要旨】ボランティア肝臓 31P MRS 計測を 3T MRI および 120 mm 径ループコイルを用いて行った。3D CSI が 17 分の検査時間で十分な感度で計測可能であった。

Introduction: 31P magnetic resonance spectroscopy (MRS) is a valuable tool to detect metabolites related to energy and lipids non-invasively. Applying that to the liver, 31P MRS signals may give us useful information in certain diseases. For introduction of 31P MRS measurements to clinical liver image examination at 3T, commercially available 31P MRS pulse sequences and an RF coil were tested.Methods: Volunteer scans were performed on a 3T (MAGNETOM Skyra, Siemens) scanner with multinuclei option. A 31P/1H loop RF coil (120-mm diameter, Takashima Seisakusho) was placed on the abdomen of supine-positioned volunteers to scan the liver. 31P MRS without localization was acquired with TR=1 s, a 0.2-ms hard RF pulse, 2500-Hz spectral width, 128 FID data points. 31P 3D chemical shift imaging (CSI) was acquired with the parameters above, (200-mm)3 3D FOV and 8 x 8 x 8 matrix. Average-weighting k-space sampling was applied. RF power for 31P MRS was previously defined using a 20 mM Na3PO4.12H2O (Wako) solution phantom.Results: 31P MRS without localization with sufficient signal-to-noise ratio could be obtained with 16-average, i.e. total scan time was 16 seconds. A phosphocreatine (PCr) peak was dominant in the spectra. 31P 3D CSI were obtained within 17-minute total scan time. PCr was dominant in volume close to the abdominal surface. In volumes under the surface, adenosine triphosphate (ATP) was dominant and PCr was negligible. It was difficult to assign peaks in low field region other than inorganic phosphate (Pi) in the liver.Discussion: 31P 3D CSI sequence could obtain spectra in the liver without contamination from abdominal muscle. These protocols with 1-s TR contribute to reduce total examination time, but not suitable for long-T1 31P metabolites.

PDF-061　MRI検査における閉所での不安感を解消する広視野バーチャル映像表示技術
Hyper-realistic display system with wide field of view to reduce the stress and anxiety for MRI examination

石崎　庄治（東芝メディカルシステムズ 株式会社）
Shoji Ishizaki[1], Yu Ueda[1], Hiromitsu Takamori[1], Takashi Sasaki[2]
[1]Toshiba Medical Systems Corporation, [2]Toshiba corporate R&D Center

【要旨】MRI装置の検査空間内で広視野・高臨場感映像を体験できる技術を開発した。ドーム形スクリーンをボア内に設置し、ボア外からスクリーンとボア内壁に映像を投影する。患者はボア内であっても、広視野のバーチャル空間を体感できる。本システムを体験したすべての人から、圧迫感は低減されているとのアンケート結果を得た。

The inspection space (bore) in MRI causes anxiety and stress to a patient. In the case of head imaging, a mirror on head coil has been used. And patients can look at images installed outside the bore. However, the equipment is insufficient to relax because of its small visual field. In the light of human vision, it is known that visual stimuli with wide field of view (stimulating both of central and peripheral vision) is able to provide a presence of hyper-realistic visual space. We have developed a hyper-realistic display system to provide images with wide field of view. The system can provide the patients with central and peripheral vision.
Our hyper-realistic display consists with the dome screen and the mirror that placed at front of patient's face. The projected the image illuminate both the dome screen and the inner bore surface. A patient observes both the images and illuminated inner bore with reflected by the mirror, and obtains wide visual space.
We evaluated the effect of the system from questionnaire survey for experienced person. It could be confirmed that pressure is reduced substantially compared with the past with all people even in the case of claustrophobia.

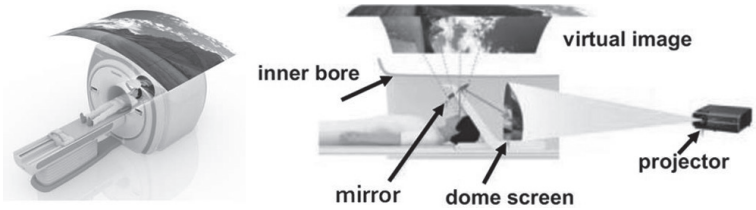

PDF-062　3T MRI装置の設置面積削減の検討
Considering minimized installation space for a 3T MRI system

石原　隆尋（東芝メディカルシステムズ株式会社）
Takahiro Ishihara, Naoki Imamura, Kazuyuki Soejima
TOSHIBA MEDICAL SYSTEMS

【要旨】構成要素の整理、キャビネット統合、メンテナンススペースの最適化により、静音化機構などの装置性能を犠牲にすることなく、従来3T装置に比べ22%の面積削減を達成した。これにより、一般的な1.5T MRI装置からの置き換えは、設置スペースの再検討や電源設備の増設も最小限に実施可能となった。

[Purpose] In general, 3T MRI provides high quality images when compared with low magnetic field system. Therefore, 3T MRI systems can be considered to replace 1.5T systems that have been installed in existing locations over the past 10 years. In the past, it has been difficult to replace these existing 1.5T MRI systems due the large footprint required for 3T MRI systems. Now a wide bore high performance 3T MRI system can be considered for installation in small footprint without constraints in the area for an existing space.[Methods] The footprint reduction was examined by following two approaches.A) We organized the MRI components and developed a cabinet that can be installed beside the magnet in order to effectively utilize the dead space of the scan room. We assembled some electric circuits that are not affected by magnetic fields, including digital RF circuit, into this cabinet. As a result, the number of parts in the computer room was reduced and the integration of the cabinet was realized.B) We analyzed the maintenance space in order to reduce the minimum required area while keeping the maintainability.[Results] Compared to the conventional 3T MRI.A) Total 12% footprint has been reduced by 1) Relocation of the A/D converter and some control circuits to the cabinet beside the magnet and 2) Reduction of the number of units by the integration of the control unit and the RF unit.B) Total 45% maintenance space has been reduced by limiting the access direction by relocating the internal components in the cabinets.[Conclusion] The installation space was reduced by 24% compared with the conventional 3T MRI and resulted in 27 m2 approximately. New 3T MRI is equipped with the latest features now allows replacement of the conventional1.5T MRI in existing space.

PDF-063　VRFA撮像後のMPR処理における空間分解能の方向依存性の検討
Evaluation of the directional dependency of spatial resolution at MPR processing after using VRFA

加々美　智（福岡リハビリテーション病院）
Satoshi Kagami

Fukuoka rehabilitation hospital

【要旨】VRFAを用い表示分解能が1mmアイソボクセルとなるように設定し、櫛ファントムを3D撮像した。3軸のMPRを作成すると、分解能の方向依存性が生じた。感度補正マップ、VRFAの角度、ETL、Echo Space、スライス厚等のパラメーターによる画質への影響を視覚評価し、方向依存性が少ない条件を検討した。

[Background] Increase of ETL and shortening of echo space with FSE enabled the measurement in the short time. Optimizing VRFA permitted reduction of the bullring artifact and SAR, and this refinement facilitated 3D-FSE measurement in the whole body.After 3D measurement, you can observe images multidirectionally by MPR, so the observation in any direction is possible after inspection. However, in spite of isotropic voxel, direction dependence occurred in MPR.[Purpose]Optimization of the condition that influence spatial resolution of VRFA.[Method] I made comb phantom (1mm interval), and changed the photography condition of sensitivity revision map and VRFA-FSE and evaluate visually. The spatial resolution set 1*1*1mm.[Considerations]Influence of the sensitivity correction map. Influence of ETL. Influence of echo space. Influence of the angle of the VRFA. Influence of Slice thickness. [Result]In comparison with frequency direction and the phase direction, the resolution of the slice direction decreased. When the slice thickness sets to 0.9 mm, the resolution became equal. The influences of sensitivity revision map, ETL, echo space, and VRFA are little.[Summary]I examined parameters that affect the resolution in the VRFA. Imaging conditions were able to set to parameter of less direction dependence.

PDF-064　model-based iterative reconstructionを利用したT2マッピングの定量化
Quantitative t2 mapping accelerated by model-based iterative reconstruction

小林　謙一（獨協医科大学病院 放射線部）
Kenichi Kobayashi[1], Kiyotaka Kato[1], Kiyoshi Oguro[1], Yasushi Kaji[2], Hiroshi Imai[3]

[1]Dokkyo Medical University Radiologic part, [2]Dokkyo Medical University Radiology, [3]Siemens Healthcare K.K.

【要旨】T2値の測定には時間がかかるが最近開発されたmodel-based iterative reconstructionを使用することにより大幅な時間短縮が出来る可能性がある。従来の方法と同様の結果を示すための条件を検討し5倍速まで短縮可能であった。

Quantitative T2 mapping accelerated by model-based iterative reconstruction [Background] T2 value has been widely used for a quantitative index. However, conventional multi echo SE method requires long scan time. Recently developed model-based iterative reconstruction method could largely shorten imaging time by direct pixel-wise estimation of T2 values from highly undersampled raw data.[Purpose] To evaluate the accuracy of T2 values estimated with model-based iteration method.[Methods] We prepared a T2 phantom which was consisted of thirteen small containers with diluted solutions of Bothdel (Kyowa Hakko Kirin) having different concentrations. It was scanned by clinical MR scanner MAGNETOM Skyra (SIEMENS, Erlangen, Germany) and 3 types of multi echo T2 mapping protocols, which were based on SE, TSE and prototype undersampled SE. Moreover, the influence of iPAT, the number of multi-echo, maximum echo time and undersampling factor were evaluated. [Results] The estimated T2 values with model-based method showed good agreement with it from a conventional SE method in our target T2 value range of 20-200ms. 5-fold acceleration to conventional method was available by decreasing maximum echo time.

PDF-065　乳輪再建術に使用するインクが磁場不均一を及ぼす影響についての検討
Influences of cosmetic pigments for nipple areola tattoo after breast reconstruction on artifacts and magnetic attractive force in MR imaging

前田　晋義（社会医療法人 生長会 府中病院）
Masayoshi Maeda[1], Mamoru Ishimoto[1], Kazuhiro Kawano[1], Miho Kita[2], Kenichi Takenaka[1], Gouichi Haraoka[3], Morio Sato[4]

[1]Department of Radiological Technology, Seichokai Fuchu Hospital., [2]Department of Radiology, Seichokai Fuchu Hospital., [3]Department of plastic and reconstructive surgery, Seichokai Fuchu Hospital., [4]Department of Radiology, Hannann Municipal Hospital

【要旨】乳房形成術施行時に使用する顔料(7種)がMRIに及ぼす影響を 1.磁気吸引力2.アーチファクトについて検討を行った結果、磁気吸引力は2種、アーチファクトは3種の顔料にて出現した。中でも酸化鉄含有量が多いと思われる顔料:MUD PIEにて、両者の影響が最も強く現れた。

[Objective]
Breast reconstruction has been prevailed for patients with breast cancer. Nipple areola tattoo is being performed following breast reconstruction. The objective of this study is to investigate the influences of cosmetic pigments used for nipple areola tattoo on artifacts and magnetic attractive force in MR imaging.
[Materials and Methods]
Seven cosmetic pigment-solutions (PURE; Biotouch, USA) were used; 1.MUSHROOM 2.TOFFEE 3.PINK BRICK 4.MAGIC COLOR 5.MUD PIE 6.NUDE 7.MILK CHOCO.
(1) One droplet of each pigment solution was dropped to each of seven small gauzes which was hung down with a cotton thread at the bore of the magnet of 3T MR scanner (Magnetom Skyra; Siemens, Germany). The angle of the thread attracted from the vertical axis was measured to assess the magnetic attraction force.
(2) The seven gazes were stuck on copper sulfate solution phantom. Then, MR images were obtained using TSE, GRE, and DWI sequences for MR mammography to assess the degree of the artifacts.
[Results]
(1) Two of the seven gazes with pigment solutions showed magnetic attraction. The attraction angle of the gaze with No.5 MUD PIE solution was the greatest(37°) of the seven pigments solutions.
(2) Three of the seven pigments solutions produced artifacts on MR images.The artifacts on MR images were most prominent in No.5 MUD PIE solution.
[Discussions and Conclusions]
Three of the seven pigments solutions produced artifacts on MR images and two of them showed magnetic attraction. All of the pigments tested are known to contain valuable amounts of iron oxide particles. Of the seven pigments solutions, MUD PIE solution affected MR imaging most greatly in artifacts and magnetic attraction. Iron oxide particles may cause artifacts and magnetic attractive force in MR imaging.

PDF-066　MRI検査時に生じるストレス　－脈波解析－
Psychological Stress in Patients Undergoing MR Imaging -Plethysmogram analysis-

門間　正彦（茨城県立医療大学 保健医療学部 放射線技術科学科）
Masahiko Monma[1], Rika Kikuti[1], Naho Mitimura[1], Suzuka Wakui[1], Yoshikazu Shimada[1], Hiraku Kawamura[1], Yoshiyuki Ishimori[1], Mitihiro Kawano[2]

[1]Ibaraki Prefectural University of Health Science, School of Health Science, Department of Radiological Sciences, [2]Ibaraki Prefectural University of Health Science, School of Health Science, Department of Nursing

【要旨】 生体の自律神経活動を示す脈波データから得られる脈波高（PWA）より、MRI検査時に生じるストレスについて検討した。　検査前・検査中・検査後のPWAに対しt検定を行った結果、統計的な有意差があった。また、PWAと主観的ストレスとの相関を調べるためにt検定を行った結果、相関の有意差は無いという結果になった。

Purpose: MRI can cause physical and mental stress due to its various characteristics. We investigated the level of stress experienced during MRI. As an indicator of stress, we focused on pulse wave amplitude (PWA) obtained from the photoplethysmography, which indicates autonomic activity in the body. we investigated relationships between simultaneously obtained questionnaire results (visual analog scale [VAS]) and these indicators. Methods: Finger plethysmography was continuously performed before, during, and after MRI for a total of 14 healthy individuals (9 men, 5 women) who gave their consent to participate.In the present study, the following definitions from a preceding study were used: promotion of sympathetic activity indicates a "state of stress", whereas promotion of parasympathetic activity indicates a "state of relaxation". In other words, a low PWA indicate a state of stress. Measurements were taken for 3 min before and after MRI, and for 20 min during MRI. Finger plethysmography measurements were initiated after a 5-min rest period. In addition, subjective stress was measured using VAS before and after MRI.Results: Comparison of data for the 14 subjects before, during, and after MRI showed that the PWA decreased during MRI in 12 subjects. Mean values for PWA decreased during MRI. Measurements of subjective stress showed that most subjects experienced more stress during MRI than either before or after. T-test performed to investigate correlations between PWA and subjective stress showed that no significant differences existed.Conclusion: The results for PWA obtained from the photoplethysmography showed that most subjects experienced stress during MRI indicates, which indicates the need to pay attention to patient stress when conducting MRI.

PDF-067 生体MRAのB1不均一性に対する超音波検査用ジェルを用いた自作誘電パッドのファントム実験による検証
The effect of a homemade dielectric pad with using commercially available ultrasound gel to correct B1 inhomogeneity in body MRA - a phantom study-

黒木　佑椰（社会医療法人 共愛会 戸畑共立病院）
Yuuya Kuroki[1], Akiyoshi Yamamoto[1], Hiroki Matoba[1], Daiji Uchiyama[1], Seigo Yosida[1], Katsumi Nakamura[1], Mitsue Miyazaki[2]

[1]Tobatakyouritsu hospital, [2]Toshiba Medical Research Institute USA

【要旨】3T装置を用いたFBI法では、しばしば被験者の体型によってB1の不均一性が主な原因と思われる画質の劣化が発生する。この問題に対処するために超音波検査用ジェルを用いた誘電パッドを作成してファントム実験にて検証を行った。その結果、B1不均一性の改善の可能性が示唆された。

PURPOSE To evaluate an effect of a homemade ultrasound gel pad to correct the B1 inhomogeneity, which would degrade the image quality of non-contrast MR angiography especially at 3T.MATERIALS and METHODSA pair of two cylindrical phantoms contained copper sulfate with different concentration of 0.32% and 0.055% was made, which gave different B1 values. The phantom was supposed to mimic as left and right thighs with inhomogeneous B1 circumstances. Commercially available ultrasound gel was placed into a plastic bag (20 x 15cm) and adjusted its thickness to 2 cm. The pads were placed on the surface of the cylindrical phantoms in seven different manners. The effect of US gel pad was compared with those of other pads made with water, BB bullets, and rinse-free rice. B1 value ratio index (BRI) was calculated using ROI analysis as follows; BRI = (B1 value of A) - (B1 value of B) / B1 value of A x100.Acquisition parameters of 2D SSFSE were as follows; TR 3000msec, TE 30msec, ETS 5msec, slice thickness 10mm, FOV 40cm X 40cm, and matrix 128 X 128.RESULTSBRI was significantly decreased from 24.1 of without US gel pad to 15.6 % with US gel pad. The effects of US gel pads were greater than those of water pads. BB bullets pads and rinse-free rice pads showed little effect for B1 value.CONCLUSIONThe US gel pad improves the RF penetration and can correct B1 inhomogeneity.

PDF-068 木質材料による良好なSNRと異方性を持つ位置決め用皮膚表面マーカの提案と検証
Surface marker localization devices with sufficient signal-to-noise ratio: verification with wood

鈴木　政司（首都大学東京 大学院 放射線）
Masashi Suzuki, Atsushi Senoo

Tokyo Metropolitan University

【要旨】MRI検査に使用される皮膚表面マーカには，SNRの不足や，異方性がないなどの問題点がある．そのため木材をマーカ材料として提案し検証した．ブレスケアやベビーオイルは脂肪抑制でSNRが低下し，MR-SPOTSは異方性がなかった．木材はいずれのシーケンスでも十分なSNRと異方性を持つためFAmapでも観察が可能であった．

Introduction: Surface markers are utilized in MRI examination to highlight the existence and location of masses and the cause of pain. Conventional surface markers pose problems such as incorrect shape, low signal-to-noise ratio(SNR), and high cost. The improvement of surface markers facilitates the identification of findings on images and contributes to their interpretation. The aim of the present study was to suggest and verify materials as surface markers with a sufficient SNR for various sequences.
Materials and Methods: An Achieva 3.0T TX Philips MRI System with a QD head coil was used. Protocols included SURVEY (FFE), T1W (SE, TE/TR 10/600), T2W (TSE, TE/TR 100/3000), PDW (TSE, TE/TR 30/3500), T2-star weighted (TE/TR 16/300), T1W SPIR (SE, TE/TR 10/600), T2W SPAIR (TSE, TE/TR 100/3000), PDW SPAIR (TSE, TE/TR 30/3500), STIR (TE/TR 30/5000), DWI (TE/TR 79/5000), and DTI (TE/TR 65/5000), with the following parameters: FOV 170 mm × 127.5 mm, matrix 256 × 192, slice thickness/gap 4 mm/1 mm. Other parameters were used as Philips' default. SNR estimates were assessed using breath care, MR-SPOTS, baby oil, and wood. The SNR data were analyzed by the ImageJ.
Results: The breath care had SNR under 46 for three of the fat-suppression sequences and a low signal value. In DWI/FAmap, SNR was not observed, and in the others, it was above 125. The baby oil had SNR under 25 for three of fat-suppression sequences and a low signal value. In DWI/FAmap, SNR was not observed, and in the others, it was above 64. The MR-SPOTS had SNR above 172 for all sequences, with the exception of FAmap, in which it was not observed. The wood had SNR of 88.5 in FAmap, and in the others, it was above 117.
Conclusion: The wood has sufficient SNR and anisotropy.

PDF-069　3D-eTHRIVEにおけるk-space充填配列によるMR画像への影響
Influence of MR Imaging by changing the k-space Ordering Scheme in 3D - eTHRIVE

大塚　和人（独立行政法人 国立病院機構 宇都宮病院）
Kazuto Ohtsuka

National Hospital Organization Utsunomiya National Hospital

【要旨】e-THRIVEは、最初にエコーをk-space orderingする方向をinner loopとして設定が行われ、この設定方向（スライス・位相エンコード）を任意に変えることができるが、撮像時間・SPAIR TR・null pointも大きく変化する。そこで、k-space orderingの方向によって画像に与える影響について検討したので報告する。

[Purpose] To verify influence of the MR Imaging by k-space Ordering Scheme in 3D – eTHRIVE.[Materials and Methods] All examinations were performed on a 1.5T clinical system (Achieve 3.2 Release) with a 4-channel body coil. We used 3D-e THRIVE without SENSE / Half Scan / Oversampling, combined the turbo direction (Z and Y) and k-space ordering scheme(innerloop/outerloop=linear/linear;linear/high-low;linear/low-high;linear/rev-linear;low-high/linear;low-high/high-low;low-high/low-high;low-high/rev-linear;rev-linear/linear;rev-linear/high-low; rev-linear/low-high; rev-linear/rev-linear).1) I calculated scan time, using the following expressions a) and b). a) Scan time = SPAIR TR x (phase encodings -1) +SPAIR inv. delay + Shot duration/2 = SPAIR TR x phase encodings (inner loop is slice encode.) b) Scan time = SPAIR TR x (slice encodings -1) + SPAIR inv. delay + Shot duration/2 = SPAIR TR x slice encodings (inner loop is phase encode.)2) I calculated contrast to noise ratio (CNR) from the following expressions c), using the signal intensity of the baby oil and water. c) CNR = (SI fat – SI water) / (SI fat + SI water)3) I measured the spatial resolution of MR images using the Image J.[Results] 1) At scan time, the turbo direction Y shortened than turbo direction Z. 2) The CNR showed a high value in the turbo direction Y than turbo direction Z, when using SPAIR.In addition, CNR showed about the same value, when using no SPAIR. 3) The difference was hardly seen in spatial resolution of turbo direction of Z and Y, when using no SPAIR.[Conclusion] The choice of turbo direction Z or Y have an important influence for k-space ordering scheme. Particularly, it is thought that a value of SPAIR TR and SPAIR inversion delay greatly affects the scan time and contrast of the MR image.

PDF-070　MRI患者の満足度影響をSERVQUAL解析
A Patient-Satisfaction Survey for MRI Using the SERVQUAL Model

小檜山奈津留（一般財団法人脳神経疾患研究所附属総合南東北病院）
Natsuru Kobiyama

Southern Tohoku General Hospital

【要旨】MRI検査を受ける多くの患者は、検査を受けることに不安を感じている。SERVQUALモデルを用いた患者満足度調査にて、こうした患者の満足度を高めるためには、どのような要因を高めることが重要かを検証した。放射線科にて調査票を配布し、多変量解析を行った結果、確実性及び信頼性の次元を重点的に高めることが必要である。

Purpose: Most patients have an uneasy feeling for taking MRI examination as compared with other examinations. However, we think that patient satisfaction should be evaluated by medical process in radiation technologist (RT) involved in providing medical service. The purpose of this study was to conduct a patient satisfaction survey for MRI by using the SERVQUAL model to analyze the factors increasing patient satisfaction.**Methods**: The survey subjects were patients visiting outpatient clinic ($n = 81$). We asked the patients to fill a questionnaire reflected the five characteristics of the SERVQUAL model (five ranks evaluation). First, we performed multiple regression analysis by the stepwise method. We considered the degree of patient satisfaction as an explanatory variable to evaluate the degree of influence RT factor exerted on the degree of patient satisfaction.Second, we performed hierarchical cluster analysis using the ward method for clustering. **Results**: Regarding the evaluation of the SERVQUAL dimensions, the multiple regression analysis revealed a significant standard partial regression coefficient for general outpatient satisfaction that was significantly influenced, by the interaction; first, with the assurance ($\beta = 0.431$, $P < 0.01$); second, with the reliability ($\beta = 0.380$, $P < 0.01$).These are the results of the hierarchical cluster analysis. The first group involved with the assurance and empathy. The second group involved with the reliability and responsiveness. The remaining a group involved a lone parameter, with the tangibles. **Conclusion**: In our patient for MRI general satisfaction survey, we clarified the contribution of general patient satisfaction in SERVQUAL dimensions. We observed that the influence of assurance was significantly high.

PDF-071　MRI検査の患者におけるSERVQUALモデルを用いたロイヤリティ評価
A Patient-Loyalty for MRI with the SERVQUAL Model

小檜山奈津留（一般財団法人脳神経疾患研究所附属総合南東北病院）
Natsuru Kobiyama
Southern Tohoku General Hospital

【要旨】患者ロイヤリティは経済的成果を達成するために必要である。MRIを受ける多くの患者は、検査を受けることに不安を感じている。そこで、SERVQUAL次元において、MRIを受ける患者のロイヤリティを高めるためには、どのような要因が重要かを検証した。多変量解析を行った結果、確実性の次元を重点的に高めることが必要である。

Purpose: In medical services, it is important to increase the cumulative patient satisfaction in order to increase patient loyalty.However, we think that patient loyalty should be evaluated by medical process in radiation technologist (RT) involved in providing medical service.The purpose of this study was to conduct a patient satisfaction survey for MRI by using the SERVQUAL model to analyze the factors increasing patient loyalty. **Methods**: The survey subjects were outpatients (n = 81). We asked the patients to fill a questionnaire reflected the five characteristics of the SERVQUAL model (five ranks evaluation).First, we performed multiple regression analysis by the stepwise method to evaluate the degree of influence RT factor exerted on the degree of patient loyalty.Second, we performed hierarchical cluster analysis using squared Euclidean distance for measurement and the ward method for clustering.Moreover, we calculated NPS (net promotor score) as an indicator to measure the loyalty.**Results**: Regarding the evaluation of the SERVQUAL dimensions, the multiple regression analysis revealed a significant standard partial regression coefficient for patient loyalty that was significantly influenced, by the interaction; first, with the assurance ($\beta = 0.361$, $P < 0.05$); second, with the reliability ($\beta = 0.328$, $P < 0.05$).These are the results of the hierarchical cluster analysis. The first group involved with the assurance and empathy. The second group involved with the reliability and responsiveness. The remaining a group involved a lone parameter, with the tangibles.**Conclusion**: In our patient for MRI general satisfaction survey, we clarified the contribution of patient loyalty in SERVQUAL dimensions. We observed that the influence of assurance was significantly high.

PDF-072　MRI受検者における閉所恐怖症の切り分けと恐怖症に合った対策の検討
Classification of MRI examinee claustrophobia and examine countermeasures matched each phobia

田泉　智明（市立敦賀病院 放射線室）
Tomoaki Taizumi, Satoshi Matsuyama, Atsuyuki Shimizu, Takeshi Yamazaki, Takeshi Hibi
Municipal Tsuruga hospital , radiology

【要旨】閉所恐怖症という言葉にいくつかの恐怖症が包括されていると仮定し患者アンケートによって切り分けた。結果、狭所、閉所、暗所、孤独においての恐怖症が混在していることが示唆され、各種対策においても恐怖症ごとに効果に差があることが推察された。

Purpose: Nomally, some phobias are classified into one phobia, claustrophobia. To realize better environment for patients and MRI staffs, We conducted questionnaires toward patients. By analyzing them, we want to classify claustrophobia into some detailed phobias and think about countermeasures matched each phobia.
Methods: We conducted questionnaires toward 112 patients that had MRI scan in my hospital from 2015.4.3 to 2016.6.14. We analyzed between correlation phobias that every single person had and desired countermeasures.
Results: First of all, 48 patients (42.9%) have some kind of phobia in 112 patients. Among them, only 2 patients (1.8%) answered that they have 4 phobias, cramped place phobia, claustrophobia, the dark phobia and eremophobia. Also, 14 patients (12.5%) answered that they have 3 phobias, cramped place phobia, claustrophobia and the dark phobia. This rate is totally different from the rate of a single phobia(cramped place phobia:22 patients (19.6%), claustrophobia:28 patients (25%), the dark phobia: 22 patients (19.6%), eremophobia:10 patients (8.9%)). Also, countermeasures that every single person desired were different depending on the characteristic of each phobia.
Examinations: Generally speaking, the word of claustrophobia includes cramped place phobia, claustrophobia, the dark phobia and eremophobia. Even though each phobia has correlation with each other, we can know that each phobia exists by itself. In fact, the treatment that we thought was effective for claustrophobia in not effective against some particular phobias. Therefore, we have to listen to what phobia the patient have and think about the countermeasures matched each patient in order to realize the better environment for both patients and MRI staffs.

PDF-073　mUTE シーケンスにおける撮像条件とコントラストの関係についての基礎的検討
Basic Study on the Relationships between the Scanning Parameters of the mUTE Sequence and Image Contrast

菅野　康貴（東芝メディカルシステムズ株式会社 MRI営業部）
Yasutaka Sugano[1], Yuichi Yamashita[1], Miho Kitamura[1], Naotaka Sakashita[2]
[1]TOSHIBA Medical Systems Co., Ltd. MRI Sales Department, [2]TOSHIBA Medical Systems Co., Ltd. Center for Medical Research and Development

【要旨】UTEシーケンスの静音化、ASL法の適応およびMulti-phase撮像を可能としたmUTEシーケンスを開発したため、シーケンスの特性における基礎的な検討を行った。ファントムを用いた実験の結果、撮像条件の画像への影響がFFE3Dと異なる部分が認められた。本研究により、mUTEシーケンスの特長を認識して使用する必要性が示された。

Purpose: The ultra-short echo time (UTE) sequence is known to be useful for the visualization of short-T2* tissues such as lung and ligament. More recently, it has also been reported that the UTE sequence can be used to reduce acoustic noise in head MRA. We have therefore developed the mUTE sequence by applying the ASL technique, multi-phase imaging, and acoustic noise reduction to the UTE sequence. In this study, we investigated the characteristics of the mUTE sequence as compared to FFE3D.Methods: A 3T scanner (Toshiba Medical Systems) and an MRI phantom were used. The characteristics of the mUTE sequence were evaluated and compared against FFE3D under fixed conditions (TR = 3.0msec, TE = 0.1 ms, matrix size = 256 × 256). The relationships between image contrast and the shot interval, number of segments, number of k-space trajectories, and inversion time (TI) were also investigated.Results: For the mUTE sequence, the results showed a tendency for the SNR to increase as the shot interval became longer. The effect of the IR pulses tended to vary significantly with the number of trajectories per segment. Regarding the relationship between TI and the number of phases, TI contributed strongly to image contrast, but the number of phases did not. In addition, TI showing the same contrast was different from the FFE3D and depends greatly on number of segments and number of trajectoriesConclusion: The differences in the characteristics of mUTE and FFE3D were investigated. The results of this study have demonstrated that there are differences between mUTE and FFE3D in terms of the effects of various scanning parameters on image contrast. It is therefore suggested that when mUTE is used, it is important to take into consideration the particular characteristics of this sequence.

PDF-074　IR パルス併用 Ultra-short echo-time imaging を用いた T1 緩和時間測定
T1 relaxation time measurement using ultra-short echo-time imaging with inversion recovery pulse

増山　　研（医療法人 渓仁会 手稲渓仁会病院 診療技術部）
Ken Masuyama[1,2], Masakazu Shioda[1], Shun Akimoto[1], Kazuya Akiyoshi[1], Hiroyuki Aoki[1], Yuka Inoko[1], Hajime Adachi[1], Toru Yamamoto[3]
[1]Department of Medical Radiation Technology, Teine Keijinkai Hospital, [2]Graduate School of Health Sciences, Hokkaido University, [3]Faculty of Health Sciences, Hokkaido University

【要旨】現在、UTEによる骨のT1値の報告はなく、IRパルス併用UTEから得られるT1値の精度を調査した。Gd造影剤希釈ファントムのT1値をIR併用PETRA(IR-PETRA)とIR併用SE(IR-SE)で取得した。IR-PETRAとIR-SEのT1値は長いT1値の範囲で高い相関を示し、IR-PETRAは長いT1値の測定が可能である。

[Purpose]The ultra-short echo-time (UTE) imaging detects signal from protons with short T2 such as bound water in bone. Utilizing this advantage, T2 values of the MR signal from bone have been investigated. However, T1 values from the bone have not been obtained. In this study, we investigated the reliability of the T1 values obtained by using UTE with IR pulse.[Materials and Methods]The T1 values of saline solution with Gd-DTPA contrast agent (0, 0.1, 0.25, 0.5, 1.0, 5, 10, and 20 mmol/L) in each phantom were obtained by using IR-PETRA (Pointwise encoding time reduction with radial acquisition, TE = 70 μs) and IR-SE (TE = 10 ms) with a 1.5-T MRI. TR was 10 s for both pulse sequences, and TI were varied from 100 to 2000 ms (IR-PETRA) and 50 to 4000 ms (IR-SE). The values of T1 were obtained by the least mean square method with iteration of the assumed MR signal of infinite TI. The concentration dependency of Gd-DTPA on T1 was obtained.[Results and Discussion] The T1 obtained from IR-SE decreased with the Gd-DTPA concentration clearly as in the paramagnetic relaxation theory. The T1 values obtained from IR-PETRA and IR-SE were linearly correlated (r = 0.999) in the Gd-DTPA concentration range from 0 to 1 mmol/L. However, the T1 values obtained from IR-PETRA deviate from those obtained from IR-SE in the Gd-DTPA concentrations above 5 mmol/L. This is because the lowest TI value was 100 ms in IR-PETRA; that was 50 ms in IR-SE. The T2 values of the bound water are as small as in the detectable range of UTE. While on the other hand, its T1 values are large as well as those of ice (a few seconds). Therefore, UTE with IR pulse is promising to measure the T1 value of the bound water. [Conclusion]IR-PETRA can measure the rather long T1 value of bound water.

索　　引

座長・筆頭著者索引

数字は演題番号を示す

S：シンポジウム，SS：緊急シンポジウム，KJS：KSMRM-JSMRM Joint Session，
EL：教育講演，O：一般演題(口演)，P：ポスター，PDF：PDFポスター，
LS：ランチョンセミナー，ES：イブニングセミナー

【き】

【く】

【こ】

【さ】

座長・著者索引

数字は演題番号を示す

S：Symposium，SS：Special Symposium，KJS：KSMRM-JSMRM Joint Session，
EL：Educational Lecture，O：Oral，P：Poster，PDF：PDF Poster，
LS：Luncheon Seminar，ES：Evening Seminar

【I】

【J】

【K】

【L】

【M】

【N】

【O】

【T】

【Y】

【Z】

JSMRM2016 第44回日本磁気共鳴医学会大会
協賛企業・団体一覧

株式会社AZE
GEヘルスケア・ジャパン株式会社
PSP株式会社
アミン株式会社/ザイオソフト株式会社
医療法人社団 豊智会
エーザイ株式会社
株式会社エルエイシステムズ
株式会社ガリバー
株式会社杏林システマック
コニカミノルタジャパン株式会社
産業科学株式会社
シーメンスヘルスケア株式会社
住商ファーマインターナショナル株式会社
スター・プロダクト株式会社
セント・ジュード・メディカル株式会社
第一三共株式会社
大陽日酸株式会社
東芝メディカルシステムズ株式会社
東洋メディック株式会社
トーレック株式会社
ナモト貿易株式会社
日本メドトロニック株式会社
株式会社根本杏林堂
バイエル薬品株式会社
バイテックグローバルエレクトロニクス株式会社
株式会社日立製作所
株式会社フィジオテック
株式会社フィリップスエレクトロニクスジャパン
フジデノロ株式会社
富士フイルムメディカル株式会社
富士製薬工業株式会社
ブルカー・バイオスピン株式会社
株式会社文光堂書店
ボストン・サイエンティフィック ジャパン株式会社
株式会社メディテックファーイースト

（2016年8月8日現在　50音順・敬称略）

支援団体一覧

公益財団法人埼玉県産業文化センター

ご協力ありがとうございました。

2016年8月23日
大会長　新津　守

お 知 ら せ

平成29年度 第45回日本磁気共鳴医学会大会について

会　期：2017年9月14日（木）～ 9月16日（土）

会　場：栃木県総合文化センター／宇都宮東武ホテルグランデ

大会長：瀬尾　芳輝
（獨協医科大学医学部生理学教室）

平成30年度 第46回日本磁気共鳴医学会大会について

会　期：2018年9月7日（金）～ 9月9日（日）

会　場：ホテル日航金沢／金沢市アートホール

大会長：宮地　利明
（金沢大学医薬保健研究域保健学系）

日本磁気共鳴医学会雑誌

略称：日磁医誌（JJMR）

Vol. 36 SUPPLEMENT
2016年9月6日発行
定価 4,000円（税込）

〒105-0012　東京都港区芝大門2-12-8
浜松町矢崎ホワイトビル2F
TEL: 03-6721-5388
FAX: 03-6721-5433

印　刷　所　山菊印刷株式会社

年1回発行　